ETSI TR 145 912 V17.0.0 (2022-05)

TECHNICAL REPORT

**Digital cellular telecommunications system (Phase 2+) (GSM);
Feasibility study for evolved GSM/EDGE Radio Access
Network (GERAN)
(3GPP TR 45.912 version 17.0.0 Release 17)**

**GLOBAL SYSTEM FOR
MOBILE COMMUNICATIONS**

Reference

RTR/TSGR-0045912vh00

Keywords

GSM

ETSI

650 Route des Lucioles
F-06921 Sophia Antipolis Cedex - FRANCE

Tel.: +33 4 92 94 42 00   Fax: +33 4 93 65 47 16

Siret N° 348 623 562 00017 - APE 7112B
Association à but non lucratif enregistrée à la
Sous-Préfecture de Grasse (06) N° w061004871

Important notice

The present document can be downloaded from:
http://www.etsi.org/standards-search

The present document may be made available in electronic versions and/or in print. The content of any electronic and/or print versions of the present document shall not be modified without the prior written authorization of ETSI. In case of any existing or perceived difference in contents between such versions and/or in print, the prevailing version of an ETSI deliverable is the one made publicly available in PDF format at www.etsi.org/deliver.

Users of the present document should be aware that the document may be subject to revision or change of status. Information on the current status of this and other ETSI documents is available at
https://portal.etsi.org/TB/ETSIDeliverableStatus.aspx

If you find errors in the present document, please send your comment to one of the following services:
https://portal.etsi.org/People/CommiteeSupportStaff.aspx

If you find a security vulnerability in the present document, please report it through our
Coordinated Vulnerability Disclosure Program:
https://www.etsi.org/standards/coordinated-vulnerability-disclosure

Notice of disclaimer & limitation of liability

The information provided in the present deliverable is directed solely to professionals who have the appropriate degree of experience to understand and interpret its content in accordance with generally accepted engineering or other professional standard and applicable regulations.
No recommendation as to products and services or vendors is made or should be implied.
No representation or warranty is made that this deliverable is technically accurate or sufficient or conforms to any law and/or governmental rule and/or regulation and further, no representation or warranty is made of merchantability or fitness for any particular purpose or against infringement of intellectual property rights.
In no event shall ETSI be held liable for loss of profits or any other incidental or consequential damages.

Any software contained in this deliverable is provided "AS IS" with no warranties, express or implied, including but not limited to, the warranties of merchantability, fitness for a particular purpose and non-infringement of intellectual property rights and ETSI shall not be held liable in any event for any damages whatsoever (including, without limitation, damages for loss of profits, business interruption, loss of information, or any other pecuniary loss) arising out of or related to the use of or inability to use the software.

Copyright Notification

ETSI

Intellectual Property Rights

Essential patents

IPRs essential or potentially essential to normative deliverables may have been declared to ETSI. The declarations pertaining to these essential IPRs, if any, are publicly available for **ETSI members and non-members**, and can be found in ETSI SR 000 314: *"Intellectual Property Rights (IPRs); Essential, or potentially Essential, IPRs notified to ETSI in respect of ETSI standards"*, which is available from the ETSI Secretariat. Latest updates are available on the ETSI Web server (https://ipr.etsi.org/).

Pursuant to the ETSI Directives including the ETSI IPR Policy, no investigation regarding the essentiality of IPRs, including IPR searches, has been carried out by ETSI. No guarantee can be given as to the existence of other IPRs not referenced in ETSI SR 000 314 (or the updates on the ETSI Web server) which are, or may be, or may become, essential to the present document.

Trademarks

The present document may include trademarks and/or tradenames which are asserted and/or registered by their owners. ETSI claims no ownership of these except for any which are indicated as being the property of ETSI, and conveys no right to use or reproduce any trademark and/or tradename. Mention of those trademarks in the present document does not constitute an endorsement by ETSI of products, services or organizations associated with those trademarks.

DECT™, **PLUGTESTS™**, **UMTS™** and the ETSI logo are trademarks of ETSI registered for the benefit of its Members. **3GPP™** and **LTE™** are trademarks of ETSI registered for the benefit of its Members and of the 3GPP Organizational Partners. **oneM2M™** logo is a trademark of ETSI registered for the benefit of its Members and of the oneM2M Partners. **GSM**® and the GSM logo are trademarks registered and owned by the GSM Association.

Legal Notice

This Technical Report (TR) has been produced by ETSI 3rd Generation Partnership Project (3GPP).

The present document may refer to technical specifications or reports using their 3GPP identities. These shall be interpreted as being references to the corresponding ETSI deliverables.

The cross reference between 3GPP and ETSI identities can be found under http://webapp.etsi.org/key/queryform.asp.

Modal verbs terminology

In the present document "**should**", "**should not**", "**may**", "**need not**", "**will**", "**will not**", "**can**" and "**cannot**" are to be interpreted as described in clause 3.2 of the ETSI Drafting Rules (Verbal forms for the expression of provisions).

"**must**" and "**must not**" are **NOT** allowed in ETSI deliverables except when used in direct citation.

Contents

Foreword

This Technical Report has been produced by the 3rd Generation Partnership Project (3GPP).

The contents of the present document are subject to continuing work within the TSG and may change following formal TSG approval. Should the TSG modify the contents of the present document, it will be re-released by the TSG with an identifying change of release date and an increase in version number as follows:

Version x.y.z

where:

x   the first digit:

1   presented to TSG for information;

2   presented to TSG for approval;

3   or greater indicates TSG approved document under change control.

y   the second digit is incremented for all changes of substance, i.e. technical enhancements, corrections, updates, etc.

z   the third digit is incremented when editorial only changes have been incorporated in the document.

Introduction

GERAN is a result of over a decade of radio interface evolution that is still ongoing. While GERAN is or is being deployed worldwide also in emerging markets, evolving further the GERAN radio interface needs to be studied to ensure not only that the same services are available regardless of the underlying radio technology UTRAN or GERAN, but essentially that service continuity exists across these radio technologies supported by core network evolution e.g. IMS. Such an evolution is also needed to maintain GERAN competitiveness as well as UTRAN competitiveness.

1 Scope

The present document is an output of the 3GPP work item "Future GERAN Evolution" [1].

The scope of this document is to capture the results of the feasibility study on the GERAN, the objectives of which are to: increase capacity, coverage and data rates; reduce latency; and enhance service continuity with other RATs; while minimising impacts to infrastructure.

2 References

The following documents contain provisions which, through reference in this text, constitute provisions of the present document.

- References are either specific (identified by date of publication, edition number, version number, etc.) or non-specific.

- For a specific reference, subsequent revisions do not apply.

- For a non-specific reference, the latest version applies. In the case of a reference to a 3GPP document (including a GSM document), a non-specific reference implicitly refers to the latest version of that document *in the same Release as the present document*.

[1] 3GPP TSG-GERAN#24 Tdoc GP-051052 "Work Item Description: Future GERAN Evolution".

3 Abbreviations

For the purposes of the present document, the following abbreviations apply:

ACP	Adjacent Channel Power
ACR	Adjacent Channel Rejection
AGI	Antenna Gain Imbalance
AMR	Adaptive Multi-Rate
AOA	Angle Of Arrival
BEP	Bit Error Probability
BLEP	BLock Error Probability
BLER	BLock Error Rate
BN	Bit Number
BTS	Base Transceiver Station
CDCU	Constrained Dual-Carrier Uplink
CDF	Cumulative Density Function
CIR	Carrier to Interference Ratio
CR	Conventional Receiver
DA	Dynamic Allocation
DARP	Downlink Advanced Receiver Performance
DSR	Dual Symbol Rate
EDA	Extended Dynamic Allocation
EFL	Effective Frequency Load
EGPRS	EDGE General Packet Radio Service
GEV	GERAN EVolution
HOMTC	Higher Order Modulation and Turbo Codes
HSN	Hopping Sequence Number
IM	InterModulation
IR	Incremental Redundancy
IRC	Interference Rejection Combining
LQC	Link Quality Control
MCS	Modulation and Coding Schemes
MDSR	Modified Dual Symbol Rate
MIP	Multipath Intensity Profile

MRC	Maximal Ratio Combining
MSRD	Mobile Station Receive Diversity
OOR	Out-Of-Range
PA	Power Amplifier
PAR	Peak-Average Ratio
RMS	Root Mean Square
SAIC	Single Antenna Interference Cancellation
SF	Stealing Flag
TTI	Transmission Time Interval
TU	Typical Urban
VSRB	Variable Sized Radio Block

4 Objectives

4.1 General

The general objective of this study is to improve the service performance and to provide efficient bearers for GERAN to meet enhanced demands for different types of services. Some examples of services considered are given below.

- Interactive and Best-effort services (like web browsing, file download and image or video clip upload) typically gain from increased mean bit rates, but also gain from reduced latency, e.g. throughput is limited by the TCP window size divided by the round trip time.

- Conversational services (like Voice over IP (VoIP) and enhanced Push to talk over Cellular (PoC)), as well as, e.g. on-line gaming services typically have high requirements on latency and fast access.

- All services may gain from improved coverage, e.g. video-telephony is a service that will need (better) coverage for higher bit rates for both uplink and downlink.

- All services may gain from a mobile station always being connected to the most appropriate base station, i.e. as seen from a radio performance perspective, as this may yield higher capacity, reduce latency etc. due to improved interference conditions.

- Particular requirements may be set by services like broadcast TV over MBMS bearers. Typically, high bit rates are required at the same time as robustness is important to fulfil coverage and latency requirements as well as providing interactivity.

A GSM/EDGE network may interoperate with WCDMA RAT, either within an operator's network or with different operators. There are also standalone GSM/EDGE networks. Both the GSM/WCDMA networks and the GSM only networks will benefit from the increased GSM/EDGE service portfolio. A combined WCDMA & GSM/EDGE network will benefit from better service continuity between the accesses resulting in an easier resource utilisation and service provisioning. GSM/EDGE only networks can give their users an increased range of end user services/applications and possibly make use of applications/services that do not require adaptations to access specific capabilities. This could potentially lead to reduce cost of provisioning and create a wider use of services.

As a general guideline, the following subclauses detail the performance requirements and design constraints the proposed features/candidates should take into account. Taking those in consideration would enable easy network evolution and be able to efficiently use existing network equipment and support legacy mobile stations.

Each candidate should describe the compliance to the following relevant assumptions and pre-requisites. If non-compliant the reasons and consequences need to be detailed.

4.2 Performance objectives

The enhancements are expected to provide (either a single one or as a group of enhancements per listed requirement):

- Spectrum efficiency/capacity (interference limited scenario):

  - 50 % better (measured in kbps/MHz/cell for data and Erl/MHz/cell for speech).

- Increase peak data rates:

    - 100 % better in downlink and uplink.

- Improved coverage (noise limited scenario):

    - Speech and data:

        - Sensitivity increase in downlink of 3 dB.

- Improved service availability (when cells are planned for speech):

    - Increase mean bit rate by 50% at cell edges for uplink and downlink.

- Reduced latency:

    - Initial access ("no TBF assigned"):

        - A round trip time less than 450 milliseconds (in non-ideal radio conditions on the radio interface).

    - After initial access:

        - A round trip time less than 100 milliseconds (in non-ideal radio conditions on the radio interface).

NOTE: Round trip time means end-to-end; i.e. the time between sending an echo request from the end user to the server and receiving the response, but in this document only contributions from the mobile station up to the Gi interface and vice versa are included in the RTT figure.

- Balanced performance improvements:

    - Throughput improvements should be supported by available round trip time e.g. RTT-bit rate-product should not increase over typical TCP window size.

    - Relatively similar uplink and downlink improvements on bit rates, coverage, capacity and latency.

    - Peak bit rate or improvements in ideal conditions should not be primary optimisation goal, but typical performance in real network.

4.3   Compatibility objectives

The proposals should consider the following compatibility objectives:

- Coexist with existing legacy frequency planning:

    - This will enable an operator to deploy the enhancements in existing network given already existing adjacent frequency protection levels, sensitivity and interference levels.

    - This will enable an operator to do plug-and-play deployment of new enhanced radio bearers in existing networks.

- Coexist with legacy mobile stations:

    - This will enable compatibility with legacy (E)GPRS terminals by allowing multiplexing of shared resources and thereby avoiding radio resource segregation.

- Avoid impacts on existing BTS, BSC and CN hardware:

    - This will enable use of already existing hardware and only require a software upgrade.

- Be based on the existing network architecture and minimal impact on core network:

    This will enable an operator to re-use existing network nodes.

- Be applicable also for Dual Transfer Mode.

- Be applicable for the A/Gb mode interface.

5 Conclusions and recommendations

Within a relatively short period of time a significant number of proposals has been put forward to determine the next steps on future GERAN evolution. The general viability of proposals can be determined by comparing how those fit with the given objectives in chapter 4, which are summarised in table 1. Conclusions and recommendations for downlink, uplink and latency enhancements are summarised in subclauses 5.1, 5.2 and 5.3 respectively.

Numbers in the table refer to the related chapter of the feasibility study. Some proposals are combined to achieve better performance. Some performance objectives like "balanced performance improvements" are considered as general objectives, thus not included in the table. Downlink and uplink performance objectives are separated, since most of the proposals are meant only for one link.

Table 1 should be seen as giving the current status for each proposal and is subject to change with each forthcoming meeting.

Table 1: Comparison of different proposals versus performance and compatibility objectives

GP-061312 rev 1 Source: TSG GERAN Ad-Hoc on GERAN Evolution Sophia Antipolis 25-26 May, 2006	MS Rx diversity	Dual-carrier and multi-carrier (DL)	Dual-carrier and multi-carrier (UL - wideband)	Dual-carrier and multi-carrier (UL - Independent carriers)	New modulation schemes and Turbo Codes (Downlink)	New modulation schemes and Turbo Codes (Uplink)	Dual symbol rate	Modified dual symbol rate	New burst structures and new slot formats	Latency Enhancements HS-HARQ not evaluated	Uplink TP enhancements with low standard impact
Downlink performance											
50% spectrum efficiency gain *Common definition as reported in AHGEV-0034.* *- Figure(s) for sufficient QoS not agreed* *- "50%" figure to be redefined* *Note: alternative definitions possible, however at least the common one shall be used*	FFS	0%	N.A.	N.A.	FFS (report range, use agreed definition)	N.A.	N.A.	N.A.	N.A.	N.A.	N.A.
100% peak data rate increase (theoretic)	0%	100%	N.A.	N.A.	33.3% vs. 8PSK	N.A.	N.A.	N.A.	N.A.	N.A.	N.A.
3dB sensitivity increase in DL	>3dB	0%	N.A.	N.A.	No	N.A.	N.A.	N.A.	N.A.	N.A.	N.A.
50% bit rate gain at cell border	>50%	100%	N.A.	N.A.	FFS	N.A.	N.A.	N.A.	N.A.	N.A.	N.A.
Uplink performance											
50% spectrum efficiency gain *Common definition as reported in AHGEV-0034.* *- Figure(s) for sufficient QoS not agreed* *- "50%" figure to be redefined* *Note: alternative definitions possible, however at least the common one shall be used*	N.A.	N.A.	0%	0%	N.A.	[40% - 60%] / FFS *Common definition; 15kbps sufficient QoS per timeslot; 10th percentile*	FFS (60%, 1TRX) FFS (0%, 2TRX) *Definition as reported in AHGEV-0035*	FFS (60%, 1TRX) FFS (0%, 2TRX) *Definition as reported in AHGEV-0035*	FFS (max. theoretic 41.3% with 4 TS aggregations *) ** Raw-bit level. Not in-line with common definition*	N.A.	0%
100% peak data rate increase (theoretic)	N.A.	N.A.	100%	100%	N.A.	33.3% vs. 8PSK	100%	100%	41.3% * (4 TS aggregation) ** Raw-bit level*	N.A.	100%
50% bit rate gain at cell border	N.A.	N.A.	FFS	FFS	N.A.	FFS	50% (coverage limited, 1TRX); 55% (capacity limited, 1TRX) / FFS	90% (coverage limited w/QPSK, 1TRX); 67% (capacity limited, 1TRX) / FFS	FFS (max. theoretic 41.3% with 4 TS aggregations *) ** Raw-bit level*	N.A.	50%
Multiplexing limitations *Potential multiplexing losses*	None	None	None	None	Yes (USF) *0%-100% loss depending on network allocation/scheduling policy*	None	None	None	None	No *NOTE: RTTI implies limitations for RTTI operation e.g. USF decoding*	No
Latency											
Initial RTT < 450 ms	N.A.	N.A.	N.A.	N.A.	N.A.	N.A.	N.A.	N.A.	N.A.	**Not studied**	N.A.
RTT < 100 ms	N.A.	N.A.	N.A.	N.A.	N.A.	N.A.	N.A.	N.A.	N.A.	Yes	N.A.
Initial Access ("no TBF assigned"): A round trip time less than 450 milliseconds (in non-ideal radio conditions on the radio interface) *After initial access: A round trip time less than 100 milliseconds (in non-ideal radio conditions on the radio interfac*											
Compatibility											
Coexist with existing legacy frequency planning *- This will enable an operator to deploy the enhancements in existing network given already existing adjacent frequency protection levels, sensitivity and interference levels* *- This will enable an operator t*	Y	Y	No: fixed carrier spacing / FFS *As of yet no solution allowing coexistence with legacy frequency planning: further studies (Extended Frequency Allocation?) expected until GERAN#30*	Yes Freq. range of 20MHz	FFS	Yes	Yes (1/3 re-use, 1TRX) Yes (1/3 re-use, 2TRX, radio freq. hopping) No (2TRX, Baseband hopping) FFS (other scenarios)	Yes (1/3 re-use, 1TRX) Yes (1/3 re-use, 2TRX, radio freq. hopping) No (2TRX, Baseband hopping) FFS (Other scenarios)	Yes	Yes	Yes
Coexist with legacy MSs *This will enable compatibility with legacy (E)GPRS terminals by allowing multiplexing of shared resources and thereby avoiding radio resource*	Y	Y	Yes	Yes	Yes	Yes	Yes	Yes	Yes	Yes	Yes
Avoid HW impacts on BSS *'May' indiactes that a hardware upgrade might be required from at least one network vendor (see GP-061083)*	Y	Y	FFS (IRC) *Need for IRC to be evaluated.* *Impact of IRC to be evaluated*	Yes	May	May	May	May	Yes / FFS (e.g. buffering, tracking)	Yes	Yes
No NW architecture impacts	Y	Y	Yes	Yes	Yes	Yes	Yes	Yes	Yes	Yes	Yes
Applicable for DTM	Y	Y	Yes	Yes	Yes	Yes	Yes	Yes	Yes/No (CS in the "middle" of PS slots)	Yes (RTTI=10ms)	Yes
Applicable for the A/Gb mode	Y	Y	Yes	Yes	Yes	Yes	Yes	Yes	Yes	Yes	Yes
Feasible MS implementation	Y	Y	Yes/No	No (not feasible for all MS formats) / FFS	FFS	Yes	Yes	Yes	Yes	Yes / FFS *(Reduced MS response time)*	FFS

N.A.= not measurable or not used as criteria in evaluating the proposal.

5.1 Conclusions and recommendations for Downlink

Mobile Station Receive Diversity (MSRD) is a downlink feature, which improves the receiver performance of the mobile station by means of an additional antenna. The introduction of Single Antenna Interference Cancellation (SAIC) characterised by the Downlink Advanced Receiver Performance (DARP) requirements has already shown that receiver enhancements in the MS can provide significant gains in terms of spectral efficiency. MS receive diversity offers the possibility of enhanced channel diversity and the potential for further improved interference cancellation performance for GMSK modulated signals. Also, as opposed to SAIC, receive diversity enables significant gains for 8PSK-modulated signals. It has been noted that MSRD has significant impact on the MS hardware, and may impact both terminal power consumption and size.

Simulations and literature surveys in clause 6 have shown that considerable gains are achievable for both 8-PSK and GMSK modulated signals, although it is recognized that factors such as antenna performance and terminal design may impact the performance in a live network. To study the performance in more detail a simple channel model was derived, which includes antenna correlation and gain imbalance between the receiver antennas.

Subclauses 6.3.4.2 to 6.3.4.4 have assessed the impact of these parameters using the MSRD channel models as well as provided a small literature survey of publications related to the achievable performance MS receive diversity. Several contributions have shown the impact in terms of receiver performance for different architectures and in general it seems that the diversity receivers are relatively insensitive to parameter variations. That is, large gains are achieved even for high values of correlation and antenna gain imbalance. Link- and system level simulations have been provided for speech services (AMR) and data services (EGPRS).

Based on the results reported in chapter 6, it has been decided to open a work item on MSRD characterised by DARP Phase II. This was agreed at TSG GERAN#27.

Multi-carrier is a performance-enhancing feature whereby data to a single user can be transmitted on multiple carriers (see clause 7). The feature is aimed at enabling higher data rates in GERAN with minimal impacts to infrastructure. Currently, the theoretical peak data rate of EGPRS is 473.6 kbps for a single user. In a real network, average bit rates in the order of 100 kb/s to 200 kb/s are feasible on four timeslots. With multi-carrier, both peak and average user throughput are increased proportionally to the number of carriers. With a dual-carrier configuration, the peak data rate would be close to 1 Mb/s. With this feature, peak and average bit rates can be increased in a very flexible and backwards-compatible manner.

Given the current technical and implementation limitations, it is considered acceptable in an initial phase to restrict the number of carriers to two. The need for higher bit rates could make it desirable to support more than two carriers in future releases of the GERAN standards.

Dual Carrier in the Downlink has been shown to meet some of the performance objectives of GERAN Evolution (in particular it enables an increase in the peak downlink data rate) without impairing any of the other performance metrics. Also, it satisfies all the compatibility objectives for candidate features; in particular, it is expected that it will have no impact on BSS hardware, given that there are no changes to the modulation and to the coding schemes. It is also anticipated that implementation in the MS is feasible.

Dual Carrier in the Downlink can optionally be combined with MS Receive Diversity. Provided that the MS supports this capability, it could be possible for a dual antenna terminal to switch between dual carrier reception and MS receive diversity (see clause 12).

Based on the results of the Feasibility Study (as detailed in clause 7), it has been decided to open a work item on Dual Carrier in the Downlink. This was agreed at GERAN#28.

5.2 Conclusions and recommendations for Uplink

5.3 Conclusions and recommendations for Latency enhancements

6 Mobile station receiver diversity

6.1 Introduction

Mobile Station receiver diversity is a downlink feature, which improves the receiver performance of the mobile station by means of an additional antenna. The introduction of Single Antenna Interference Cancellation (SAIC) characterised by the Downlink Advanced Receiver Performance (DARP) requirements has already shown that receiver enhancements in the MS can provide significant gains in terms of spectral efficiency [1]. MS receiver diversity offers the possibility of enhanced channel diversity and the potential for further improved interference cancellation performance for GMSK modulated signals as well as significant gains for 8PSK-modulated signals. As stated in clause 4 one of the key objectives of the GERAN evolution is to improve the end user performance, for instance by increasing the average data rates, and the receiver performance improvement introduced by MS receiver diversity has the potential to do exactly that by e.g. improving user throughput for downlink EGPRS services.

6.2 Concept description

The aim of MS diversity is to enhance the reception of a given link in the downlink direction, by means of diversity provided by an additional antenna. Thus, receiver diversity is based on reception of the *same* signal on two antennas in the MS. Therefore no changes are made to the transmissions schemes in the Base Transceiver Station (BTS).
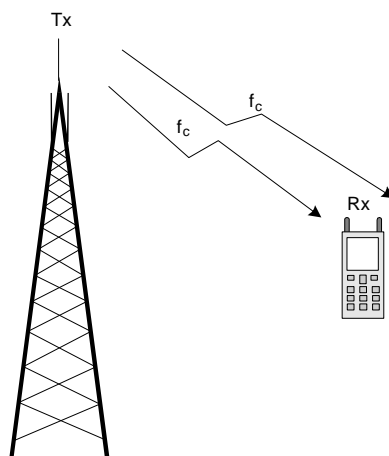
Figure 1: Concept of MS Receive Diversity

Seen from the Layer 1 in the MS, the introduction of MS Receiver diversity will be a general *link level* improvement. That is, the signals received by the two antennas are to be combined as one link. Therefore existing algorithms and procedures such as link adaptation, bit error probability estimation and RXQUAL are expected to remain unchanged in the sense that these measures simply reflect improved link quality.

6.3 Modelling Assumptions and Requirements

To evaluate the performance of dual-antenna terminals, the channel models currently used in TSG GERAN must be extended to model two parallel channels. Figure 2 depicts a model of the environment surrounding a dual antenna MS.
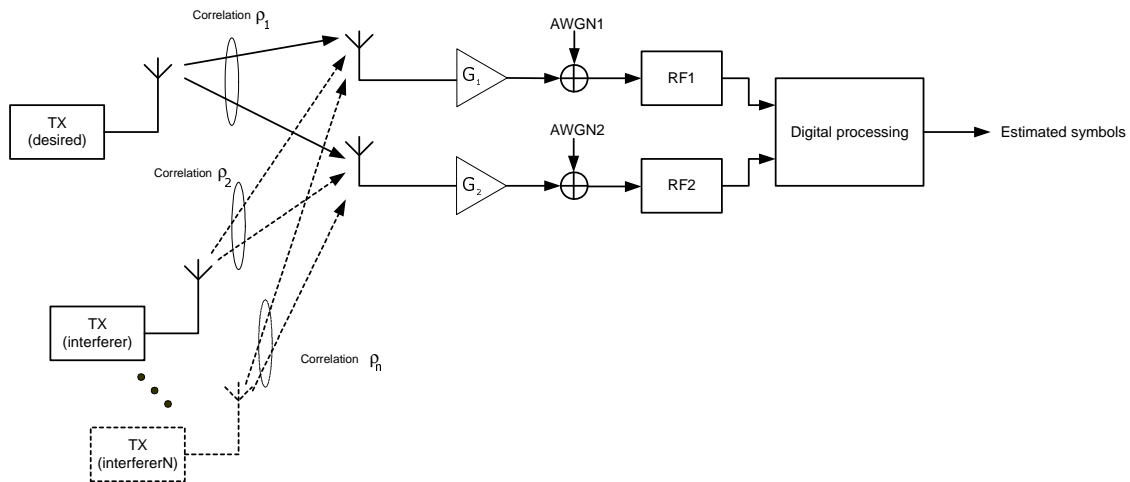
Figure 2: Interferer environment for a dual antenna MS

As seen from the figure, the MS has two receiver branches, each influenced by both interference and thermal noise (modelled by AWGN). The figure also illustrates how the signal received at one antenna will be correlated with the signal received at the other. For instance, the desired signal received at the two antennas is correlated with a correlation factor ρ_1. This correlation factor is a function of the radio propagation environment, the physical design of the MS as well as the presence of a user.

Besides the correlation factors, the model shows individual gain for each antenna, G_1 and G_2. The difference between these values is sometimes referred to as the branch power difference (BPD) or the Antenna Gain Imbalance (AGI). This difference is dependent on the physical design of the transmitting and receiving antennas, the scattering medium and also on other factors including user interaction. For example, the user may cover one of the two antennas with his/her hand during reception. The BPD is only considered most relevant for noise-limited scenarios (i.e. at, or close to the minimum supportable received power level), since - to a first-order approximation - the carrier to interference ratio (CIR) can be considered the same for each antenna although one has less gain than the other. That is, both carrier and interferer are attenuated thus maintaining the same CIR.

In order to evaluate the performance of dual antenna mobiles, a dual channel model must be defined, which takes the impact of antenna correlation and gain differences into account. The following subclauses deals with how to define such as model and the parameters associated with it.

6.3.1 Spatial Modelling

As a starting point, a 2x2 MIMO channel model [3] is assumed, where the first transmit antenna transmits the signal of the desired user, and the second transmit antenna transmits the signal of the interferer. For convenience, flat fading is assumed, where the transmission coefficients h_{mn} describe the transmission paths of between transmit antenna n and receive antenna m (see note), see figure 3.

NOTE: The first index of the transmission coefficients denotes the receive antenna and the second index the transmit antenna.
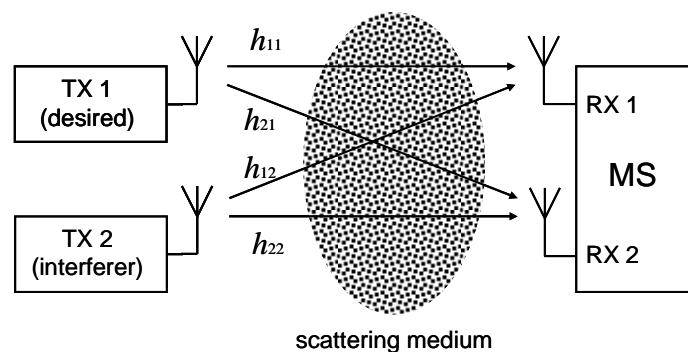
Figure 3: Scattering environment for a dual antenna MS [13]

It is assumed that the channel coefficients h_{mn} are superpositions of L multipath components (MPC), each of which interacting with the scattering medium through a different path. Each MPC is described by its angle of departure (AOD), denoted as θ_l, and its Angle Of Arrival (AOA), denoted as ϕ_l, and its complex amplitude $\alpha_l, l = 1 \ldots L$. Note that nothing is assumed on the relationship between AOD and AOA of a MPC. A MPC may arise due to single scattering, multiple scattering, or line-of-sight transmission.

First, we consider the TX antennas to be far-distanced, and the TX antennas of the desired user and the interferer illuminate different scatterers. Such a situation arises as inter-site interference, i.e. the BTS antennas of the desired user and the interferer belong to different BTS sites, see figure 4.
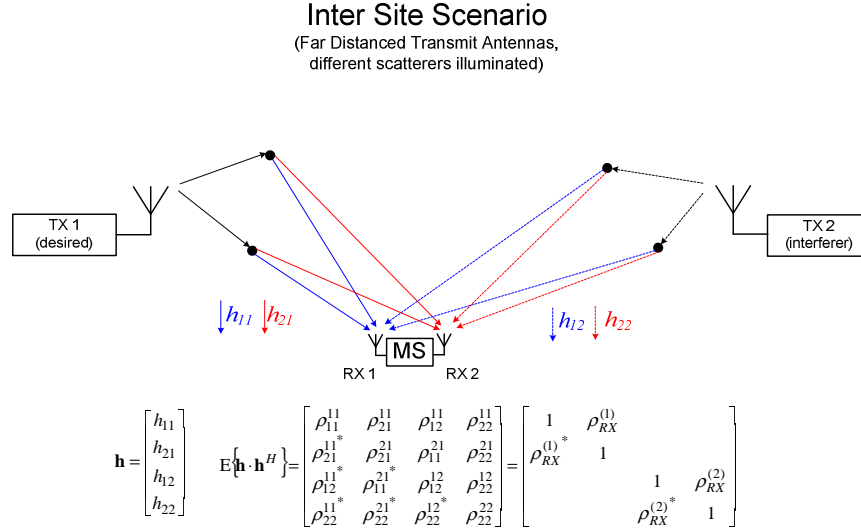
Figure 4: Inter-site interference scenario [13]

We denote the complex amplitudes of the MPCs between TX antenna 1 and RX antenna 1 as $\alpha_l^{(1)}$ and between TX antenna 2 and RX antenna 1 as $\alpha_l^{(2)}$. The phase shifts between the RX antennas are denoted as $\varphi_l^{(1)}$ for the MPCs from the first TX antenna and $\varphi_l^{(2)}$ for the MPCs of the second TX antenna, respectively. Note that the far-field and the narrow-band condition is assumed to be valid for the RX antennas.

The transmission coefficients are:

$$
\begin{aligned}
h_{11} &= \sum_{l=1}^{L^{(1)}} \alpha_l^{(1)} \\
h_{12} &= \sum_{l=1}^{L^{(2)}} \alpha_l^{(2)} \\
h_{21} &= \sum_{l=1}^{L^{(1)}} \alpha_l^{(1)} \, e^{j\varphi_l^{(1)}} = \sum_{l=1}^{L^{(1)}} \alpha_l^{(1)} \, e^{j\frac{2\pi}{\lambda}\left\langle \vec{e}\left(\phi_l^{(1)}\right), \vec{r}_2^{\,\mathrm{RX}} - \vec{r}_1^{\,\mathrm{RX}}\right\rangle} \\
h_{22} &= \sum_{l=1}^{L^{(2)}} \alpha_l^{(2)} \, e^{j\varphi_l^{(2)}} = \sum_{l=1}^{L^{(2)}} \alpha_l^{(2)} \, e^{j\frac{2\pi}{\lambda}\left\langle \vec{e}\left(\phi_l^{(2)}\right), \vec{r}_2^{\,\mathrm{RX}} - \vec{r}_1^{\,\mathrm{RX}}\right\rangle}
\end{aligned}
\tag{1}
$$

Here, λ is the wavelength, $\vec{e}\left(\phi_l^{(n)}\right)$ is a unit vector pointing toward the AOA of the $l-$th MPC, and $\vec{r}_n^{\,\mathrm{TX}}$ and $\vec{r}_m^{\,\mathrm{RX}}$ are the locations of the transmit and receive antennas, respectively, relative to an arbitrary coordinate system. Moreover, $\langle\cdot,\cdot\rangle$ denotes the scalar product of two vectors. With regard to the statistics of the transmission coefficients, it is assumed that each h_{mn} is a zero-mean complex circularly symmetric Gaussian random variable, i.e. $\mathrm{E}\{h_{mn}\} = 0$ and

$E\left\{\left|h_{mn}\right|^2\right\} = 1$ for all m, n. Moreover, it is assumed that the complex amplitudes of the MPC are mutually uncorrelated, i.e. $E\left\{\alpha_l^{(n)}\left(\alpha_{l'}^{(n)}\right)^*\right\} = 0$ for $l' \neq l$.

Receive Correlation

Since the signals of TX antenna 1 and TX antenna 2 are transmitted over two completely different propagation paths, the two correlation factors between the RX signals are different:

$$\rho_{RX}^{(1)} = E\left\{h_{11}h_{21}^*\right\} = \sum_{l=1}^{L^{(1)}} E\left\{\left|\alpha_l^{(1)}\right|^2\right\} e^{-j\varphi_l^{(1)}}$$

$$\rho_{RX}^{(2)} = E\left\{h_{12}h_{22}^*\right\} = \sum_{l=1}^{L^{(2)}} E\left\{\left|\alpha_l^{(2)}\right|^2\right\} e^{-j\varphi_l^{(2)}}$$

(2)

The RX correlation factors may differ in their absolute value, but also in their phase angle. The phase angle of the correlation factor depends on the main direction at which the received signal arrives at the MS. When the latter differs much for desired user and interferer, there is also a huge difference in the phase angle.

Transmit Correlation

Due to uncorrelated MPC between TX antenna 1 and the receiver and TX antenna 2 and the receiver, respectively, the TX correlation factors are zero:

$$\rho_{TX}^{(1)} = E\left\{h_{11}h_{12}^*\right\} = 0$$

$$\rho_{TX}^{(2)} = E\left\{h_{21}h_{22}^*\right\} = 0$$

(3)

Therefore, considering only correlation on the receiver side a suitable channel model can be implemented as described in subclauses 6.3.2 and 6.3.3.

6.3.2 Single input - dual output channel model

Figure 5 shows a simple linear model that can be used to generate a two branch fading signal.
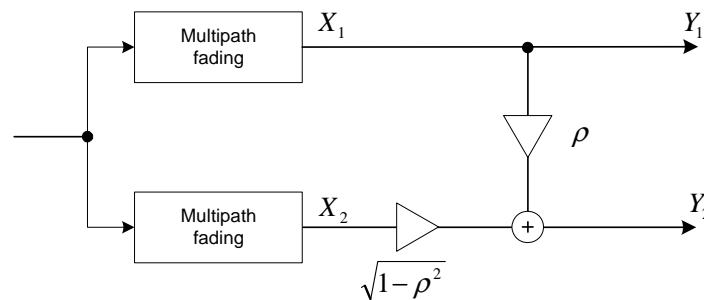
Figure 5: Single input - dual output channel model for MS Receiver Diversity

The model consists of a single input signal, which is sent through two fading channels. The multipath fading is independent Rayleigh fading processes but the channel profile, e.g. TU50 is the same for each branch. The correlation between the two branches is generated using the weighting factor ρ. The system equations of the linear model are:

$$y_1 = x_1$$

$$y_2 = \rho \cdot x_1 + \sqrt{1 - \rho^2} \cdot x_2$$

The magnitude of the complex cross-correlation between the two received signals Y_1 and Y_2 is then:

$$R_{y_1,y_2} = \frac{E[Y_1 Y_2^*]}{\sqrt{E[Y_1 Y_1^*] E[Y_2 Y_2^*]}} = \frac{\rho E[X_1 X_1^*] + \sqrt{1-\rho^2}\, E[X_1 X_2]}{\sqrt{E[Y_1 Y_1^*] E[Y_2 Y_2^*]}}$$

Assuming that X_1 and X_2 are independent processes and thus orthogonal results in:

$$R_{y_1,y_2} = \frac{E[Y_1 Y_2^*]}{\sqrt{E[Y_1 Y_1^*] E[Y_2 Y_2^*]}} = \frac{\rho}{\sqrt{E[Y_1 Y_1^*] E[Y_2 Y_2^*]}}$$

Since:

$$E[X_1 X_1^*] = 1,$$
$$E[X_1 X_2] = 0$$

Similarly the denominator reduces to:

$$R_{y_1,y_2} = \frac{E[Y_1 Y_2^*]}{\sqrt{E[Y_1 Y_1^*] E[Y_2 Y_2^*]}} = \frac{\rho}{\sqrt{E[X_1 X_1^*] \cdot \left(\rho^2 E[X_1 X_1^*] + (1-\rho^2) E[X_2 X_2] + 2\rho\sqrt{1-\rho^2}\, E[X_1 X_2] \right)}} = \frac{\rho}{\sqrt{1}} = \rho$$

An alternative description of the correlation, the envelope correlation, is sometimes used in the literature. The relation between these two correlation measures can be approximated as [19]:

$$\rho_e = \rho_p^2$$

Figure 6 show the coupling between the two measures.
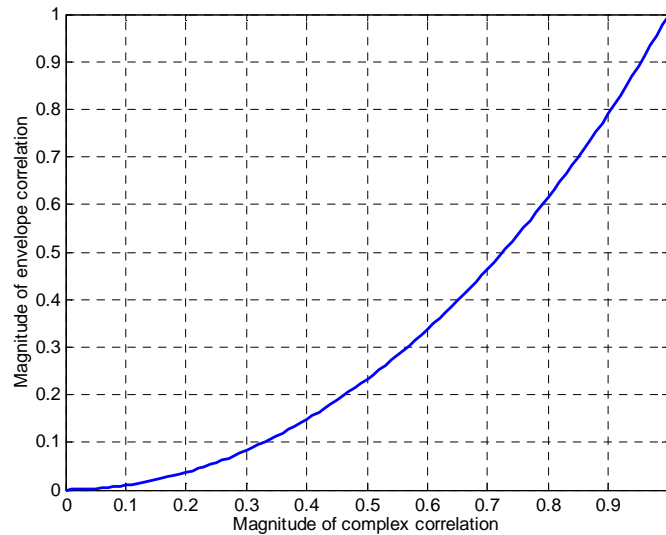
Figure 6: Coupling between the envelope correlation and the magnitude of the complex correlation for Gaussian fading I and Q-part of the complex channel taps

6.3.3   Multiple interferer model

The single input-dual output model is easily extended to a multi-interferer scenario as shown in figure 7. The model uses instances of the single input dual output channel model to instantiate the interfering signals. After summation of the interfering signals and the desired signal an AWGN signal is added to the received signal at each antenna to model the internal noise of the receiver. A gain scaling is also applied to model the difference in antenna gains.
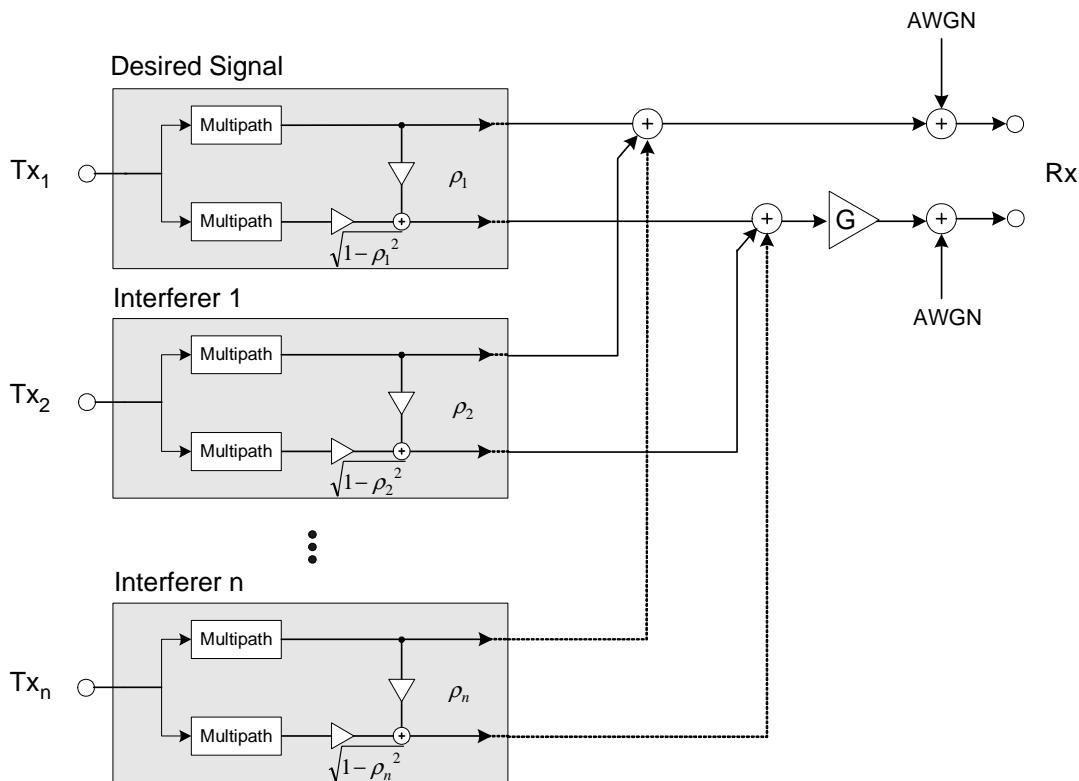
Figure 7: Multi interferer model

Figures 8 and 9 show the correlation as a function of time when applying a sliding window on a TU3nFH channel @ 945 MHz using the channel model above. The mean correlation was set to 0.7 and a single cochannel interferer was applied. Additional plots can be found in [26].
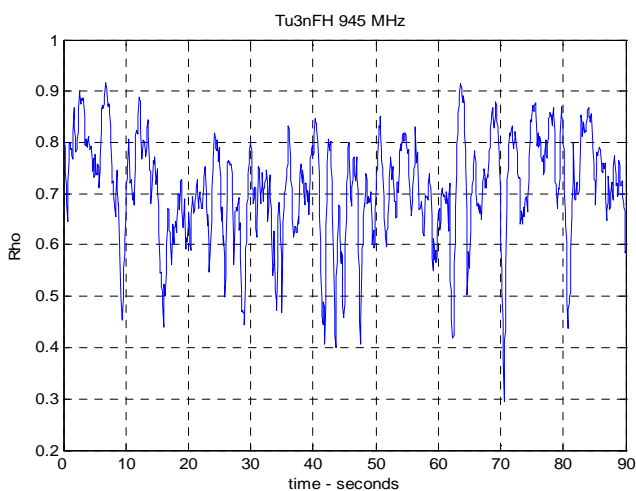
Figure 8: Antenna correlation values in steps of 100ms using a window width of 1s. C/I of 5 dB - TU3nFH945
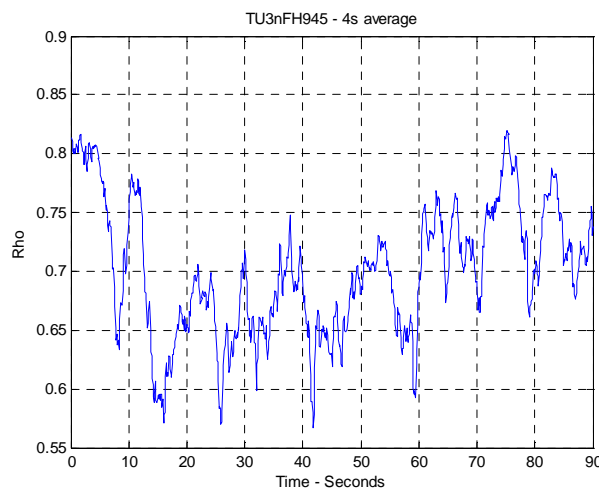
Figure 9: Antenna correlation values in steps of 100ms using a window width of 4s. C/I of 5 dB - TU3nFH945

6.3.4 Channel Model Parameters

In this subclause the parameters of the channel model is studied in more detail in order to be able to select a suitable parameter set for evaluation of the MSRD feature. The studies are based on measurements, surveys and simulations showing the characteristics and impact of the antenna correlation and the antenna gain imbalance.

6.3.4.1 Measurement results on Antenna Correlation

The following subclauses provide correlation measurements for three routes, with a full view and a zoomed view into one of the more interesting areas. The routes/scenarios are:

1. Indoor, Pedestrian Speed. No repeater.

2. Indoor, Pedestrian Speed. With Repeater.

3. Outdoor (U.S. Highway 163-South).

These field data were taken with a QUALCOMM MSM6500 diversity FFA. The phone has an external stubby dipole antenna and an internal meander line antenna. Data were recorded during traffic calls on Verizon's San Diego network at 800 MHz. Note that Verizon's network is not a GSM network but the correlation measurements do not depend on the employed airlink.

The measurements are derived from complex estimates from each receive chain correlated over a sliding 1-second period. The plots show $|\rho|^2$ on the y-axis.

In all of the following plots some of the BTS's are collocated, i.e. signals from different BTS's come from the same physical site. This will be indicated when applicable.

6.3.4.1.1 Indoor, Pedestrian Speed. No repeater

Figures 10 and 11 come from measurements performed at pedestrian speed in an indoor scenario. In this scenario, BTS B and BTS C are from the same site. However, due to the rich scattering environment, even the correlation of those signals is not the same.
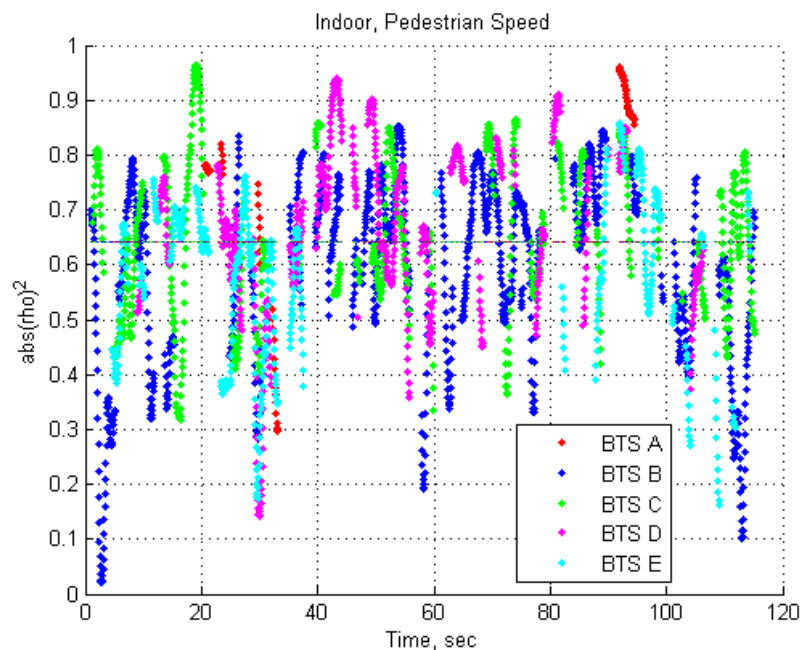
Figure 10: Indoor, Pedestrian Speed. No repeater - Full view [15]
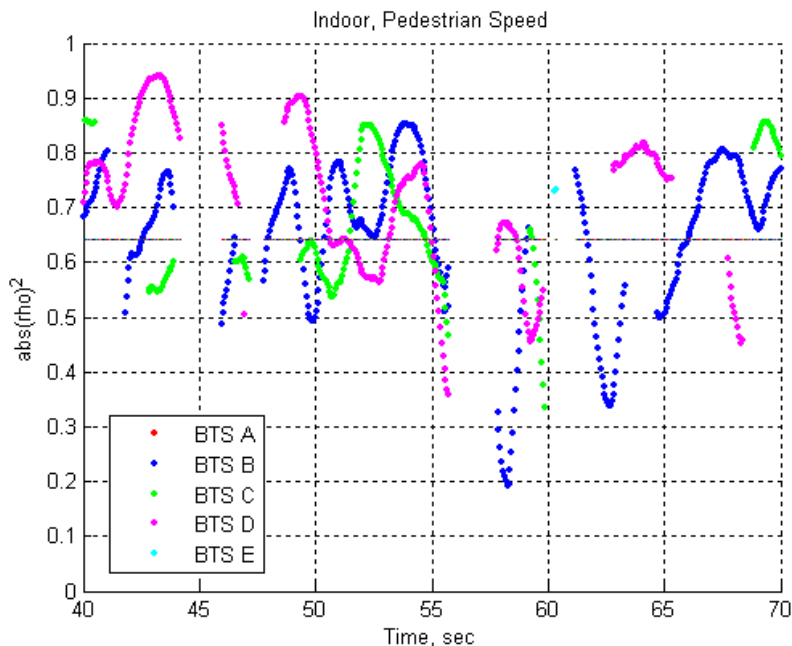
Figure 11: Indoor, Pedestrian Speed. No repeater - Zoom view [15]

6.3.4.1.2   Indoor, Pedestrian Speed. With repeater

Figures 12 and 13 come from measurements performed at pedestrian speed in an indoor scenario with the presence of a repeater. In this scenario, BTS A and BTS B are from the same site, while BTS C is not. However, due to the repeater, the correlation of all signals is the same. The verification of this obvious conclusion can be considered as a validation of the measurement process.
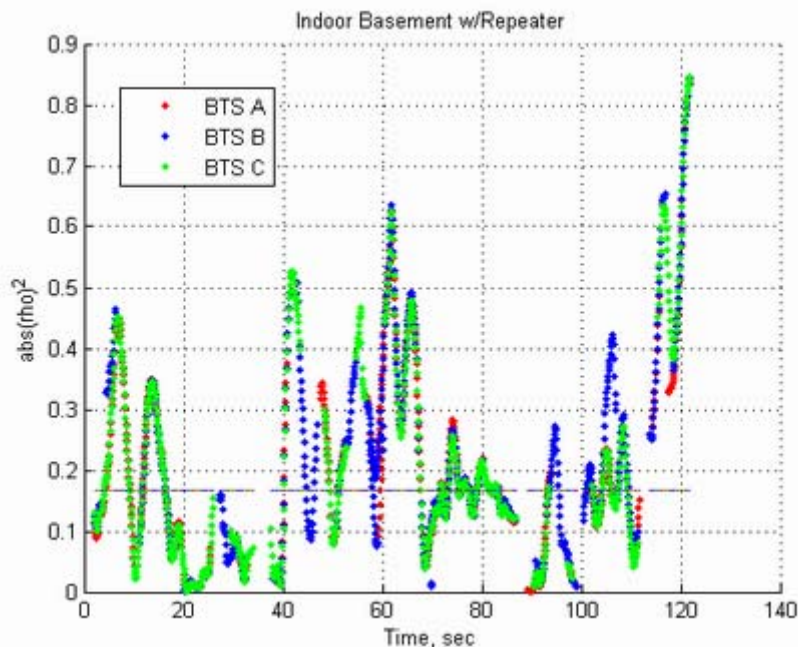
Figure 12: Indoor, Pedestrian Speed. With repeater - Full view [15]
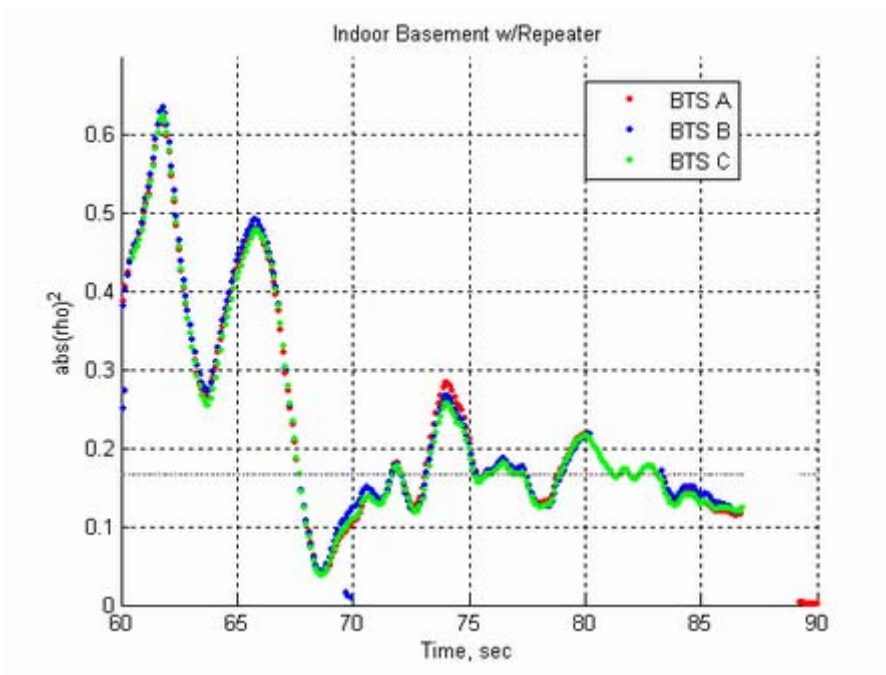
Figure 13: Indoor, Pedestrian Speed. With repeater - Zoom view [15]

6.3.4.1.3   Outdoor (highway)

Figures 14 and 15 come from measurements performed at driving speed along U.S Highway 163 Southbound. In this scenario, BTS A and G are from the same site, and BTS C and F are from the same site. This explains e.g. why the correlations of C and F match in the zoom view.
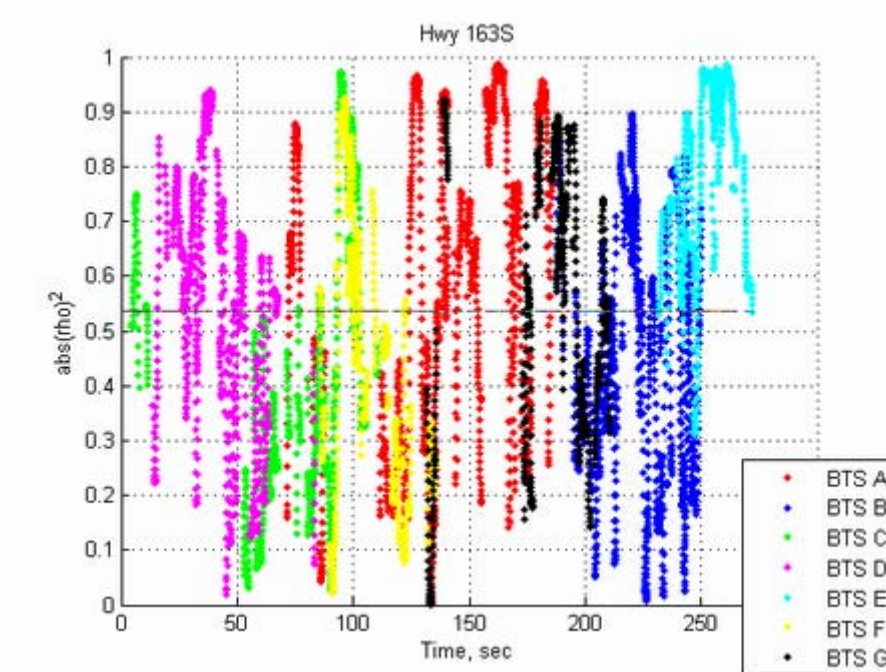
Figure 14: Outdoor, Highway Speed - Full view [15]
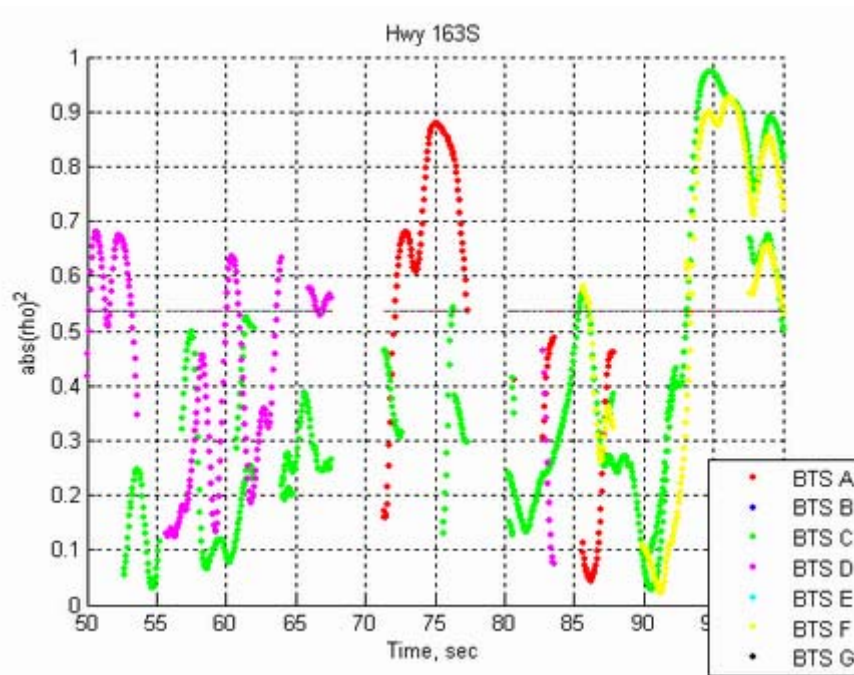
Figure 15: Outdoor, Highway Speed - Zoom view [15]

6.3.4.2 Literature Survey

This subclause summarises measurements of the envelope correlation and mean branch power imbalance found in scientific publications [4], [5] and [6].

6.3.4.2.1 Envelope correlation

The correlation between the two branches can vary considerably and depend on many factors. These include the scattering environment, handset orientation, head-and-hand-to-handset interaction, antenna spacing and the antenna design.

6.3.4.2.2 Spatial diversity

Spatial diversity is achieved by using two antennas separated in space. The correlation between the two signals is related to the distance between the antennas relative to the wavelength of the signal. The possible separation is limited by the size of the mobile station. A reasonable separation could be 4 cm (1.6 inches), which corresponds to roughly 0.1 wavelengths at 800 MHz to 900 MHz and 0.25 wavelengths at 1 800 MHz to 1 900 MHz.

The measurement results in [4] show the effect of antenna spacing on the envelope correlation for a 2.05 GHz carrier frequency system. In an urban canyon NLOS (non-line-of-sight), the mean envelope correlation is roughly 0.75 at an antenna spacing of 0.1 of the wavelength and stays at roughly 0.6 across 0.15 to 0.45 of the wavelength. Additional measurements in the same paper show lower correlation values for other environments, ranging from 0.4 to 0.65 (mean values for the respective environments) at 0.1 wavelength antenna distance and 0.3 to 0.6 at 0.25 wavelength antenna distance. It is interesting to note that the difference between 0.1 and 0.25 wavelengths separation is quite small and clearly smaller than expected from theory. This is further discussed in subclause 6.3.4.2.4.

Additional measurement distributions for various channel and test conditions in an operational GSM network are described in [6], according to which the correlation coefficient can have a mean and standard deviation of (0.44, 0.3) in rural measurements with a wide yet fairly flat distribution from roughly 0.2 to 0.8. In an urban environment, the measured correlation coefficient has a mean and standard deviation of (0.23, 0.33) and a wide non-uniform distribution. It should be noted that the measurements in [6] are conducted on the uplink, with antenna spacing significantly larger than what is possible in a mobile station. Nevertheless, the results are similar to the downlink measurements in [4].

In [23] the performance of different antenna types (dipole, patch in 3 configurations) on a small handset is studied with and without the presence of a user by means of measurements. The correlation is found to be below 0.4 in free space and rises to around 0.6 when the user is present for the different antenna types. In [24] the diversity gains of handheld phones are assessed by means of measurements. Also here the presence of a user's head is included, and low correlation

is obtained (~ 0.1). In [25] the potential diversity performance of a handheld phone is studied in a UMTS bandwidth scenario. 150 test persons used the handset in a normal speaking position, and for all 150 persons the correlation was always below 0.7. The antenna gain imbalance had a maximum of around 4 dB when using a dipole and a patch antenna for certain users.

6.3.4.2.3   Polarization diversity

Polarization diversity is achieved by using two antennas with different (typically orthogonal) polarization relative to each other.

With polarization diversity, a very good de-correlation between the branches can be achieved. Measurements in e.g. [4] and [6] typically show average values below 0.3.

6.3.4.2.4   Antenna pattern diversity

Diversity can also be achieved by using antennas with different antenna patterns (i.e. the antenna gain varies with the direction in the horizontal plane and the elevation angle). Due to this the received signals of the two antennas will be composed by reflections from different scatterers in the local environment.

As with polarization diversity, a very good de-correlation between the branches can be achieved with antenna patterns diversity. Again, measurements in [4] show average values below 0.3.

It should be noted that also a pair of omnidirectional antennas used for spatial diversity will experience antenna pattern diversity [4]. This is since the antennas will be coupled if their distance to each other is small. This in turn will change the individual antenna patterns from omnidirectional to directional. Therefore, the correlation of a spatial antenna pair with small separation will be lower than expected from theory for omnidirectional antennas (as indicated by the measurements recited in subclause 6.3.4.2.2).

6.3.4.2.5   Mean branch power imbalance

This parameter models the difference in mean received signal power between the two antennas. It is affected, for example, by the handset orientation, the head-and-hand-to-handset interaction, the antenna spacing and the dual-antenna design.

The power imbalance has a large range depending on the environment. In [4], values from 0 dB to 7 dB are reported for different types of dual-antennas for mobile station, except in one situation where 13 dB imbalance is shown. In [5] and [6], values are presented (for uplink) in a large range mainly below 10 dB for polarization diversity.

6.3.4.3   Results from measurements at Ericsson Research

This subclause summarises not yet published results from experiments conducted at Ericsson Research.

Various dual terminal antenna prototypes have been tested, giving different combinations of spatial, polarization and antenna pattern diversity. The experiments were conducted in an indoor office environment at 1 880 MHz. The effects of a user were included. The user either held the prototype close to the right ear ("talk mode") or in a position in front of the body, typical for viewing the terminal screen ("data mode").

The base station was transmitting at 22 dBm. Both horizontal and vertical polarization of the base antenna was evaluated with similar results.

6.3.4.3.1   Envelope correlation

The measurements show similar results as in subclause 6.3.4.2. The envelope correlation is found to range mainly from 0 to 0.7, both in talk mode and data mode.

6.3.4.3.2   Mean branch power imbalance

Again, the measurements resemble those in subclause 3.1 The measured mean branch power imbalance is in the range 1 dB to 4.5 dB in data mode, while it is in the range 2 dB to 13 dB in talk mode.

6.3.4.4 Results From Simulations

In this subclause some preliminary simulation results are presented to show how the choice of parameters for the channel/antenna model impacts the performance of an interference cancellation algorithm. Note that results are not yet available with the multiple-interferer model in figure 7. Instead, results with a single co-channel interferer are shown.

The following simulation assumptions were used:

- TU3 channel with ideal frequency hopping.

- Realistic MS receiver impairments.

- Noise level is 25 dB below carrier.

- Desired signal is GMSK modulated (MCS-3).

- Interferer is 8PSK modulated.

- Interference cancellation was used.

6.3.4.4.1 Impact of branch correlation

The impact of branch correlation is shown in figure 16 for envelope correlations in the range 0 to 0.9 for the carrier and interferer signals. It can be seen that the performance (gain at BLER=10 %, compared to a conventional single-antenna receiver) is relatively insensitive to the correlation. The largest gain is achieved when the correlation of the carrier is low while the correlation of the interferer is high. With equal correlation of the carrier and interferer, the gain is more or less constant regardless of the correlation value chosen.
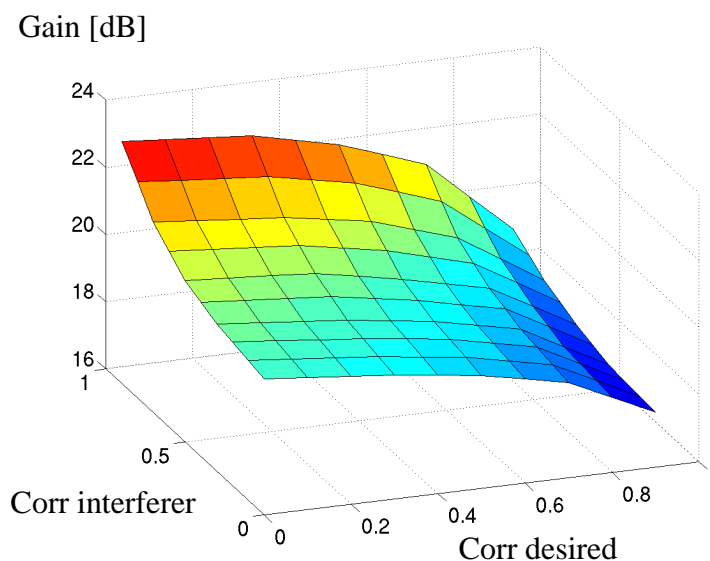
Figure 16: Impact of antenna correlation [11]

It should be noted that a random phase offset was applied to one of the antenna branches when deriving the results of figure 14.

6.3.4.4.2 Impact of branch power imbalance

Figure 17 shows the impact of branch power imbalance. In this figure, the correlation of the carrier and interferer are the same. The results indicate that the branch power imbalance is more important than the correlation. However, for imbalance levels less than 10 dB, the gain is more or less the same. For imbalance levels larger than 10 dB the gain is reduced. This is likely due to the noise component at 25 dB below the carrier (on average).
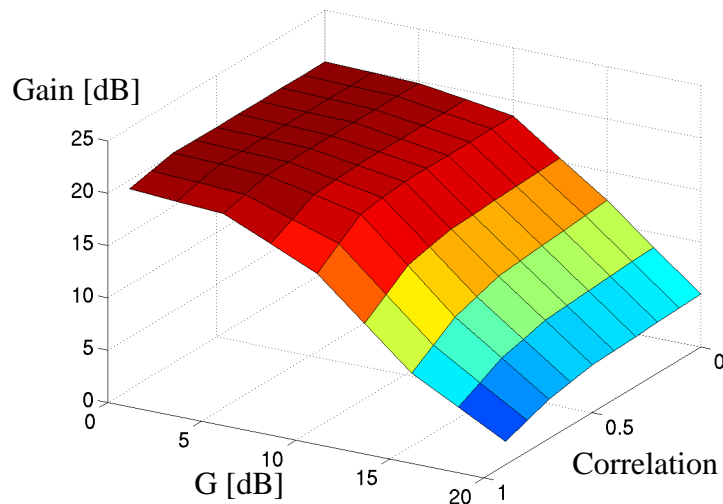
Figure 17: Impact of mean branch power imbalance (G) [11]

The results are consistent with those presented to GERAN in [7] and [8]. Note though that the results in [8] are in a sensitivity-limited environment, which explains the larger impact of the branch power imbalance. Generally, the branch power imbalance does not significantly impact the performance in purely interference limited scenarios, since the attenuation impacts carrier and interference equally. However, when the received signal level is close to the sensitivity level, the imbalance will degrade performance.

6.3.4.4.3   Phase offset

As mentioned in subclauses 6.3 and 6.3.1, there may be a phase offset between the signals received at the two antennas in the MS, This phase offset may originate from different antenna spacing and/or angle of arrival in a line of sight scenario. In [13], [22], [14], [26], [28] and [29] it has been discussed whether or not to implement such a phase offset in the MSRD channel models, considering that different branches of the channel model fade independently. In the following, the effect of applying both a random and a constant phase offset is studied by means of simulations.

To study the effect of applying a random phase offset in one of the antenna branches, a set of simulations was run for a sensitivity limited scenario as well as DTS-1 and DTS-2. A TU50 nFH channel was used and 5 000 blocks were simulated. The phase shift was randomly selected per burst in the range $[0;2\pi]$, and correlation factors in the range from 0 to 1.0 were applied. The results are presented in figures 18 to 20.
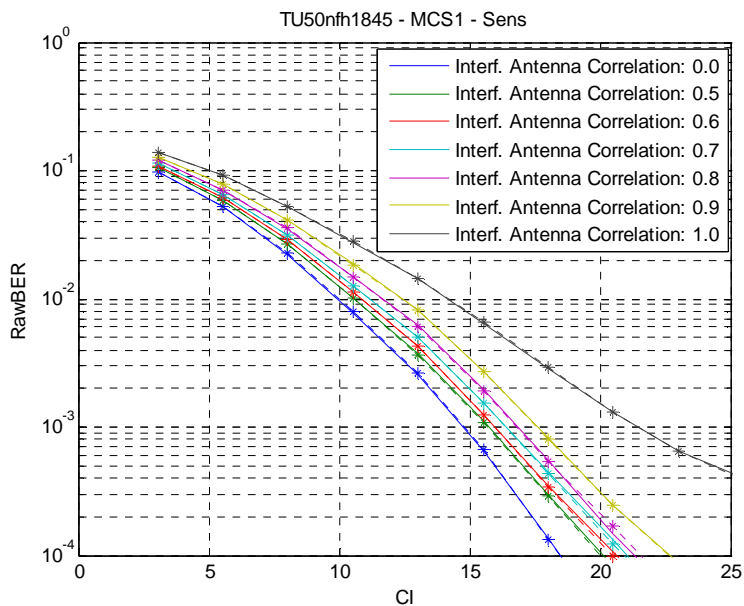
Figure 18: BER performance. TU50nFH1845. Sensitivity - With and without phase offset [26]
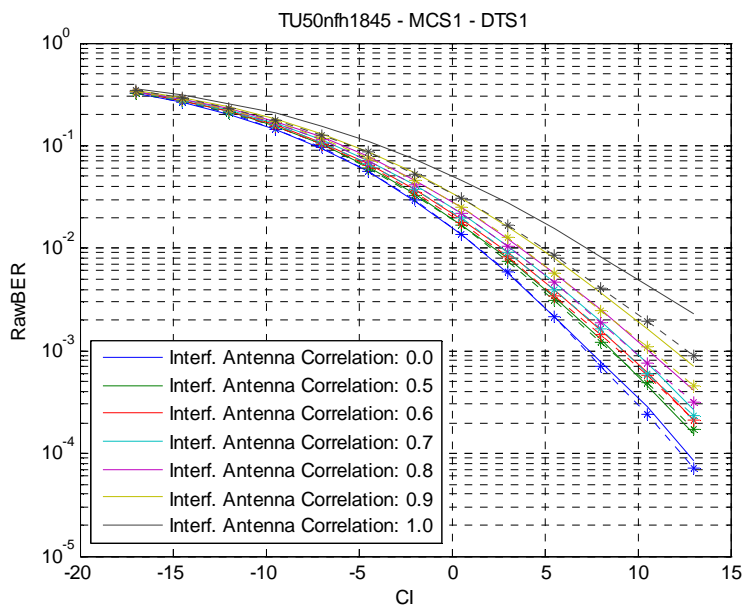
Figure 19: BER performance. TU50nFH1845. DTS-1 - With and without phase offset [26]
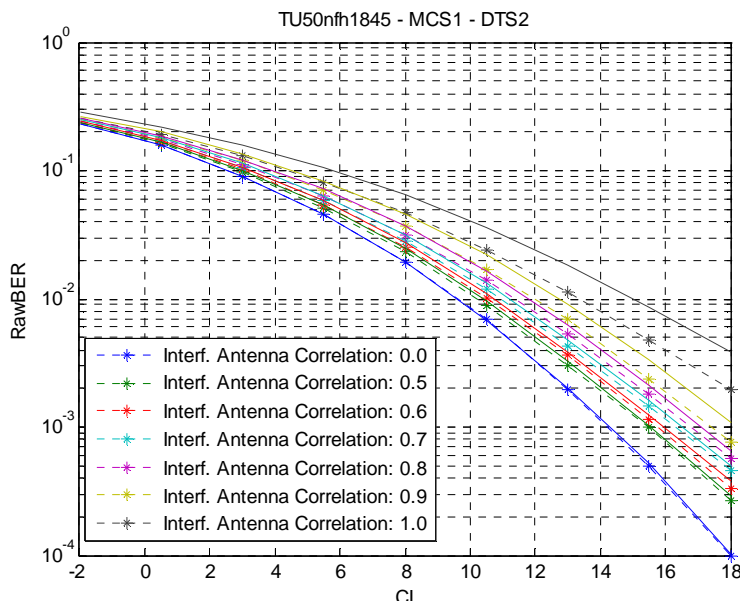
Figure 20: BER performance. TU50nFH1845. DTS-2 - With and without phase offset [26]

The conclusion of the simulations can be summarized as:

- Co-channel: For correlation values in the range of 0 to 0.8 the largest impact of the phase offset is 0.5 dB. For correlations of 0.9 and 1.0 there is a gain of 1 and 2.5 dB when applying a phase offset.

- Adjacent: For correlation values in the range of 0 to 0.9 the largest impact of the phase offset is 0.4 dB. For a correlation of 1.0 there is a gain of 1 dB when applying a phase offset.

- Sensitivity: The phase offset has no impact.

The impact on MSRD performance originating from a constant difference in phase angle on the desired and interfering user was studied in [22]. The studies were based on a scenario comprising of two direct incoming waves as shown in figure 21.
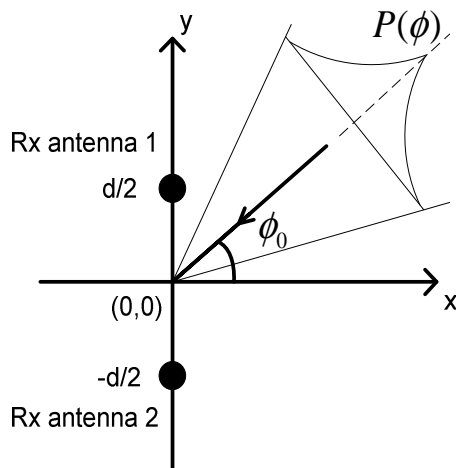
**Figure 21: Antenna setup at MS side for evaluation of the impact
on phase difference between antenna correlations [22]**

In [22] examples of the relationship between phase angle and envelope correlation are given assuming an angular spread of 35 degrees and three different antenna spacings. Based on this a set of simulations were run to study the impact of phase difference between desired and interfering signals.

For the simulations, an 8-PSK modulated transmission in a co-channel interference scenario is considered, and the multiple interferer model shown in [1], figure 4 is assumed. The channel profile is TU3iFH.

The signals of desired user and interferer may arrive from different incidence directions, resulting in different phase angles in the correlation factors. The absolute value of the correlation factor is assumed to be 0.9 for both users.

Figure 22 depicts the raw bit error rate of the desired user as a function of the carrier-to-interferer ratio. For comparison, the raw BER of a conventional single-antenna 8-PSK receiver is also shown.
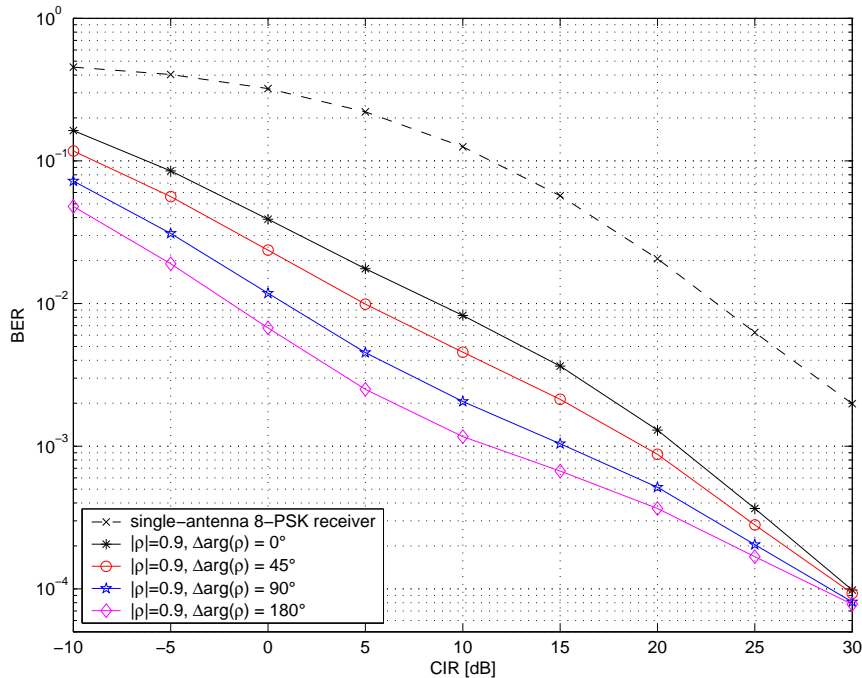
Figure 22: Raw bit error rate of an 8-PSK receiver in a co-channel interferer scenario [22]

It becomes obvious that receiver performance improves for increasing phase difference of the correlation factors. At a BER level of 10^{-2} for example, the improvement between $0°$ and $180°$ phase difference is around 10 dB. With the findings of the previous subclause, it can be concluded that the performance of interference cancellation schemes is significantly dependent on the incidence direction of the incoming signals in the scenarios applied here. The worst-case is when the signals of desired user and interferer arrive from the same direction.

The dependency of receiver performance on the correlation factors' phase difference is at maximum for a correlation factor of 1.0 and decreases for lower correlation factors. This becomes obvious when considering the multiple interferer of subclause 6.3.3. For an absolute value of the correlation factors of 1.0 and a phase difference of 0 degrees, no interference can be cancelled at all. On the other hand, for a phase difference of 180 degrees, interference can be cancelled perfectly just by adding the signals of the two antenna branches. In the other extreme, when the correlation factors of both users are equal to zero, the phase angle just plays no role. Simulations showed that the phase angle of the correlation factors should be considered for envelope correlation factors above 0.7.

6.3.4.4.4 Impact of Antenna correlation Factors in desired and interfering branches

In [14], plots showing performance as a function of correlation in the interferer signal branch for a fixed correlation in the desired branch of 0.4 and 0.6 were presented. In the following results are provided for a correlation range of [0, 0.3 0.5 0.6 0.7 0.8 0.9 1.0] for both desired and interferer. The multi-interferer model specified in subclause 6.3.3 was used.

Figure 23 shows the performance for the MSRD receiver, as a function of the correlation in the desired and interferer branch. The performance is measured as the C/I level in dB at which a raw BER of 1 % is reached.
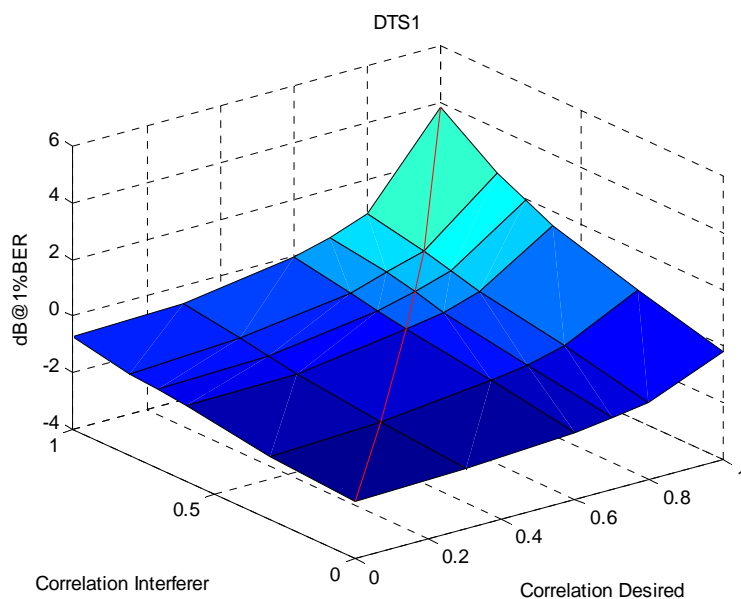
Figure 23: Impact of correlation in desired and interfere branch. DTS-1 - GMSK [26]

As seen on figure 23, the performance is relatively constant across the performance surface, except when the correlation is close to one. At this point the performance becomes similar to the performance of a single branch receiver with SAIC (see note). Applying the same correlation in desired and interferer branch seems to result in average to worst-case performance.

NOTE: A SAIC receiver would cross the 1 % raw BER at around 5 dB.
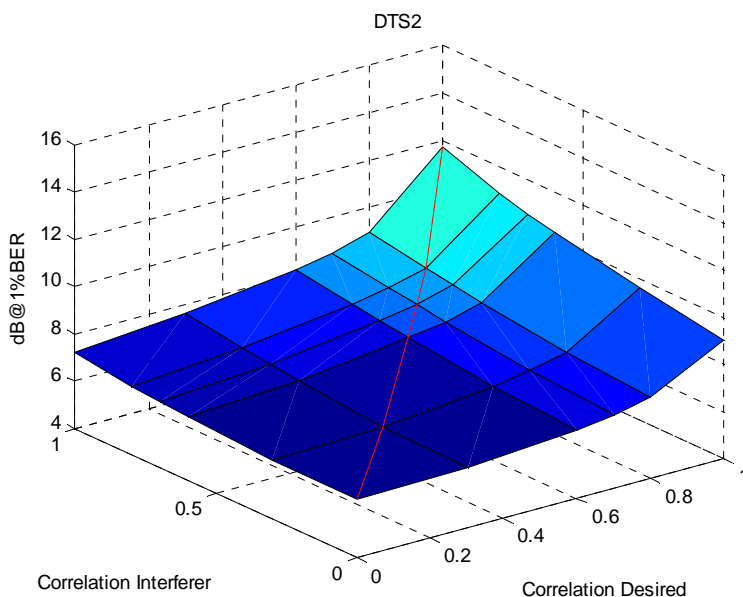
Figure 24: Impact of correlation in desired and interfere branch - DTS-2 - GMSK [26]

Figure 24 shows the corresponding plots for DTS-2, which contains multiple interferers. The MSRD receiver shows a performance surface similar to the DTS-1 scenario. That is, a relatively flat performance surface except for very high correlations.

In [21], the impact of antenna correlation and antenna gain imbalance was studied for the GERAN configuration 2 scenario [1]. The performance obtained when applying a correlation coefficient of 0.7 and a gain imbalance of 3 dB is shown in figures 25 and 26.
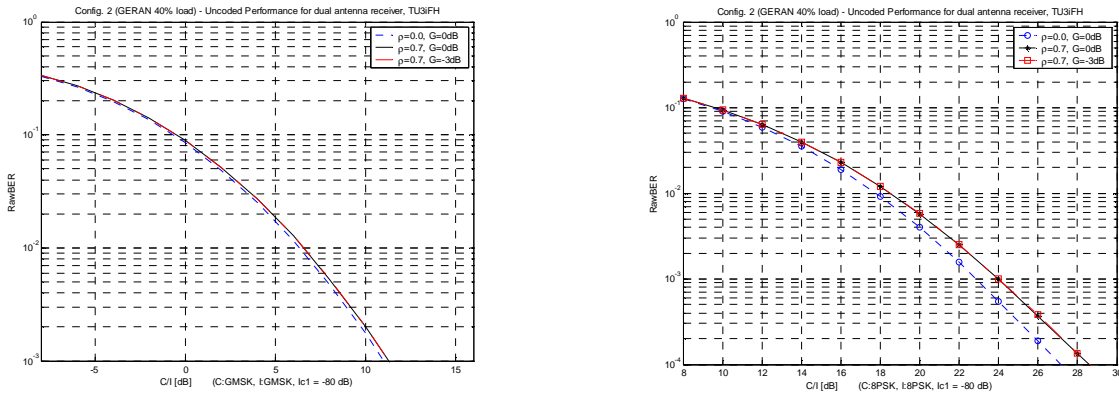
Figure 25: Uncoded BER of MS RX diversity for GMSK (left figure) and 8PSK (right figure), configuration 2 and different antenna gain imbalances and correlations [21]
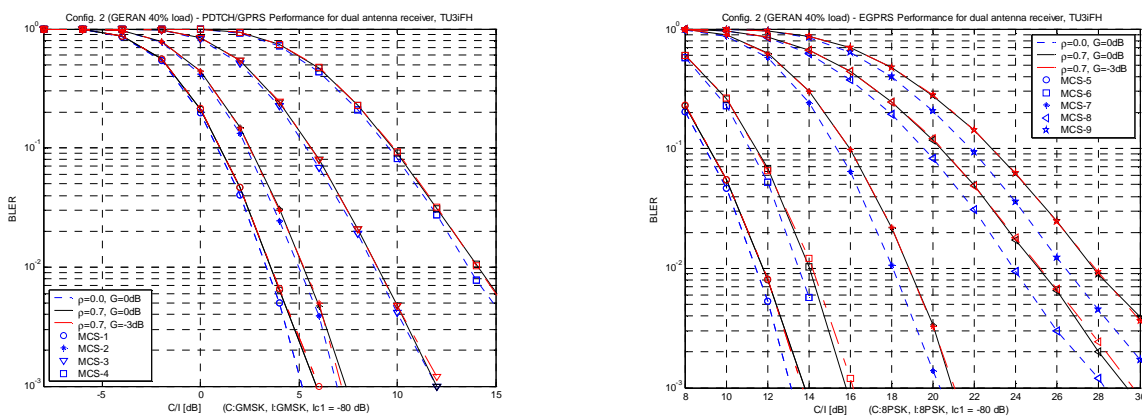
Figure 26: BLER of MS RX diversity for MCS-1 to MCS-4 (left figure) and MCS-5 to MCS-9 (right figure), configuration 2 and different antenna gain imbalances and correlations [21]

6.3.4.5 Discussion

Subclauses 6.3.4.2 to 6.3.4.4 have assessed the impact of various parameters of the MSRD channel models as well as provided a small literature survey of publications related to the achievable performance of diversity in mobile terminals. It seems clear that the performance of a diversity terminal is impacted by several factors, such as antenna correlation, gain imbalance, presence of a user, antenna spacing, etc.

In order to evaluate the gains of MS receive diversity, these values should be carefully selected so that when used in simulations, the results will reflect realistic link level performance. Now, since both parameters are influenced by a number of MS implementation and user dependent factors it may be most suitable to specify a set of parameters that would reflect the performance bounds. That is, best and worst case values. Obviously, best case values would be uncorrelated signals and no gain imbalance.

As for selecting the worst case or typical values, several contributions have proposed values and shown the impact in terms of receiver performance for different architectures [7], [8], [11], [17], [18] and [21]. In general, it seems that the diversity receivers are relatively insensitive to parameter variations. That is, large gains are achieved even for high values of both correlation and antenna gain imbalance. Based on these studies and simulations, it has been agreed that the parameters of table 2 is to be used for specifying the link level performance of MS receive diversity.

6.3.4.6 Parameter Selection

Table 2: Proposed values for simulation of MSRD Performance

Parameter set	Magnitude of complex Correlation	Antenna gain imbalance
A	0.0	0 dB
B	0.7	6 dB

6.4 Performance Characterization

This subclause provides link- and system level simulation results in order to characterize the performance of MS receive diversity in different scenarios. The basis of the simulations is the performance models developed for SAIC/DARP [1]. That is, the GERAN SAIC models and the DARP Test Scenarios (DTS) [20].

6.4.1 Link Level Performance

6.4.1.1 SAIC GERAN Configurations

This subclause presents simulation results using the GERAN network configurations developed during the GERAN SAIC Feasibility Study [1]. The properties of the desired signals and interferers are shown below [1].

Table 3: Interferer levels for network configuration 1 to 4

Link Parameter	Configuration 1	Configuration 2 40% Load	Configuration 3 70% Load	Configuration 4
Desired signal, C TSC Fading	TSC0	TSC0	TSC0	TSC0
Dominant Coch. Interf. TSC Fading	Random TSC excluding TSC0	Random TSC excluding TSC0	Random TSC excluding TSC0	Random TSC excluding TSC0
2nd Strongest Coch. Interf. Ic1/Ic2 TSC Fading	10 dB Random TSC	6 dB Random TSC	4 dB Random TSC	9 dB Random TSC
3rd Strongest Coch Interf. Ic1/Ic3 TSC Fading	20 dB Random TSC	10 dB Random TSC	8 dB Random TSC	17 dB Random TSC
Residual Coch. Interf. (filtered AWGN) Ic1/Icr TSC No Fading	- NA	9 dB NA	5 dB NA	20 dB NA
Dominant Adj. Interf. Ic1/Ia (see note) TSC Fading	15 dB Random TSC	14 dB Random TSC	14 dB Random TSC	16 dB Random TSC
Residual Adj. Interf. (filtered AWGN) Ic1/Iar[1] TSC No Fading	20 dB NA	15 dB NA	14 dB NA	21 dB NA
NOTE: After the Rx filter assuming an 18dB ACP.				

6.4.1.1.1 GMSK BER

The uncoded BER curves of the DAIC receiver are compared to the conventional receiver curves in figures 27 and 28. The interferers are all GMSK.

The results demonstrate very high gains of 6.4dB to 7.1dB. The gain seems robust for different interferer distributions.
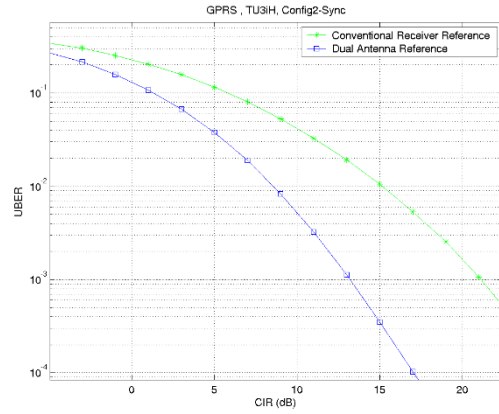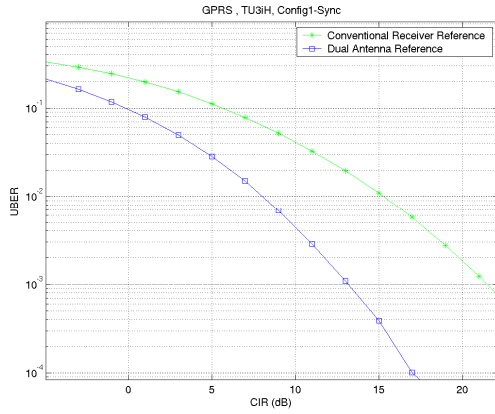
(a)   (b)

Figure 27: Uncoded BER Performance comparison of the DAIC and conventional GMSK receivers for Synchronized Network (a) Config1, and (b) Config2 [18]
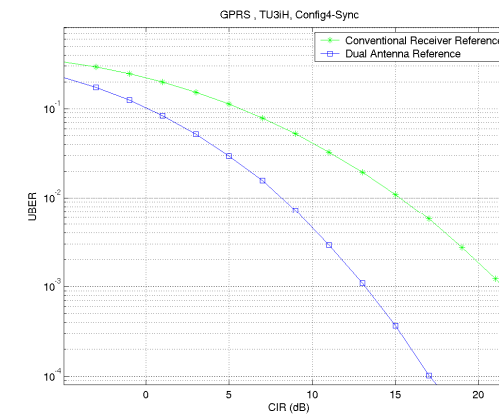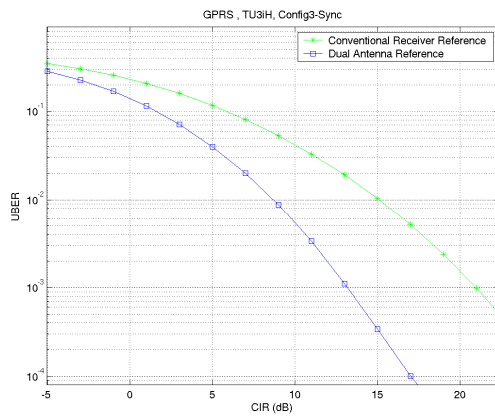
(a)   (b)

Figure 28: Uncoded BER Performance comparison of the DAIC and conventional GMSK receivers for Synchronized Network (a) Config3, and (b) Config4 [18]

6.4.1.1.2   8-PSK BER

The uncoded BER curves of the DAIC receiver are compared to the conventional receiver curves in figures 29 and 30. The interferers are all 8PSK. The results demonstrate that, unlike SAIC techniques, DAIC yields huge gains of 7.0 dB to 7.5 dB at 1 % BER for 8-PSK channels in loaded network scenarios.
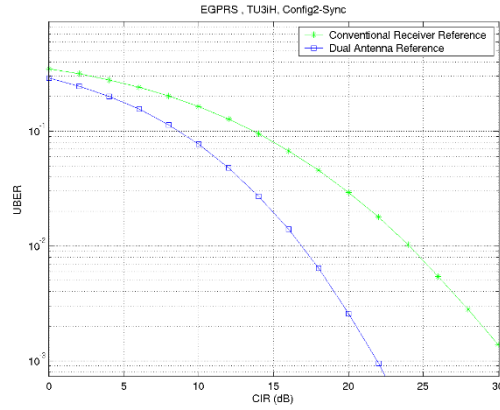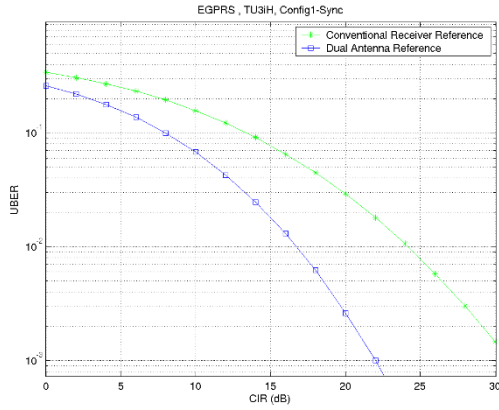
(a)   (b)

Figure 29: Uncoded BER performance comparison of the DAIC and conventional 8PSK receivers for Synchronized Network (a) Config1, and (b) Config2 [18]
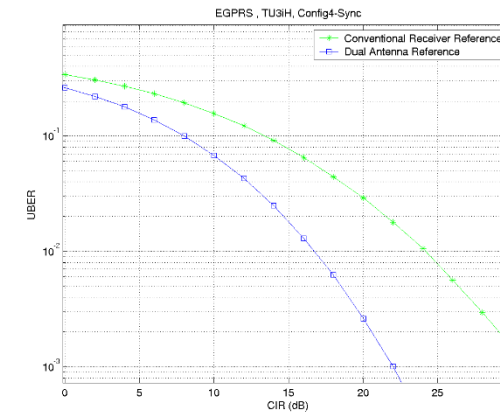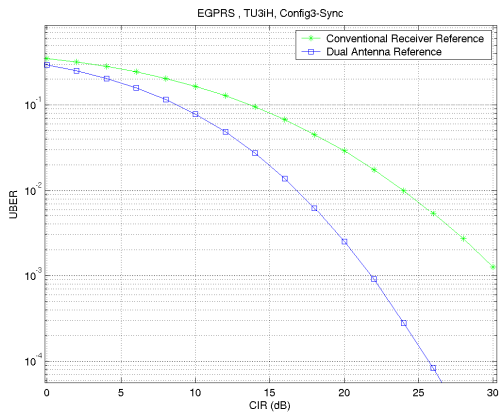
(a)   (b)

Figure 30: Uncoded BER performance comparison of the DAIC and conventional 8PSK receivers for Synchronized Network (a) Config3, and (b) Config4 [18]

6.4.1.1.3   AMR FER

The TCH/AFS FER curves of the DAIC receiver are compared to the conventional receiver curves for AMR 12.2, 7.95 and 5.9 in figures 31 and 32. The interferers are all GMSK. The results show DAIC performance gains of 3.8 dB to 6.3 dB at 1 % FER in loaded network scenarios.
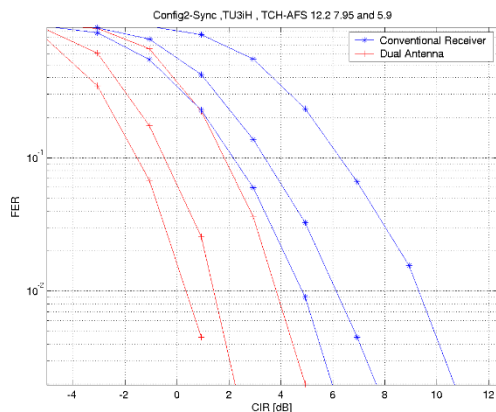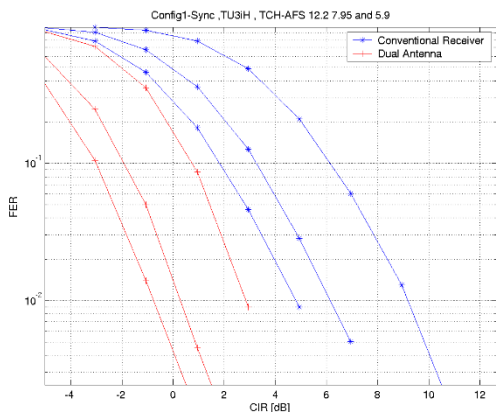
(a) (b)

Figure 31: TCH/AFS FER Performance comparison of the DAIC and conventional receivers for Synchronized Network (a) Config1 and (b) Config2 [18]
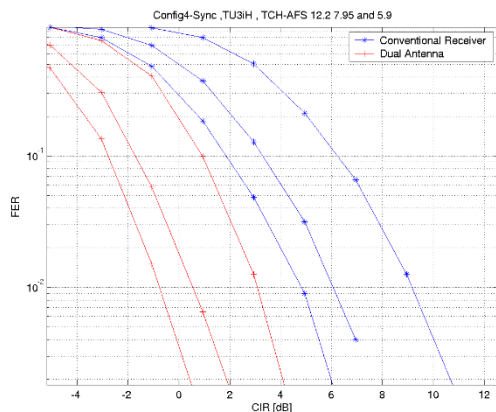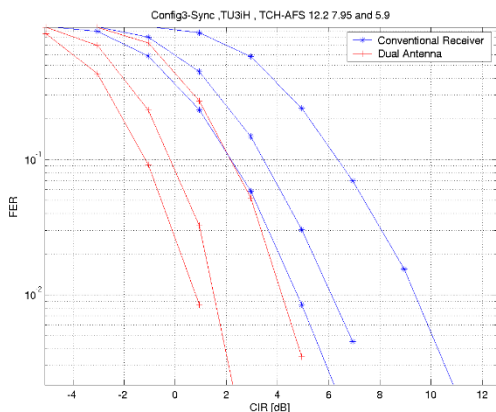
(a) (b)

Figure 32: TCH/AFS FER Performance comparison of the DAIC and conventional receivers for Synchronized Network (a) Config3 and (b) Config4 [18]

The performance of an alternative MSRD receiver for configuration 2 is shown in figure 33. Different antenna gain imbalances and correlation values were applied as described in [21].
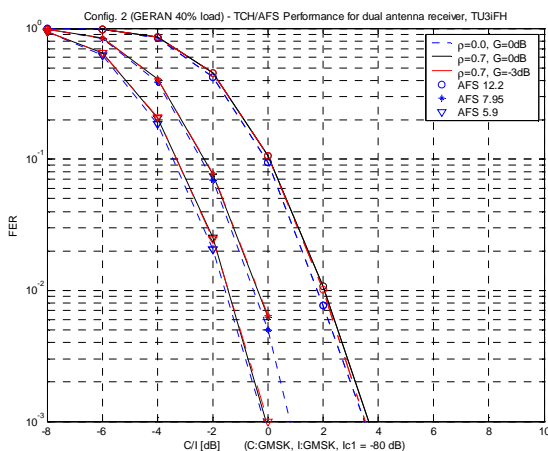
Figure 33: FER of MS RX diversity for voice traffic channels AFS5.9, AFS7.95 and AFS12.2, configuration 2 and different antenna gain imbalances and correlations

6.4.1.1.4 GPRS BLER

The PDTCH BLER curves of the DAIC receiver are compared to the conventional receiver curves for CS1-4 in figures 34 and 35. The interferers are all GMSK. The results show DAIC performance gains of 4.7 dB to 7.2 dB at 10 % BLER in loaded network scenarios.
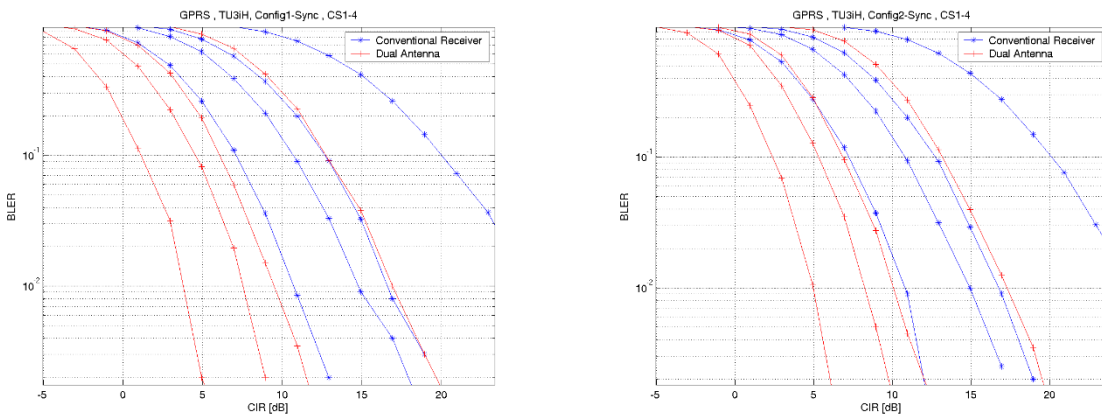
(a)   (b)

Figure 34: GPRS BLER Performance comparison of the DAIC and conventional receivers for Synchronized Network (a) Config1 and (b) Config2 [18]
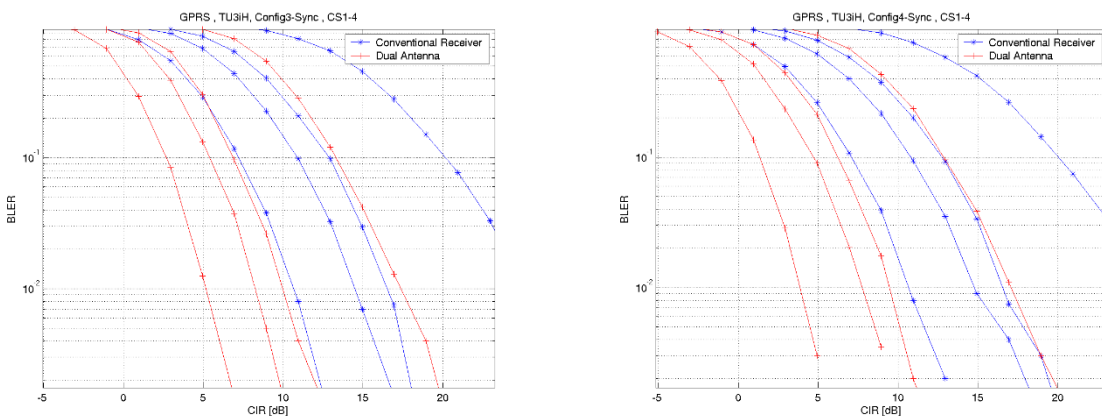
(a)   (b)

Figure 35: GPRS BLER Performance comparison of the DAIC and conventional receivers for Synchronized Network (a) Config3 and (b) Config4 [18]

6.4.1.1.5 EGPRS BLER

The PDTCH BLER curves of the DAIC receiver are compared to the conventional receiver curves for MCS5-9 in figures 36 and 37. The interferers are all 8PSK. The results show DAIC performance gains of 5.1 dB to 7.6 dB at 10 % BLER in loaded network scenarios.
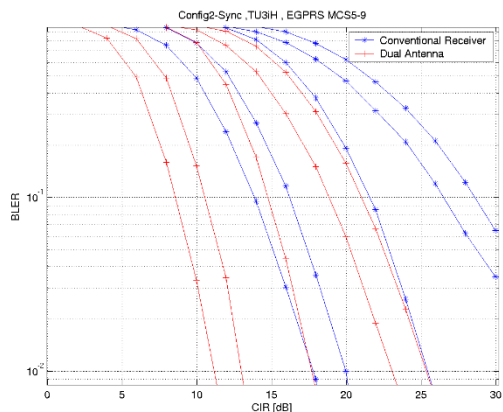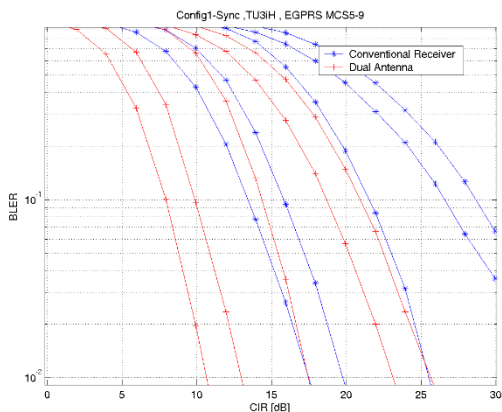
(a)   (b)

Figure 36: EGPRS BLER Performance comparison of the DAIC and conventional receivers for Synchronized Network (a) Config1 and (b) Config2 [18]
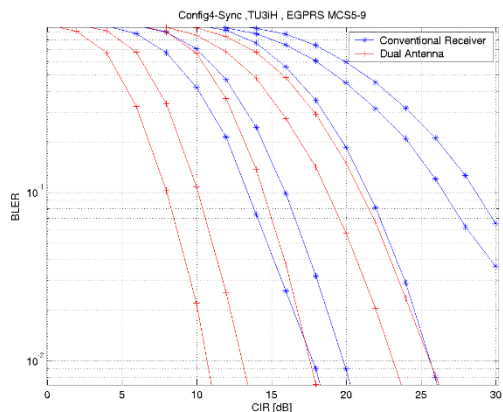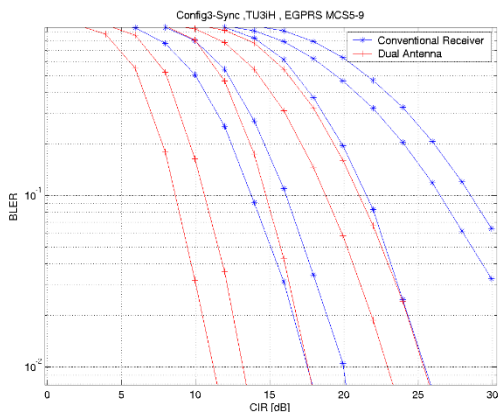
(a)   (b)

Figure 37: EGPRS BLER Performance comparison of the DAIC and conventional receivers for Synchronized Network (a) Config3 and (b) Config4 [18]

The performance of an alternative MSRD receiver for configuration 2 is shown in figure 38. Different antenna gain imbalances and correlation values were applied as described in [21].
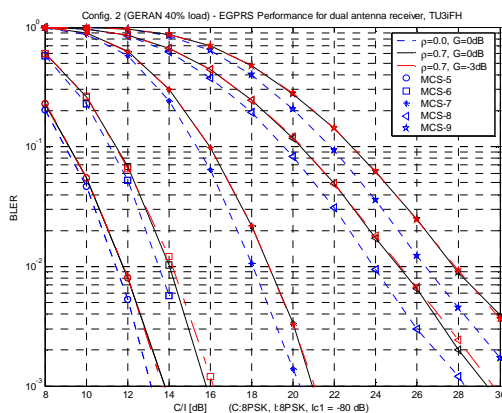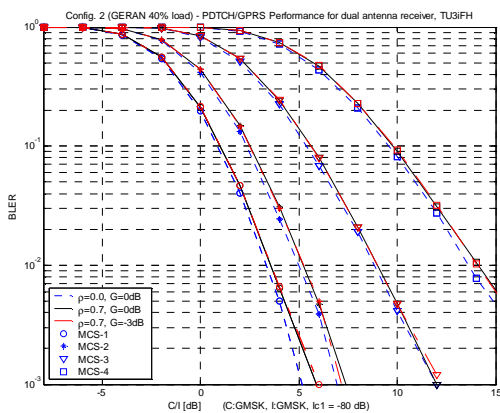
Figure 38: BLER of MS RX diversity for MCS-1 to MCS-4 (left figure) and MCS-5 to MCS-9 (right figure), configuration 2 and different antenna gain imbalances and correlations [21]

6.4.1.1.6 EGPRS Throughput

The optimal throughput curves for GPRS and EGPRS are shown in this subclause. These curves are obtained by selecting the CS or MCS that yields the maximal throughput for each C/I.

Figure 39 compares the hull curves of the DAIC and SAIC receivers to that of a conventional receiver for GPRS CS1-4 in loaded network scenarios.

Figure 40 compares the hull curve of the DAIC receiver to that of a conventional receiver for EGPRS MCS5-9 in loaded network scenarios.

It could be appreciated how much better the throughput performance of DAIC with respect to SAIC or conventional receivers, and what enormous performance boost EGPRS gets at typical C/I levels of 10 dB to 20dB.

$$R_{EFFECTIVE} = \underset{k}{MAX}[(1 - BLER_{MCSk}) \cdot R_{MCSk}]$$
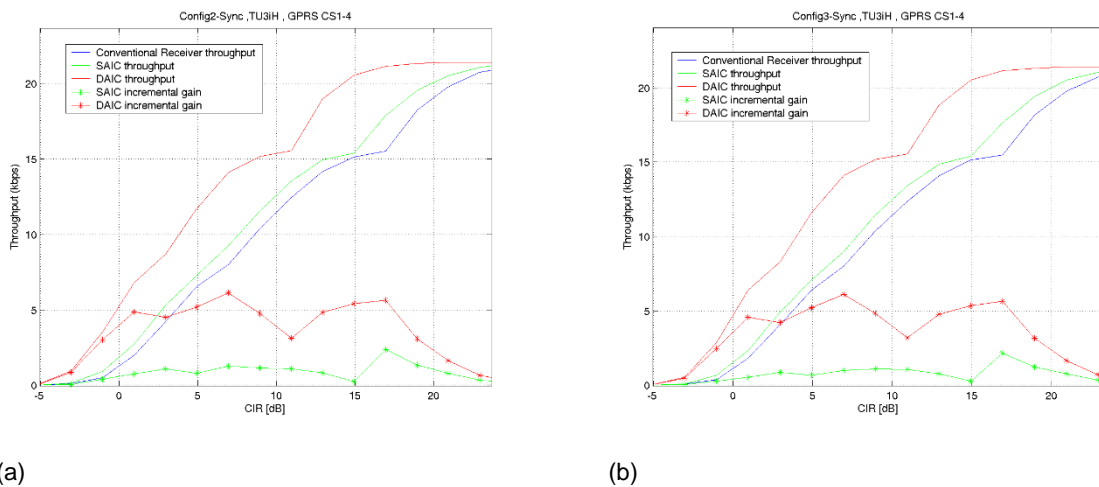
(a) (b)

Figure 39: GPRS Hull-curve comparison of the DAIC, SAIC and conventional receivers for Synchronized Network (a) Config2 and (b) Config3 [18]
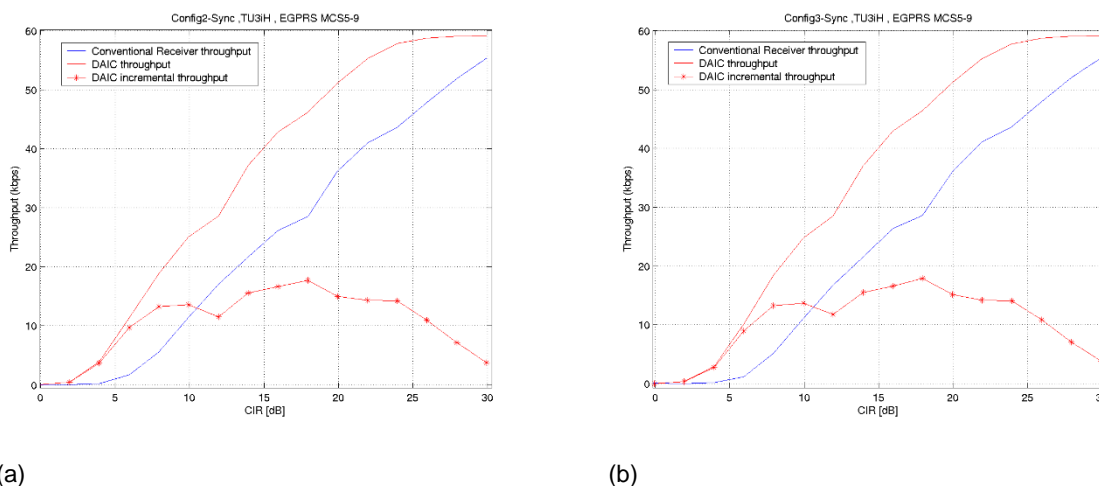
(a) (b)

Figure 40: EGPRS Hull-curve comparison of the DAIC and conventional receivers for Synchronized Network (a) Config2 and (b) Config3 [18]

6.4.1.2 DARP Test Scenarios (DTS)

This subclause contains simulation results using the test scenarios defined for DARP [20]. Assuming identical signal correlations for the wanted signal and all interferers, simulations are run with parameter sets 1 to 3 for antenna gain imbalance and correlation (see table 4) while choosing for all users the same multipath profile and frequency bands.

Table 4: Gain and correlation parameters used for tests

Parameter set	Antenna Gain Imbalance G [dB]	Correlation ρ
PS 1	0	0
PS 2	0	0.7
PS 3	-3	0.7

By applying these parameter sets, the performance of MS RX diversity is evaluated under following conditions:

- PS 1: uncorrelated signals/antennas and equal average receive power.

- PS 2: highly correlated signals/antennas, e.g. due to angle of arrival or small antenna spacing, and equal average receive power.

- PS 3: highly correlated signals/antennas, e.g. due to angle of arrival or small antenna spacing, and unequal average receive power, e.g. due to shadowing of one antenna by hand or head.

Note that the reference single antenna receiver is favoured by allowing only negative values for G as in practice a second antenna might also have a larger gain than the first one.

Please note that the assumption of identical correlations is backed by the observation that the actual choice of interferers' signal correlations has minor influence on the performance compared to the number of interferers, their modulation schemes and signal powers [7], [8] and [9].

The interferers' statistics itself is chosen according to test cases DTS-1 and DTS-2 specified in 3GPP TS 45.005 for DARP/SAIC, i.e. the interference robustness improvement is investigated for:

- a single synchronous co-channel interferer (DTS-1);

- multiple synchronous co- and adjacent channel interferers (DTS-2).

Table 5: DARP Test Scenarios, DTS-1 and DTS-2

Test case	Interfering Signal	Interferer relative power level	Interferer TSC	Interferer delay range
DTS-1	Co-Channel 1	0 dB	None	No delay
DTS-2	Co-Channel 1	0 dB	None	No delay
	Co-Channel 2	-10 dB	None	No delay
	Adjacent 1	3 dB	None	No delay
	AWGN	-17 dB	---	---

For both interferer models, the performance is studied for the combination of:

- GMSK modulated wanted signal and GMSK modulated interferer(s).

- 8PSK modulated wanted signal and 8PSK modulated interferer(s).

Like for DARP/SAIC, the wanted signal always uses training sequence 0 while the midamble of the interferers is filled with random data bits.

The power of the co-channel and adjacent channel interferer is measured in the signal r1 before any receiver filtering and during the active part of the desired burst. All power levels are relative to the signal level of the strongest co-channel interferer. The level of the strongest co-channel interferer (Co-channel 1) is -80 dBm and the AWGN power is measured over a bandwidth of 270,833 kHz (see DARP test cases in 3GPP TS 45.005).

Performance results in interference-limited scenarios are provided for packet switched channels in table 6. The carrier-to-dominant co-channel interference ratio (C/I1) is given in dB for which a block error ratio of 10 % and 30 % is achieved for MCS-1 to MCS-9 and MCS-8/MCS-9, respectively.

For benchmarking of MS RX diversity and GMSK modulated signals, the corresponding DARP-phase 1 limits (3GPP TS 45.005, table 2o) as well as the co-channel interference performance limits (derived1 from 3GPP TS 45.005, table 2a) are included in table 4 for MCS-1 to MCS-4.

For assessment of MS RX diversity and 8PSK modulated signals, the 8PSK co-channel interference performance limits specified for MCS-5 to MCS-9 are used (derived1 from 3GPP TS 45.005, table 2c).

NOTE 1: The limits given in tables 2a and 2c of 3GPP TS 45.005, which correspond to a single synchronous interferer test case (DTS-1), are applied to C/I and increased by 0,61 dB when used as reference for C/I1 in DTS-2.

Table 6: Diversity receiver performance for DTS-1 and DTS-2 - TU50nFH 1 1800/1900 MHz, [17]

	DTS-1 – TU50 nFH 1800/1900 C/I1 = C/I					DTS-2 – TU50 nFH 1800/1900 C/I1				
	TS 45.005 Tables 2a, 2c	TS 45.005 Table2o (DARP)	DAIC - PS 1 (G 0dB, corr. 0%)	DAIC - PS 2 (G 0dB, corr. 70%)	DAIC - PS 3 (G -3dB, corr. 70%)	TS 45.005 Tables 2a,2c [1]	TS 45.005 Table 2o (DARP)	DAIC - PS 1 (G 0dB, corr. 0%)	DAIC - PS 2 (G 0dB, corr. 70%)	DAIC - PS 3 (G -3dB, corr. 70%)
GMSK(C)/GMSK(I)										
PDTCH MCS-1 (BLER 10%)	10,0	3,5	-5,5	-5,0	-4,9	10,6	9,0	0,8	1,5	1,9
PDTCH MCS-2 (BLER 10%)	12,0	6,5	-5,1	-4,6	-4,5	12,6	11,0	2,3	3,1	3,5
PDTCH MCS-3 (BLER 10%)	17,0	11,5	-1,7	-1,0	-0,9	17,6	15,0	6,8	7,4	7,9
PDTCH MCS-4 (BLER 10%)	23,0	19,5	3,9	4,4	4,6	23,6	22,0	12,5	13,1	13,5
8PSK(C)/8PSK(I)										
PDTCH MCS-5 (BLER 10%)	15,0		-2,4	-1,9	-1,5	15,6		9,8	10,1	10,4
PDTCH MCS-6 (BLER 10%)	18,0		1,6	2,2	2,4	18,6		13,3	13,6	13,9
PDTCH MCS-7 (BLER 10%)	27,5		10,8	11,1	11,3	28,1		19,5	20,0	20,2
PDTCH MCS-8 (BLER 10%)	--		21,3	22,1	22,1	--		25,5	26,5	26,5
PDTCH MCS-8 (BLER 30%)	29,5		12,8	12,9	13,1	30,1		20,0	20,6	20,8
PDTCH MCS-9 (BLER 10%)	--		26,6	28,0	28,0	--		29,4	30,7	30,7
PDTCH MCS-9 (BLER 30%)	--		19,2	19,9	19,9	--		23,6	24,5	24,7

Table 7: Diversity receiver performance for DTS-1 and DTS-2. TU3nFH 900 MHz, [21]

	DTS-1 – TU3 nFH GSM900 C/I1 = C/I				DTS-2 – TU3 nFH GSM900 C/I1			
	TS 45.005 v6.10.0 Table 2a,2c	DAIC - PS 1 (G 0dB, corr. 0%)	DAIC - PS 2 (G 0dB, corr. 70%)	DAIC - PS 3 (G -3dB, corr. 70%)	TS 45.005 v6.10.0 Table 2a, 2c	DAIC - PS 1 (G 0dB, corr. 0%)	DAIC - PS 2 (G 0dB, corr. 70%)	DAIC - PS 3 (G -3dB, corr. 70%)
GMSK(C)/GMSK(I)								
PDTCH MCS-1	13	-1,6	-0,4	-0,4	13,6	3,8	4,6	5,0
PDTCH MCS-2	15,0	-1,5	-0,3	-0,3	15,6	4,8	5,6	5,9
PDTCH MCS-3	16,5	1,4	2,7	2,7	17,1	7,5	8,3	8,7
PDTCH MCS-4	19,0	2,8	4,2	4,3	19,6	11,1	11,8	12,1
8PSK(C)/8PSK(I)								
PDTCH MCS-5	19,5	0,4	1,2	1,5	20,1	12,7	13,1	13,5
PDTCH MCS-6	21,5	4,7	5,1	5,6	22,1	16,2	16,6	16,8
PDTCH MCS-7	26,5	13,2	13,5	13,6	27,1	21,3	21,8	22,0
PDTCH MCS-8 (10%BLER)	30,5	20,4	20,9	21,0	31,1	25,0	26,0	26,1
PDTCH MCS-8 (30%BLER)	--	9,5	9,9	10,2	--	19,4	20,0	20,2
PDTCH MCS-9 (10%BLER)	--	25,1	26,1	26,2	--	28,1	29,3	29,4
PDTCH MCS-9 (30%BLER)	25,5	16,5	17,0	17,1	26,1	22,6	23,4	23,5

Tables 8 and 9 shows the performance of another receiver using the same parameter sets as applied above. Furthermore the gains compared to the performance requirements for DARP [1] are presented. As before, DTS-1 and DTS-2 is considered here.

Table 8: Diversity receiver performance DTS-1 - Correlation 0.0 and 0.7 [16]

DTS-1 - TU50nFH 1845 MHz				
Parameter Set: Logical Channel	PS1 $\rho = 0.0$	PS2 $\rho = 0.7$	3GPP TS 45.005	Gain
PDTCH MCS-1	-12,0	-8,0	3,5	**11,5 dB**
PDTCH MCS-2	-10,0	-6,0	6,5	**12,5 dB**
PDTCH MCS-3	-5,5	-1,5	11,5	**13,0 dB**
PDTCH MCS-4	1,0	5,5	19,5	**14,0 dB**

Table 9: Diversity receiver performance DTS-2 - Correlation 0.0 and 0.7 [16]

DTS-2 - TU50nFH 1845 MHz				
Parameter Set Logical Channel	PS1 $\rho = 0.0$	PS2 $\rho = 0.7$	3GPP TS 45.005	Gain
PDTCH MCS-1	1,0	1,5	9,0	7,5 dB
PDTCH MCS-2	2,5	3,0	11,0	**8,0 dB**
PDTCH MCS-3	6,5	6,5	15,0	**8,5 dB**
PDTCH MCS-4	12,0	12,5	22,0	**9,5 dB**

6.4.1.3 Sensitivity

This subclause presents simulation results in sensitivity limited scenarios. The combinations of antenna gain imbalance G and correlation ρ given in table 10 are used.

Table 10: Gain and correlation parameters used for tests

Parameter set	Antenna Gain Imbalance G [dB]	Correlation ρ
PS 1	0	0
PS 2	0	0.7
PS 3	-3	0.7

The sensitivity performance of MS RX diversity is shown in table 11 for packet switched channels PDTCH MCS-1 to MCS-9. The signal levels are given in dBm for which an MS RX diversity mobile terminal meets the block error rates specified in subclause 6.2 of 3GPP TS 45.005. For comparison, the corresponding signal levels specified in tables 1a and 1c of 3GPP TS 45.005 for MCS-1 to MCS-4 and MCS-5 to MCS-9, respectively, are also included.

Table 11: Feasible specification values for diversity receiver sensitivity performance [17]

	3GPP TS 45.005 tables 1a and 1c	DAIC - PS 1 (G 0 dB, corr. 0 %)	DAIC - PS 2 (G 0dB, corr. 70 %)	DAIC - PS 3 (G -3 dB, corr. 70 %)
GMSK				
PDTCH MCS-1 (BLER 10%)	-100,5	-107,7	-106,9	-105,6
PDTCH MCS-2 (BLER 10%)	-98,5	-106,2	-105,5	-104,0
PDTCH MCS-3 (BLER 10%)	-94,5	-102,4	-101,3	-99,9
PDTCH MCS-4 (BLER 10%)	-88,5	-97,2	-96,1	-94,6
8PSK				
PDTCH MCS-5 (BLER 10%)	-93,5	-98,9	-98,3	-96,9
PDTCH MCS-6 (BLER 10%)	-91,0	-96,9	-96,2	-94,8
PDTCH MCS-7 (BLER 10%)	-81,5	-91,9	-90,9	-89,6
PDTCH MCS-8 (BLER 10%)	--	-87,8	-86,6	-85,2
PDTCH MCS-8 (BLER 30%)	-80,0	-90,7	-89,7	-88,3
PDTCH MCS-9 (BLER 10%)	--	-84,4	-83,0	-81,5
PDTCH MCS-9 (BLER 30%)	--	-87,5	-86,5	-85,0

Tables 12 and 13 shows the performance of another receiver using the same parameter sets as applied above. Furthermore the gains compared to 3GPP TS 45.005 are presented.

Table 12: Sensitivity - Correlation 0.0 and 0.7 - BPD of 0 dB [16]

Sensitivity - TU50nFH 1845 MHz				
BPD = 0.0 LOGICAL CHANNEL	PS1 $\rho = 0.0$	PS2 $\rho = 0.7$	3GPP TS 45.005	Gain
PDTCH MCS-1	-107,0	-105,5	-100,5	5,0 dB
PDTCH MCS-2	-105,0	-104,5	-98,5	**6,0 dB**
PDTCH MCS-3	-102,5	-101,5	-94,5	**7,0 dB**
PDTCH MCS-4	-97,5	-96,5	-88,5	**8,0 dB**

Table 13: Sensitivity - Correlation 0.0 and 0.7 - BPD of 3 dB [16]

Sensitivity - TU50nFH 1845 MHz				
BPD = 3.0 LOGICAL CHANNEL	$\rho = 0.0$	PS3 $\rho = 0.7$	3GPP TS 45.005	Gain
PDTCH MCS-1	-105,5	-104,5	-100,5	4,0 dB
PDTCH MCS-2	-104,0	-103,0	-98,5	**4,5 dB**
PDTCH MCS-3	-101,0	-100,0	-94,5	**5,5 dB**
PDTCH MCS-4	-96,5	-95,0	-88,5	**6,5 dB**

6.4.2 System level Performance

6.4.2.1 Voice Capacity

This subclause provides results of system level simulations from [7], [12] evaluating the potential gains in voice capacity when introducing MS receive diversity.

6.4.2.1.1 Link to System Mapping

The link-to-system mapping was validated by comparing the actual link simulator to a "mapped link simulator". The "mapped link simulator" read the desired and interfering signal levels from the actual link simulator on every burst and translated them to estimated BEP and FEP with the stage-1 and stage-2 maps. The actual and estimated FER for one antenna are shown in figure 41. The degradation from the mapping process is considered negligible.

For two antennas, we showed in [7] that Maximal Ratio Combining (MRC) and Single Antenna Interference Cancellation (SAIC) could be used as a conservative estimate of the performance of Dual Antenna Interference Cancellation (DAIC). In this method, the MRC branch gains were determined and applied to the desired and interfering signals. The CIR and DIR were calculated from the resulting summed branches, and then used to estimate BEP and FEP through the stage-1 and stage-2 maps derived from non-diversity link simulations.
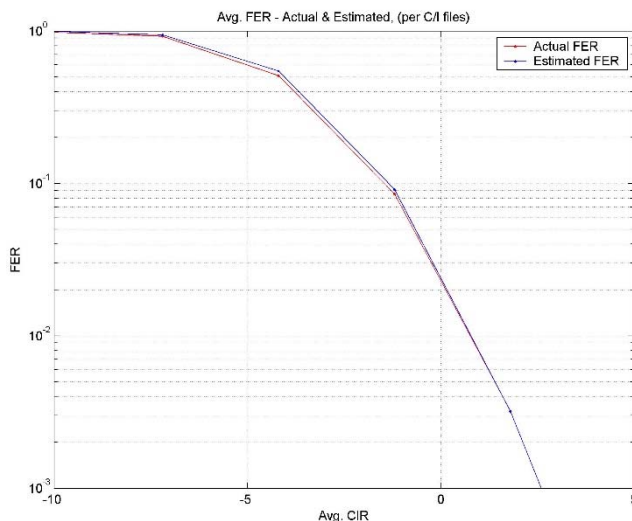
Figure 41: Actual and estimated link FER for one antenna [12]

Table 14: System Assumptions and Parameters [12]

Parameter	Value	Unit
Frequency	1 900	MHz
Bandwidth	1.2	MHz
Reuse	1/1 (TCH)	-
Voice Codec	AMR 5.9 FR	-
Cell Radius	1 000	m
Sectors (cells) per Site	3	-
Sector Antenna Pattern	UMTS 30.03	-
Propagation Model	UMTS 30.03	-
Log-Normal Fading: Standard Deviation	8	dB
Log-Normal Fading: Correlation Distance	110	m
Log-Normal Fading: Inter-Site Correlation	50	%
Adjacent Channel Interference Attenuation	18	dB
Handover Margin	3	dB
Antenna Gain Imbalance (AGI)	0 or 2.0	dB
Antenna Correlation (ρ)	0 or 0.4	-
Fast Fading	Flat or TU	-
Mobile Speed	3 or 50	km/hr
Hopping	Ideal FH, Random RF	-

The system voice capacity is Effective Frequency Load (EFL) at which 95 % of the calls have less than 2% FER over the call duration. Blocked calls are counted against the call satisfaction statistics.

Figures 42 and 43 show the system capacity at 3 km/hr and 50 km/hr, respectively. Both figures show the Conventional Receiver (CR), 1-antenna DARP, or DARP+MSRD. The DARP+MSRD receiver is shown with or without the combined antenna impairments of 2 dB Antenna Gain Imbalance (AGI) and an antenna correlation of 0.4. The antenna correlation is the magnitude of the complex correlation. Note that the curves with DARP+MSRD use the MRC+SAIC conservative approximation to dual antenna interference cancellation, as presented in [7]. Table 15 contains a summary of the performance curves at the 95 %-ile point, which is defined as the system capacity.

With only one antenna, the channel model has quite a significant effect, the TU channel being much more benign than flat fading. With DARP+MSRD, TU is slightly better than flat fading. Both MSRD and the TU channel tend to reduce the deep nulls experienced in flat fading.

The effects of antenna gain imbalance and correlation are shown together, and only compared to the case of no impairments with flat fading. The degradation is insignificant, which is consistent with previous link simulations [7] and [8] that showed a smaller impact to interference-limited situations than noise -limited situations.
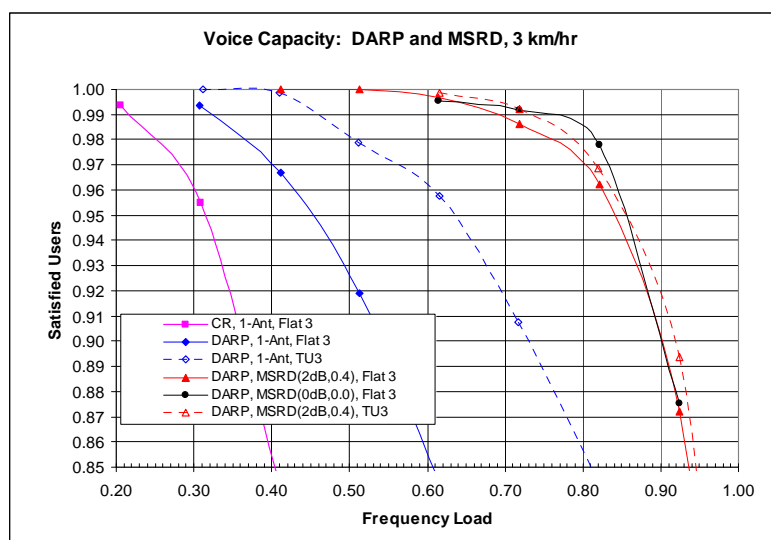
Figure 42: Voice system capacity with DARP and MSRD, 3 km/hr [12]
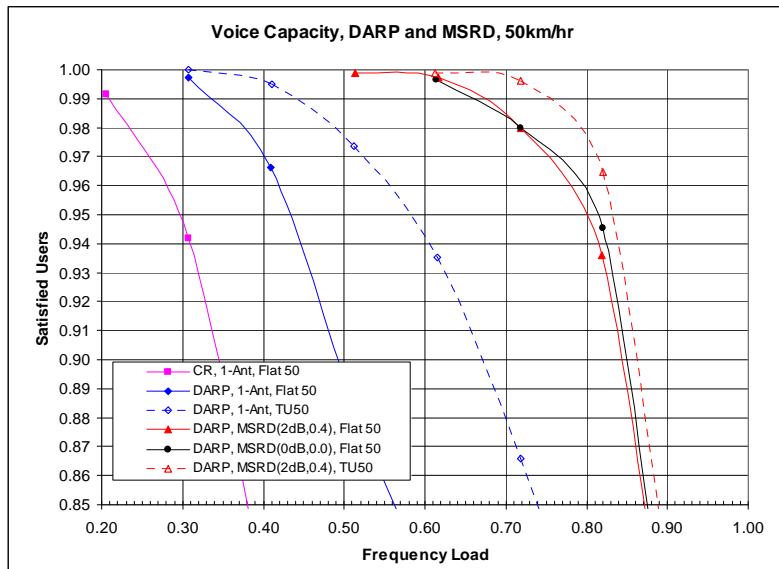
Figure 43: Voice system capacity with DARP and MSRD, 50 km/hr [12]

Table 15: System voice capacity (EFL for 95 % < 2 % FER) [12]

	Conventional Receiver	DARP	DARP+MSRD (2 dB AGI, 0.4 ρ)	DARP+MSRD (0 dB AGI, 0 ρ)
Flat, 3 km/hr	32 %	45 %	84 %	85 %
Flat, 50 km/hr	30 %	42 %	80 %	82 %
TU, 3 km/hr	-	64 %	84 %	-
TU, 50 km/hr	-	58 %	83 %	-

6.4.2.2   Mixed Voice and HTTP traffic

Voice and HTTP traffic were generated in a static simulation in accordance with the system configuration description in table 17 and the HTTP traffic model in table 18. The HTTP traffic model is similar to that in [27], with minor changes. A dedicated 32 kbps backhaul resource was assumed for each user, and as a consequence, the network delay for each packet is a deterministic function of the packet size. Also, Out-Of-Range (OOR) draws of random variables used in the generation of the HTTP traffic were either limited or re-cast to better match the mean values reported in [27].

For two antennas, it was shown in [7] that maximal ratio combining (MRC) and Single Antenna Interference Cancellation (SAIC) link mappings could be used to conservatively estimate the performance of Dual Antenna Interference Cancellation (DAIC). In this method, the CIR and DIR are calculated for the max-ratio sum of the outputs of the two antennas, and are then used to estimate BEP and FEP through the stage-1 and stage-2 maps derived from the non-diversity SAIC link simulations.

In the simulation, 3 time slots were reserved for data. Handsets were limited to a single receive slot for simplicity. In the absence of this restriction, we would expect the user throughput to increase with the number of slots, and the relative performance gains of DARP and MSRD to remain unchanged. All sites were assumed to be time synchronized. However, because voice and data slots may have significantly different loadings, the time slots reserved for data at each site were chosen randomly to provide a common interference environment for the voice and data slots.

The simulation used MCS-1, MCS-2, and MCS-3, but without Incremental Redundancy (IR). IR may be added to the simulation in the future. Link Adaptation was based on a filtered measure of FER, to avoid speculative decoding of multiple MCS rates.

A mix of 70 % voice and 30 % HTTP was used, where the percentage denotes the fraction of total population using the particular application. For circuit voice traffic alone, the (Voice) Effective Frequency Load (EFL) was defined as the number of current voice users divided by the total slots (frequencies x slots) in a sector. It may be useful to consider the circuit voice load to be "reservation Erlangs", and define an associated "interference Erlangs" as the reservation Erlangs reduced by the voice activity factor. Similarly, an effective interference load can be associated with HTTP and FTP calls, though the relationship is not fixed because the total number of times slots associated with a call depends on the (M)CS. Thus, for any loading of voice and data traffic, we define the Effective Interference Load as the average fraction of slots which are occupied by either voice or data.

In this contribution, the system voice capacity is defined as the Effective Frequency Load (EFL) at which 98 % of the calls have less than 2 % FER over the call duration. Blocked calls are counted against the call satisfaction statistics. The performance metric for HTTP is the average of the per-user throughput. The reading time for packet calls is not included in the calculation of throughput.

Figure 44 shows the average per-user data throughput of a mixed voice-data system, in flat fading at 50 km/hr. The concurrent voice capacity of the system in the presence of the data traffic is illustrated in figure 45.

Figures 46 and 47 are similar to figures 1 and 2, but differ in that user throughput and voice satisfaction are shown against the Effective Interference Load instead of the (Voice) Effective Frequency Load (EFL). The "DARP - Voice Only" curves in Figures 2 and 4 denote the result of previous system simulations without HTTP traffic. By referring to Figure 4, it is apparent that the impact of interference on voice performance is represented better by using the Effective Interference Load.

In the Figures, results are presented for the conventional receiver (CR), 1-antenna DARP, and DARP+MSRD. The DARP+MSRD receiver is shown with the combined antenna impairments of 2 dB Antenna Gain Imbalance (AGI) and an antenna correlation of 0.4, where the antenna correlation is defined here as the magnitude of the complex correlation. Note that the curves with DARP+MSRD use the conservative MRC+SAIC approximation for the performance of dual antenna interference cancellation, as presented in [7].

Table 16 contains a summary of the figures 44 and 45 curves. The voice capacity is defined as the EFL at which 98 % of the calls have an FER < 2 %. For data, the average per-user throughput (for 1 slot) is compared at an EFL loading of 20 %.
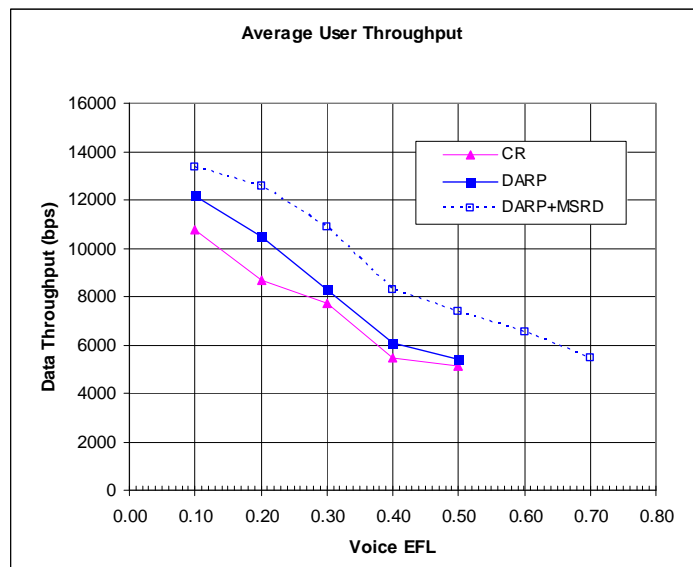
Figure 44: User data throughput versus Voice EFL, 50 km/hr
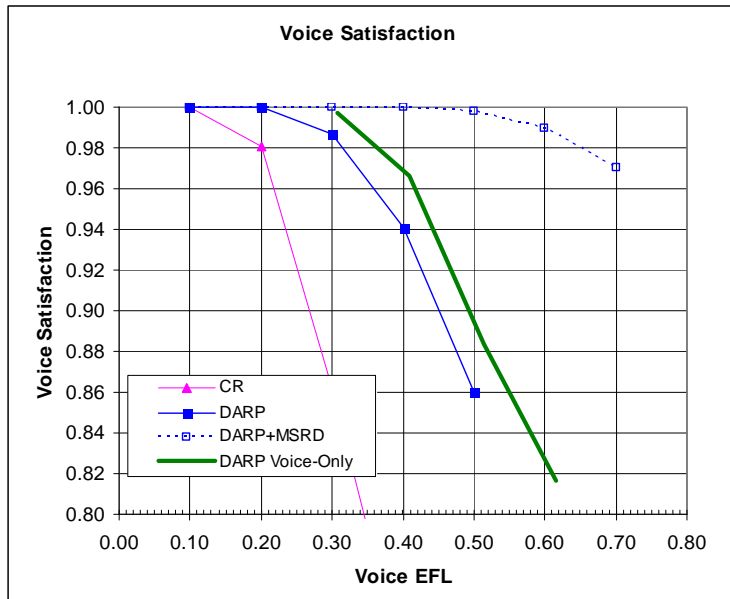
Figure 45: Voice satisfaction versus Voice EFL, 50 km/hr
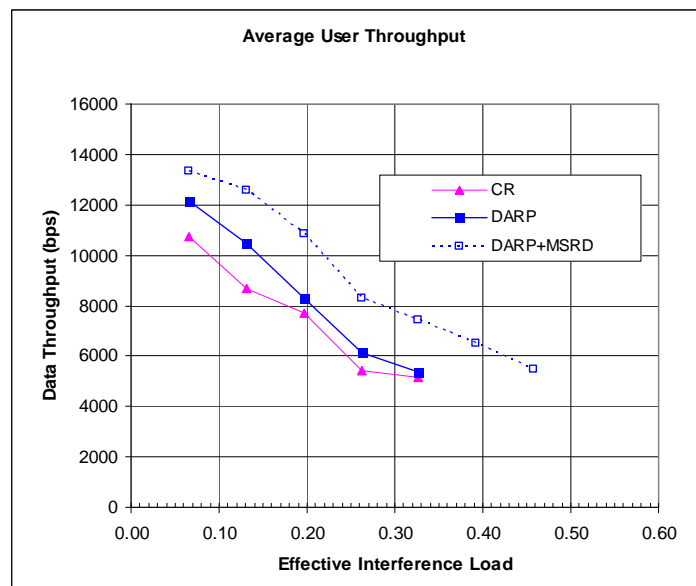
Figure 46: User data throughput versus Effective Interference Load, 50 km/hr
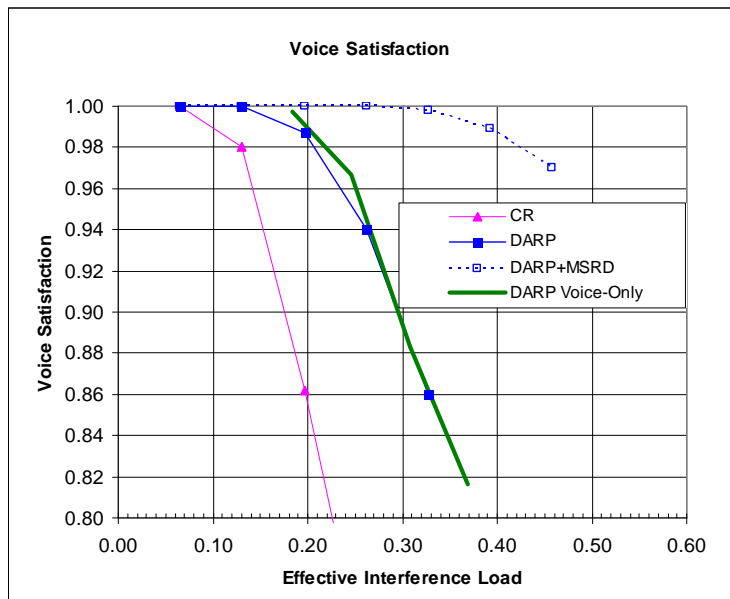
Figure 47: Voice satisfaction versus Effective Interference Load, 50 km/hr

Table 16: System performance, flat 50 km/hr

	Conventional Receiver	DARP	DARP+MSRD (2 dB AGI, 0.4 ρ)
System Voice Capacity (EFL at 98 % FER < 2 %)	20 %	32 %	65 %
Avg. User Throughput (bps) at 20 % EFL	8,690	10,485	12,579

Table 17: System assumptions and parameters

Parameter	Value	Unit
Frequency	1 900	MHz
Bandwidth	1.2	MHz
Reuse	1/1 (TCH)	-
Voice Codec	AMR 5.9 FR	-
Cell Radius	1 000	m
Sectors (cells) per Site	3	-
Sector Antenna Pattern	UMTS 30.03	-
Propagation Model	UMTS 30.03	-
Log-Normal Fading: Standard Deviation	8	dB
Log-Normal Fading: Correlation Distance	110	m
Log-Normal Fading: Inter-Site Correlation	50	%
Adjacent Channel Interference Attenuation	18	dB
Handover Margin	3	dB
Antenna Gain Imbalance (AGI)	2.0	dB
Antenna Correlation (ρ)	0.4	-
Fast Fading	Flat	-
Mobile Speed	50	km/hr
Hopping	Random RF, uncorrelated fading	-

Table 18: HTTP traffic model for MSRD system level simulations

	Parameter	Value	Note
1	Session arrivals	Poisson	Mean 5 arrivals/hr
2	Number of packet calls in session	Geometric	Mean 5, max. 15 (Re-cast OOR RVs)
3	Packet call size	Pareto	alpha = 1.1, k = 2.25 Kbytes, m = 225 Kbytes (Limit OOR RVs)
4	Packet call reading time	Geometric	Mean 5 s, no max
5	Packet size:	Semi-empirical	40 % 40 bytes, 20 % 576 bytes, 20 % 1 500 bytes, 20 % Uniform (40 bytes to 1 500 bytes)
6	Number of packets in packet call	-	Depends on packet call size (RV) and packet size (RV)
7	Packet inter-arrival time	-	Depends on packet size and backhaul rate (32 kbps)
8	Data Erlangs/HTTP User	0.043	At MCS-2 (MCS-dependent)

6.5 Impacts to the Mobile Station

MS receiver diversity has significant impacts to the MS design. The additional antenna and corresponding RF module is likely to increase the size and thus also the cost of the MS. Assuming a parallel receiver structure, MS Diversity can in terms of signal processing be considered as somewhat comparable to twice the complexity of SAIC.

Beyond the increase in size cost and complexity, there is also the impact on power consumption that needs to be considered.

In IDLE DRX the increase in MS power consumption would substantially degrade the waiting time supported with a specific battery. Substantial degradation of battery life is also expected for high-multislot packet switched channel allocations.

It is therefore proposed to allow the MS to disable the 2nd receive branch in DRX mode, since in such cases the link budget is expected to be more favourable than in packet, or CS traffic modes.

It has already been proposed to allow the flexibility to reuse the 2nd receive branch to support either Multi-Carrier (MC) or receive diversity by network control [10].

We propose to introduce further signalling that will allow the network to delegate the decision to a DAIC capable MS whether to disable the 2nd branch altogether.

For example in areas where the network is not expecting high cell loading, or coverage issues the network may decide to let the MS utilize Rx level, and interference measurement to further optimize the power consumption vs. performance tradeoff.

6.6 Impacts to the BSS

The introduction of MS receiver diversity is likely to require the optimisation of BSS algorithms such as link adaptation and power control.

6.7 Impacts to the Core Network

As with SAIC/DARP it is desirable that the network is able to take the improvement in link level performance into account. That is, it should be possible for the MS to signal its capabilities to the network. This could be implemented as a DARP phase 2.

The network should be able to signal the MS how to use the dual receive paths, e.g.:

- RxDiv - The MS must utilize its diversity capabilities.

- MC - The MS should switch its 2nd receive branch to the 2nd carrier.

- RxDiv-Optional - The MS may decide to switch off its 2nd receive branch.

6.8 Impacts to the Specification

As was the case with SAIC/DARP, MS receiver diversity can be implemented with limited impacts to the 3GPP specifications.

Table 19: Impacted 3GPP specifications

Specification	Description
3GPP TS 45.005	Radio transmission and reception
3GPP TS 24.008	Mobile radio interface Layer 3 specification; Core network protocols; Stage 3 (Release 7)
3GPP TS 51.010 (series)	Mobile Station (MS) conformance specification

6.9 References

[1]   3GPP TR 45.903: "Feasibility study on Single Antenna Interference Cancellation (SAIC) for GSM networks (Release 6)".

[2]   3GPP TS 25.101: "User Equipment (UE) radio transmission and reception (FDD) (Release 6)".

[3]   IEEE Journal on Selected Areas in Communications, Vol. 20, No., 6 August 2002: "A Stochastic MIMO Radio Channel Model With Experimental Validation", J.P. Kermoal, L. Schumacher, K.I. Pedersen, P.E. Morgensen and F. Frederiksen.

[4]   IEEE Transactions on Antennas and Propagation, vol. 49, no. 9 September 2001, pp. 1271-1281: "Spatial, Polarization, and Pattern Diversity for Wireless Handheld Terminals", C.B. Dietrich Jr., K. Dietze, J.R. Nealy and W.L. Stutzman.

[5]   IEEE Trans. on Vehicular Technology, vol. 44, no. 2, May 1995, pp. 318-326: "An Experimental Evaluation of the Performance of Two-Branch Space and Polarization Diversity Schemes at 1800 MHz", A.M.D. Turkmani, A.A. Arowojolu, P.A. Jefford and C.J. Kellet,.

[6]   VTC'98, pp. 741-746: "Performance of Two-Branch Polarisation Antenna Diversity in an Operational GSM Network", T.B. Sorensen, A.O. Nielsen, P.E. Morgenensen, M. Tolstrup, K. Steffensen.

[7]   GP-051504: "Observations on Receive Diversity Implementation and Performance", source Motorola

[8]   GP-051459: "Proposed text on MS Diversity for the GERAN evolution feasibility study", source Nokia

[9]   AHGEV-018: "Link Level Simulation Specification for MS RX Diversity", source Philips, Copenhagen, May 2005

[10]   TDoc AHGEV-004: "Combined capabilities Switching for GERAN Evolution, Qualcomm".

[11]   GP-052145: "Mobile station receive diversity - antenna and channel models", source Ericsson.

[12]   GP-051979: "System Capacity of Mobile Station Receive Diversity With DARP", source Motorola.

[13]   GP-052114: "Modelling of Antenna Correlation for Dual-Antenna RX Diversity and Interference Cancellation", source Siemens.

[14]   GP-052124: Channel modelling for MS Receive Diversity", source Nokia.

[15]   GP-052102: "On correlation modelling for GERAN Receive Diversity", source QUALCOMM.

[16]   GP-052125: "Example Link level performance for MS Receive Diversity", source Nokia.

[17]   GP-051901: "Link level simulations for MS RX diversity", source Philips.

[18]   GP-052101: "Dual Antenna MS Evaluation", source Intel.

[19]   Microwave Mobile Communication, William C. Jakes Jr., John Wiley 1974.

[20]   3GPP TS 45.005: "Radio transmission and reception".

[21]   GP-052332: "On the impact of antenna gain imbalance and correlation on MS RX diversity performance", source Philips.

[22]   GP-052624: "Dependency of Dual-Antenna RX Diversity and Interference Cancellation Schemes on Complex Antenna Correlation", source BenQ Mobile.

[23]   Review of Radio Science 1996-1999, August 1999 Chapter 5: "Handset Antennas for Mobile Communications; Integration, Diversity and Performance", G.F Pedersen, J. Bach Andersen.

[24]   The 8th international symposium on Personal, Indoor and Mobile Radio Communications, 1997: "Handset Antenna diversity evaluation in a DCS-1800 small cell", G.F Pedersen, S. Widell, T. Ostervall.

[25]   Proceedings of the 10th IEEE International Symposium on Personal, Indoor and Mobile Radio Communications, September 1999: "Antenna Diversity on a UMTS Handheld Phone". G.F. Pedersen, J.Ø. Nielsen, K. Olesen and I.Z Kovacs.

[26]   GP-052647: "Channel modelling and parameter selection for MS Receive Diversity", source Nokia.

[27]   GP-040408: "A GPRS traffic model for SAIC performance evaluation", source Nokia.

[28]   GP-051980: "On Channel models for evaluation of GMSK and 8PSK with Receive Diversity and Interference Cancellation", source Motorola.

[29]   AHGEV-013: "Dual Antenna terminals - Evaluation principles and scenarios", source Ericsson.

7   Dual-carrier and multi-carrier

7.1   Introduction

Multi-carrier GERAN is a performance-enhancing feature aimed at improving peak and average user throughput, increase trunking gain, and to reduce latency. Currently, the theoretical peak data rate of EGPRS is 473.6 kbps. In a real network, bit rates in the order of 100 kb/s to 200 kb/s are feasible on four timeslots. With multi-carrier, both peak and average user throughput is increased proportionally to the number of carriers. With a dual-carrier constellation, the peak data rate would be close to 1 Mb/s. The need for higher bit rates could make it desirable to support multi-carrier GERAN in future releases of the GERAN standard. With this feature, peak and average bit rates can be increased in a very flexible and backwards-compatible manner. The improved data rates are needed in order to ensure that the same services are available regardless of the underlying radio technology, GERAN or UTRAN.

The most obvious benefit of multi-carrier GERAN is that it overcomes one limitation of the GSM radio interface - the 200 kHz carrier bandwidth. This limitation puts a restriction on the rate of data transfer to one and the same user, and is the fundamental difference between GSM/EDGE and other radio access technologies such as WCDMA. Multi-carrier GERAN gives increased flexibility in how the system throughput is divided among users.

Conceptually, dual-carrier is a special case of multi-carrier. Since there may be differences mainly in terms of MS implementation, special consideration is sometimes given to dual-carrier is the descriptions below.

In this chapter, it is assumed that the dual-carrier and multi-carrier concept applies to the downlink and uplink except where explicitly indicated.

7.2   Concept description

7.2.1   Basic concept

Multi-carrier GERAN means that multiple GERAN carriers on independent carrier frequencies (or MAIO:s in the frequency hopping case) are received or are transmitted by the same terminal. A straightforward solution would be to split the data flow of one user onto multiple carriers below RLC/MAC, reusing the current physical layer per carrier without modifications. This could be seen as a natural extension to the multi-slot principle, where a multi-slot allocation is now allowed to span across more than one carrier. This is illustrated in figure 48.
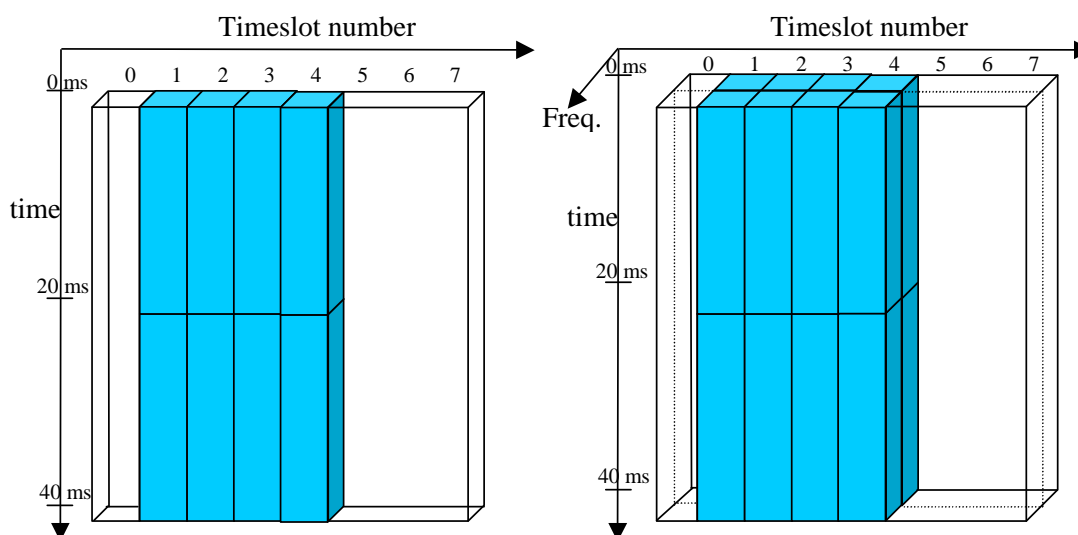
**Figure 48: Left: Illustration of radio blocks in a 4-slot single-carrier allocation.
Right: Illustration of radio blocks in a 2*4-slot dual-carrier allocation. The two frequencies
(MAIO:s in case of frequency hopping) are typically not adjacent.**

7.3   Modelling assumptions and requirements

There are no special requirements for the modelling of the multi-carrier concept. The same principles as with EGPRS can be used.

7.4   Performance characterization

7.4.1   Peak data rates

The peak data rates for EGPRS for different number of carriers are shown in table 20. The increase in average data rate is also proportional to the number of carriers. Since there are also some additional degrees of freedom in the channel allocation and link adaptation (trunking gain), the improvement can be somewhat larger.

Table 20: Peak data rate for EGPRS versus number of carriers

# of carriers	Air interface peak data rate (4 slots per carrier) [kbps]	Air interface peak data rate (8 slots per carrier) [kbps]
2	473	947.2
3	710.4	1 420.8
4	947.2	1 894.4
5	1 184	2 368
6	1 420.8	2 841.6
7	1 657.6	3 315.2
8	1 894.4	3 788.8
9	2 131.2	4 262.4
10	2 368	4 736

7.4.2 Window size limited TCP throughput

The high latency is a potential problem for the transport layer protocol. In particular, the throughput and RTT should satisfy the "throughput x RTT = TCP window size" limit, which gives the maximum throughput for a given TCP round trip delay and TCP window size. This relation is illustrated in figure 22, which shows the maximum RTT for throughputs between 50 kbit/s to 1 500 kbit/s.
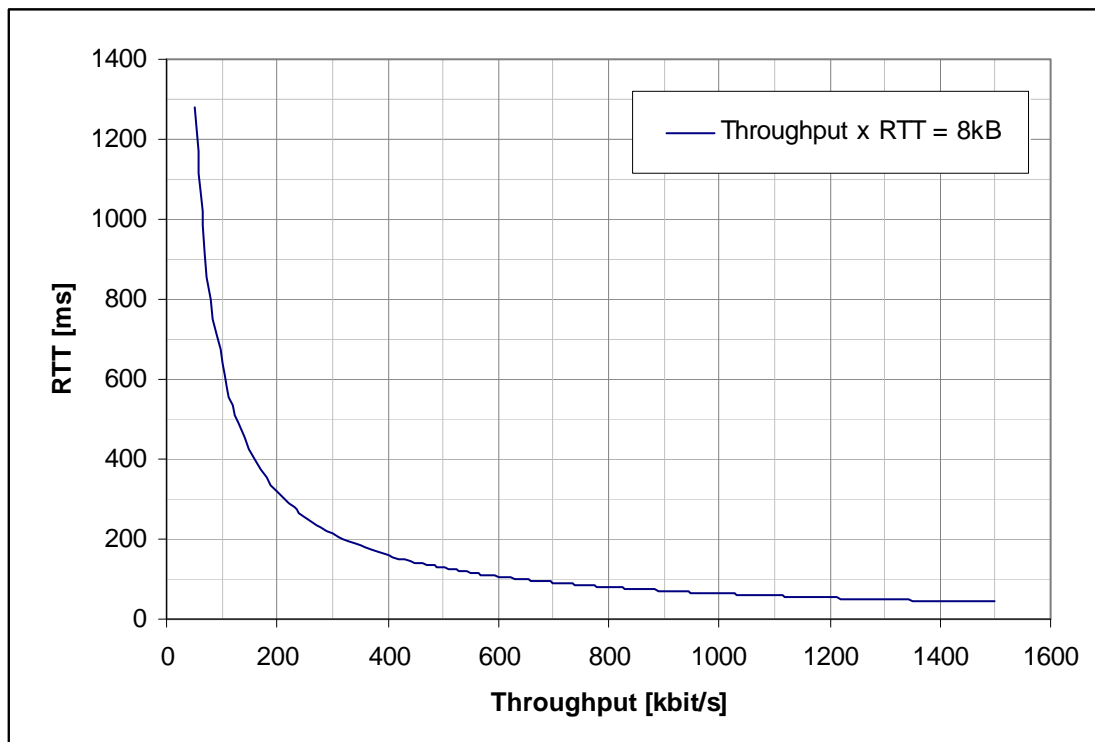
Figure 49: TCP throughput boundary

7.4.3 Error-limited TCP throughput

7.4.3.1 Introduction

The TCP throughput may also be limited by the segment error rate and by the delay. This is generally referred to as the error-limited TCP throughput. In this subclause, the performance of TCP is considered as not limited by the TCP window.

7.4.3.2 TCP modelling

The error-limited TCP throughput has been analyzed in the literature, and is modelled by the following empiric formula (see [1] in clause 2):

$$throughput[bps] = \frac{MSS}{RTT \cdot \sqrt{1.33 \cdot p} + T_0 \cdot \min\left(1,3 \cdot \sqrt{0.75 \cdot p}\right) \cdot p \cdot \left(1 + 32 \cdot p^2\right)}$$

Where the following parameters are defined.

Table 21: TCP modelling parameters

Parameters	Description
MSS	IP segment size (bits)
RTT	Round-trip time
T_0	Timeout (assumed = 5 * RTT)
p	Probability of IP segment loss
No limit on window size	

7.4.3.3 Multi-carrier GERAN modelling

Air Interface

The air interface peak data rate for Multi-carrier GERAN has been computed as the simple multiplication of the per-carrier peak data rate times the number of carriers. Two cases have been considered: the ideal case of 8 allocated slots per carriers, and the more realistic case of 4 allocated slots per carrier. The peak data rates are shown in table 20 in subclause 7.4.1.

TCP related figures

The TCP error-limited throughput has been modelled by the following set of parameters.

Table 22: Figures used to model the TCP error-limited throughput

Parameter	Figure(s)
IP segment size [bytes]	1 500
IP segment error rate	[10e-4, 5*10e-4]
RTT (*) [ms]	[100, 200, 300, 400, 500, 750]
NOTE: (*) Includes internet/backhaul delay + radio-related delay (including retransmission overhead).	

In reality, there will be some relationship between the number of carriers, the IP segment error rate, and the associated delay. In that sense, by neglecting such association we have performed some level of approximation. However, given that the result is essentially driven by the delay figure, and, within this, by its fixed component, we believe the formula yield an accurate enough model of the expected behaviour.

7.4.3.4 Results

The plots provided in annex A show how the error-limited TCP throughput may turn into a performance upper bound, no matter how many carriers are combined for MC GERAN.

When the two curves (i.e. the air interface peak data rate and the TCP error-limited throughput) cross, it means that the increase of air interface peak data rate is not translating into increase of TCP throughput. In these cases, the TCP throughput is de-facto bounded by its error-limited performance (which is in turn driven by the delay component).

Table 23 summarizes for the considered cases of multislot allocation and IP error rate the number of carriers at which performance is bounded by the TCP error-limited throughput.

Table 23: Max number of carriers before performance becomes TCP-limited

RTT	IP error rate = 10e-4		IP error rate = 5*10e-4	
	4-slot case	8-slot case	4-slot case	8-slot case
750 ms	5	2	2	1
500 ms	8	4	3	1
400 ms	> 10	5	4	2
300 ms	> 10	7	6	3
200 ms	> 10	9	9	4
100 ms	> 10	> 10	> 10	9

The limit would obviously be reached earlier for if a more pessimistic IP error rate were assumed.

7.5 Impacts to protocol architecture

7.5.1 Physical Layer

7.5.1.1 Modulation, multiplexing, and radio transmission

No changes are expected.

7.5.1.2 Channel coding

The channel coding of the basic multi-carrier concept (without inter-carrier interleaving) can be carried out with the existing modulation and coding schemes of EGPRS (MCS 1-9).

7.5.1.3 Mobile capabilities

The multi-carrier capability could be defined either as a simple indication, or as a set of dedicated multi-slot classes for multi-carrier. The first option implies that the multi-carrier mobile would act like a time-slot multiplier, the time and frequency domains being fully independent from each other. With the latter option, there would be more flexibility to control the number of time slots, but a set of new multi-slot classes would need to be specified.

7.5.1.4 Channel quality measurements

The current EGPRS mobiles are required to support the reporting of four different types of measurements: MEAN_BEP measurements, CV_BEP measurements, interference measurements (γ_{CH}), and slot-wise MEAN_BEP measurements (MEAN_BEP_TS).

For multi-carrier mobiles, the MEAN_BEP and CV_BEP reporting could be done either in a carrier wise or combined manner. In the carrier wise scheme, the MEAN_BEP and CV_BEP figures are individually calculated for each carrier, whereas in the combined scheme, the MEAN_BEP and CV_BEP values are averaged over multiple carriers.

The main benefit of the carrier wise MEAN_BEP and CV_BEP reporting is that the potential imbalance between the carriers is taken into account. This is especially important for the network deployments, where one carrier is placed on the BCCH layer and the other carriers on the hopping layer. In such case, the averaging over several carriers would produce an erroneous result, because the fading statistics of hopping and non-hopping carriers are different. The evident drawback of the carrier wise reporting is the increased size of the channel quality report. The increased message size can be avoided by using the poll-based reporting strategy, which is explained in subclause 7.5.2.6.

The main benefit of the combined MEAN_BEP and CV_BEP reporting is that the size of the channel quality report remains unchanged. The obvious drawback is the degraded estimation accuracy, when at least one of the carriers is deployed on a non-hopping layer. This problem could be avoided by limiting the scope of multi-carrier on the hopping layer, i.e. by using the same frequency parameters (except MAIO) for both carriers. Besides enabling a more reliable measurement reporting, such strategy would also simplify assignment procedures.

Regardless of the reporting strategy for MEAN_BEP and CV_BEP measurements, the interference and MEAN_BEP_TS measurements need to be reported per time slot. Again, the method of subclause 7.5.2.6 can be exploited to avoid the increased message size.

7.5.2 RLC/MAC

7.5.2.1 Multiplexing with legacy MSs

The same principles apply for multiplexing on multiple carriers as on a single carrier. There is no radio resource segregation: provided that the intra-carrier interleaving is not used, the multi-carrier data flows can be multiplexed with the single carrier data flows on the same timeslots.

7.5.2.2 Multiplexing data on multiple carriers

7.5.2.2.1 Simultaneous transmission over multiple carriers

The most straightforward way to allow for transmission over multiple carriers is to allow a TBF to span over two carriers, like it would span over several timeslots. The same TFI can be used over all carriers (even a different TFI could be used per carrier, if deemed necessary). However RLC limitations (window size) may come into effect if the total amount of timeslots exceeds 8: this is looked at in subclause 7.5.2.4.

7.5.2.2.2 Time-divided transmission over multiple carriers

Uplink transmission is ruled by dynamic allocation i.e. through USF. RRBP is also used for reserving uplink radio blocks for transmission of RLC/MAC control blocks by the mobile station.

With multi-carrier on the downlink, receiving over multiple carriers brings about the transmission over multiple carriers (distinctively, as opposed to simultaneously). The following behaviour is proposed:

- Reception of an assigned USF on a given carrier grants uplink transmission on the same carrier.

- Reception of a valid RRBP on a given carrier grants uplink transmission on the same carrier.

- In case of a conflict (abnormal case, from the network side), i.e. more than one uplink radio block reserved on the same time slot and TDMA frames (see note) it is proposed that:

  - If one of the uplink radio block is reserved by means of RRBP for an RLC/MAC control message, the MS shall respond in that uplink radio block.

  - If more than one uplink radio block are reserved by means of RRBP, the MS shall respond in one of them (e.g. randomly selected). The MS shall send the RLC/MAC control message according to the priorities defined in 3GPP TS 44.060.

  - If more than one uplink radio block are reserved by means of USF, the MS shall respond in one of them (e.g. randomly selected).

  NOTE: This may occur in case of colliding USF allocations (i.e. USFs detected in the same block on more than one carrier at the same time), RRBP allocation on one carrier colliding with a USF allocation on another carrier, or colliding RRBP allocations hence granting the same uplink block on more than one carrier at the same time.

7.5.2.3 Segmentation / reassembly

Reassembly in multi-carrier case is comparable to reassembly in multi-slot case; additional timeslots are monitored on the allocated carriers. Note that additional requirement is put on mobile station side given all carriers have to be monitored simultaneously: the MS has to monitor all allocated timeslots on both carriers. While timeslots on a carrier are separated in time, carriers are separated in frequency (hence timeslots (with same TN) on different carriers occur at the same time).

7.5.2.4 RLC window size

The RLC window size needs to cope with the maximum amount of outstanding RLC data blocks within RLC roundtrip time. Otherwise too small a window starts to limit the peak throughput. This amount is given as follows when N carriers, all timeslots (8 per carrier) and two RLC data blocks per radio block (20ms) are used:

$$Max\_RLC\_Window = N \times \frac{RTTms}{20ms} \times 2 \times 8 \qquad (4)$$

Typical RLC roundtrip time is 160 ms corresponding with BS_CV_MAX value of 6. The RLC roundtrip time could however be significantly higher if Abis transport is arranged by geo-stationary satellite hop, yielding to about 640ms RTT.

As can be seen from the Equation 1, the current maximum RLC Window Size for EGPRS (1024) is well adapted for multi-carrier (except possibly in case of Abis over satellite hop), but definitely too small for GPRS (64). The usage of multi-carrier could be hence restricted to EGPRS.

7.5.2.5 Incremental redundancy

In order to retain full retransmission flexibility, the incremental redundancy (IR) within all carriers should be supported. This feature would be mandatory for MS and optional for BSS.

7.5.2.6 Link adaptation

Link quality measurements are reported in acknowledgement message, upon request from the network. As described in subclause 7.5.1.4, it would be beneficial to report the measurements separately for all carriers. In order to avoid reporting a large amount of measurement data in a single EGPRS channel quality report, the following approach could be considered.

Report measurements for only one carrier in the acknowledgement message (i.e. report measurements for the carrier on which the poll was received). Indication of the reported carrier is needed.

7.5.2.7 Signalling

The allocation of multiple carriers needs to be supported through signalling (assignment, reconfiguration of resources) between the network and the mobile station. This will increase the likelihood for segmentation of the corresponding RLC/MAC control messages. Note however that extended RLC/MAC control message segmentation was introduced in Rel-6 for messages that span over more than two radio blocks, and can be used in this case as well.

7.5.3 Higher layers

The support of multi-carrier by the mobile station needs to be indicated with sufficient flexibility as part of the mobile station's capabilities.

It is assumed that the indication (broadcast) of the network support for multi-carrier is not needed, given no need is identified for the MS to request a multi-carrier transmission.

7.6 Downlink Dual Carrier

7.6.1 Overall throughput considerations for dual carrier on the downlink

A preliminary assessment is that multi-carrier is most feasible for the downlink. Whether is can be applied also to the uplink depends on MS implementation constraints which are studied in further subclauses. However, even by just allowing multi-carrier reception in the downlink, it is possible to increase the uplink data rates since receiving more effective downlink time slots in a shorter period of time allows to accommodate more uplink timeslots. For instance, the definition of higher multi-slot classes with effective sum=9 could be studied for the case of dual-carrier reception, as shown in figure 50. Although fast frequency synthesizers are assumed, the monitoring slot will be a little bit shorter to allow for tuning from the Tx to the monitoring frequency and from the monitoring to the Rx frequency. As figure 50 shows, this concept is compatible with DTM. This allocation gives a gain of 80 % in the overall throughput compared with a state of the art multislot class 12 MS (sum = 5).

Downlink	0	1	2	3	4	5	6	7
f1	Monitoring	TCH/AFS	PDTCH					
f2	PDTCH	PDTCH	PDTCH					
Uplink	5	6	7	0	1	2	3	4
f1'					TCH/AFS	PDTCH	PDTCH	PDTCH

Legend: **Neigbour cell Monitoring** | **MS - Reception** | **MS - Transmission**

**Figure 50: Example of higher multislot classes with effective sum=9
using a second receiver for downlink reception**

If multi-carrier is not applied in the uplink, it would still be advantageous if the MS was capable of alternating between the uplink carriers corresponding to the allocated downlink carriers according to the dynamic allocation (see subclause 7.5.2.2 for detailed description).

The multi-carrier operation is illustrated in figure 51, which shows a dual-carrier mobile (4+1) multiplexed with two legacy mobiles (2+1). Note the multiplexing of the dual-carrier MS on two uplink carriers.

DL slot	0	1	2	3	4	5	6	7	0	1	2	3	4	5	6	7
UL slot	5	6	7	0	1	2	3	4	5	6	7	0	1	2	3	4
DL (f1)	A	A	A	B					A	A	B	B				
DL (f2)	A	A	C	C					A	A	A	A				
UL (f1)							A								B	
UL (f2)							C								A	

A: Dual Carrier MS 4+1 (=8+1)   **B**: Legacy MS 2+1 on frequency 1   **C** Legacy 2+1 MS on frequency 2

Figure 51: Dual carrier multiplexing

7.6.2 Inter-carrier interleaving

This is investigated in clause 10.

7.6.3 Dual-carrier diversity

The same baseband signal is transmitted over two carrier frequencies. At the receiver, the signals on the two carriers are converted to baseband, providing two diversity branches.

7.6.4 Adaptation between dual carrier and receive diversity

In many cases, the dual-carrier on the downlink would be deployed in a network that already supports the MS RX diversity. In order to guarantee the most optimal utilization of network resources, it should be possible to switch between the two modes. The performance evaluation of this scheme is studied in clause 12.

7.6.5 Impacts to the mobile station

7.6.5.1 Multiple narrowband receivers

There are different options for the implementation of the multi-carrier RF in the MS receiver. One option, suitable mainly for a small number of carriers (e.g. dual-carrier), is to have separate receiver chains for each carrier. This means that the multi-carrier terminals exploit an architecture, where the receiver branches can be tuned to different frequencies (see figure 52). The receiver branches can use either the same antenna or separate antennas.
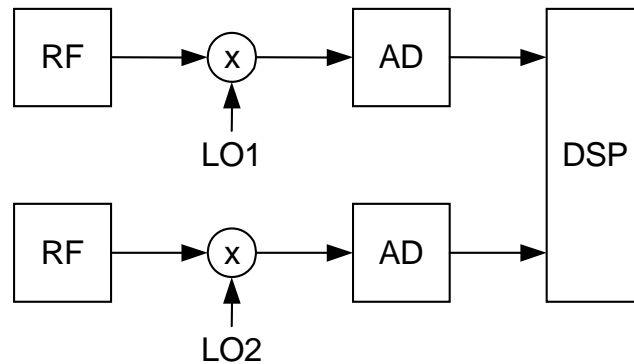
Figure 52: RF architecture for dual-carrier receiver with separate receiver chains for each carrier

7.6.5.2 Wideband receiver

Another option, mainly suitable for a larger number of carriers, is a wideband receiver. This option may have additional impacts to the network since it may be necessary to limit the carrier spacing of the multi-carrier assignment. Also, blocking requirements may be an issue.

7.6.5.2.1 Larger bandwidth

Simultaneous reception of n carriers would obviously imply larger bandwidth for the receiver front-end. This is in itself a source for additional complexity. However, it is difficult to assess such complexity without a clear requirement on the width of the wideband front-end.

Given that most, if not all, of the GERAN carriers of the multi-carrier allocation will effectively be MAIO's, the receiving interval (from the lowest frequency carrier to the highest frequency carrier) might even be variable. Obviously the receiver shall be dimensioned for the worst case. Thus, it would be beneficial to establish some assumptions in that sense. In other words:

- Can there be any assumption on the maximum interval between carriers for which the multi-carrier receiver shall be dimensioned for?

7.6.5.2.2 Channel separation

As mentioned in a previous contribution (see [2] in subclause 7.12), channel separation may be performed with known techniques, e.g. digitally.

However, it is important to note that the complexity of digital channel separation is also dependent on the width of the wideband receiver, which shall maintain the same C/N applicable today for GERAN (see note), which in turn is likely to have an effect on power consumption.

NOTE: The C/N requirement for GERAN is 28 dB, while the C/N requirement for WCDMA is 16 dB.

7.6.5.2.3 Blocking requirements

Blocking requirements are described in 3GPP TS 45.005.

In-band blocking requirements are obviously defined assuming that there is one "useful" carrier, and the receiver has to fulfil some blocking requirements towards all frequencies higher and lower than the "useful" carrier.

This can be illustrated pictorially by figure 53, which refers to a "small MS" in the GSM900 band.
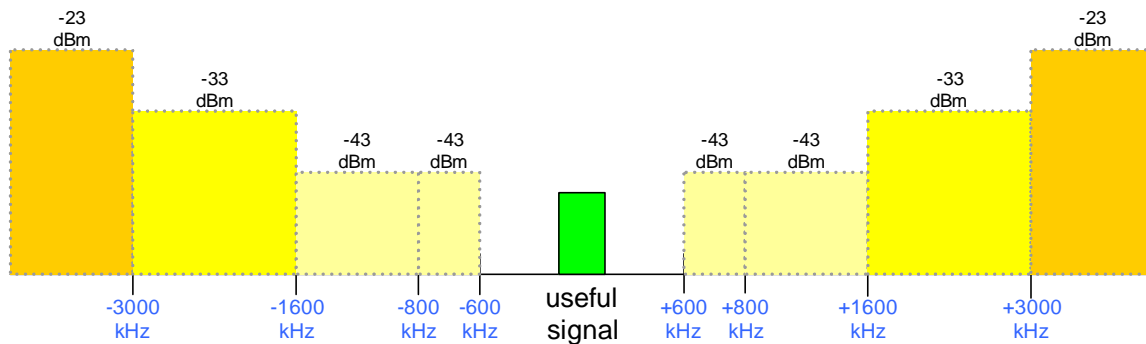
Figure 53: In-band blocking requirements for a Rel-6 "small MS" in GSM900

It is very unlikely that a similar blocking requirement structure can be maintained for a wideband multi-carrier receiver.

In essence, we would now have multiple "useful signals", around each of which we should depict a structure as in figure 53. This is obviously not a practicable option as we would end with drawing a blocking requirement on top of a "useful signal".

Thus, it seems that blocking requirements should be relaxed. A qualitative sketch of such relaxation is illustrated in figure 54.
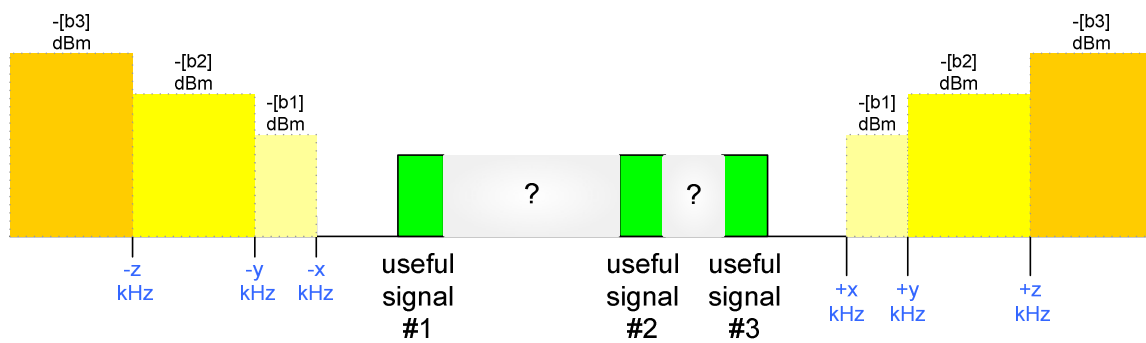
Figure 54: Possible relaxation of blocking requirements for a multi-carrier "small MS" in GSM900

Note that the "grey area" between the "useful signals" corresponds to the area where the performance requirements for adjacent interference apply. A redefinition of these requirements may also be needed, depending on the respective spacing of the "useful signals".

Further, it is important to consider that, if the frequencies of "useful signals" are effectively MAIO's, then also the respective spacing are changing on a TDMA frame basis. Thus, it should be discussed

- Whether any bound on the respective spacing of the multiple carriers can be assumed.

- How blocking should be defined (qualitatively) for a receiver expected to receive multiple carriers at once (i.e. should it look like figure 54?).

7.6.5.3 Baseband

On baseband, the receiver is required to process multiple RLC/MAC blocks per time slot. This requirement may have an impact on meeting the timing requirements of baseband processing. The baseband complexity is directly proportional to the number of carriers.

The support for multi-carrier incremental redundancy may have an impact on the baseband design. In practice, it is required that the channel decoder of a multi-carrier mobile is able to store and retrieve soft decisions from a common pool of soft values.

7.7 Uplink Dual Carrier

7.7.1 Concept description for dual carrier on the uplink

Dual Carrier in the Uplink shall be operated in such a way that it is compatible with legacy network operation. Multiplexing with existing GSM/EDGE bearers and a minimized BSS impact should therefore be ensured according to the objectives of the Feasibility Study.

It may be applied on non-hopping carriers as well as on hopping carriers. In case of configured frequency hopping, independent frequency hopping sequences are assumed to be present on both carriers.

7.7.2 Mobile Station Capabilities

The mobile station is required to include a second transmitter for Dual Carrier in the Uplink. It is also possible that a second transmit antenna at the mobile station might be necessary in order to avoid additional insertion loss. The impacts on the mobile station are described in subclause 7.6.1.

7.7.3 Increase in Peak Data Rate

The performance gain in peak data rate can be up to 100 % for dual carrier. Specifically, in interference limited scenarios which are typical for high traffic densities, it is expected that dual carrier leads to a doubled average data rate on UL. In sensitivity limited scenarios the average data rate may be doubled for a large portion of cell locations. Depending on the mobile station capabilities, even at the cell boundary an increase of the average data rates can be achieved when compared to single carrier.

7.7.4 Decrease of Latency

The main impact on latency would be the decrease in delays due to the higher bit rates that would be possible with dual carrier in the uplink. However, a reduced TTI could also be implemented, bringing additional improvements for the latency of small amounts of data. By using dual carrier on uplink with inter carrier interleaving of the bursts to reduce the latency, air interface latency of 10 ms could be achieved (see clause 10).

7.7.5 Impact on Cell Coverage

The cell coverage is dependent on the propagation conditions, the cell overlap and the required Eb/No for a particular service.

At cell edges when 8PSK can not be supported, the GMSK transmission can be used on two carriers with appropriate back off as pointed out in subclause 7.7.1 and thus data rates even at the cell edges can be improved when compared to single carrier transmission.

7.7.6 Impacts to the mobile station

7.7.6.1 RF Architecture options

Dual carrier requires duplication of the whole TX path e.g. from DSP to PA including own VCOs for both carriers. The architecture for a Dual Carrier RF in UL could be based on the following options:

   A) Combined single carrier transmitters with single antenna.

   B) Single carrier transmitters with separate antennas.

   C) Wideband multicarrier transmitter with single antenna.

For a wideband multicarrier transmitter with single antenna architecture option it may be challenging to keep intermodulation (IM) products and spectral growth due to high PAR below acceptable level. Also, TX bandwidth may be limited by DAC or used PA linearization technique. Efficiency may also be significantly worse than with a single carrier transmitter options A) and B). Restricting frequency spacing of carriers e.g. to 800 kHz would not be compatible with the existing frequency definitions or any frequency planning either.
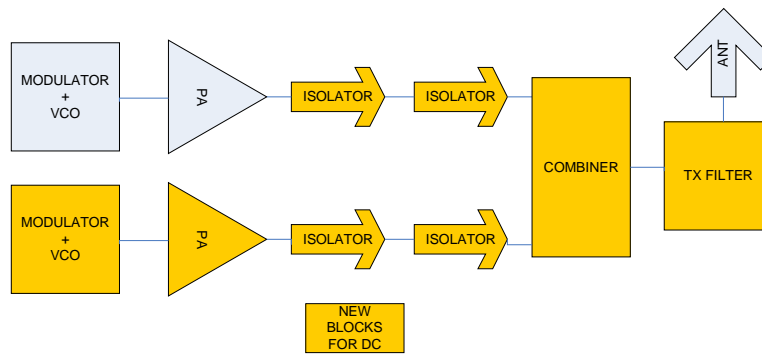
Figure 55: RF architecture of Dual Carrier MS with single antenna (Option A)
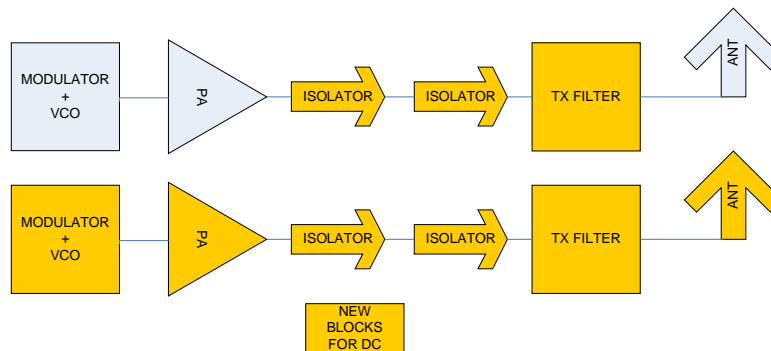
Figure 56: RF architecture of Dual Carrier MS with separate antennas (Option B)
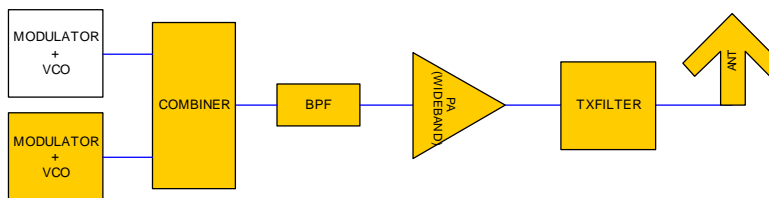
Figure 57: RF architecture of Dual Carrier MS with wideband PA and single antenna (Option C)

For option B, the Modified Concept for Uplink Dual Carrier (see subclause 7.7.3) could mean that no TX filters are required.

7.7.6.2   Evaluation of option A and option B (Taken from GP-060188)

7.7.6.2.1   Combining loss

With single antenna option A) a combiner is needed. Insertion loss of hybrid combiner is about 3 dB to 3.5dB, and that loss should be included to the RF loss budget in the architecture option A).

7.7.6.2.2   Intermodulation (IM)

Intermodulation products, due to various mechanisms are a challenge for systems with multiple carriers. Good isolation between transmitters is essential to avoid IM products. In this subclause, so called reverse intermodulation is assumed to have highest IM contribution.

Typically 3rd order IM results are dominating and those fall to the frequencies 2 x f_1- f_2 and 2 x f_2 - f_1, where f_1 and f_2 are carrier frequencies. Other products than 3rd order IM products may also exist e.g. sum of 900 MHz carriers (f_1+ f_2) may fall to the 1 800 band.

IM products may reduce link and system performance in uplink; furthermore IM products falling to receiving band of MS may block adjacent MSs to perform DL reception.

7.7.6.2.2.1 Reverse Inter Modulation (RIM)

Reverse intermodulation products are generated in the transmitter by wanted signal and external signal coming to transmitter's output port e.g. from an adjacent transmitter. Typically the reverse IM is tested at -40 dBc level of external signal thereby indicating needed level of isolation between transmitters. With that 40dB isolation it's possible, but not trivial, to obtain about -70 dBc IMD levels, e.g. to meet current spectrum due to modulation limits at > 6 MHz offsets. Typical reverse IM attenuation in the EDGE PAs is slightly above 20dB i.e. reverse IMD level is slightly less than -60 dBc at -40 dBc test level. Linearization of the PA would also improve the reverse IM characteristics, however this would mean in practice lower efficiency and higher current consumption.

The needed isolation may be reduced by amount of antenna isolation in case of architecture option B) and by amount of antenna return loss in case of option A). It needs to be noted that e.g. a hand on top of the MS antennas may reduce the obtainable antenna isolation e.g. down to a level of 6 dB to 12 dB and also reduce the antenna return loss e.g. down to a level of 6 dB to 12 dB. Isolation of 12 dB is assumed in the following for both. Thus additional isolation requirements are likely about the same ~30 dB to 40 dB for both options with the same susceptibility of transmitter for reverse IM.

7.7.6.2.2.1.1 Isolators

This ~30 dB isolation requirement between transmitters should be taken into account with both architecture options A) and B). It would mean e.g. to use isolators at the transmitter output. Isolators are narrow band devices, thus multiband MS should have separate isolators on lower and upper bands. Furthermore 2 to 4 isolators may be needed in series because one provides typically about 10 dB to 12dB isolation. These isolators introduce also insertion loss e.g. 0.8 dB per isolator. For example quad band MS and dual carrier transmitter MS could need up to 8 to 16 isolators.

7.7.6.2.2.1.2 RX band rejection of TX filter

Assuming IM level of -70dBc and spurious requirement of < -79 dBm at 900 RX band and assuming also that number of allowances (5) up to -39 dBm is exceeded with frequency hopping, the TX filtering of dual carrier transmitter with 27 dBm output should have ~37 dB rejection at RX band. This may not be obtained by the existing TX filtering. Improving of filtering may increase size and insertion loss. Indeed this filtering requirement should be fulfilled by both TX filters with architecture option B). Additional insertion loss of such a TX filter could be e.g. 2 dB to 4 dB. 10 MHz separation between TX and RX bands at 900 MHz would likely increase insertion loss related to other bands. Quad band MS would likely to have a bank of these filters.

7.7.6.2.3 Decreased efficiency due to reduced output power

The efficiency of a transistor gets smaller when a smaller part of the supply voltage is used for the actual signal. Thus the efficiency of the PA is reduced due back-off. It's assumed that dual carrier transmitter should not have higher total transmitter power than single carrier transmitter. This will introduce 3dB back-off at least for GMSK mode which may cause about 50 % increase in the peak power consumption.

7.7.6.2.4 Peak power consumption

The efficiency of MS transmitter has high impact on the MS design, e.g. in size and battery life. It needs to be noted that the whole TX path need to be duplicated, and not only PA, which may further increase power consumption and also in idle mode. In table 24 peak power consumption for options A) and B) are compared. The effect of reduced TX power due to dual carrier e.g. 3 dB reduction may increase peak power consumption of typical PA by about 50 % is included to the last row of the table.

Table 24: Increase in power consumption due to dual carrier transmitter

Item	DC option A)	DC Option B)
Combiner Loss	3.5 dB	0
Loss due to isolators (3 x 0.8)	2.4 dB	2.4 dB
Loss due to additional TX band filtering	3 dB	3 dB
Total loss	8.4 dB	5.4 dB
Increase in peak power consumption due to losses	**6.9 x**	**3.5 x**
Total increase of peak power consumption	**~10 x**	**~5 x**

It needs to be noted that insertion losses would increase peak power consumption also for normal single carrier voice, if e.g. some by-pass switches, which need to have sufficient IM properties, low loss and possibly fast enough to be switched during guard periods e.g. for DTM, are not used. Insertion loss of pair of switches could be in order of 1 dB.

Note that power consumption may be less when considering synergies with DL DC such as component re-use. Also note that analysis assumed equal gain for both antennas and excluded the option where 2nd PA is optimized for 3 dB backoff (this last option is considered further in subclause 7.7.2).

7.7.6.3 Evaluation of option B (Taken from GP-052723)

For uplink transmission the dual carrier approach requires the implementation of one further transmitter in the MS. This will cause an increase both of thermal power and battery peak current consumption, if appropriate countermeasures are not followed.

Due to the prerequisite of independent frequency hopping on both carriers a second transmitter will use a separate power amplifier and thus power consumption of both power amplifiers need to be considered.

7.7.6.3.1 PA and battery considerations

Current PA technologies are not yet optimised for dual carrier transmission. A second state-of-the-art power amplifier will double peak current consumption in the mobile. Even if a power amplifier is backed off by 3 dB, the power consumption is decreased by only about 25 %. Hence if two power amplifiers are operated with 3 dB back-off, a 50 % increase of peak current consumption will occur. However, talks to terminal manufacturers confirm that this drawback can be overcome in the near term if new developments are being looked at. Advanced power management technologies are required in this case. In particular, PA manufacturers are improving the PA efficiency at reduced output power. Hence reduction in peak current consumption can be expected. Moreover, as far as 8-PSK is concerned, peak current consumption is less critical than for GMSK with maximum output power.

Without output power back-off, the peak output power in the worst case for 8-PSK transmission will be 27 dBm + 3.2 dB (peak-to-average ratio) = 30.2 dBm. The current under this condition is expected to be 75 % of the current at GMSK with 33 dBm. Hence, if both PAs happen to transmit simultaneously with peak power for 8-PSK, the peak current consumption is 50 % higher than in the single carrier GMSK case.

By reducing the MS' Tx power by 1 dB (equivalent to the link budget of dual symbol rate), the peak current increase is expected to amount to only 40 %. Additional improvements on the receiver side as proposed above in the order of 1 dB to 2 dB will lower the peak current increase further to just 30 % to 35 % as shown in table 25.

The concept is foreseen to use either two 8-PSK modulated carriers or one 8-PSK modulated carrier and one GMSK modulated carrier, the latter being backed off by 4 dB.

At cell edges when 8-PSK can not be supported, the GMSK transmission can be used on two carriers with appropriate back-off of 4 dB as shown in table 25.

Table 25: Approximate peak current rise for the MS with dual carrier on UL

Parameter	Dual Carrier (8-PSK)	Dual Carrier (GMSK)
Usual output power per carrier	+27 dBm	+33 dBm
Peak-to-average ratio	+3.2 dB	0 dB
Power back-off	0 dB	-4 dB
Sum of output powers for dual carrier	+33.2 dBm	+32 dBm
Estimated increase of peak current consumption in case of (additional) back-off, compensated by receiver gain		
- without receiver gain	50 %	40 %
- with 1 dB receiver gain	40 %	35 %
- with 2 dB receiver gain	35 %	30 %
- with 3 dB receiver gain	30 %	25 %

It has to be noted that the peak current consumption issue is of less importance for other devices than small mobiles. A laptop computer with a double carrier data card will not experience the same relative increase of peak current consumption.

7.7.6.3.2 Antenna considerations

For dual carrier transmission in the UL it is required to implement a second transmit antenna at the MS in order to isolate both transmitters and at the same time avoid an insertion loss due to a combiner. None of the antennas should be covered by the user's hand. This can be achieved e.g. by the combination of a conventional internal antenna with a conventional external (stub) antenna. Since Rx diversity is likely to be standardised as part of GERAN evolution and since the same antenna can be used for Rx and Tx, the second antenna is not believed to be an obstacle in normal sized handsets. For particularly small handsets which cannot be equipped with a second antenna, a fallback solution with reduced throughput based on dual carrier on downlink and single carrier on uplink is already proposed in subclause 7.6.1. Currently advanced MS antenna designs are subject to research. For instance a dual polarized antenna design is investigated in [6]. Such a design allows both for Rx diversity as well for dual carrier transmission.

Furthermore it is believed that the additional power consumption through the activation of the second transmitter can be minimised for good and average C/I situations expected anyway for data transfer where a reduced transmit power can be assumed.

In a second phase additional interference diversity due to intercarrier interleaving applied to dual carrier on the uplink and addition of new coding schemes will reduce further the increase of power consumption while keeping the current EGPRS transmission time interval of 20 ms.

It is believed that for mobile stations implementing Rx diversity and dual carrier in the downlink, the additional complexity to implement dual carrier also in the uplink is reasonably limited as a number of components in the RF chain could be reused.

7.7.6.4 Evaluation of option C (Taken from GP-060609)

This subclause presents a third implementation option for the uplink, with the dual carrier generation at baseband utilizing a common PA and transmitter antenna. Some possibilities such as introducing restrictions on the frequency allocation are investigated to improve implementation feasibility.

7.7.6.4.1 Concept Description

Possible architectures based on a single TX path are proposed and illustrated in figures 58 and 59. These possibilities avoid the drawbacks associated with fully duplicated TX paths.
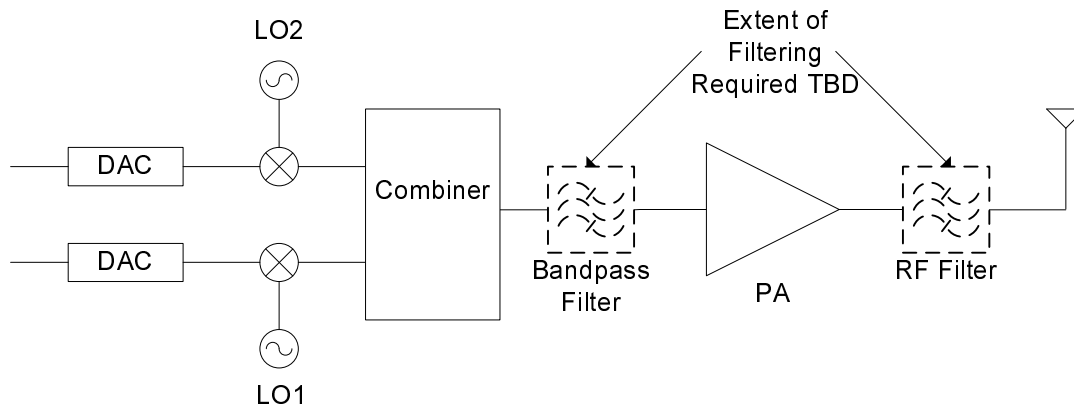
Figure 58: Architecture with separate modulators and common wideband transmitter

For the architecture in figure 58, the bandpass filter between the combiner and the PA and the RF filter following the PA may or may not be required depending on the implementation.
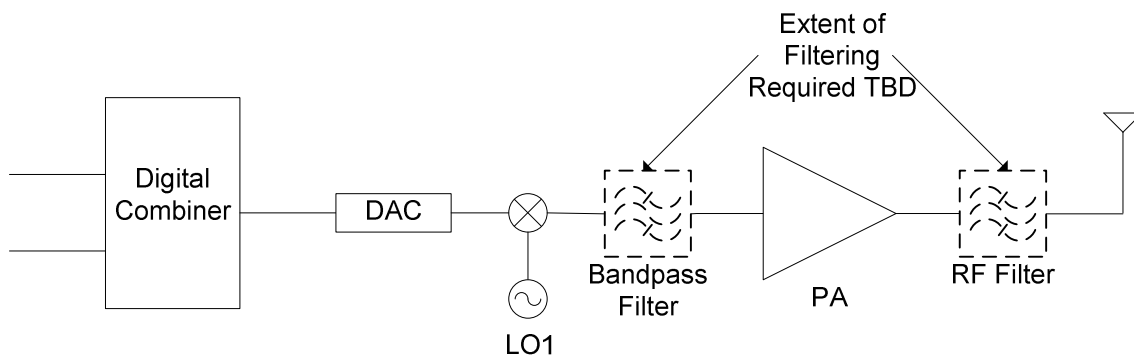
Figure 59: Architecture with common modulator and wideband transmitter.

For the architecture in figure 59, the two carriers are implemented in the digital baseband domain. This is achieved by expanding the bandwidth of the baseband signal chain by increasing the sampling rate.

7.7.6.4.2   System Impacts

The uplink "digital" dual carrier proposals only affect part of the baseband and the TX chain. Therefore, impacts to higher layers (RLC/MAC) are very similar to the generic downlink dual carrier architecture and are not addressed.

7.7.6.4.3   Output Power

The output power generated by the single PA is divided between the two carriers. Depending on the frequency separation of the two carriers the fading profile of the associated radio channels will be more or less identical. However the interference profile seen by each of the carriers could vary significantly. The ability to have separate power control for each carrier is desirable from a frequency planning point of view. The power control range may be limited, however pseudo-independent power control per carrier should be possible provided the total output power of the PA is not exceeded. In a situation where the mobile is using a single carrier downlink and dual carrier uplink, this presents challenges with uplink power control implementation. Issues related to these topics are for future study.

7.7.6.4.4   Power Efficiency

The peak to average power ratio (PAR) of a single 8-PSK carrier is approximately 3.2 dB. Adding a second carrier increases the PAR to approximately 6.2 dB. Therefore, in digital dual carrier mode with a single PA and two 8-PSK modulated carriers, the power level into the PA would need to be 3 dB lower than in the single 8-PSK carrier case. This increased back-off required to achieve PA linearity can potentially impact power efficiency. Increased back-off may be needed to meet the power spectrum mask due to modulation.

To improve power efficiency and increase output power, techniques to reduce PAR should be considered. This may imply allowing minor deviations from the normal spectrum mask for the unused frequency channel(s) between the two carriers.

The peak to minimum power ratio of two 8 PSK carriers is also increased over the single carrier case. This leads to PA linearity requirements over an enhanced input signal level range.

Operating the uplink digital dual carrier MS in single-carrier GMSK mode with the PA in saturation, the same power efficiency can be achieved as with current implementations. Stand-by time and talk time for legacy voice services will not be affected.

7.7.6.4.5 Coverage

The increased back-off to compensate for the higher PAR can potentially impact coverage. Applying the reduction of MS maximum output power specified in 3GPP TS 45.005 to an uplink dual carrier transmission, no significant changes to cell coverage is expected compared to a single-carrier multislot transmission with the same total number of time slots assigned.

The increased service provided by uplink digital dual carrier could be useful, even if the power-limited coverage is not the same as for existing services. When 8 PSK was initiated, it was clear it could not be used over the entire cell radius. Recall that the effective cell radius (based on TX power considerations) is often much larger than the actual cell radius (as deployed in the field), and the coverage of a cell is not always RF power limited. There are significant instances in time/location/frequency where signal and interference conditions permit such an enhancement.

7.7.6.4.6 Frequency Planning, Frequency Hopping

The carrier spacing for uplink digital dual carrier is assumed to be fixed within each cell. For non-hopping scenarios this does not impose any restrictions other than that both carriers have to be available.

In the case of frequency hopping, the carrier spacing has to be preserved, i.e. the two carriers have to hop in pairs. Only one of the carriers has an assigned MAIO. For the second carrier no MAIO is used, but it is specified by its frequency offset to the primary carrier (with MAIO). Frequency planning aspects are covered in more detail in subclause 7.10.1.

7.7.6.4.7 Intermodulation Interference

Restricting the maximum permitted frequency distance between the carriers makes it possible to reuse the technique and experience from WCDMA transmitters. This may make it possible to reduce the unwanted intermodulation products to acceptable levels, provided that these products fall into the active bandwidth of the error-corrected amplifier. To achieve sufficient suppression of intermodulation products, up to 5th order products may need to be taken care of. This implies that the maximum frequency offset between the pair of carriers from the same mobile needs to be no more than 1 MHz.

IM3 performance may be crucial and modified requirements in the close vicinity of the two carriers may be considered. A combined spectral mask would be an appropriate way to characterize the intermodulation. A linear power summation of two spectrum masks offset by the carrier spacing could create this combined spectral mask. In addition, IM suppression may be sensitive to variation in antenna characteristics due to different user behaviour (e.g. position of hand, distance to head or other obstructions).

7.7.6.5 Observations on the implementation options (Taken GP-060732)

The three possible implementation approaches described in subclause 7.7.6.1 can be summarised as follows:

a) dual, single-carrier PA's, driving either one of the two antennas, post-combining;

b) dual, single-carrier PA's, with each PA coupled to one of two antennas; or

c) a single wideband PA supporting dual carriers, driving a single antenna.

Options A and B were observed, however, to suffer from either significant combining losses (in the case of option A) or significant reverse intermodulation (RIM) vulnerability due to inter-antenna coupling (option B) leading to likely unacceptable losses of effective PA conducted output power levels.

Consider, for example, the dual-antenna option B. One estimate of the impact on conducted radiated power levels at the antenna connector for both GMSK and 8PSK modulation types (low band) appears in table 26. Assuming dual PA's are available rated at +33dBm and +27dBm for GMSK and 8PSK respectively, effective per-carrier total radiated power levels drop to +28dBm (GMSK) and +22dBm (8PSK). This analysis is consistent with that reported in subclause 7.7.6.2.

In the option B architecture, of course, the MS must also support dual PA's - with associated thermal and mechanical impact - plus approximately 2x larger peak current drain and power consumption in the RF subsystem. This may be difficult to support in mobile devices given current and anticipated battery technologies.

Table 26: Option B effective conducted power levels at antenna connector

	Units	GMSK	8PSK
Single-carrier PA rated power	dBm	33.0	27.0
Composite isolator loss	dB	3.0	3.0
Post-PA filtering loss	dB	2.0	2.0
Available conducted power per PA	dBm	28.0	22.0

The need for post-PA combining in option A means that approach offers few advantages over option B.

This leaves option C. The restricted carrier separation method described in subclause 7.7.3 appears inconsistent with straightforward frequency planning. If that modification is unavailable, the PA linearity and predistortion loop bandwidth requirements for option C may exceed contemporary PA design capabilities. For example, figure 60 shows the measured output power spectrum (i.e. power in a 30kHz bandwidth according to 3GPP TS 45.005, subclause 4.2.1) as a function of total *per-carrier* output power for a contemporary dual-mode GSM/EDGE PA with a dual-carrier 8PSK input signal.

Each 8PSK carrier was pseudo-randomly modulated with a carrier-specific sequence (the same sequence was applied in sequence to each burst) at carrier frequencies $f_1 = 900$ MHz and $f_2 = 901$ MHz. Also shown on the same plot are the power spectrum limits from 3GPP TS 45.005, subclause 4.2.1, referenced to +24dBm. It can be seen that at the +24 dBm per carrier output power level, the 3rd-order products at {899,902} MHz are suppressed by as little as 30 dB with respect to the primary carriers, while 5th order products were also significant. Accordingly, such a mode of operation appears no more attractive than options A and B.
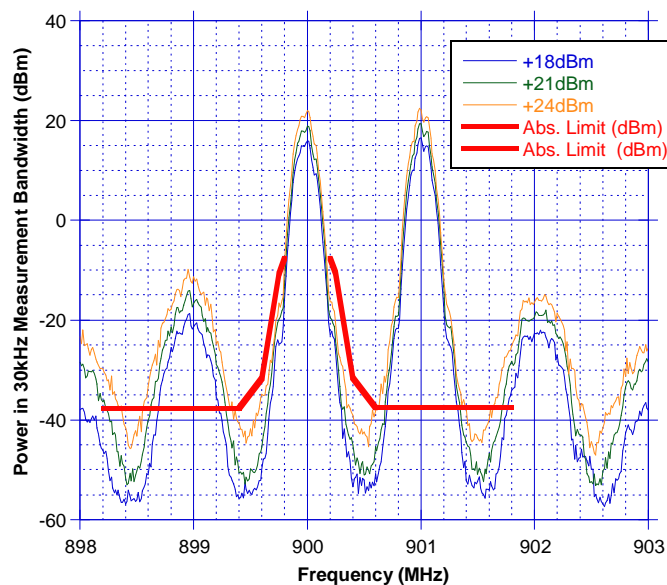
Figure 60: Measured PA output spectrum, dual-carrier input, 1 MHz carrier separation.

Figure 61, however, shows the output spectrum from the same PA when the dual-carriers were constrained to be separated by only a single ARFCN index (i.e. 200 kHz). Again, the 3GPP TS 45.005 spectrum limits are plotted, referenced to the +24 dBm case.
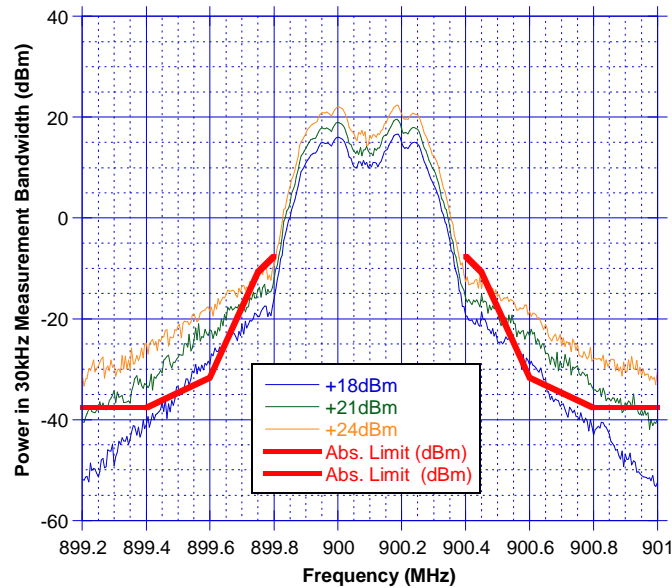
Figure 61: Measured PA output spectrum, dual-carrier input, 200kHz carrier separation.

It can be seen that in this case, while the power spectrum still exceeds the specified mask, there is significantly less adjacent channel leakage compared to the case of unconstrained carrier separation, and that the location in frequency of the non-compliant radiated power spectrum is relatively compact and predictable (largely impacting adjacent and 1st- and 2nd-alternate carriers).

It is, of course, quite predictable that the power spectrum of a constrained dual carrier uplink is significantly worse than the single-carrier case. This is a simple function of the complex envelope trajectory and peak-average ratio of the respective baseband waveforms, as illustrated in figures 62 and 63 for the single- and dual-carrier cases. Each figure shows a) the constellation, or combined 'constellation' of the waveform, plus b) the Peak-Average Ratio (PAR) distribution or Cumulative Density Function ( ). It can be seen that at the 99.9% CDF point, the PAR of the single-carrier waveform is approximately 3.2 dB, while the dual-carrier waveform has a PAR of almost 6.1 dB - i.e. approximately 3 dB greater.

Figure 61 suggests, however, that - depending on the allowable power spectrum - single PA operation for dual-carrier modes where the component carriers are constrained to be frequency-adjacent could *conceivably* permit per-carrier radiated power levels in the range of 20 dBm to 21 dBm without critically impacting MS complexity or power consumption, and so Constrained Dual-Carrier Uplink (CDCU) merits further discussion.
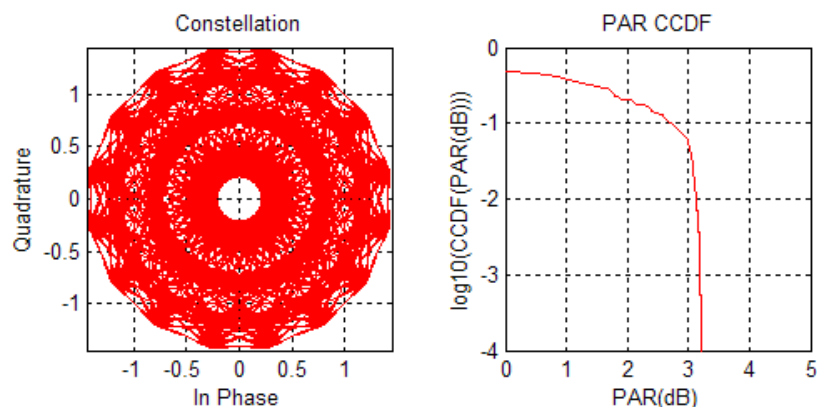
Figure 62: Single-carrier 8PSK constellation and PAR CDF
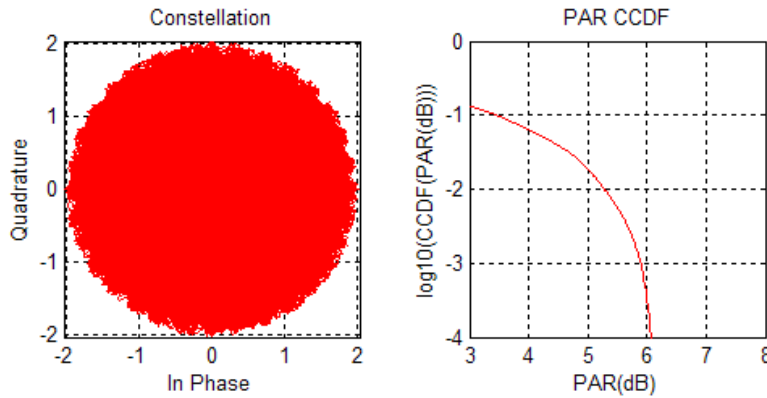
Figure 63: Dual-carrier 8PSK constellation and PAR CDF

7.7.6.5.1 Base Station Architecture Impact

One of the advantages of DCU is the potential for low impact on the BTS hardware, and constrained DCU can be viewed similarly. One important consideration, however, is the effect of a continuous adjacent companion carrier on achievable per-carrier receiver CINR, and the corresponding impact on reception of logical channels requiring high signal-noise ratios (e.g. uplink PDTCH using MCS 7-9).

In more detail, constrained DCU implies that the uplink one-sided carrier to adjacent channel interference ratio C/I_a input to the receiver does not exceed 0dB. Classically, 18dB of adjacent channel rejection has been assumed for GSM receivers, with contemporary GSM base stations frequently exceeding that specification. Further, the common use of Interference Rejection Combining (IRC) and other techniques in current BTS architectures suggests greater adjacent channel interferer rejection levels are achievable in practice, provided the interferer environment is not excessively complex. It is also important to recognise, however that IRC techniques based on differentiating the spatio-temporal interferer covariance matrix from the desired waveform could be limited in the constrained DCU application since - as illustrated in the dual-port receiver model of figure 64 - the multipath channel to the respective desired and interfering signals are identical since a single transmit antenna is used.
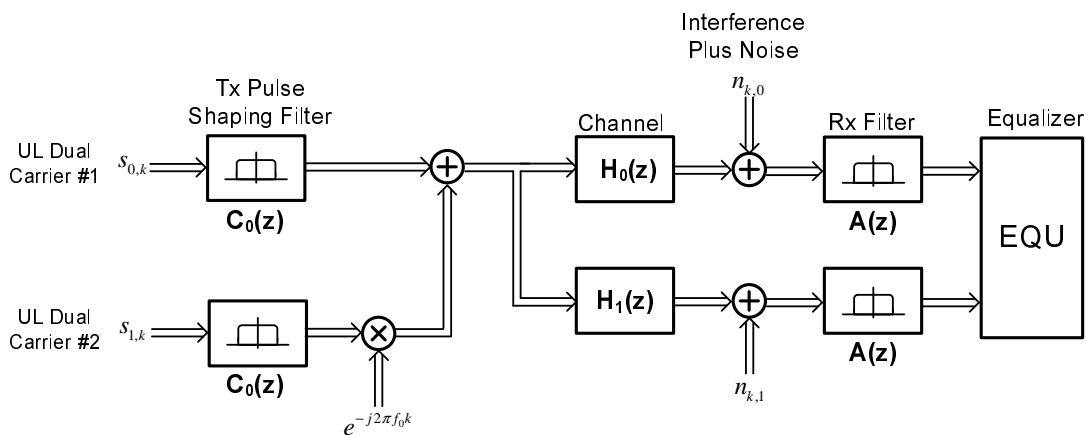
Figure 64: Conceptual dual-carrier, dual-port link

Nevertheless, *if* additional Adjacent Channel Rejection (ACR) is required, the synchronous nature (time and frequency offset) of dual-carrier transmission can be exploited in the BTS equalizer by using dual-carrier joint detection. Note that the use of separate, per-carrier equalizer processing resources (or resources with limited inter-resource communication) in the BTS is not necessarily an obstacle here provided there are sufficient per-carrier memory and computational resources to track the trellis state of the adjacent interferer.

7.7.6.5.2 Dual Carrier Interleaving and Constrained Dual Carrier Uplink

Constraining uplink dual-carriers to be immediately adjacent in frequency also has the potential to reduce any additional frequency diversity gain achieved through intra-burst interleaving beyond that attributable to conventional frequency hopping.

Table 27 provides guidance on E_b/N_0 values (reference to the coded bit rates for GMSK and 8PSK) required to achieve 10 % BLER for a TU50 channel at 850 for different combinations of single-carrier and dual-carrier intra-burst interleaving and frequency hopping.

Table 27: Performance of single- and dual-carrier interleaving, 10 % BLER, TU50 at 850MHz, both with no frequency hopping and with random frequency hopping over 45 contiguous carriers

| Carrier | Random FH over 45 contiguous carriers | | | | No FH | |
| | Dual Independent | Dual Adjacent | Single | | Dual Adjacent | Single |
Interleaving	With ICI	With ICI	Without ICI		With ICI	Without ICI
MCS1	8.3	8.2	8.6		9.2	9.6
MCS2	9.3	9.5	10.0		10.3	10.7
MCS3	12.8	13.1	13.8		13.6	14.2
MCS4	20.0	20.0	19.7		20.7	20.2
MCS5	8.4	8.7	9.1		9.5	9.9
MCS6	10.6	10.9	11.3		11.6	12.0
MCS7	16.0	16.3	16.6		16.4	16.7
MCS8	22.1	21.9	22.2		22.0	22.2
MCS9	27.2	27.1	26.0		27.0	25.9

The simulation results indicate that that:

a) random frequency hopping with dual independent carriers and intra-burst interleaving can provide up to 1dB in link performance gain for some logical channels, but losses of up to 1.2 dB are observed for MCS-4 and MCS-9;

b) when the dual carrier frequencies are constrained to be adjacent in frequency, the maximum gain is reduced to 0.7 dB while the maximum performance loss is reduced to 1.1 dB.

Accordingly, intra-burst, inter-carrier interleaving appears to offer mixed results in terms of link enhancement. Furthermore, constraining the dual carriers to be adjacent does appear to slightly reduce both the gains and losses in performance resulting from inter-carrier interleaving. Note that the case of widely separated, non-hopped carriers remains to be assessed.

7.7.6.5.3 System Frequency Re-Use Impact

The availability of sufficiently large cell allocations to support constrained DCU re-use patterns of the same dimension as traditional (3,3,9) or (4,3,12) BCCH patterns may be unlikely except in deployments with unusually rich resources. Accordingly, use of CDCU may often be limited to frequency hopping pairs. In this case, however, there is no obvious obstacle to the allocation of pairs of adjacent MAIO's. If a radiated power level of 18 dBm to 21 dBm per carrier were to be achievable, then reasonable uplink coverage for higher-order MCS's in dual-carrier configurations may be possible. Example link budgets for single- and dual-carrier MCS-9 operation assuming a target E_c/N_0 value of 25 dB appear in figure 65.

		UL	UL	
		EDGE	EDGE	
		8PSK	8PSK	
Logical Channel		PDTCH MCS-9	PDTCH MCS-9	
Carrier Configuration		Single Carrier	Dual Carrier	kbps
MS Transmitter Parameters				
Average Transmitter Power per Carrier		27.0	21.0	dBm
Cable, Connector, and Combiner Losses		0.0	0.0	dB
Transmitter Antenna Gain		0.0	0.0	dBi
EIRP per Traffic Channel		27.0	21.0	dBm
BTS Receiver Parameters				
Receiver Antenna Gain		17.0	17.0	dBi
Cable and Connector Losses		3.0	3.0	dB
Receiver Noise Figure		5.0	5.0	dB
Thermal Noise Density		-174.0	-174.0	dBm/Hz
Receiver Interference Density		-169.0	-169.0	dBm/Hz
Coded Symbol Rate (3x270.83kbps)		59.1	59.1	dB-Hz
Ec/Nt (Ec = Coded Bit)		25.00	25.00	dB
Receiver Sensitivity		-84.9	-84.9	dBm
Ancillary Parameters				
Handoff or Fast Cell Selection		0.0	0.0	dB
Inter-sector Antenna Rolloff w Combining Gain		-1.0	-1.0	dB
Smart Antenna Gain (e.g. beamforming)		0.0	0.0	dB
Other Diversity Gain (e.g. rx antenna diversity, MIMO)		0.0	0.0	dB
Other Gain (Vehicle or Building Penetration Loss + Body Loss)		0.0	0.0	dB
Log-Normal Fade Margin		12.1	12.1	dB
Total Gains/Margins		-13.1	-13.1	dB
Pathloss Model (UMTS 30.03 Section B.1.4.1.3)				
Loss (dB) = A * log10(R(km)) + B				
Height BS Above Rooftop		15.0	15.0	m
Carrier Frequency		900.0	900.0	MHz
Loss Coefficient - Parameter A		37.6	37.6	
Loss Offset - Parameter B		120.9	120.9	
Range Computation				
Maximum Path Loss		112.8	106.8	dB
Maximum Range (PL model: 128.1+37.6log10(.R))		0.61	0.42	km

Figure 65: Example link budget, MCS-9 single- and dual-carrier modes

7.7.7 Impact of reduced MS power

7.7.7.1 Introduction

The major problem of the uplink DC is the increased power consumption, which is a direct consequence of the simultaneous transmission on two uplink carriers. To maintain the same total transmitted power, both transmitters of a dual-carrier terminal need to be backed off by 3 dB. Unfortunately, the backoff decreases the efficiency of the power amplifier, hence increasing the peak current consumption. It has been estimated that the increase in peak current consumption would be approximately 50 % (see subclause 7.7.6.2). It has been also estimated that additional isolators and TX filtering may be needed to reduce the intermodulation products. These extra components are estimated to increase the peak power consumption by 250 % (see subclause 7.7.6.2). As a consequence, the peak power consumption of an uplink capable dual-carrier mobile could be up to ~5 times higher than the peak power consumption of a downlink-only dual-carrier mobile.

The aim of this study is to evaluate the impact of the additional backoff on the system level performance of uplink dual-carrier.

7.7.7.2 Simulation setup

7.7.7.2.1 Network

Two network scenarios are considered:

- Network 1: Interference-limited.

- Network 2: Coverage-limited.

The main parameters of these scenarios are listed in table 28.

Table 28: Network scenarios

Parameter	Interference limited scenario	Coverage limited scenario
Site separation	2.25 km	12 km
Bandwidth	2.4 MHz (BCCH), 2.4 MHz (TCH)	2.4 MHz (BCCH), 7.2 MHz (TCH)
Re-use	4/12 (BCCH), 1/1 (TCH)	4/12 (BCCH), 3/9 (TCH)
Number of TRXs	1 BCCH, 5 hopping	1 BCCH, 4 hopping
Load (EFL for single-carrier)	26 %	2.3 %

The load for the interference limited case is selected so that the speech outage (proportion of bad quality calls) would be around 5 %. Similarly, the cell radius for the coverage limited case is selected to yield the 5 % speech outage, the network load being low.

Some important network parameters (common to both cases) are listed in table 29.

Table 29: Common network parameters

Parameter	Value
Frequency band	900 MHz
Channel model	TU3
Traffic model	AMR / FTP
Synchronization	Synchronized BSS
MS mobile class	4+1
EGPRS penetration	30 %
DC penetration	100 %
DL power Control	Disabled
UL power Control	Enabled
MAIO management	Enabled
Incremental redundancy	Enabled
Frequency hopping	Random RF hopping
Propagation parameters	As in 3GPP TR 45.903, table 4-2

7.7.7.2.2   Dual-carrier Deployment

Two dual-carrier deployment scenarios are considered:

- Deployment scenario 1: BCCH / Hopping.

- Deployment scenario 2: Hopping / Hopping.

In the first case it is assumed that the PS traffic originally resides on the BCCH TRX. When deploying dual-carrier, one hopping TRX is reserved for the dual-carrier traffic. In the second case it is assumed that the PS traffic originally resides on one hopping TRX. When deploying dual-carrier, another hopping TRX is dedicated for the dual-carrier traffic.

In both cases, the size of the PS territory is fixed to two TRXs, i.e. there are no dynamic territory updates. The dual-carrier TRX is taken among the existing hopping TRXs, meaning that the size of the CS territory is decreased by 8 time slots and some additional interference is generated towards the speech calls. This approach was possible in the simulated network, because one TRX could be taken away from the CS layer without significantly increasing the number of blocked calls. In practical network implementations, an additional TRX for dual-carrier may be needed.

7.7.7.2.3   Backoff

Three different backoff scenarios are considered (powers relative to 33 dBm):

- Reference: 0 dB backoff for GMSK, 6 dB backoff for 8PSK.

- Backoff case 1: 3 dB backoff for GMSK, 6 dB backoff for 8PSK.

- Backoff case 2: 3 dB backoff for GMSK, 9 dB backoff for 8PSK.

In the first case (backoff case 1), the GMSK power is backed off by 3 dB in order to comply with the nominal power reduction for 2 GMSK time slots (according to 3GPP TS 45.005), whereas the 8PSK power remains the same.

In the second case (backoff case 2), the 8PSK power has also been backed off in order to optimise for power efficiency, size and cost. In this case, it is assumed that the first PA is optimised for a maximum power of 33 dBm and the second PA for a maximum power of 30 dBm. If efficiency was maintained for the first PA and if no additional losses occurred, the total peak power consumption would remain equal to a single carrier device. However, the peak power consumption of dual-carrier is still considerably higher than the peak power consumption of single carrier, since the first PA cannot be optimised for dual-carrier and there are considerable losses from the extra isolation and TX filtering (as explained in subclause 7.7.7.1).

7.7.7.3 Results

This subclause summarizes the results from the dynamic network simulations. The throughput is given as net session throughput per user, which means that only the times when the mobile has had a TBF or it has been in the TBF establishment procedure are included.

7.7.7.3.1 Coverage limited network

The results from the coverage limited simulations (BCCH/hopping deployment scenario) are shown in figure 66.
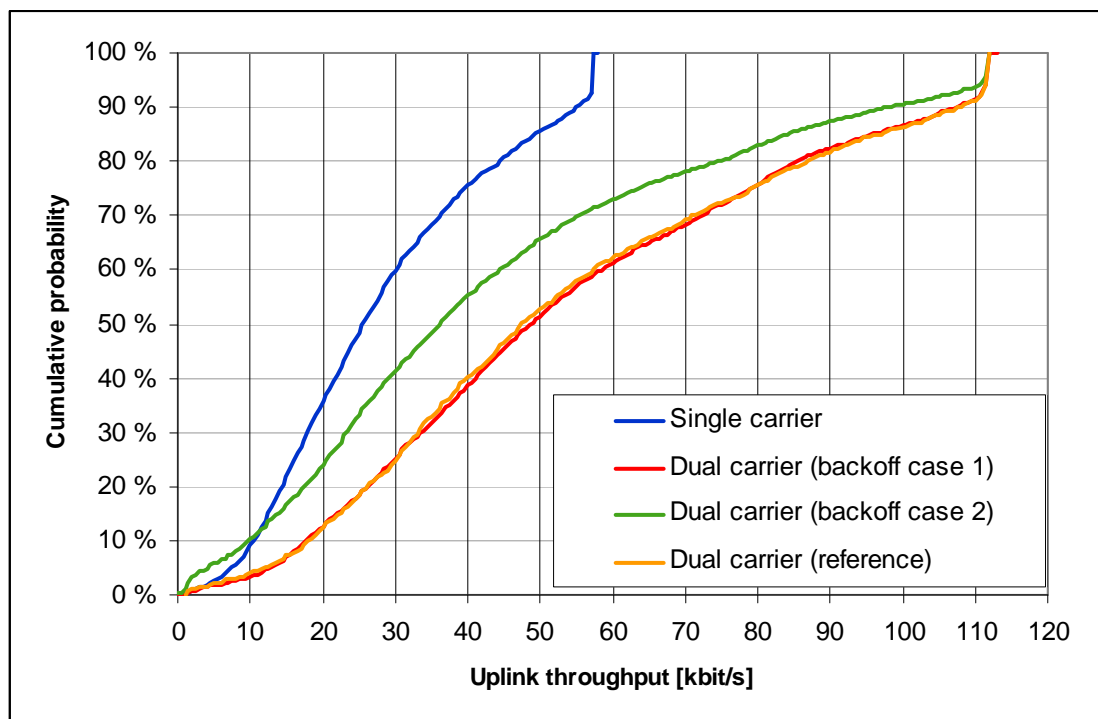
Figure 66: Dual-carrier UL performance in the coverage limited network

As can be seen from the results, there is no performance loss due to the GMSK backoff. This is due to the fact that in this scenario only a small fraction of the radio blocks were transmitted with the GMSK modulation.

In contrast, there is a significant performance loss due to the 8PSK backoff. This degradation is a direct consequence from the 3 dB loss in the link budget for 8PSK modulated blocks. It is important to note that nearly all radio blocks were transmitted at the full power, hence implying that nearly all 8PSK blocks were experiencing a 3 dB performance loss compared to the single carrier transmission. As can be seen from the figure, the effective doubling of the multislot-class is not able to compensate this loss at the cell border, where the dual-carrier does not give any gain over single-carrier. At the cell median, the dual-carrier gives 38 % gain compared to the single-carrier.

The throughput gains are summarized in table 30.

Table 30: Throughput gain of the simulated backoff scenarios

	Single carrier	Dual carrier		
		Reference	Case 1	Case 2
Cell border (10 percentile)	10 kbit/s	+80 %	+80 %	+0 %
Cell median (50 percentile)	26 kbit/s	+88 %	+81 %	+38 %
Peak TP (90 percentile)	55 kbit/s	+96 %	+96 %	+78 %

7.7.7.3.2 Interference limited network

The results from the interference limited simulations (hopping/hopping deployment scenario) are shown in figure 67.
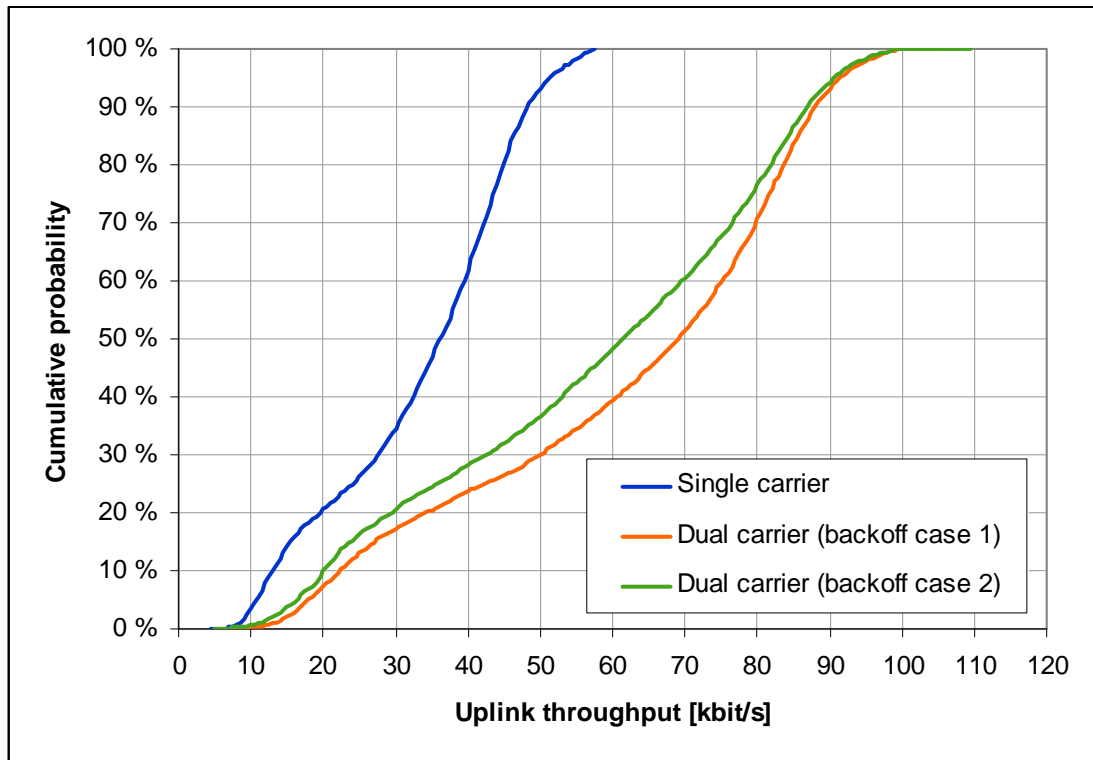
Figure 67: Dual-carrier UL performance in the interference limited network

As can be seen, the impact of the additional backoff is less severe in an interference-limited environment. This is largely due to the fact that the maximum power levels are less frequently used, and because the higher transmit power increases the interference levels, hence mitigating the gain from the lower backoff.

Dual-carrier has a negative impact on the speech capacity, since part of the PS interference is moved to the hopping layer. In the simulated network, the proportion of bad quality speech calls increased from 3.1 % to 5.6 % when dual-carrier was deployed. Note that this impact might not be applicable to balanced networks employing downlink dual carrier.

7.7.8 Modified Concept for Dual Carrier in the Uplink

7.7.8.1 Introduction

It is stated in subclause 7.7.6.2 that additional TX filtering is required in the TX paths of the mobile station to counteract the generation of 3rd order intermodulation products, falling into the RX band. This filter is estimated to have at least a 37 dB RX band rejection, which is judged difficult for a small MS. In this subclause we investigate solutions to mitigate this implementation issue.

7.7.8.2 Modified Concept

In order to avoid such interference injection into RX band of the mobile station, the dual carrier in UL concept is modified below.

In fact most relevant are 3rd order intermodulation products of the form $2*f_1 - f_2$ and $2*f_2 - f_1$ as well as 5th order intermodulation products of the form $3*f_1 - 2*f_2$ and $3*f_2 - 2*f_1$. These are generated assuming that the signal is sent on carrier frequency f_1 to antenna 1 and on carrier frequency f_2 to antenna 2 and that reverse intermodulation due to insufficient antenna isolation occurs. In subclause 7.7.6.2 it is shown that in order to prevent that 3rd order intermodulation products causing spurious emissions fall into the RX band, the transmitter needs to implement additional TX filtering providing a further insertion loss of 2 dB to 4 dB. Hence if additional TX filtering in the MS shall be avoided, it must be ensured, that these 3rd order intermodulation products lie outside the RX band. This is illustrated in figure 68 for two different scenarios.
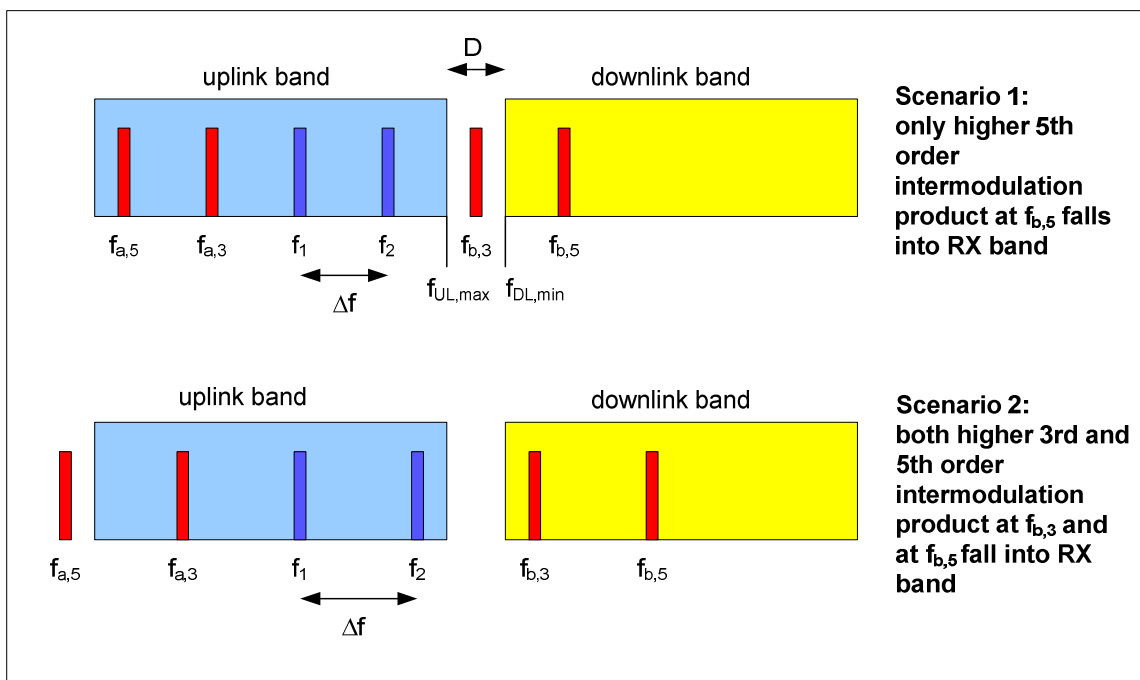
**Figure 68: 3rd order and 5th order intermodulation products
for uplink carrier frequencies f_1 and f_2 for different frequency spans Δf**

Assuming that $f_2 = f_1 + \Delta f$ with $\Delta f > 0$, then 3rd order intermodulation products are generated at;

-   $f_{a,3} = f_1 - \Delta f$; and

-   $f_{b,3} = f_2 + \Delta f$;

as well as 5th order intermodulation products are generated at:

-   $f_{a,5} = f_1 - 2*\Delta f$; and

-   $f_{b,5} = f_2 + 2*\Delta f$.

In the following it is assumed that 3rd order intermodulation products are dominating and that it is sufficient to avoid that these fall into the RX band. This assumption needs to be proven by measurements (see subclause 7.7.8.4).

The receive band of the mobile is always at higher frequencies than the transmit band, hence the 3rd order intermodulation product at $f_{b,3}$ is of interest here.

If the condition is satisfied that:

-   $f_{b,3} < f_{DL,min}$;

-   i.e: $\Delta f < f_{DL,min} - f_2$;

with f_2 being the highest carrier frequency in an assigned mobile allocation, then no 3rd order intermodulation product is generated in the receive band and consequently no additional TX filtering in the mobile station is required.

This means that the frequency span Δf of the mobile allocation is dependent on the lower band edge of the corresponding downlink and the highest frequency in the mobile allocation. Thus it cannot surmount the guard band D in case the highest carrier frequency $f_{UL,max}$ is part of the mobile allocation. Else if the highest carrier frequency is lower it can surmount D.

Two implementation options are considered here:

1. In order to decrease complexity the allowable frequency span Δf of the mobile allocation may be fixed per GSM band and is defined to be equivalent to the guard band D.

2. The allowable frequency span Δf of the mobile allocation is 20 MHz where possible. This means, if the highest frequency in mobile allocation is lower than $f_{DL,min}$ - 20 MHz, a frequency span up to 20 MHz can be chosen, else the frequency span is equivalent to the guard band D.

Table 31 provides an overview of the guard band D and the allowable frequency span Δf of the mobile allocation for option 1 and option 2 for various (not all) GSM bands. Note that the given figures are valid for geographical regions where this band is allowed for operation, not related to individual systems. For instance in the 900 MHz band the requirement for a system using P-GSM frequencies in an E-GSM environment are given under E-GSM here.

Table 31: Guard band D and allowable frequency span Δf for mobile allocations for various GSM bands for option 1 and option 2 - K identifies a reduction factor

GSM band	450	480	710	750	850	P-GSM 900	E-GSM 900	R-GSM 900	DCS 1800	PCS 1900
D [MHz]	2.8	2.8	12.0	15.0	20.0	20.0	10.0	6.0	20.0	20.0
Option 1: Δf [MHz]	2.8 - K	2.8 - K	12.0 - K	15.0 - K	20.0 - K	20.0 - K	10.0 - K	6.0 - K	20.0 - K	20.0 - K
Option 2: Δf [MHz]	2.8 - K	2.8 - K	12.0 - K	15.0 - K	20.0 - K	20.0 - K	10.0 - K or 20.0 - K	6.0 - K or 20.0 - K	20.0 - K	20.0 - K

Thus for the main bands GSM 850, P-GSM 900, E-GSM 900, R-GSM 900, DCS 1800 and PCS 1900 allowable frequency spans of 20.0 MHz are possible. Note that a reduction factor K is added to avoid that a 3rd order intermodulation product just falls onto the lowest downlink channel. It is assumed that this factor is FFS and is equal for all GSM bands.

The reduced frequency span of the mobile allocation is not seen as a major performance restriction for operation of dual carrier in the UL. Only in case of E-GSM 900 and R-GSM 900 a reduction of the frequency span of mobile allocations close to the upper band edge is expected, as well as in general for GSM 450, GSM 480, GSM 710 and GSM 750.

7.7.8.3   Intermodulation measurements

In this subclause, measurements related to the most relevant impact from 3rd order and 5th order intermodulation products due to dual carrier implementation are presented.

Note that IM products due to near-far scenarios have not been considered.

7.7.8.3.1   Measurement setup

All the measurements are made with an EDGE mobile station module. Three different setups shown below are used for the measurements. The interference signal is generated using a separate signal generator. At this point a continuous wave signal is used to simulate the interference signal from the other antenna. An isolator is used to shield the signal generator from the output of the EDGE module. The insertion loss of the isolator and the power divider were taken into account while measuring the levels of intermodulation products. The spectrum analyser is always shielded from the carrier using a notch filter at the carrier frequency and in order not to exceed the dynamic range of the spectrum analyser an additional 6 dB attenuator is used and the insertion losses of these devices were also taken into account while measuring the intermodulation products.

Common spectrum analyser settings

- VBW = 100 kHz.

- RBW = 100 kHz.

- Span= 925MHz-960 MHz.

- Averaging over 50 Bursts.

Setup 1: Used to measure only IM3

Isolator — Signal Generator SMIQ f = 880.2 MHz CW signal

EDGE MS 914.8 MHz → Power Divider 6 dB → 6 dB Attenuator → Notch at fc = 914.8 MHz → Spectrum Analyser
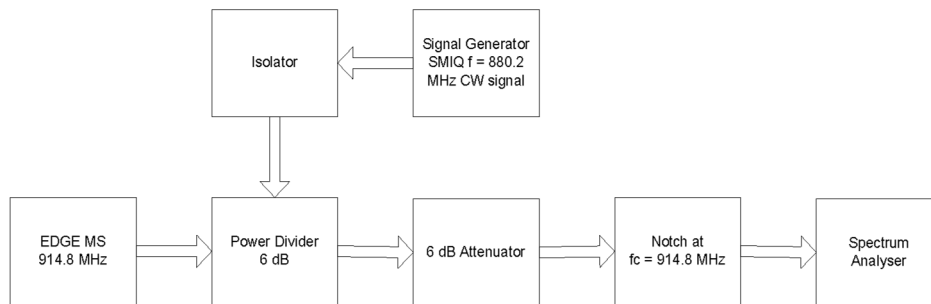
Setup 2 Used to measure IM3 and IM5

Isolator — Signal Generator SMIQ f = 903 MHz CW signal

EDGE MS 880.2 MHz → Power Divider 6 dB → 6 dB Attenuator → Notch at fc - 880.2 MHz → Spectrum Analyser
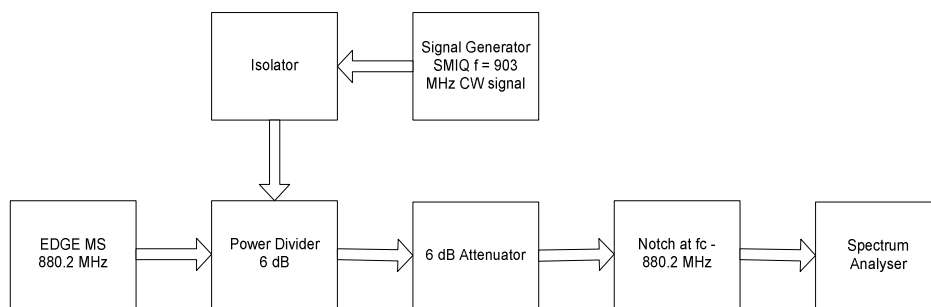
Setup 3 Used to measure IM3 and IM5

Isolator — Signal Generator SMIQ f = 880.2 MHz CW signal

EDGE MS 903 MHz → Power Divider 6 dB → 6 dB Attenuator → Notch at fc - 903 MHz → Spectrum Analyser
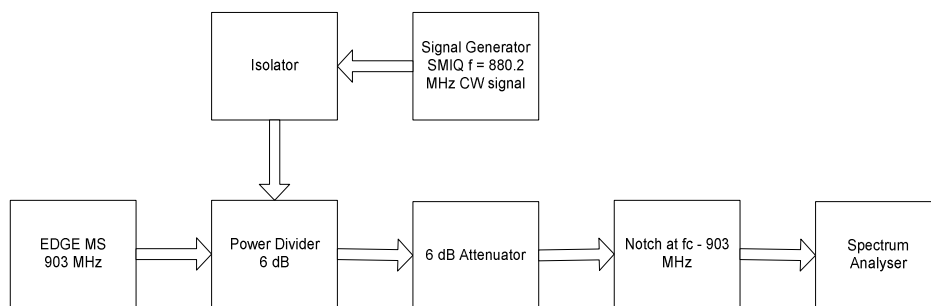
The intermodulation products of 3rd (IM3) and 5th (IM5) order are of special interest here since they have high amplitudes. Note that the carrier frequencies selected for the signal (f1 - for the EDGE Module) and the interferer (f_2 - SMIQ signal generator) are not consistent with the modified approach described in subclause 7.7.8. Hence some intermodulation products fall in downlink band. However, the idea here is to simply measure the levels of various intermodulation products. Hence, though IM3 falls in the downlink band in this case, the restrictions applicable for the emissions in uplink band (i.e. up to -36 dBm allowed see 3GPP TS 45.005) are used here and it is assumed that during practical deployment, the frequency span between the uplink carriers is chosen as stated in subclause 7.7.8 thus avoiding IM3 falling into downlink band. However it is expected that IM5 could fall in the downlink band in this case and hence IM5 measurement results are compared with the limit for the GSM900 downlink band (i.e. up to -79 dBm allowed, see 3GPP TS 45.005).

7.7.8.3.2 Analysis of IM3 measurements

The measurements shown in figure 69 are made using setup 1. IM3 occurs at:

$$2 \times 914.8 - 880.2 = 949.4 \text{ MHz}$$

SoftPlot Measurement Presentation

Interferer=-10dBm Interferer=0dBm Interferer=10dBm Interferer=off

Interferer=-30dBm

1	949.408818 MHz
∇	-83.3348 dBm
2	Interferer=-30dBm
∇	949.408818 MHz
	-56.3588 dBm
3	Interferer=-10dBm
∇	949.408818 MHz
	-35.9945 dBm
4	Interferer=0dBm
∇	949.408818 MHz
	-25.6376 dBm
5	Interferer=10dBm
∇	949.408818 MHz
	-17.1392 dBm

Start: 925.000000 MHz   Stop: 960.000000 MHz
Res BW: 100 kHz   Vid BW: 100 kHz   Sweep: 72 ms
17.02.2006 10:26:33   FSEA 30

Figure 69: Measurements for IM3 in GMSK mode - f1 at 32 dBm - Setup 1

It can be seen from the figure that in order to satisfy the requirement for the IM3 falling in uplink band (i.e. < -36 dBm), the power of the interferer should be lower than -10dBm. Assuming the interferer power also to be 32 dBm, a total isolation of 32 dBm - (-10 dBm) = 42 dB is necessary. Assuming that an isolation of around 12 dB is possible with separate TX antennas (see Option B in subclause 7.7.6.2), a further 30 dB isolation is necessary and hence two cascaded isolators are expected to be necessary for this purpose. (Each isolator is assumed to provide around 15 dB isolation, see figure 70). However, if the maximum GMSK output power in an uplink dual carrier configuration is reduced to 29 dBm (see subclause 7.7.6.2 or [3]), less isolation would be sufficient.
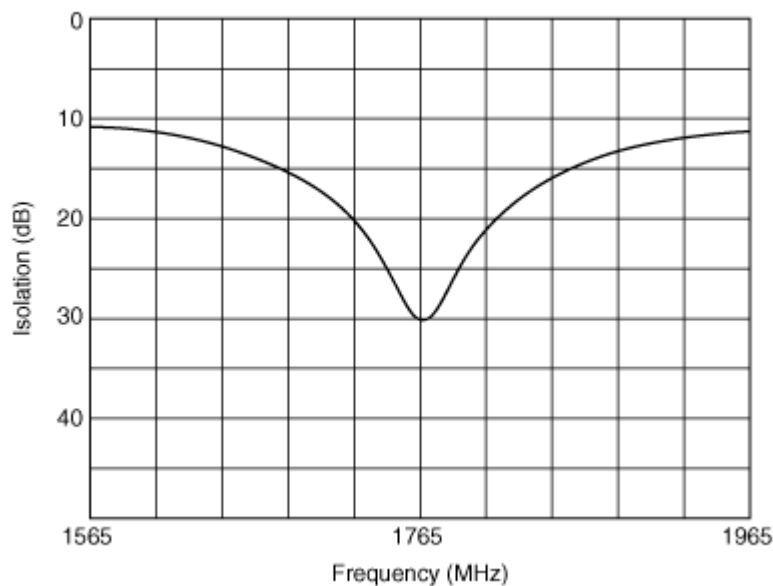
Figure 70: Example isolator characteristics (Source: MURATA - Part no: CES301G76CCB000)

Similar measurements are made also for 8PSK with the carrier signal (f1) at 27 dBm. The results are shown in figure 71.

SoftPlot Measurement Presentation

Interferer=off   Interferer=-30dBm Interferer=-10dBm Interferer=-0dBm

Interferer=10dBm

1	949.408818 MHz
▽	-84.8606 dBm
2	Interferer=-30dBm
▽	949.408818 MHz
	-51.8288 dBm
3	Interferer=-10dBm
▽	949.408818 MHz
	-30.8497 dBm
4	Interferer=-0dBm
▽	949.408818 MHz
	-22.3512 dBm
5	Interferer=10dBm
▽	949.408818 MHz
	-11.9989 dBm

Start: 925.000000 MHz   Stop: 960.000000 MHz
Res BW: 100 kHz   Vid BW: 100 kHz   Sweep: 72 ms
17.02.2006 10:40:53   FSEA 30

Figure 71: Measurements for IM3 in 8-PSK mode - f1 at 27 dBm - Setup 1

It can be seen that for the interferer level at -10dBm, the generated IM3 is approximately -31dBm. Hence it is expected that a reverse intermodulation level from the interferer up to -15 dBm could be tolerated (giving an IM3 of -36 dBm which is the limit). Assuming maximum power for the interferer frequency (f2) i.e. 27 dBm, again the required isolation could be calculated as above: 27 dBm - (-15dBm) = 42 dB. This again requires 2 isolators in cascade as highlighted above.

Thus it is expected that a total of 2 isolators are necessary to satisfy the current GSM uplink band requirements from the IM3 perspective.

7.7.8.3.3   Analysis of IM5 measurements

IM5 is investigated with both setup 2 and setup 3.
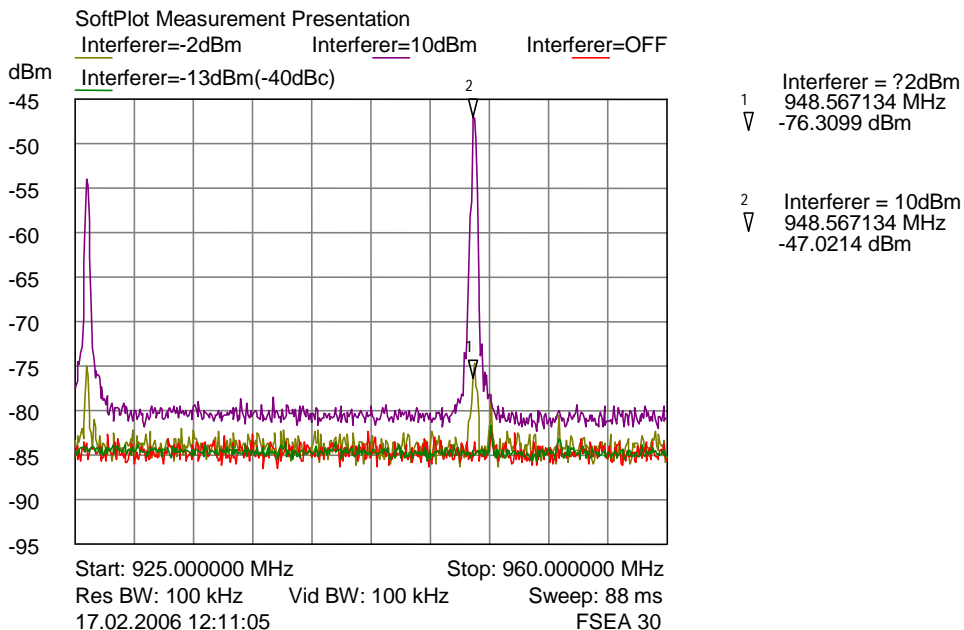
Figure 72: IM5 Measurements for 8-PSK 27 dBm mode - Setup 2

For IM5, it is assumed that a level of up to -79 dBm is allowed (downlink band requirements). Since at approximately -2 dBm interferer level there is an IM5 of approximately -76 dBm, we can assume that up to -3 dBm for the level of interferer is acceptable.
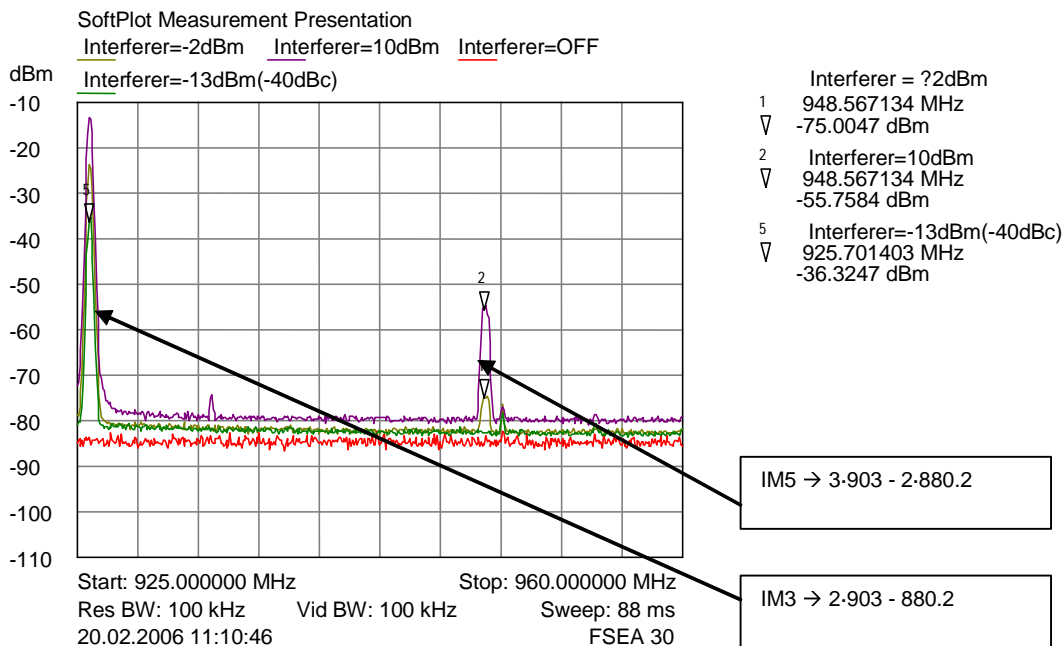
Figure 73: IM5 Measurements for 8-PSK 27 dBm mode - Setup 3

Figure 73 shows for setup 3 (frequencies of EDGE MS and signal generator are swapped compared with figure 72) that the IM5 product in the downlink band is slightly higher in this case, requiring the interferer level to be < -4 dBm. This means that it is necessary to have an isolation of 27 dBm - (-4 dBm) = 31 dB. Clearly IM5 is less critical than IM3 and hence the two isolators used to avoid too high IM3 levels are expected to provide sufficient isolation for IM5 requirements in the downlink band as well.

7.7.8.3.4 Analysis of IM2

There were concerns that there could be some impact of IM2 products from GSM900 band falling into the DCS1800 downlink band. Hence the impact of IM2 was also investigated. Setup 3 is reused for this purpose. Figure 74 shows the measurement results.
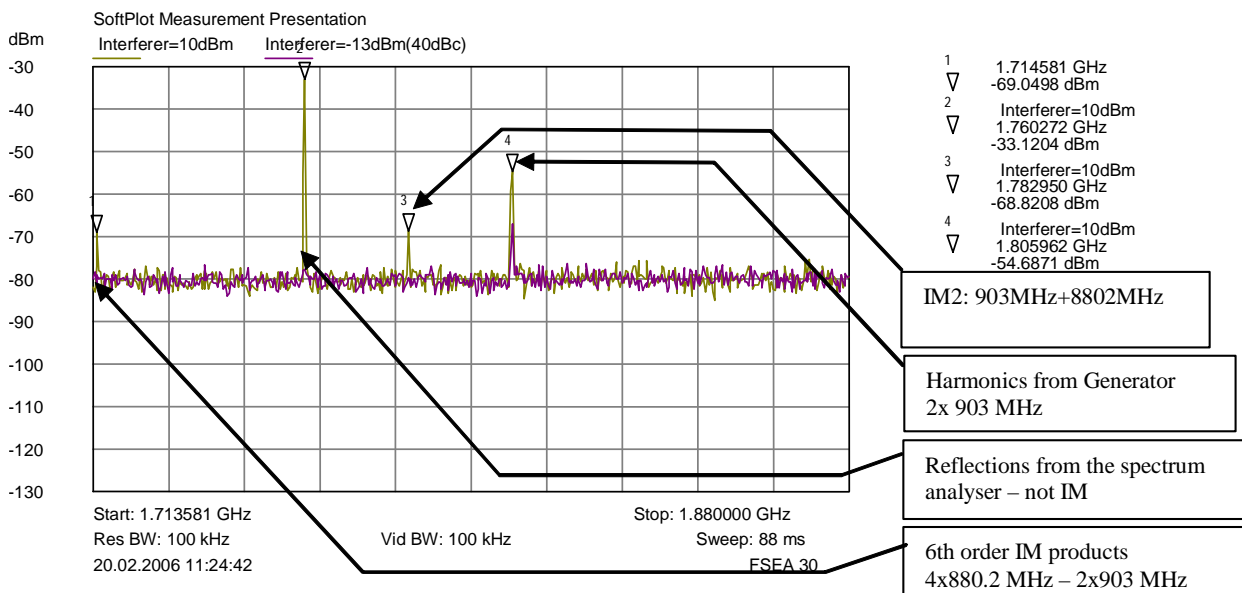
Figure 74: IM2 measurement for 8-PSK 27 dBm mode - Setup 3

At an interferer level of 10 dBm, an IM2 product (903 MHz + 880.2 MHz) was found at -69 dBm. At an interferer level of -13 dBm, this IM2 product has disappeared in the noise floor (-80 dBm). Thus it can be seen that IM2 is not critical.

7.7.8.4 Dual carrier architecture with minimal single-carrier operation impact

7.7.8.4.1 Introduction

In subclause 7.7.8.4, measurement results for uplink dual carrier were shown and it has been shown that to satisfy the requirements for emissions in TX and RX bands two isolators are needed in series in the TX paths of an uplink dual carrier mobile with two PAs. In this subclause, a possible architecture for the new dual carrier mobile stations is shown with an option to bypass the isolators in one TX path when in single carrier mode, thereby minimizing the impact on the talk time in single carrier mode.

7.7.8.4.2 TX architecture

Figure 75 shows the proposed TX architecture of the dual carrier mobile.
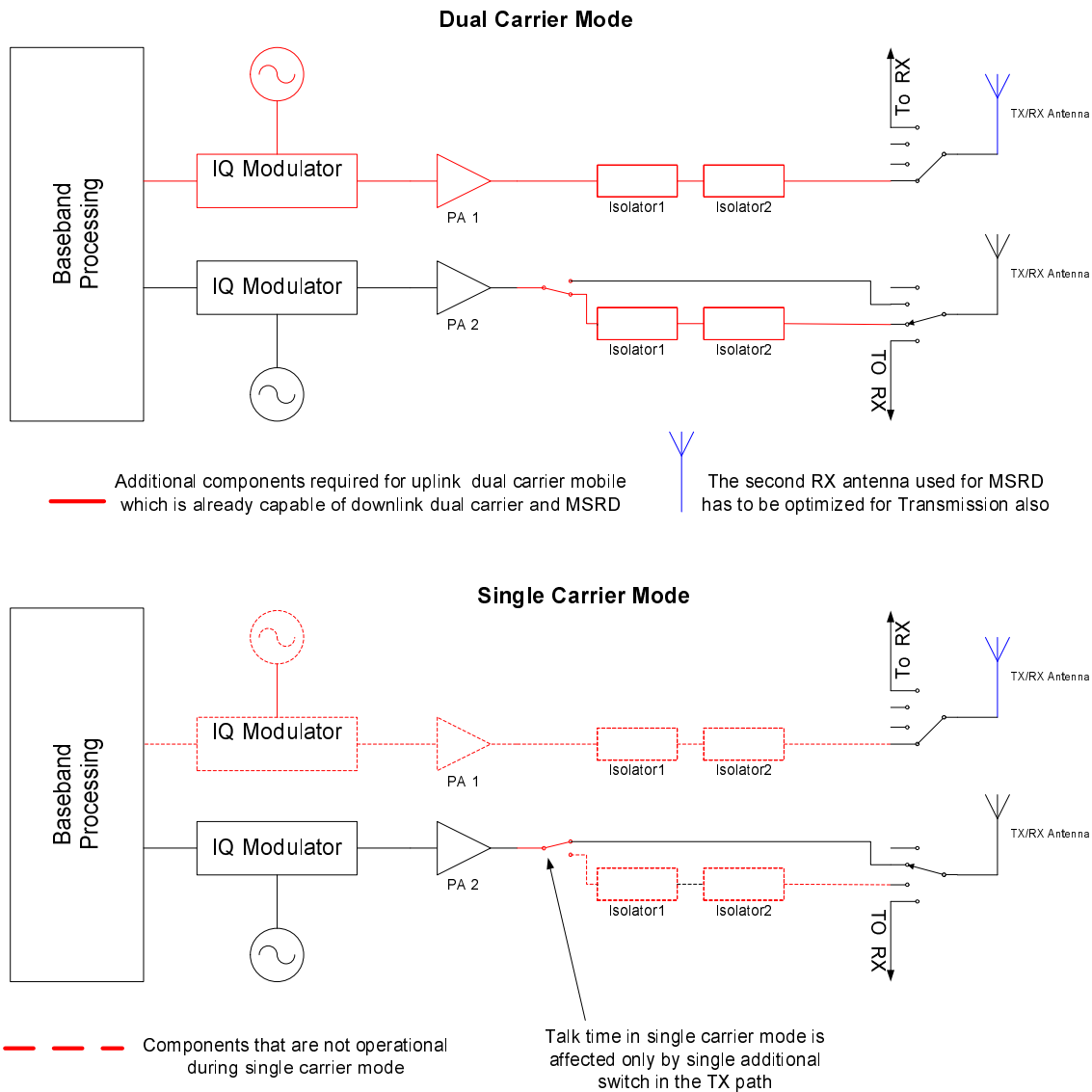
Figure 75: Architecture of uplink dual carrier mobile

Note that only a single band is shown in the above figure for the sake of simplicity. Additional switch positions at the antenna switchplexer could be used for inputs/outputs of other bands. This diagram shows transmitters using direct modulators, but a polar architecture is possible too.

As can be seen, the isolators in the lower TX path could be bypassed during single carrier mode using a switch. It is expected that the insertion loss of such a switch is in the order of 0.5 dB. As the switch is the only additional component present in the TX path, reduction in talk time because of the switch is expected to be only around 10 % which is reasonably low.

If having two TX antennas is of concern and TX power of the MS in dual carrier mode is not critical, a design with only one TX antenna can be used. In this case, the signals are combined after the isolators and before the TX antenna which would introduce a combiner loss around 3dB in dual carrier mode. The combiner could also be bypassed together with the isolators in a similar way as shown in figure 75 and the talk time in single carrier mode will be the same as for the design shown in figure 75.

7.7.8.4.3   Throughput in coverage limited scenario

In this subclause the median uplink throughput (at received signal level of -98 dBm) as a function of the number of uplink time slots is compared for single carrier EGPRS and dual carrier EGPRS mobiles. For this purpose, the link level throughput curves shown in [8] are used.

It is assumed that the mobile station follows a multi slot power reduction according to MULTISLOT_POWER_PROFILE 3 (see 3GPP TS 45.005).

From figure 75, it can be seen that the total insertion loss during dual carrier mode is not same in the two TX paths. This is because in the upper TX path, dedicated for uplink dual carrier, there is no additional switch. Hence, assuming that each isolator has an insertion loss around 0.8 dB and that the switch has an insertion loss of 0.5 dB, it is possible to conclude the following:

- Insertion loss in the upper TX path, used only during dual carrier mode = 0.8 + 0.8 = 1.6 dB (path 1).

- Insertion loss in the lower TX path, reused for single carrier mode = 0.5 + 0.8 + 0.8 = 2.1 dB (path 2).

It should be noted that the output power reduction caused by the insertion losses is inside the allowed tolerance for 8-PSK (±3 dB in low band). Hence the nominal output power of 27 dBm in low band can still apply.

The following formulae based on 3GPP TS 45.005 are used according to MULTISLOT_POWER_PROFILE 3 to calculate the actual output power depending on the number of timeslots and the respective insertion loss:

- Output power for normal EGPRS = min (27, [27 + 6 - 10*log10(#Timeslots)]) dBm.

- Output power for the TX path1 = min (27 - 1.6, [27 + 6 - 10*log10(#Timeslots)]) dBm.

- Output power for the TX path2 = min (27 - 2.1, [27 + 6 - 10*log10(#Timeslots)]) dBm.

The throughput as a function of the number of used timeslots is shown in figure 76.
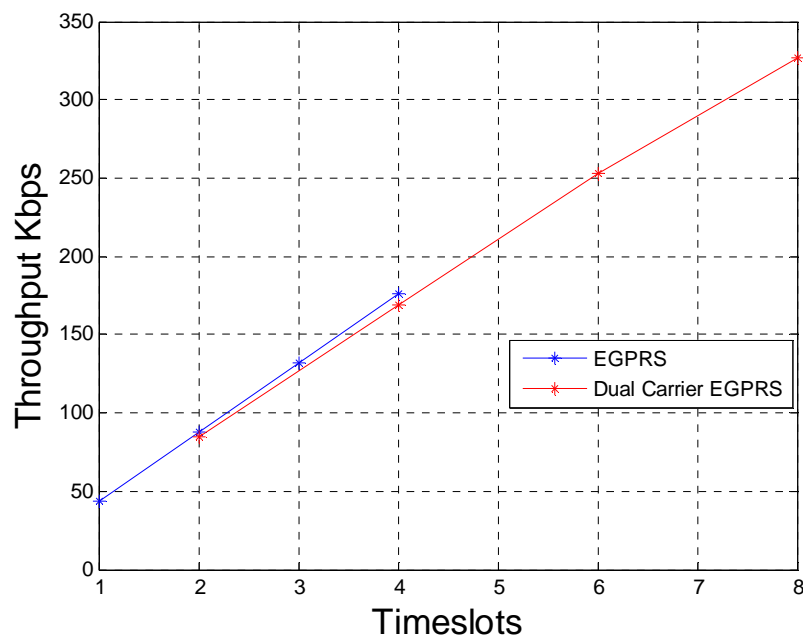
Figure 76: Throughput of dual carrier and single carrier EGPRS mobiles as a function of the number of uplink timeslots under coverage limited conditions

The proposed architecture for an uplink dual carrier mobile provides almost normal talk time in single carrier mode.

It can be seen that even under coverage limited conditions, very high uplink throughputs can be achieved, and at the same number of uplink slots, the throughput is almost as high as with a single carrier EGPRS MS.

In this subclause, the assumption has been made that the antenna imbalance is zero. However, this is considered to be very optimistic; in particular, it may not be economically feasible to build a mobile with very low antenna imbalance.

7.7.9 Discussion on Uplink Coverage

7.7.9.1 Introduction

In this subclause coverage aspects for some uplink proposals are discussed. Coverage analysis includes multislot power reduction with different multislot profiles and also impact of insertion losses e.g. due to duplexers and isolators. Analyzed proposals include DSR, MDSR, UL DC with independent carriers, modified UL DC with constrained frequency separation and Type-2 MS. 16QAM combined with turbo coding were not included, because no coverage gain at median is shown so far. UL DC with wideband transmitter was also excluded, because output power constraints due to IMD [12] will likely make this option unviable for coverage improvements.

It should be noted that both capacity and coverage should be improved in a balance, since performance in real networks is limited by both of them and typically worst of them.

7.7.9.2 Assumptions for power reductions and power consumption

Multi slot power reduction was taken into account by applying multi slot profiles (0 and 3) for all the cases. For 8PSK modulation in the case of EGPRS and DSR 4 dB power reduction was applied related to GMSK [9]. For MDSR 16QAM 6 dB power reduction was applied at highest power level and 4 dB for other levels [10].

The uplink dual carrier has 5 dB lower output power related to EGPRS due to IMD constraints [11] and [12]. The modified UL DC has 2 dB lower power related to EGPRS. Multi slot power profiles were applied for UL DC so that actual number of transmitted slots was divided by 2, although this leads to double power consumption related to single carrier transmission. 3 dB duplexer loss was assumed for Type-2 MS. Transmitter output powers versus number of time slots are shown in figures 77 and 78.
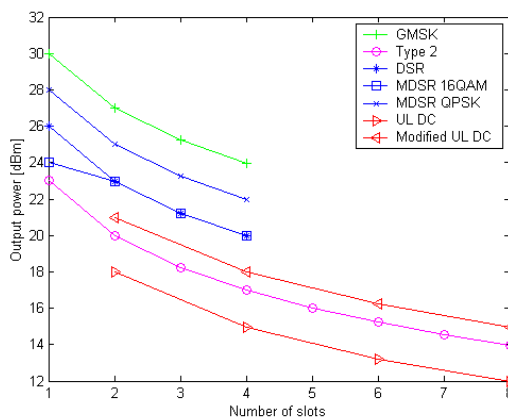
Figure 77: TX power with multislot profile 0
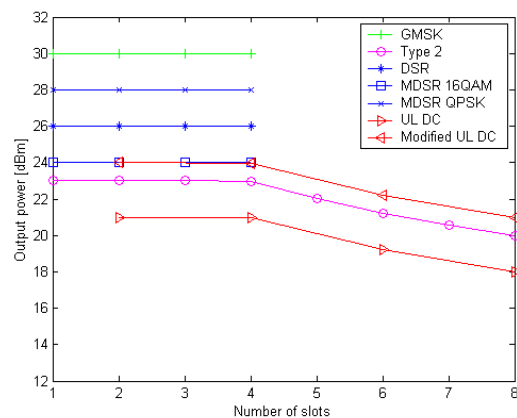
Figure 78: TX power with multislot profile 3

7.7.9.3 Receiver and Network model

The BTS receiver and network model was as in [10]. Median RX level under interest was -98 dBm and RX level at cell border was -108 dBm.
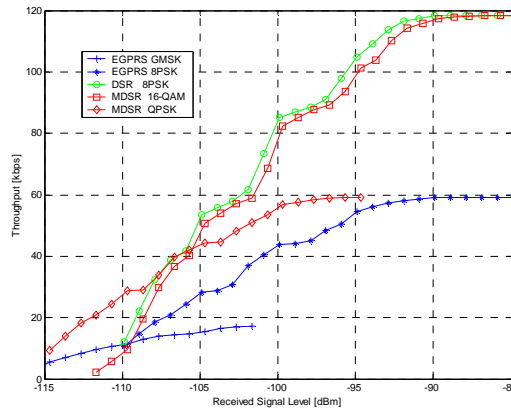
Figure 79: Throughput versus received signal level, TU3iFH, NF=5dB

7.7.9.4 Results

7.7.9.4.1 Cell border

Figures 80 and 81 show throughput versus timeslots at cell border for multislot profile 0 and 3 respectively.

MDSR seems to outperform other schemes at cell border.

Type-2 MS with multislot profile 3 would need 6 or more slots to exceed throughput obtained by EGPRS already with 4 slots.

Dual carrier seems not to provide any gain at cell border.
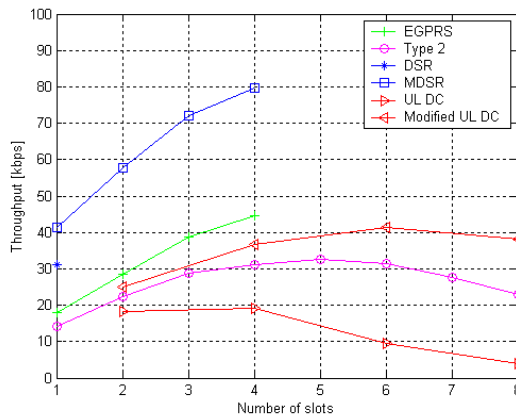
Figure 80: Throughput at cell border (-108 dBm) with multislot profile 0
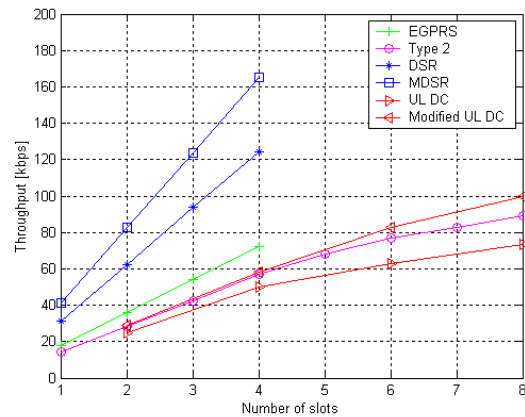
Figure 81: Throughput at cell border (-108 dBm) with multislot profile 3

7.7.9.4.2 Median coverage

Figures 82 and 83 show median uplink throughput versus number of time slots used for multislot profile 0 and 3 respectively.
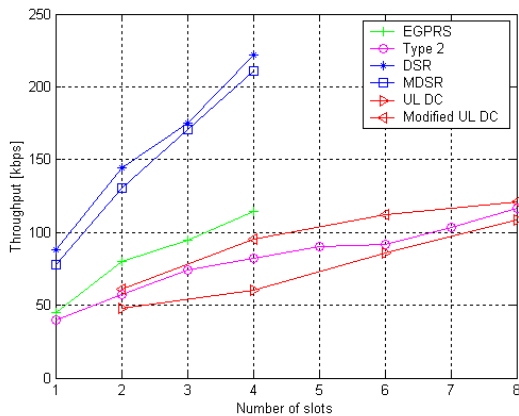
Figure 82: Median throughput (-98 dBm) with multislot profile 0
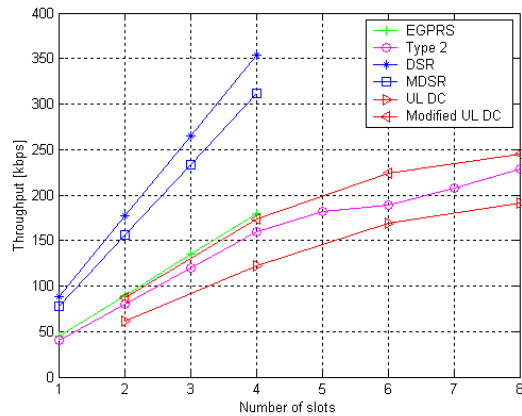
Figure 83: Median throughput (-98 dBm) with multislot profile 3

Figures 84 and 85 show median uplink throughput gain related to EGPRS with 4 slots versus number of time slots used for multislot profile 0 and 3 respectively.
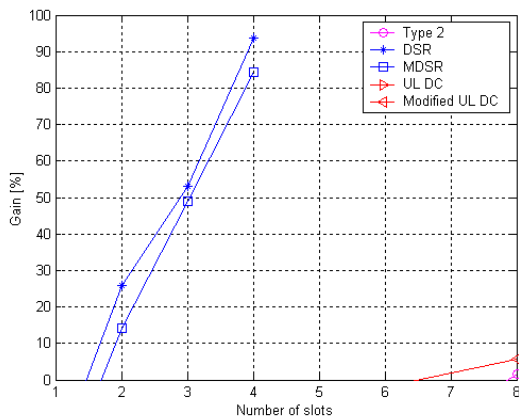
Figure 84: Median coverage gain related to EGPRS with 4 slots with multislot profile 0
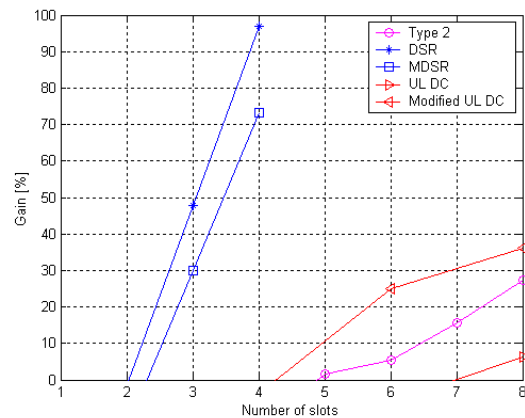
Figure 85: Median coverage gain related to EGPRS with 4 slots with multislot profile 3

7.7.10   Improvements for DTM and MBMS

This subclause highlights the additional gains for MBMS and DTM in terms of added flexibility for resource allocation and additional downlink throughput that can be obtained if mobile stations support dual carrier on the uplink.

7.7.10.1   Assumptions

The following assumptions are made about the dual carrier technology applicable to the MS:

-    The MS cannot transmit and receive in the same slot.

-    The MS can receive on both carriers on a given timeslot. (Dual Carrier in the downlink).

-    The MS cannot transmit on any carrier on the slot immediately following a slot it is receiving on (due to the timing advance).

-    The MS can receive on both receivers in a slot immediately after transmitting.

-    Only one Tx->Rx and one Rx->Tx transition is allowed in a TDMA frame per radio transceiver.

- Frequency Hopping is used.

- CS traffic takes up one DL+UL TS pair.

7.7.10.2   Gains for DTM Multislot Capacity

With dual carrier only in the downlink, it is shown in [7] that the maximum capacity for a downlink biased DTM call is 10 TSs for reception and up to 2 TSs for transmission (with sum = 12). For an uplink biased allocation the corresponding figures are shown to be up to 4 TSs for reception and 5 TSs for transmission (with Sum = 9).
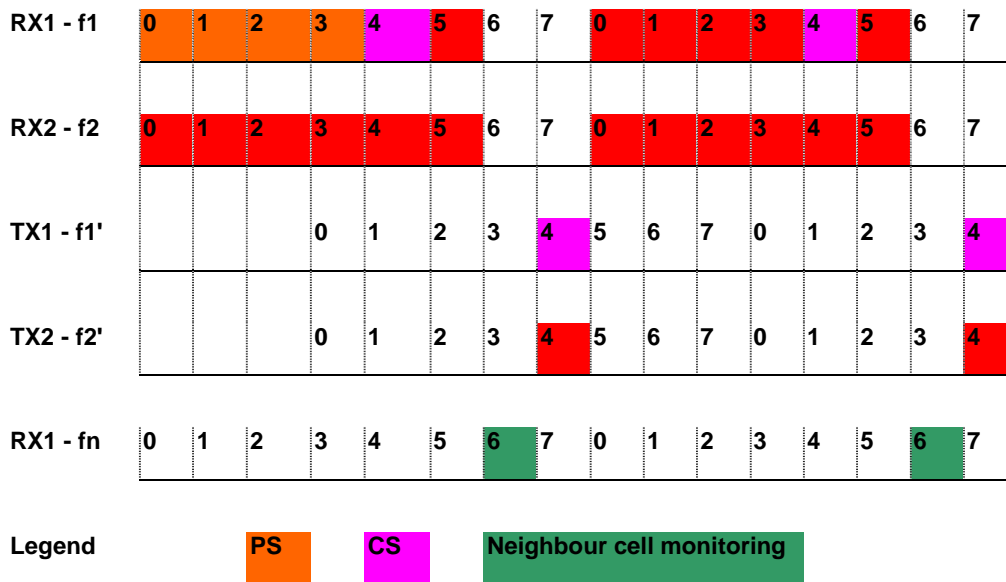
Figure 86: DL DTM DC Mobile Multislot Capability (DC in UL and DL)

With dual carrier transmission on the uplink it is possible to receive on 12 downlink TSs and transmit on 2 uplink TSs as shown in figure 86 (Sum = 14) as the uplink PS TS can be provided in parallel with the uplink CS timeslot.

Similarly, for uplink biased asymmetric allocation, it is shown in [7] that it is possible to receive on as many as 4 TSs and transmit on up to 10 TSs (Sum = 14).

In addition to gains for downlink throughput, there is also added flexibility in resource allocation for the BSS. For a given number of DL or UL TSs, the BSS can choose to allocate the required resources in a flexible way, as it now has the option to allocate resources on two downlink and two uplink carriers. There is an additional benefit that the unit of allocation now could be smaller on each carrier. For instance, if 6 uplink time slots are needed for a service, then it can be distributed among the two uplink carriers in many ways (3+3 or 4+2, etc.). As described in subclause 7.7.10.3, this avoids the need for any resource re-allocation during call setup thus reducing the signalling load on the BSS.

7.7.10.3   CS Connection setup while in packet transfer mode

According to the existing Rel-6 DTM behaviour, if the network wishes to establish an SDCCH for CS connection set-up before allocating a TCH, the likelihood is that the existing packet resources will first have to be moved to be next to an SDCCH, and then moved again when a TCH is required for speech. This involves two resource re-allocations which is inefficient in terms of radio resource management and increases processing and signalling load for the BSS.

Figure 87 shows how an SDCCH can be allocated on the second carrier pair (on any free frequency) without disturbing existing packet resources on the first carrier pair. The example shows 2 DL TSs and one UL TS allocated to packet resources on the first carrier pair (f1, f3). The second carrier pair can be changed by the network to select an appropriate TCH without disturbing the existing PS resources.
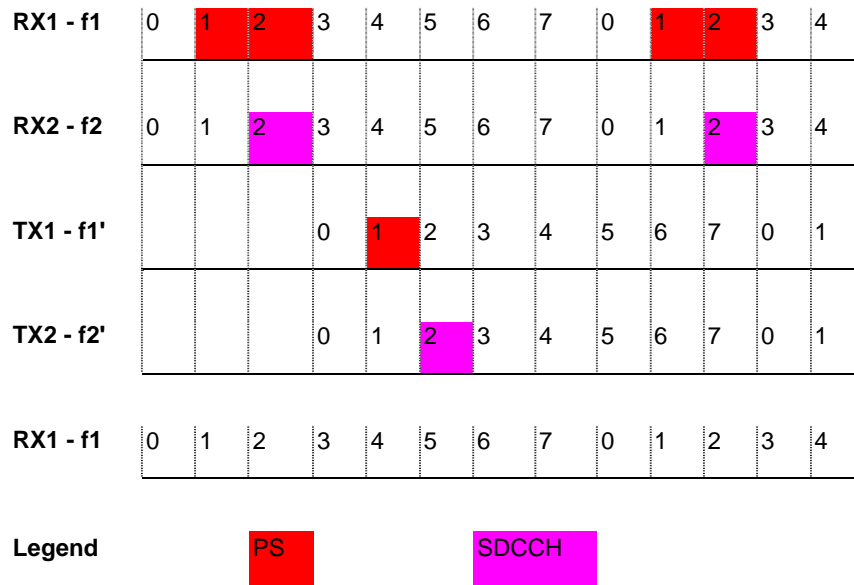
Figure 87: Allocation of SDCCH on Second Carrier Pair

7.7.10.4 Gains for MBMS + CS

Increased capabilities of Mobile stations like dual carrier in DL/UL etc may in the future allow users to receive MBMS and CS calls simultaneously. Currently, it is not possible to support a CS call for any mobile which is already receiving the MBMS session with feedback if the mobile is not capable of transmitting or receiving on dual carrier.

If the mobile is capable of receiving on two carriers, then it is possible to allow 1 mobile in the cell to have a CS call in parallel with the MBMS session as shown in figure 88. This requires that PBCCH is deployed and has the same hopping sequence as the MBMS carrier. It can be seen that in figure 88, the frequency pairing for uplink and downlink has to be violated either for the MBMS session or for the CS call.
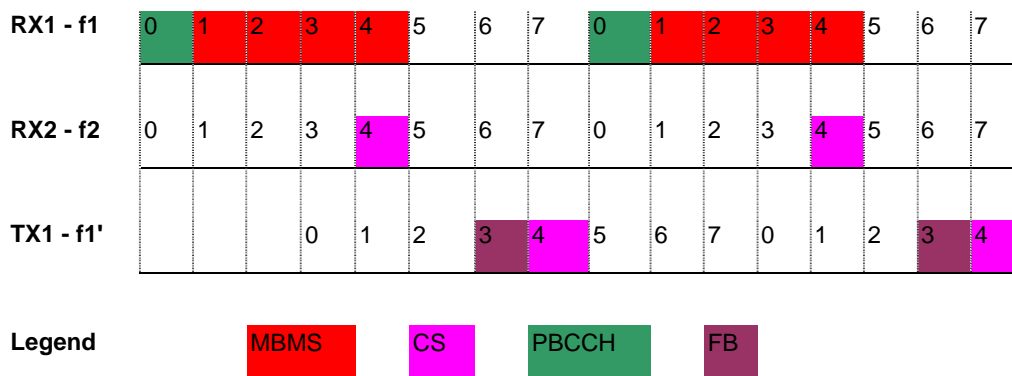
Figure 88: MBMS session with parallel CS calls - Dual Carrier DL only

With dual carrier on the uplink however, it is possible to support up to 2 mobiles per non-MBMS carrier in the cell to receive the MBMS session with feedback and have a parallel CS call. Moreover, there is no problem with correspondence of the uplink and downlink CS time slots with this arrangement as shown in figure 89.
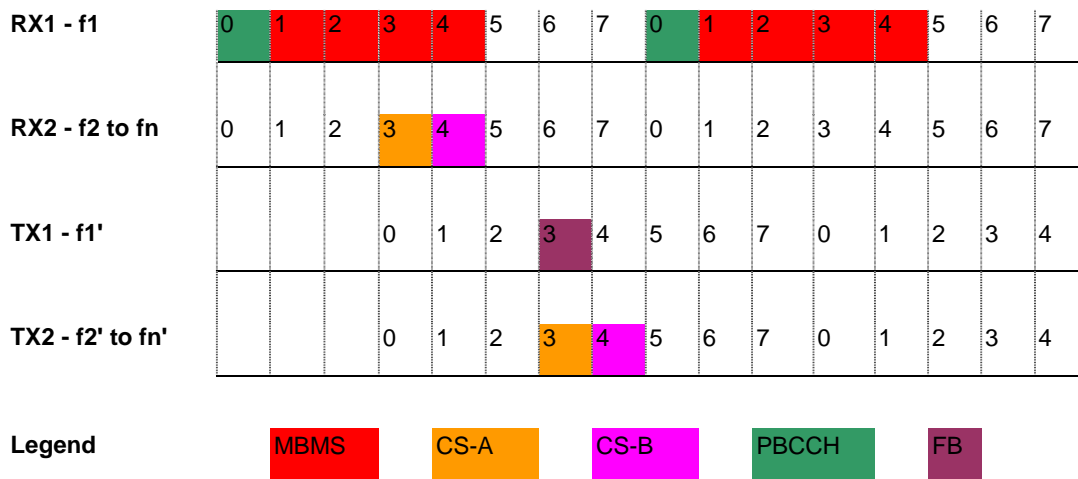
Figure 89: MBMS session with parallel CS calls Dual Carrier UL and DL

7.7.11 Performance enhancing features

7.7.11.1 Intercarrier Interleaving

7.7.11.1.1 Introduction

Diagonal intercarrier interleaving can be used to gain additional frequency diversity for dual carrier transmission on the uplink (see clause 10 on the use of intercarrier interleaving for reducing latency). This concept is likely not applicable as-it-is on the downlink because, downlink is a shared channel and old and new mobiles shall be multiplexed on the same shared channel on the downlink and hence, the header (and in particular the Uplink State Flag (USF)) can not be interleaved across the carriers because of interworking requirements with legacy mobiles. Hence to extend the concept to downlink it might be necessary to leave the header and the USF bits as-they-are now and perhaps interleave only the data across the carriers.

On the uplink, diagonal interleaving across two carriers is used for this purpose. The header and the payload data are interleaved across the two carriers. The interleaving scheme used is based on existing block rectangular interleaving defined for MCS schemes with a different burst mapping to achieve the diagonal interleaving across two carriers on the uplink. The interleaved blocks are redistributed across the two carriers on the uplink as shown in figure 90.
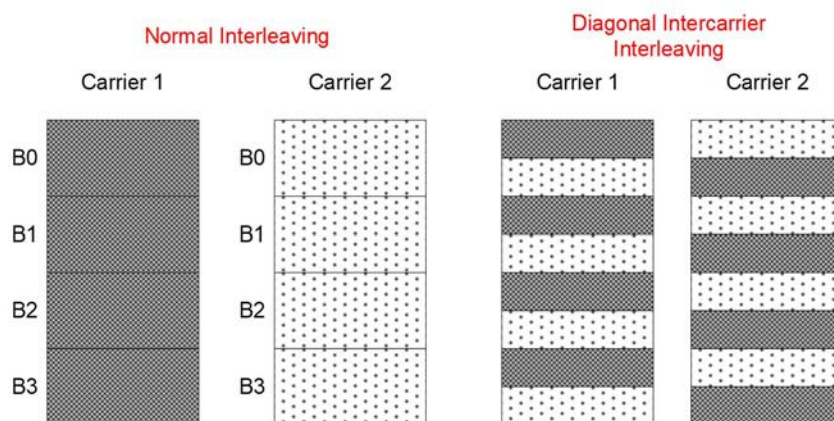
Figure 90: Inter-carrier interleaving modes

7.7.11.1.2   Link level gains by intercarrier interleaving

7.7.11.1.2.1   Used Simulation Parameters

Simulations are performed for TU50 channel model for receiver sensitivity case. Initial simulations show the performance comparison for MCS-5 and MCS-6 with and without intercarrier interleaving. Both ideal frequency hopping and no frequency hopping cases are simulated.

7.7.11.1.2.2   Impairments

Transmitter and receiver impairments have not been included in the currently presented set of simulation results.

7.7.11.1.2.3   Simulation Results

The results presented here are only for the sensitivity limited scenarios as the sensitivity limited scenarios are of main concern when applying dual carrier on the uplink as there is a reduced power transmission on the uplink.

It can be observed in figure 91 for a non frequency hopping channel and in figure 92 for a frequency hopping channel that gains of around 1 dB (for 10 % BLER) to 2dB (for 1 % BLER) could be obtained by using intercarrier interleaving for uplink dual carrier. Intercarrier interleaving shows high link level gains for lower MCS. The gain will be reduced as the amount of coding reduces with higher MCS. However it is expected that when incremental redundancy is used, even higher MCS schemes will show some gains for subsequent retransmissions.
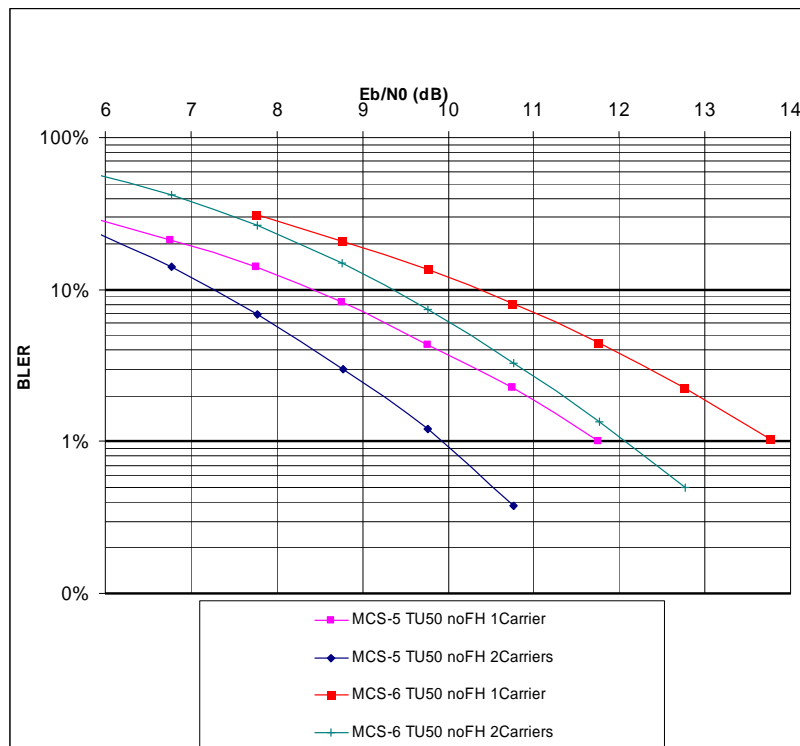
Figure 91: Receiver sensitivity simulation results for various MCS schemes for TU50 channel without Frequency Hopping
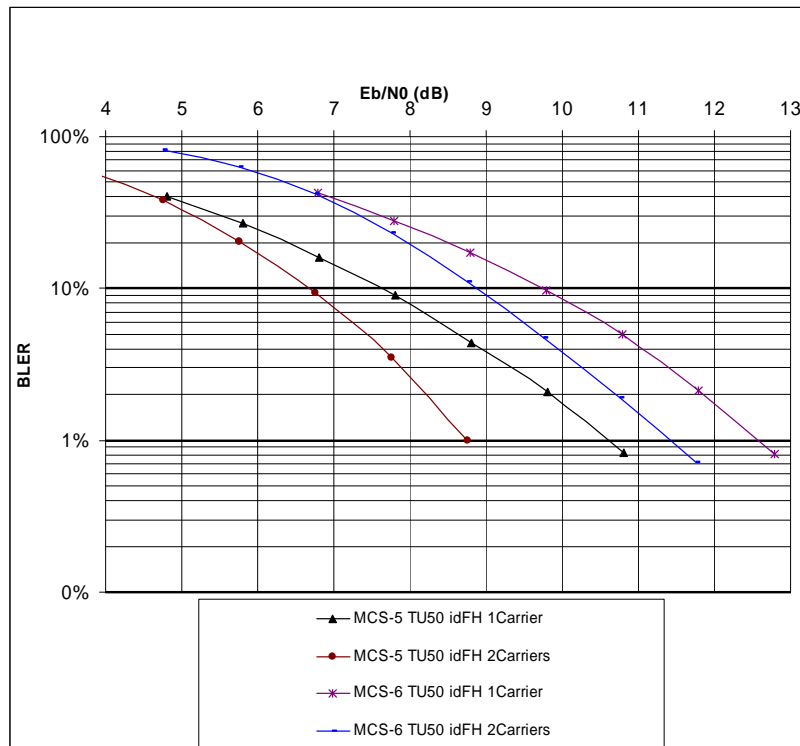
**Figure 92: Receiver sensitivity simulation results for various MCS schemes
for TU50 channel with Frequency Hopping**

7.7.11.2 Advanced Coding Schemes

Advanced coding schemes like turbo coding [5] etc are known to perform better with longer input block lengths. Further link level gains are foreseen with dual carrier transmission on uplink with turbo coding. The idea is to compensate the loss in coverage due to reduced power transmission of the MS using additional link level gains.

Doubled block sizes can be used with dual carrier transmission on the uplink and this, when combined with the additional frequency diversity that can be obtained using intercarrier interleaving, is expected to compensate for the loss in power due to additional backoff at the MS.

7.8 Impacts to the BSS

Multi-carrier is expected to have no impact on EDGE transceivers, but the BSS needs to perform data transfer (possibly including incremental redundancy transmission), resource allocation and link control for more than one carrier.

Dual Carrier in the UL enables maximum reuse of the existing BSS infrastructure, avoiding HW impacts both to the BTS and BSC. Some SW impacts are foreseen due to the need of combining the data streams over both carriers if intercarrier interleaving is used. Incremental redundancy if no intercarrier interleaving is applied will be dedicated to one carrier and hence operate as for the single carrier approach. If intercarrier interleaving is in operation, it is required that the soft decision values of the transmission and retransmission related to a particular RLC block can be exchanged between the transceivers. The complexity increase in the BTS is reduced to combining the data streams of both receivers. A doubled data rate must be supported by Abis as well.

7.9 Impacts to the Core Network

No changes are expected to the core network except that new capabilities shall be signalled by the MS to the network. For DC in the uplink, no further changes to Gb interface are required.

7.10   Radio network planning aspects

7.10.1   Analysis for Option C

7.10.1.1   Introduction

Due to the issues and complexity regarding dual carrier in uplink with two separate transmitters, the use of a wideband transmitter has been proposed in order to simplify the implementation (see subclause 7.7.11.4).

The maximum carrier separation for a wideband transmitter is estimated to be 1 MHz. The impact of this limitation on the legacy frequency planning is described in this subclause.

7.10.1.2   Legacy Frequency Planning

There exists a number of different frequency planning techniques all depending on numerous parameters as e.g. geographical environment, traffic load, frequency hopping etc. In this report we will focus on two main techniques - Fractional Load Planning (FLP) and Multiple Reuse Planning (MRP).

FLP: A FLP network is planned with two or more frequency groups, one for the non-hopping BCCH and one or several for the hopping TCHs. The BCCH is normally planned with a 4/12 or sparser reuse whiles the hopping TCHs normally is planned with a 1/1 or 1/3 reuse.

The available frequency spectrum can either be divided in blocks between the BCCH and the TCHs or it can be evenly spread between them.

MRP: The fundamental idea with MRP is to apply different reuse patterns with different degrees of tightness. MRP uses base-band frequency hopping, which means that the number of transceivers in a cell is equal to the number of assigned frequencies. A benefit with MRP is that the BCCH can be included in the hopping sequence. In figure 93 it is shown how the available frequency spectrum is divided into different frequency groups. The number of frequency groups corresponds to the maximum number of transceivers in a cell.
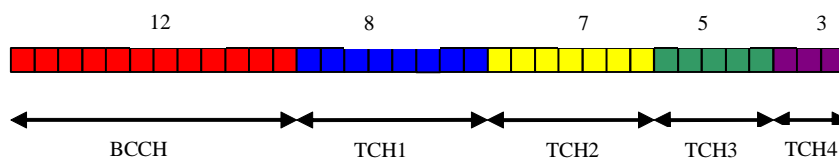
Figure 93: Frequency planning using MRP technique

7.10.1.3   Impact of Wideband transmitter on legacy frequency planning

The maximum carrier separation in a wideband transmitter is e.g. 1 MHz, due to InterModulation (IM) products and the linearization of the PA. From a system point-of-view there is a requirement on the minimum carrier separation in order to ensure a certain quality level in a cell. The minimum carrier separation is 400 kHz (measured from the centre of each carrier), i.e. adjacent frequencies should not be used in the same cell.

One drawback with the limited carrier separation is in the case of inter-carrier interleaving, where a reduced carrier separation will have negative impact on the frequency diversity.

7.10.1.3.1   FLP-1/1 or 1/3

When considering frequency planning for a wideband transmitter there is no difference between the 1/1-frequency reuse or 1/3. Two different cases have been considered for the FLP network: in the first case both carriers are placed in the same TCH hopping group and in the second case one of the carriers is placed on the BCCH.

7.10.1.3.1.1   Both Carriers in the TCH hopping group

In figure 94 a blocked configuration is used and each cell has two transceivers in the TCH hopping group. There are two different Mobile Allocation alternatives, and only alternative 2 is applicable for dual carrier in the uplink with a wideband transmitter.
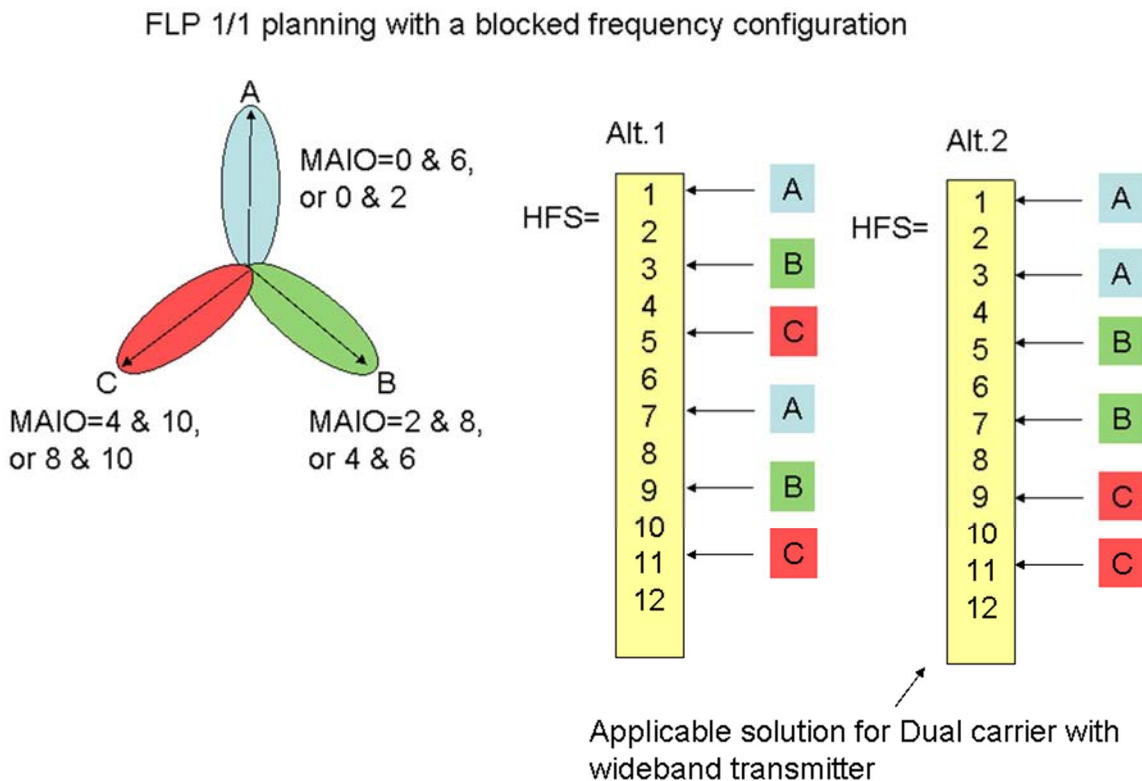
Figure 94: Different Mobile Allocation alternatives in a FLP network

However, also with alternative 2 there will be occasions when the separation between the carriers is too large. For example this will occur when carrier 1 is using ARFCN 12 and carrier 2 is using ARFCN 2 (due to wrap-around). This problem can be avoided if the allocated Hopping Frequency Set (HFS) for one of the two TRXs is slightly modified, see figure 95.
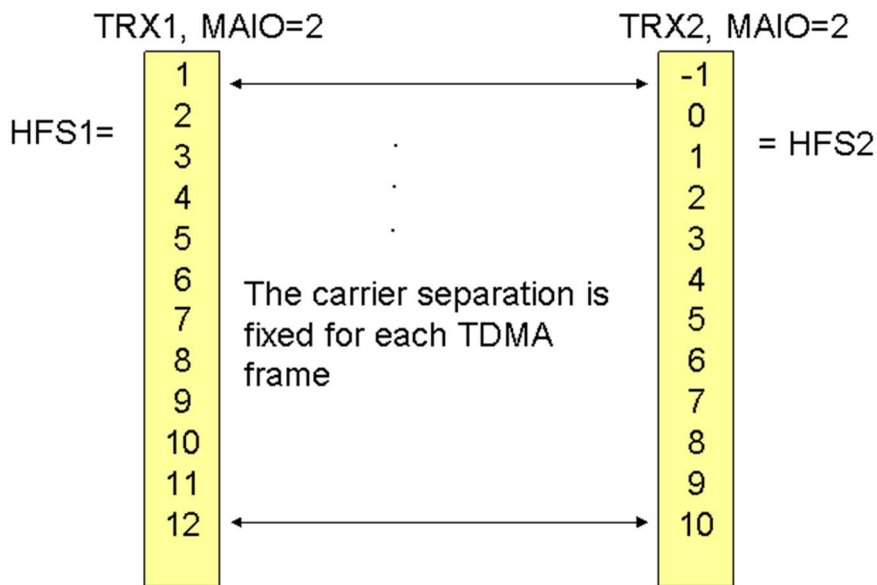
Figure 95: Two different HFS are used in a cell to avoid a too large carrier separation for a dual carrier in uplink configuration

7.10.1.3.1.2   One of the carriers on the BCCH

If the two carriers are separated between the BCCH and the TCH hopping group it will be more or less impossible to fulfil the requirement on the maximum carrier separation. If the requirement is to be fulfilled in this configuration the MS must be able to support a carrier separation that is equal to the total bandwidth of the BCCH and TCH group. In the example in figure 96 the requirement on the maximum carrier separation is 5 MHz.
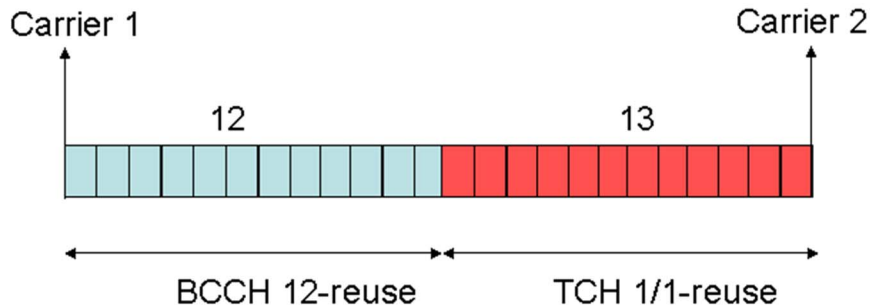
**Figure 96: Maximum carrier separation when the two carriers are placed
in different frequency groups**

If one of the carriers shall be configured on the BCCH there is only one alternative left and that is to allocate a new non-hopping frequency to the cell. This will require a re-planning of the BCCH frequencies and will require that the operator has more frequencies than needed today, otherwise the total capacity in the system will be reduced. An example of this configuration is shown in figure 97.
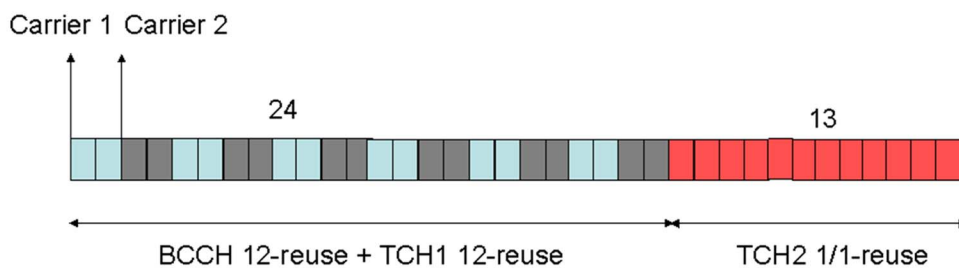
**Figure 97: An extra frequency group with the same reuse as the BCCH has been added
to comply with the requirement on maximum carrier separation**

7.10.1.3.2   MRP

Most MRP networks are including the BCCH frequency in the hopping set, the separation between two carriers in a MRP cell is therefore >> 1 MHz. This makes it impossible to include dual carrier in uplink using a wideband transmitter in a MRP network.

However, if a re-planning of the frequencies is allowed it could be possible to have two non-hopping carriers with the same sparse reuse as the BCCH in a cell. This is the same solution as described at the end of subclause 7.10.1.3.1.2. An example of this solution for an MRP network is presented in figure 98, the same frequency spectrum as in figure 93 is used.
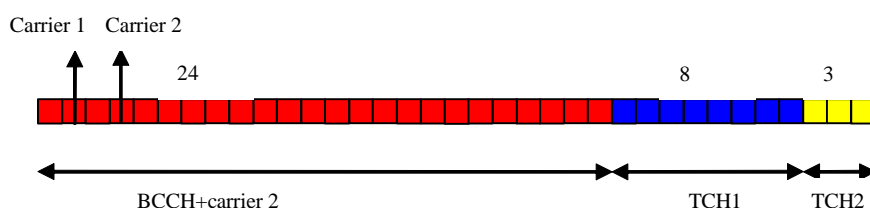
Figure 98: Strict MRP technique planned for dual carrier in uplink

7.10.1.4 Extended frequency allocation

7.10.1.4.1 Introduction

A conclusion from subclause 7.10.1.3 is that in some networks it will be rather tricky to implement dual carrier in uplink using a wideband transmitter without any impact to the legacy frequency planning. A solution that removes this obstacle is therefore investigated in this subclause. Note that some operators do not consider Extended Frequency Allocation described here as feasible due to the high impact on frequency planning.

7.10.1.4.2 Description of Extended Frequency Allocation

The idea with the solution is to temporarily assign an uplink frequency for carrier two that is within the maximum carrier separation to carrier one. This temporarily used frequency does not need to be a frequency that is normally allocated in the cell. This solution will work in all kinds of networks and there is no impact on the legacy frequency planning. However, simulations are needed in order to estimate the impact on the system performance.

Two examples of this solution are shown in figures 99 and 100. In the first example (figure 99) both carriers are allocated in a TCH hopping group and in the second example the carriers are divided between the BCCH and the TCH hopping group.

In figure 99 it is illustrated how this would work in a FLP network when both carriers are placed in the TCH hopping group.
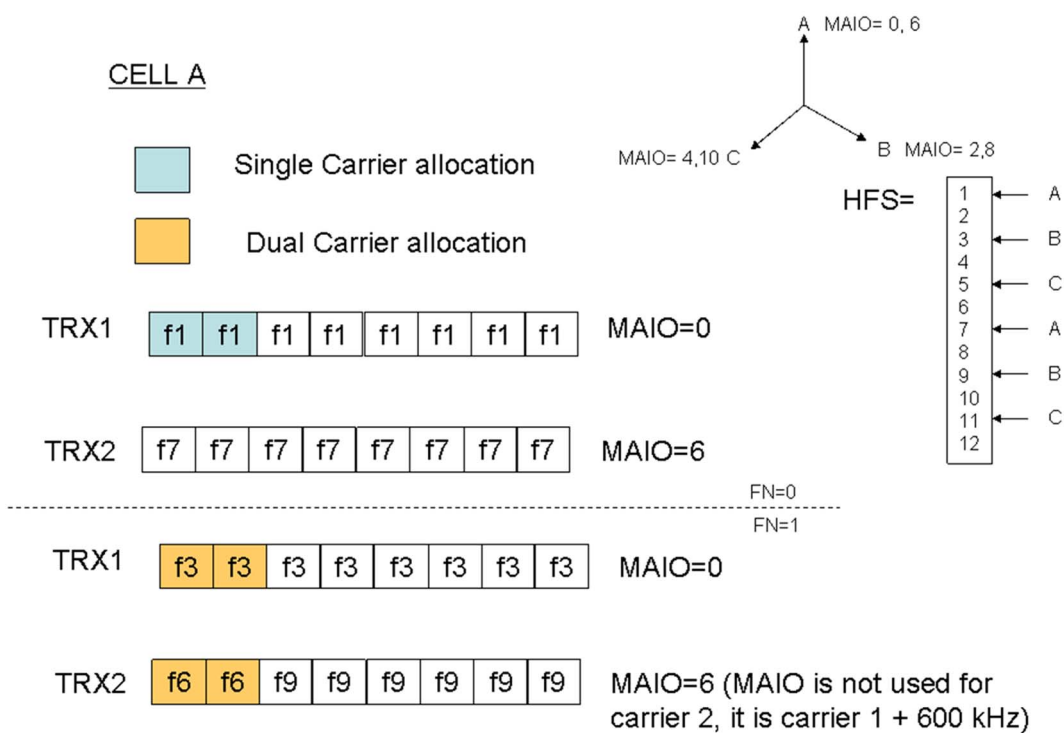
**Figure 99: Dual carrier in uplink using extended frequency allocation
with a carrier separation of 600 kHz**

In figure 100 is the example where the dual carrier is divided between the BCCH and the TCH hopping group.
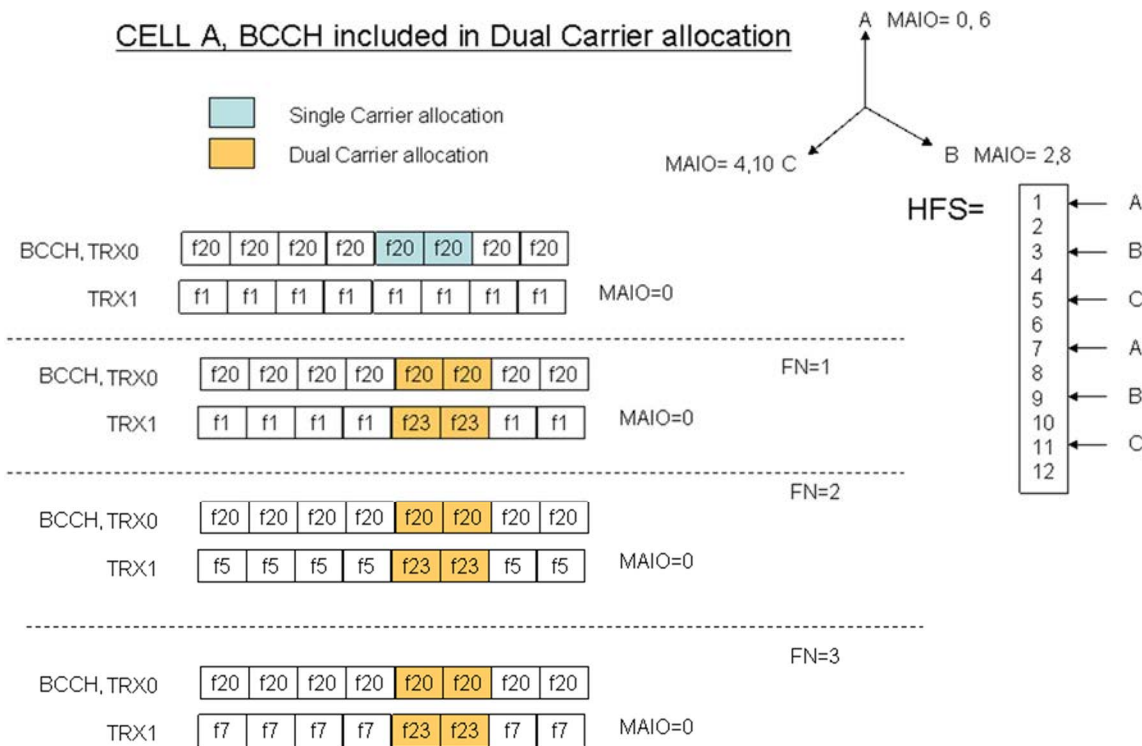
**Figure 100: Dual carrier in uplink using extended frequency allocation
with a carrier separation of 600 kHz**

7.10.1.4.3 Impact of EFA on the BTS

EFA shall only be applied to the timeslots that are used by dual carrier in uplink and the duplex distance can therefore be different between the timeslots within a TRX. The impact of changed duplex distance can be implementation dependent and needs to be investigated by each network vendor. In the Ericsson BTS there is no problem to handle the change of duplex distance as the TX and RX part of a TRX can have different frequency lists allocated. When EFA is used the RX part will receive two different frequency allocation lists, one to use in normal mode and one to use in EFA mode.

In some BTS configurations there are requirements on minimum frequency separation when distributing several frequencies on to the same antenna. This requirement is related to the combiner on the TX side and should therefore not been an issue for EFA. In figure 101 is a diagram over the different filters that are used in the BTS.
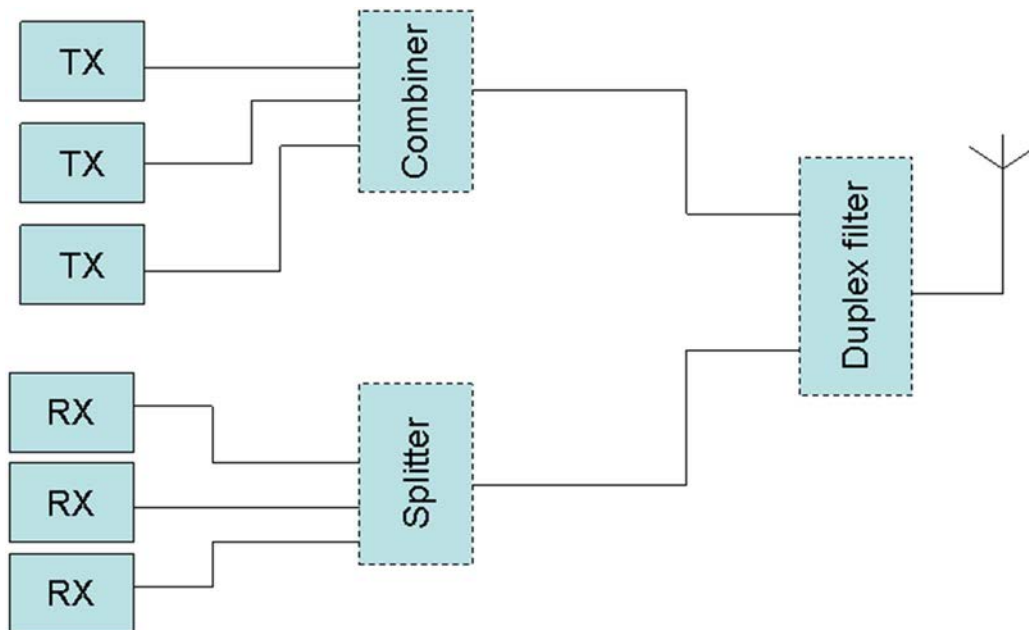
Figure 101: Schematic picture of BTS filters

The splitter on the RX side has no problem to handle adjacent frequencies.

7.10.1.4.2.1 Non-frequency hopping

The use of EFA with a fixed frequency has already been described in subclause 7.10.1.4.2, but in this subclause is an example with EFA in a network with a frequency reuse of 12 presented. Each cell in table 32 has two TRXs with a frequency reuse of 12, but when resources are assigned for dual carrier in uplink this reuse distance is decreased for the uplink. The cells with the same letter belong to the same site. Simulations have been performed to evaluate how large impact this decrease in frequency reuse has on the system performance, results from these simulations are shown in subclause 7.10.1.5.

Table 32: Frequency allocation for dual carrier in uplink, the frequency separation is set to 400 KHz

Cell name:	A1	B1	C1	D1	A2	B2	C2	D2	A3	B3	C3	D3
Frequency TRX 1	1	2	3	4	5	6	7	8	9	10	11	12
Frequency TRX 2	13	14	15	16	17	18	19	20	21	22	23	24
Frequency Dual Carrier TRX 2	3	4	5	6	7	8	9	10	11	12	13	14

7.10.1.4.2.2 Frequency Hopping

It has already been shown in subclause 7.10.1.3 that dual carrier in uplink could work in a network using synthesized frequency hopping and legacy frequency allocation. However, it could be needed to decrease the number of frequencies allocated per TRX in order to avoid the "wrap-around" problem. If this reduction in allocated frequencies is not possible in a network an alternative solution could be to use EFA as described in figure 102.
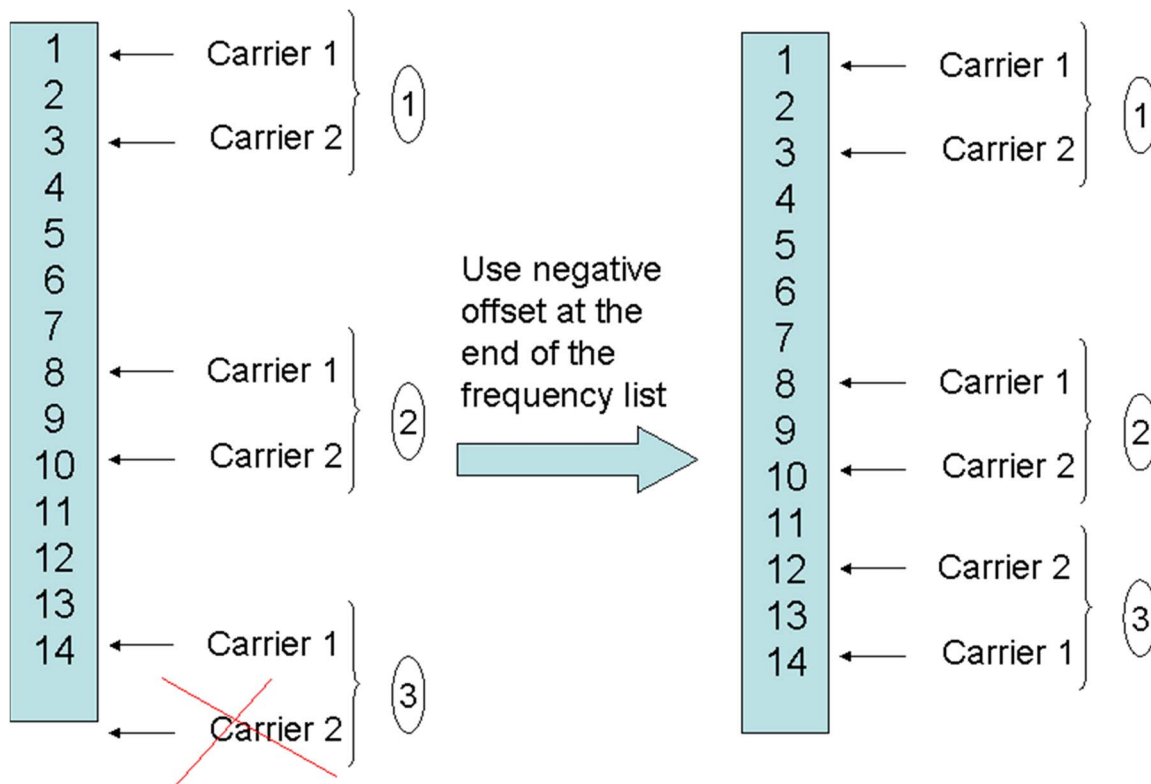
Figure 102: How EFA should work when frequency hopping is used

Both carriers in figure 102 have the same MAIO but carrier two has an additional frequency offset of 400 kHz. The sign of the additional frequency offset for carrier two is changed when a frequency above the highest allocated frequency is to be used. In this way it is ensured that the dual carrier in uplink MS will not use other operators' frequency spectrum.

Baseband hopping:

In figure 103 is the method described in the previous text applied to a baseband frequency hopping cell. The TX part has only one configured frequency at baseband frequency hopping, the different bursts for a connection must therefore be distributed between the different TXs to achieve frequency hopping in the downlink. The RX part of a TRX is only used by the MSs that has been assigned resources on that particular TRX.
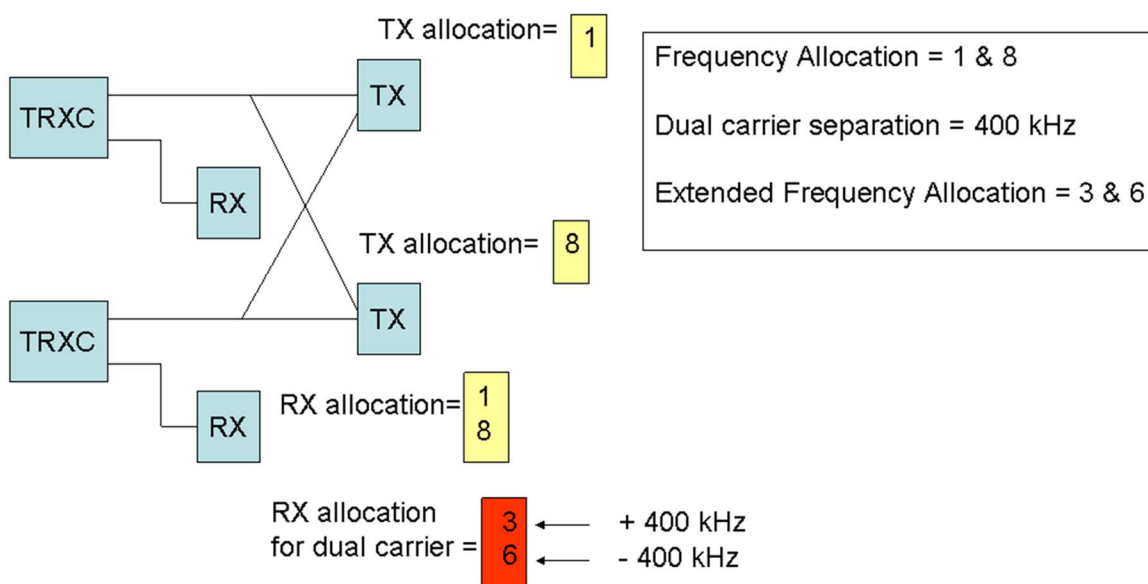
Figure 103: A block diagram for the BTS and frequency allocation for baseband frequency hopping

Synthesized frequency hopping:

In figure 104 EFA is applied to a cell that is configured for synthesized frequency hopping.
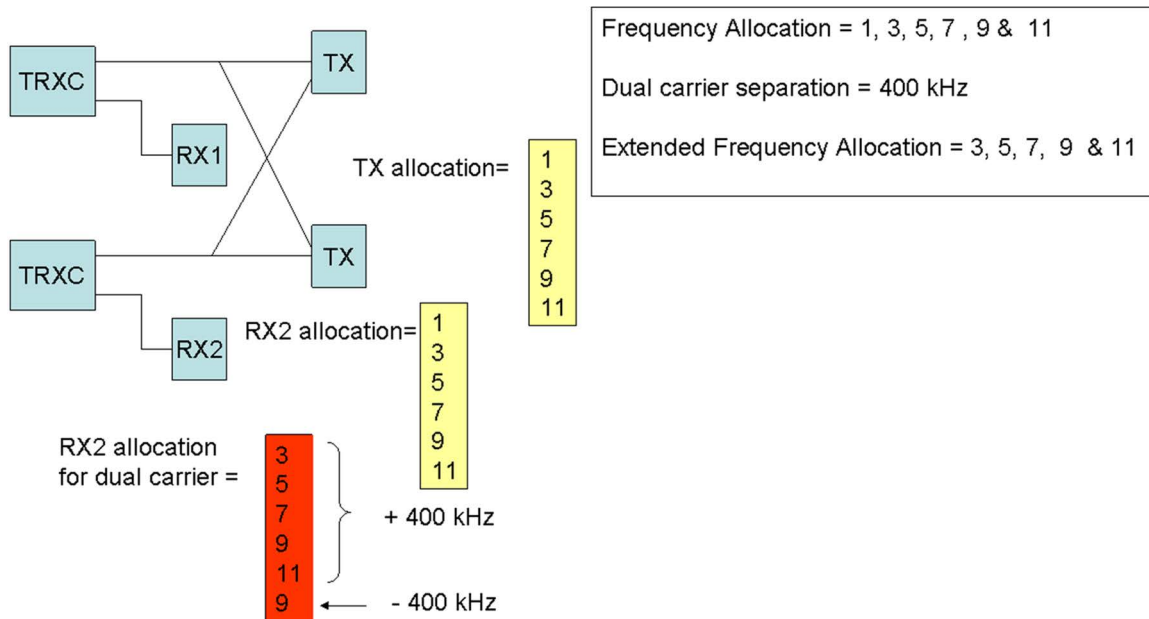
Figure 104: A block diagram for the BTS and frequency allocation for synthesized frequency hopping

All TXs are configured with the same frequencies and is only separated with a MAIO value. The RX part is the same as for baseband frequency hopping.

7.10.1.4.3 Separation of carriers

Different separation between the carriers can be needed in order to avoid co-channel and adjacent channel interference within a site.

7.10.1.5 Evaluation of network performance

7.10.1.5.1 Setup

Simulations have been performed to evaluate the system impact from the introduction of dual carrier in uplink with EFA. The following settings have been used.

Frequency reuse	12
Sectors (cells) per site	3
Number of TCH frequencies	36 (7.2 MHz), not including BCCH
Number of cells simulated	75 + wrap around
IRC	No
Cell radius	500 m
Frequency Hopping	No
Rayleigh fading	Yes
Coherence Bandwidth	1 MHz
Frequency Band	900 MHz
Log-normal fading standard deviation	8 dB
Log-normal fading correlation distance	110 m
Simulation time	200 s
Terminal speed	3 m/s

The service mix was 80 % speech users and 20 % data users, where data users were one of EDGE, or Dual Carrier EDGE, in two different scenarios. Speech and data users were modeled as:

- Speech users: Normal speech users on 1TS, with DTX on and Power control.

- EDGE users: Continuous transmission on 1TS, no Power control and output power 27 dBm.

- Dual Carrier EDGE users: Simply by doubling the EDGE load, i.e. in practice twice as many EDGE users. Output power for dual carrier is 2×21 dBm.

7.10.1.5.2 Results

The results are presented in the form of a CDF of the uplink C/I distribution for the speech users of each case. C/I is averaged over measurement periods of 480 ms.
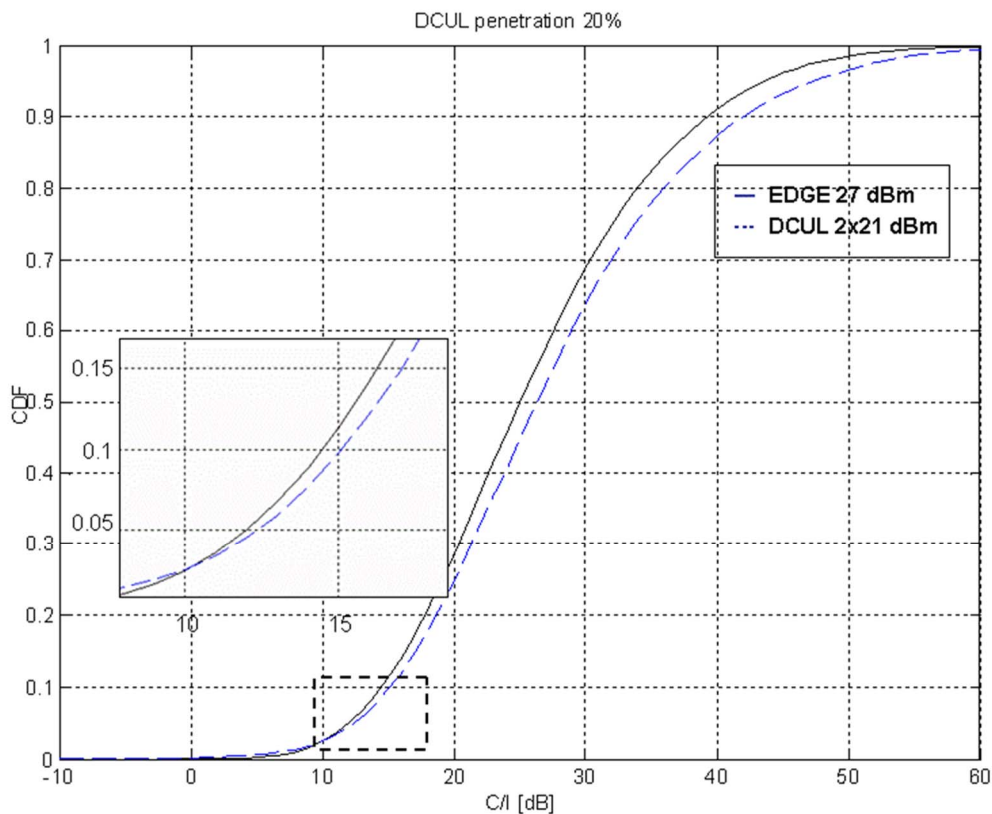
**Figure 105: C/I distribution for speech users in a network with a frequency reuse of 12
The dashed line is for dual carrier in uplink with EFA**

From figure 105 it can be seen that the negative impact of dual carrier in uplink and EFA is very small, and instead an improvement can be seen for almost the whole C/I range. The improvement comes from the reduced output power for dual carrier in uplink and it is the connections that had good quality before that is improved. What it is more important is that the percentage of samples with a C/I below 10 dB has not increased, this indicates that speech quality can be maintained in a network at introduction of dual carrier in uplink with EFA.

7.11 Impacts to the specifications

The impacted 3GPP specifications are listed in 33.

Table 33: Impacted 3GPP specifications

Specification	Description	Comments
43.055	DTM Stage 2	
43.064	GPRS Stage 2	
45.001	Physical layer one radio path; general description	
45.002	Multiplexing and multiple access on the radio path	
45.005	Radio transmission and reception	Possibly new radio requirements if wideband receivers are to be used.
45.008	Radio subsystem link control	
44.060	Radio Link Control / Medium Access Control (RLC/MAC) protocol	
44.018	Radio Resource Control (RRC) protocol	
24.008	Mobile radio interface Layer 3 specification	

It is envisaged that a common RLC/MAC layer (see subclause 7.5.2) would help minimize the impact on existing specifications and would allow enhancements of the existing mechanism for data recovery (ARQ II could be optimized over several carriers).

7.12   References

[1]   Padhye & al. "Modeling TCP Reno Performance: A simple model and its empirical validation" IEEE/ACM Transaction on Networking, vol. 8, no. 2, April 2000.

[2]   AHGEV-020, "Multi-carrier GERAN", 3GPP GERAN-EV Ad Hoc #1.

[3]   GP-052723, "GERAN Evolution - Proposed Text on Dual Carrier in the Uplink for Technical Report", GERAN#27.

[4]   GP-052742, "RF Aspects for dual carrier in UL", GERAN#27.

[5]   GP-052099, "GERAN Evolution - Proposed text on New Coding Schemes for technical report", GERAN #26.

[6]   Oliver Klemp, Oliver Schmitz, Hermann Eul, "Polarization Diversity Analysis of Dual Polarized Log.-Per. Planar Antennas", PIMRC 2005 Conference, 11-14 September 2005, Berlin.

[7]   GP-052587: "DTM Capabilities with Dual Carrier Technology", GERAN#27.

[8]   AHGEV-060016: "Discussion on Uplink Coverage", GERAN AdHoc on GERAN Evolution, May 2006.

[9]   3GPP TR 45.912 (V0.5.0): "Feasibility study for evolved GSM/EDGE Radio Access Network (GERAN)".

[10]   Tdoc GP-060775: "Modified Dual Symbol Rate", Nokia.

[11]   Tdoc GP-060188: "RF aspects for Dual Carrier in uplink", Nokia.

[12]   Tdoc GP-060732: "Observations on Evolution of the GERAN Uplink", Motorola.

8   Higher Order Modulation and Turbo Codes

8.1   Introduction

Higher order modulations should be considered as a candidate to increase peak rates and, more importantly, to increase the mean bit rates. Convolutional coding is currently used for MCS coding for packet service over EGPRS. As a replacement to these within Future GERAN Evolution, Turbo Coding schemes can also be considered as a candidate to increase the mean bit rates.

This subclause analyses the impact of introducing higher order modulation based on QAM and Turbo coding in EGPRS. Simulations to evaluate link performance have taken reasonable practical impairments in the receiver and transmit implementations into consideration.

8.2   Concept Description

The coding and modulation schemes that are already available for the current EDGE system are enhanced with the introduction of higher order modulations and Turbo coding. Since the higher order modulations enable higher data rates, new coding schemes may also be introduced.

8.2.1   Higher Order Modulations

8.2.1.1   Square 16QAM Modulation

New modes for MCS-8 and MCS-9 schemes are introduced that use 16-QAM modulation. With the same payload, 16-QAM allows lower coding rate (as it enables a higher modem bit rate). Note that 8-PSK, 16-QAM and 32-QAM modulations allow modem bit rates of 1224, 1688 and 2152 per block respectively (excluding the RLC/MAC header bits, USF and stealing bits). The payloads for MCS-8 and MCS-9 are 2X564 = 1128 and 2X612 = 1224 (including the CRC bits) respectively. Therefore, 8-PSK with MCS-8 coding scheme allows a coding rate of 1128/1224 = 0.92, whereas 16-QAM modulation allows a coding rate of 1128/1688 = 0.67. More coding power introduces more diversity, and thus achieving significant gains over existing EDGE schemes.

Similarly, for MCS-9 coding scheme, using 16-QAM instead of 8-PSK enables lower rate coding 0.73 instead of 1.00.

The new proposed coding schemes MCS-10 and MCS-11 use higher order modulations with increased data rates.

The data and coding rates for a number of possible alternative schemes can be found in table 34, together with the current EGPRS coding schemes.

Table 34: Coding configurations and parameters for modified and new coding schemes proposed.

Modulation and coding scheme	Family	User PDU (bytes)	User Data Rate (kbps)	Modulation	Payload Length (see note 1)	Overhead (see note 2)	Payload Coding Rate	Interleaving depth
MCS-1	C	1×22	8.8	GMSK	1×196	92	0.53	4
MCS-2	B	1×28	11.2	GMSK	1×244	92	0.66	4
MCS-3	A	1×37	14.8	GMSK	1×316	92	0.85	4
MCS-4	C	1×44	17.6	GMSK	1×372	92	1.00	4
MCS-5	B	1×56	22.4	8PSK	1×468	144	0.37	4
MCS-6	A	1×74	29.6	8PSK	1×612	144	0.49	4
MCS-7	B	2×56	44.8	8PSK	2×468	144	0.76	4
MCS-8	A	2×68	54.4	8PSK	2×564	168	0.92	2
MCS-9	A	2×74	59.2	8PSK	2×612	168	1.00	2
MCS-8-16QAM	A	2×68	54.4	16QAM	2×564	170	0.67	4
MCS-9-16QAM	A	2×74	59.2	16QAM	2×612	170	0.73	4
MCS-10-16QAM	B	3×56	67.2	16QAM	3×468	191	0.83	4
MCS-10-32QAM	B	3×56	67.2	32QAM	3×468	190	0.65	4
MCS-11-32QAM	A	3×68	81.6	32QAM	3×564	190	0.79	4
MCS-7-16QAM-2	B	2×56	44.8	16QAM	2×468	168	0.55	4
MCS-8-16QAM-2	A	2×68	54.4	16QAM	2×564	168	0.67	4
MCS-9-16QAM-2	A	2×74	59.2	16QAM	2×612	168	0.73	4
NOTE 1: Including FBI, E bits and CRC.								
NOTE 2: Encoded RLC/MAC header, USF and stealing bits.								

The information bits are always coded using convolutional coding with coding rate of 1/3 and constraint length of 7. The coded bits are then punctured using uniform puncturing to obtain desired coding rate.

The signal constellations for QAM are used in figure 106. The bits are mapped to the symbols using Gray mapping.
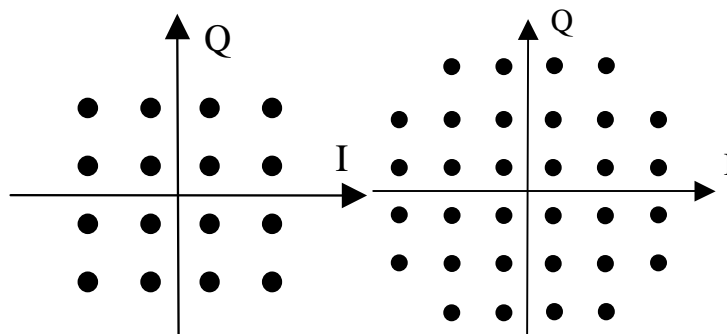
Figure 106: Signal constellations for QAM. Left: 16QAM. Right: 32QAM

The Peak-to Average-Ratio (PAR) for different modulation constellations is shown in table 35.

Table 35: PAR for different modulations

Modulation	PAR (dB)
8-PSK with 3π/8 rotation	3.3
16-QAM	5.9
16-QAM with π/4 rotation	5.3
32-QAM	5.7

The PAR of 32 QAM is lower than that of 16 QAM due to the shaping gain of the 32-QAM cross arrangement. There are other methods to modify the modulations to reduce the PAR, e.g. PAR for Q-O-QAM is 4.6 dB, see Feasibility report on EDGE [4].

In simulations for Implementation B (see subclause 8.3), 45 deg shifted constellation for 16-QAM has been used, but this has no impact on PAR.

8.2.1.2   Other 16-ary Modulations

The performance of square 16QAM modulation and Turbo coding schemes (HOMTC) has been evaluated [14], [12], [9]. It has been shown to have much improved performance as compared with EGPRS. However, inherent in using a square 16QAM constellation, there are some practical implementation issues that arise.

- The higher peak-to-average power ratio (PAPR) typically requires a larger backoff of the PA at maximum output power; This affects coverage areas in noise-limited environments. The 99.99 % PAPR of square 16QAM is higher by about 2dB than that of 8PSK.

- The higher backoff may also cause issues when using 16QAM on the BCCH channel. See [33], [45] and subclause 8.7b for more details.

- The dynamic range of square 16QAM modulation reaches 40dB. This leads to wider linearity range requirements in the RF front end, and may be more difficult to implement on legacy BTSs.

A comparison of circular 16APK (Amplitude Phase Keying) constellations (see [34] and [35]) to the square 16QAM constellation is presented in subclause 8.7.

8.2.1.3   32QAM Modulation

16QAM and circular 16-ary modulation schemes for enhancements in GERAN Evolution [9], [12] and [14]. 32QAM modulation is considered as an additional, and possibly alternative, modulation to 16QAM. 32QAM presents the opportunity to achieve higher peak throughput bit rates, and possibly also more robust channel coding schemes for existing MCSs.

The 32QAM constellation used in implementation D is shown in figure 107. The constellation follows the structure described in [40]. It is a cross constellation that has almost Gray coding between adjacent symbols in the constellation.

A rotation of the 32QAM constellation is applied between symbol periods, as was done for 8PSK and the square 16QAM modulation, in order to avoid transition through the origin between symbols. The rotation used is $\pi/4$.
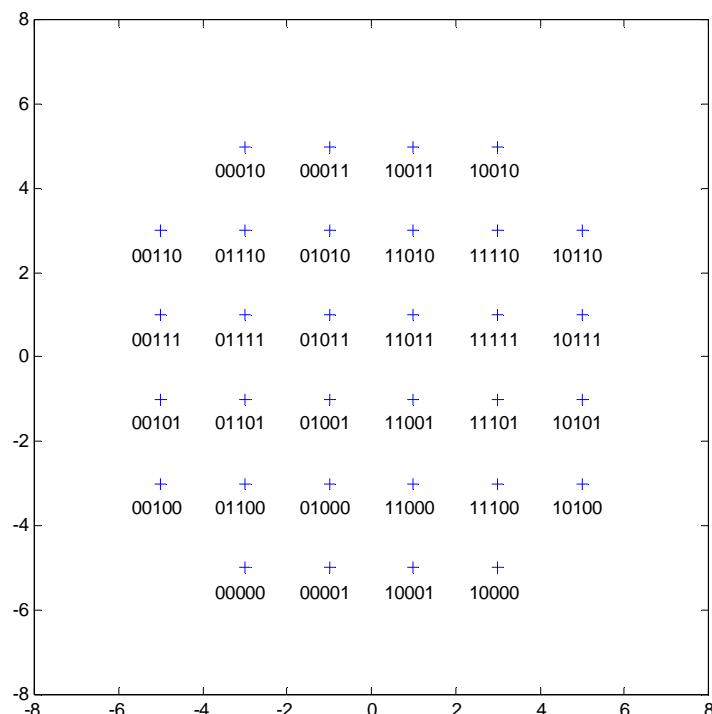
Figure 107: 32 QAM Cross Constellation

8.2.2   Channel Coding

Much work has been done within the framework of 3GPP RAN standardization with Turbo coding. This chapter takes the turbo coding scheme, and subsequent rate matching as it is used in RAN [15].

The reference configuration used is the existing EGPRS coding schemes MCS-1 to MCS-9. This is compared to the performance of Turbo Coding schemes with the same coding rate.

The performance of convolutional coding with 16-QAM modulation is also considered.

Also, it is known in the literature that, unlike Convolutional coding schemes, the performance of turbo codes tends to improve with source code block length. The basic simulations were extended to investigate the potential of this property. Doubling of the source code block length was considered.

8.2.3   Symbol Mapping and Interleaving

For non-MCS coding schemes, rectangular interleaving is done across the bursts. For basic block, it is done across 4 bursts. For a doubling of the source code word, interleaving across 8 bursts is used to transmit the block. Bit-wise interleaving is performed. The structure for interleaving over 8 bursts, and the structure for interleaving for 16-QAM modulation are similar to that for EGPRS interleaving.

Further performance enhancement is achieved by introducing a symbol mapping method of turbo coded bits for 16-QAM modulation in order to improve the performance of such turbo coded systems. The symbol mapping follows the rule that systematic bits are assigned into higher reliability positions while parity bits into lower reliability positions on 16-QAM symbols. This symbol mapping method has already been included as part of the coding chain for HS-DSCH [15]. For further details and for simulation results see subclause 8.5.

8.2.4   Header Block

The header block would most likely require modification. Since the header is relatively short, a change from Convolutional to Turbo coding is probably not relevant. However, some improvement of the header coding may be required to be properly aligned with the improvement in the performance of the data block reception. This aspect is left for further study.

8.2.5   USF Signaling

The USF signaling to instruct transmission from MS would probably not be affected for a finally selected scheme for 8-PSK modulation.

For 16-QAM modulation a stronger block code would have to be devised to maintain robustness, and the network would probably be limited for the case that it was required to signal to legacy mobiles that support only EGPRS. This is similar to the case today for GPRS-only legacy mobiles in a EGPRS environment.

8.2.6   Link Adaptation

The current mechanism for EGPRS link adaptation is based on BEP reporting. BEP measurements are independent of specific coding scheme used as it essentially estimates the expected uncoded BER. So it is anticipated that the current BEP scheme could be utilized with appropriate modifications to the link adaptation mapping.

8.2.7   Incremental Redundancy Combining

The current mechanism for incremental redundancy combining is based on a "family" of MCSs where the members of the family have multiples of a basic payload unit [7]. A modified form of this could be used for Turbo codes MCSs.

8.2.8   Multislot Classes

For configurations that interleave a block over 4 bursts, there should be no need for modifications to the Multislot classes. There may be a need for additional multislot class to support signalling of configurations that interleave across dual carriers.

8.2.9 Non-core Components

The components described below are not necessary to the core concept of turbo coding within GERAN. However, during the work we observed, particularly for 16-QAM modulation, that the combined effect together with Turbo coding was greater than the sum of the parts. They have therefore been included as sub-components as an addition to the core concept, and the combined performance is also reported.

8.2.9.1 Dual Carrier

The dual carrier concept has been described in detail in [7]. We have investigated the improvement in throughput performance that can be obtained by defining a configuration where the turbo-coded RLC block is interleaved between the different carriers (or hopping sequences). This is a specific example of doubling the source block length which can fit within the same TTI and be interleaved over 8 essentially decorrelated bursts.

It is considered unlikely that a dual carrier configuration would be deployed on 2 carriers in the non-hopping layer. However, as a lower limit, the performance under these conditions is considered.

Note, it is instructive to consider what frequency separation is needed in order to have carrier channels that can be considered as largely independent for fast fading. For channels such as TU which has rms delay spread of ~1 µs, which corresponds to a coherence bandwidth of ~160 kHz, significant decorrelation may be assumed for channels even 600 kHz apart.

8.2.9.2 MS Receiver Diversity

The potential interdependence of performance enhancements of MSRD and Higher order modulations (with or without Turbo coding) has been investigated in reference [26], when the features are used simultaneously. A particular aim was to assess whether 16QAM/TC would bring a similar improvement also in the case of MSRD, i.e. whether the gains from 16QAM/TC and MSRD are additive.

Furthermore, the performance of 16QAM/TC EGPRS in a sensitivity limited environment is shown, taking into account the additional back off for 16QAM modulated radio blocks.

These issues are presented in subclause 8.6.

8.3 Modelling Assumptions and Requirements

The impairments include typical imperfections like I/Q modulator/demodulator imbalance, receiver and transmitter synthesizer (phase) noise, frequency error and non-linear characteristics of the power amplifier.

The impairment models used for the simulations are described in SMG2 EDGE workshop contributions from Toulouse meeting March 1999 (see reference [3] and [4]).

The frequency error is added as a rotation of the received signal.

The impairments in I/Q modulator and demodulator (gain imbalance and phase imbalance) are added.

The phase noise (synthesizer impairment) is added as a normal distributed AWGN source filtered through a low pass filter.

The power amplifier (PA) is characterized by amplitude and phase transfer characteristics, and it is memoryless.

Simulations from different sources have used different assumptions. The sets of assumptions are denoted Implementation set A, Implementation set B, Implementation set C and Implementation D in the following. Further details are found for Implementation set A are described in reference [1] and [17], for Set B in reference [7], for set C in reference [6] and [8], and for set D in reference [11], [12], [13] and [14].

8.3.1 Transmitter Impairments

The transmitter impairments that are used in this report are:

- IQ phase imbalance (phase deviation from 90 degrees between I and Q) and IQ gain imbalance (gain difference between I and Q) which are due to the I/Q modulator that produces the analogue baseband signal from the I and Q signals;

- Phase noise due to the synthesizer that converts the baseband signal into an RF signal;

- Non-linearities in the Power Amplifier (PA) that introduces a certain EVM and phase noise depending on the back off (PA back off) from the 1-dB compression point.

The following values have been used in the simulations.

Table 36: TX impairments

Impairment	Values, set A	Values, set B	Values, set C	Values, set D (see note)
I/Q gain imbalance	0.2 dB	0.5 dB	0.1 dB	0.1dB
I/Q phase mismatch	0.5 degrees	4 degrees	0.2 degrees	0.2 degrees
DC offset	-	-30 dBc	-45 dBc	-45 dBc
Phase noise	1.2 degrees RMS	2 degrees RMS	0.8 degrees RMS	0.8 deg. RMS
PA model	Yes	No	Yes	No
				NOTE: Where explicitly stated as used

The average EVM values are calculated by averaging the EVM values among all the blocks. The average EVM measures depend on the transmitted impairments as well as the modulation method. One major factor that contributes to the EVM measurement is the PA back off. Table 37 shows the average EVM values with different PA back off values and modulations for the PA model used in TX impairment set A.

Table 37: PA model characteristics

Modulation	Back off (dB)	Average EVM (%)
8-PSK with 3π/8 rotation	4.3	3.9
16-QAM	6.3 see *)	3.8
32-QAM	6.3	3.7
NOTE: *) in TX impairment set B a back off of 6 dB was used in spectrum calculations.		

8.3.2 Receiver Impairments

The receiver impairments that are used in this report are:

- the I/Q demodulator has IQ phase and gain imbalances as in the transmitter;

- the receiver synthesizer introduces phase noise like the transmitter synthesizer;

- the frequency error can be seen as a constant frequency offset between the reference oscillator and the received signal.

The following values have been used in the simulations.

Table 38: RX impairments

Impairment	Value set A	Value set B	Value set C	Value set D
I/Q gain imbalance	0.4 dB	0.125 dB	0.2 dB	0.4dB
I/Q phase mismatch	1 degrees	1 degrees	1.5 degrees	2.8 degrees
DC offset	-	-30 dBc	-40 dBc	None
Phase noise	1.5 degrees RMS	1.2 degrees RMS	1.0 degrees RMS	None
Frequency error	50 Hz	0	25 Hz	50Hz

8.3.3   Equalizer

Set A: A DFSE is used, where 2-taps are handled by MLSE and the rest of the taps are handled by DFE structure. In 8-PSK modulation the number of states is 8, while in 16-QAM and 32-QAM, the number of states are 16 and 32, respectively.

Set B: The equalizer utilizes the reduced-state sequence estimation (RSSE) with set partitioning, the number of states being 16 for 16-QAM and 4 for 8-PSK. The trellis length is one for both modulations.

Set C: A 4-state RSSE receiver has been used. The complexity of the 16QAM RSSE is just 20 % higher than a conventional 8-PSK receiver.

Set D: DFSE is used, where 2-taps are handled by MLSE and the rest of the taps are handled by DFE structure. In 8-PSK modulation the number of states is 8, while in 16-QAM the number of states is 16.

8.4   Performance Characterization

8.4.1   Implementation Set A

Source: reference [1] and [6].
Implementation set A evaluates the performance of introduction of higher order modulation only using the EGPRS convolutional channel coding. This is now superseded by other implementations where the performance is evaluated for Higher Order Modulation as well as combination of Higher Order Modulation and Turbo Codes (HOMTC).

8.4.1.1   Modelling assumptions and requirements

The results are obtained in a co-channel interference limited environment.

A Typical urban channel with 3 km/h mobile speed (TU-3) at 900 MHz carrier frequency is considered.

Single transmit and receive antenna receivers are used.

A linerarised GMSK pulse shaping filter with BT product 0.3 was used.

Blind detection for different modulation schemes is not considered in the simulations (i.e. it is assumed that the modulation scheme that is used in the transmitter is known by the receiver). An evaluation of blind detection performance can be found in subclause 8.7a.

8.4.1.2   Comparison of BLER Performance

The results indicate that higher order modulations are more sensitive to the impairments compared to 8-PSK modulation for the same back off. However, a good alternative is to increase the back off for QAM modulations to a level that maintains constant impairment. According to our calculations in table 36 the back off value of 6.3 dB for the QAM modulations is selected.

Figures 108 and-109 show block-error-rate (BLER) results for constant EVM. The results are obtained with different PA back offs for 8PSK and 16 QAM and identical average EVM values. Significant amounts of gain are observed with MCS-8 and MCS-9 coding schemes. For example, gains of 4 dB and 5.5 dB with respect to the 8PSK equivalents are observed when 16 QAM is used. The results show that with transmit and receiver impairments 16-QAM and 32-QAM modulations perform well subject to back off being increased.

Figures 110 and 111 plot the performance of the new coding schemes MCS-10 and MCS-11 with different modulation schemes. It is seen that 32-QAM, if used, should give better performance for both these coding schemes.
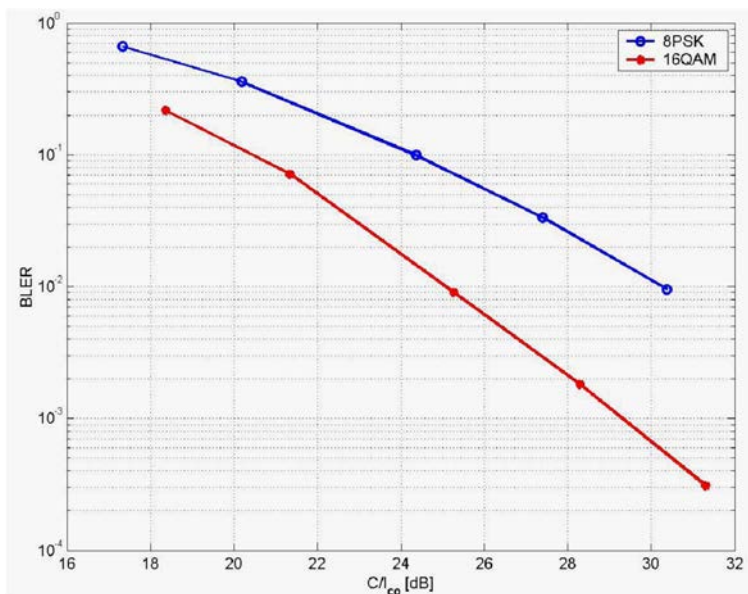
Figure 108: MCS-8 with EVM around 3.9. Back off for 8PSK was 4.3 dB and Back off for 16 QAM was 6.3 dB
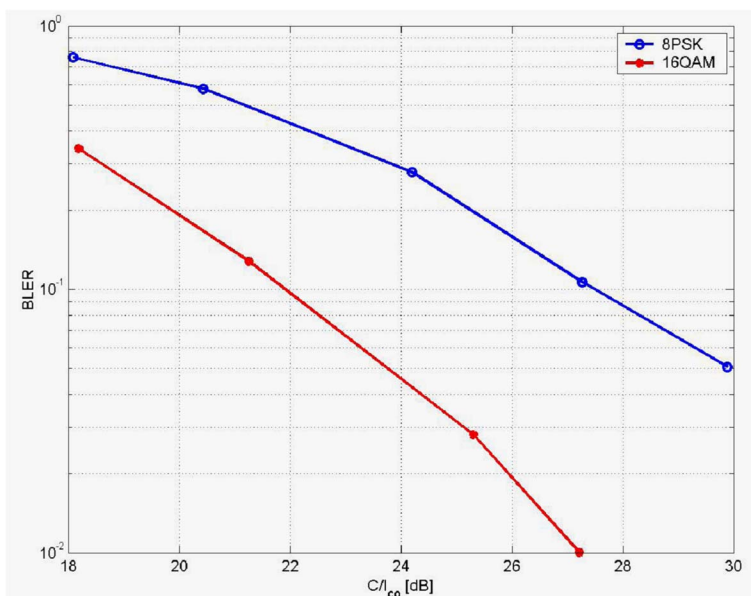
Figure 109: MCS-9 with EVM around 3.9. Back off for 8PSK was 4.3 dB and Back off for 16 QAM was 6.3 dB
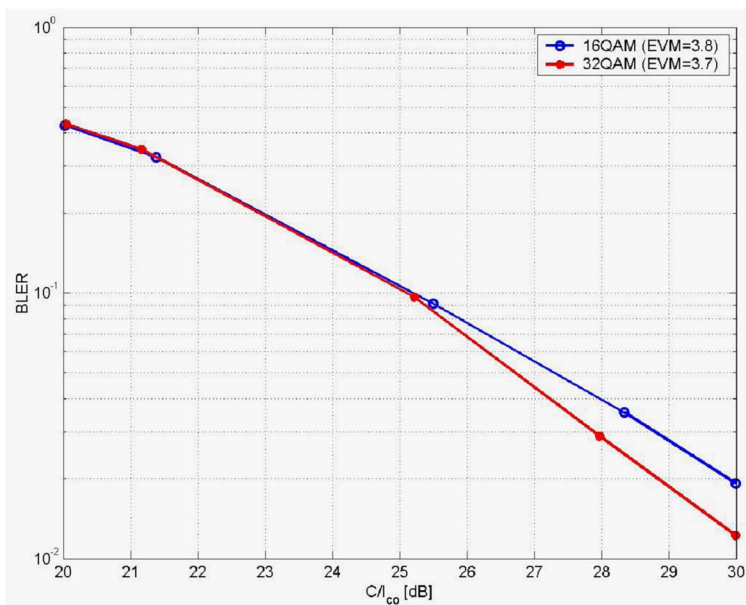
Figure 110: MCS-10 coding scheme with PA back off =6.3
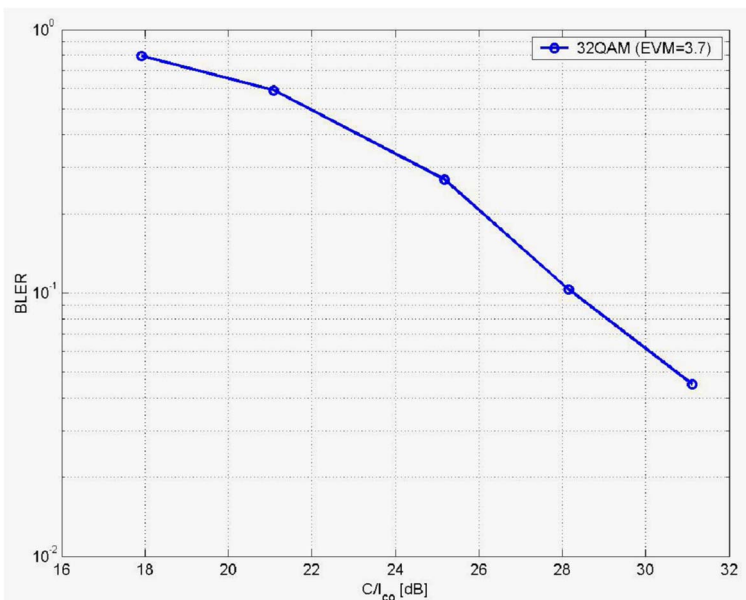
Figure 111: MCS-11 coding scheme with PA back off=6.3

Higher order modulation than 32 QAM was not considered relevant any longer, as the impact of impairments was very high.

8.4.1.3 Link Performance with Link Adaptation

Link performance for three cases with modified and new modulation schemes according to table 39 including the impact of transmitter/receiver impairments are investigated and compared to existing 8-PSK.

Table 39: Used modulation and bit rate [kbps] for the investigated cases

Coding scheme	Case A		Case B		Case C		Case D	
	Modulation	Rate	Modulation	Rate	Modulation	Rate	Modulation	Rate
MCS-1	GMSK	8.8	GMSK	8.8	GMSK	8.8	GMSK	8.8
MCS-2	GMSK	11.2	GMSK	11.2	GMSK	11.2	GMSK	11.2
MCS-3	GMSK	14.8	GMSK	14.8	GMSK	14.8	GMSK	14.8
MCS-4	GMSK	17.6	GMSK	17.6	GMSK	17.6	GMSK	17.6
MCS-5	8PSK	22.4	8PSK	22.4	8PSK	22.4	8PSK	22.4
MCS-6	8PSK	29.6	8PSK	29.6	8PSK	29.6	8PSK	29.6
MCS-7	8PSK	44.8	8PSK	44.8	8PSK	44.8	8PSK	44.8
MCS-8	8PSK	54.4	16QAM	54.4	16QAM	54.4	16QAM	54.4
MCS-9	8PSK	59.2	16QAM	59.2	16QAM	59.2	16QAM	59.2
MCS-10	-	-	-	-	16QAM	67.2	32QAM	67.2
MCS-11	-	-	-	-	-	-	32QAM	79.2

The throughput of case A-D is shown the figure 112. Note that the rightmost parts of the curves (the thin part of the curves) are extrapolated. Simulation results for this region need to be provided.
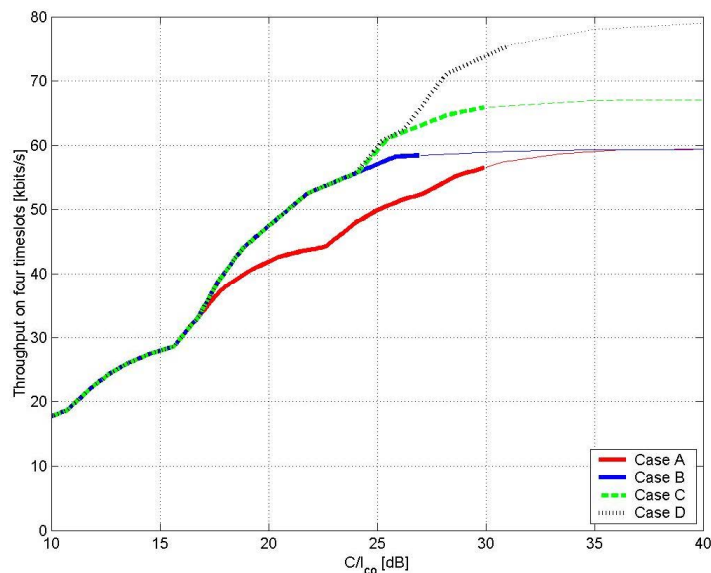
Figure 112: Throughput vs. C/I with transmitter/receiver impairments in TU3

Figure 112 plots the improvement of throughput (calculated as 1-error rate) with link adaptation. It is seen that significant increases in throughput are observed over the range of C/I where EDGE will currently be used.

8.4.1.4 System Simulation Results

Systems simulations have been performed with no impairments included. These are not included in this subclause, as we need to consider the impact of impairments comparable with existing HW.

No system simulation results including impairment consideration are available today. To further estimate the throughput gains in this case, the link results were mapped to the C/I distribution measured in live network, presented by TeliaSonera in GP-042355 [5]. The resulting CDF is shown below.
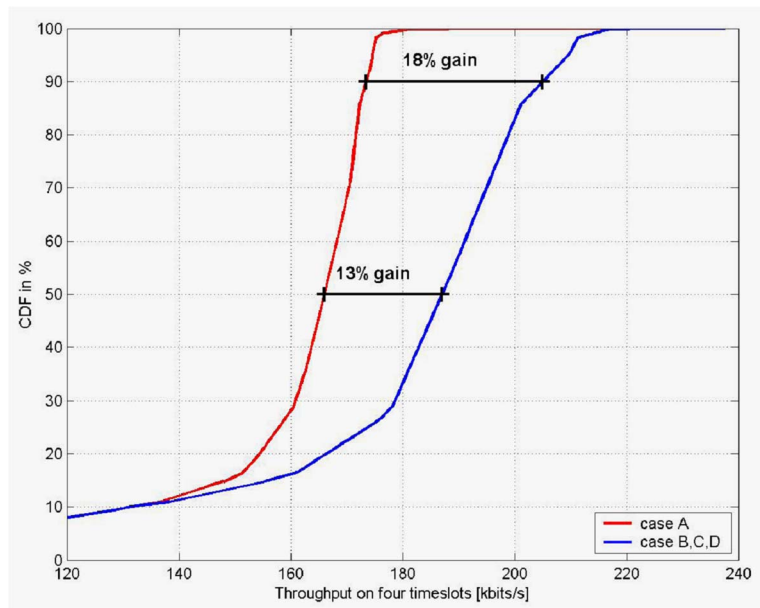
**Figure 113: Estimated throughput CDF by mapping link performance with impairments
to C/I distribution of live TeliaSonera network**

From this curves the median value of the throughput increase is estimated to be 13 % in case B and about the same for case C and D. For the 10 percentile with best C/I the improvement increases 18 % in case B. The additional improvement in case C and D is very small in this scenario as the increase in peak rate is effective for C/I> 24 dB and there are very few reported values in this C/I range. Thus the addition of MCS-10 (16-QAM or 32-QAM) and MCS-11 (32-QAM) will contribute very little to the overall improvement. This could be different for other scenarios. It is anyway worth noting that the main part of the gain is found when improving MCS-8 and MCS-9 codings by replacing 8-PSK with 16QAM.

The CDF of C/I above indicates very few occurrences of C/I above 22 dB. This would indicate little use of MCS-9 in such an environment, but this is not the case in reality. Probably this is due to limited reporting capability of the measuring device for high C/I. The Telia measurements are based on measuring equipment optimised for good accuracy in the C/I range less than 20 dB. The accuracy above 20 dB is lower and probably the equipment does not distinguish between 25 and 30 dB C/I. To find a CDF describing the real situation better, a CDF from simulations of a similar 3/9 frequency reuse scenario with approximately the same mean C/I value is used. The table below summarises the system parameters:

Table 40: System parameters for simulation of C/I distribution

Parameter	Value	Unit
Reuse	3/9	
Frequency spectrum	7.2	MHz
Frequencies per cell	4	
Blocking limit	2 %	
Traffic	Speech	
DTX	No	
Cell radius	500	m
Power control	No	
Log-normal fading standard deviation	8 dB	

The resulting CDF is shown in figure 114. To be able to map link throughput curves to this C/I mapping, the effects of fast fading are not included in the C/I distribution (since fast fading is modeled in the link level simulations).
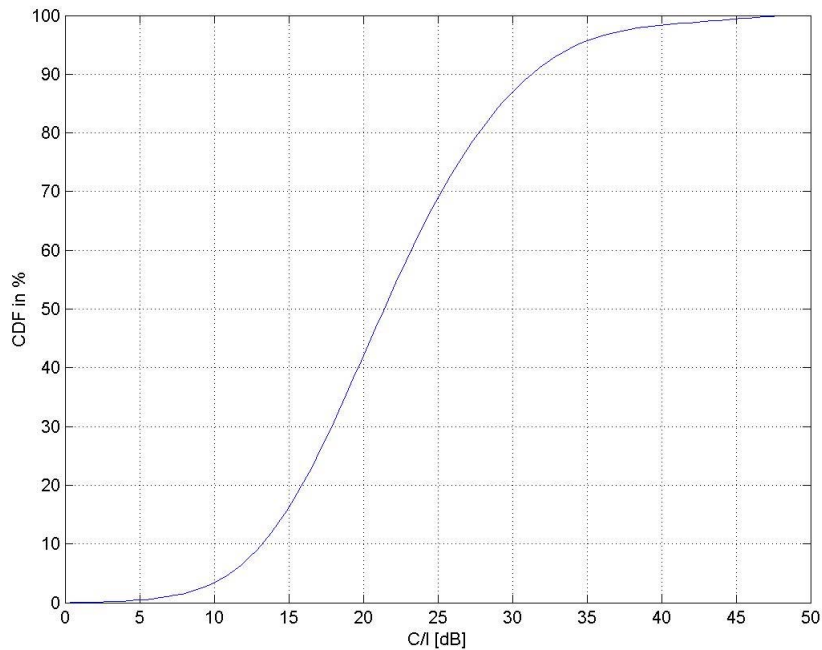
Figure 114: C/I distribution in a 3/9 reuse, excluding effects of fast fading

Mapping the link results in figure 112 on this CDF results in the estimated throughput CDF shown in figure 115 (note that since figure 112 is extrapolated above 30 dB, the throughput distribution for the 13 % best users is preliminary in figure 115)
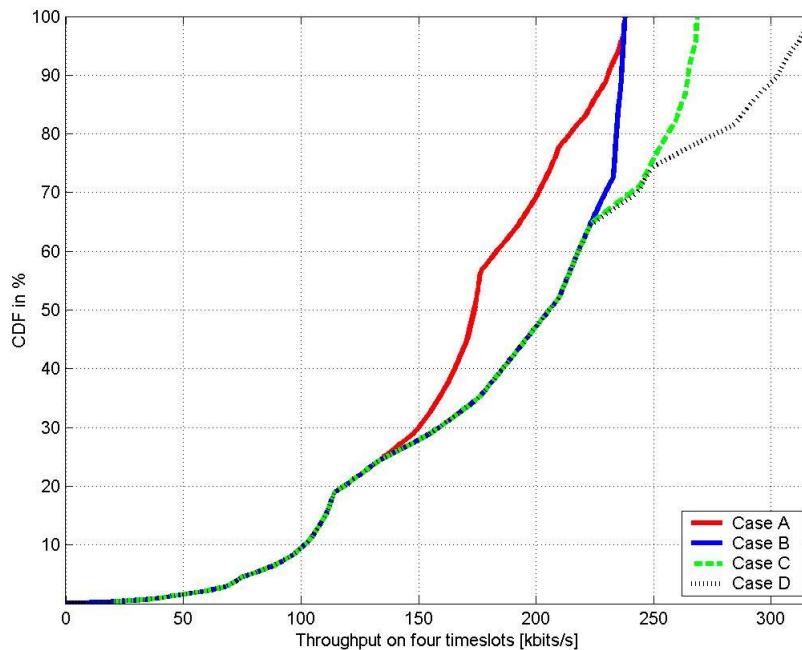
Figure 115: Throughput distribution in a 3/9 reuse

The throughput gain for case B, C and D (relative to case A, EGPRS) is shown in figure 116.
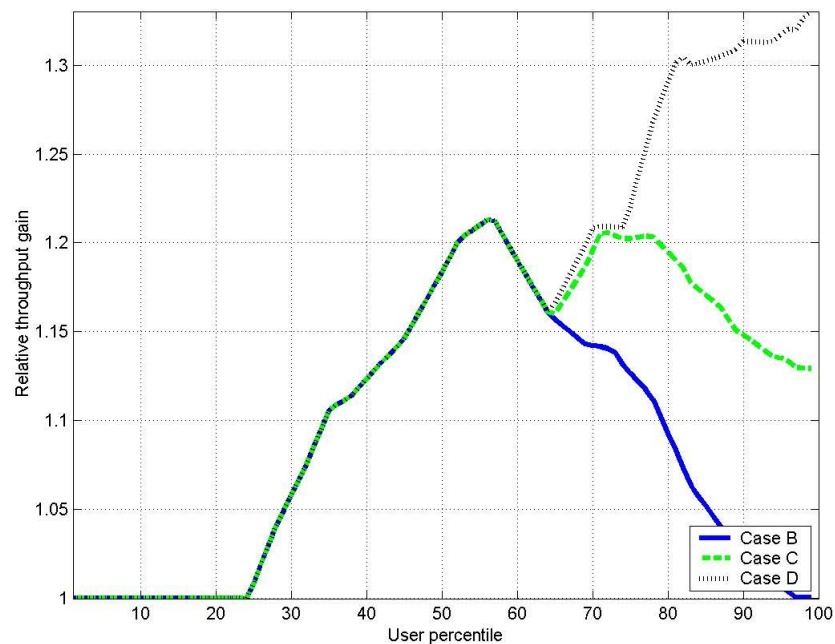
Figure 116: Relative gain distribution.

8.4.2 Implementation B

Source: Reference [7].

8.4.2.1 Introduction

The impact of the following factors is evaluated:

- Frequency hopping.

- Incremental redundancy.

- Propagation environment.

- RX and TX impairments.

- RRC pulse shaping: Linearized Gaussian pulse (BT=0.3) or Root-raised cosine pulse (rolloff=0.3).

8.4.2.2 Basic Link Layer Performance

The purpose of this subclause is to assess the basic link layer performance of the 16-QAM coding schemes. The simulations are carried out without frequency hopping, impairments, and incremental redundancy, which are separately evaluated in the later subclauses. The applied pulse shaping method is linearized Gaussian (BT=0.3).

8.4.2.2.1 BER Performance

The raw BER performance is illustrated in the figure 117. As can be seen, 16-QAM is approximately 2 dB to 3 dB less sensitive than 8-PSK.
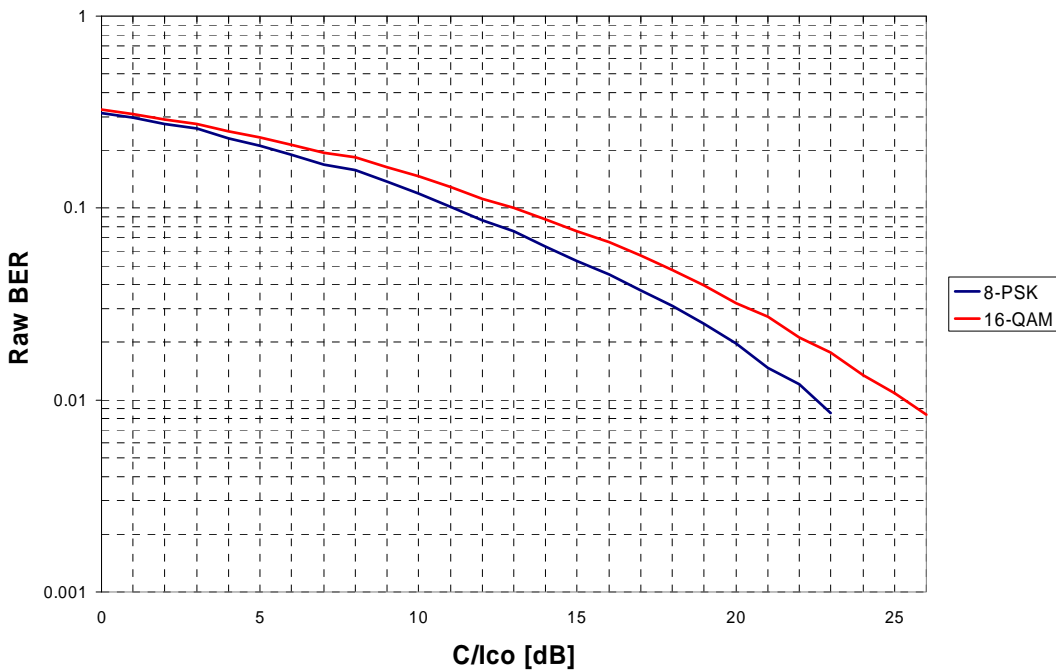
Figure 117: Raw BER (TU3nFH@900MHz, no impairments)

8.4.2.2.2 BLER Performance

The BLER performance of the three highest MCSs is shown in figures 118, 119 and 120 and summarized in table 41.
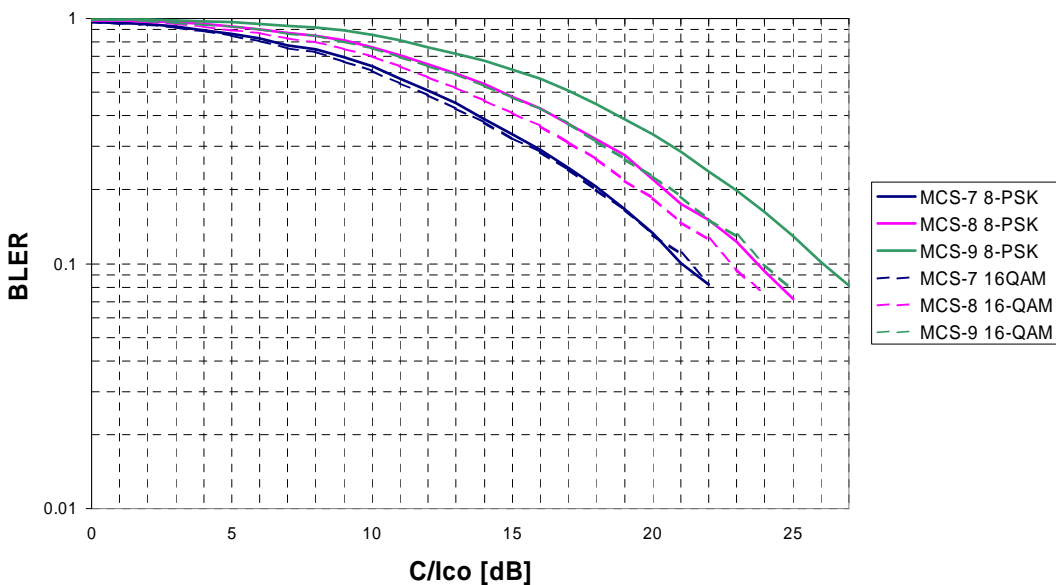
Figure 118: BLER performance for 8-PSK and 16-QAM without impairments

Link performance of 8-PSK with and without FH for TU3 channel
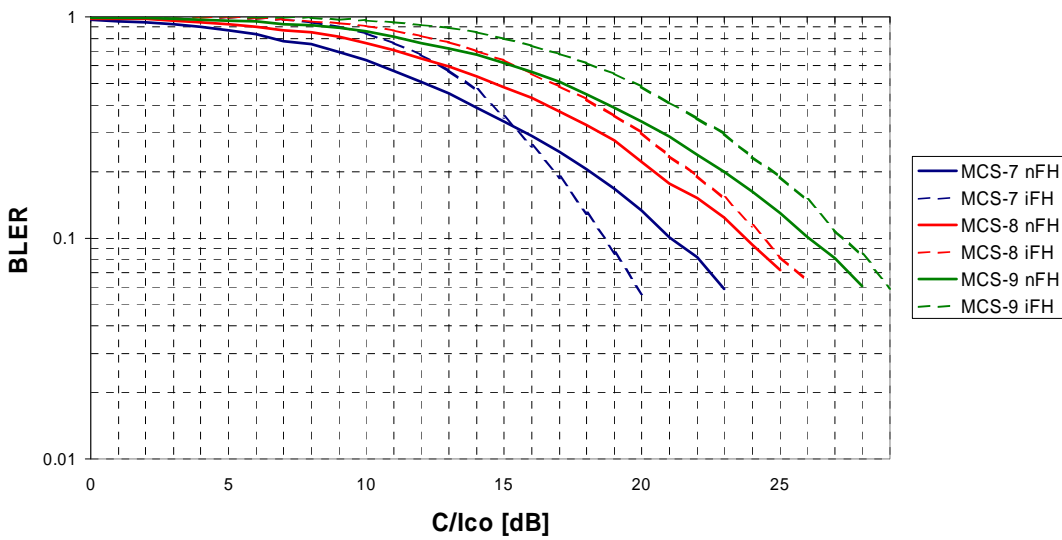
Figure 119: BLER performance for 8-PSK with and without frequency hopping

Link performance of 16-QAM with and without FH for TU3 channel
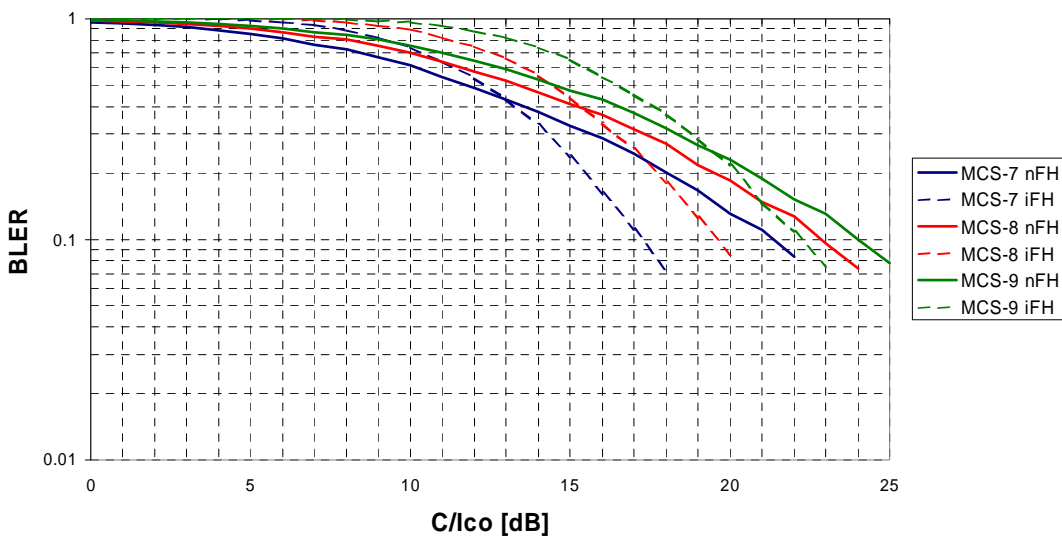
Figure 120: BLER performance for 16-QAM with and without frequency hopping

Table 41: BLER performance (TU3nFH@900MHz, no impairments)

MCS	C/Ico [dB]@BLER=10 %		gain [dB]
	8-PSK	**16-QAM-2**	
7	21.04	21.38	-0.35
8	23.77	22.86	0.91
9	26.05	23.98	2.07

As can be seen, the gain due to 16-QAM modulation is approximately 2 dB for MCS-9, 1 dB for MCS-8, and 0 dB for MCS-7.

8.4.2.2.3 Throughput

The slot-wise throughput is illustrated in figure 121. As can be seen from the figure, 16-QAM brings some improvement to the range of medium and high CIR values, the throughput gain varying between 0 and 10 %. The applied LA switching points are marked with squares.
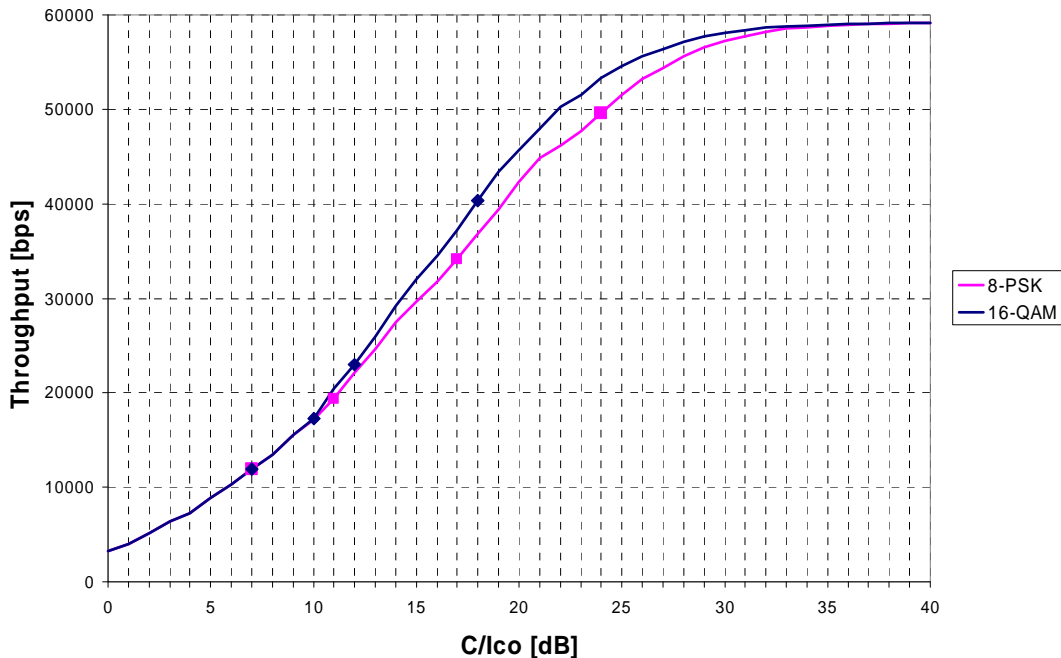
Figure 121: Throughput (TU3nFH@900MHz, no impairments, ideal LA)

8.4.2.3 Impact of Frequency Hopping

The results from the frequency hopping simulations are shown in Appendix A and summarized in tables 42 and 43. Due to the lower coding rate and increased interleaving depth, the FH gain is larger for 16-QAM than for 8-PSK. It is good to note that also MCS-8 and MCS-9 benefit from the frequency hopping in the case of 16-QAM.

Table 42: Frequency hopping gain for 8-PSK

MCS	C/Ico [dB]@BLER=10 %		Gain [dB]
	TU3nFH	TU3iFH	
7	21.04	18.68	2.36
8	23.77	24.43	-0.66
9	26.05	27.36	-1.31

Table 43: Frequency hopping gain for 16-QAM

MCS	C/Ico [dB]@BLER=10 %		gain [dB]
	TU3nFH	TU3iFH	
7	21.38	17.29	4.09
8	22.86	19.63	3.23
9	23.98	22.25	1.73

The FH gain is also illustrated in figure 122, which shows the throughput for both modulation methods with and without FH. As can be seen, the throughput gain is approximately 0 to 20 % in the case of FH, while in the case of nFH it is only 0 to 10 %.
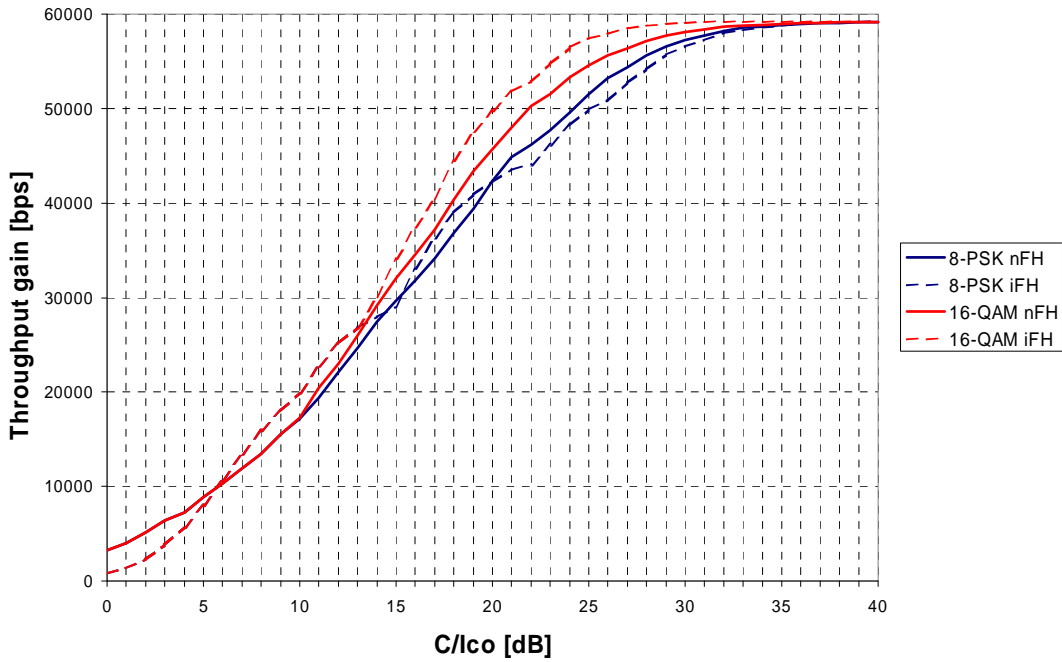
Figure 122: Impact of frequency hopping (TU3nFH/iFH@900MHz, no impairments, ideal LA)

8.4.2.4   Impact of Incremental Redundancy

The results from the IR simulations are shown in figure 123, which shows the performance of MCS-9 with and without IR. As can be seen, 8-PSK benefits more from the incremental redundancy than 16-QAM. This is due to the already lower coding rate of 16QAM, which mitigates the gain from the further increases in the redundancy.
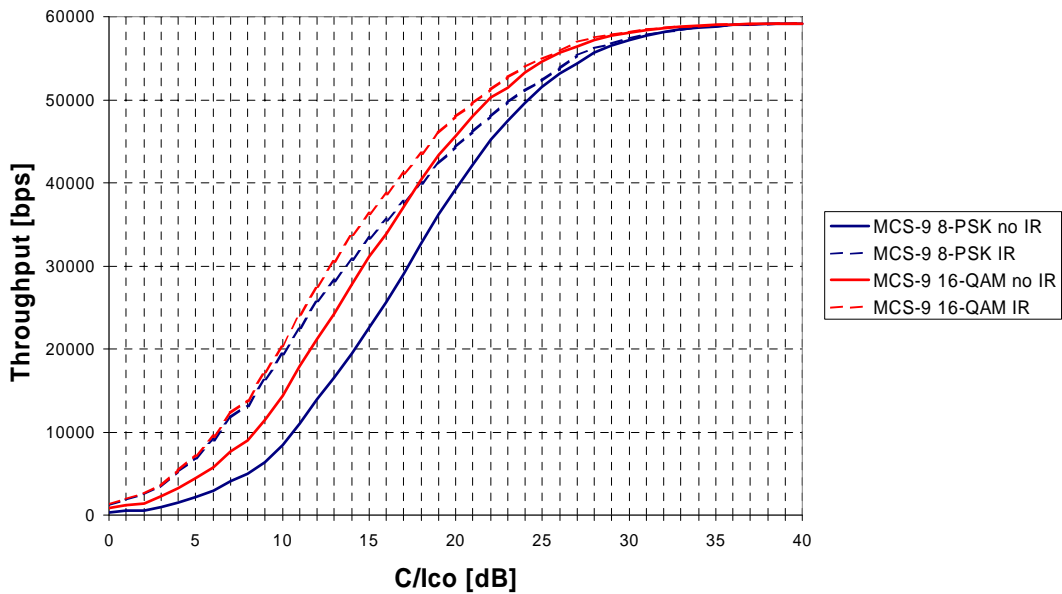
Figure 123: Impact of incremental redundancy
(TU3nFH@900MHz, no impairments, ideal IR for MCS-9)

8.4.2.5 Impact of Propagation Environment

The impact of the propagation environment is illustrated in figure 124. As can be seen, the Doppler effect degrades the throughput of the highest MCSs in the case of fast-moving terminals. In addition, the high delay spread of the HT channel manifests itself as a reduced throughput.
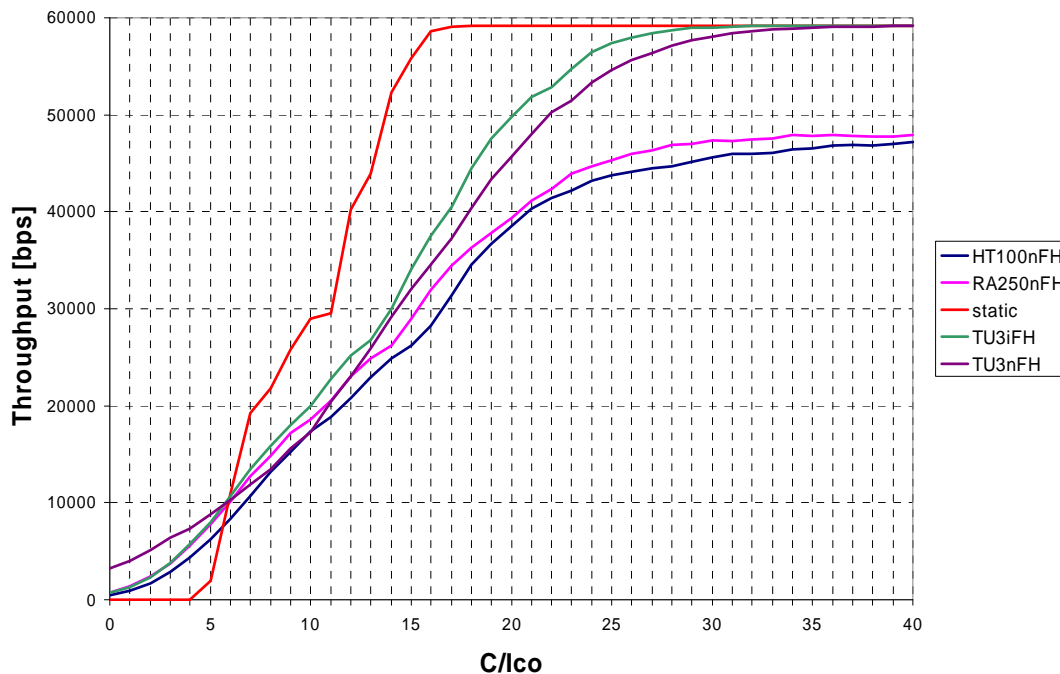
Figure 124: Impact of the propagation environment (no impairments, ideal LA)

8.4.2.6 Impact of RX and TX Impairments

Given equal coding rates, it is obvious that 16-QAM is more sensitive to the RX and TX impairments than 8-PSK. However, when comparing 8-PSK and 16-QAM with equal payload sizes, the lower operating point of 16-QAM effectively compensates the sensitivity loss due to tighter constellation. This fact can be easily seen from figure 125, which shows that the MCS-9-16QAM is less sensitive to the impairments than the MCS-9-8PSK.
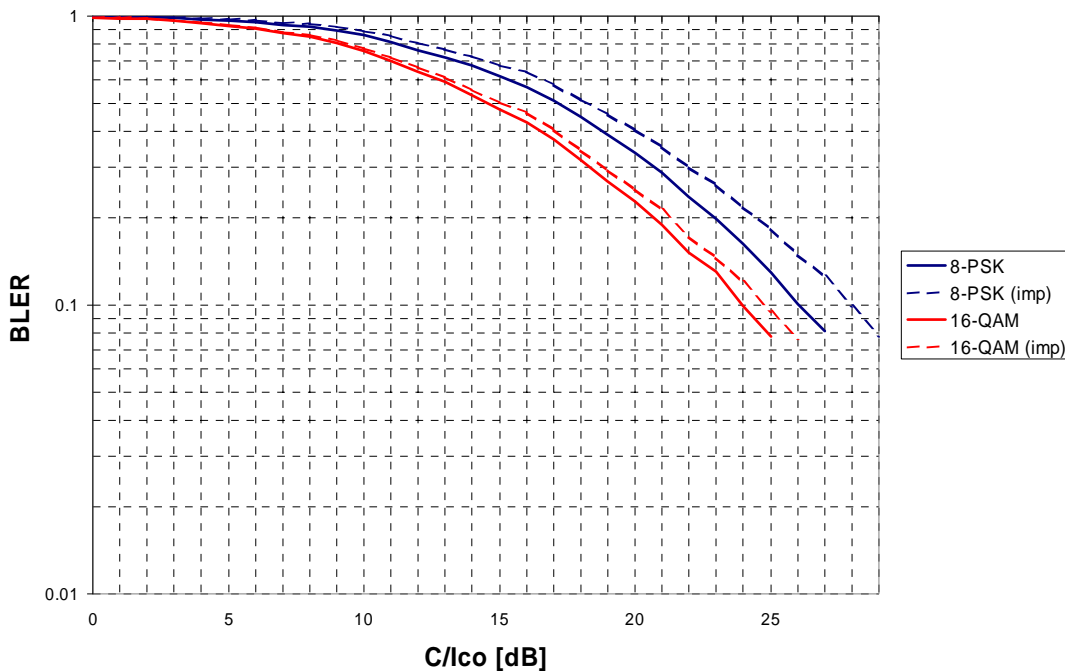
Figure 125: Impact of RX and TX impairments (TU3nFH@900MHz, MCS-9)

In order to evaluate the potential of 16-QAM coding schemes above MCS-9, a set of high coding rates (0.8, 0.9 and 1.0) are evaluated. The results from these simulations are shown in figure 126.

As can be seen, the higher coding rate means also higher sensitivity to the RX/TX impairments. While the uncoded 16-QAM is heavily impaired, the slightly lower coding rates are considerably less affected by the impairments. Hence, it could be possible to increase the peak data rates by adopting MCS10 and MCS11 with coding rates 0.8 and 0.9, respectively.
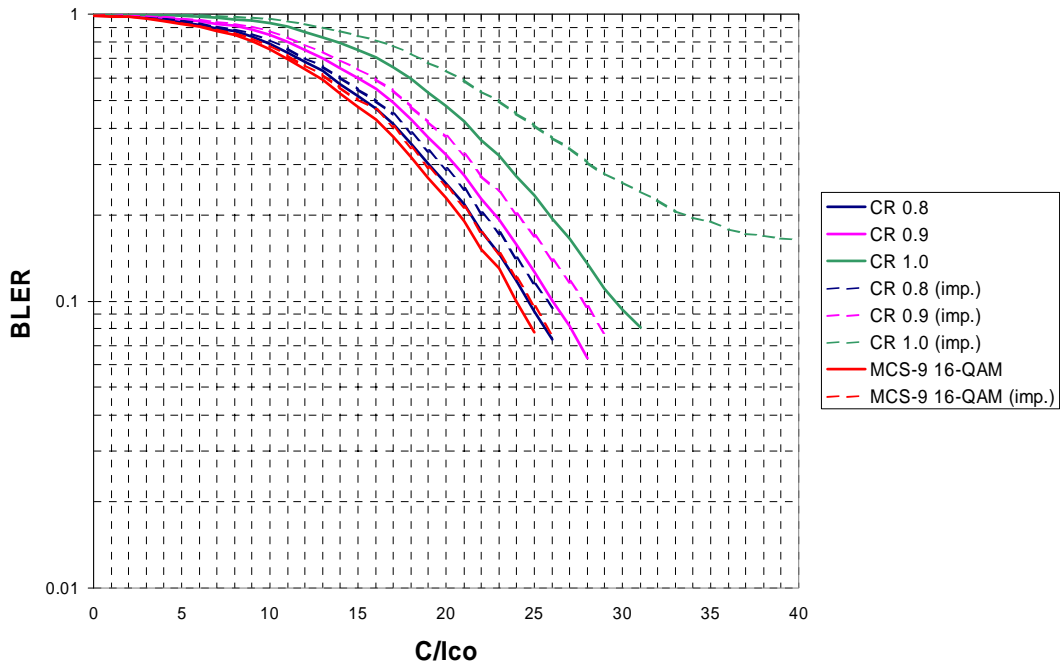
Figure 126: Impact of high coding rates (TU3nFH@900MHz)

8.4.2.7 Impact of RRC Pulse Shaping

The performance of 16-QAM could be, in principle, enhanced by replacing the Gaussian pulse with an RRC pulse. The impact of the improved TX filtering is shown in figure 127, which shows the throughput curves for Gaussian and RRC pulse shapes.
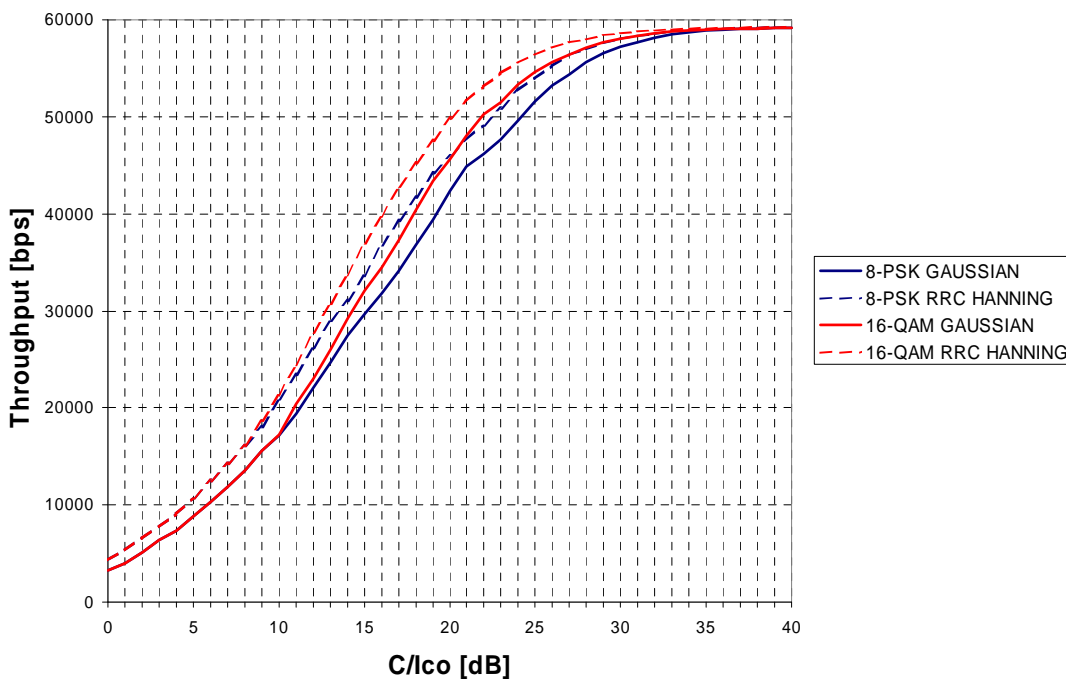
Figure 127: Impact of RRC pulse shaping (TU3nFH@900MHz, no impairments, ideal LA)

The main drawback of the RRC filtering is that the signal spectrum cannot be fitted into the existing GSM spectrum mask. This can be clearly seen from figure 128, which shows the RRC spectrum with all relevant TX impairments included. The adoption of RRC would hence require a specification of a new spectrum mask.
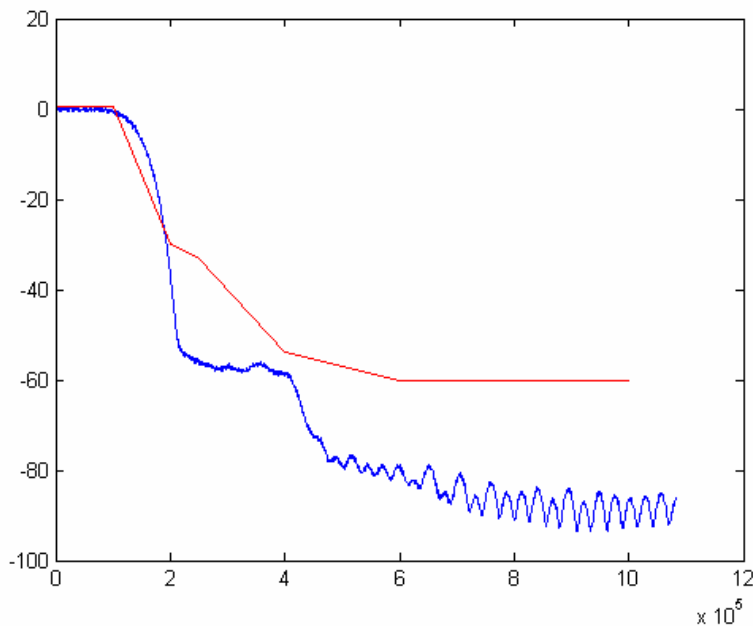
Figure 128: RRC spectrum (backoff=6dB, typical impairments)

8.4.2.8   Evaluation of Performance

The throughput gain (versus 8-PSK) for different C/I values is shown in figure 129.
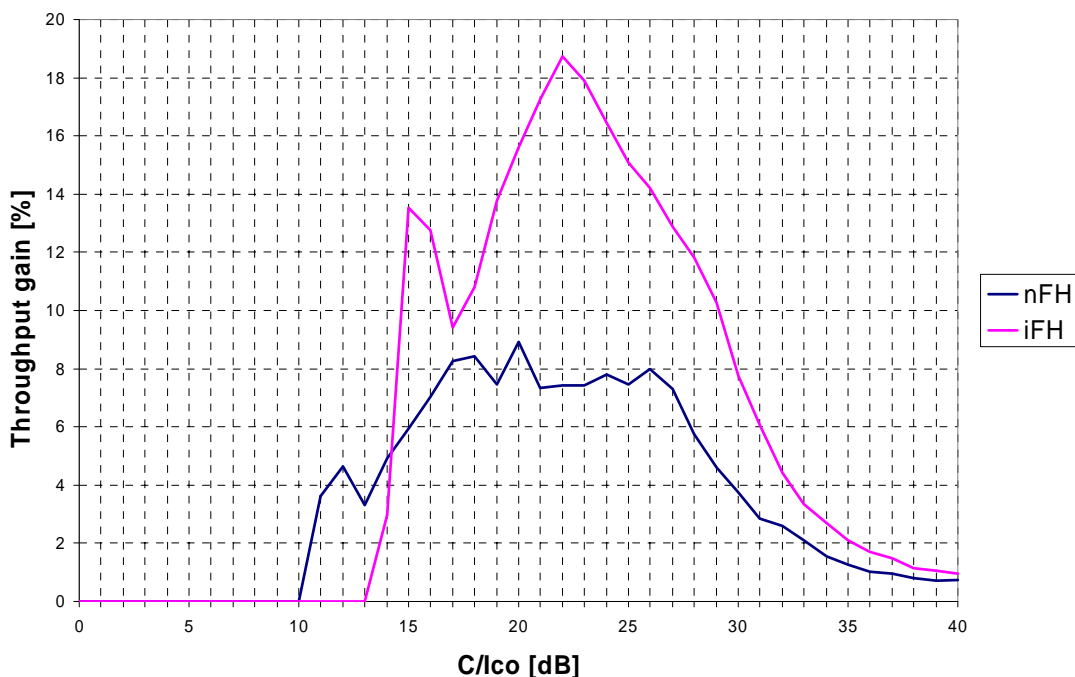
Figure 129: Throughput gain from 16-QAM (TU3, typical impairments, ideal LA)

As can be seen, the throughput gain for 16-QAM modulation varies between 0 to 19 % in the case of ideal frequency hopping, and between 0 to 9 % when no hopping is applied. The requirement for 50 % throughput improvement at cell border is not reached, because 16-QAM does not improve the performance of the most robust coding schemes at all. The peak data rates are neither improved, given that the current payloads for MCS7-9 are used. By introducing less robust MCSs, the peak data rates could be improved by 24 % (assuming code-rate 0.9 MCS), but the coverage of these high bit rates would be extremely limited.

As a summary, the following improvements could be (ideally) achieved by the use of 16-QAM:

- 24 % gain for peak data rates (with limited coverage).

- 0 to 19 % throughput gain over cell range.

- 0 % gain for throughput at cell border in power-limited conditions due to increased PA backoff (up to 2 dB).

In a real network, the following characteristics should be considered as well:

- The increased PA backoff degrades the link layer performance of 16-QAM by some 2 dB in power-limited conditions. By considering that the link level gain for 16-QAM modulation can be as low as 0-2 dB (nFH), it is possible that, in some cases, no improvements in performance is seen for 16-QAM compared to 8-PSK (e.g. a sensitivity-limited non-hopping network).

- 16-QAM benefits less from the incremental redundancy than 8-PSK due to the already lower coding rate of 16QAM, which mitigates the gain from the further increases in the redundancy.

- 16-QAM benefits less from the BTS antenna diversity than 8-PSK for the same coding rate, because the degree of diversity is already higher due to lower coding rate and longer interleaving depth.

8.4.3 Implementation C

Source: Reference [6], [19], [8], [28], [30], [42] and [43]. Note that there are additional details of simulation results in annex B.

Higher order modulations and turbo codes have been proposed as candidates for the GERAN continued evolution feasibility study. The performance gains of 16QAM, 32QAM, turbo codes and the combination of these are evaluated on link and system level.

In addition a short investigation is included regarding the impact on performance if the 16QAM DFSE equalizer is replaced by RSSE.

8.4.3.1 Channel coding

8.4.3.1.1 EGPRS

As reference, the regular EGPRS coding schemes MCS-1 to MCS-9 are used, see table 34. The only deviation from table 34 is that Tail bits are viewed as channel coding redundancy.

8.4.3.1.2 Convolutional Codes with 16QAM

Three 16QAM-modulated coding schemes with convolutional codes are evaluated. These are called MCS-7-16QAM-2, MCS-8-16QAM-2 and MCS-9-16QAM-2 in table 34 and have the same payload size as MCS-7, MCS-8 and MCS-9, respectively. The mother code of EGPRS (R=1/3, k=7) has been used. Uniform (FLO) puncturing has been used for the RLC/MAC header and RLC data blocks. Interleaving is done over four bursts. The only deviation from table 34 is that Tail bits are viewed as channel coding redundancy.

8.4.3.1.3 Turbo Codes with 8-PSK Modulation

Two new 8PSK-modulated coding schemes with turbo codes are evaluated. These are called MTCS-5 and MTCS-6 and have the same payload size as MCS-5 and MCS-6, respectively, as defined in table 44.

The RLC/MAC header, USF and stealing flags have the same channel coding as MCS-5 and MCS-6. The RLC data block has been encoded with a turbo code. For the turbo codes, the constituent codes, internal interleaver and rate matching defined for UTRAN [12] have been reused. Uniform (FLO) puncturing has been used for the RLC/MAC header and RLC data blocks. Interleaving is done over four bursts.

Table 44: 8PSK-modulated coding schemes with turbo codes.

Modulation and coding scheme	Family	User PDU (bytes)	User Data Rate (kbps)	Modulation	Payload Length (see note 1)	Overhead (see note 2)	Payload Coding Rate (see note 3)	Interleaving depth
MTCS-5	B	1×56	22.4	8PSK	1×462	144	0.37	4
MTCS-6	A	1×74	29.6	8PSK	1×606	144	0.49	4
NOTE 1: Including FBI, E bits and CRC.								
NOTE 2: Encoded RLC/MAC header, USF and stealing bits.								
NOTE 3: Tail bits are viewed as channel coding redundancy.								

8.4.3.1.4   Turbo Codes with 16QAM Modulation

Three new 16QAM-modulated coding schemes with turbo codes are evaluated, called MTCS-7-16QAM, MTCS-8-16QAM and MTCS-9-16QAM, as defined in table 45. These have the same payload size as MCS-7, MCS-8 and MCS-9, respectively.

The RLC/MAC header, USF and stealing flags have the same channel coding as MCS-7-16QAM, MCS-8-16QAM and MCS-9-16QAM. The RLC data block has been encoded with a turbo code. For the turbo codes, the constituent codes, internal interleaver and rate matching defined for UTRAN [12] have been reused. Uniform (FLO) puncturing has been used for the RLC/MAC header and RLC data blocks. Interleaving is done over four bursts.

Table 45: 16QAM-modulated coding schemes with turbo codes

Modulation and coding scheme	Family	User PDU (bytes)	User Data Rate (kbps)	Modulation	Payload Length (see note 1)	Overhead (see note 2)	Payload Coding Rate (see note 3)	Interleaving depth
MTCS-7-16QAM	B	2×56	44.8	16QAM	2×462	168	0.55	4
MTCS-8-16QAM	A	2×68	54.4	16QAM	2×558	168	0.66	4
MTCS-9-16QAM	A	2×74	59.2	16QAM	2×606	168	0.72	4
NOTE 1: Including FBI, E bits and CRC.								
NOTE 2: Encoded RLC/MAC header, USF and stealing bits.								
NOTE 3: Tail bits are viewed as channel coding redundancy.								

8.4.3.2   Modulation

Simulations are run with 8PSK and 16QAM modulation. The 8PSK modulation is according to the definition in 3GPP TS 45.003.

The 16QAM modulation constellation is shown in figure 106. To reduce the Peak-to-AveRage ratio (PAR), the constellation is rotated by π/4 radians per symbol.

8.4.3.3   Pulse Shaping

For both 8PSK and 16QAM, the regular linearized GMSK pulse shape is used.

8.4.3.4   Link performance Evaluation

8.4.3.4.1   Simulation Assumptions

Scenario

The link level scenario is summarized in table 46.

Table 46: Summary of link simulation parameters.

Parameter	Value
Channel profile	TU
MS speed	3 km/h
Frequency hopping	Ideal
Interference	Co-channel
Radio blocks per simulation point	10 000

Impairments

Realistic transmitter and receiver impairment levels have been used. The details are described in tables 36 and 38 respectively. The power amplifier model reflects a state-of-the-art power amplifier with sufficient back-off. The distortion from the PA is in the order of 0.25 % EVM rms, which does not give noticeable impact on performance.

The downlink direction is studied, i.e. the transmitter is a BTS transmitter and the receiver is a terminal receiver.

Demodulator

8PSK: A state-of-the-art receiver is used.

16QAM: A 4-state RSSE equaliser is used. Channel tracking/frequency error correction is not implemented (for further study; the results for 16QAM may be slightly pessimistic). This receiver complexity is about 20 % higher than the 8PSK receiver.

Decoder for turbo codes

The turbo decoder is run eight iterations per decoding attempt. The constituent decoders are sub-optimum LOGMAX decoders.

8.4.3.4.2   Link Level Results

The link level performance at 10 % BLER and 1 % BLER is summarized in tables 47 and 48. Detailed simulation results can be found in annex B.

Table 47: Summary of link level performance @ 10 % BLER

Modulation/coding scheme	C/I @ 10 % BLER [dB]				Total gain (see note) [dB]
	Cc/8PSK	Tc/8PSK	Cc/16QAM	Tc/16QAM	
5	11.2	10.4	-	-	0.8
6	13.6	12.8	-	-	0.8
7	18.8	-	17.5	16.4	2.4
8	23.9	-	19.9	19.2	4.7
9	26.1	-	21.8	20.6	5.5
					NOTE: Best scheme vs EGPRS

Table 48: Summary of link level performance @ 1% BLER

Modulation/coding scheme	C/I @ 1% BLER [dB]				Total gain (see note) [dB]
	Cc/8PSK	Tc/8PSK	Cc/16QAM	Tc/16QAM	
5	15.0	13.9	-	-	1.1
6	17.1	16.2	-	-	1.1
7	23.1	-	21.4	20.3	2.8
8	30.5	-	24.3	23.4	7.1
9	32.8	-	26.3	24.9	7.9
					NOTE: Best scheme vs EGPRS

NOTE: Turbo coded equivalents of MCS-7, MCS-8 and MCS-9 with 8PSK modulation have also been evaluated but no gains were seen compared to convolutional codes. Therefore these results are not included in this report.

8.4.3.5 Link-to-system Interface

A two-stage mapping has been used. With this approach, the C/I is mapped to a block error ratio (BLEP) in two stages. In stage one, the model takes burst level C/I samples as input and maps them onto the (raw) Bit Error Probability (BEP) for a burst. In stage two, the BEP samples of one radio block are grouped together and used to estimate the BLEP. This is done by calculating the mean and the standard deviation of the burst BEP samples of the block, and mapping these parameters onto the BLEP. Finally, the BLEP value is used to calculate whether the particular radio block was in error.

8.4.3.6 System Level Results

8.4.3.6.1 Simulation Assumptions

Three different sets of modulation and coding schemes are compared. They are summarized in table 49.

Table 49: Evaluated sets of modulation/coding schemes.

Modulation and coding scheme	Set 1 ("EGPRS")	Set 2 ("16QAM")	Set 3 ("16QAM+turbo")
1	MCS-1	MCS-1	MCS-1
2	MCS-2	MCS-2	MCS-2
3	MCS-3	MCS-3	MCS-3
4	MCS-4	MCS-4	MCS-4
5	MCS-5	MCS-5	MTCS-5
6	MCS-6	MCS-6	MTCS-6
7	MCS-7	MCS-7-16QAM	MTCS-7-16QAM
8	MCS-8	MCS-8-16QAM	MTCS-8-16QAM
9	MCS-9	MCS-9-16QAM	MTCS-9-16QAM

A dynamic system level simulator has been used to evaluate performance for packet data. The simulator models the network with 5 ms granularity (i.e. on burst level).

The system level scenario is summarized in table 50.

Table 50: Summary of system simulation parameters.

Parameter	Value						
	Scenario 1	Scenario 2	Scenario 3	Scenario 4	Scenario 5	Scenario 6	Scenario 7
Reuse	1	4/12	4/12	1/3	1/3	3/9	3/9
Spectrum allocation	7.2 MHz (excluding BCCH)	7.2 MHz (excluding BCCH)	7.2 MHz (excluding BCCH)	7.2 MHz (excluding BCCH)	7.2 MHz (excluding BCCH)	7.2 MHz (excluding BCCH)	7.2 MHz (excluding BCCH)
Frequencies per cell	36	3	3	12	12	4	4
Transceivers per cell	12	3	3	12	12	4	4
Frequency hopping	Random	No	Random	Random	No	Random	No
Traffic model	FTP, 100 kB file size	FTP, 100 kB file size	FTP, 100 kB file size	FTP, 100 kB file size	FTP, 100 kB file size	FTP, 100 kB file size	FTP, 100 kB file size
Cell radius	500 m	500 m	500 m	2 km	2 km	2 km	2 km
Power control	No	No	No	No	No	No	No
Pathloss model	Okumura-Hata	Okumura-Hata	Okumura-Hata	Okumura-Hata	Okumura-Hata	Okumura-Hata	Okumura-Hata
Log-normal fading standard deviation	8 dB	8 dB	8 dB	8 dB	8 dB	8 dB	8 dB
Rayleigh fading	Yes	Yes	Yes	Yes	Yes	Yes	Yes
Multi-slot allocation per session	4 timeslots	4 timeslots	4 timeslots	4 timeslots	4 timeslots	4 timeslots	4 timeslots
Link quality control	Measurement based link adaptation	Measurement based link adaptation	Measurement based link adaptation	Measurement based link adaptation	Measurement based link adaptation	Measurement based link adaptation	Measurement based link adaptation
Power backoff 8PSK	3.3 dB	3.3 dB	3.3 dB	3.3 dB	3.3 dB	3.3 dB	3.3 dB
Power backoff 16QAM	5.3 dB	5.3 dB	5.3 dB	5.3 dB	5.3 dB	5.3 dB	5.3 dB

The system performance is measured as the average FTP session bit rate versus offered load. Offered load is defined as the total amount of transferred bits in the system averaged over all available timeslots and time.

8.4.3.6.2   Results

The three different modulation and coding sets have been investigated in the above described radio network scenarios. Below, the system level results are summarised. Power backoff according to table 50 is included in all simulations. A comparison of performance with and without backoff is presented in subclause 8.4.3.6.2.4.

8.4.3.6.2.1   Scenario 1: 1-reuse with Random Frequency Hopping

Scenario 1, 1-reuse with random frequency hopping, is the tight reuse scenario of the investigation and could for example be users on traffic channels that are tightly planned due to limited spectrum.

Figure 130 shows the average session bit rate for different user percentiles (10th, 50th and 90th percentile). This allows for an analysis of how users in different radio quality situations are affected by the introduction of higher order modulation and turbo coding.
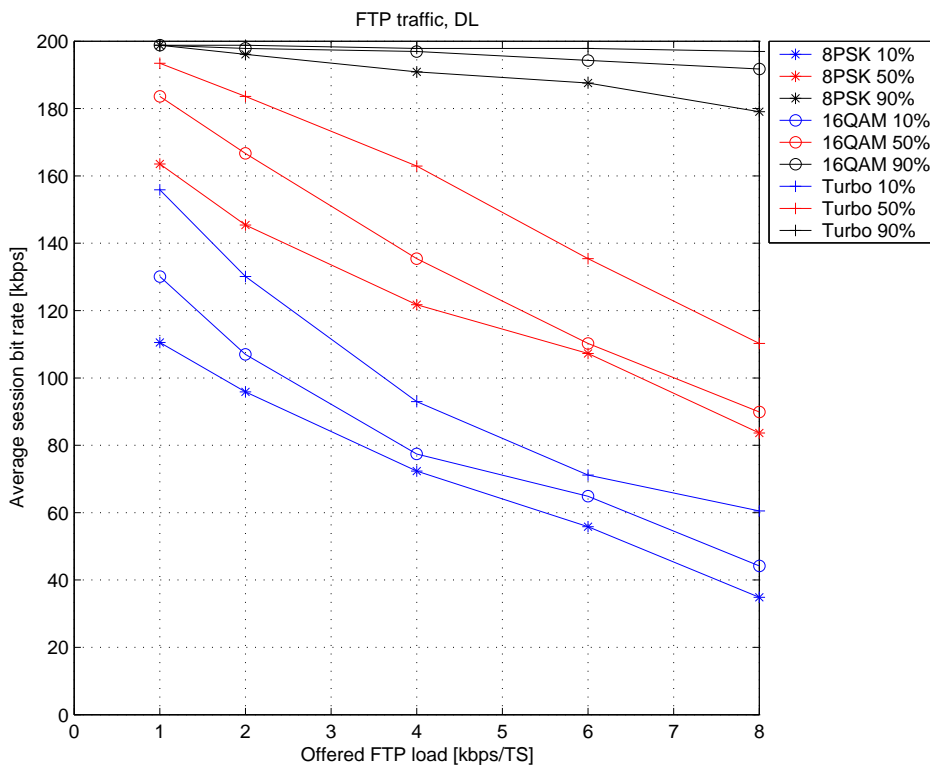
**Figure 130: Average session bit rate percentiles, 10th percentile (blue), 50th percentile (red)
and 90th percentile, as a function of offered FTP load, for MCS set 1, 2 and 3**

In figure 130 it can be seen that the users with the best radio quality (90th percentile) do not gain very much, up to approximately 10 % gain for the highest load case. However, the users with worse radio quality (10th and 50th percentiles) experience significantly higher gains. The general gains on the 10th percentile are approximately 35 % to 40 % for 16QAM + turbo, and 15 % to 20 % with plain 16QAM. For the median users (50th percentile) the general session bit rate gains are approximately 20 % to 30 % for the 16QAM + turbo set, and 5 % to 15% for the 16QAM set.

Furthermore, the improvement in bit rate performance lowers the load of the system, since the staying time of each user gets shorter. This improves the capacity of the system. Figure 131 shows an example where the normalised spectrum efficiency is shown for different service requirements. It is important to note that the relative capacity gain depends highly on the chosen service requirement. If the bit rate requirement is higher, the relative capacity gain from higher order modulation and turbo coding gets higher, but the total capacity gets lower. Taking that into account and choosing for example a 60 kbps bit rate requirement, it can be seen in figure 131 that the capacity gain with 16QAM + turbo is just below 50 %.
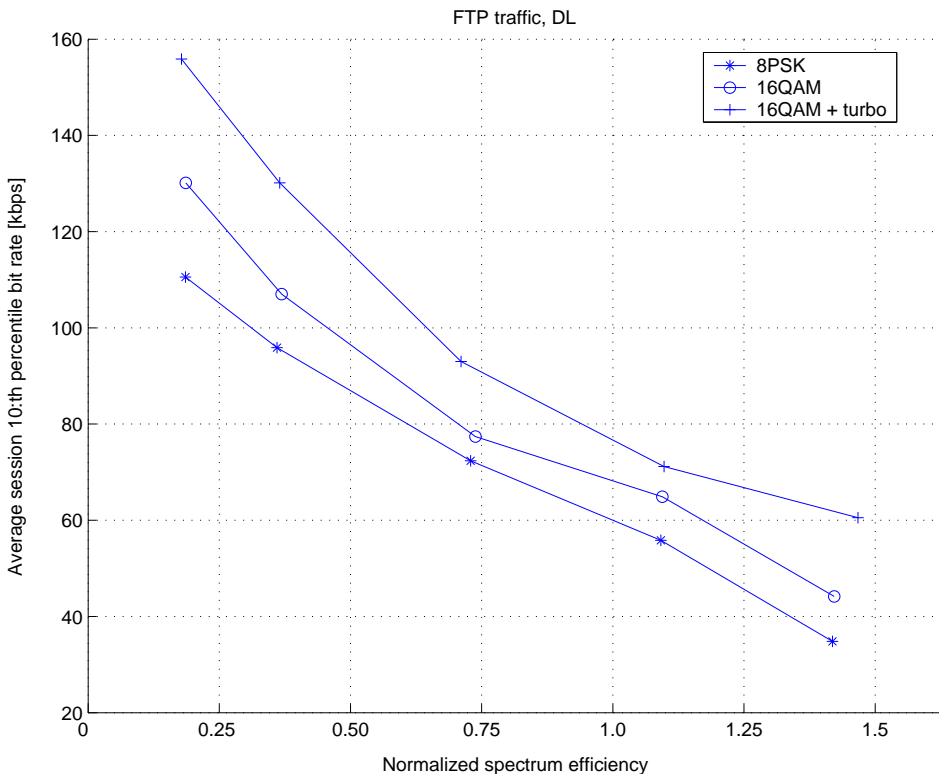
Figure 131: Normalised spectrum efficiency as a function of different service requirements, for 1-reuse with frequency hopping

8.4.3.6.2.2   Scenario 2: 12-reuse without Frequency Hopping

Scenario 2, 12-reuse without frequency hopping, is one of the sparse reuse scenarios investigated and could for example be users on a broadcast channel (see Note) that is sparsely planned to ensure secure signalling operation.

NOTE : three non-hopping frequencies are used per cell in this scenario, thus it is not identical to a scenario where EDGE is deployed on BCCH frequencies. However, similar performance can be expected. This scenario was chosen to allow a comparison with the other scenarios.

Figure 132 shows the average session bit rate for different user percentiles (10th, 50th, and 90th percentile). This allows for an analysis of how users in different radio quality situations are affected by the introduction of higher order modulation and turbo coding.
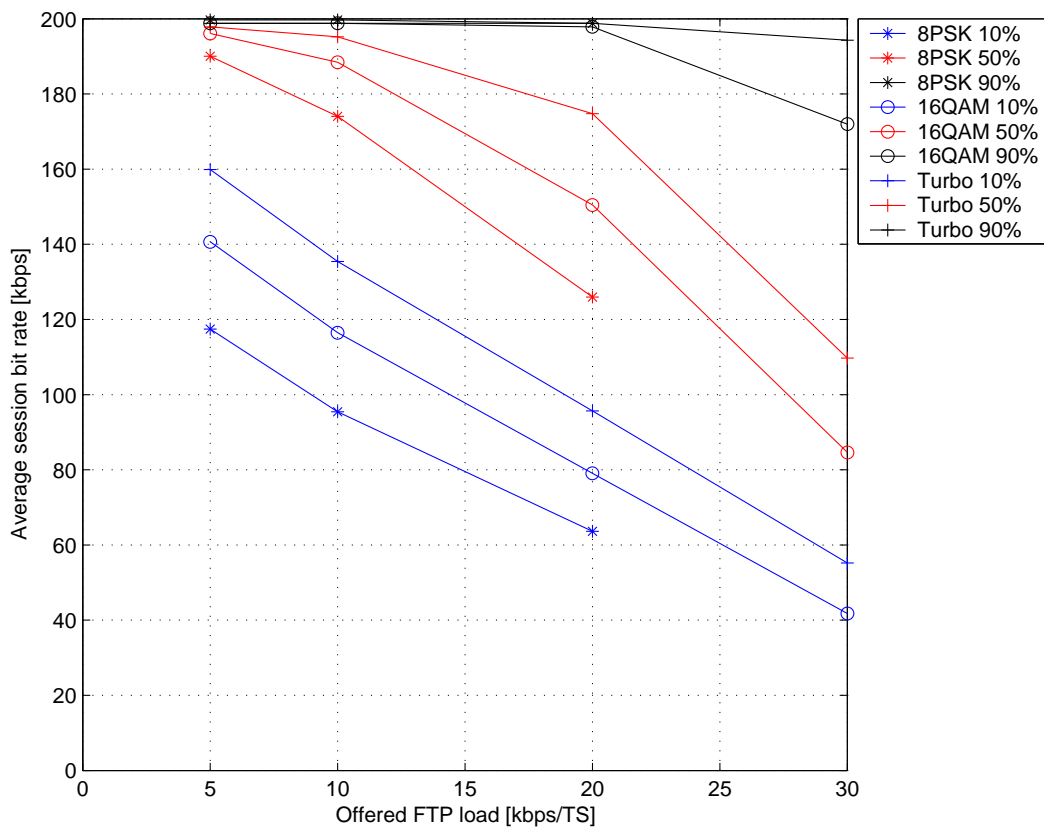
Figure 132: Average session bit rate percentiles, 10th percentile (blue), 50th percentile (red), 90th percentile (black), as a function of normalised system load, for MCS set 1, 2 and 3

In figure 132 it can be seen that also for the 12-reuse, the gains for the 90th percentile users are limited. For the users with lower radio quality (10th and 50th percentiles) the gain is substantial. The general gain at the 10th percentile is approximately 40 % to 45 % with the 16QAM + turbo set and 20 % to 25 % with the 16QAM set, depending on system load. For the 50th percentile these general gains are approximately 20 % to 40 % for 16QAM + turbo and 10 % to 20 % for 16QAM, depending on system load.

NOTE: The bit rate curves for EGPRS do not reach an offered load of 30 kbps/TS since that load cannot be offered with EGPRS in this scenario.

Furthermore, the improvement in bit rate performance lowers the load of the system, since the staying time of each user gets shorter. This improves the capacity of the system. Figure 133 shows an example where the normalised spectrum efficiency is shown for different service requirements. It is important to note that the relative capacity gain depends highly on the chosen service requirement. If the bit rate requirement is higher, the relative capacity gain from higher order modulation and turbo coding gets higher, but the total capacity gets lower. Taking that into account and choosing for example a 80 kbps bit rate requirement (see Note), it can be seen in figure 133 that the capacity gain with 16QAM + turbo is just above 60 %.

NOTE : A different level is chosen here since all curves do not reach the 60 kbps/TS level used in the 1-reuse scenario.
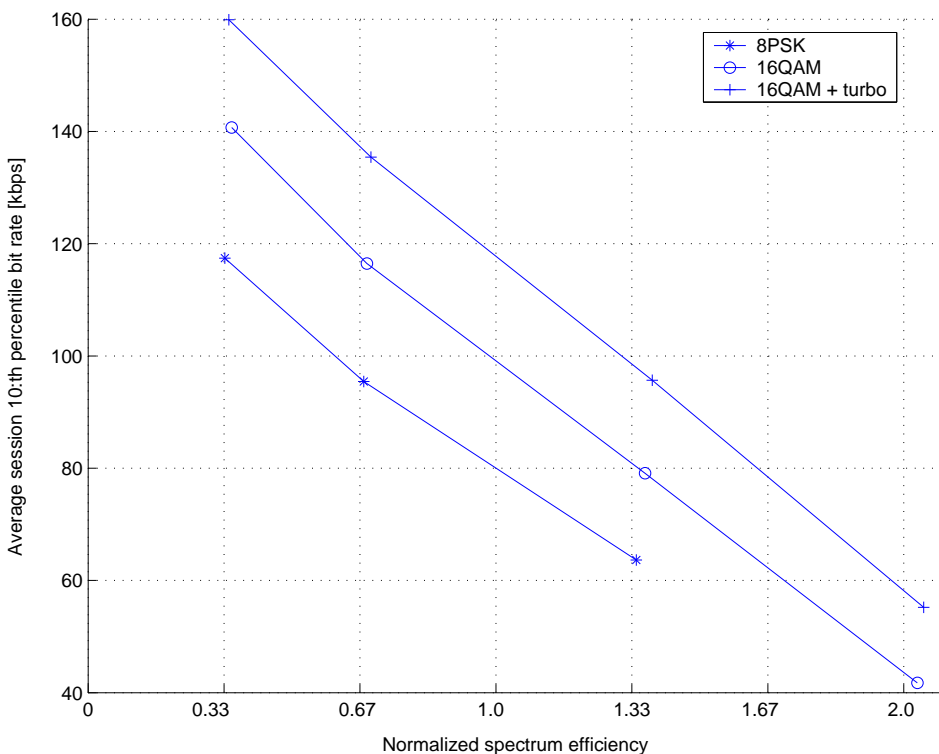
Figure 133: Normalised spectrum efficiency as a function of different service requirements, for 12-reuse without frequency hopping

8.4.3.6.2.3 Scenario 3: 12-reuse with Random Frequency Hopping

Scenario 3, 12-reuse with frequency hopping, is the other of the sparse reuse scenarios investigated and could for example be users on a traffic channel that is sparsely planned due to more generous spectrum availability.

Since frequency hopping does not make very large differences in performance for packet data services in sparse reuse scenarios, performance with and without frequency hopping are given in the same plot.

Figure 134 shows the same curves as in figure 132 only the corresponding results with frequency hopping have been added with dashed lines.
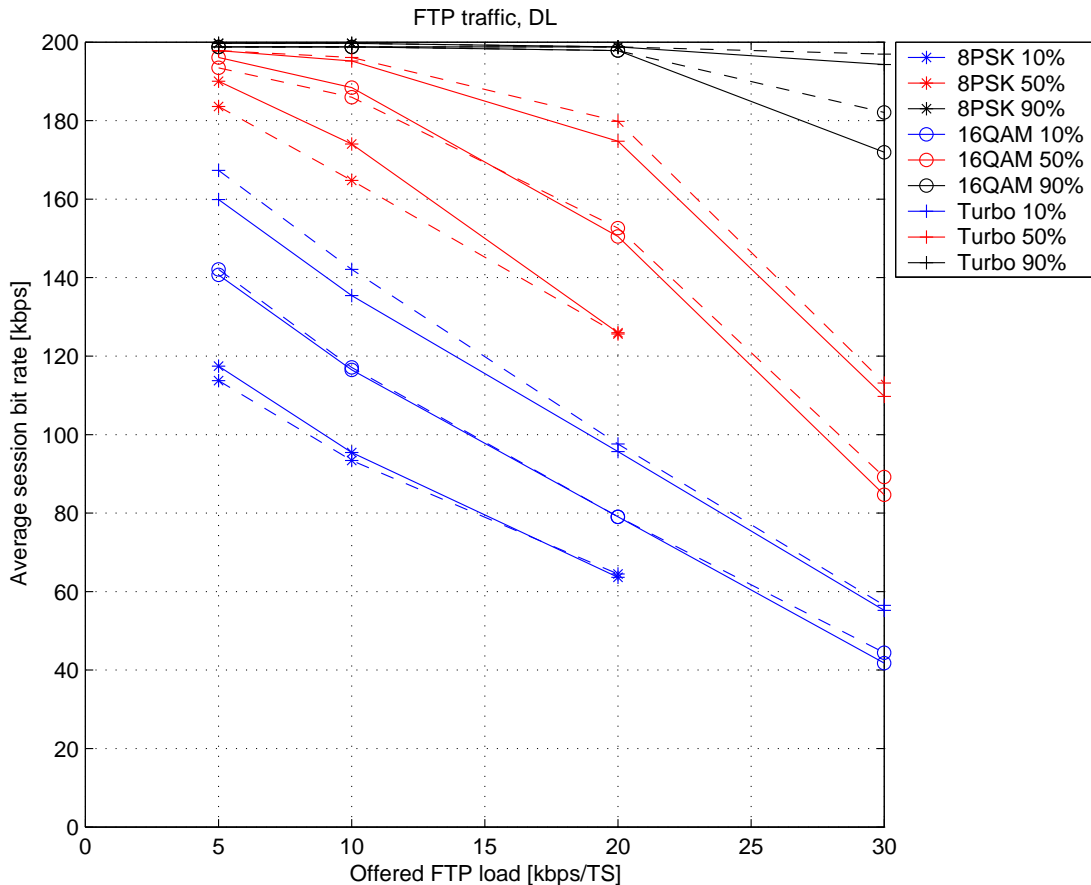
Figure 134: Average session bit rate percentiles, 10th percentile (blue), 50th percentile (red), 90th percentile (black). 12-reuse without frequency hopping (solid) and with frequency hopping (dashed), for MCS set 1, 2 and 3

Figure 134 shows that the performance is quite similar both with and without frequency hopping in the 12 reuse scenario. It is however visible that frequency hopping gives a very slight decrease in performance for standard 8PSK, while it gives a very small improvement for 16 QAM and a slightly higher performance with 16QAM + turbo, where the increased diversity can be exploited. In total, the general improvements in session bit rates are further increased by a few percent with 16QAM and slightly more with 16QAM + turbo, by the introduction of frequency hopping.

8.4.3.6.2.4 Scenario 4 and 5: 1/3-reuse

Figure 135 shows the average session bit rate for different user percentiles (10th, 50th and 90th percentile). Dashed lines are with frequency hopping, solid lines are without frequency hopping. As in [4], the gains for the 90th percentile of users (session bit rates) are small since they are near the peak bit rate already with EGPRS. The gains on the 10th percentile are 35 % to 50 % for 16QAM+turbo codes and 10 % to 15 % from 16QAM alone. On the 50th percentile, the gains are 10 % to 30 % for 16QAM+turbo codes and 5 % to 15 % from 16QAM. The lower end of the gain intervals corresponds to the lowest offered FTP load. Note that the lower gain (5 % or 10 %) of the 50th percentile is due to that the peak rate is almost reached.
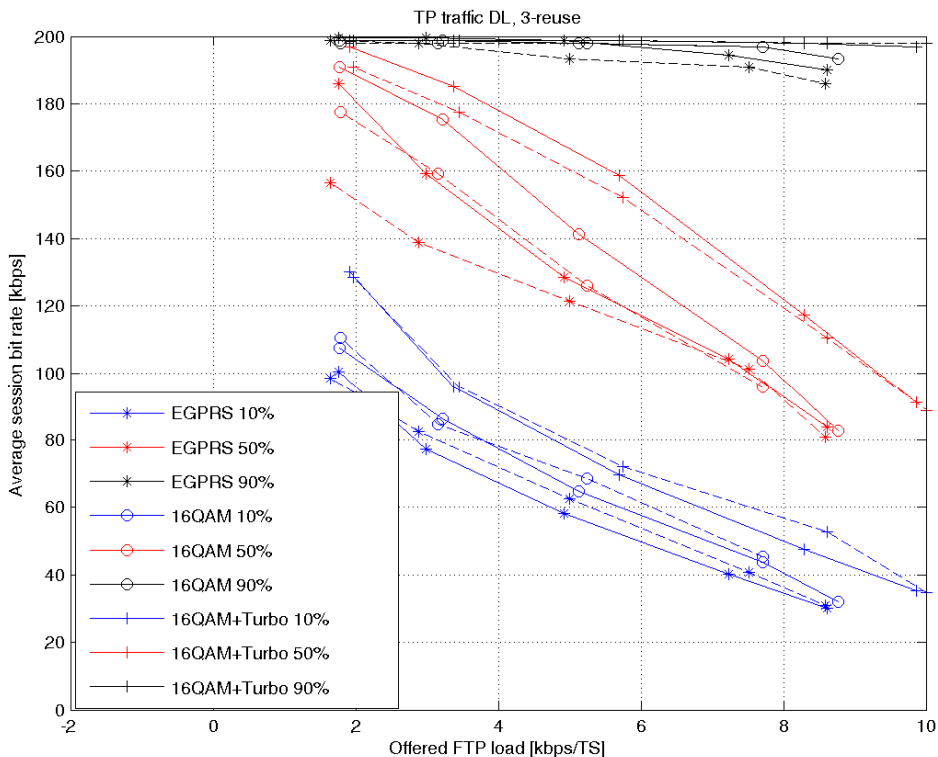
Figure 135: Average session bit rate percentiles, 10th percentile (blue), 50th percentile (red), 90th percentile (black), as a function of offered FTP load, for EGPRS, 16QAM and 16QAM+turbo Dashed lines are with frequency hopping, solid lines are without frequency hopping

Figure 136 shows normalized spectrum efficiency. The spectrum efficiency depends on the required bit rate (for the 10th percentile, i.e. for 90 % of the sessions). If for example the requirement is 60 kbps (shown as a red dashed line in the figure), the spectrum efficiency gain for 16QAM+turbo codes is 44 % without frequency hopping and 42 % with frequency hopping. For plain 16QAM, the gain is 21 % without frequency hopping and 16 % with frequency hopping.

FTP traffic DL
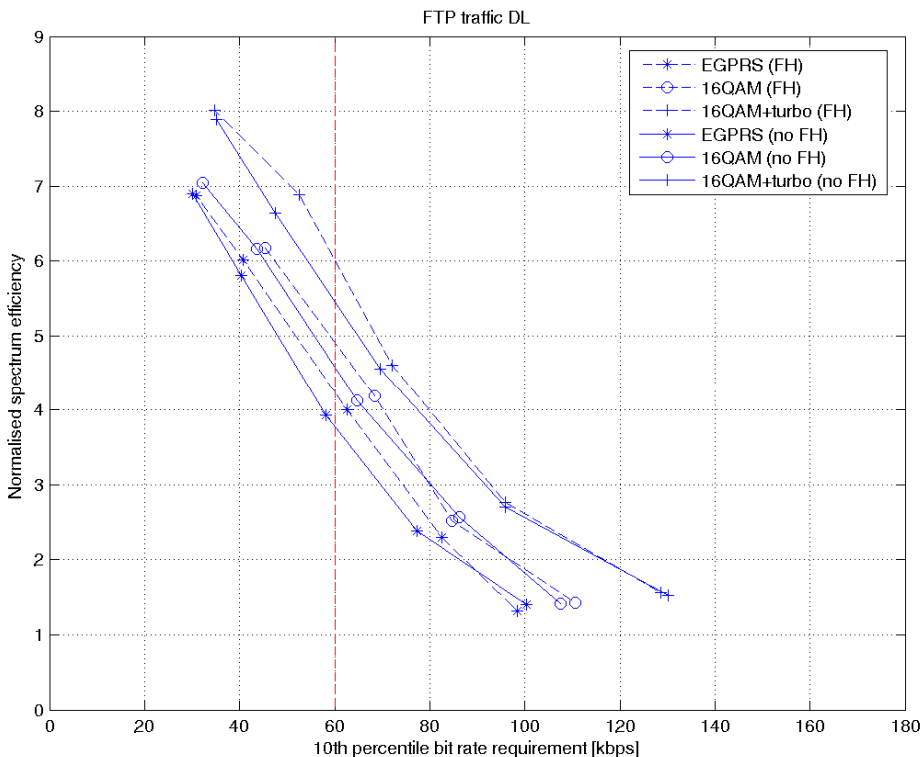
**Figure 136: Normalised spectrum efficiency as a function of different service requirements
Dashed lines are with frequency hopping, solid lines are without frequency hopping**

8.4.3.6.2.5 Scenario 6 and 7: 3/9-reuse

Figure 137 shows the average session bit rate for different user percentiles (10th, 50th, and 90th percentile). Dashed lines are with frequency hopping, solid lines are without frequency hopping. Again, the gains for the 90th percentile of users (session bit rates) are small since the bit rates are near the peak bit rate already with EGPRS. The gains on the 10th percentile are 30 % to 40 % for 16QAM+turbo codes and 10 % to 25 % from 16QAM alone. On the 50th percentile, the gains are 2 % to 35 % for 16QAM+turbo codes and 2 % to 20 % from 16QAM. The lower end of the gain interval corresponds to the lowest offered FTP load. Note that the lower gains (2 %) at the 50th percentile are due to that the peak rate is almost reached.
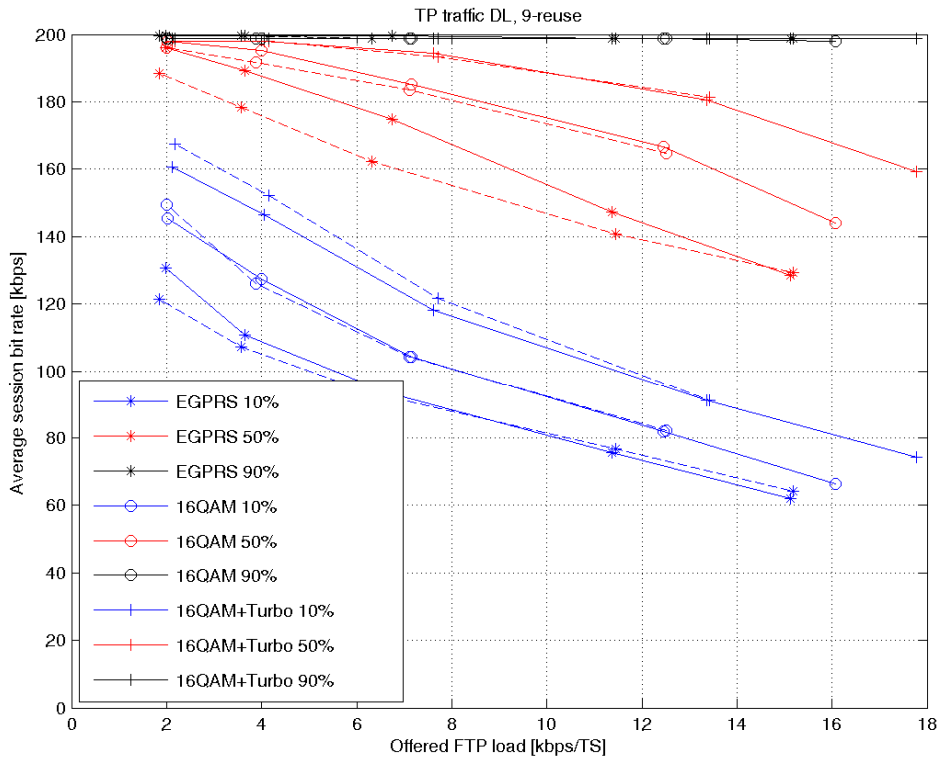
Figure 137: Average session bit rate percentiles, 10th percentile (blue), 50th percentile (red), 90th percentile (black), as a function of offered FTP load, for EGPRS, 16QAM and 16QAM+turbo Dashed lines are with frequency hopping, solid lines are without frequency hopping

Figure 138 shows normalised spectrum efficiency. The spectrum efficiency depends on the required bit rate (for the 10th percentile, i.e. for 90 % of the sessions). If for example the requirement is 90 kbps (shown as a red dashed line in the figure), the spectrum efficiency gain for 16QAM+turbo codes is 82 % without frequency hopping and 87 % with frequency hopping. For plain 16QAM, the gain is 40% without frequency hopping and 44% with frequency hopping.
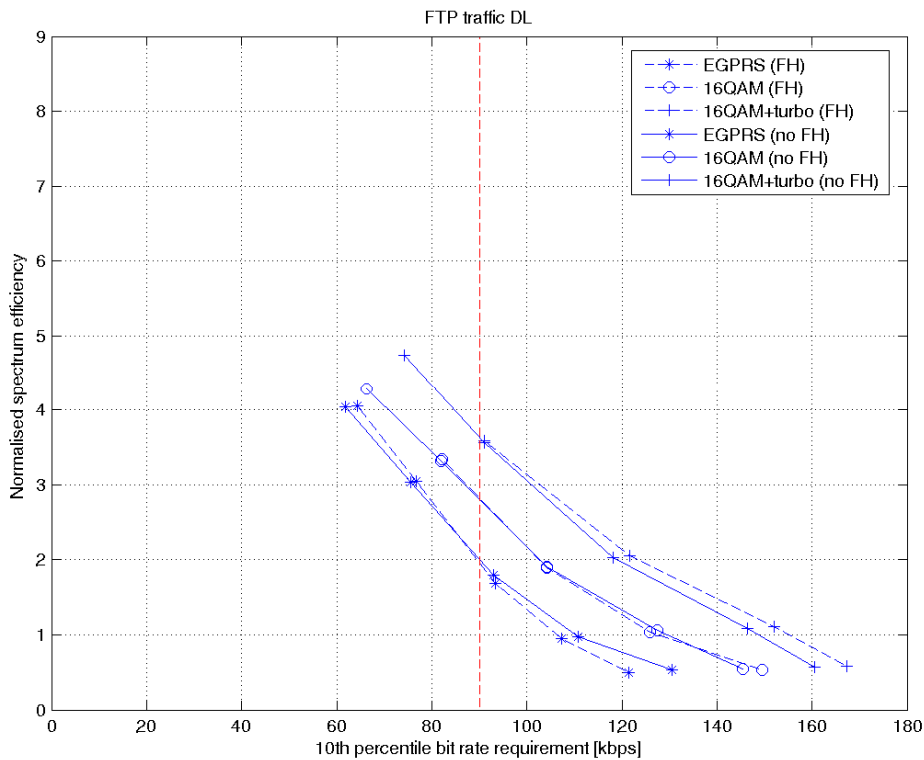
**Figure 138: Normalised spectrum efficiency as a function of different service requirements
Dashed lines are with frequency hopping, solid lines are without frequency hopping**

8.4.3.6.2.6   The Impact of Power Back Off

In the above results, the power back off factors given in table 50 have been used. In a similar manner as with frequency hopping, it has also been investigated how the removal of the power back off factors affects the results. This means that all the three modulations (GMSK, 8PSK, and 16QAM) will be using the same output power.

Figure 139 shows the same plot as in figure 132, but the corresponding results without power back off have been added with dashed lines.
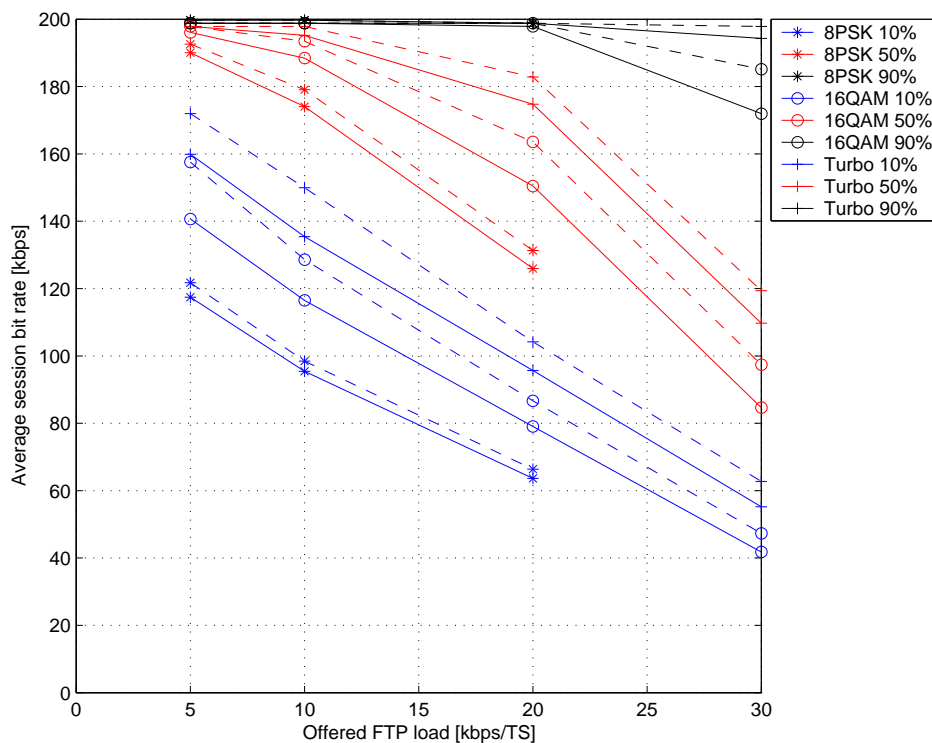
Figure 139: Average session bit rate percentiles, 10th percentile (blue), 50th percentile (red), 90th percentile (black). 12-reuse with power back off (solid) and without power back off (dashed), for MCS set 1, 2 and 3

Figure 139 shows that average session bit rates are slightly higher without power back off. However, the relative gains achieved by using higher order modulation and turbo coding are quite similar both with and without power back off.

8.4.3.7 Increased Peak Throughput with 16QAM and Turbo Codes

In this subclause two new MCSs are defined that increase the peak throughput compared to the conventional MCSs in EDGE today.

8.4.3.7.1 Modulation, Coding and Interleaving

To increase the peak throughput higher than MCS-9, new modulation and coding schemes need to be defined. Two new MCSs have been considered, MCS-10 and MCS-11, the former one has also been evaluated in combination with turbo codes (MTCS-10). MCS-11 has been chosen to be un-coded and thus the addition of turbo codes will not have an impact on the performance. In table 51 the PDU sizes, code rates of the data and header and interleaving depth are shown. Note that in table 51 only the uplink is considered but the MCSs can also be defined for the downlink. The only difference will be an addition of USF bits, resulting in a slightly less robust header.

Table 51: Block sizes, code rates and interleaving depth of MCS-10 and MCS-11

MCS	Family	Dir.	User PDU [bytes]	User data rate [kbps]	Payload [bits]	Interleaving depth	Data code rate	Header code rate
MCS-10	B	UL	3x56	67.2	3x448	4	0.83	0.42
MTCS-10	B	UL	3x56	67.2	3x448	4	0.82	0.42
MCS-11	A	UL	3x68	81.6	3x544	2	1	0.42

It can be seen that both MSC-10 and MCS-11 consist of 3 RLC-blocks which fall into the families B and A respectively. Thus MCS-10 contains three MCS-7 RLC blocks and MCS-11 contains three MCS-8 RLC blocks.

8.4.3.7.1.1   Coding

Each RLC block is encoded separately (joint coding is for further study). The same mother convolutional code as used today in combination with linear puncturing has generated the coded header and data bits. For MCS-10 with turbo coding (MTCS-10) the turbo code defined for UTRAN has been used [15]. The puncturing schemes for the turbo codes have been generated by prioritizing the systematic bits and additionally puncturing the two parity bits streams (rate 1/3 code) in a linear manner with minimal overlap between IR puncturing schemes.

8.4.3.7.1.2   Interleaving

For the MCS used today, depending on what MCS is used the number of bursts over where the interleaving is performed differs. For MCS-7 the data bits in the RLC block is interleaved over all four bursts while for MCS-8-9 the interleaving is performed over two bursts for each RLC block. The reason for this is the coding rate of the MCSs; a high code rate will experience small gains (or even lose) in performance with increased diversity. This also applies to MCS-10 and MCS-11 where the RLC blocks for MCS-10 are interleaved over all four bursts while for MCS-11 the interleaving is performed over two bursts. One difference between MCS-11 compared to MCS-8-9 is that the RLC block errors will be more correlated since the different blocks are not entirely separated, as is depicted in figure 140.
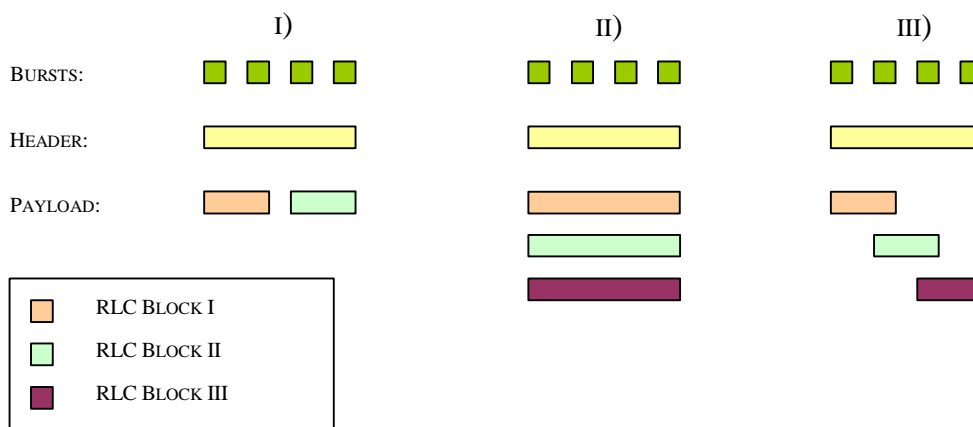
**Figure 140: Schematic figure of header and RLC block interleaving for
I) MCS-8 & MCS-9; II) MCS-10; III) MCS-11**

8.4.3.7.2   Link Performance

A state-of-the art link level simulator for GSM/EDGE has been used to evaluate the performance of the new modulation and coding schemes. The simulator parameters are shown in table 52.

Table 52: Link simulator settings

Parameter	Value
Channel profile	Typical Urban (TU)
Terminal speed	3 km/h
Frequency band	900 MHz
Frequency hopping	Ideal
Interference	Single co-channel interferer
Direction	Uplink
Antenna diversity	No
Impairments: - Phase noise - I/Q gain balance -I/Q phase imbalance - DC offset - Frequency error - PA model	Tx / Rx 0.8 / 1.0 [degrees (RMS)] 0.1 / 0.2 [dB] 0.2 / 1.5 [degrees] -45 / -40 [dBc] - / 25 [Hz] Yes/ -

Figure 141 shows the throughput curves of MCS-10 and MCS-11 both using 16QAM modulation. For MCS-10 the performance when adding turbo codes is also shown. MCS-9 as used in EDGE today is shown as reference.
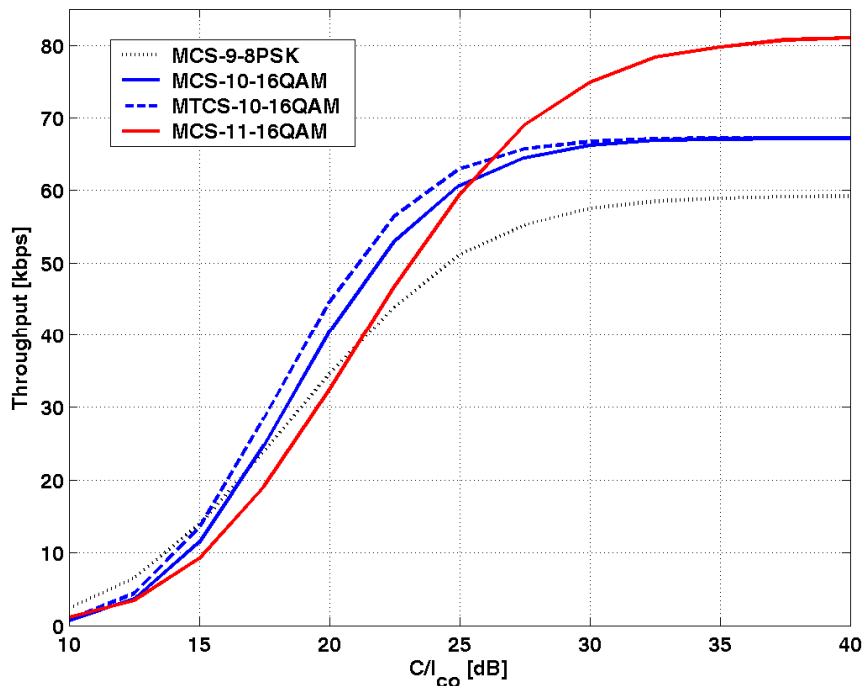
**Figure 141: Throughput gain by using HOMTC including MTCS-10 and MCS-11
The different sets are defined in table 53**

It can be seen that MTCS-10 is superior to MCS-9 at C/I levels above 17 dB. When turbo coding is added the point is moved to 15 dB. It should be noted that the puncturing scheme for MTCS-10 has been improved since the results in [29] giving an additional improvement of approximately 0.5 dB. From the figure it can also be seen that the peak throughput can be increased from 59.2 kbps to 81.6 kbps by using MCS-11 - an increase of 38 %. The peak throughput available today, 59.2 kbps, is exceeded at C/I levels above 23 dB.

Figure 142 evaluates the throughput performance at different C/Is when MCS-10 and MCS-11 is combined with MCS-5-9 with and without turbo codes and 16QAM, see table 53.

Table 53: Sets of MCSs used for ideal LA in figure 142

Set	Utilized MCSs
EDGE	MCS-5-9: 8-PSK
Set 1	MCS-5 and MCS-6: 8-PSK MCS-7-11: 16QAM
Set 2	MCS-5 and MCS-6: 8-PSK and TC MCS-7-10: 16QAM and TC MCS-11: 16QAM
Set 3	MCS-7-9: 8-PSK and IR
Set 4	MCS-7-11:16QAM and IR
Set 5	MCS-7, MCS-9 and MCS-10: 16QAM, TC and IR MCS-11: 16QAM and IR

Ideal link adaptation has been assumed for the sets both with and without incremental redundancy. Thus, for a certain C/I level the MCS giving the largest throughput is chosen.
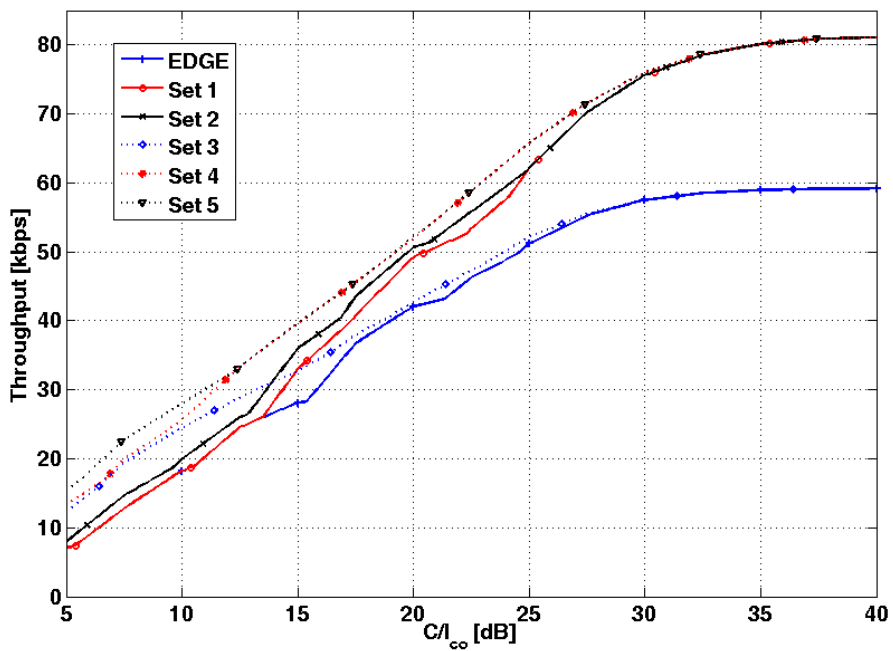
Figure 142: Throughput as a function of C/I. Ideal LA assumed

Figure 142 shows that there are substantial gains by introducing the MCSs for increased peak throughput. The peak throughput increased by 38 %. Without IR, the peak throughput of today is exceeded for C/I above 23 dB (comparing Set 2 with the EDGE set). Similar gains are shown when IR is introduced as shown in Set 3 and 5. Comparing Set 4 and Set 5 it is seen that, in IR mode (two retransmissions included), MCS-11 is actually used until C/I = 12 dB.

In table 143 the throughput gains by using HOM and TC are compared to the MCSs used today in EDGE. As was also seen in figure 142 there is a gain in the whole C/I region. The largest gains are at high C/I and is a result from the introduction of MCS-10 and MCS-11. Similar gains are seen when IR is introduced. The average gain in throughput is approximately 25 % both with and without incremental redundancy.
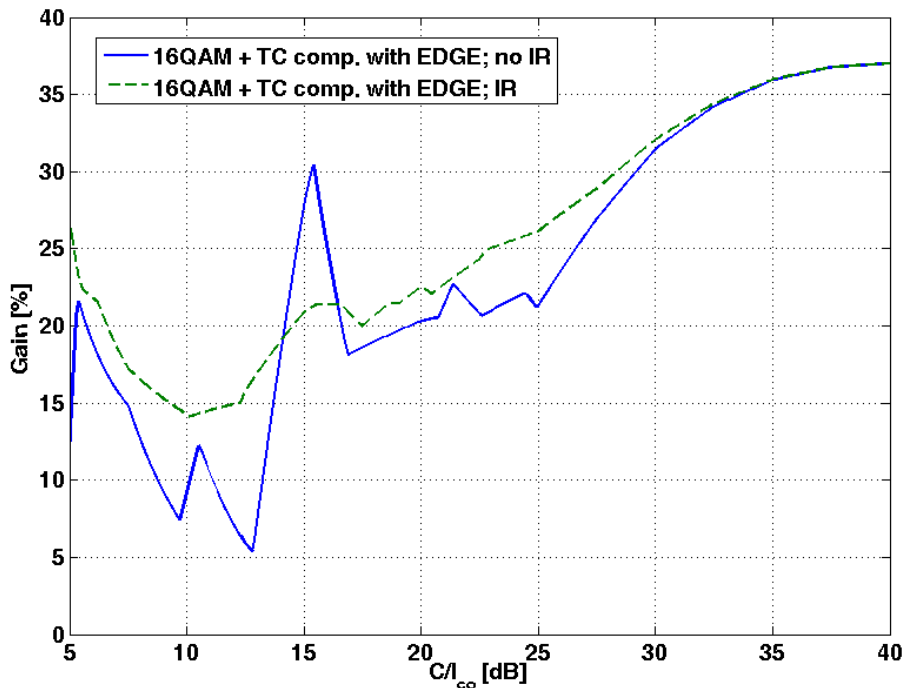
Figure 143: Throughput gain by using HOMTC including MTCS-10 and MCS-11
The different sets are defined in table 53

8.4.3.7.3   System Performance

System simulations in subclause 8.4.3.6 have shown significant gains in spectral efficiency and average session bit rates when introducing HOM and/or TC for robustness (MCS-5-9), see [8], [9] and [29]. It was shown that the spectral efficiency could be increased up to 40 % to 60 % depending on the frequency reuse in the system. Also, gains in average session bit rates were shown to be between 30 % to 45 % for the median and worst users. For users in good radio conditions the gain was not seen as clear, thus the performance limitation lied clearly in the peak throughput that was reached both with and without HOM+TC. In this subclause additional results are shown where MCS-10 and MCS-11 also have been included in the simulations. Since these MCSs increase the peak throughput, an increase of mean throughput in the system is expected, especially for the users in good radio conditions. Also, since the staying time in the system will be shorter for users utilizing these higher MCS, the overall interference level will decrease and giving rise to a more spectrally efficient system and an increase of average user bit rates.

It should be noted that the simulations presented in this subclause have used a link quality controller (LQC) not optimized for the addition of MCS-10 and MCS-11.

In table 54 the simulation parameters are shown for the simulated scenario. Frequency reuse 1 is used where the traffic model consists of each user downloading a file of 100 kB with FTP.

Table 54: System simulator settings

Parameter	Value
Reuse	1
Spectrum allocation	7.2 MHz (excluding BCCH)
Frequencies per cell	36
Transceivers per cell	12
Frequency hopping	Random
Traffic model	FTP, 100 kB file size
Cell radius	500 m
Power control	No
Pathloss model	Okumura-Hata
Log-normal fading standard deviation	8 dB
Rayleigh fading	Yes
Multi-slot allocation per session	4 timeslots
Average MS speed	3 m/s
Link quality control - Initial MCS - MCS selection criteria	Measurement based link adaptation MCS-3 Throughput maximisation
Power backoff 8PSK	3.3 dB
Power backoff 16QAM	5.3 dB

Simulations with two different sets of MCSs have been performed. Both sets use the newly defined 16QAM MCSs with turbo coding, but Set B also include MTCS-10 and MCS-11; details are shown in table 55.

Table 55: Sets of MCSs used in the simulations

Modulation and coding scheme	Set A	Set B
1	MCS-1	MCS-1
2	MCS-2	MCS-2
3	MCS-3	MCS-3
4	MCS-4	MCS-4
5	MTCS-5	MTCS-5
6	MTCS-6	MTCS-6
7	MTCS-7-16QAM	MTCS-7-16QAM
8	MTCS-8-16QAM	MTCS-8-16QAM
9	MTCS-9-16QAM	MTCS-9-16QAM
10	-	MTCS-10-16QAM
11	-	MCS-11-16QAM

In figure 144 the average session bit rates versus offered load are shown. It can be seen that there is a significant throughput gain for the 90th percentile of between 12 % to 20 % depending on the load. For the 10th and 50th percentile the session bit rates seem to be unchanged since the small difference in bit rates that are seen can rather be explained by statistical effects than difference in performance. With an optimized LQC gains are expected also for these percentiles.
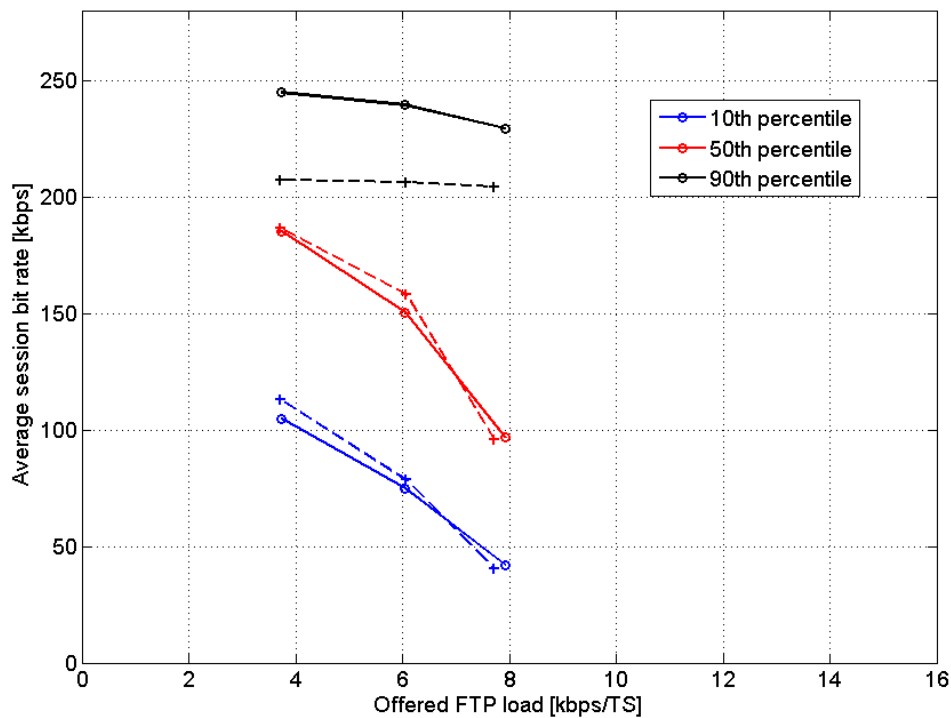
**Figure 144: Average session bit rates versus frequency load for the 10th, 50th and 90th percentile
The two sets of MCSs used are defined in table 54
In the figure Set A is dotted**

8.4.3.8   16QAM with Alternative Transmit Pulse Shaping

Since decoding of turbo codes is computationally complex, it may not be feasible in all legacy BTS equipment without hardware impacts. Hardware impacts to legacy networks should be avoided according to the objectives of the GERAN Evolution Feasibility Study [2]. It is therefore of interest to look at alternative improvement methods for the uplink that can be combined with higher order modulations.

One such enhancement is to use other transmit pulse shapes than the linearised GMSK pulse normally used for EDGE. In the following subclauses, root-raised cosine (RRC) pulses are evaluated.

8.4.3.8.1   Link Performance

Link simulations have been run to evaluate the performance of different RRC Tx pulses.

8.4.3.8.1.1   Simulation Conditions

The simulation assumptions are summarised in table 56.

Table 56: Simulation parameters

Parameter	Value
Modulation/coding scheme	MCS8-16QAM
Channel	TU3 iFH (co-channel) TU50 noFH (sensitivity)
Tx and Rx pulse shaping filter	RRC, rolloff=0.3, rectangular window, length=51 symbols
RRC Tx and RX pulse single sided 3 dB-bandwidth	110 kHz 120 kHz 135 kHz
Tx impairments	None
Rx impairments	Phase noise: 1.0 deg. RMS I/Q amplitude gain imbalance: 0.2 dB I/Q phase imbalance: 1.5 deg Frequency error: 25 Hz DC offset: -40 dBc
Backoff	Not included
Simulation length	10 000 bursts per simulation point

8.4.3.8.1.2   Simulation Results

Figure 145 shows co-channel interference limited link level performance with different RRC Tx pulses and Rx filters. Performance with a linearised GMSK Tx pulse is shown as reference. The interferer is a legacy GMSK modulated signal.
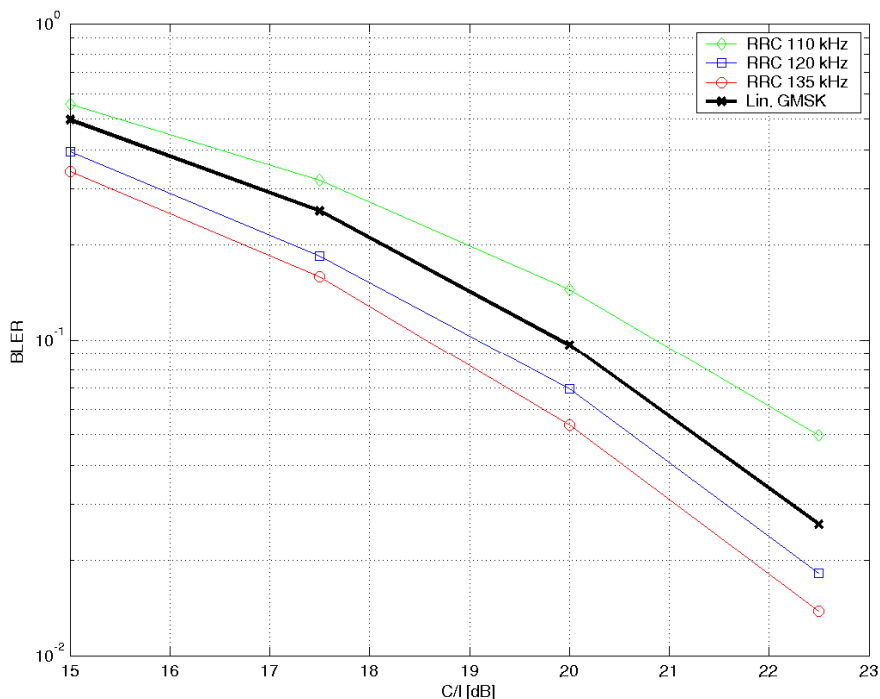
Figure 145: Co-channel performance for MCS8-16QAM with different Tx pulse shaping filters and Rx filters. The filter bandwidths shown in the plots are single sided

Figure 146 shows sensitivity limited link level performance with different RRC Tx pulses and Rx filters. Performance with a linearised GMSK Tx pulse is shown as reference.
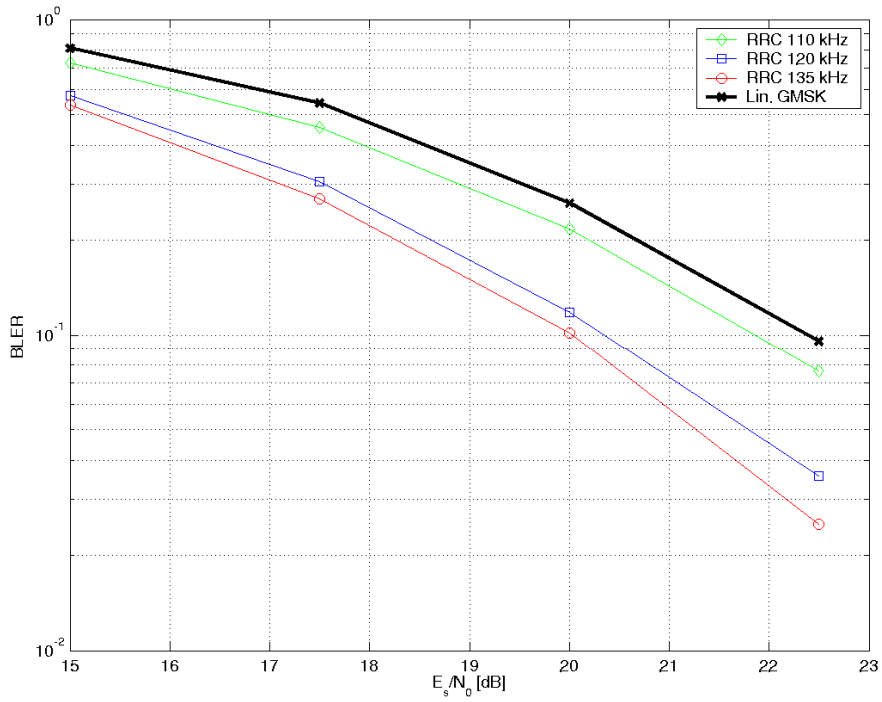
Figure 146: Sensitivity performance for MCS8-16QAM with different Tx pulse shaping filters and Rx filters. The filter bandwidths shown in the plots are single sided

8.4.3.8.2   Spectrum

Figure 147 shows the spectrum of 16QAM with different Tx pulse shaping filters. It can be seen that the RRC pulse with 110 kHz ssb bandwidth fulfils the GSM spectrum mask.
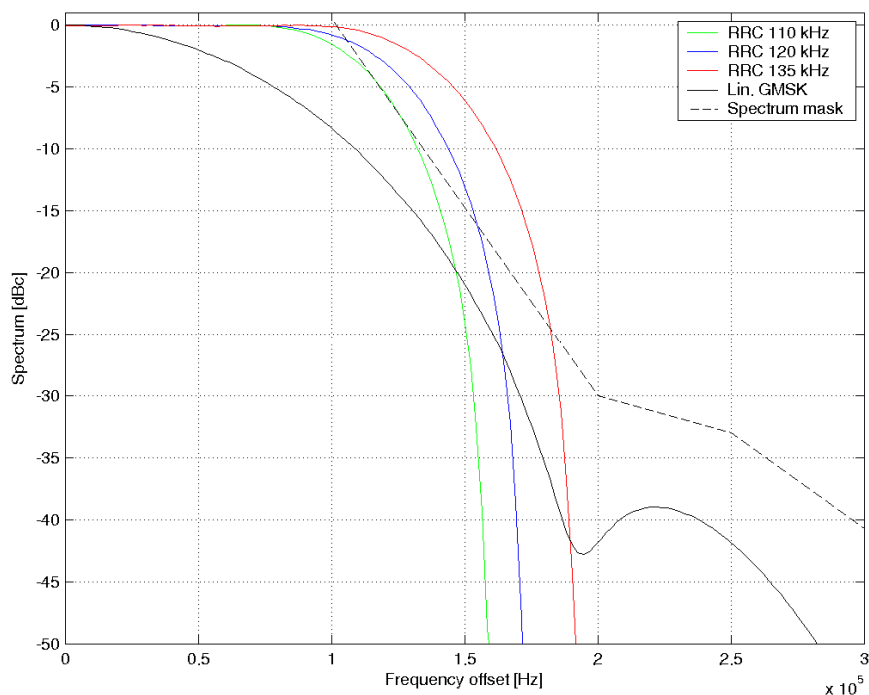
**Figure 147: Spectrum of 16QAM with linearised GMSK pulse and different RRC pulses
The 8PSK spectrum mask for MS [8] is also shown**

8.4.3.8.3   Discussion

Figure 145 shows that a RRC Tx pulse with a SSB bandwidth of 135 kHz gives gains of 1.5 dB in a co-channel interference limited scenario. Figure 146 shows that the gain in a sensitivity limited scenario is 2.5 dB for the same Tx pulse. With a narrower RRC Tx pulse, the gain is reduced. A pulse with a SSB bandwidth of 110 kHz gives a loss of 1 dB in the co-channel scenario but a sensitivity gain of 0.5 dB.

The gains with a wide RRC Tx pulse are in the same order as those of turbo codes, or even larger. A preliminary conclusion is therefore that the system level gains in the order of 30 % shown previously for 16QAM+turbo codes can be achieved with this alternative method (i.e., higher order modulation combined with a wider Tx pulse).

Note that the gains from turbo codes and the gains from a new transmit pulse shape are likely additive. Therefore, it can be considered to have an option of turbo codes in addition to the higher order modulation with new transmit pulse shape.

8.4.3.9   Higher order modulation than 16-QAM

Increasing the modulation order will make the symbols more susceptible to interference and thus the higher order the modulation the better radio conditions are needed to gain in performance. Also, increasing the modulation order to 32QAM, or maybe even to 64QAM, will probably result in such an increase of receiver complexity that new hardware is needed in both base stations and mobile stations.

Three new MCSs have been defined for 32QAM, giving a peak throughput of up to 99.2 kbps.

8.4.3.9.1   Modulation, coding and interleaving

The new MCSs for 32QAM are used to increase the robustness of the previously defined 16QAM MCSs, MCS-10 and MCS-11, but also to increase the peak throughput even further to 99.2 kbps with MCS-12.

The MCSs are summarized in table 57. For comparison previously defined MCS-7-11 for 16QAM are also included.

Table 57: Definitions 32QAM MCSs. Previously defined MCSs for 16QAM are also shown for comparison. Different shades of gray are used for the different modulation orders

MCS	Family	Dir.	User PDU [bytes]	User data rate [kbps]	Modulation	Payload [bits]	Int. depth	Data code rate	Header code rate
7	B	UL	2x56	44.8	16QAM	2x468	4	0.55	0.34
8	A	UL	2x68	54.4	16QAM	2x564	4	0.66	0.34
9	A	UL	2x74	59.2	16QAM	2x612	4	0.72	0.34
10	B	UL	3x56	67.2	16QAM	3x468	4	0.83	0.42
10	B	UL	3x56	67.2	32QAM	3x468	4	0.67	0.35
11	A	UL	3x68	81.6	16QAM	3x564	2	1	0.42
11	A	UL	3x68	81.6	32QAM	3x564	4	0.80	0.35
12	A / B	UL	2x68 + 2x56	99.2	32QAM	2x564 + 2x 468	1 and 2	0.98	0.35

It can be seen that MCS-12 is actually a multi-family MCS, i.e. it consists of PDU sizes from both family A and B. Only the code rates of the UL MCSs are shown in the table but worth noting is that the basic difference in performance for the DL MCSs would be the addition of USF bits which could result in a slightly less robust header.

In table 58 the conventional 8PSK MCSs and the currently defined HOM MCSs are shown with corresponding data code rate. It is seen that HOM is used for making a more robust transmission (no increase in data rates) but also for increasing the peak rates. MCSs defined both with and without turbo coding are shadowed in gray.

Table 58: Set of MCSs for different modulation orders

Modulation	MCS							
	5	6	7	8	9	10	11	12
8PSK	0.375	0.49	0.76	0.92	1			
16QAM			0.55	0.66	0.72	0.83	1	
32QAM						0.67	0.80	1

8.4.3.9.1.1   Coding

Each RLC block is encoded separately (joint coding is for further study). The same mother convolutional code as used today in combination with linear puncturing has generated the coded header and data bits. For the turbo coded MCSs the code defined for UTRAN has been used [15]. The puncturing schemes for the turbo coded data have been generated by prioritizing the systematic bits and additionally puncturing the two parity bits streams (rate 1/3 code) in a linear manner with minimal overlap between IR puncturing schemes.

8.4.3.9.1.2   Interleaving

The interleaving depth used for an MCS will basically depend on the number of RLC blocks in one radio block and the code rate of the data. For example, conventional MCS-9 is uncoded and will therefore not gain from an increased diversity. Thus, each RLC data block is interleaved over 2 bursts: interleaving depth 2. MCSs with low code rates on the other hand will gain from diversity and the RLC blocks are interleaved over all four bursts: interleaving depth 4. Figure 148 shows the implementation of the interleaving for all HOM MCSs in table 57.
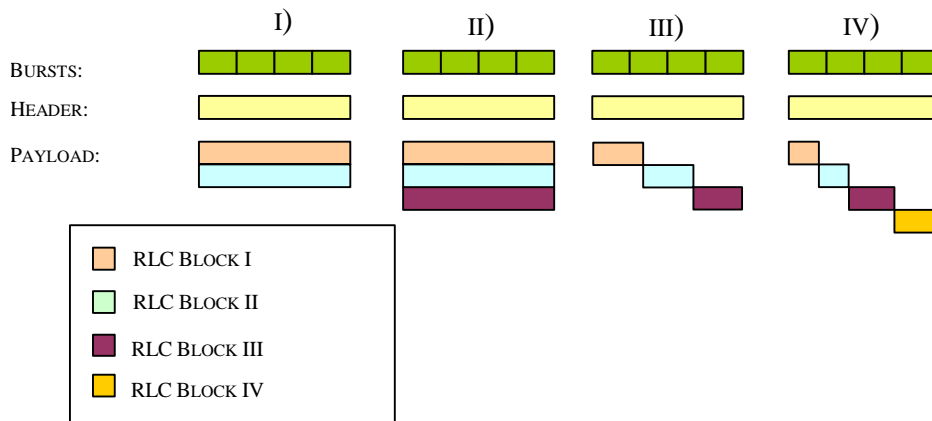
Figure 148: Schematic figure of header and RLC block interleaving for I) MCS-7/8/9/-16QAM; II) MCS-10-16QAM & MCS-10/11-32QAM; III) MCS-11-16QAM; IV) MCS-12-32QAM

Worth noting is that the RLC-blocks for MCS-12-32QAM (uncoded) is interleaved over either one or two bursts. This is a result of the different RLC block sizes shown in table 57.

8.4.3.9.2 Interference Rejection Combining, IRC

Interference rejection combining, IRC, is a diversity combining method that can be used in a multiple antenna system for suppressing mainly CO-channel interference. The suppression is possible by utilizing the cross-covariance of the interference received in the different antennas. Figure 149 shows the basic principle of IRC.
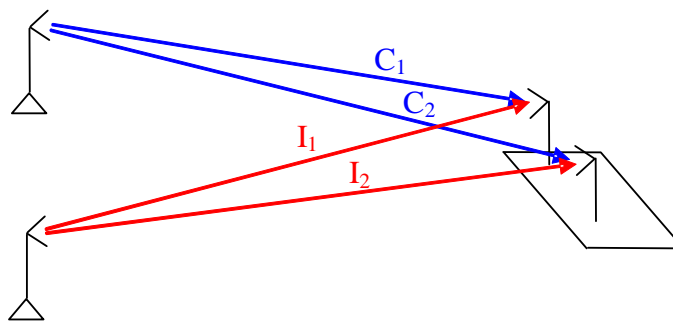
Figure 149: Illustration of the principle of IRC with two receiving antennas

IRC is basically an expansion of Maximum Ratio Combining, MRC, in which only the noise variance is utilized. The performance of the IRC algorithm will largely depend on the interference scenario, the synchronization of the interfering and carrier burst and the correlation of the receiving antennas. Synchronization between carrier and interferer is assumed in the simulations. Table 59 shows the interference scenario that has been used in the simulations.

Table 59: Interference scenario used in the IRC simulations

Scenario	Interference		
	Co-channel	**Adjacent**	**AWGN**
DTS2	1) 0 dB rel. pow. GMSK mod. 2) -10 dB rel. pow. GMSK mod.	1) 3 dB rel. pow. GMSK mod. 200 kHz freq. offset	1) -17 dB (see note 1) rel. pow. 2) -30 dB (see note 2) rel. pow.
NOTE 1: Approximates the remaining interference, apart from the already defined co-interference and adjacent interference, as AWGN.			
NOTE 2: Noise source modulating e.g. the thermal noise in the receiver.			

The fewer interferers there are, the more efficient the IRC performs. The chosen scenario, DTS2 [21], is a complex interference model containing two co-channel interferers, one adjacent interferer and two AWGN sources, which corresponds to the interference of a heavily loaded system. The first AWGN source is a Gaussian approximation of the remaining interferers, apart from the strong co and adjacent interferers, while the second source is modelling the Gaussian noise in the receiver, e.g. thermal noise.

8.4.3.9.3 Results

8.4.3.9.3.1 Link simulator settings

Simulations have been conducted using a state-of-the-art GSM/EDGE link simulator. The new modulation schemes utilizing 32QAM have been evaluated but also previously defined MCSs in combination with IRC. The simulation parameters are summarized in table 150.

Table 60: Link simulator settings

Parameter	Value
Channel profile	Typical Urban (TU)
Terminal speed	3 km/h
Frequency band	900 MHz
Frequency hopping	Ideal
Interference	Co-channel DTS2 (see note)
Direction	Uplink
Antenna diversity	Single Two antennas, IRC
Antenna correlation	0
Carrier/interf. time sync.	Ideal
Equalizer - 8PSK - 16/32QAM - Hyper States	 Decision Feedback Seq. Est. (DFSE) Reduced State Seq. Est. (RSSE) 4 (16QAM) 8 (32QAM)
Impairments: - Phase noise - I/Q gain imbalance - I/Q phase imbalance - DC offset - Frequency error - PA model	Tx / Rx 0.8 / 1.0 [degrees (RMS)] 0.1 / 0.2 [dB] 0.2 / 1.5 [degrees] -45 / -40 [dBc] - / 25 [Hz] Yes / -
NOTE: See table 59 for a thorough description.	

8.4.3.9.3.2 Link Simulations

In this subclause the link level results of the 32QAM MCSs are shown. Both results with and without turbo coding are presented.
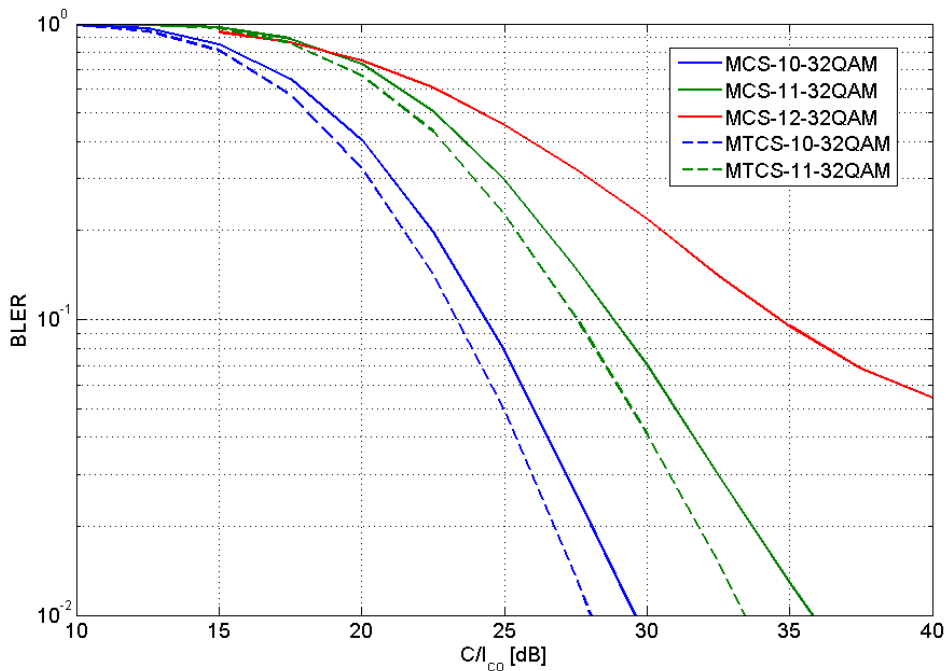
**Figure 150: Link performance (without antenna diversity)
of MCS-10/11/12-32QAM and MTCS-10/11-32QAM**

It can be seen that the turbo coding gives an additional gain in performance of approximately 1 dB at 10 % BLER (as has been seen before in e.g. [28]). The performance of uncoded 32QAM, MCS-12, seems to experience an error floor at high C/I. This is due to the transmitter and receiver impairments that are not dependent on the radio conditions.

In table 61 the performance of MCS-7-12 at a BLER of 10 % is shown.

Table 61: Performance of difference modulations @ 10 % BLER

MCS	C/I @ 10% BLER [dB]					Gain [dB]	
	Cc/8PSK	**Cc/16QAM**	**Tc/16QAM**	**Cc/32QAM**	**Tc/32QAM**	**Cc**	**Tc (see note)**
7	18.8	17.5	16.4			1.3	2.4
8	23.9	19.9	19.2			4.0	4.7
9	26.1	21.8	20.6			4.3	5.5
10		25.0	24.2	24.3	23.3	0.7	0.9
11		28.8		28.8	27.6	0.0	1.2
12				34.7			
NOTE:	If there is no turbo code performance result for different modulations of one MCS, the performance of the convolutional code is used instead.						

It can be seen that there is a performance gain when HOM is used for robustness. The gain is however smaller between 16QAM and 32QAM compared to 8PSK and 16QAM. For all MCSs the turbo coding gives an additional gain of around 1 dB.

In figures 151 and 152 the achieved throughput with ideal Link Adaptation, LA, is shown (no IR is used). The sets of MCSs used are defined in table 62.

Table 62: Different sets of MCSs used in the link adaptation

Set	MCS
EDGE	**MCS-5/6/7/8/9-8PSK**
1	MTCS-5/6-8PSK MTCS-7/8/9/10-16QAM MCS-11-16QAM
2	MTCS-5/6-8PSK MTCS-7/8/9-16QAM MTCS-10/11-32QAM MCS-12-32QAM
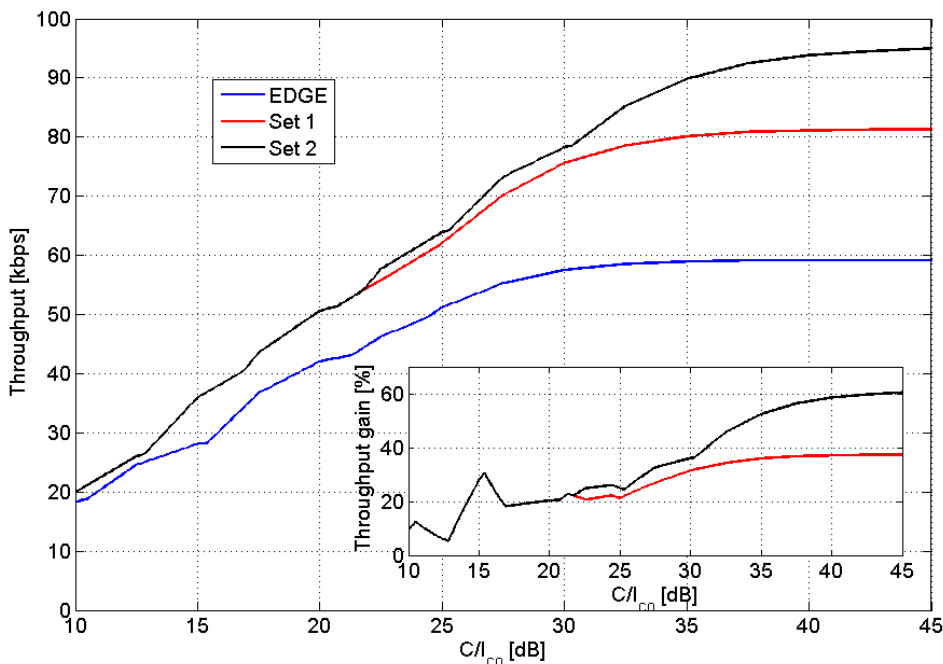
**Figure 151: Throughput of different sets of MCSs with no antenna diversity
or incremental redundancy**

Using 16QAM to increase robustness and to increase peak throughput (Set 1) gives gains at high C/I of, at the most, 38 %. Gains of more than 20 % are however achieved at C/I > 20 dB. 32QAM will increase performance even further (Set 2) with performance improvements compared to 16QAM from approximately a C/I of 22 dB. Throughput gains of higher than 50 %, compared to EDGE, are experienced at C/I > 34 dB.

Even further gains are achieved when combining the HOM with receiver diversity as figure 152 shows.
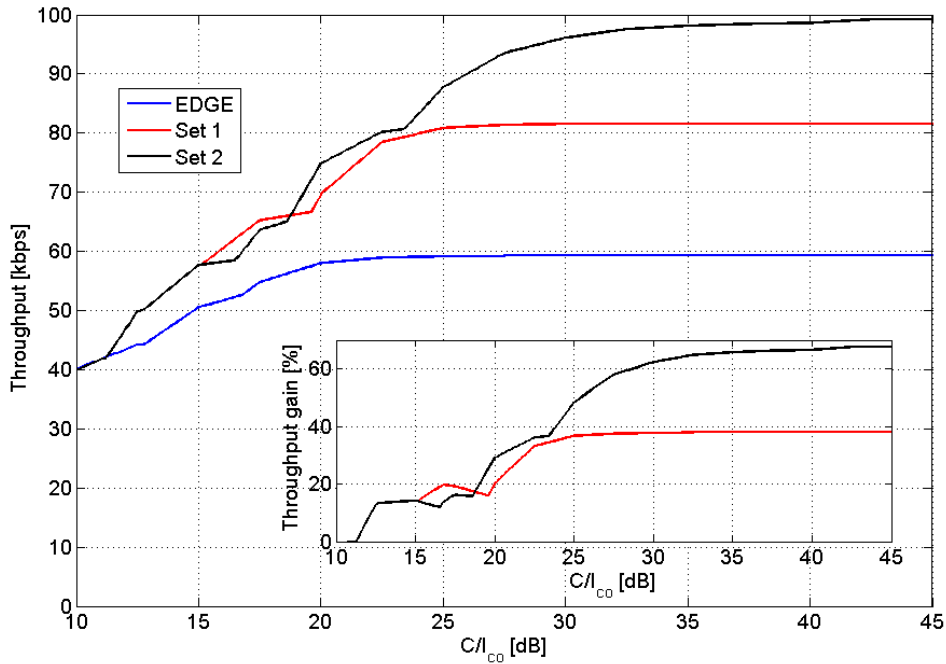
Figure 152: Throughput of different sets of MCSs with two receiving antennas using IRC Interference scenario 'DTS2'

The same sets of MCSs have been used as in figure 151, but there are two receiving antennas and in the equalizer IRC is used. It can be seen that the gains are approximately the same, or somewhat less, up to approximately C/I of 17 dB. Gains of more than 20 % are experienced with 16QAM at C/I > 20 dB and the gain with 32QAM is above 50 % for C/I > 25 dB.

In figure 153 the throughput of the highest MCS of set EDGE, Set 1 and Set 2 is shown when using incremental redundancy, IR (but no antenna diversity). The number of IR retransmissions has been limited to 2. It can be seen that the throughput gains are similar to the ones in figure 151 where ideal LA without IR was utilized.
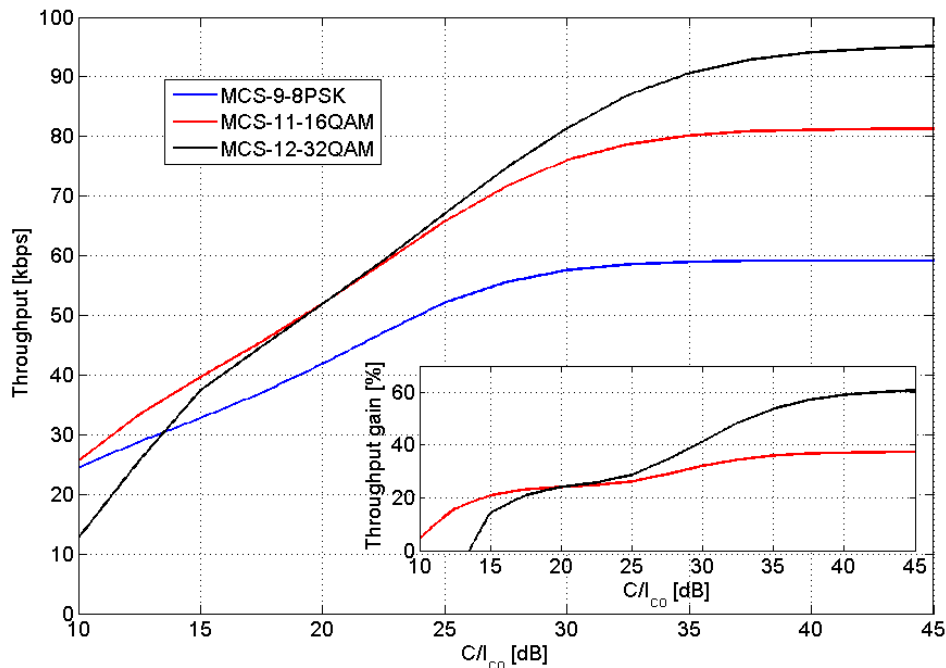
Figure 153: IR throughput (without antenna diversity) for the highest MCS of EDGE, Set 1 and Set 2 respectively. The number of IR retransmissions have been limited to 2

To estimate the impact on mean user throughput, calculations with a C/I-distribution have been performed. The distribution used is from a 3/9 freq. reuse with a 2 % blocking limit, see annex B, figure B.9.

Table 63: Estimation of average user throughput

Set	Mean user bit rates [kbps]			
	Single antenna div.	Dual antenna div. w. IRC	Throughput gain (see note) single antenna div. [%]	Throughput gain (see note) dual antenna div. [%]
EDGE	43.5	54.6		
1	54.3	70.0	25 %	28 %
2	56.5	75.5	30 %	38 %
NOTE:	Gain is presented relative to EDGE performance.			

In table 63 it can be seen that there are substantial gains by using both 16QAM and 32QAM, both with and without IRC. Previously it has been shown that 32QAM can increase the peak bit rate with 66 % and in this calculation it is shown that the average throughput gain for all users can be close to 40 %. The gains shown when IRC is used are expected also for downlink if MSRD is used.

8.4.3.9.3.3   System simulator settings

The same simulator as in subclause 8.4.3.6.1 has been used. The system level scenarios are summarised in table 63a.

Table 63a: Summary of system simulation parameters.

Parameter	Value	
	Scenario 1	Scenario 8
Reuse	1	1/3
Spectrum allocation	7.2 MHz (excluding BCCH)	7.2 MHz (excluding BCCH)
Frequencies per cell	36	12
Transceivers per cell	12	12
Frequency hopping	Random	Random
Traffic model	FTP, 100 kB file size	FTP, 100 kB file size
Cell radius	500 m	500 m
Power control	No	No
Pathloss model	Okumura-Hata	Okumura-Hata
Log-normal fading standard deviation	8 dB	8 dB
Rayleigh fading	Yes	Yes
Multi-slot allocation per session	4 timeslots	4 timeslots
Link quality control	Measurement based link adaptation	Measurement based link adaptation
Power backoff 8PSK	3.3 dB	3.3 dB
Power backoff 16QAM	5.3 dB	5.3 dB
Power backoff 32QAM	5.6 dB	5.6 dB

8.4.3.9.3.4   System simulation results

Figure 153a shows the average session bit rate for different user percentiles (10th, 50th, and 90th percentile) in scenario 1. The gains on the 10th percentile are 15-60% for HOT level 2 (where the higher value corresponds to higher load). On the 50th percentile, the gains are 35-45% while the gain on the 90th percentile is ~37%.
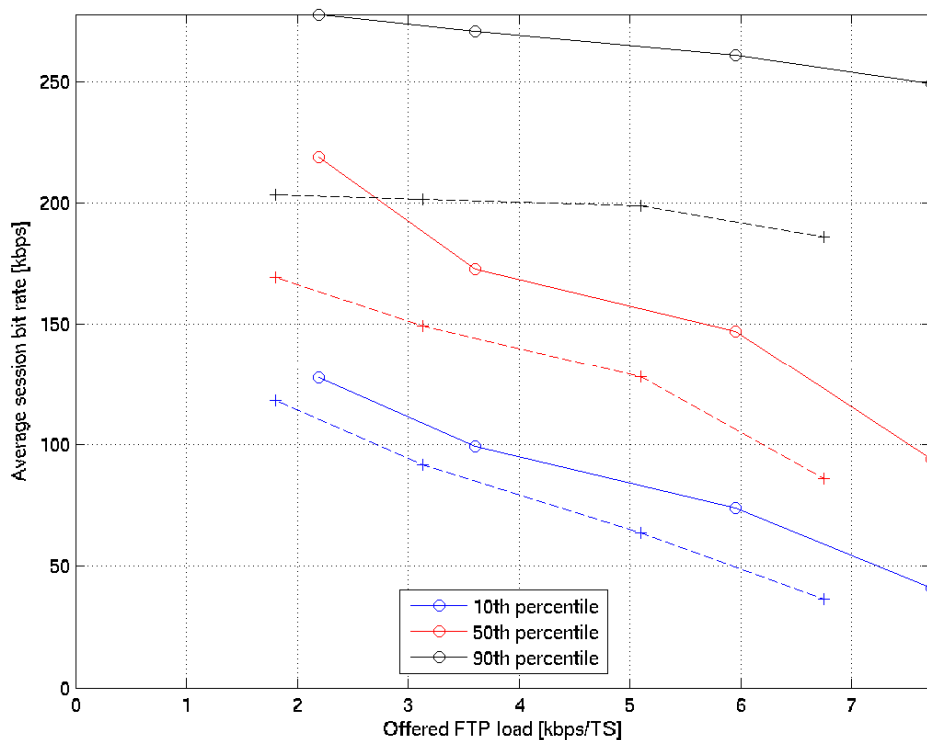
Figure 153a. Average session bit rate percentiles, 10th percentile (blue), 50th percentile (red), 90th percentile (black), as a function of offered FTP load, for EGPRS (dashed) and HOT level 2 (solid), in a 1-reuse.

Figure 153b shows the average session bit rate for different user percentiles (10th, 50th, and 90th percentile) in scenario 8. The gains on the 10th percentile are 13-55% for HOT level 2. On the 50th percentile, the gains are 34-42% while the gain on the 90th percentile is 34-38%.
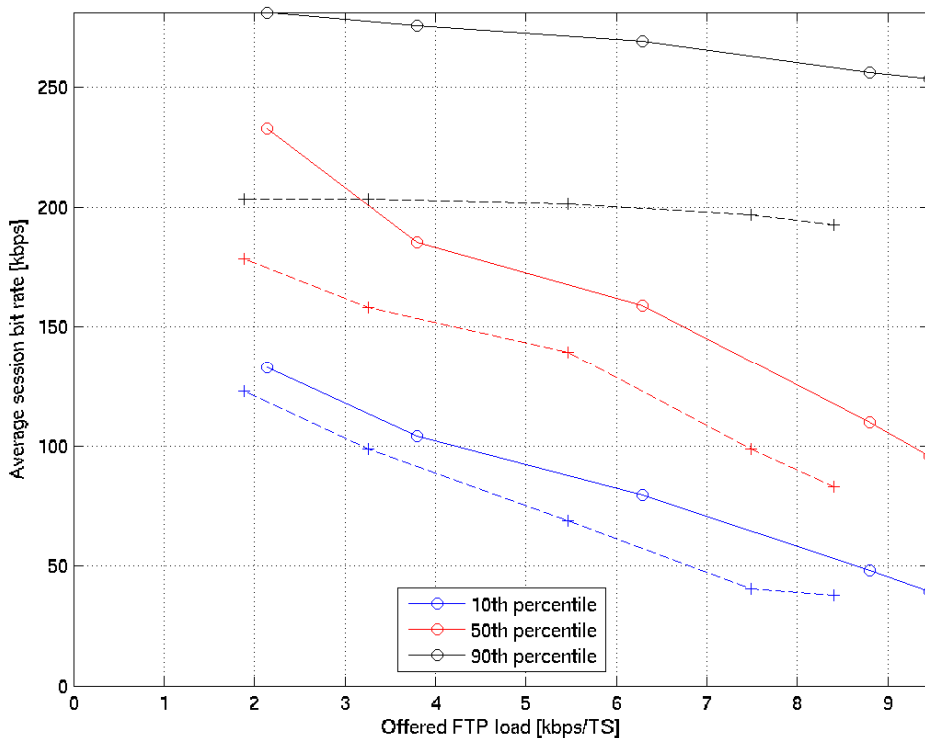
Figure 153b. Average session bit rate percentiles, 10th percentile (blue), 50th percentile (red), 90th percentile (black), as a function of offered FTP load, for EGPRS (dashed) and HOT level 2 (solid), in a 3-reuse.

8.4.3.10   Comparison between DFSE and RSSE Performance

To evaluate the impact on performance when using the RSSE of implementation set C and a DFSE, MCS-9 performance has been simulated on a TU3 channel with ideal frequency hopping at 900 MHz. For the receiver impairments mainly the contribution from phase noise was included while transmitter impairments were not. These simulations were run with a $\pi/4$ rotation per symbol of the 16QAM constellation, which will reduce the peak-to-average (PAR) ratio to 5.3 dB. This should be compared to the PAR of 3.3 dB for 8PSK with $3\pi/8$ rotation and the PAR of 16QAM without rotation of 6 dB.

In figure 154 it is shown that the loss is less than 0.5 dB.
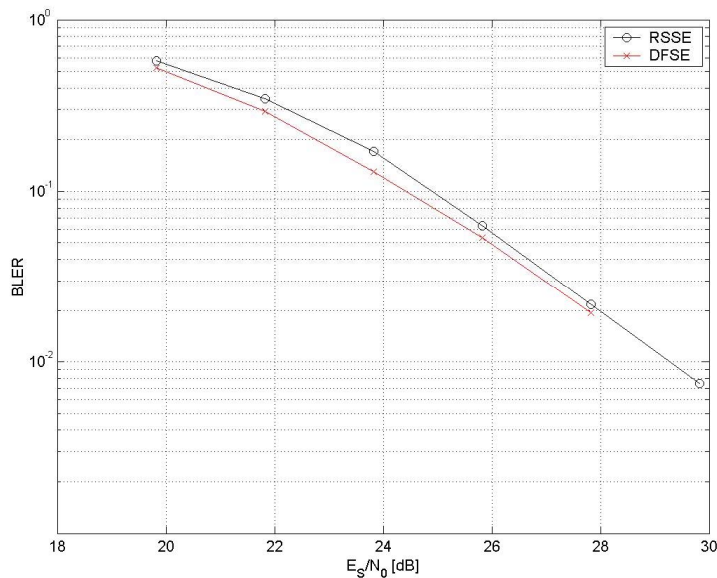
Figure 154: Performance of 16QAM receivers with DFSE and RSSE

8.4.3.11 Discussion

8.4.3.11.1 Link Level Performance

Turbo codes show gains in the order of 1 dB in all evaluated cases (MTCS-5, MTCS-6, MTCS-7-16QAM, MTCS-8-16QAM, MTCS-9-16QAM), compared to convolutional codes. No gains have been found for 8PSK-modulated turbo-coded equivalents of MCS-7 to MCS-9 (simulation results not shown in this report). It is clear that in order to get gains with turbo codes for a wide range of MCSs, they need to be combined with higher order modulations. The combination of 16QAM and turbo codes gives gains up to 5.5 dB at 10%BLER and up to 7.9 dB at 1 % BLER.

8.4.3.11.2 System Level Performance

Turbo codes together with 16QAM will give significant gains in average session bit rate also in a 1-reuse network. The gains are present (and even seem to increase) with higher loads. At 8 kbps/timeslot offered FTP load, the average session bit rate gain is about 20 % to 25 % (see figure 130). 8 kbps/timeslot offered FTP load corresponds to a frequency load of 10 % to 15 %, which is a higher load than in most networks deployed today.

It is interesting to notice (see figure 130) that all users benefit from the improvements. In fact, the relative gains are larger, about 30 % to 40 %, for the average users and the users experiencing the worst conditions (50th and 10th percentile).

The reason why lower percentiles are so positively affected is that users in worse radio conditions have very varying radio conditions, but high MCSs are still sometimes used. With 16QAM, and particularly with the addition of turbo coding as well, these radio quality variations can be exploited through interference diversity gains. This is not the case with traditional EGPRS, where the higher MCS:s cannot benefit from interference diversity due to the high coding rates.

Users with high average radio quality (higher percentiles) will use the high MCSs far more regularly, which increases the possibilities to gain from the enhanced robustness. However, due to the fair and stable radio conditions the robustness gains are limited and the bit rates are high, resulting in a smaller relative gain than what is seen in lower percentiles.

Turbo codes together with 16QAM also give significant gains in average session bit rate in a 12-reuse scenario, regardless of if frequency hopping is used or not. In the 12-reuse scenario the users with the best radio quality (90th percentile) will experience only small gains. However, for the 10th and 50th percentiles, performance increases by as much as 40 % to 45 %.

Thus, higher order modulation and turbo coding improves session bit rate performance significantly, both in tight and sparse reuse.

In addition, regardless of reuse scenario, since 16QAM and turbo codes make the transmission more efficient, FTP session airtime will be reduced. Thereby less interference will be generated in the system, which benefits all users- and increases the capacity of the system. It is important to note that the relative capacity gain depends highly on the chosen service requirement. If the bit rate requirement is higher, the relative capacity gain from higher order modulation and turbo coding gets higher, but the total capacity gets lower. Taking that into account the gains in spectral efficiency where around 50 % for a 60 kbps bit rate requirement in 1-reuse, and around 60 % for an 80 kbps requirement in 12-reuse.

The performance of adding 32QAM has also been evaluated. Also the performance gain of higher order modulation with turbo codes has been evaluated in combination with IRC.

The results have shown that 32QAM can increase the peak data bit rates up to 99.2 kbps - an increase from EDGE of 68 %. In interference limited scenario, the throughput with 32QAM reaches above 59.2 kbps (peak rate of MCS-9) at C/I > 22.5 dB and throughput gains above 40 % are achieved at C/I > 31 dB. When using antenna receiver diversity in combination with IRC the respective C/I-levels are at 17 dB and 23.5 dB respectively. An estimation of the mean user throughput using a C/I-distribution from a 3/9 freq. reuse shows mean throughput gains of 38 % with 32QAM and IRC. The gains shown when IRC is used are expected also for downlink if MSRD is used.

Thus, a combination of higher order modulation and turbo coding improves capacity significantly.

8.4.4   Implementation Set D

Source: References [10], [11], [12], [13], [14], [31], [41] and [47]. Note that there are additional details of simulation results in annex C.

8.4.4.1   Performance Characterisation

8.4.4.1.1   Uncoded BER Performance

Figure 155 shows the uncoded BER performance of the basic receiver for 8-PSK and 16-QAM modulation. This shows good alignment of the basic receiver performance with previously reported results by other contributors [6].
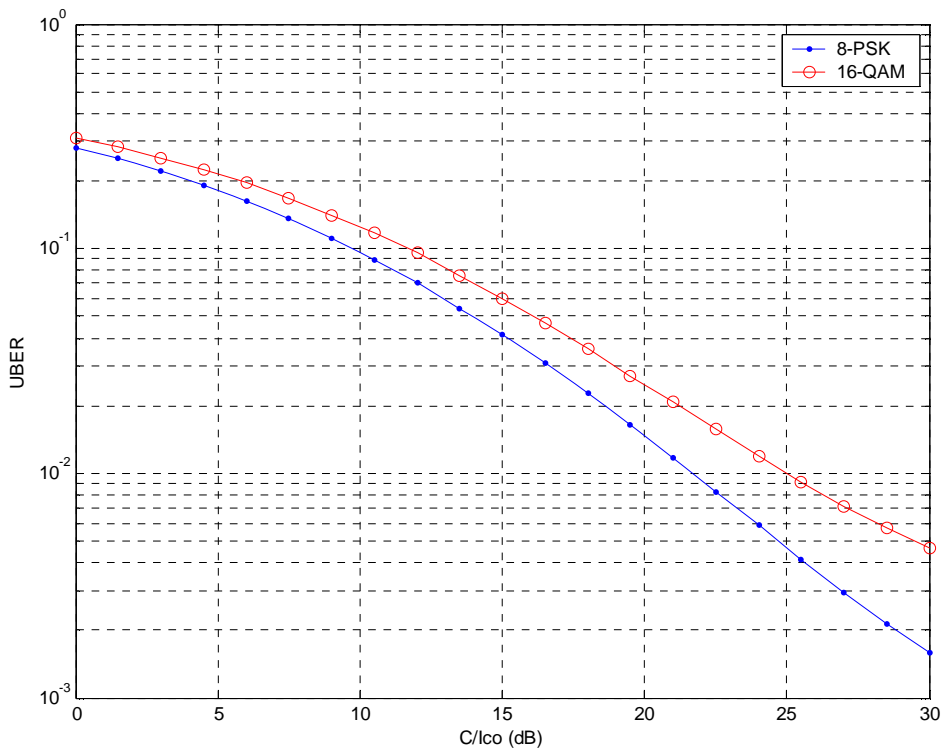
Figure 155: Uncoded BER for 8-PSK under TU3 Channel

8.4.4.1.2 BLER Performance of Turbo Coding with 8PSK

This subclause reports the results of simulations using logical channel configurations defined in table 64. These define combinations of Turbo coding with 8-PSK modulation only.

Table 66 shows the relative gains for TU3iFH Co-Channel scenario. As can be observed, the gains are relatively modest, in the region of 1 dB to 1.5 dB for a 4 slot interleaver, improving to 1.5 dB to 2.5 dB for 8 slot interleaver.

Note that for MCS-9 there is no improvement in basic BLER to be made, since the code rate is already 1.

It was assessed that the relatively modest improvements were most likely due to the relatively high code rates (MCS-6 already has code rate 0.76), and that a combination of Turbo Coding with 16-QAM would provide more potential for gain. The performance results for this are reported in the following subclauses.

Table 64: Modulation and Coding Configurations

Modulation and Coding Scheme	Data Block Length (bits)	Coding	Data Code Rate	Interleaving Depth	Data Rate (per 200kHz channel)
MCS-5	450	Conv	0.37	4	22.5
MCS-5-T4	450	Turbo	0.37	4	22.5
MCS-5-T8	900	Turbo	0.37	8	22.5
MCS-6	594	Conv	0.49	4	29.7
MCS-6-T4	594	Turbo	0.49	4	29.7
MCS-6-T8	594*2	Turbo	0.49	8	29.7
MCS-7	450*2	Conv	0.76	2	45.0
MCS-7-T4	900	Turbo	0.76	4	45.0
MCS-7-T8	1800	Turbo	0.76	8	45.0
MCS-8	546*2	Conv	0.92	2	54.6
MCS-8-T4	1092	Turbo	0.92	4	54.6
MCS-8-T8	2184	Turbo	0.92	8	54.6
MCS-9	594*2	Conv	1	2	59.4

8.4.4.1.3 BLER Performance of Turbo Coding with 16QAM

This subclause reports the results of simulations using logical channel configurations defined in table 65. These define combinations of Turbo coding with 8-PSK or 16-QAM modulation.

Table 65: Modulation and Coding Configurations - with 16QAM

Modulation and Coding Scheme	Data Block Length (bits)	Coding	Data Code Rate	Interleaving Depth	Data Rate (per 200 kHz channel)
MCS-6-16QAM	594	Conv	0.37	4	29.7
MCS-6-T4-16QAM	594	Turbo	0.37	4	29.7
MCS-6-T8-16QAM	594*2	Turbo	0.37	8	29.7
MCS-7-16QAM	450*2	Conv	0.57	2	45.0
MCS-7-T4-16QAM	900	Turbo	0.57	4	45.0
MCS-7-T8-16QAM	1 800	Turbo	0.57	8	45.0
MCS-8-16QAM	546*2	Conv	0.69	2	54.6
MCS-8-T4-16QAM	1 092	Turbo	0.69	4	54.6
MCS-8-T8-16QAM	2 184	Turbo	0.69	8	54.6
MCS-9-T4-16QAM	1 188	Turbo	0.75	4	59.4
MCS-9-T8-16QAM	2 376	Turbo	0.75	8	59.4
MCS-10-T4-16QAM	1 400	Turbo	0.89	4	70.0
MCS-10-T8-16QAM	2 800	Turbo	0.89	8	70.0
MCS-11-T4-16QAM	1 500	Turbo	0.95	4	75.0
MCS-11-T8-16QAM	3 000	Turbo	0.95	8	75.0

The BLER performance has been considered under a number of different channel configurations and conditions. In the main body of the text, the results for TU3 channel with ideal hopping are presented, for both co-channel interferer and sensitivity limited scenarios.

The other detailed BLER results, from which the throughput curves in subclause 8.4.4.1.7 are derived, are presented in annex C. Those results look at the impact of non hopping channels.

Figures 161 to 162 show the BLER performance curves for TU3iFH under co-channel scenario; figures 168 to 169 show the BLER curves for TU3iFH under sensitivity limited scenario. The performance improvements for BLER=10 % are shown in tables 66 and 68.

The results for the Turbo coded configurations are consistently better than both the current MCS configurations, and equivalent configurations using 16-QAM modulation. The improvement increases in going from MCS-5 to MCS-9 with gains in the region of 1.5 dB to 12 dB for 4 slot interleaving, rising to gains of 2.6 dB to 13.7 dB for 8 slot interleaving.

Significant gains of up to 4.2 dB are obtained for equivalent configurations to MCS-5 and MCS-6, compared to both standard MCS codes, and a configuration using 16-QAM with convolutional coding. These are gains that are particularly helpful at a system level in improving throughput for the worst condition users. This will be noted in more detail in subclause 8.4.4.1.9.

8.4.4.1.4 Comparison to Ericsson Results

These results have been compared to those reported by [19] for the co-channel scenario. Although, there is not an exact alignment, the Ericsson results also confirm the assertions based on the results presented here. It should be noted that the improvements (both as absolute C/Ico and relative) are larger than those reported in [19].

It should also be noted that there is also substantial further gain to be achieved by interleaving blocks over 8 slots (for example using dual carrier to maintain TTI value).

**Table 66: Performance Improvement of Turbo Coding with 8-PSK
only vs. EGPRS Logical Channels in TU3iFH Co-Channel Scenario**

Modulation and Coding Scheme	Co-Channel	
	C/Ico (dB) @ 10 % BLER	Gain (dB) v MCS @ 10 % BLER
MCS-5	9.5	-
MCS-5-T4	8	1.5
MCS-5-T8	7	2.5
MCS-6	12	-
MCS-6-T4	10.5	1.5
MCS-6-T8	9.5	2.5
MCS-7	18	-
MCS-7-T4	17	1.0
MCS-7-T8	16	2.0
MCS-8	24	-
MCS-8-T4	23	1.0
MCS-8-T8	22.5	1.5

Table 67: Performance Improvement vs EGPRS Logical Channels in TU3iFH Co-Channel Scenario

Modulation and Coding Scheme	C/Ico (dB) @ 10 % BLER	Gain (dB) v MCS @ 10 % BLER
MCS-5	9.5	-
MCS-5-T4	8	1.5
MCS-5-T8	7	2.5
MCS-6	12	-
MCS-6-16QAM	12	0
MCS-6-T4-16QAM	10	2
MCS-6-T8-16QAM	9	3
MCS-7	18	-
MCS-7-16QAM	15.5	2.5
MCS-7-T4-16QAM	14.5	3.5
MCS-7-T8-16QAM	13.5	4.5
MCS-8	24	-
MCS-8-16QAM	18.5	5.5
MCS-8-T4-16QAM	17.5	6.5
MCS-8-T8-16QAM	16.5	7.5
MCS-9	29	-
MCS-9-16QAM (see note)	21	8
MCS-9-T4-16QAM	19.5	9.5
MCS-9-T8-16QAM	18	11
MCS-10-T4-16QAM	26.5	-
MCS-10-T8-16QAM	24.8	-
MCS-11-T4-16QAM	~31	-
MCS-11-T8-16QAM	~31	-

NOTE : Assume that MCS-9 achieves 1% BLER @ ~35dB

Table 68: Performance Improvement vs EGPRS Logical Channels in TU3iFH Sensitivity Scenario

Modulation and Coding Scheme	Eb/No(dB) @ 10% BLER	Gain (dB) v MCS @ 10 % BLER
MCS-5	4.4	-
MCS-5-T4	2.9	1.5
MCS-5-T8	1.8	2.6
MCS-6	6.8	-
MCS-6-16QAM	6.8	0
MCS-6-T4-16QAM	3.6	3.2
MCS-6-T8-16QAM	2.4	4.2
MCS-7	12.5	-
MCS-7-16QAM	9.3	3.2
MCS-7-T4-16QAM	8	4.5
MCS-7-T8-16QAM	6.5	6
MCS-8	19.5	-
MCS-8-16QAM	12	7.5
MCS-8-T4-16QAM	11	8.5
MCS-8-T8-16QAM	9.8	9.7
MCS-9	25	-
MCS-9-16QAM	14.5	10.5
MCS-9-T4-16QAM	13	12
MCS-9-T8-16QAM	11.3	13.7
MCS-10-T4-16QAM	20.2	-
MCS-10-T8-16QAM	18	-
MCS-11-T4-16QAM	25.5	-
MCS-11-T8-16QAM	25	-

8.4.4.1.5   Graphs for Co-Channel Interferer Case (TU3iFH)
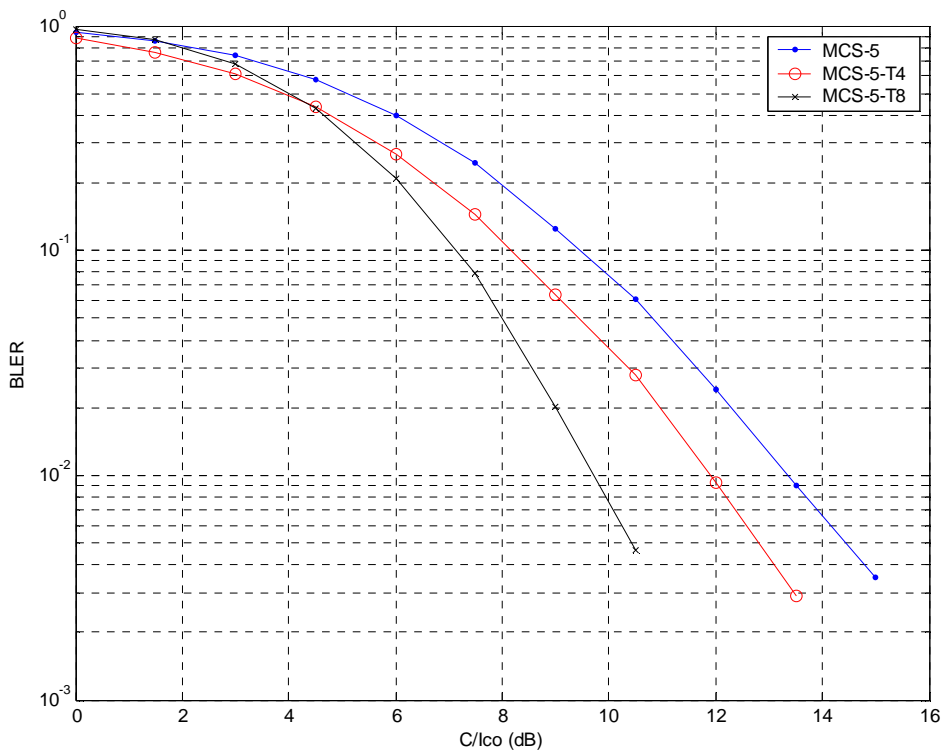
Figure 156: TU3iFH Co-Channel Performance (MCS-5)
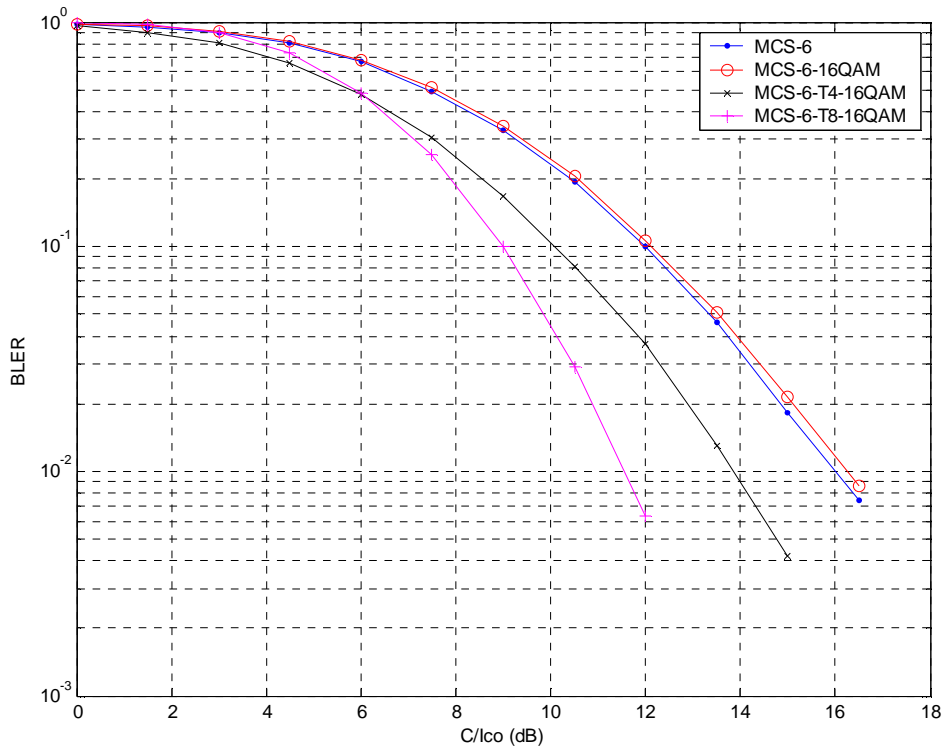
Figure 157: TU3iFH Co-Channel Performance (MCS-6)
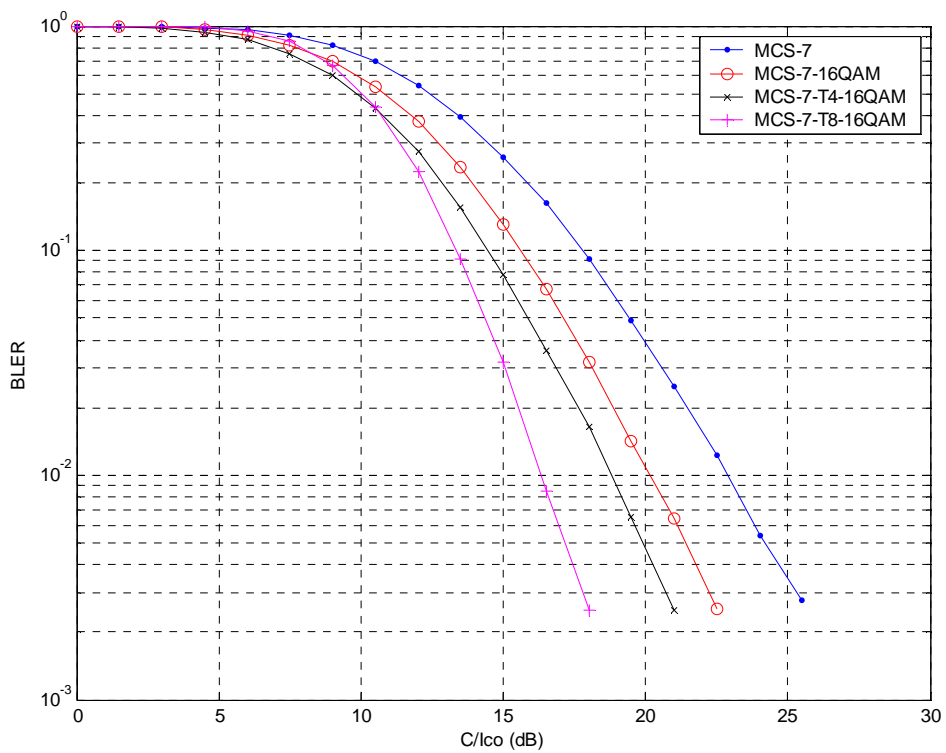
Figure 158: TU3iFH Co-Channel Performance (MCS-7)
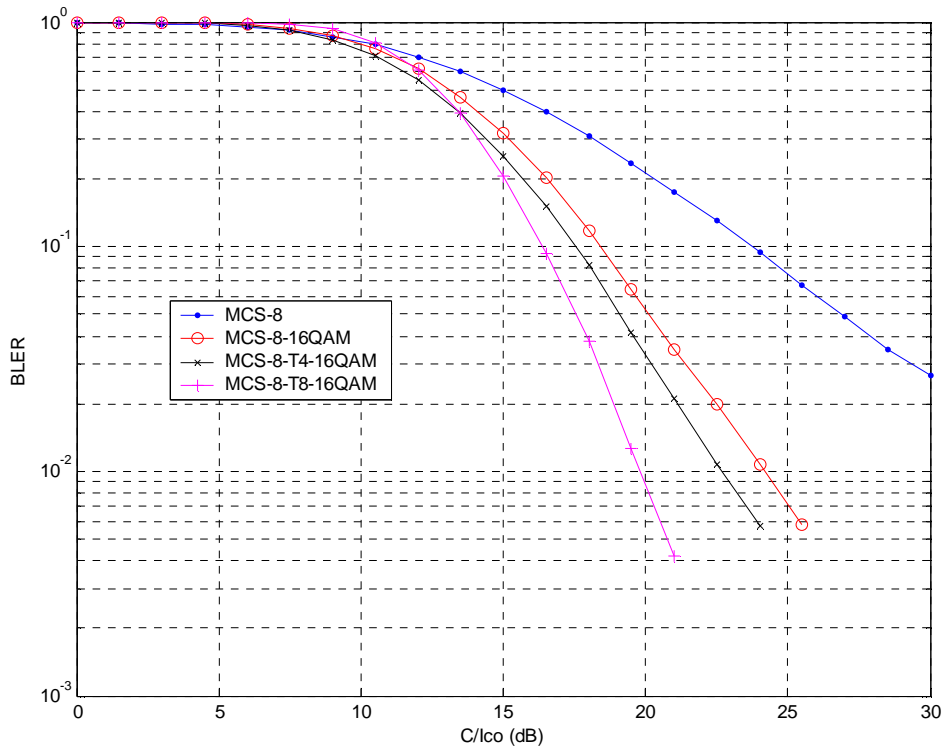
Figure 159: TU3iFH Co-Channel Performance (MCS-8)
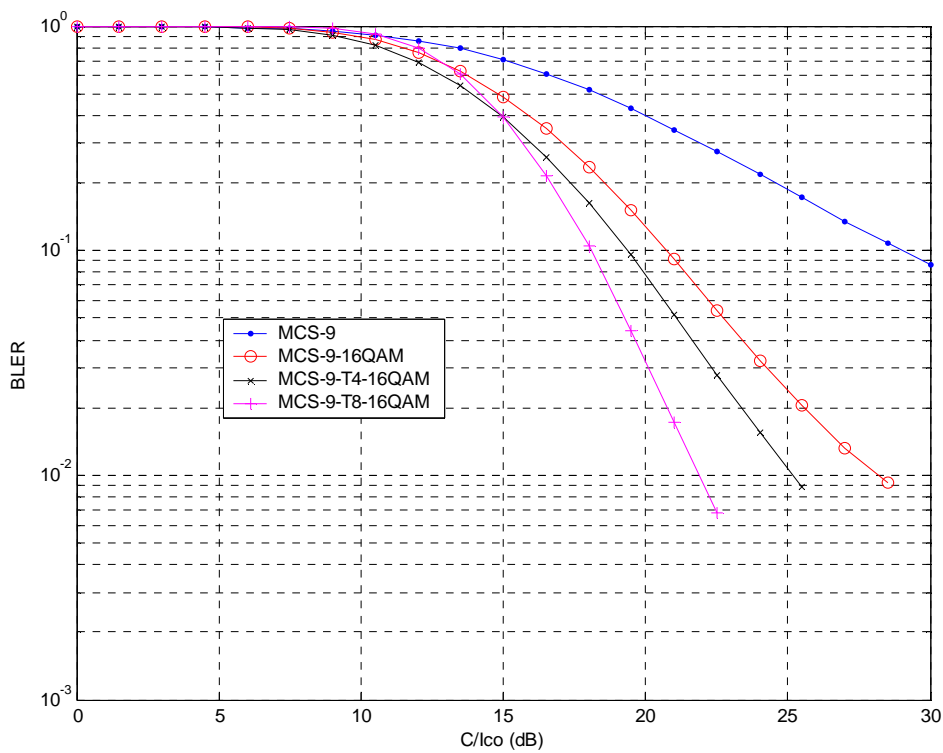
Figure 160: TU3iFH Co-Channel Performance (MCS-9)
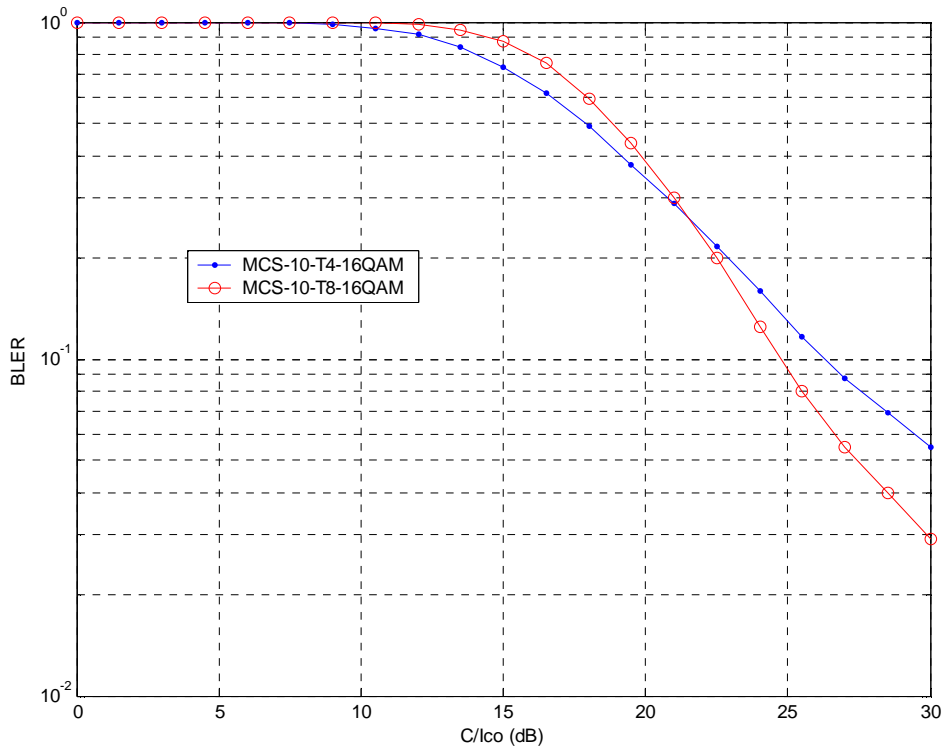
Figure 161: TU3iFH Co-Channel Performance (MCS-10 16-QAM)
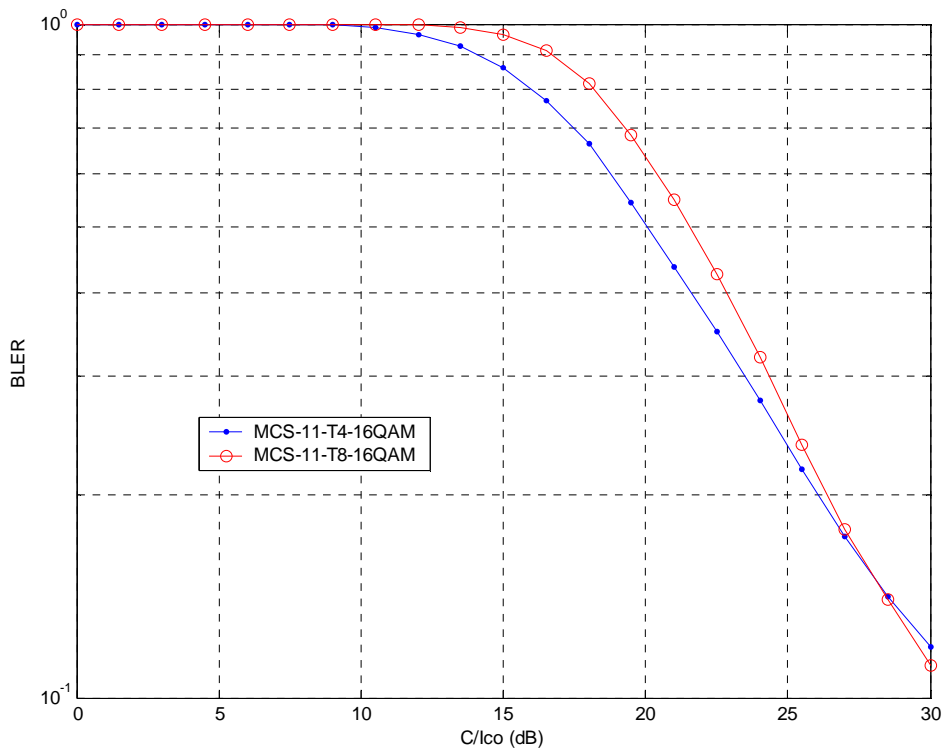
Figure 162: TU3iFH Co-Channel Performance (MCS-11 16-QAM)

8.4.4.1.6 Graphs for Sensitivity Limited Case (TU3iFH)
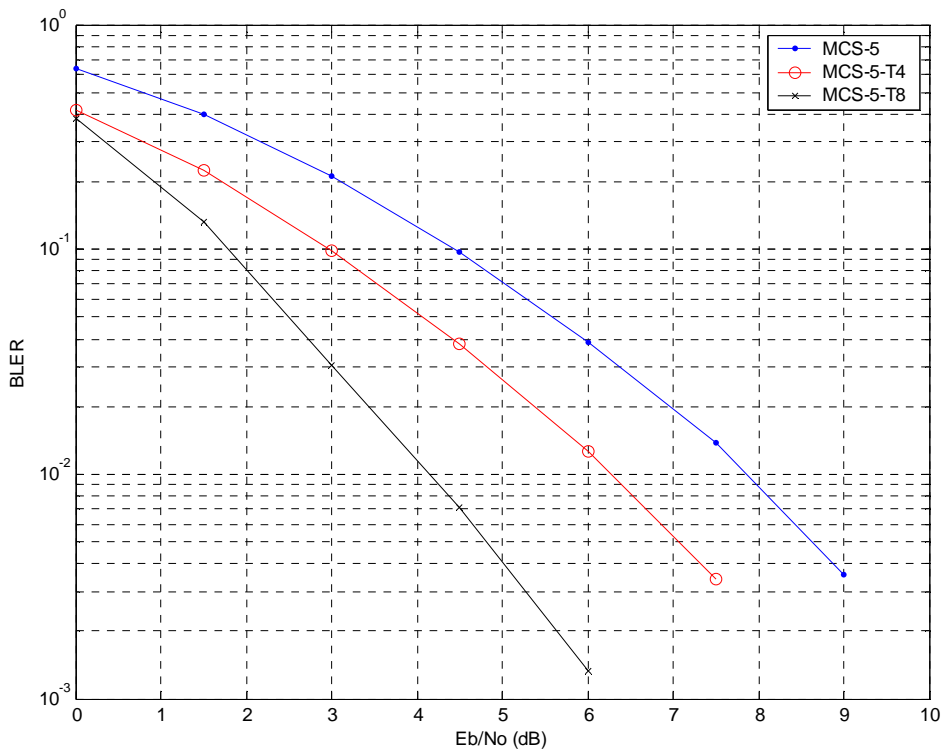
Figure 163: TU3iFH Sensitivity Performance (MCS-5)
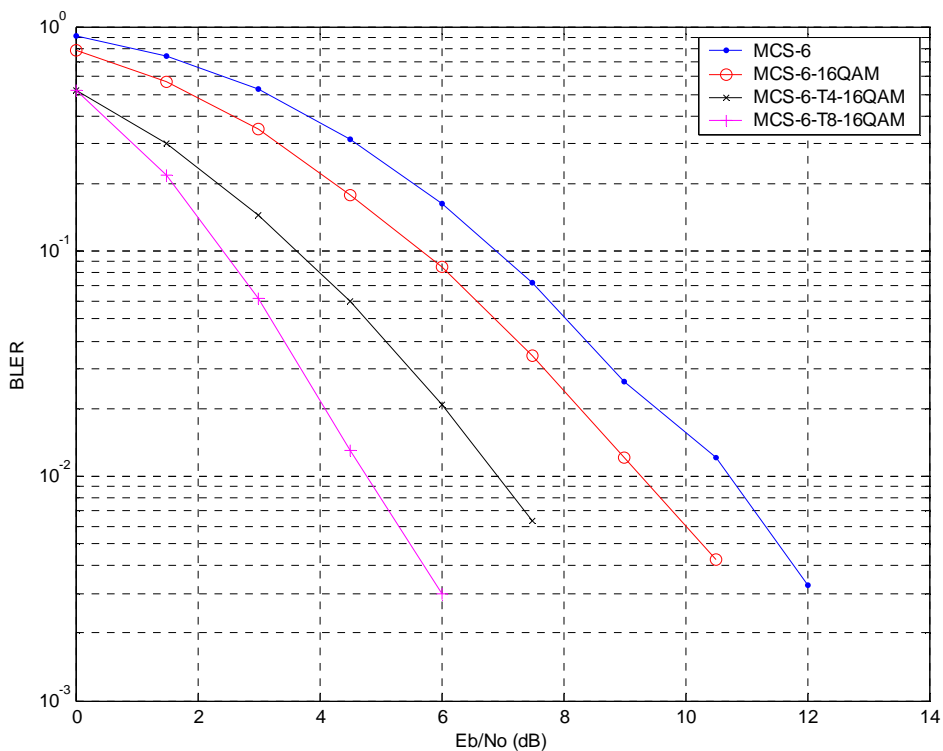
Figure 164: TU3iFH Sensitivity Performance (MCS-6)
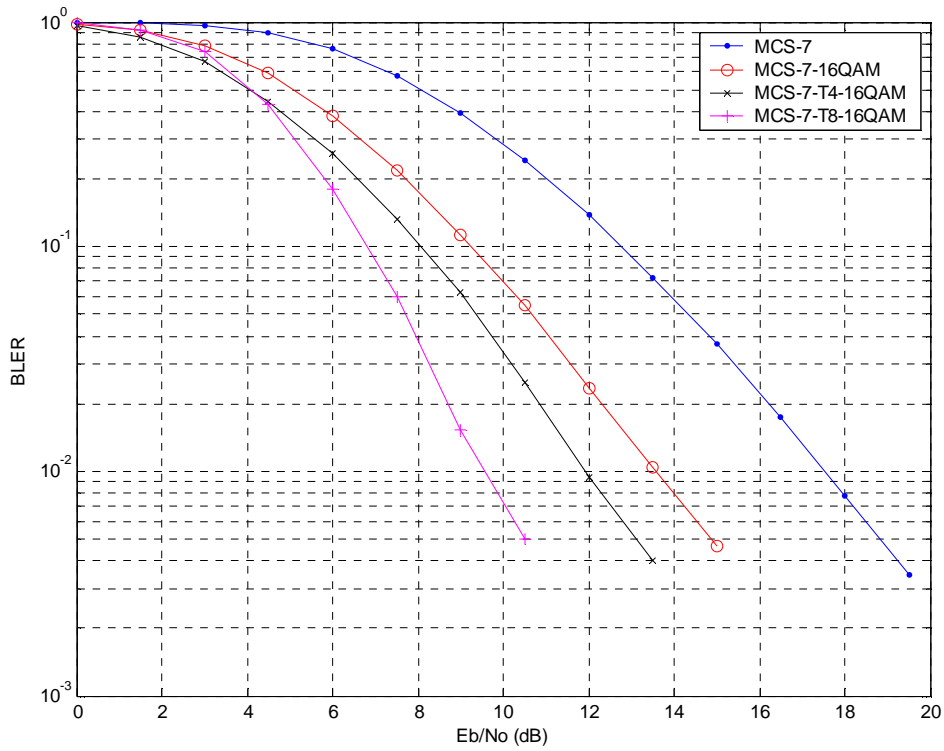
Figure 165: TU3iFH Sensitivity Performance (MCS-7)
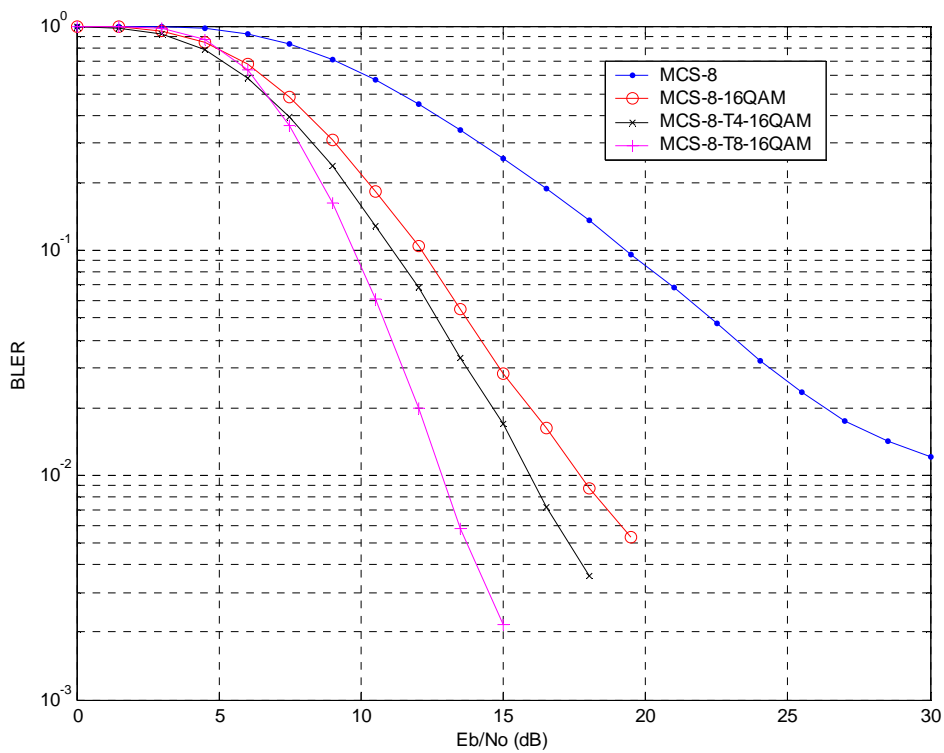
Figure 166: TU3iFH Sensitivity Performance (MCS-8)
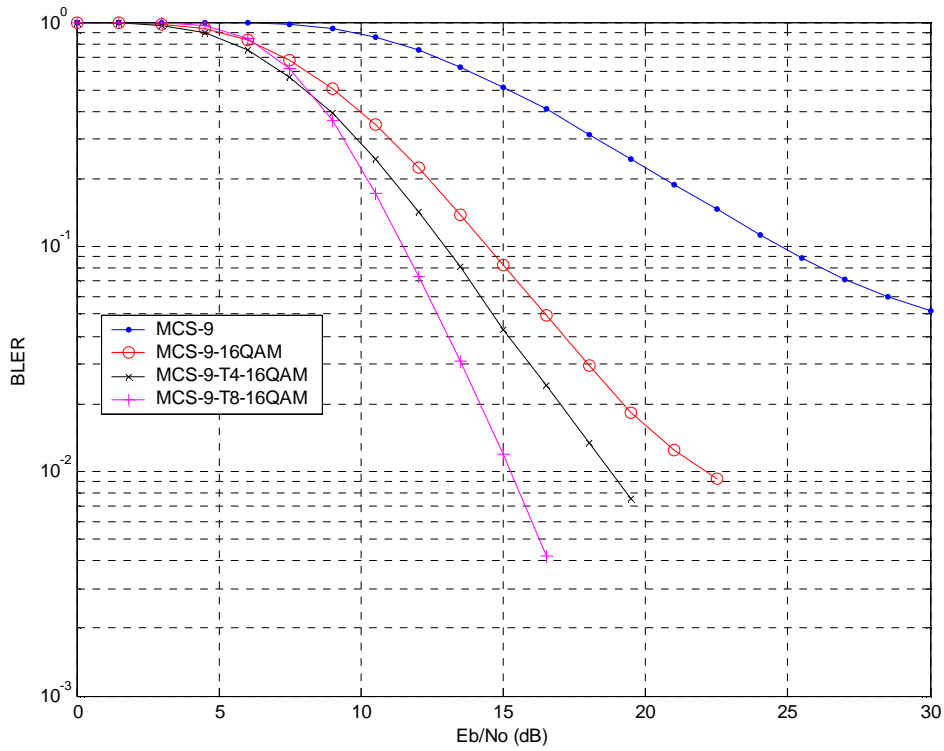
Figure 167: TU3iFH Sensitivity Performance (MCS-9)
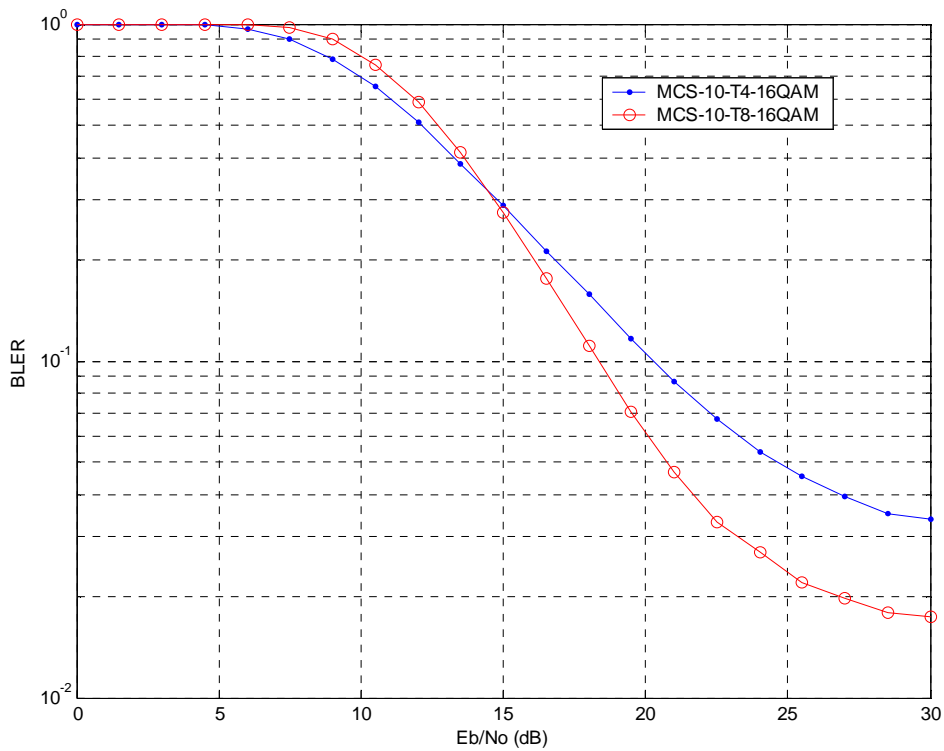
Figure 168: TU3iFH Sensitivity Performance (MCS-10 16-QAM)
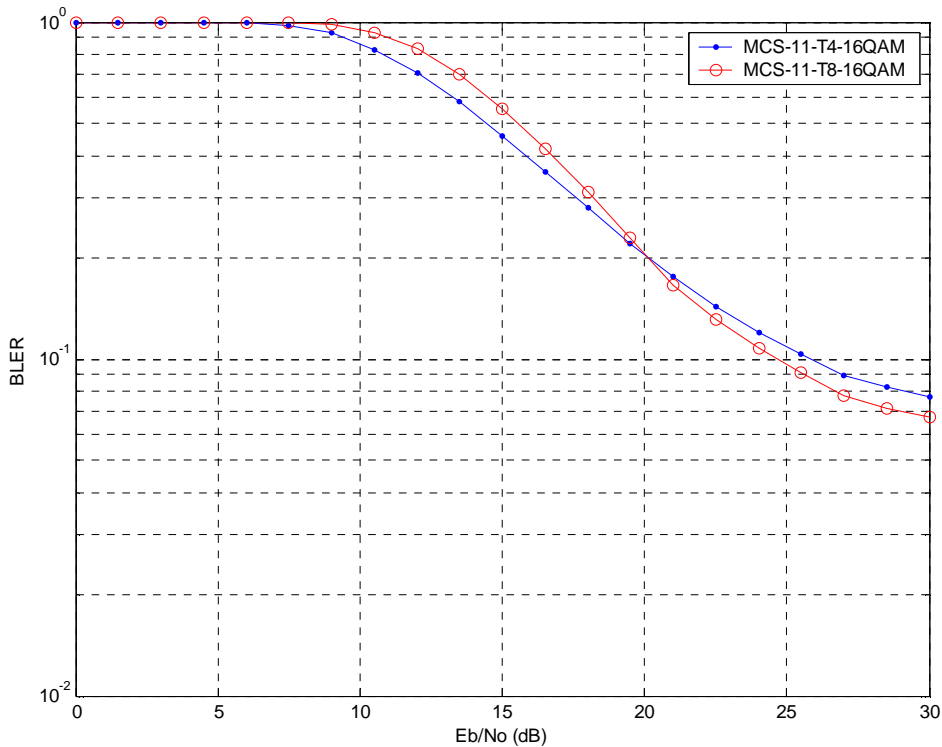
Figure 169: TU3iFH Sensitivity Performance (MCS-11 16-QAM)

8.4.4.1.7 Throughput Performance Gain

8.4.4.1.7.1 Approximation for Throughput Gain

This subclause presents the performance gain of a number of different logical channel set combinations under the physical channel scenarios considered. It is assumed that there is ideal Link Adaptation. The throughput of a logical channel combination is approximated as:

$$\text{Throughput} = (1\text{-BLER}) * \text{DataPayloadPerBlock} * \text{BlockPerSecond}$$

The logical channel configuration combinations used are shown in table 69. Figures 170 to 175 show the absolute throughput and throughput gains for these schemes under the different channel scenarios.

Performance results were not available for MCS-x-16QAM using data rates above 59kb/s. Therefore that throughput gain curve has been curtailed above 95 % * 59 kb/s.

For the TU3iFH co-channel case (figures 170 and 171) and sensitivity case (figures 178 and 179) the average throughput gains are approx 20 % and 30 % respectively.

For the non-hopping case under TU50 conditions (figures 174 and 175) the throughput gains are in the region of 15 % to 20 %.

Table 69: Configurations Used for Throughput Graphs

Scheme A	Scheme B	Scheme C
MCS-5	MCS-5	MCS-5-T8
MCS-6	MCS-6	MCS-6-T8-16QAM
MCS-7	MCS-7-16QAM	MCS-7-T8-16QAM
MCS-8	MCS-8-16QAM	MCS-8-T8-16QAM
MCS-9	MCS-9-16QAM	MCS-9-T8-16QAM
		MCS-10-T8-16QAM
		MCS-11-T8-16QAM

Note that figures 170, 173 and 174 all show a "knee" effect in throughput for Scheme C (Turbo) at around 59 kb/s. This occurs because of the superior performance of the turbo code, and a relatively large jump in maximum throughput changing from MCS-9 to MCS-10 (59 kb/s to 70 kb/s) as it has been defined here. As an updated proposal we would modify the definitions of MCS-10/11 (and probably add a further MCS) to cover the range of data rates above 59 kb/s.
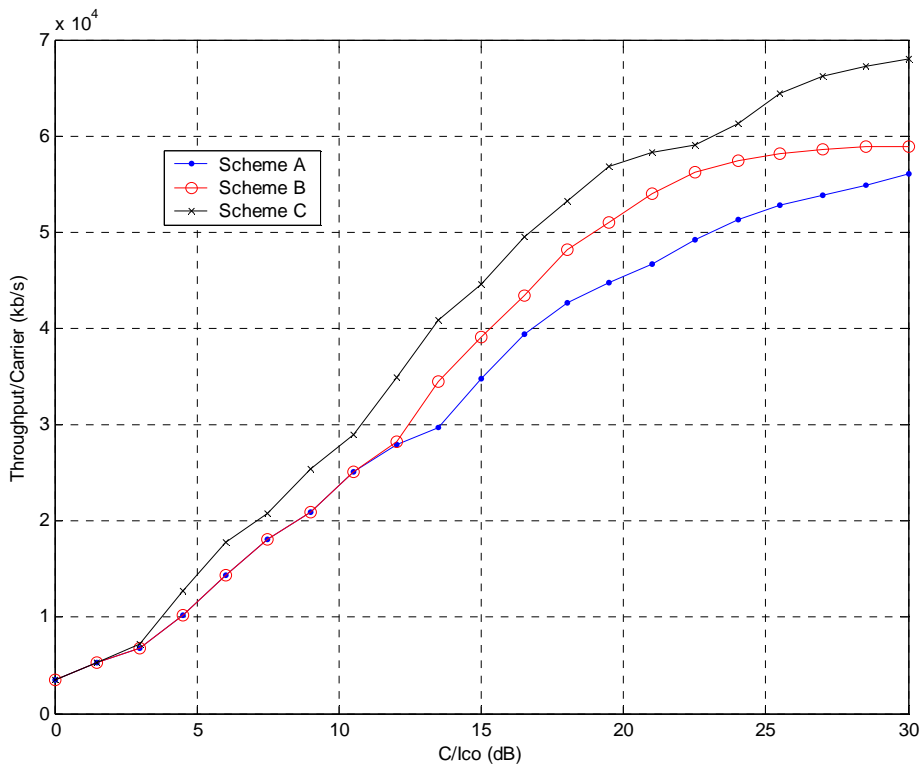
Figure 170: Throughput for TU3iFH Co-Channel
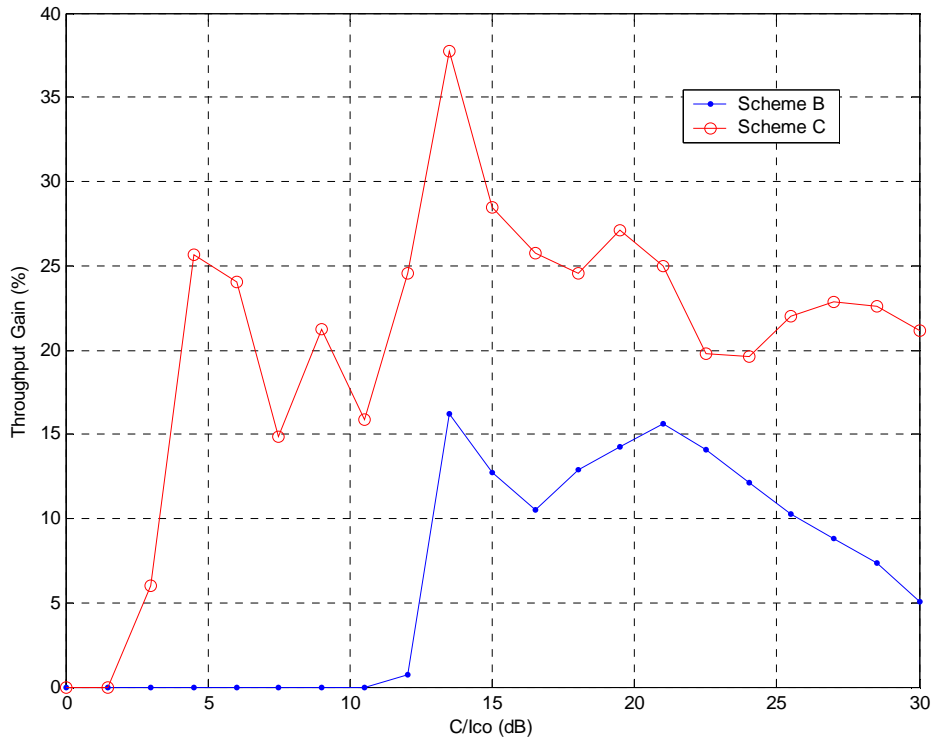
Figure 171: Throughput Gain (%) for TU3iFH Co-Channel
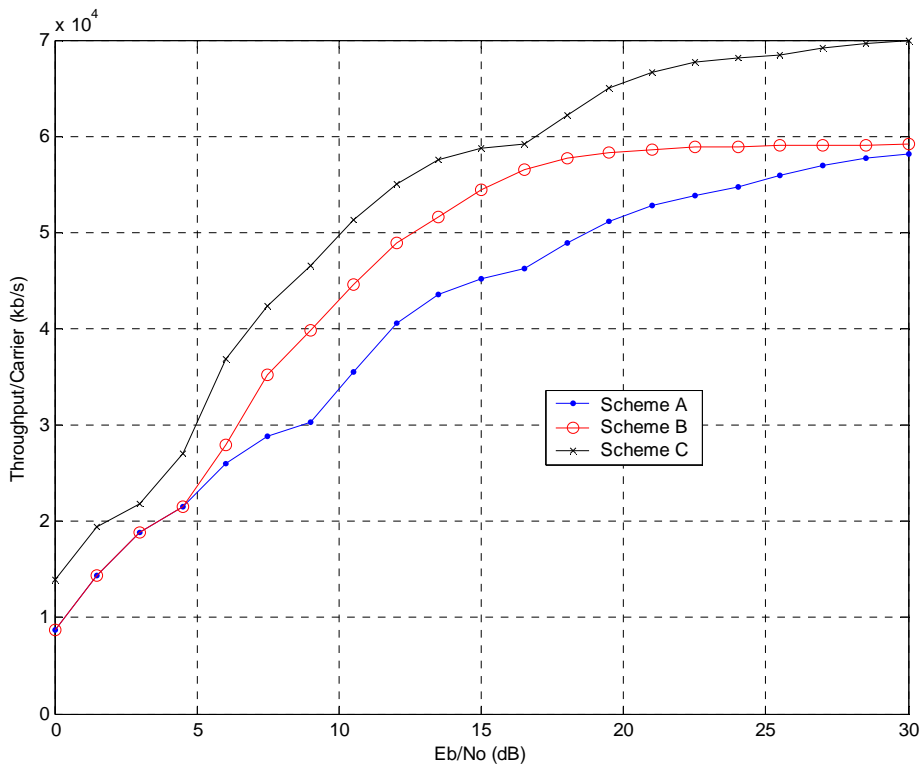
Figure 172: Throughput for TU3iFH Sensitivity
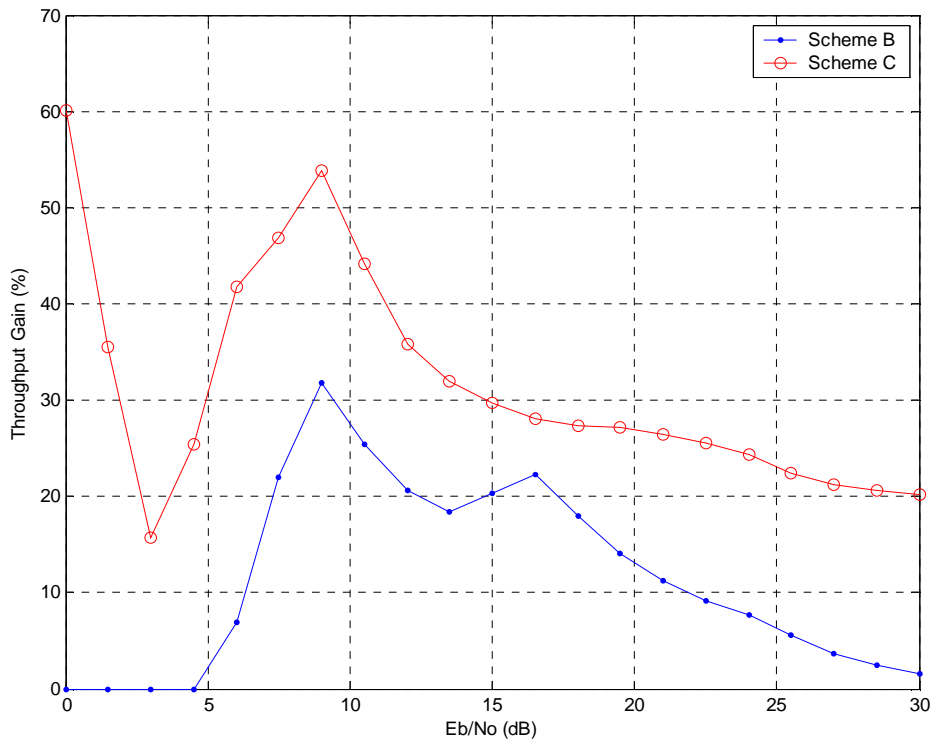
Figure 173: Throughput Gain (%) for TU3iFH Sensitivity
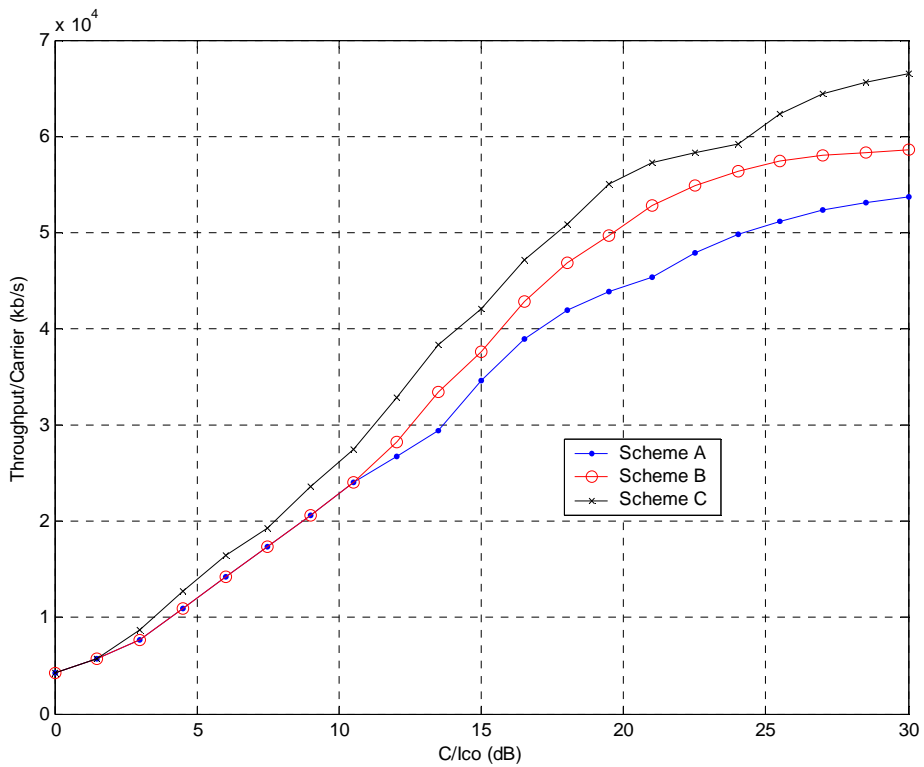
Figure 174: Throughput for TU50nH Co-Channel
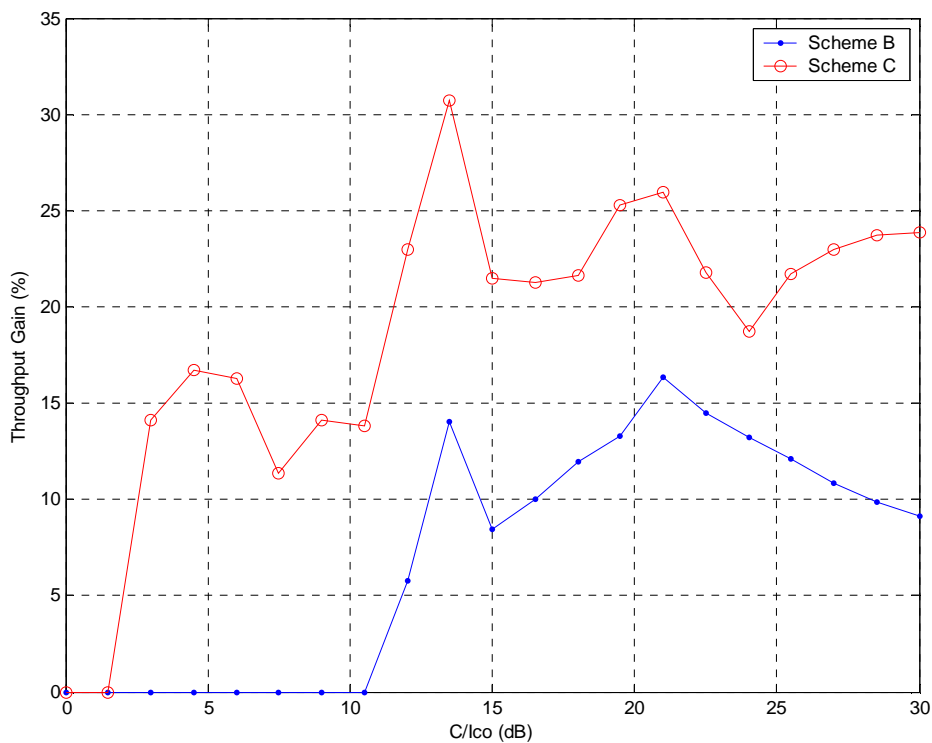
Figure 175: Throughput Gain (%) for TU50nH Co-Channel

Although different Modulation and Coding Schemes (MCS) are typically compared on a scale of Eb/No, this does not give a clear indication of what will be the relative performance under thermal noise limited conditions when different MCSs are transmitted at the same power. Also, in the case that the transmitter is operating at close to maximum power, there will be a different backoff for each modulation scheme.

Figures 176 to 179 show the performance of the selected coding schemes as a function of received power. It has been assumed that the receiver has a constant noise figure of 7 dB.

The logical channel configuration combinations used are shown in table 69. Figures 176 and 177 show the absolute throughput and throughput gain for the TU3iFH channel scenario.

If the transmitter is operating at close to maximum output power, a different backoff is needed in order to maintain EVM for the different modulations. As per [5], back offs of 4.3dB and 6.3dB are used for 8PSK and 16QAM respectively for the graphs that include the impact of transmitter backoff. The resulting throughput and throughput gain graphs are shown in figures 178 and 179. For these graphs, the Power (dBm) scale shows the power received for a non-backed off (i.e. GMSK) signal. In building the hull curves, the 8PSK and 16QAM performance have been shifted to account for the reduced output power from the transmitter.

It can be seen that the improvement from the Turbo coding extends down to a receive power of about -102dBm for the configurations tested, in the case that there is transmitter backoff.
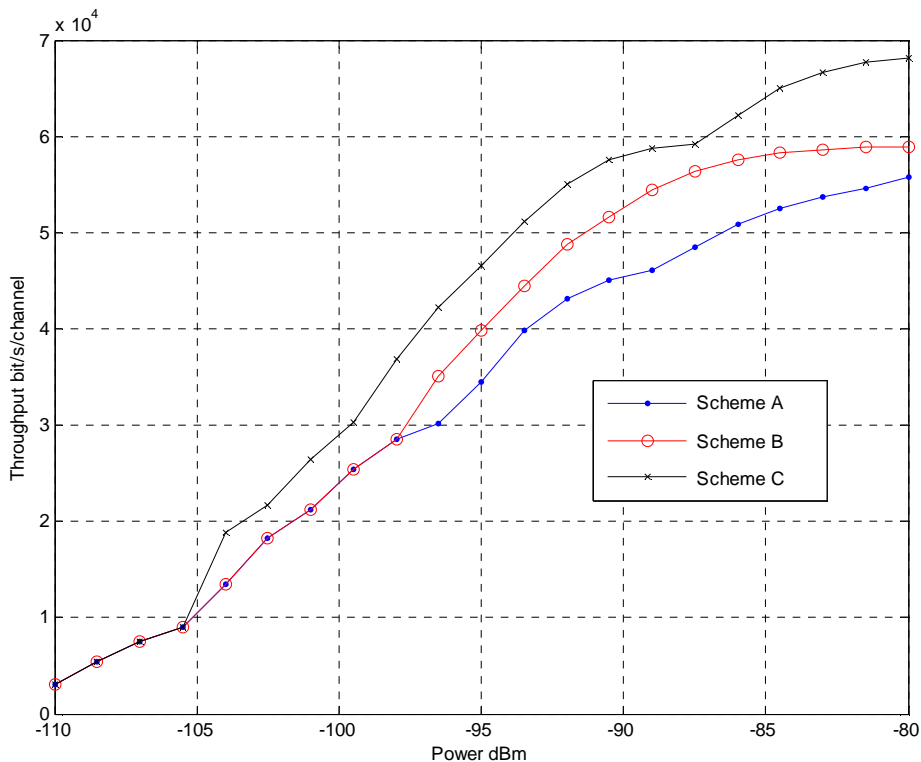
Figure 176: Throughput for TU3iFH Sensitivity
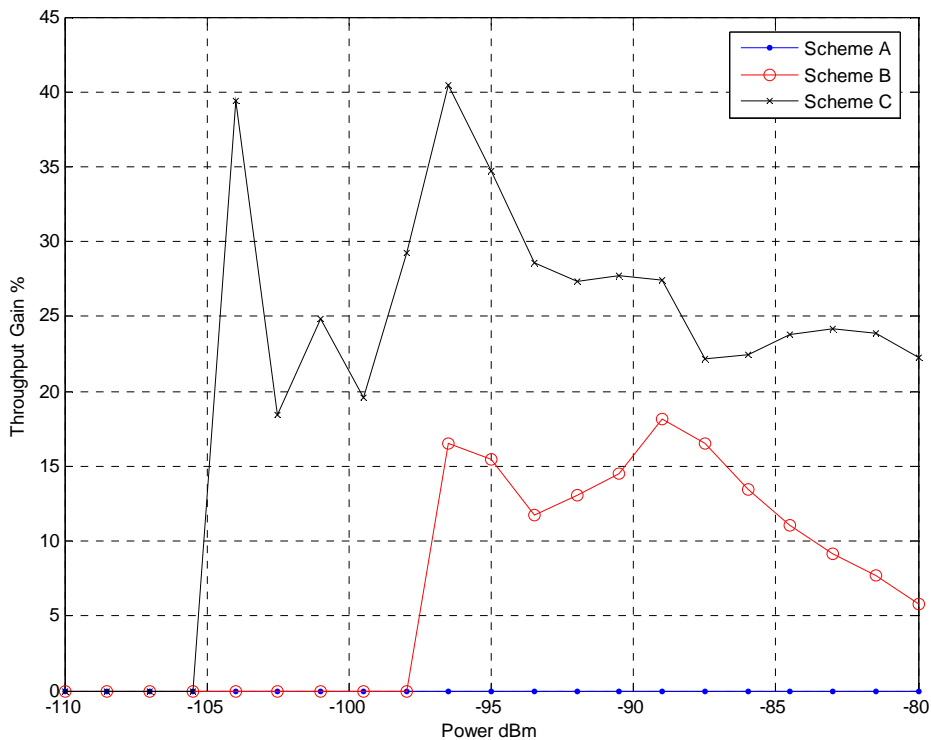
Figure 177: Throughput Gain for TU3iFH Sensitivity
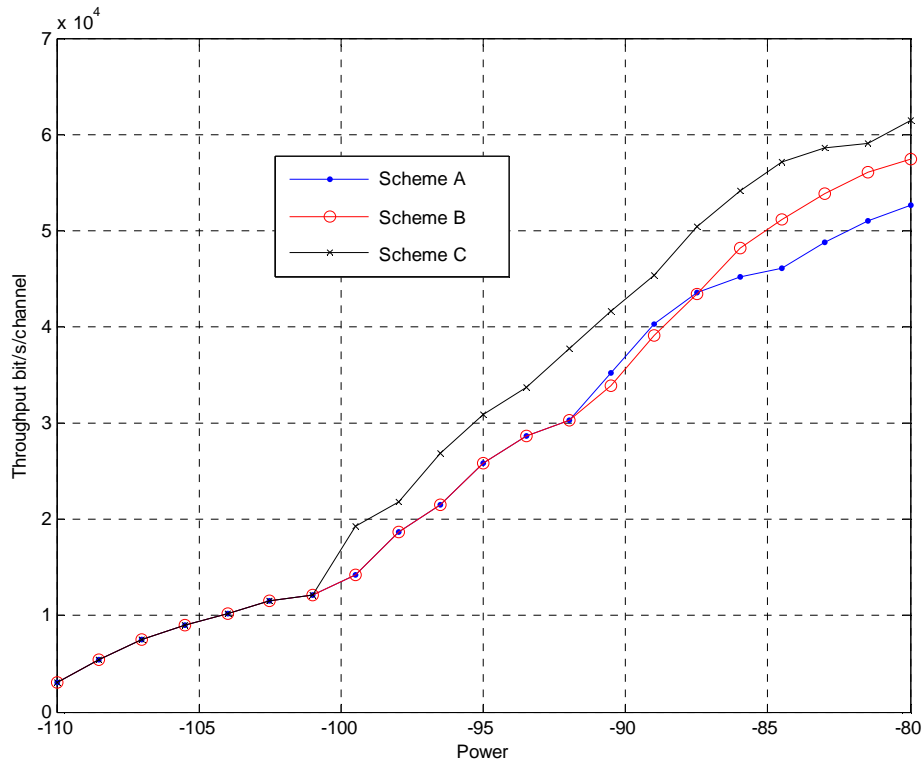
Figure 178: Throughput for TU3iFH Sensitivity, with backoff
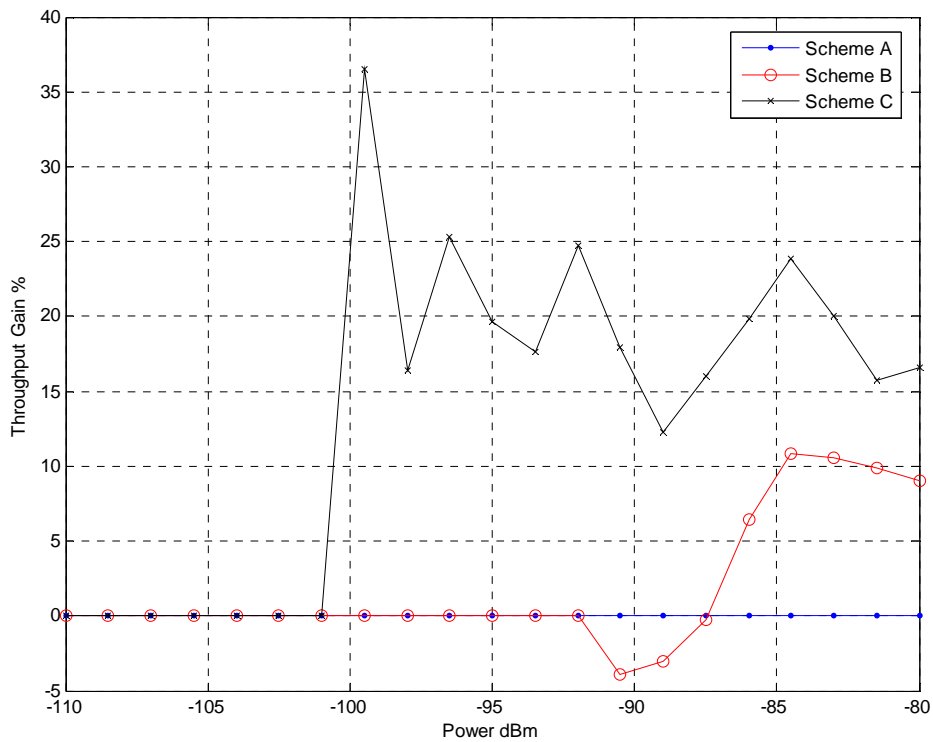
Figure 179: Throughput Gain for TU3iFH Sensitivity, with backoff

8.4.4.1.7.2 Full Incremental Redundancy

Incremental redundancy is now included for simulation of throughput for EGPRS and the Turbo coded logical channels. This is now using RLC/MAC to perform Incremental Redundancy rather than throughput approximations previously used. Puncturing (or repetition) is applied as defined in 3GPP RAN [15]. For a target coding rate greater than R=0.75, the RAN rate matching scheme is not optimal, as some of the parity symbols are never transmitted. For these cases, some modification to the scheme has been made to ensure that all symbols are transmitted at least once after 3 transmissions of a block. This improves throughput performance for regions relevant to the 1st re-transmission and onwards by 1 dB to 2.5dB.

In this subclause, results have been included that compare MCS9-T4-16QAM throughput performance to EGPRS MCS9

8.4.4.1.7.2.1 Impact of Mobile Speed

The variety of mobile speeds in the network is taken into consideration here. Performance results are included for speeds of 3 km/h, 50 km/h and 120 km/h. An example of expected distribution of users as a function of speed is taken from the Nortel OFDM study that pre-dates the current RAN LTE work [23]. Table 70 shows this distribution and the relative importance of higher mobile speeds.

Table 70: Distribution of velocities selected in Nortel OFDM study

Speed (km/h)	Percentage of total
3	60 %
30	20 %
120	20 %

The throughput performance of MCS9 and MCS9-T4-16QAM in the TU channel are shown in this subclause. It has been noted that many operators prefer to use EGPRS on the non-hopping layer rather than the hopping, as it allows superior throughput performance for the MCS7, MCS8 and MCS9 schemes. So to make a fair comparison to the proposed schemes we have used as a reference MCS9 performance on non-hopping channel.

Figures 181, 182 and 183 show the throughput of MCS9-T4-16QAM as compared to MCS9 for different vehicle speeds (3 km/h, 50 km/h and 120km/h). Figure 184 shows the throughput gain provided by MCS9-T4-16QAM as compared to MCS9 at the same speed. [Note that a test was done to extend to (unrealistically) high C/Ic with MCS9 at TU 3km/h. We saw that full throughput is achieved, and that the limiting effect is not due to equalizer limitations.]

Looking for example at the 3km/h curve, it can be seen that gains of 20-60% are achieved in the range C/Ic ~5 dB to 22 dB.

Below C/Ic of 5dB there are larger gains; however, these seem to be less relevant because of the system delay incurred by the many repetitions to work in this region. It is expected that this would be covered by link adaptation to lower MCSs.

It can also be seen that the MCS9 performance reduces fairly rapidly with increasing vehicle speed - this severely limits the maximum throughput with EGPRS. The MCS9-T4-16QAM configuration shows minimal impact with increasing mobile speed. This is seen as a marked gain improvement in figure 184, with gains of 30 % to 60 % for 120 km/h in the expected relevant C/Ic range.

The improvement is larger at higher speeds is expected, since MCS9 on its first transmission has no coding protection, while the 16QAM allows for a reasonable coding rate (0.75), which can then correct some errors due to fading. As speed increases, the probability to have a fading event in a block increases, and therefore MCS9 tends to fail more.

8.4.4.1.7.2.2 Hilly Terrain Channel

Figure 185 shows the throughput for MCS9 and MCS9-T4-16QAM in the HT 100 km/h channel. The throughput performance gain is shown in figure 186. It can be seen that for SNR above 10 dB that throughput improvements of up to 50 % are achievable.

[Note that the scale PathGain represents SNR in dB for GMSK modulation. For 8PSK and 16QAM modulations, backoffs of 3.3 dB and 5.3 dB respectively are applied. Thus, for example, the performance at a PathGain=0dB for 16QAM modulation is generated from 16QAM performance at SNR=5.3dB.]
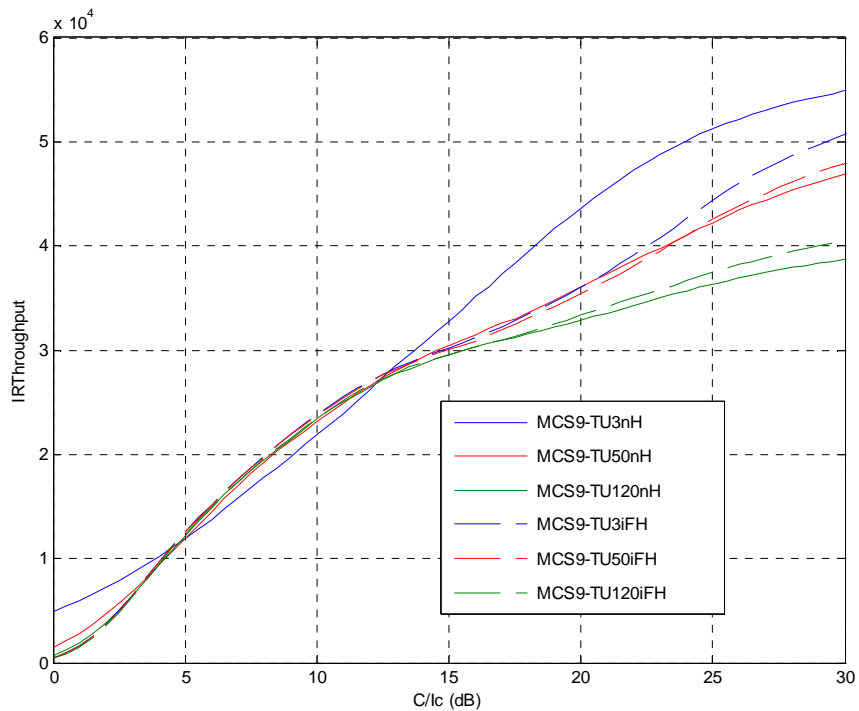
**Figure 180: Throughput Performance of MCS9 with IR for TU channel
at 3 km/h, 50 km/h and 120 km/h, both hopping and non-hopping**
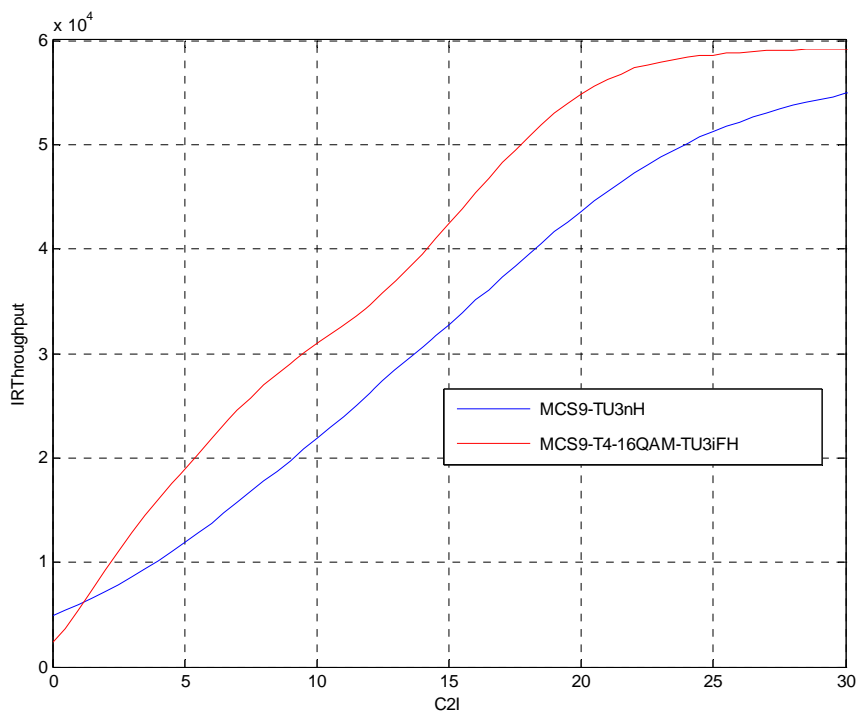
Figure 181: Throughput Performance of MCS9 and MCS9-T4-16QAM with IR at 3 km/h
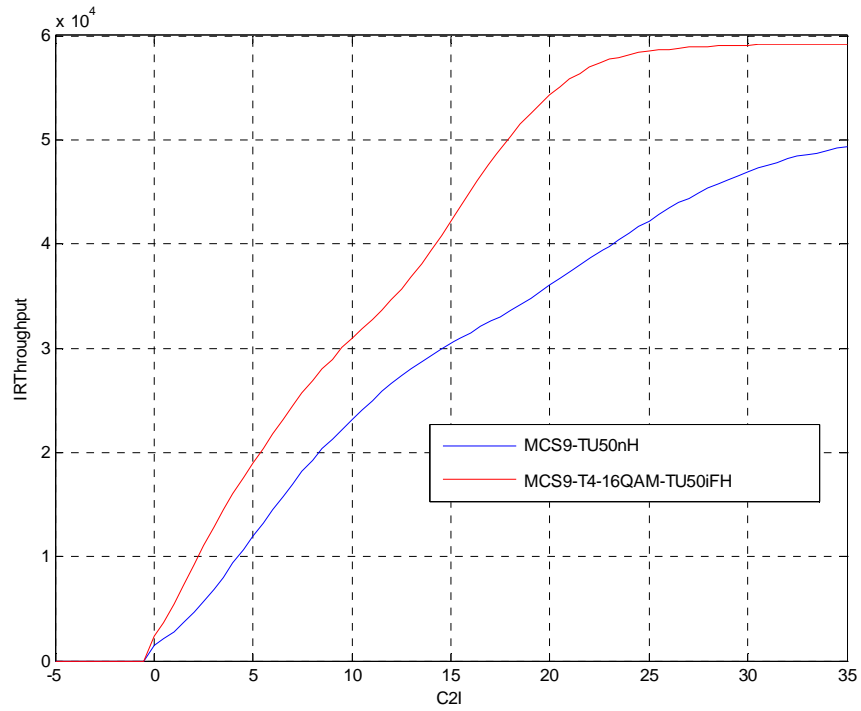
Figure 182: Throughput Performance of MCS9 and MCS9-T4-16QAM with IR at 50 km/h
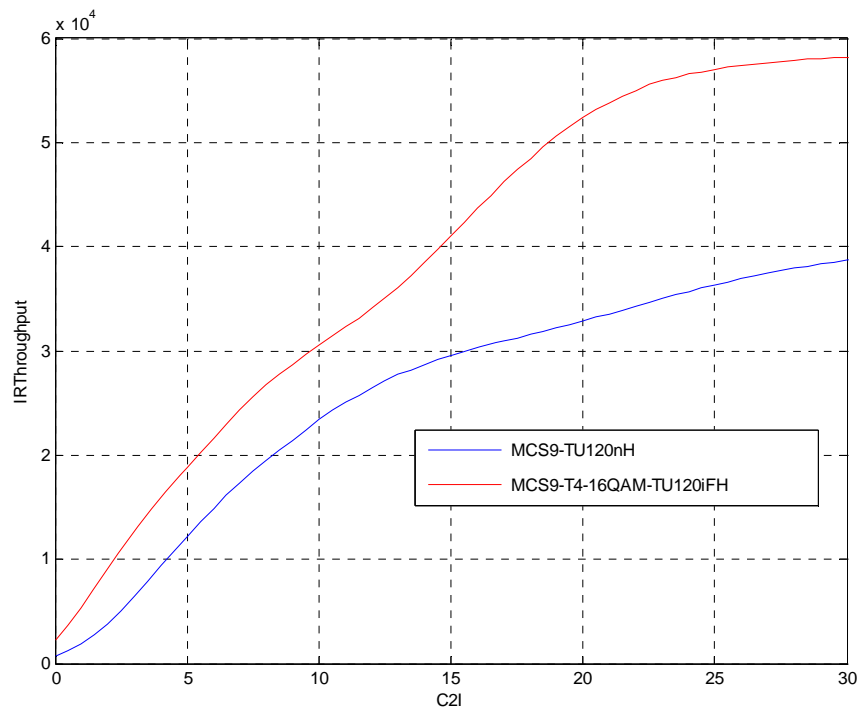
Figure 183: Throughput Performance of MCS9 and MCS9-T4-16QAM with IR at 120 km/h
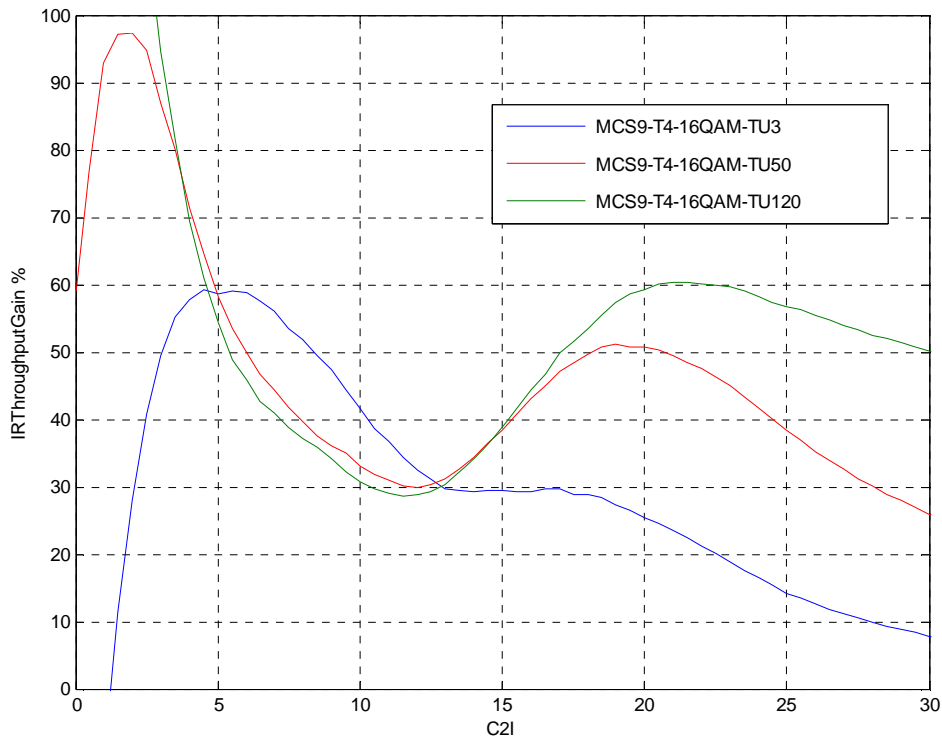
Figure 184: Throughput Performance Gain (%) of MCS9-T4-16QAM with IR at different speeds
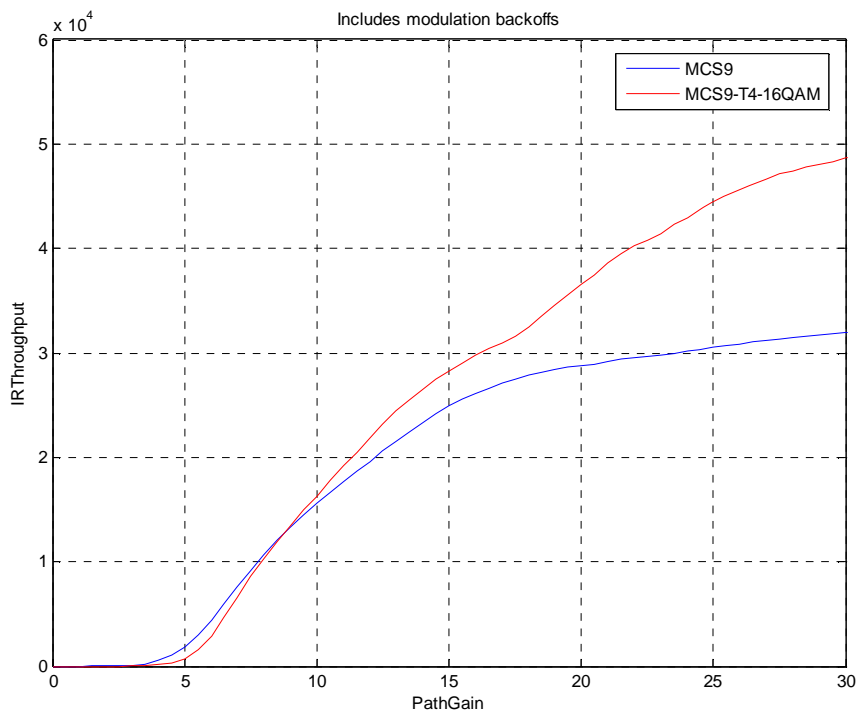
Figure 185: Throughput Performance of MCS9 and MCS9-T4-16QAM with IR for HT100 km/h Non Hopping channel
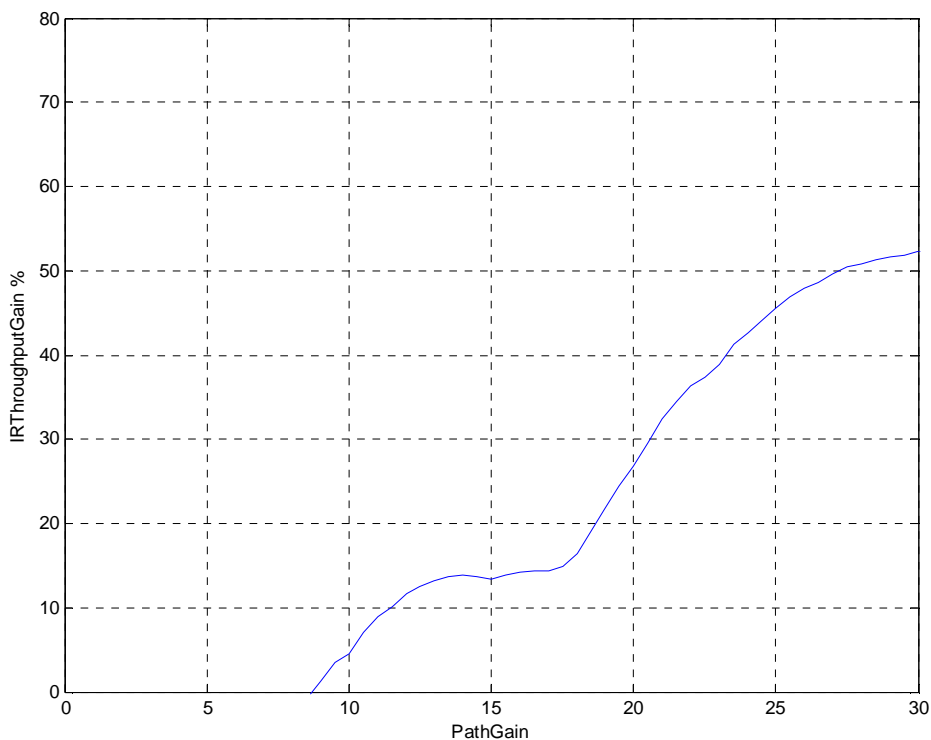
**Figure 186: Throughput Performance Gain (%) of MCS9-T4-16QAM v MCS9
with IR for HT100km/h Non Hopping channel**

8.4.4.1.7.2.3   Performance of HOMTC in Non Hopping Configuration

A comparison of throughput performance for both hopping and non-hopping layers, and at different mobile speeds, is shown in figure 187 for the MCS9-T4-16QAM logical channel. Also included for reference is the MCS9 throughput for TU 3 km/h non-hopping; remember from figure 180 that MCS9 performance decreases with speed. It can be seen that the MCS9-T4-16QAM throughput is largely unaffected under the differing conditions. There is some degradation for low speed non-hopping; though it still substantially increases throughput as compared to MCS9.
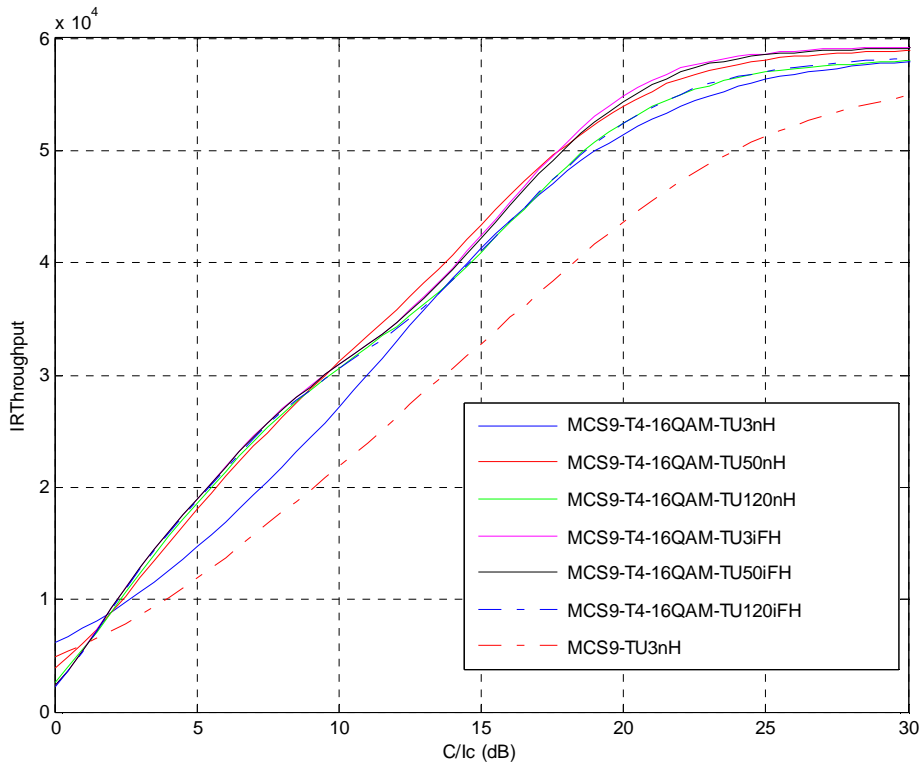
Figure 187: Throughput Performance of MCS9-T4-16QAM with IR for TU channel at 3 km/h, 50 km/h and 120 km/h, both hopping and non-hopping, plus MCS9 with IR TU 3 km/h non-hopping

8.4.4.1.8 Number of Turbo Decoding Iterations

Figures 188 and 189 (zoomed version of figure 188) show the impact on performance of reduced iterations in the Turbo decoder. As expected there is some degradation of throughput performance with reduced Turbo iterations, but it is by no means catastrophic. This would make use of Turbo coding on the uplink easier to employ; in the case of low loading on the uplink, more iterations could be used for a certain block, and for higher loading processing could be allocated between a number of blocks.
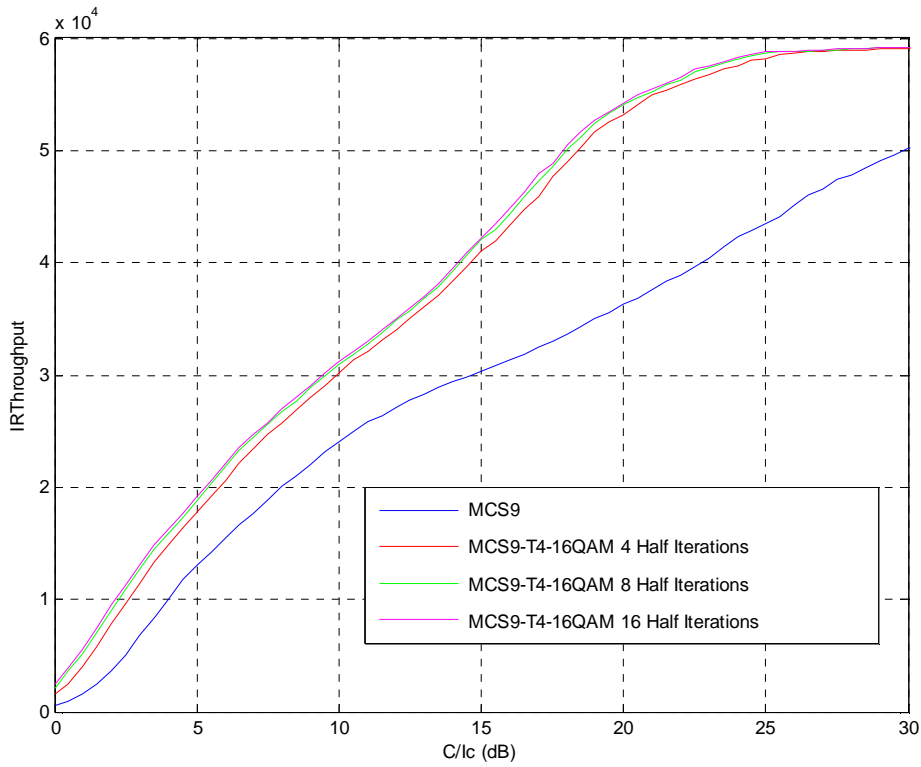
**Figure 188: Throughput Performance for MCS9 and MCS9-T4-16QAM in TU3iFH Channel
with Variable Number of Turbo Decoding Iterations**
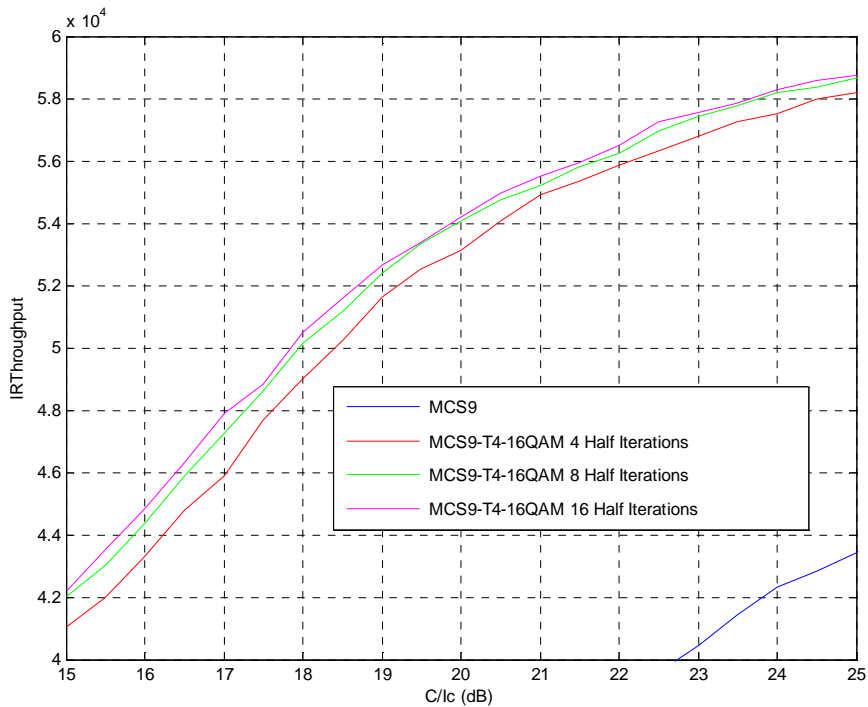
**Figure 189: Throughput Performance for MCS9 and MCS9-T4-16QAM in TU3iFH Channel
with Variable Number of Turbo Decoding Iterations (Zoomed)**

8.4.4.1.9 Improved Cell Edge Performance

This subclause shows initial results of investigation to improve throughput performance at the cell edge. As described earlier, 8PSK modulated Turbo coded schemes have been compared to the current EGPRS GMSK modulated schemes, MCS1 to MCS4. The new MCSs are defined in table 71 such that the new logical channels carry the same payloads as MCS1 through MCS4. The BLER results for MCS1 to MCS4 compared to Turbo coded schemes are shown in figures 192 to 193. The performance gains at 10 % BLER are shown in table 72. It can be seen that gains of up to 10dB are achieved. The throughput performance curves for the schemes are shown in figure 194 for ideal link adaptation; both hopping and non-hopping are shown for EGPRS.

As with the 16QAM case, the lower coding rate afforded by 8PSK modulation is advantageous, as it gives better immunity to fading.

Table 71: Modulation and Coding Configurations

Modulation and Coding Scheme	Data Block Length (bits)	Coding	Data Code Rate	Interleaving Depth	Max Data Rate (kbit/s)
MCS-1	178	Conv	0.53	4	8.9
MCS-1-T4-8PSK	178	Turbo	0.17	4	8.9
MCS-2	226	Conv	0.66	4	11.3
MCS-2-T4-8PSK	226	Turbo	0.22	4	11.3
MCS-3	298	Conv	0.8	4	14.9
MCS-3-T4-8PSK	298	Turbo	0.26	4	14.9
MCS-4	354	Conv	1	4	17.7
MCS-4-T4-8PSK	354	Turbo	0.33	4	17.7

Table 72: Performance Improvement vs EGPRS Logical Channels in TU3iFH Co-Channel Scenario

Modulation and Coding Scheme	C/Ico (dB) @ 10 % BLER	Gain (dB) v MCS @ 10 % BLER
MCS1	6.3	-
MCS1-T4-8PSK	3.1	3.2
MCS2	8.6	-
MCS2-T4-8PSK	4	4.6
MCS3	13.2	-
MCS3-T4-8PSK	5.5	7.7
MCS4	16.6	-
MCS4-T4-8PSK	6.5	10.1
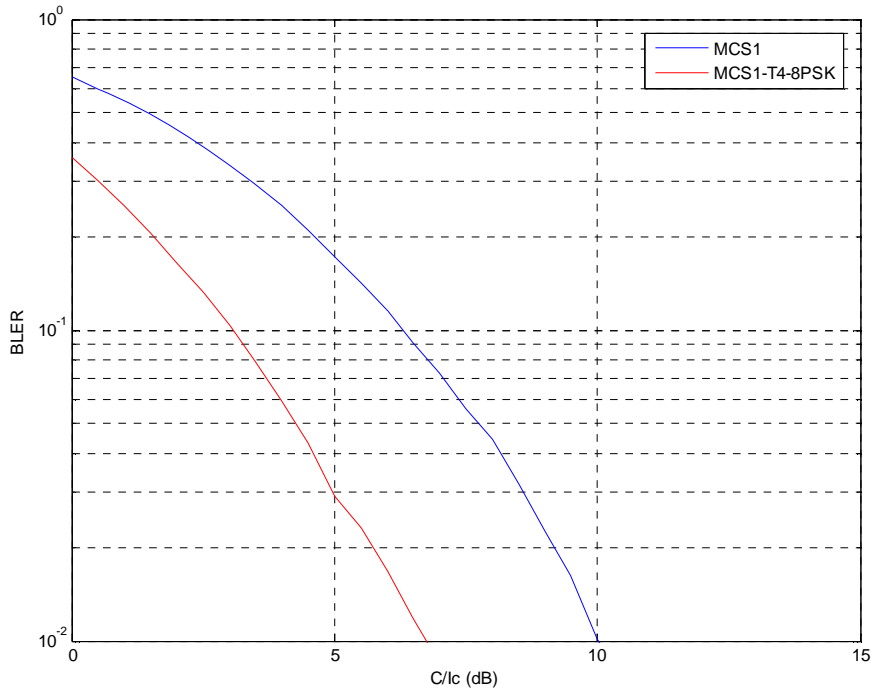
Figure 190: BLER Performance for MCS1 and MCS1-T4-8PSK in TU3iFH Channel
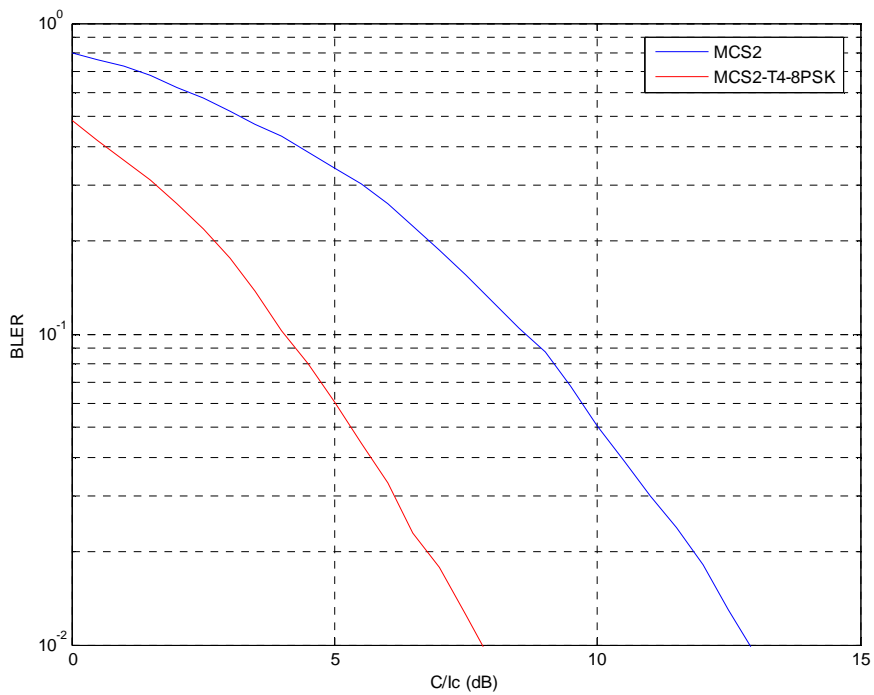
Figure 191: BLER Performance for MCS2 and MCS2-T4-8PSK in TU3iFH Channel
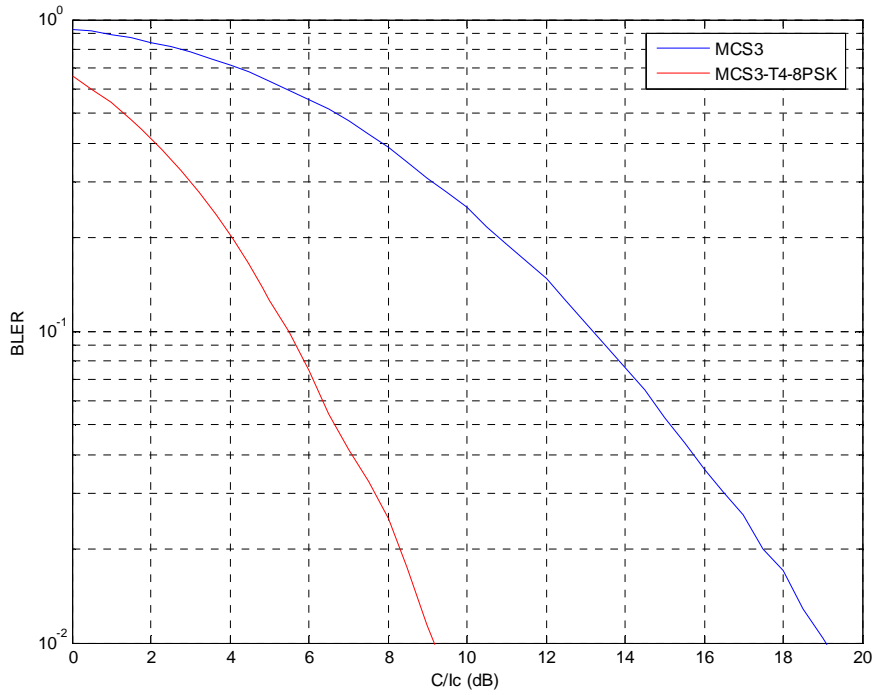
Figure 192: BLER Performance for MCS3 and MCS3-T4-8PSK in TU3iFH Channel
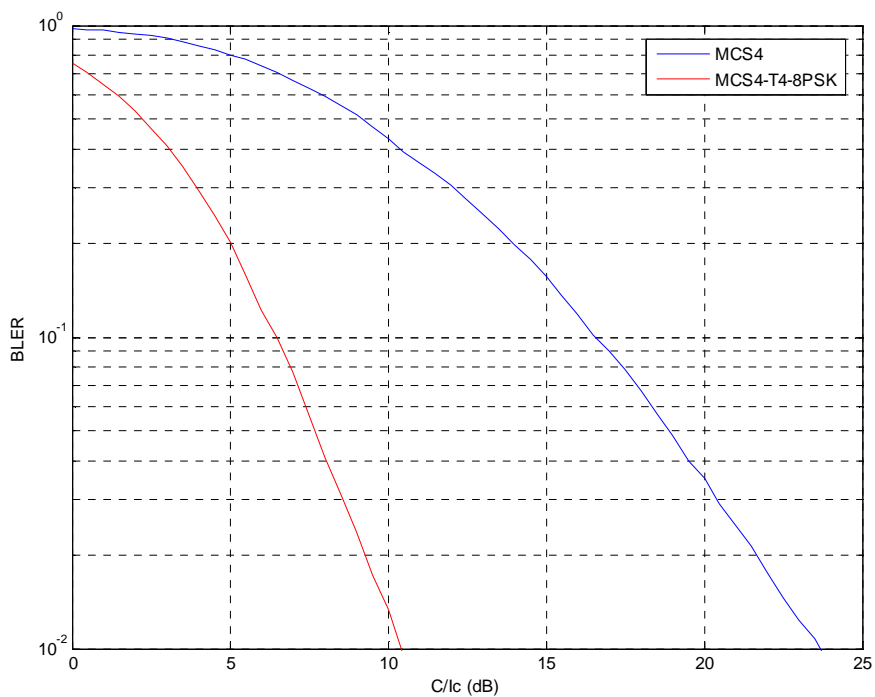
Figure 193: BLER Performance for MCS4 and MCS4-T4-8PSK in TU3iFH Channel
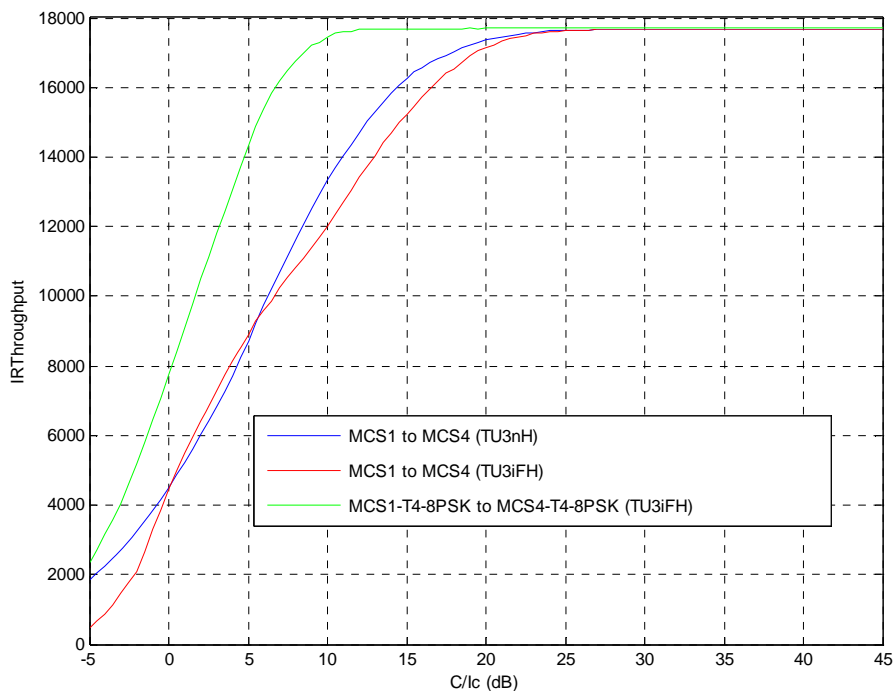
Figure 194: Throughput Performance for EGPRS MCS1-4 v MCS1-T4 to MCS4-T4

8.4.4.1.10   System Performance

A full system analysis has not been performed. However, based on the results it is possible to make some general comments.

In order to understand relevant C/I operating values, the C/I CDFs presented recently in contributions by Ericsson [8] and TeliaSonera [5] have been used. The curves are shown in figure 195.

Turbo codes together with 16QAM modulation give a significant increase in the average throughput across all the C/I range. The increase is in the region of 15 % to 30 % across the scenarios reported.

The increases are not limited to certain user conditions; the benefit is observed across the range of conditions, so that the 5 % worst case users also benefit substantially. From figure 179 the throughput gains for the relevant C./Ico range (3 dB to 12 dB) is in the region of 15 % to 35 %.

The maximum throughput is ultimately determined by the modulation scheme as the code rate tends to 1. This is not dependent on the channel coding scheme used.

It should also be noted that the block lengths used here do not lead to smooth throughput hull curves. Further study will be required to optimize the selection of new MCS configurations.
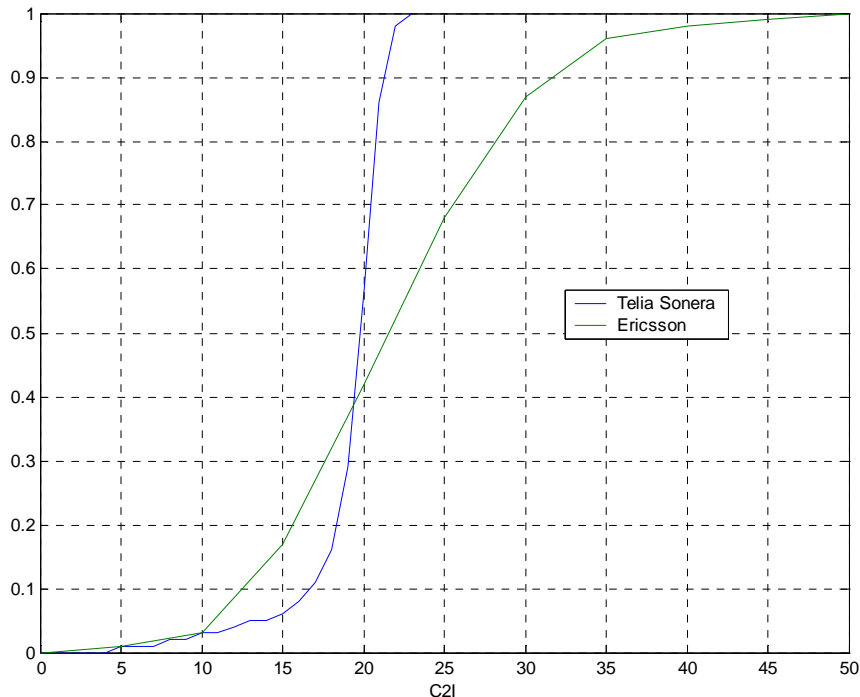
Figure 195: CDFs of C/Ico Distribution

8.4.4.1.11 32QAM Modulation

8.4.4.1.11.1 Logical Channel Configurations Used

The logical channel configurations used for the simulations are shown in tables 73 and 74. The configurations are used to compare performance of 16QAM and 32QAM modulations with that of MCS7, MCS8 and MCS9. A simple rectangular interleaver was used. It is noted that coding schemes with coding rates greater than 0.9 have not yet been included in the results.

Table 73: Modulation and Coding Schemes for EGPRS

Modulation and Coding Scheme	Data Code rate	RLC blocks per radio block	Raw Data (octets)	Interleaving depth	Data rate kb/s/slot
MCS7	0.76	2	2x56	4	44.8
MCS8	0.92	2	2x68	2	54.4
MCS9	1.0	2	2x74	2	59.2

Table 74: HOMTC Modulation and Coding Schemes

Modulation and Coding Scheme	Data Code rate	RLC blocks per radio block	Raw Data (octets)	Interleaving depth	Data rate kb/s/slot
MCS7-T4-16QAM	0.55	1	4x28	4	44.8
MCS8-T4-16QAM	0.67	1	4x34	4	54.4
MCS9-T4-16QAM	0.73	1	4x37	4	59.2
MCS10-T4-16QAM	0.82	1	6x28	4	67.2
MCS7-T4-32QAM	0.44	1	4x28	4	44.8
MCS8-T4-32QAM	0.54	1	4x34	4	54.4
MCS9-T4-32QAM	0.58	1	4x37	4	59.2
MCS10-T4-32QAM	0.66	1	6x28	4	67.2
MCS11-T4-32QAM	0.80	1	6x34	4	81.6
MCS12-T4-32QAM	0.88	1	8x28	4	89.6

8.4.4.1.11.2   BLER Performance

Link simulations were carried out for both a noise limited environment, and an interference limited environment. The TU3iFH channel model was used. It was assumed that for the noise limited sensitivity case full transmit power is always used, with backoff values applied for 8PSK, 16QAM, and 32QAM as 3.2dB, 5.3dB and 5.3dB respectively (note that the PAR value used for 32QAM here may be optimistic). The impairments detailed in tables 36 and 38 were used.

This uncoded BER performance of 16QAM and 32QAM modulations are shown in figure 196 for the co-channel interferer case.
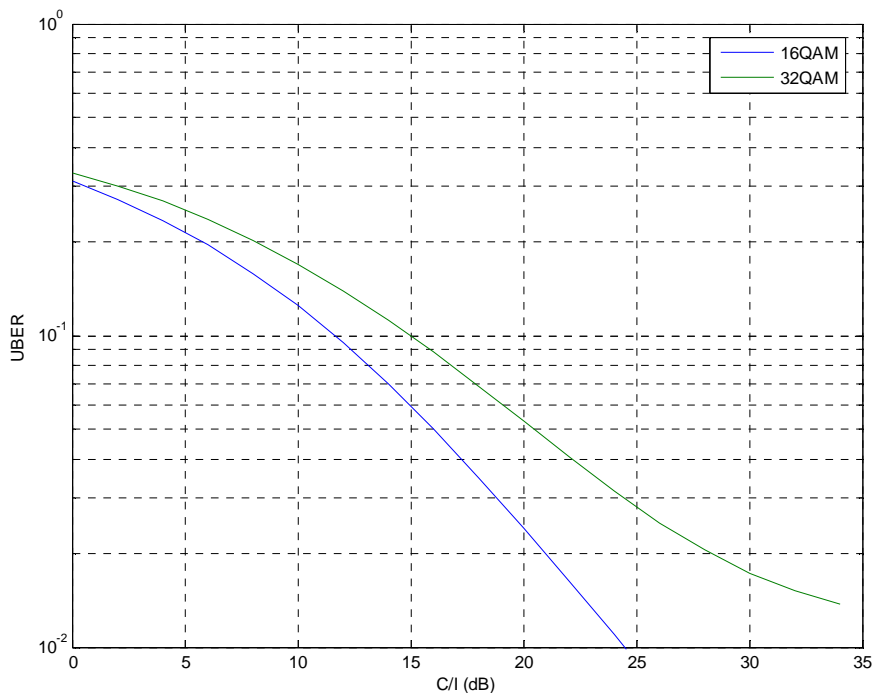
Figure 196: Uncoded BER of 16QAM and 32QAM Modulations

BLER performance graphs comparing the different logical channels are shown in figures 201 to 202 for sensitivity conditions, and figures 207 to 208 for co-channel interferer conditions. The conditions at which 10% BLER is achieved are summarized in tabular form in tables 75 and 76.

Of particular note are the performance results for MCS7/8/9 channels. It can be see that for MCS8 and MCS9 and their equivalents, the configuration using 32QAM HOMTC actually improves performance as compared to 16QAM HOMTC. For MCS7 payload, the performance of 32QAM is slightly degraded as compared to 16QAM.

On the basis of these results, it may be possible to consider an HOMTC enhancement that only requires a new 32QAM modulation, without the need to include a new 16QAM modulation as well. However, further analysis should consider channel profiles with longer delay spreads and the complexity of 32QAM verses 16QAM.

Table 75: Sensitivity limited results

MCS	EGPRS	T4-16QAM		T4-32QAM		
	SNR (dB) @ 10 % BLER	SNR (dB) @ 10 % BLER	Gain v EGPRS	SNR (dB) @ 10 % BLER	Gain v EGPRS	Gain v 16QAM
MCS7	20.7	19.2	1.5	19.5	1.2	-0.3
MCS8	27.2	22.2	5	22	5.2	0.2
MCS9	31.9	24.1	7.8	23.4	8.5	0.7
MCS10	N/A	28	N/A	26	N/A	2
MCS11	N/A	N/A	N/A	34.4	N/A	N/A
MCS12	N/A	N/A	N/A	~36 (36%)	N/A	N/A

Table 76: Interference limited results

MCS	EGPRS	T4-16QAM		T4-32QAM		
	C/I (dB) @ 10% BLER	C/I (dB) @ 10% BLER	Gain v EGPRS	C/I (dB) @ 10% BLER	Gain v EGPRS	Gain v 16QAM
MCS7	17.6	14.4	3.2	14.7	2.9	-0.3
MCS8	23.4	17.4	6	17.2	6.2	0.2
MCS9	27.9	19.2	8.7	18.5	9.4	0.7
MCS10	N/A	22.9	N/A	21.1	N/A	1.8
MCS11	N/A	N/A	N/A	29.2	N/A	N/A
MCS12	N/A	N/A	N/A	31.5 (30%)	N/A	N/A
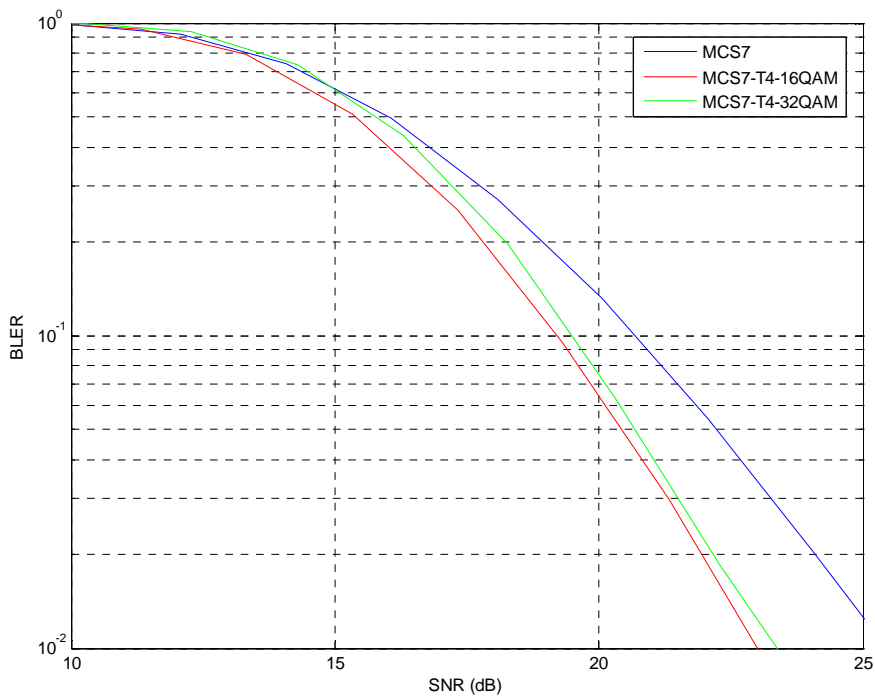
Figure 197: TU3iFH Sensitivity Performance (MCS-7)
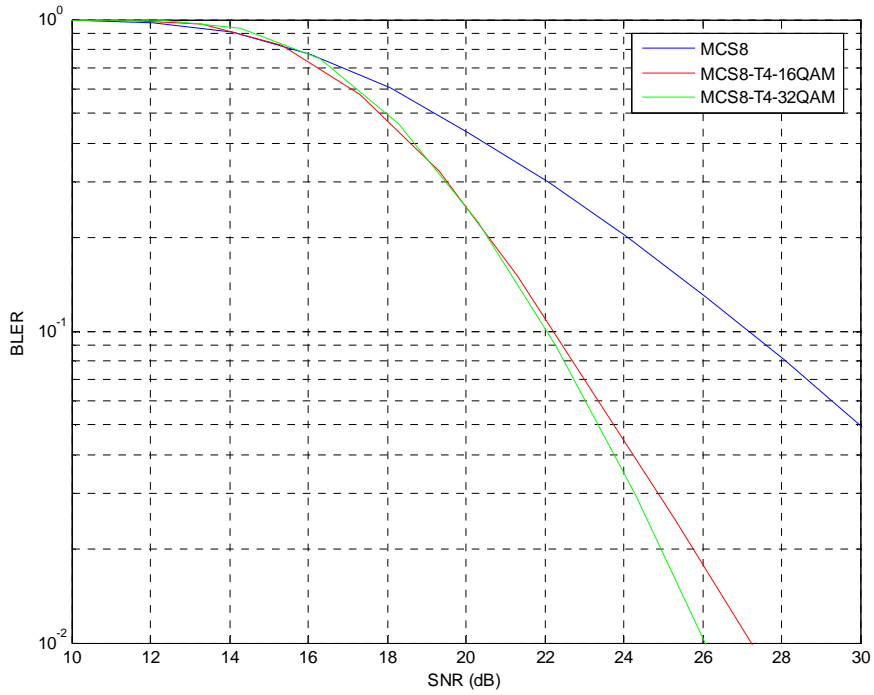
Figure 198: TU3iFH Sensitivity Performance (MCS-8)
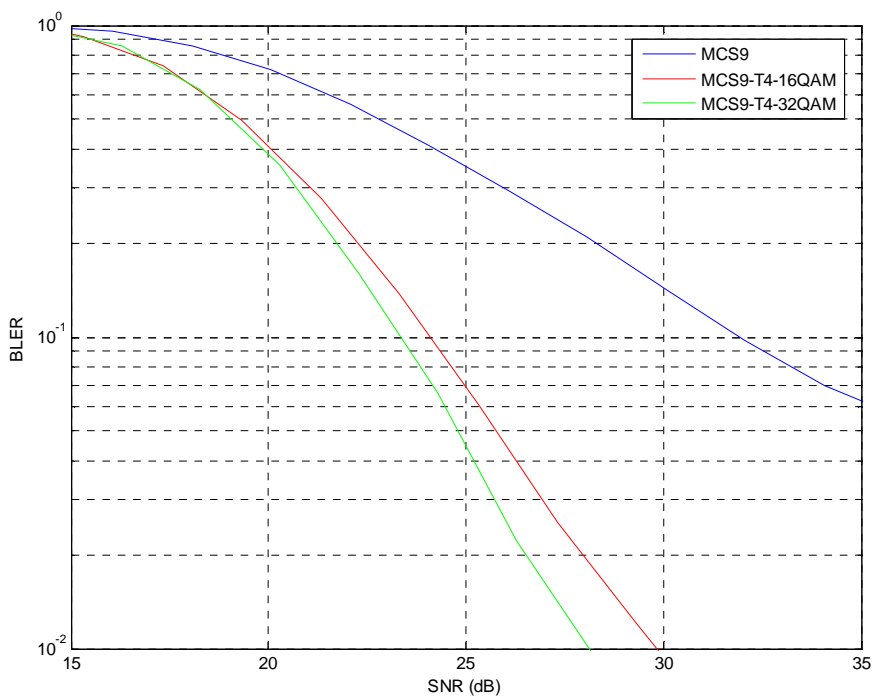
Figure 199: TU3iFH Sensitivity Performance (MCS-9)
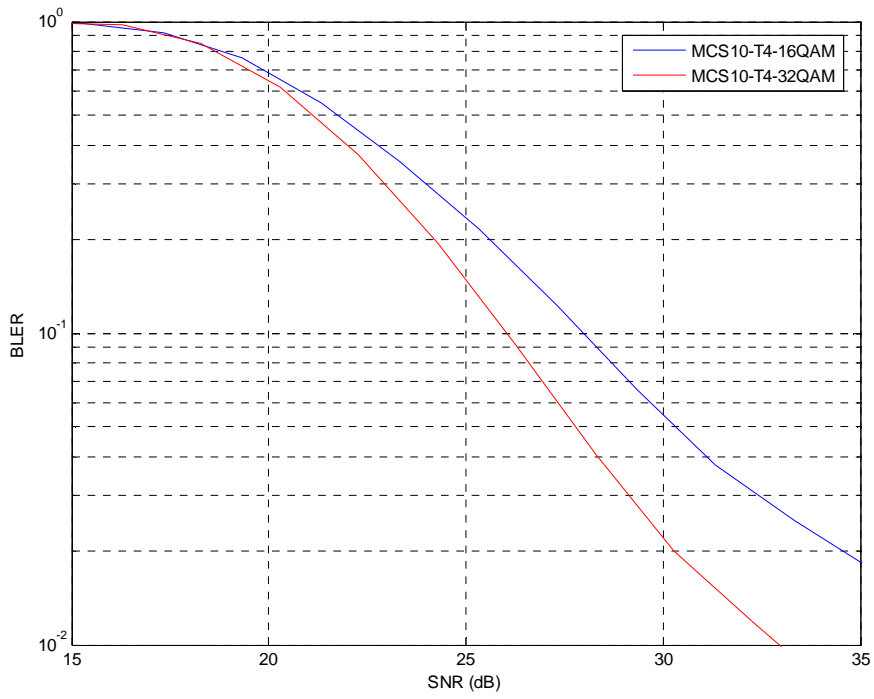
Figure 200: TU3iFH Sensitivity Performance (MCS-10)
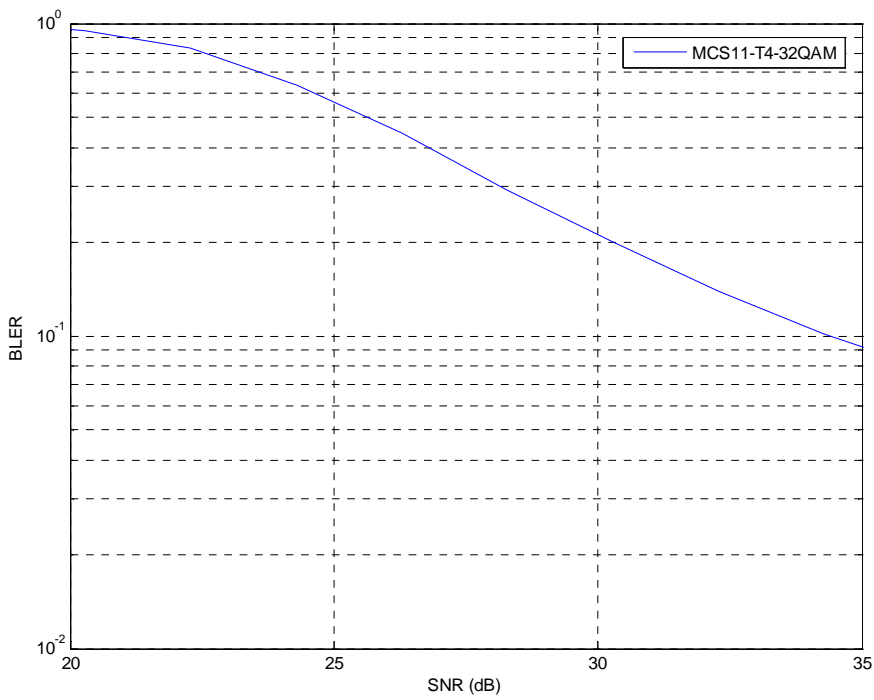
Figure 201: TU3iFH Sensitivity Performance (MCS-11)
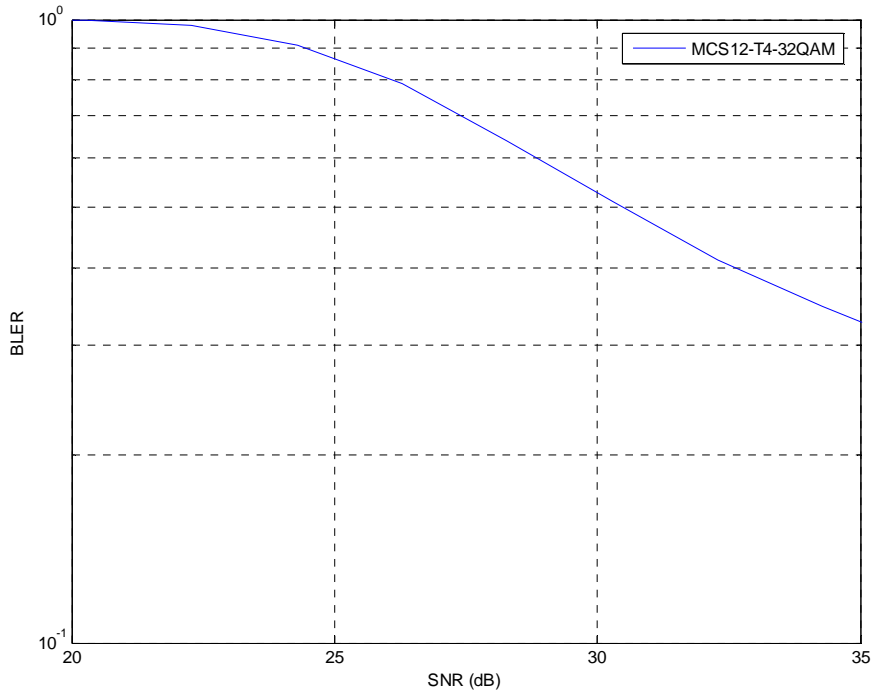
Figure 202: TU3iFH Sensitivity Performance (MCS-12)
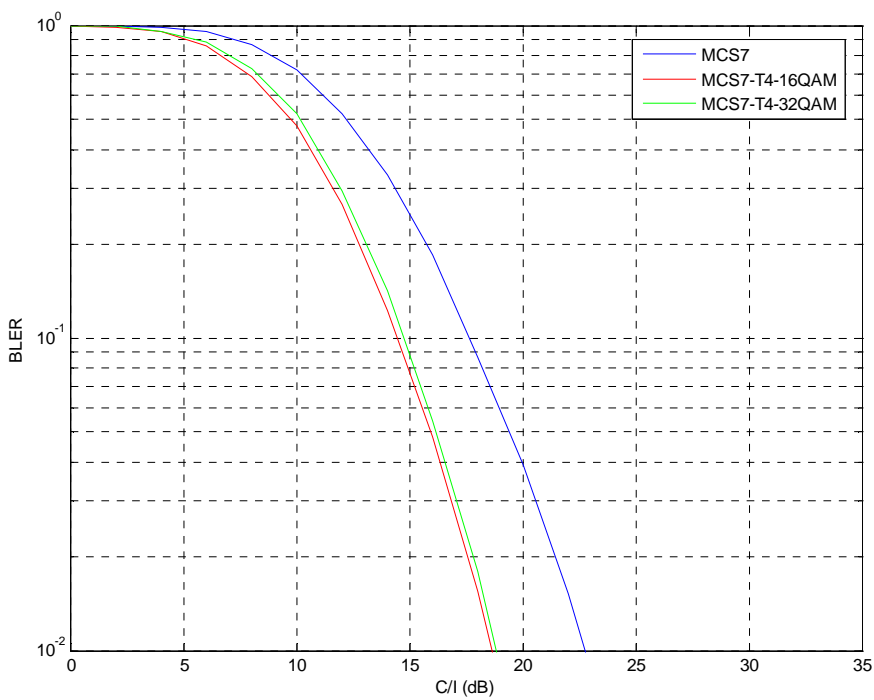
Figure 203: TU3iFH Co-Channel Performance (MCS-7)
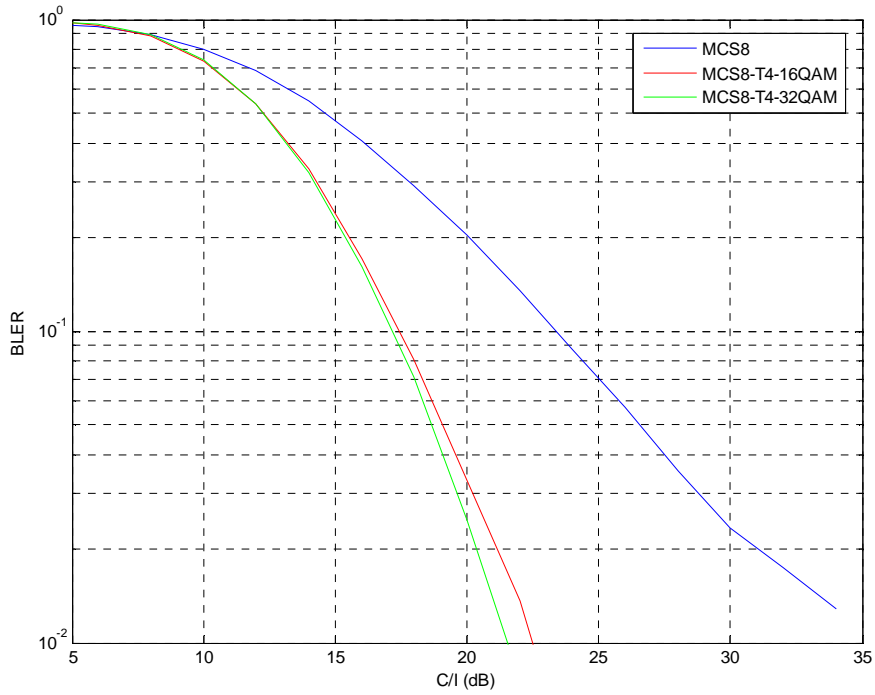
Figure 204: TU3iFH Co-Channel Performance (MCS-8)
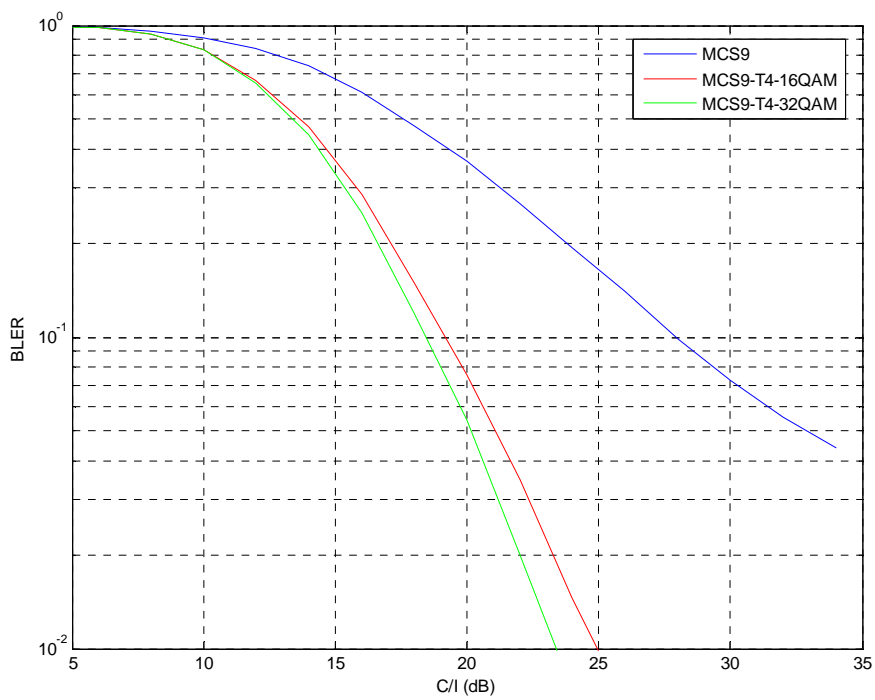
Figure 205: TU3iFH Co-Channel Performance (MCS-9)
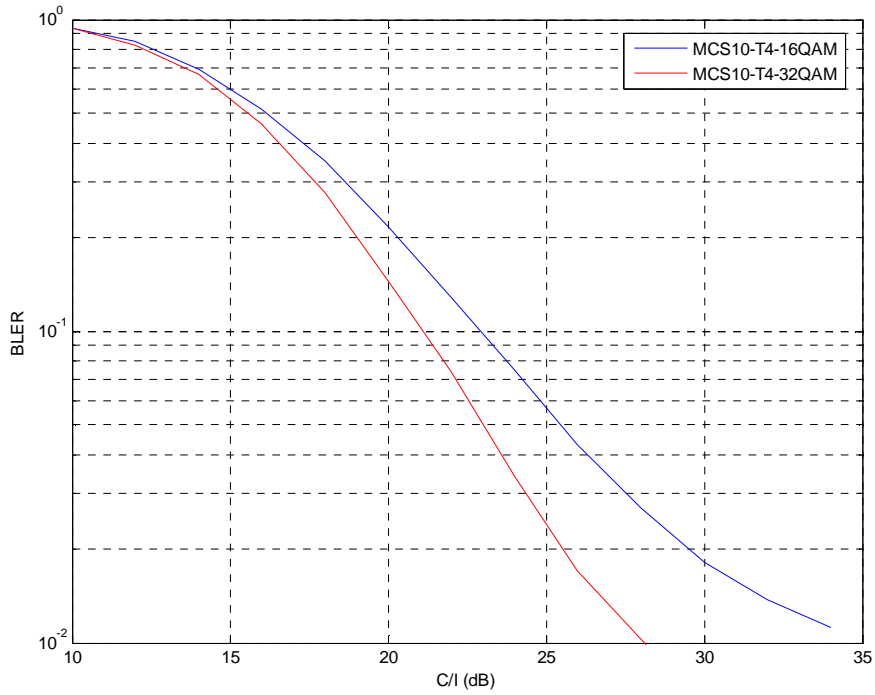
Figure 206: TU3iFH Co-Channel Performance (MCS-10)
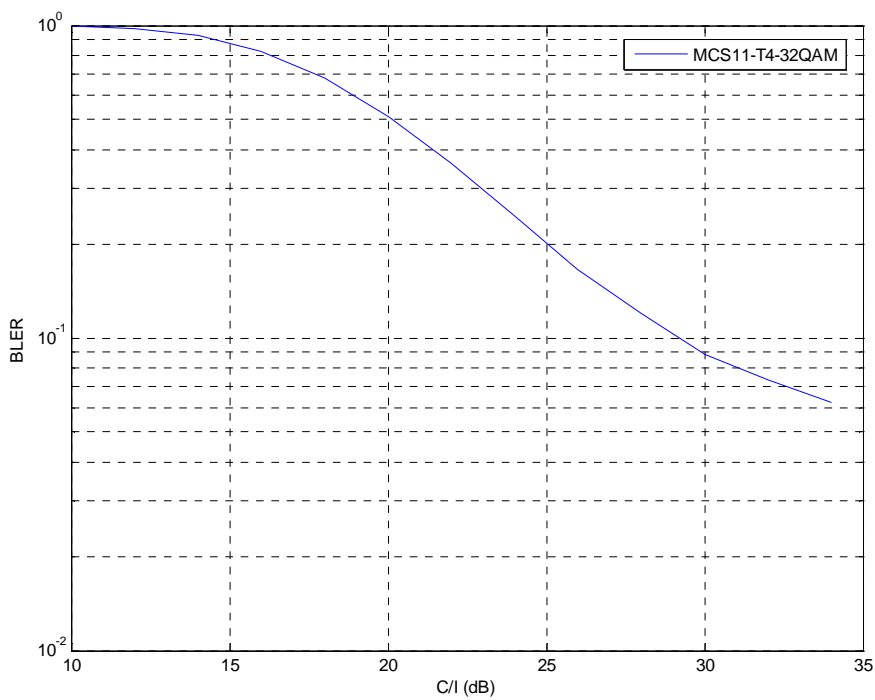
Figure 207: TU3iFH Co-Channel Performance (MCS-11)
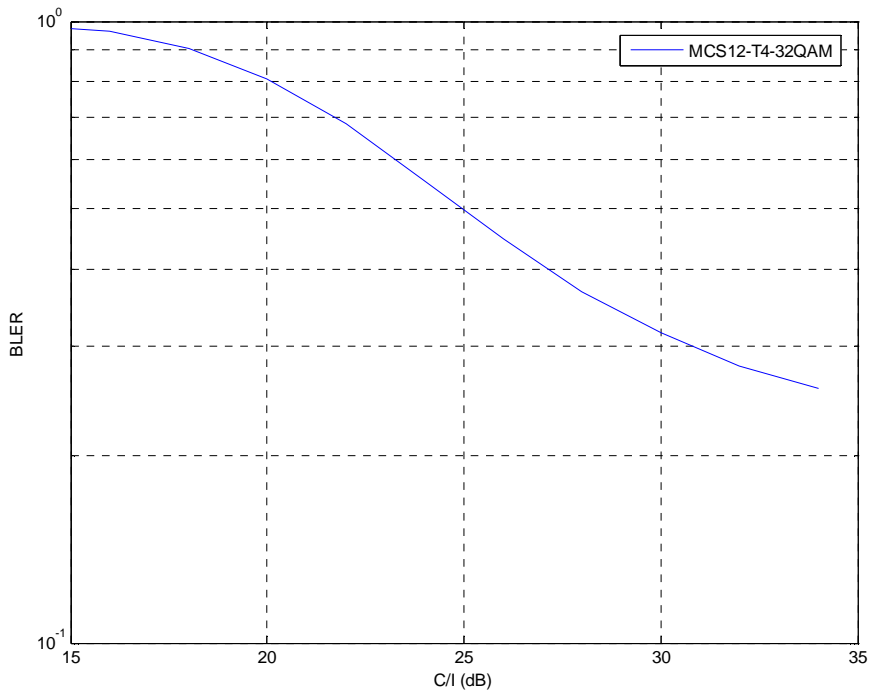
Figure 208: TU3iFH Co-Channel Performance (MCS-12)

8.4.4.1.11.3   Throughput Performance

This subclause presents the throughput performance of the HOMTC logical channel configurations as compared to EGPRS. The configurations used for each set are given in table 77. Type II Incremental Redundancy is included.

Graphs of throughput performance and gain relative to EGPRS are shown in figures 209 and 210 respectively. Set 3 in the graphs includes also 32QAM modulation. As can be seen from the graphs, the throughput gain can be further extended by use of 32QAM, as compared to 16QAM, as well as achieving higher peak bit rate.

Table 77: Throughput Performance Configurations

Set	MCS
EGPRS	MCS-7/8/9-8PSK
1	MCS-7/8/9-T4-16QAM
2	MCS-7/8/9/10-T4-16QAM
3	MCS-7/8/9-T4-16QAM MCS-10/11/12-T4-32QAM
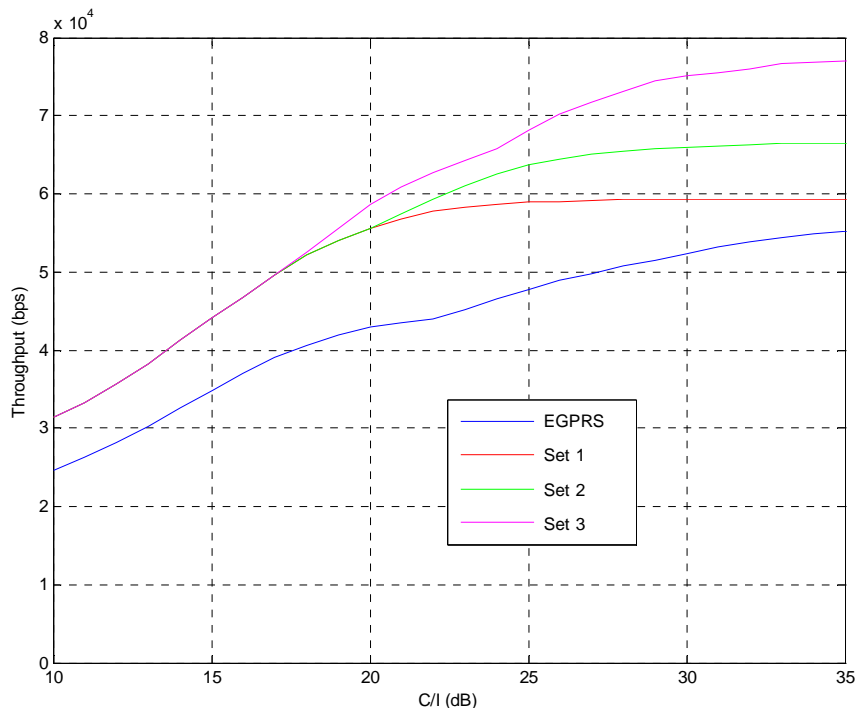
Figure 209: Throughput Performance with IR for TU channel at 3 km/h
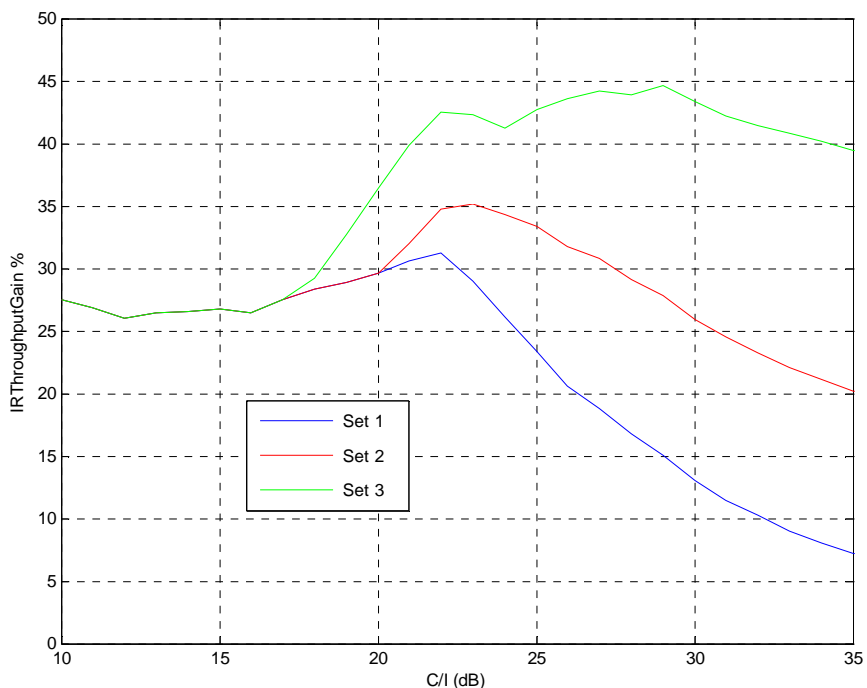
Figure 210: Throughput Gain with IR for TU channel at 3 km/h

8.4.4.1.11.4   Discussion

The results above have shown the feasibility of using 32QAM modulation with Turbo coding for GERAN Evolution. It has been seen that it may be possible to define standardization using only 32QAM, instead of both 16QAM and 32QAM.

Previous work [9] has shown that the increase in spectral efficiency using 16QAM modulation is around 40 % to 60 %. Although no system simulation data is currently available for 32QAM modulation, it is clear that, based on the link simulation data, spectral efficiency by the inclusion of 32QAM modulation will be further increased.

Peak data rate per timeslot can be increased by a factor of 1.66 as compared to EGPRS.

It is possible to allocate 5 timeslots to a Type I mobile, either DL or UL, for example using Multislot class 34. For the uplink, this would entail a 7dB backoff from maximum power, as compared to 6dB for 4 timeslots.

A combination of HOMTC including 32QAM, together with a 5 timeslot allocation, gives a factor of 1.66 x 1.25 which will exceed 100% peak data rate increase as compared to EGPRS. Thus the combination can double peak bit rate, and simultaneously improve spectral efficiency by the order of 50 %.

8.4.4.2 Comparison of Different Coding Configurations for Higher Order Modulation and Turbo Coding Schemes

For thermal noise limited scenarios, results presented in [7] and [26] indicated poor results of HOMTC as compared with EGPRS, both with and without Rx Diversity. This contradiction to performance results that are reported in subclause 8.4.4.1. This subclause reports comparative performance of configurations used in [12] and [26] and examines the source for the reported performance difference.

8.4.4.2.1 HOMTC Coding Scheme Configurations

The logical channel configurations used are defined in table 79. Two configurations of HOMTC have been used. MCSx-T4-16QAM is the configuration used in [12], where the payload is Turbo encoded as a single block. MCSx-T4-16QAM_2 is the configuration used in [26], where the payload is Turbo encoded as 2 half length blocks.

Table 78: Modulation and Coding Schemes

Modulation and Coding Scheme	Data Code rate	RLC blocks per radio block	Interleaving depth	Data rate kb/s	Turbo Decoder Scaling
MCS7	0.76	2	4	44.8	Yes
MCS8	0.92	2	2	54.4	Yes
MCS9	1.00	2	2	59.2	Yes
MCS7-T4-16QAM	0.55	1	4	44.8	Yes
MCS8-T4-16QAM	0.67	1	4	54.4	Yes
MCS9-T4-16QAM	0.73	1	4	59.2	Yes
MCS7-T4-16QAM_2	0.55	2	4	44.8	No
MCS8-T4-16QAM_2	0.67	2	4	54.4	No
MCS9-T4-16QAM_2	0.73	2	4	59.2	No

The simulations are carried out for both an interference limited environment, and a noise limited environment. The TU3iFH channel model is used.

It is assumed that, for the noise limited case, full transmit power is always used, thus implying that the power of 8-PSK modulated blocks is backed off by 3.3 dB and the power of 16-QAM modulated blocks by 5.3 dB.

Mobile station impairments are included as in table 79. No base station impairments were included.

Table 79: Impairments

Impairment	Value
MS I/Q Gain mismatch	0.2 dB
MS I/Q phase mismatch	2.8 degrees
MS Frequency Offset	50 Hz

8.4.4.2.2 Performance Characterization

8.4.4.2.2.1 Interference Limited Channel

The results from the interference limited simulations are summarized in table 80 which shows the link layer performance in terms of CIR at BLER=10 %.

Table 80: Interference limited results

Modulation and Coding Scheme	EGPRS	T4-16QAM		T4-16QAM_2	
		C/I @ 10 % BLER	Gain (dB)	C/I @ 10 % BLER	Gain (dB)
MCS7	17.9	14.6	3.3	16.2	1.7
MCS8	23.8	17.7	6.1	18.8	5
MCS9	29.1	19.4	9.7	20.3	8.8

8.4.4.2.2.2 Sensitivity Limited Channel

The results from the sensitivity limited simulations are summarized in table 216 which shows the link layer performance in terms of SNR at BLER=10 % (after 5.3 dB backoff is taken into account).

Table 81: Sensitivity limited results

Modulation and Coding Scheme	EGPRS	T4-16QAM		T4-16QAM_2	
		SNR @ 10 % BLER	Gain (dB)	SNR @ 10 % BLER	Gain (dB)
MCS7	21	19.5	1.5	21.2	-0.2
MCS8	27.5	22.6	4.9	23.8	3.7
MCS9	32.8	24.5	8.3	25.4	7.4

Figure 211: TU3iFH Co-Channel Performance (MCS-7)
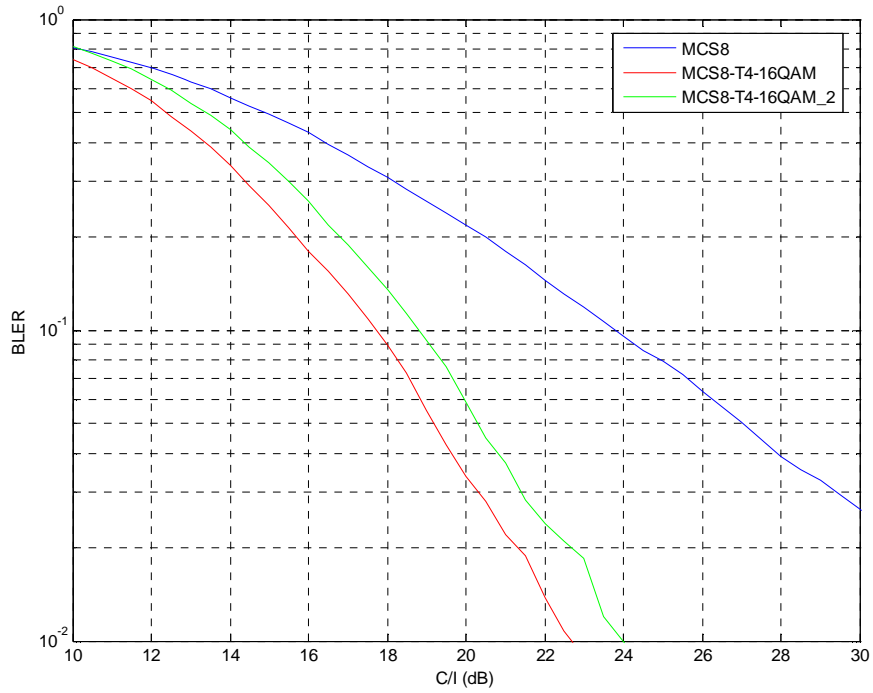
Figure 212: TU3iFH Co-Channel Performance (MCS-8)
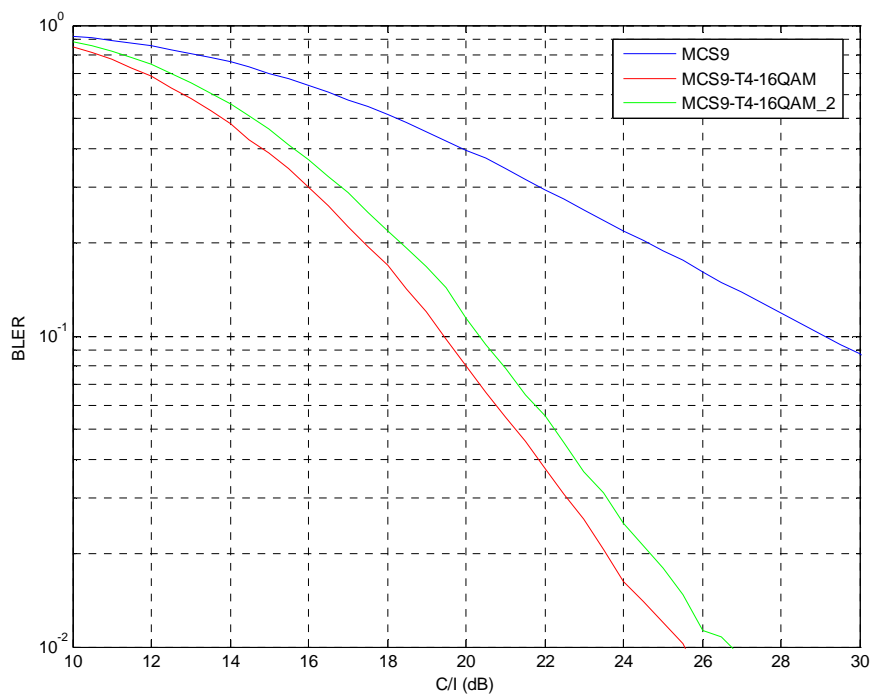
Figure 213: TU3iFH Co-Channel Performance (MCS-9)
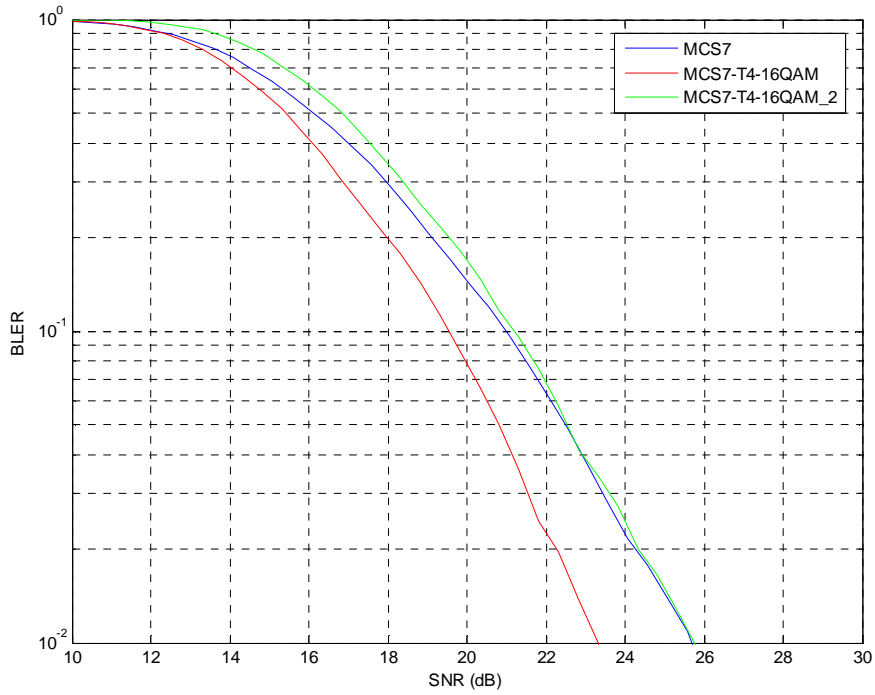
Figure 214: TU3iFH Sensitivity Performance (MCS-7)
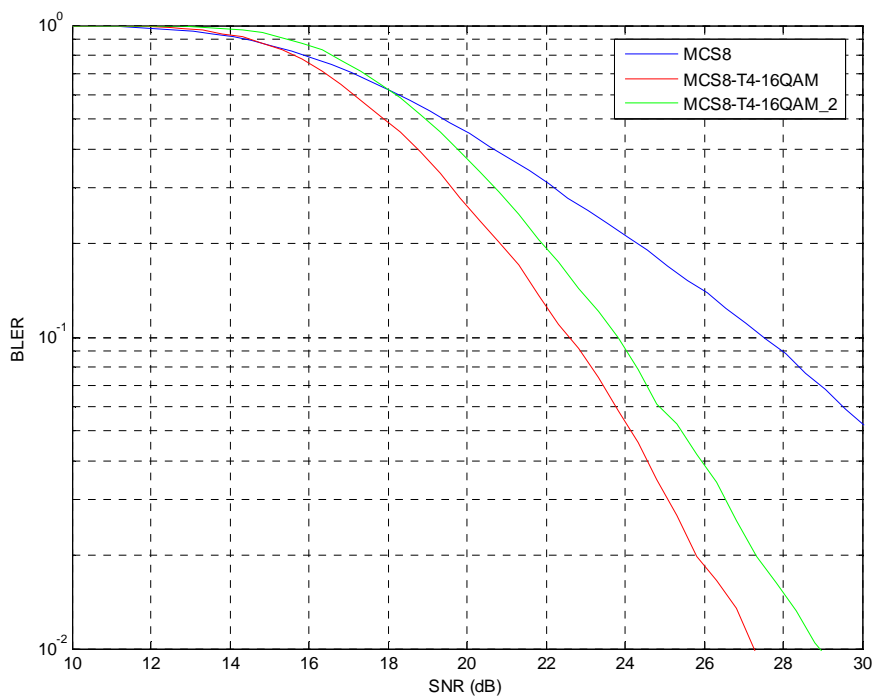
Figure 215: TU3iFH Sensitivity Performance (MCS-8)
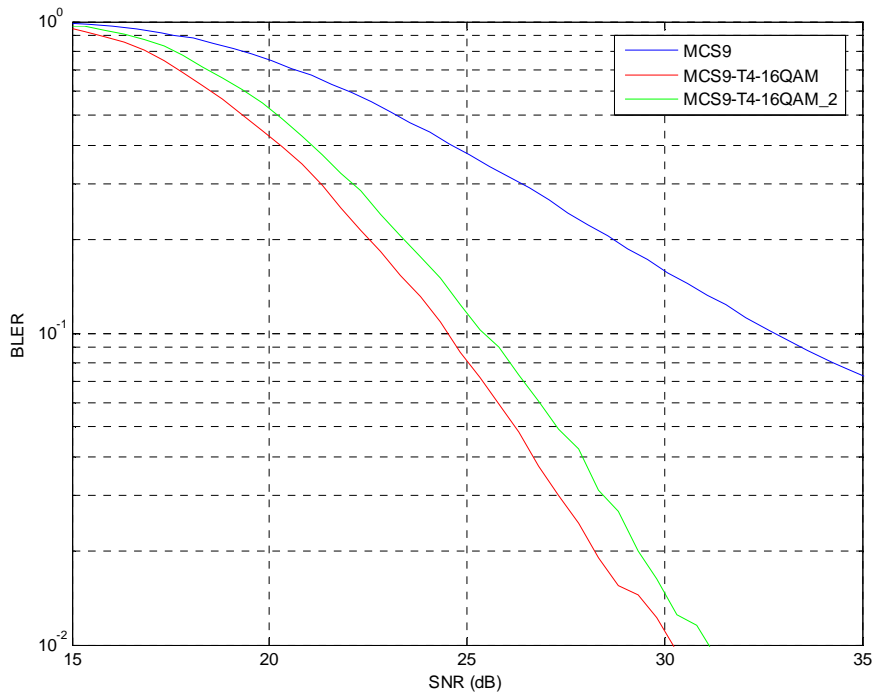
Figure 216: TU3iFH Sensitivity Performance (MCS-9)

8.4.4.2.3 Discussion

8.4.4.2.3.1 Interference Limited Channel

As can be seen from the results, the BLER performance is affected by partitioning of the block. This is particularly noticeable in the configurations equivalent to MCS7, where coding the payload as two separate blocks cuts the gain roughly in half from 3.3 dB to 1.7 dB. For the MCS8 and MCS9 equivalent cases, the loss by division of the payload block is slightly over 1 dB, reducing gain for the MCS8 cases down from 6.1 dB to 5 dB.

8.4.4.2.3.2 Noise Limited Channel

As was seen in the interference limited cases, the noise limited cases are also adversely affected by splitting the payload into 2 blocks. In particular, for the MCS7 equivalent case, the 2 block coding causes a loss in BLER performance as compared to MCS7 - this is in line with the result reported in [26]. However, if the payload is encoded as a single block, this becomes a 1.5 dB gain as compared to MCS7. For the MCS8 and MCS9 equivalent cases, the loss by division of the payload block is approximately 1 dB, reducing gain for the MCS8 cases from 4.9 dB down to 3.7 dB.

8.4.4.3 Impact of Blind Modulation Detection

8.4.4.3.1 Blind Modulation Detection

The training sequences for 8PSK modulation in EDGE were selected to be rotated versions of the original GMSK training sequences. For GMSK, the rotation was $\pi/2$ between symbols. For 8PSK, it was selected to be $3\pi/8$.

The principle is extended for 16QAM and 32QAM, with different rotations used as shown in Table 81a.

Table 81a: Rotation Angles for Different Modulation Constellations

Modulation	Rotation (rad)
GMSK	π/2
8PSK	3π/8
16QAM	π/4
32QAM	-π/4

It will be seen in the results section that incorrect modulation selection increases as the SNR or C/I decreases. But also the quality of the data from the equalizer decreases. An incorrect modulation selection will lead to a performance loss only if the output of the equalizer would have contributed to the decoding phase.

8.4.4.3.2 Simulation Configuration

The results shown are for the simulation configuration described in Section 8.3.

Results are presented for the following channel conditions:

1. Sensitivity: TU50iFH, HT100nH

2. Co-Channel: Tu3iFH, TU50iFH

8.4.4.3.3 Performance Results

The results given in the Annex B.4 show the performance of the selected logical channels at 10% BLER. The performance is shown for the cases when the modulation is known and when blind modulation detection is used in the presence of 4 possible modulations: GMSK, 8PSK, 16QAM and 32QAM. Also shown on each graph is the modulation detection error curve.

Note: A simple modulation detection scheme was used that determines the modulation on a burst by burst basis.

8.4.4.3.4 Discussion

The loss due to blind modulation is insignificant, being no more than 0.1dB in all cases. As is seen in the performance graphs, the modulation detection is far more robust than the data decoding, even when considering 4 modulations, rather than 2 in EGPRS. There are even some cases that the BLER is improved relative to the known modulation case.

8.4.4.3.5 Conclusion

Blind modulation detection does not degrade performance of HOT.

8.5 Symbol Mapping of Turbo Coded Bits

Source: Reference [24].

In this subclause, a symbol mapping method of turbo coded bits for 16-QAM modulation is introduced in order to improve the performance of such turbo coded systems. It is noted that this symbol mapping method has already been included as part of the coding chain for HS-DSCH [15].

8.5.1 Symbol mapping for 16-QAM Modulation

8.5.2.1 Concept description

In high order modulation schemes, such as 16-QAM, 32-QAM and 64-QAM, each symbol consists of bits with different reliabilities. Figure 1 shows the signal constellation diagram of 16-QAM used in 3GPP TS 25.213 [25]. A 16-QAM symbol has a set of four consecutive data bits $b_n, b_{n+1}, b_{n+2}, b_{n+3}$ with (n mod 4)=0 and this set is separated into two consecutive data bits $(i_1 = b_n, i_2 = b_{n+2})$ on the I-axis and two consecutive data bits $(q_1 = b_{n+1}, q_2 = b_{n+3})$ on the Q-axis. This four consecutive bits (i_1, q_1, i_2, q_2) are mapped to a 16-QAM symbol by the modulation mapper. It is noted that in the 16-QAM constellation shown in figure 106, the first two bits (i_1 and q_1) which are in higher reliable positions result in bit error rate (BER) than the last two bits (i_2 and q_2) which are in lower reliable positions. To justify the performance difference between the higher reliable positions and the lower reliable positions, we show simulation results for uncoded 16-QAM symbol transmission over both AWGN and Rayleigh fading channel. Figure 218(a) demonstrates that the higher reliable positions achieve a performance gain of 0.7 dB at BER of 10^{-3} over AWGN channel compared to the lower reliable positions. As shown in figure 218(b), further performance gap of about 3 dB at BER of 10^{-3} exists between the higher reliable positions and the lower reliable positions over Rayleigh fading channel.

As shown in figure 219, higher priority bits can be assigned on higher reliable positions (H part) while lower priority bits can be assigned on lower reliable positions (L part). This symbol mapping concept can be applied to turbo coded bits for 16-QAM modulation in order to attain performance gain without additional complexity.
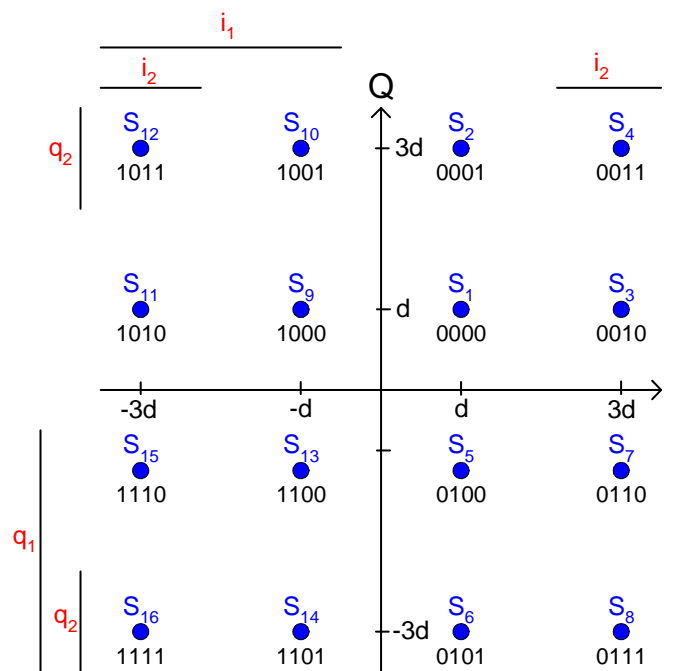
Figure 217: Signal constellation of 16-QAM modulation

8.5.2.2 16-QAM Symbol Mapping of Turbo Coded Bits

An example of transmit architecture for MCS-7, MCS-8 and MCS-9 in downlink is shown in figure 220. Differences from the architecture considered in the feasibility study of GERAN evolution [12, 13, 8] are in fact that a conventional convolutional encoder is replaced by a turbo encoder and an interleaver is replaced by a symbol mapping block. The output sequence of turbo encoder can be separated into two groups: a systematic bit stream (S) and a parity bit stream (P). Since the systematic bits have higher priority than the parity bits in turbo decoding procedure, a performance gain can be achieved by mapping higher priority bits into higher reliable positions in 16-QAM modulation.
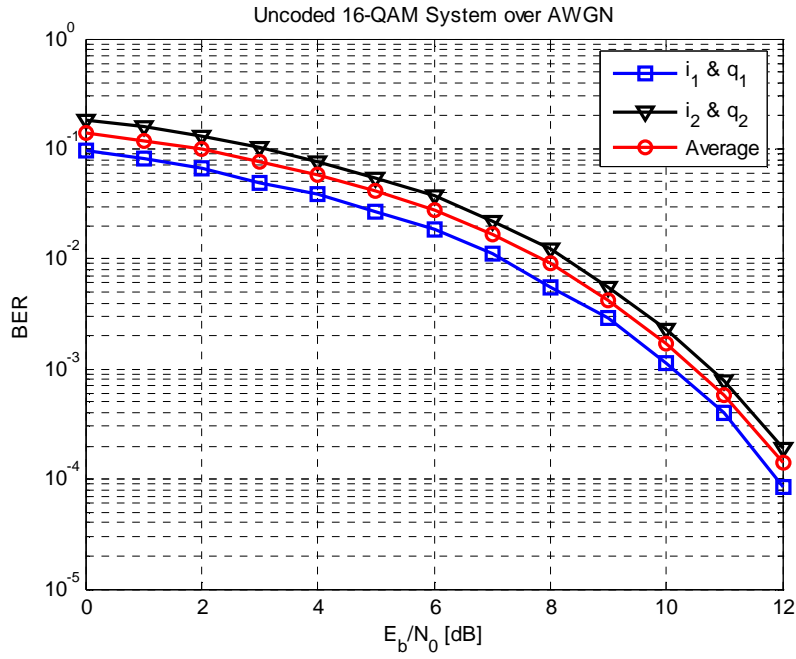
(a) AWGN Channel
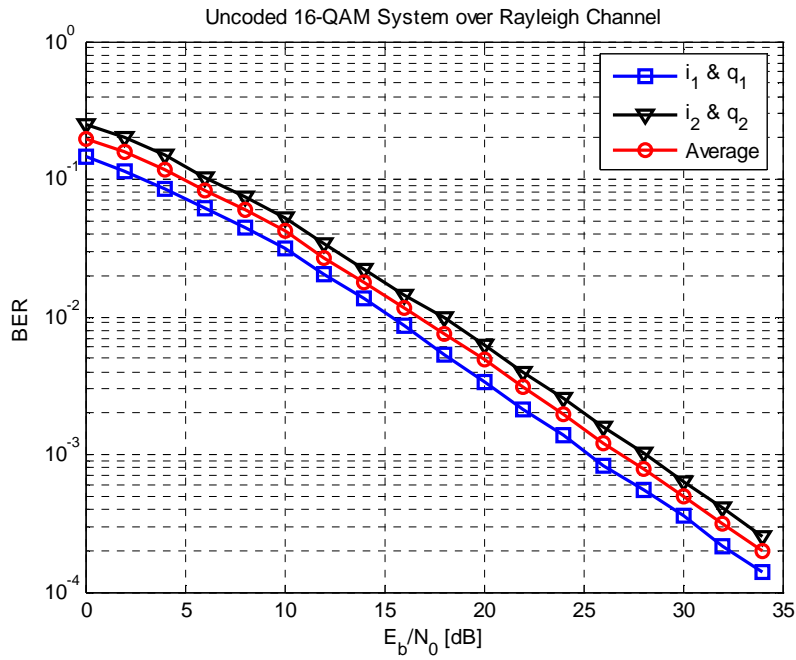
(b) Rayleigh Channel

Figure 218: BER of uncoded 16-QAM systems
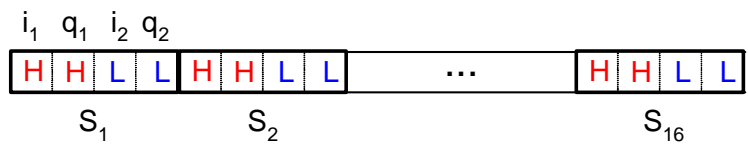
H : Higher Reliable Position
L : Lower Reliable Position

Figure 219: Reliability of bit positions in 16-QAM symbols

Figure 221 shows a structure of symbol mapping. After passing through a rate matching algorithm, turbo coded bits are separated into systematic bits and parity bits. As shown in figure 5(a), the turbo coded bits are separated into two data streams by a bit separation block: systematic bits $S = \{s_1, s_2, ..., s_M\}$ and parity bits $P = \{p_1, p_2, ..., p_N\}$. These two data streams can be the inputs to two independent block interleavers (1st and 2nd interleavers), which perform inter-column block interleaving and are identical as described in [15]. The two logically-divided interleavers make 16-QAM symbol mapping feasible, i.e. bits in the higher priority sequence (S*) can be assigned into higher reliable positions and bits in lower priority sequence (P*) can be mapped into lower reliable positions on 16-QAM symbols.

In the bit collection mechanism, two data sequences (S* and P*) are parallel-to-serial converted to a single bit stream (V), where higher priority (H) part and lower priority (L) part are allocated in an alternating sequence. Therefore, the output $V = \{v_1, v_2, ..., v_{M+N}\}$ of the bit collection block is collected two by two from the sequences S* and P*, if $M = N$. The output of the symbol mapping block is mapped into 16-QAM symbol, as shown in figure 5(b). It is noted that $M = N$ may not be held because of different data rates of MCSs. Therefore appropriate techniques will be required in implementation of the symbol mapping.
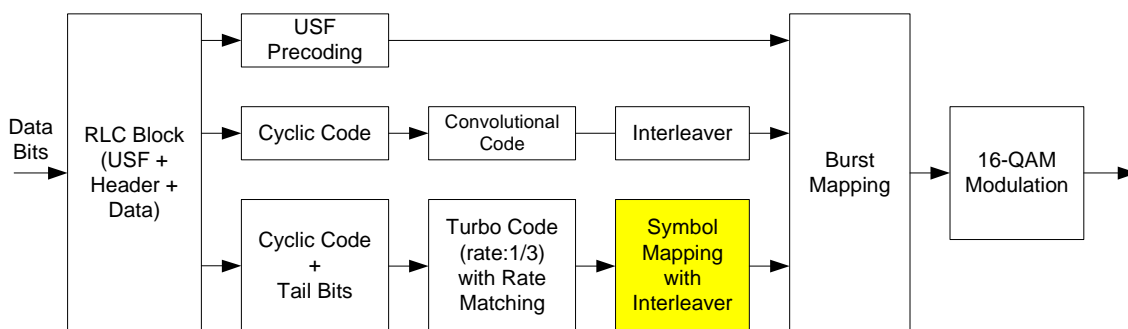
Figure 220: A transmit architecture including symbol mapping
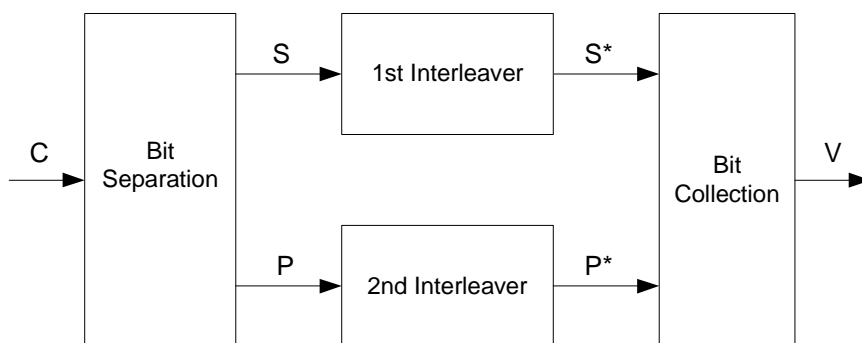
(a) Interleaving structure
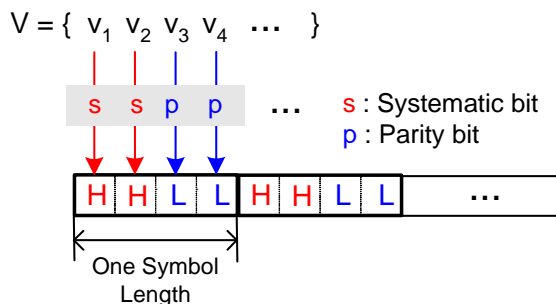
(b) 16-QAM symbol mapping

Figure 221: Structure of symbol mapping

8.5.2 Performance Evaluation

Performance of turbo coding with 16-QAM with a symbol mapping is evaluated on link level. Monte Carlo simulations for MCS-7-T4-16QAM, MCS-8-T4-16QAM and MCS-9-T4-16QAM are performed over AWGN and Rayleigh fading channels, respectively.

Table 82 depicts modulation and coding configuration used in simulations. Simulation results of each MCS are depicted in figure D.1, figure D.2 and figure D.3 in annex D, respectively, where burst mapping was not considered.

Figure D.1 shows performance gains of MCS-7-T4-16QAM in terms of BER and Block Error Rate (BLER) over AWGN and Rayleigh channel. Referring to figure D.1, by using the symbol mapping performance gains of 0.4 dB have been achieved at BER of 10^{-3} and BLER of 10^{-2}, respectively. For Rayleigh fading channel, performance gains of 0.4 dB and 0.2 dB have been attained for BER and BLER, respectively. Similarly, performance gains have been attained for MCS-8-T4-16QAM and MCS-9-T4-16QAM. The results are summarized in table 2.

Table 82: Modulation and coding configuration with turbo coding and 16-QAM

Modulation and Coding Scheme	Data Block Length (bits)	Turbo Code Rate (see note)	Interleaving Depth (bursts)
MCS-7-T4-16QAM	900	1/2	4
MCS-8-T4-16QAM	1088	2/3	4
MCS-9-T4-16QAM	1188	3/4	4
NOTE: Code rates after rate matching and without consideration of cyclic coded header (Mother code rate of turbo code is 1/3)			

Table 83: Performance gain [dB] employing the symbol mapping

	BER at 10^{-3}		BLER at 10^{-2}	
	AWGN	Rayleigh	AWGN	Rayleigh
MCS-7-T4-16QAM	0.4	0.4	0.4	0.2
MCS-8-T4-16QAM	0.2	0.18	0.2	0.12
MCS-9-T4-16QAM	0.15	0.12	0.14	0.12

Further details on simulation results are found in annex D.

8.6 Higher Order Modulation, Turbo Codes Combined with MS Receiver Diversity

Source: Reference [26].

8.6.1 Simulation Model

The simulation model is described in [7]. The following text explains the features that are not treated in that contribution.

The antenna correlation is assumed to be zero and the gain imbalance 0 dB.

The interference model is DTS-1 for the single-antenna receiver and DTS-2 for the dual-antenna receiver. The interferers are GMSK-modulated in both cases. The signal-to-interference ratio is normalized so that it represents the total received power after RX filtering, hence including an 18 dB reduction for the adjacent channel interference. Such approach is taken in order to enable a fair comparison between DTS-1 and DTS-2.

The channel coding of the MCS5 - MCS9 is carried out with 1/3-rate turbo code. The internal interleaver and generator polynomials are implemented as specified for UTRAN [15], the non-systematic parity bits being punctured with an even-spaced pattern. The number of decoding iterations is fixed to 8, the decoding algorithm being LOGMAX. No scaling is applied to the extrinsic information. Turbo coding is applied only for the data bits, while the other fields of an RLC/MAC block are encoded according to current EGPRS specification. The simulated modulation and coding schemes are summarized in table 84.

Table 84: Modulation and Coding Schemes

Modulation and Coding Scheme	Data Code rate	Header Code rate	RLC blocks per radio block	Family	Interleaving depth	Data rate
MCS-1	0.53	0.53	1	C	4	8.8
MCS-2	0.66	0.53	1	B	4	11.2
MCS-3	0.85	0.53	1	A	4	13.6/14.8
MCS-4	1.00	0.53	1	C	4	17.6
MCS-5	0.37	0.33	1	B	4	22.4
MCS-6	0.49	0.33	1	A	4	29.6/27.2
MCS-7	0.76	0.36	2	B	4	44.8
MCS-8	0.92	0.36	2	A	2	54.4
MCS-9	1.00	0.36	2	A	2	59.2
MCS-5-TC	0.37	0.36	1	B	4	22.4
MCS-6-TC	0.49	0.36	1	A	4	29.6/27.2
MCS-7-16QAM/TC	0.55	0.36	2	B	4	44.8
MCS-8-16QAM/TC	0.67	0.36	2	A	4	54.4
MCS-9-16QAM/TC	0.73	0.36	2	A	4	59.2

8.6.2 Simulation Results

The simulations are carried out in interference limited and noise limited environments. In the interference limited scenario, it is assumed that the highest power levels are never reached and no back off is hence needed. In the noise limited scenario, it is assumed that the full transmit power is always used, thus implying that the power of 8-PSK modulated blocks is backed off by 3 dB and the power of 16-QAM modulated blocks by 5 dB.

The link adaptation is assumed to occur in ideal manner without any incremental redundancy combining. The channel model is TU3iFH.

8.6.2.1 Interference Limited Scenario

The results from the interference limited simulations are summarized in table 85, which shows the link layer performance in terms of CIR at BLER=10 %.

Table 85: Interference limited results

MCS	Single antenna MS			Dual antenna MS		
	EGPRS	16QAM / TC		EGPRS	16QAM / TC	
		CIR@10%FER	Gain [dB]		CIR@10%FER	Gain [dB]
MCS-5	10.6	10.0	0.5	5.5	4.9	0.6
MCS-6	13.0	12.5	0.5	7.3	6.7	0.6
MCS-7	18.8	16.5	2.3	11.5	9.8	1.7
MCS-8	24.9	19.6	5.3	15.9	11.9	4.0
MCS-9	29.1	21.0	8.1	19.5	12.9	6.7

The interference limited throughput is shown in figure 222. In addition to the basic schemes, curves for dual carrier EGPRS and single antenna 16-QAM are given as reference.
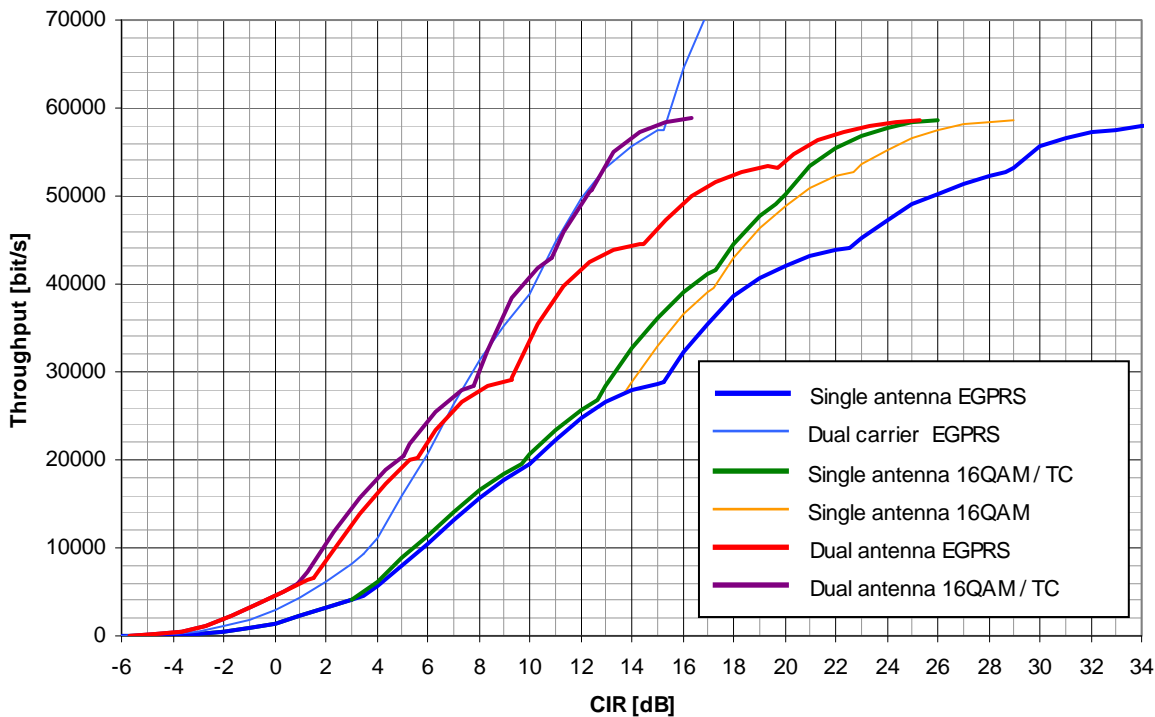
Figure 222: Interference limited throughput

8.6.2.2 Sensitivity Limited Scenario

The results from the sensitivity limited simulations are summarized in table 86.

Table 86: Sensitivity limited results

MCS	Conventional			MS receive diversity		
	EGPRS	16QAM / TC		EGPRS	16QAM / TC	
		SNR@10%FER	Gain [dB]		SNR@10%FER	Gain [dB]
MCS-5	14.1	13.4	0.7	9.5	8.8	0.7
MCS-6	16.1	15.6	0.6	11.3	10.6	0.7
MCS-7	20.9	21.9	-1.0	15.1	16.4	-1.3
MCS-8	25.8	24.3	1.5	18.9	18.3	0.6
MCS-9	29.3	24.6	4.8	22.1	19.2	2.9

The sensitivity limited throughput is given in figure 223.
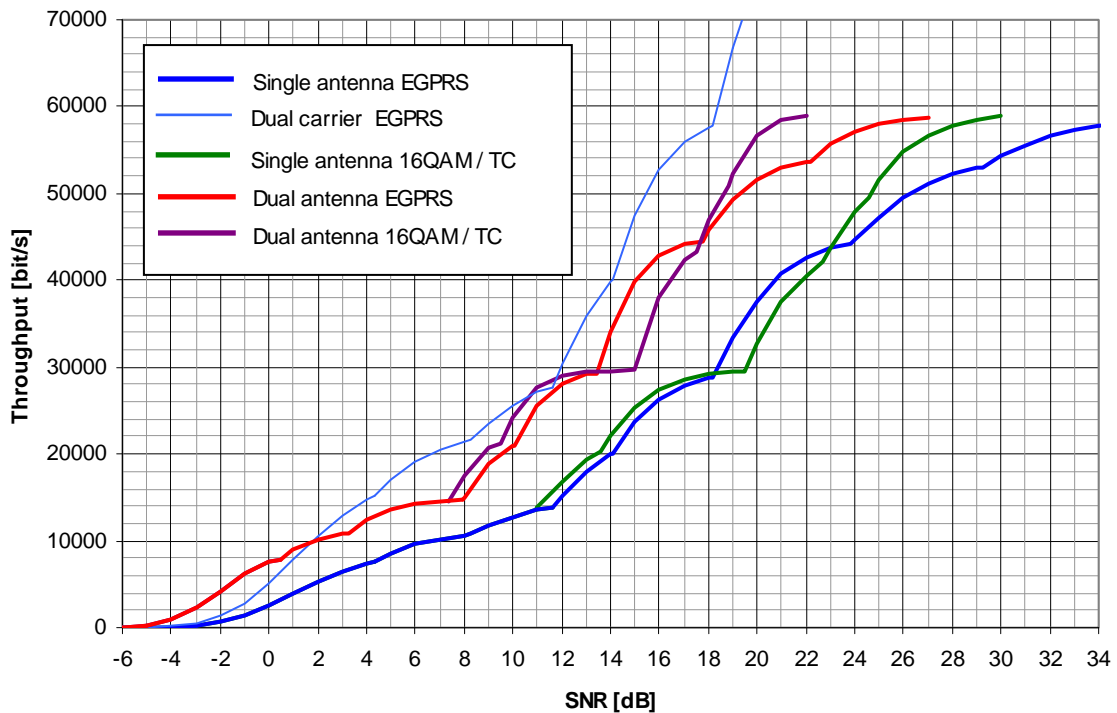
Figure 223: Sensitivity limited throughput

8.6.3   Discussion

8.6.3.1   Interference Limited Scenario

As can be seen from the results, the gains from 16QAM/TC and MSRD are rather close to additive, i.e. the total gain is close to the sum of the individual gains in decibel scale. It is also interesting to note that the throughput of the MSRD/16QAM/TC configuration is close to the throughput of the dual-carrier up to a CIR of 16 dB.

Most of the throughput gain for 16QAM/TC clearly comes from 16-QAM (see yellow curve). The only exception is MCS-7, for which about one half of the gain comes from 16-QAM and one half from the turbo codes. This result is somewhat contradictory with the system level results of [8], where most of the throughput gain in cell border and median is reported to come from turbo codes. One reason for this difference is that no IR is applied in [8], hence implying that the two highest MCSs are possibly not used very often.

It can be seen from figure 222 that the maximum throughput with MSRD/16QAM/TC is achieved with the same signal quality where the single-carrier MCS-7 is switched on. There could be hence some room for higher coding rate MCSs when MSRD is used.

The results indicate that a throughput gains up to ~30 % could be achieved with the combination of 16-QAM and turbo codes. However, it is important to notice that the evaluated scenario represents the performance of 16QAM/TC in very favourable conditions. It has been already shown in [7] that the inclusion of non-hopping environment and IR can drastically reduce the achieved gains. Another impairment that is not visible in the link layer simulations is the power back off, i.e. it is assumed that the highest power levels are never touched. This might not be a valid assumption even in the case of an interference limited network, since the downlink power control is not necessarily used at all, and on the BCCH layer a constant transmission power has to be used. As will be shown in next subclause, the inclusion of full back off can easily translate the achieved gains into loss.

One comment should be made about the performance of the dual-antenna scenarios. The average DIR of the applied interference scenario (DTS-2) is expected to be somewhat higher than the average DIR of a typical network scenario (see e.g. [27]). Hence, the gain from MSRD is expected to be somewhat optimistic in the given results.

8.6.3.2   Noise Limited Scenario

As can be seen from figure 223, the gain from 16QAM/TC is heavily impacted by the inclusion of 5 dB back off for 16-QAM modulation. For MCS-8 and MCS-9 there is a gain of ~10 %, and for MCS-7 a loss of similar magnitude. This example hence illustrates that the 16QAM/TC does not necessarily bring any improvement, but can even induce some loss compared to the current EGPRS.

8.7   Modified 16-ary Constellations for Higher Order Modulation and Turbo Coding Schemes

Source: Reference [32].

8.7.1   Introduction

A number of circular 16APK (Amplitude Phase Keying) constellations are compared to the square 16QAM constellation. The modulations are compared in terms of their PAPR and dynamic range, and their impact on BLER performance.

8.7.2   Circular 16APK Constellations

In this subclause two circular constellations are considered. The Circular 16APK(12,4) constellation consists of two concentric circles, the inner one containing four symbols while the outer one contains the remaining 12 symbols. The Circular 16APK(8,8) constellation consists of two concentric circles, with both the inner and outer circles containing 8 symbols, at coincident angles.

The constellation design parameter is the ratio R between the outer and inner circle radii. Usually values of R may range from 1.2 to 3. The effect of the parameter R is as follows: larger values of R will generally improve the performance, while smaller values of R will degrade performance but also lower the PAPR and dynamic range of the modulation. Examples of 16APK (12,4) and (8,8) with R=1.5 are given in figures 224 and 225.

In order to avoid transition through the origin between symbols, a rotation of the constellation is applied between symbol periods, as was done for 8PSK and the square 16QAM modulation. For 16APK(12,4), the optimal rotation is $5\pi/12$. For 16APK(8,8), as with 8PSK the optimal rotation is $3\pi/8$.
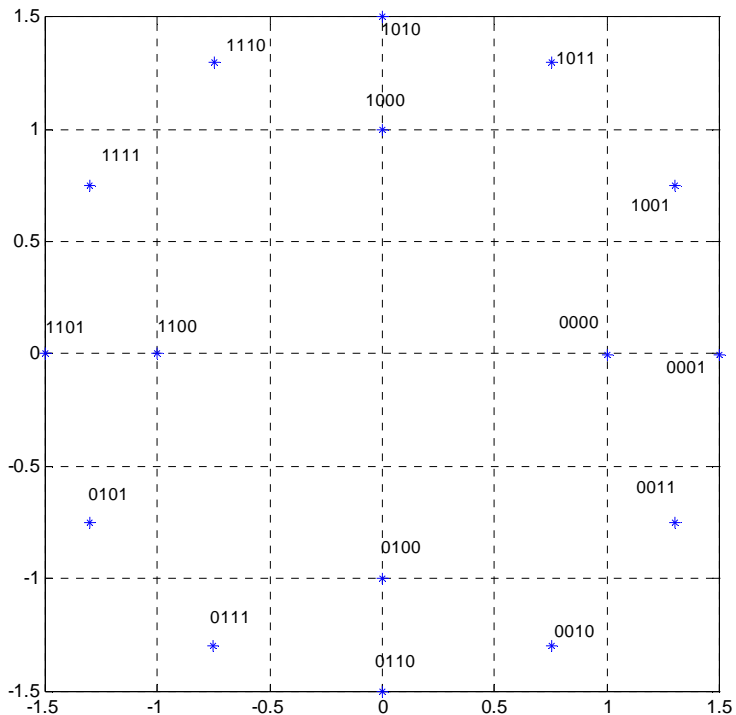
Figure 224: 16APK (12,4) Constellation
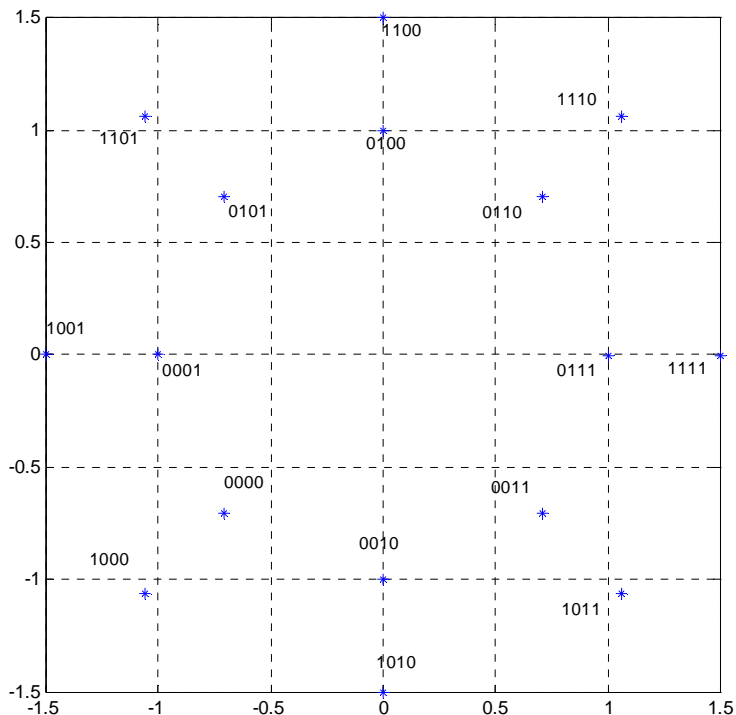
Figure 225: 16APK (8,8) Constellation

8.7.2.1 PAPR and Dynamic Range Comparison

Table 87 shows a comparison of PAPR and dynamic range for square 16QAM, 8PSK and circular 16APK in (12,4) and (8,8) constellations with R=1.5 and R=2.0. The values of PAPR (99.99 %) and Dynamic Range (99.99 %) are shown for each modulation.

As can be seen, it is possible to make a substantial reduction in PAPR to around 4dB by using 16APK modulations. From the simulations done in the EDGE Feasibility Study and reported in [33], a modulation backoff of 4dB has a minimal impact on system handover performance. It can also be seen that 16APK (8,8) reduces the dynamic range to 22dB, that is only 5dB above that of 8PSK.

The performance of the 16APK modulations is compared below, with the exception of 16APK (8,8) with R=2.0 that does not have sufficiently good PAPR and dynamic range characteristics.

Table 87: Comparison of PAPR and Dynamic range of 16APK (12,4) and (8,8) modulation schemes

Modulation	PAPR [dB]	Dynamic Range [dB]
16 QAM	5.2	40
16APK (12,4) R=2	4.2	38
16APK (12,4) R=1.5	4	29
16APK (8,8) R=2	5.2	38
16APK (8,8) R=1.5	4.6	22
8 PSK	3.2	17

8.7.3   Logical Channel Configurations

The channel configurations used for simulations are shown in table 88. The configurations are used to compare performance of circular 16QAM modulation with that of MCS7, MCS8 and MCS9. For each of the MCS schemes, 3 other options are considered, as taken from table 87.

Table 88: Modulation and Coding Schemes

Modulation and Coding Scheme	Data Code rate	RLC blocks per radio block	Interleaving depth	Data rate
MCS7	0.76	2	4	44.8
MCS8	0.92	2	2	54.4
MCS9	1.00	2	2	59.2
MCS7-T4-16QAM	0.55	1	4	44.8
MCS8-T4-16QAM	0.67	1	4	54.4
MCS9-T4-16QAM	0.73	1	4	59.2
MCS7-T4-(12,4) APK (R=2)	0.55	1	4	44.8
MCS8-T4-16APK (12,4) (R=2)	0.67	1	4	54.4
MCS9-T4-16APK (12,4) (R=2)	0.73	1	4	59.2
MCS7-T4-16APK (12,4) (R=1.5)	0.55	1	4	44.8
MCS8-T4-16APK (12,4) (R=1.5)	0.67	1	4	54.4
MCS9-T4-16APK (12,4) (R=1.5)	0.73	1	4	59.2
MCS7-T4-16APK (8,8) (R=1.5)	0.55	1	4	44.8
MCS8-T4-16APK (8,8) (R=1.5)	0.67	1	4	54.4
MCS9-T4-16APK (8,8) (R=1.5)	0.73	1	4	59.2

8.7.4   Performance Characterisation

The simulations were carried out for both a noise limited environment, and an interference limited environment. The TU3iFH channel model was used.

It was assumed that for the noise limited case, full transmit power is always used, implying that the power of 8PSK modulated blocks is backed off by 3.2 dB and the power of 16QAM/16APK modulated slots according to the relevant PAPR in table 87.

For the simulations, the impairments detailed in table 89 were used.

Table 89: Simulation Impairments

Impairment	Value
BTS I/Q Gain mismatch	0.1 dB
BTS I/Q phase mismatch	0.2 degrees
BTS Phase Noise	0.8 degree rms
BTS DC Offset	-45 dBc
MS I/Q Gain mismatch	0.2 dB
MS I/Q phase mismatch	2.8 degrees
MS Frequency Offset	50 Hz
MS Phase Noise	1.0 degree rms
MS DC Offset	-40 dBc

8.7.4.1   Uncoded BER Performance

This subclause shows the uncoded BER performance of the 16QAM and 16APK modulations from table 87. The uncoded BER results are shown in figure 226.

It can be seen that for circular 16APK(12,4) with R=2.0, UBER performance is about 0.5 dB better compared to 16QAM - helped by the 1.2 dB advantage in backoff; with R=1.5, UBER performance degraded by about 0.6dB at UBER=10% though this gap increases noticeably at higher SNRs.

For circular 16APK(8,8) with R=2.0, UBER performance is worse by about 0.2 dB. With R reduced to 1.5, the UBER as compared to 16QAM is degraded by 0.5 dB. However, as we shall see in the next subclause on BLER performance, the impact on BLER performance at the critical points is not severe.
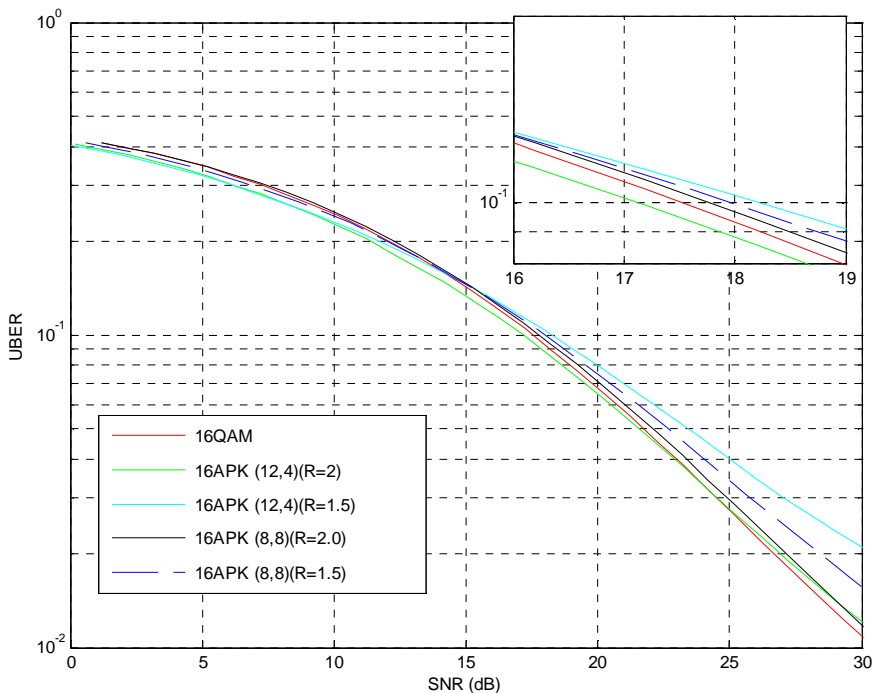
Figure 226: Uncoded BER of 16QAM, 16APK (12,4) & (8,8) Modulations

8.7.4.2 BLER Performance

8.7.4.2.1 Sensitivity Limited Channel

Figure 227 shows the BLER performance for MCS7, and the three 16-ary modulated configurations carrying the same payload as MCS7. Figures 228 and 229 show the BLER performance for MCS8 and MCS9 respectively.

The results from the sensitivity limited simulations are summarized in table 90. For each configuration the table shows the link layer performance in terms of SNR at BLER=10%. The gain relative to the relevant EGPRS MCS is also given.

It can be seen that the results for 16APK (12,4) with R=2.0 are slightly better than 16QAM. For both (12,4) and (8,8) with R=1.5, the gains are slightly reduced, though provide a good tradeoff for the less stringent modulation requirements.

8.7.4.2.2 Interference Limited Channel

Figure 230 shows the BLER performance for MCS7, and the three 16-ary modulated configurations carrying the same payload as MCS7. Figures 231 and 232 show the BLER performance for MCS8 and MCS9 respectively.

The results from the interference limited simulations are summarized in table 91. For each configuration the table shows the link layer performance in terms of C/I at BLER=10%. The gain relative to the relevant EGPRS MCS is also given.

For the interference limited cases, the 16APK (12,4) and 16APK (8,8) modulations perform less well than the 16QAM modulation. However, the gains compared to EGPRS are still substantial. The 16APK (8,8) modulation with R=1.5 has almost the same performance as the 16APK (12,4) with R=2.0. Of these modulations, the PAPR and dynamic range of the (8,8) R=1.5 modulation are far more relaxed.

Table 90: Sensitivity limited results

Modulation and Coding Scheme	EGPRS	T4-16QAM		T4-16APK (12,4) (R=2)		T4-16APK(12,4) (R=1.5)		T4-16APK (8,8) (R=1.5)	
	SNR @ 10% BLER	SNR @ 10% BLER	Gain (dB)	SNR @ 10% BLER	Gain (dB)	SNR @ 10% BLER	Gain (dB)	SNR @ 10% BLER	Gain (dB)
MCS7	20.8	19.3	1.5	18.8	2.0	19.5	1.3	19.2	1.6
MCS8	27.3	22.4	4.9	22.0	5.3	23.2	4.1	22.6	4.7
MCS9	32.7	24.3	8.4	24.1	8.6	25.7	7.0	25.7	7.0

Table 91: Interference limited results

Modulation and Coding Scheme	EGPRS	T4-16QAM		T4-16APK (12,4) (R=2)		T4-16APK(12,4) (R=1.5)		T4-16APK (8,8) (R=1.5)	
	C/I @ 10% BLER	C/I @ 10% BLER	Gain (dB)	C/I @ 10% BLER	Gain (dB)	C/I @ 10% BLER	Gain (dB)	C/I @ 10% BLER	Gain (dB)
MCS7	17.8	14.5	3.3	15	2.8	16	1.8	15	2.8
MCS8	23.8	17.6	6.2	18.2	5.6	19.6	4.2	18.3	5.5
MCS9	29.3	19.4	9.9	20.1	9.2	22	7.3	20.4	8.9
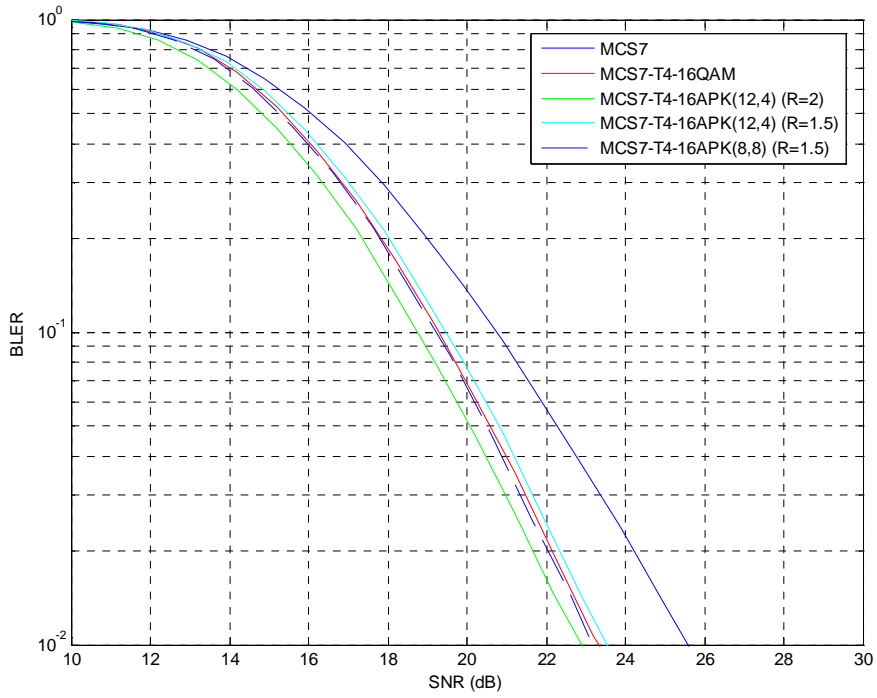
Figure 227: TU3iFH Sensitivity Performance (MCS-7)
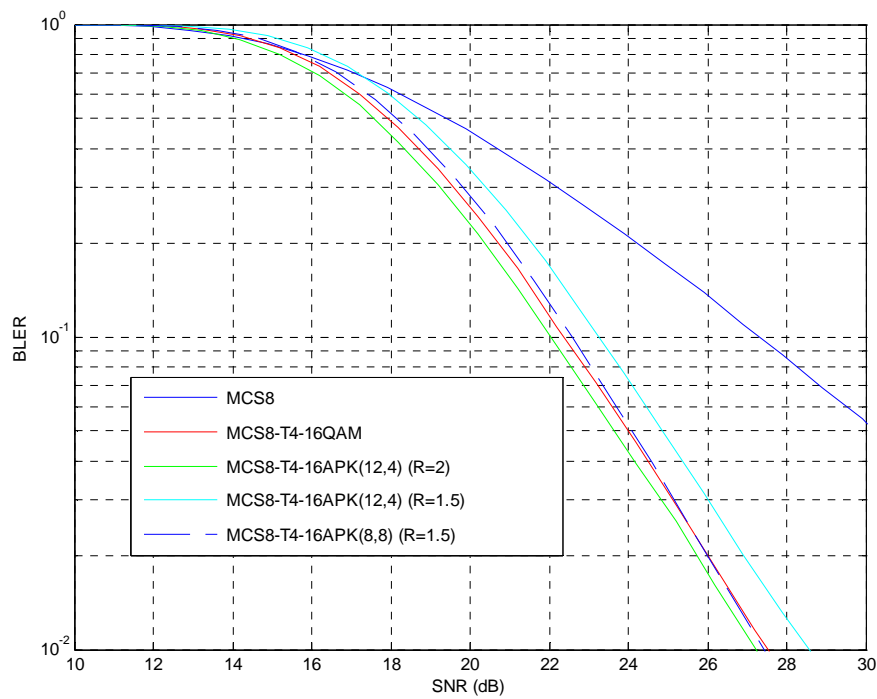
Figure 228: TU3iFH Sensitivity Performance (MCS-8)

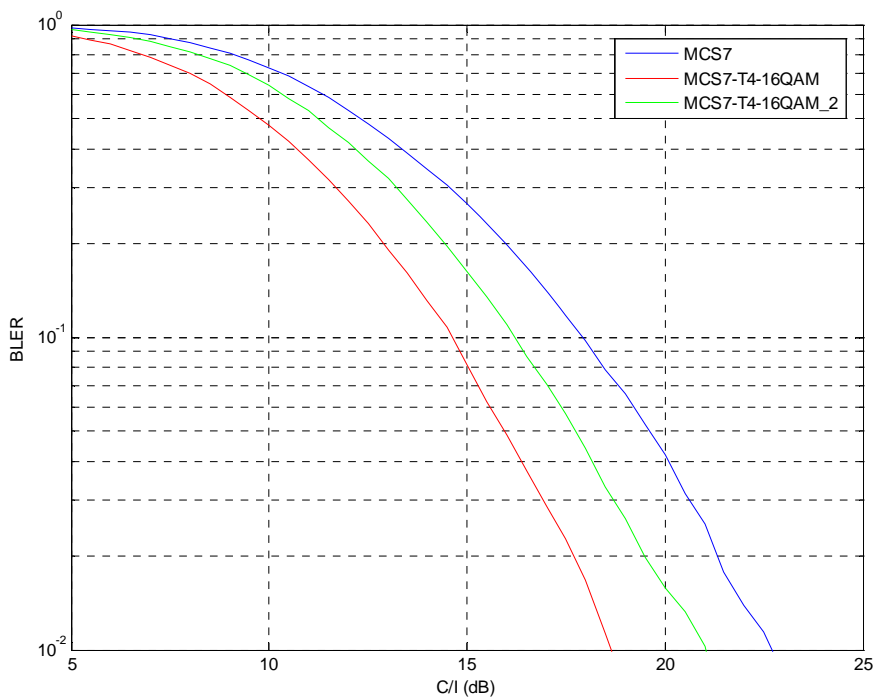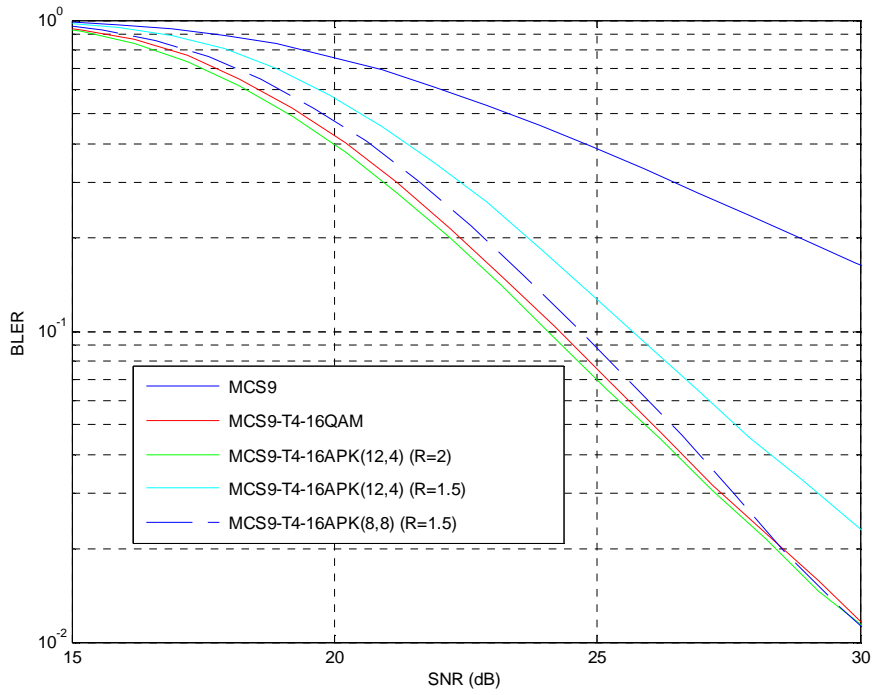**Figure 229: TU3iFH Sensitivity Performance (MCS-9)**
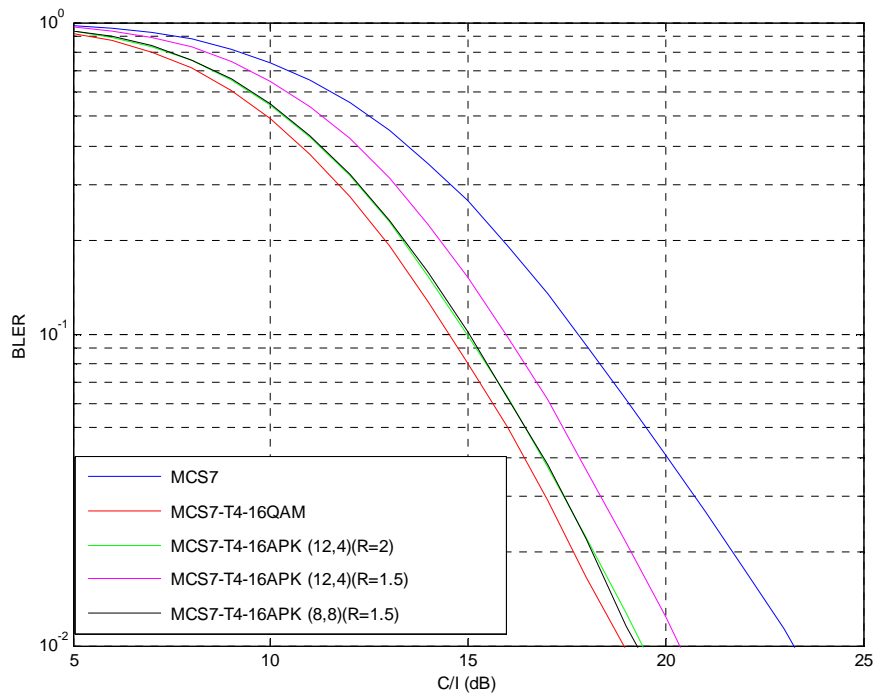
Figure 230: TU3iFH Co-Channel Performance (MCS-7)
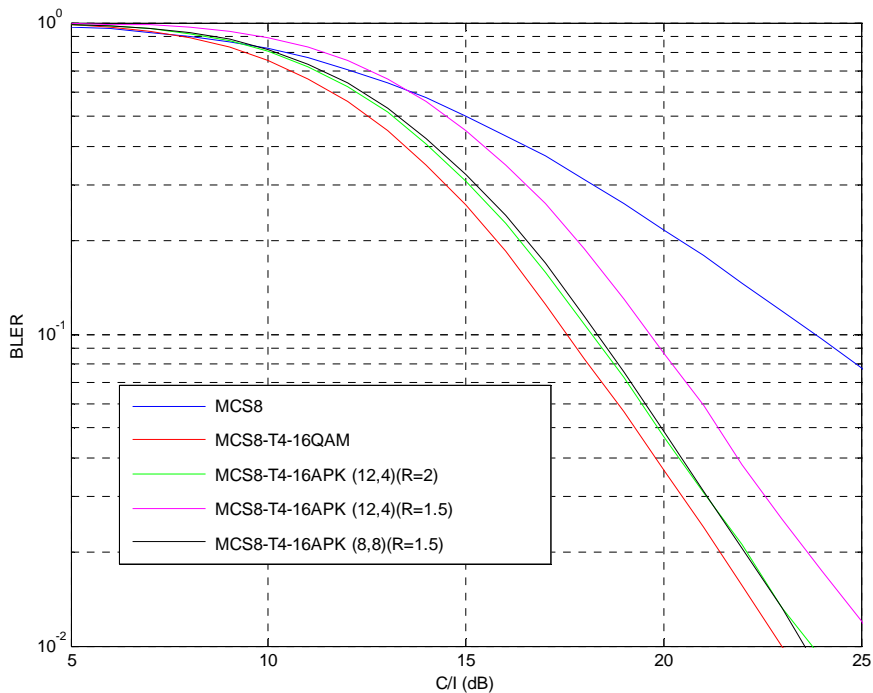
Figure 231: TU3iFH Co-Channel Performance (MCS-8)
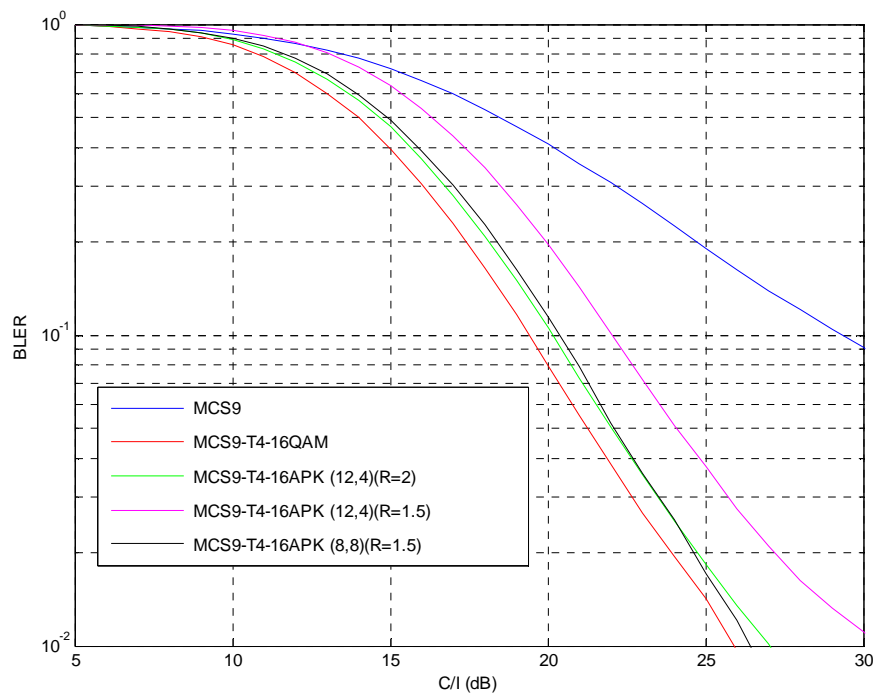
Figure 232: TU3iFH Co-Channel Performance (MCS-9)

8.7a Blind modulation detection performance

8.7a.1 Introduction

When new modulations are introduced, the receiver must blindly detect which modulation is used for each reveiced radio block. In this subclause, the performance of blind modulation detection is evaluated. The results are taken from [44].

8.7a.2   Blind modulation detection

Modulation detection in EDGE is made possible by constellation rotation during the training sequence. The same training sequence is used for GMSK and 8PSK blocks, but with different rotations; π/2 for GMSK and 3π/8 for 8PSK. This principle is straightforward to extend to more than two modulations. In this contribution, the same training sequence but different rotations have been used for all modulations. The rotation angles are listed in table 91a.

Table 91a. Constellation rotation angles for different modulations.

Modulation	Rotation angle
GMSK	π/2
8PSK	3π/8
16QAM	π/4
32QAM	-π/4

The method for modulation detection used in this contribution is a direct extension of the method used in state-of-the-art terminals. The rotation is hypothesised to each of the possible rotations (two for EDGE, four if 16QAM and 32QAM are added). The residual interference/noise during the training sequence is calculated for each hypothesis. The modulation giving the least residual noise/interference is assumed to be the correct one.

In general, the probability of a false modulation detection is higher the more interference and/or noise that is present. Further, a false modulation detection will lead to a performance loss only if the data block would have been correctly decoded with a correct modulation detection.

Therefore, the biggest challenge is not to correctly detect the modulation of a 16QAM or 32QAM modulated radio block (since these modulations are typically not used at the very lowest SNR or C/I ratios), but rather to correctly detect the modulation of a robustly encoded GMSK modulated radio block. Therefore, the main results in the next clauses show performance impact on MCS-1, the MCS that is used in the worst radio conditions. The performance impact on other MCS:s will be less. MCS-5 performance is also shown to exemplify this.

NOTE: According to the HOT proposal, the HOT MS would not use regular MCS-5 but a turbo encoded version of it. Therefore, the performance of the HOT MS would be better than the EGPRS MS. However, in order to allow a comparison with EGPRS (to assess the loss due to blind detection with more candidates), regular MCS-5 was used also for the HOT MS in the simulations. It should be noted however that with the method used in EGPRS, the modulation detection performance is not dependent on the channel coding nor the modulation, only on the number of candidate modulations and the radio conditions.

8.7a.3   Simulation conditions

Results are shown for the following scenarios (all for the 900 MHz band):

-     Sensitivity: TU50 ideal FH, HT100 no FH and RA250 no FH

-     Interference: DTS-2, TU50 ideal FH

Further, the following receiver types are evaluated:

-     Single-antenna receiver (no diversity)

-     Dual-antenna receiver with maximum ratio combining

-     Dual-antenna receiver with interference cancellation

10000 radio blocks were run per simulation point.

8.7a.4   Results

The results are presented as the relative performance loss at 10% total BLER (i.e., including errors in stealing flags, header and data) when the receiver has to blindly select between GMSK, 8PSK, 16QAM and 32QAM, compared to EDGE (that has to select only between GMSK and 8PSK). Results are show for MCS-1 and MCS-5. Detailed results can be found in [44].

8.7a.4.1   Single-antenna receiver

Table 91b shows performance losses due to blind detection of four modulations instead of two for a single-antenna receiver (no SAIC).

Table 91b. Loss in BLER performance with a single-antenna receiver.

	Relative loss @ 10% BLER [dB]			
	Sensitivity			DTS-2
	TU50 iFH	HT100 noFH	RA250 noFH	TU50 iFH
MCS-1	0.08	0.04	0.08	0.06
MCS-5	0	0	0.01	0

8.7a.4.2   Dual-antenna receiver (maximum ratio combining)

Table 91c shows performance losses due to blind detection of four modulations instead of two for a dual-antenna receiver using MRC.

Table 91c. Loss in BLER performance with maximum ratio combining.

	Relative loss @ 10% BLER [dB]			
	Sensitivity			DTS-2
	TU50 iFH	HT100 noFH	RA250 noFH	TU50 iFH
MCS-1	0.05	0.04	0.07	0.06
MCS-5	0	0	0	0

8.7a.4.3   Dual-antenna receiver (interference cancellation)

Table 91d shows performance losses due to blind detection of four modulations instead of two for a dual-antenna receiver using interference cancellation.

Table 91d. Loss in BLER performance with interference cancellation.

	Relative loss @ 10% BLER [dB]			
	Sensitivity			DTS-2
	TU50 iFH	HT100 noFH	RA250 noFH	TU50 iFH
MCS-1	0.05	0.07	0.10	0.07
MCS-5	0	0	0	0

8.7a.5   Discussion

The loss due to blind modulation detection is negligible (at most 0.1 dB) in all scenarios. The reason is that even if the modulation detection performance is slightly less robust with four candidate modulations instead of two, it is still much more reliable than the decoding of the data itself.

Still, it is possible to create artificial situations where the modulation detection performance actually has an impact on the BLER performance. For instance, in the extreme case of an MCS-1 block interfered by a single adjacent channel interferer and received by a dual-antenna receiver with interference cancellation, the C/I level required to decode the data block is in the region of -40 to -20 dB. At this level, modulation detection is more challenging. When this scenario was simulated for different channel profiles, a BLER loss of up to 1 dB was seen (see [44] for details).

8.7b   Impact of using higher order modulations on the BCCH carrier

8.7b.1   Introduction

If higher order modulations are used on the BCCH carriers, the necessary power decrease would result in biased neighbour cell measurements, which could have an impact on cell selection.

This problem was faced and evaluated when EDGE was introduced in release 99 (see [33]). Power decreases of up to 4 dB were evaluated and the impact considered acceptable.

In this subclause, larger power decreases, corresponding to the necessary levels for 16QAM and 32QAM when used on the BCCH carrier, are investigated.

8.7b.2   Impact on cell selection and reselection

8.7b.2.1   Simulation assumptions

To investigate the impact of non-constant BCCH power some simple system level simulations are run. The simulator is a static (snapshot) system simulator. The effect of the non-constant BCCH carrier power is modelled by subtracting the APD (average power decrease) from the pathgain for some of the BS candidates before cell selection is made. To model a handover hysteresis the MS randomly selects a BS within 3 dB from the strongest. Further assumptions are given in table 91e.

Table 91e. Simulation assumptions.

Simulation Assumptions	
Frequency reuse	4/12
Frequency hopping	No
Resource utilization	50%
Traffic mix	50% GMSK modulated speech 50% packet-switched data
Average Power Decrease (APD)	GMSK: 0 dB
	8PSK: 3.3 dB
	16QAM: 5.3 dB
	32QAM: 5.6 dB
Pathloss	L = C + 35 log (d)
Log-normal fading standard deviation	6 dB
Multipath fading	Not included

Four different scenarios, with different modulations of the data traffic are studied:

1. 100% GMSK

2. 100% 8PSK

3. 100% 16QAM

4. 100% 32QAM

The data traffic is assumed to be 50% of the total traffic on the BCCH carriers on average (the rest is GMSK modulated speech or control channels). This can be seen as a worst case, since a lower or higher penetration would result in a more stable power level on the BCCH carriers.

It should be noted that the assumption that all data traffic uses the highest possible modulation is pessimistic (from an APD point of view). Thus, the evaluated scenarios (especially scenario 4) should be considered as a worst case scenario.

8.7b.2.2   Results and discussion

Figure 232a to 232d show received signal strength (C) and carrier to interference ratio (C/I) distributions for up- and downlink.
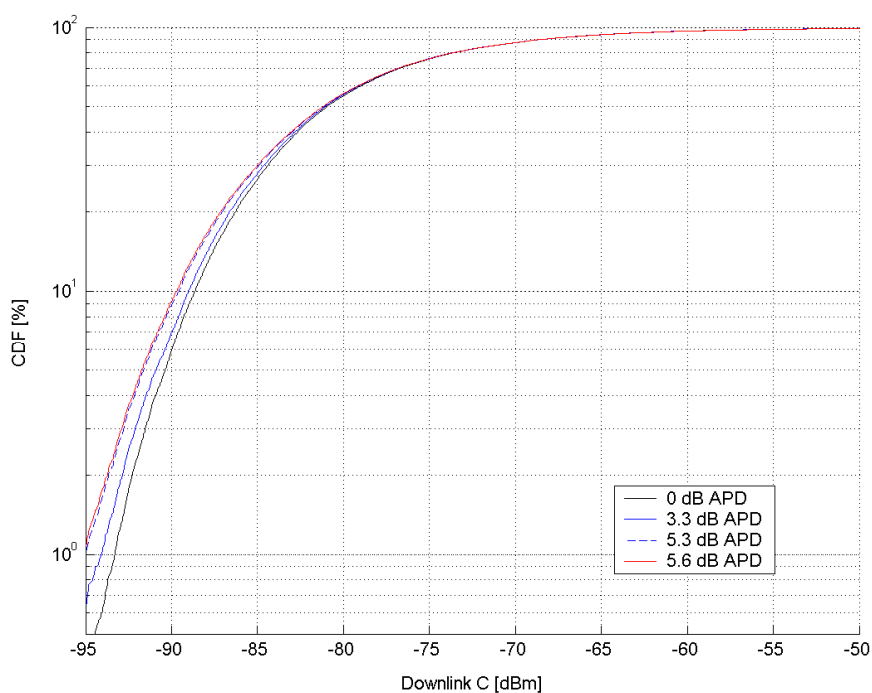
Figure 232a. Downlink distribution of C.
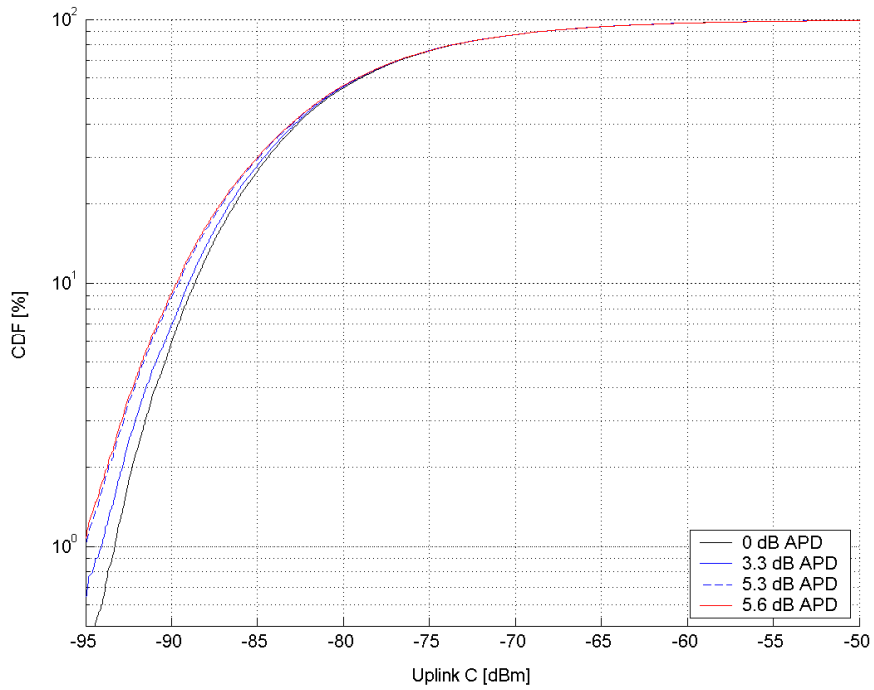
Figure 232b. Uplink distribution of C.
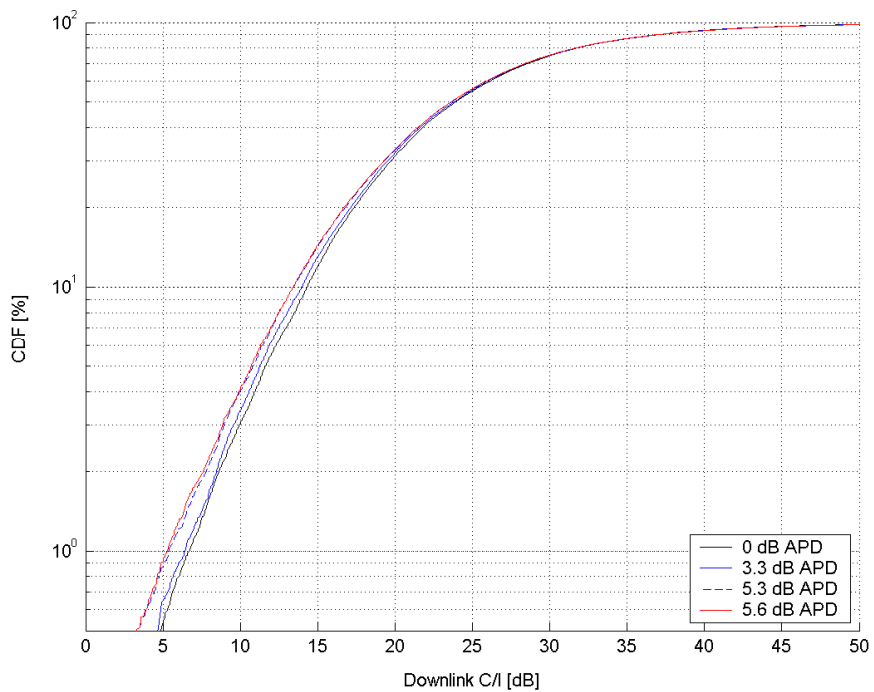
Figure 232c. Downlink distribution of C/I.
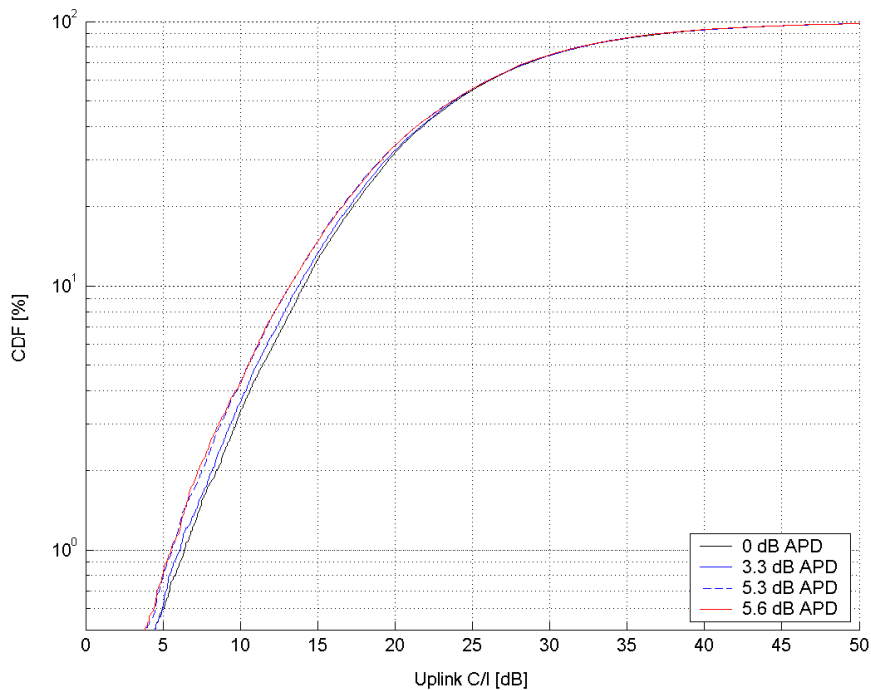
Figure 232e. Uplink distribution of C/I.

It is seen that the impact on C and C/I distributions is moderate. In scenario 4 (50% GMSK modulated speech, 50% 32QAM modulated data), 4% of the users have a downlink C/I worse than 10 dB. This should be compared to the EDGE-like scenario 2 (50% GMSK modulated speech, 50% 8PSK modulated data), in which 3.4% of the users have a downlink C/I worse than 10 dB. If all traffic on the BCCH is GMSK modulated (scenario 1), the corresponding figure is 3%. In uplink, the impact is very similar.

Fast fading is not modelled in these simulations. If fast fading was included, the variance of the MS power (RXLEV) measurements would be much larger and hence the cell selection decisions less reliable. The signal strength can easily vary by ~20 dB due to fast fading. Averaged over a measurement period, the variation is smaller but could still be in the order of several dB. In addition, the RXLEV measurements are assumed to be ideal. In reality, the RXLEV measurements are allowed a certain inaccuracy. The effect of APD is likely less if these effects are taken into account.

8.7b.3 Impact on GPRS/EGPRS MS open loop power control

In GPRS and EGPRS, the MS power is set according to the following formula:

$$P_{CH} = \min(\Gamma_0 - \Gamma_{CH} - \alpha \cdot (C + 48), PMAX)$$

where C is the received signal level at the MS on either the BCCH or PDCH, and $\alpha \in [0,1]$ is a system parameter determining the ratio between open and closed loop power control used. In case the BCCH is used for deriving C, the result of an Y dB APD on the BCCH would be that the MS in the worst case 'underestimates' the received power by Y dB, and consequently – in cases down regulation is invoked - transmits with a $\alpha \cdot Y$ dB too high power.

8.7c   Multiplexing higher order modulation MS with legacy MS

8.7c.1   Introduction

If higher order modulation MS are multiplexed with legacy GPRS/EGPRS MS on the same downlink PDCH:s, the USF (uplink state flag), when transmitted with 16QAM or 32QAM, cannot be received by a legacy MS. Therefore, multiplexing losses may occur.

This problem was faced already when EDGE was introduced in release 99, as 8PSK modulated EGPRS USF:s cannot be read by GPRS MS.

In this subclause, the multiplexing issues of higher order modulations are investigated. The higher order modulation and turbo coding feature will be referred to as *HOT* (Higher Order modulations and Turbo codes), and MS supporting it *HOT MS*.

8.7c.2   Background and problem description

In GPRS and EGPRS, the scheduling of MS transmission in the uplink is controlled by the BSS. An information field in each block on a downlink PDCH, the USF (uplink state flag), tells the MS:s listening to the PDCH on which block(s) on corresponding uplink PDCH(s) it is allowed to transmit.

When EGPRS MS are multiplexed with GPRS MS on the same PDCH, it was necessary to assure that GPRS MS could be scheduled for uplink transmission, even if EGPRS blocks were sometimes sent on the downlink. When GMSK modulated EGPRS downlink blocks are transmitted, the USF is encoded in such a way that GPRS MS can decode it. On the other hand, when 8PSK modulated EGPRS downlink blocks are transmitted, only USF:s to EGPRS MS can be transmitted. To minimise the losses due to this, the following means can be used:

1. Use USF granularity. This means that one USF schedules not one but four uplink blocks to the same MS. During the first of four downlink blocks, the USF is transmitted with GMSK modulation. In the three remaining downlink blocks, no scheduling information is needed and any modulation can be used on the downlink.

2. To the largest extent possible, coordinate the downlink and uplink scheduling, in order to transmit downlink blocks to an MS that prefers GMSK (GPRS MS or EGPRS MS in bad radio conditions) when a GPRS MS is scheduled in the uplink.

3. If, for some reason, an EGPRS downlink block has to be transmitted at the same time as a GPRS MS is scheduled in the uplink, a GMSK modulated MCS is chosen for the downlink block, even if an 8PSK modulated MCS would have been more suitable for the (good) radio conditions.

These methods are proven to work in practice, since indeed GPRS and EGPRS MS are multiplexed on the same PDCH:s. The same methods can be used when HOT MS are multiplexed with legacy MS. In the following subclauses, the performance of this is evaluated by means of simulations.

8.7c.3   Simulation setup

8.7c.3.1   Simulator description

The simulator used is a dynamic GSM/EDGE traffic simulator with channel management, DL scheduling and UL scheduling. The traffic model used is file download and file upload with fixed file sizes (100 kB). MCSs are chosen based on the specified CIR and the MS capabilities. The mix of HOT and EDGE mobile stations is specified as HOT penetration. The HOT penetration is swept from 0% to 100 % in steps of 10%. The offered traffic load is specified as a percentage (70 or 80) of the theoretical cell capacity (kbps/cell) at HOT penetration 0% and for the given CIR level (for the corresponding MCS which is chosen for that CIR).

Radio link modelling is simplified, with a fixed CIR for all users. MCSs are chosen (to maximise throughput) based on the specified CIR and the MS capabilities. Block errors are assumed to be independent.

Simulation parameters are summarised in table 91f.

Table 91f. Summary of simulation parameters.

Parameter	Value
TRXs per cell	2 (16 timeslots)
Multislot class	Class 32 (i.e., Rx=5, Tx=3, Sum=6) Up to 5+1 for downlink users Up to 3+3 for uplink users
Traffic model	FTP download/upload 100 kB packet size Poisson user arrival process. A user leaves the system when download/upload is completed.
USF granularity	1 or 4 for EDGE MS 1 for HOT MS

It is assumed that HOT MS can decode the USF of legacy blocks as well as 16/32QAM modulated blocks while the EDGE MS can only decode the USF of 8PSK modulated blocks (and GMSK modulated blocks; however, GMSK is not used in the simulations). Since HOT is a candidate Rel-7 feature, it is assumed that the fraction of MS supporting only GPRS is small and can be approximated to 0 when HOT is available on the market.

8.7c.3.2　Scheduling strategies

Two strategies are investigated:

1. Strategy 1 does not take the USF problem into account. If a downlink block is sent with 16/32QAM modulation, containing a USF to a legacy MS, the legacy MS will not receive the USF and no transmission will occur in the corresponding uplink block. The USF granularity is 1 for all users.

2. Strategy 2 is a simple attempt to reduce the USF problem. If there is a conflict between preferred downlink modulation (16/32QAM) and USF decoding, the MCS of the downlink block is reduced to an 8PSK modulated one. USF granularity 4 is used for EDGE MSs and USF granularity 1 for HOT MSs.

Strategy 2 corresponds to a combination of bullet 1 and 3 in subclause 8.7c.2. Note that this is still a very simple strategy that does not attempt to coordinate uplink and downlink scheduling. More sophisticated strategies would be used in practice.

8.7c.3.3　Performance measure

Performance is shown as the relative gain (at a certain HOT penetration) of the mean user throughput (mean over users) compared to that for HOT penetration 0%. The user throughput is defined as the number of downloaded/uploaded bits divided by the download/upload time. The download/upload time comprises transmission time, scheduling delays, TBF set-up delays and TCP impact.

8.7c.3.4　MS capabilities and MCS selection

It is assumed that HOT capable MSs can use up to MTCS-12-32QAM (i.e., HOT level 2). The MCS with the highest throughput for the given CIR is selected (i.e., no link adaptation is used). MCS choices and block error probabilities are summarised in table 91g (see Annex B for further details).

Table 91g. MCSs and block error probabilities at different CIR for EDGE and HOT MS.

C/I	15	20	25	30	35
EDGE MCS	MCS-6	MCS-7	MCS-9	MCS-9	MCS-9
EDGE BLER	5%	6%	14%	3%	0.4%
HOT MCS	MTCS-7-16QAM	MTCS-8-16QAM	MTCS-10-32QAM	MTCS-11-32QAM	MCS-12-32QAM
HOT BLER	19%	7%	5%	4%	9.5%

For the case with DL transmissions to HOT mobiles, which are adjusted for EDGE UL scheduling, MTCS-6 is used in the simulations. The block error probability versus CIR of MTCS-6 is summarised in table 91h.

Table 91h. Block error probabilities at different CIR for MTCS-6.

C/I	15	20	25	30	35
MTCS-6 BLER	3%	0.1%	~0	~0	~0

8.7c.4 Results and discussion

8.7c.4.1 Case 1: EDGE/HOT mix on downlink, EDGE on uplink

In this subclause, there is a mix of EDGE and HOT MS. In the uplink, it is assumed that all MS use EDGE.

The results are shown in figure 232e to figure 232h for two different loads (70% and 80%) and two different CIR levels (15 dB and 35 dB). Additional results can be found in [46]. The figures show significant performance gains on the downlink, but performance loss on the uplink for scheduling strategy 1. However, scheduling strategy 2 (modulation fallback and granularity 4) eliminates this loss. The large downlink gain is a combination of increased transmission bitrate and decreased scheduling delays. The reason for the decreased scheduling delays is the decrease in channel utilization (i.e. that less time is needed to serve the offered traffic).

In fact, there seems to be also a small UL gain for scheduling strategy 2. This gain (albeit small and uncertain) is probably related to the implementation of the channel handling and scheduling in the simulator. There are two factors that might affect the performance depending on HOT penetration. One is the uplink scheduling of the mix of EDGE MSs (granularity 4) and HOT MSs (granularity 1). A perfectly fair scheduling of users with different granularity might be hard to achieve. A possible result of slight unfairness can then be a gain in the mean user throughput. This would (partially) explain why there appears to be small gains at (certain) penetrations between 0% and 100%.

The other factor is the downlink channel utilization (or the number of TBFs) which decreases as the HOT penetration increases. This might have impact on the uplink performance since the uplink TBF allocation in the simulator also takes the downlink TBF occupancies into account. Depending on present multi-slot classes, a higher downlink load might lead to more uneven uplink TBF distribution over the channels and thereby more uplink channel sharing and scheduling delays. This would explain why there appears to be a small gain at 100% penetration.

NOTE: The curves are a bit shaky in some plots, due to a somewhat limited statistical confidence. Therefore, some caution is necessary when interpreting the results. E.g., in some plots, the downlink performance with scheduling strategy 2 sometimes appears to be slightly better than strategy 1. This could in principle be due to that there is some impact of the improved uplink efficiency on the downlink TBF allocation, but is more likely just due to statistical variations. Longer simulations would remove this shakiness. Still, the trend in all results clearly shows that the multiplexing issue to a large extent can be removed by simple means.

8.7c.4.1.1 Results for moderate load

Figure 232e and figure 232f show the results for a load factor of 70% at CIR=15 dB and 35 dB, respectively.
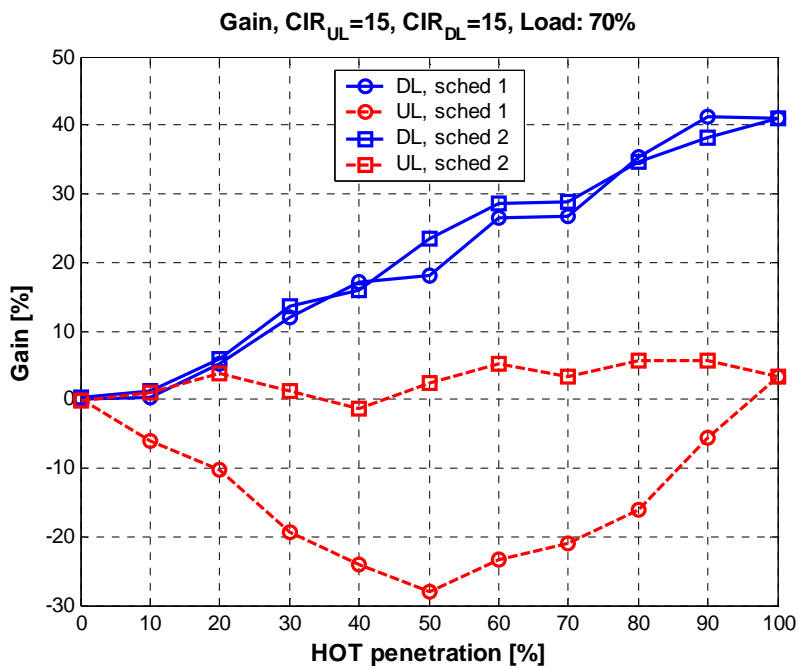
Figure 232e: CIR 15 dB, load factor: 70.0%,
DL: 314.9 kbps/cell, UL: 314.9 kbps/cell.
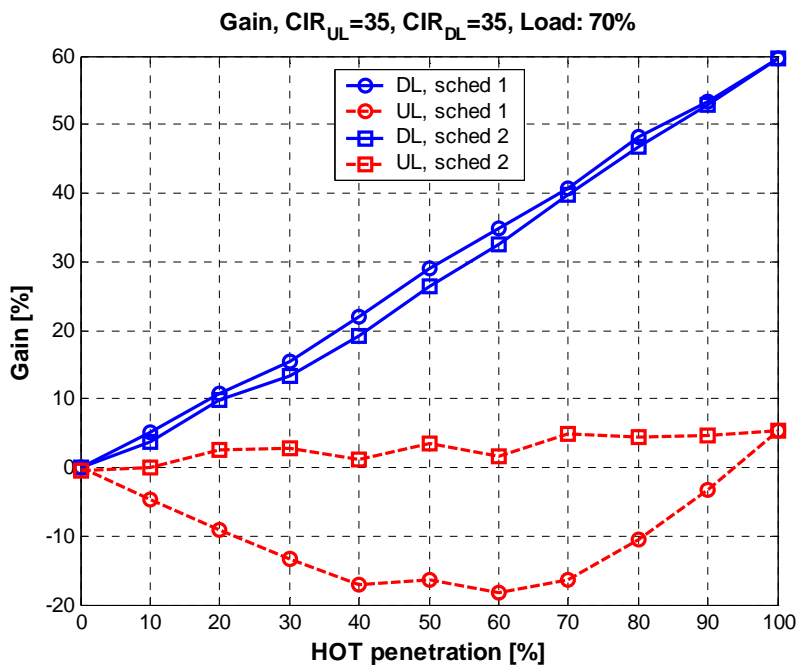
Figure 232f: CIR: 35 dB, load factor: 70.0%,
DL: 660.4 kbps/cell, UL: 660.4 kbps/cell.

8.7c.4.1.2   Results for high load

Figure 232g and figure 232h show the results for a load factor of 80% at CIR=15 dB and 35 dB, respectively.
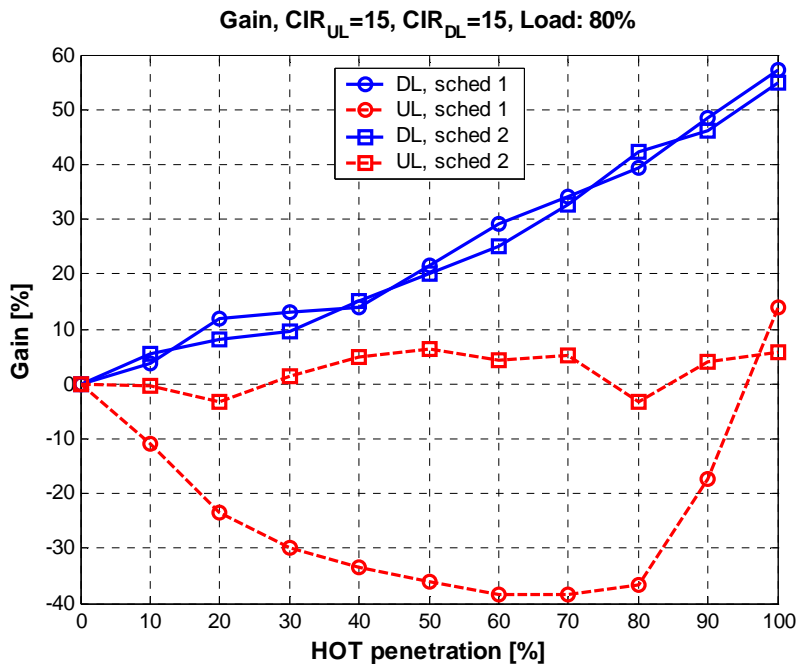
**Figure 232g: CIR: 15 dB, load factor: 80.0%,
DL: 359.9 kbps/cell, UL: 359.9 kbps/cell.**
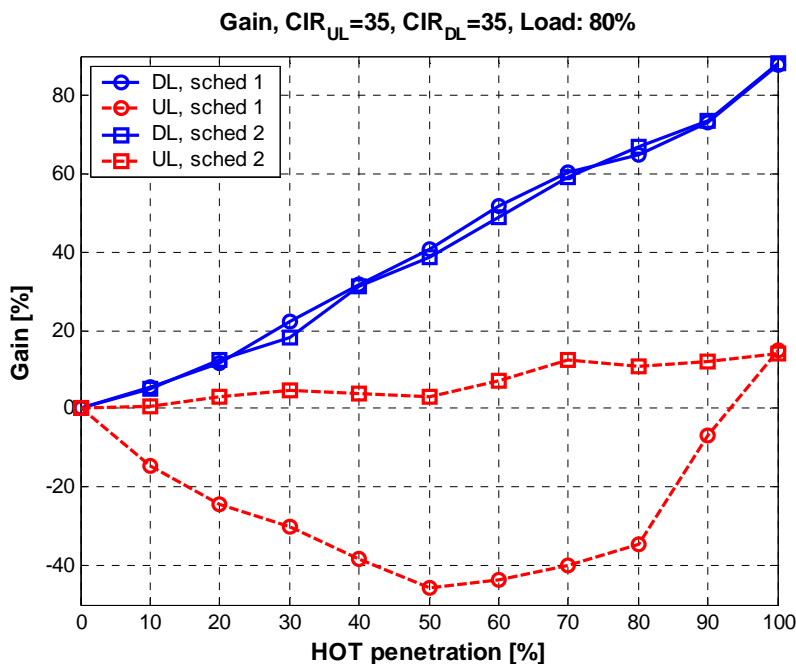
**Figure 232h: CIR 35 dB, load factor: 80.0%,
DL: 754.7 kbps/cell, UL: 754.7 kbps/cell.**

8.7c.4.2 Case 2: EDGE/HOT mix on downlink, EDGE/HOT mix on uplink

In this subclause, there is a mix of EDGE and HOT MS in both uplink and downlink. Obviously, HOT is not proposed for uplink; a better choice would have been using HUGE for uplink. However, no link performance results for HUGE were available when these simulations were run. The use of HOT performance for uplink can be seen as a (slightly pessimistic) estimate of HUGE performance.

The results are shown in figure 232i to figure 232l for two different loads (70% and 80%) and two different CIR levels (15 dB and 35 dB). Additional results can be found in annex [46]. The figures show significant performance gains on the downlink, but performance loss on the uplink for scheduling strategy 1 and low to moderate HOT penetration and low CIR. However, scheduling strategy 2 (modulation fallback and granularity 4) eliminates this loss and yields a significant performance gain.

The large gains at high penetration levels are a combination of increased transmission bitrate and decreased scheduling delays. The reason for the decreased scheduling delays is the decrease in channel utilization (i.e. that less time is needed to serve the offered traffic).

8.7c.4.2.1 Results for moderate load

Figure 232i and figure 232j show the results for a load factor of 70% at CIR=15 dB and 35 dB, respectively.
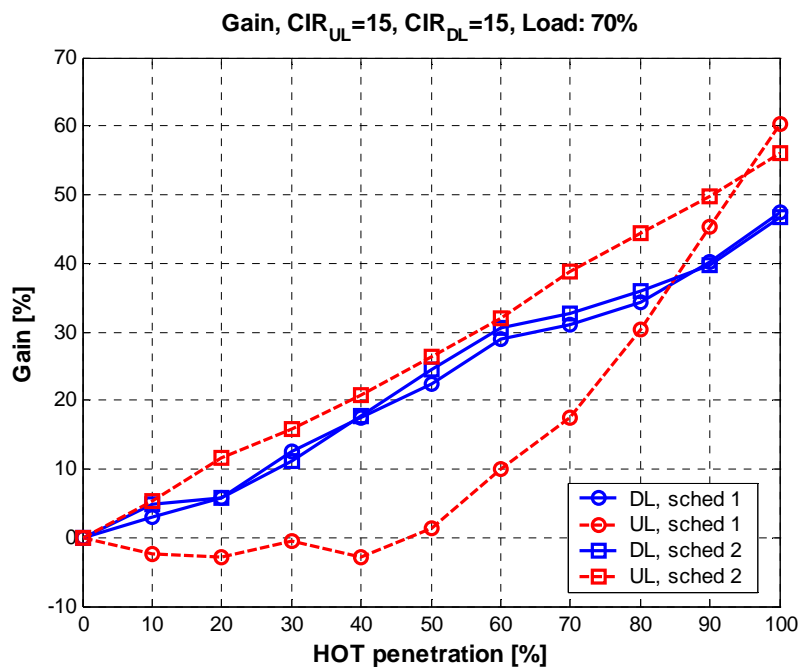
**Figure 232i: CIR 15 dB, load factor: 70.0%,
DL: 314.9 kbps/cell, UL: 314.9 kbps/cell.**
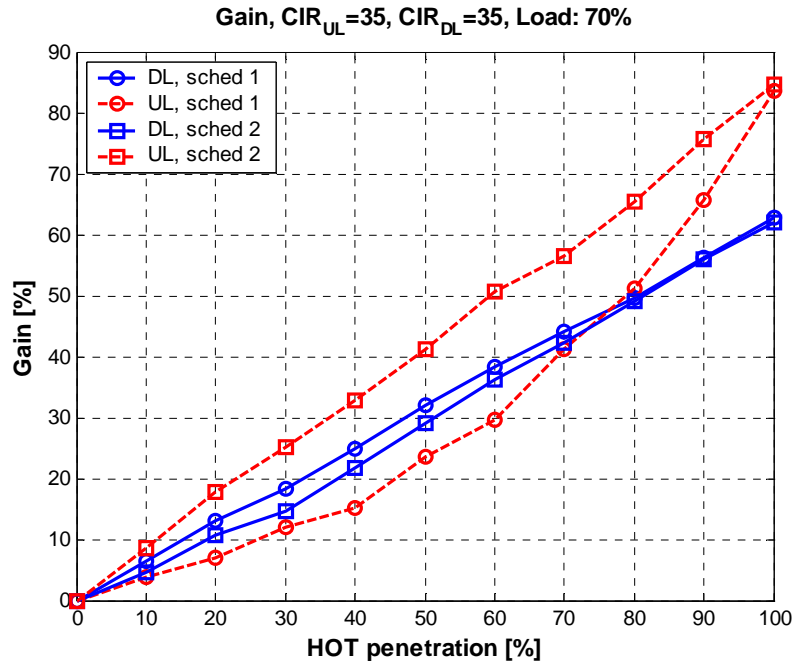
Figure 232j: CIR: 35 dB, load factor: 70.0%,
DL: 660.4 kbps/cell, UL: 660.4 kbps/cell.

8.7c.4.2.2 Results for high load

Figure 232k and figure 232l show the results for a load factor of 80% at CIR=15 dB and 35 dB, respectively.
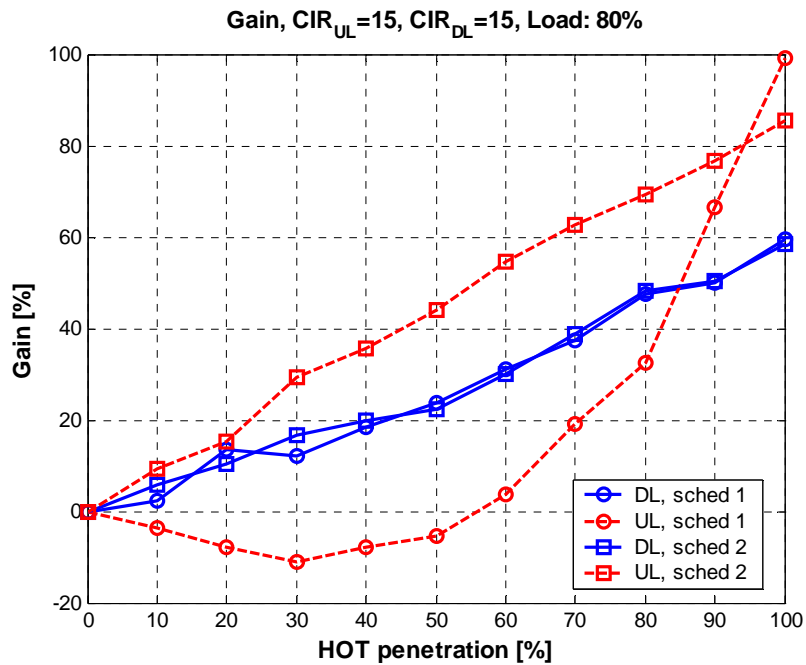
Figure 232k: CIR: 15 dB, load factor: 80.0%,
DL: 359.9 kbps/cell, UL: 359.9 kbps/cell.
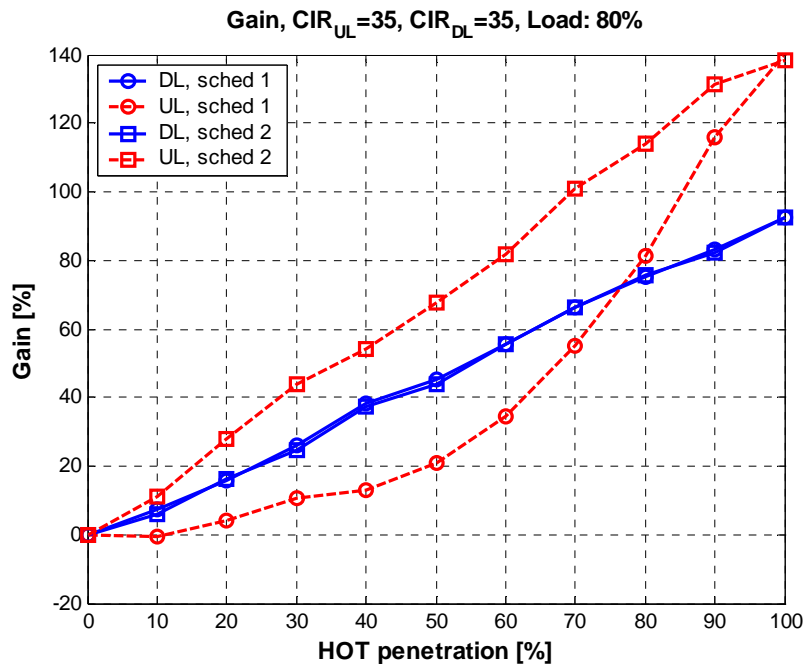
**Figure 232I: CIR 35 dB, load factor: 80.0%,
DL: 754.7 kbps/cell, UL: 754.7 kbps/cell.**

8.7c.4.3   Discussion

The simulations show that if no means are taken to solve the issue of multiplexing HOT MS and EDGE MS, there are indeed multiplexing losses. They also show that the losses can be almost completely avoided with a very simple strategy.

8.8   Incremental Redundancy for Higher Order Modulation and Turbo Coding Schemes (HOMTC)

Source: Reference [36].

8.8.1   Introduction

The current EGPRS capability includes an ARQ mechanism [22]. This allows for re-transmission of blocks that have failed to be decoded correctly on first or subsequent transmissions, using Link Adaptation and/or Incremental Redundancy. The receiver side signals back to the transmission side using ACK/NACK messages, and the relevant block can be re-transmitted using either different puncturing of the initial MCS for the block, or a MCS in the same family. Hybrid ARQ using IR was an important conceptual step in the transition from GPRS, and provides considerable additional throughput. This is a component that is important to retain for inclusion within HOMTC.

This subclause discusses how Type I and Type II ARQ capabilities can be included for the HOMTC proposal.

8.8.2   EGPRS ARQ Scheme

The payload structure currently used in EGPRS is currently built around 3 "families" of MCSs as shown in 233. This format was originally proposed during the EDGE Feasibility Study (e.g.[37]). The family structure is constructed such that units of data already segmented from the Logical Link Control (LLC) layer can be transmitted using different MCSs depending on prevailing signal conditions. Alternatively, the punctured redundancy versions for each MCS allow for incremental redundancy.

For example, consider Family A. The data is segmented in multiples of 37 octet units. Say a MCS9 block is transmitted. This contains 2 RLC packet data units (PDU) each one of 74 octets (2x37). Suppose that one of the PDU fails to be

decoded on reception. If the separately (very robustly) coded header block is decoded, or if a higher block sequence number (BSN) is received, then the block is known by the receiver to have failed. This failure is indicated by MS uplink ACK/NACK signalling to the base station (BTS) for the case of downlink transmissions (and vice versa for uplink). There are then a number of options for re-sending the data (the detailed explanation is given in [38], subclause 8.1.1):

   i) the failed PDU can be re-transmitted either as a PDU in another MCS9 block using a different redundancy version;

   ii) it can be re-transmitted as the content of an MCS6 block; or

   iii) the 74 octet PDU can be split down into 2 separate 37 octet blocks, each of which is re-encoded separately as 2 MCS blocks. These are transmitted using MCS3 with signalling that the original PDU has been re-segmented.

It is noted that the MCS7, MCS8 and MCS9 channel coding schemes have 2 RLC PDUs, each of which is separately encoded before combination into the MCS. This was done because for convolutional coded blocks the probability of a block error reduces as the length of the block decreases. As noted during the EDGE Feasibility study [37], if this split is not done, and a 4x37 octet PDU is encoded with a single convolutional coded block the BLER performance becomes poor.

Turbo codes perform in the opposite manner. As is well known [39], the performance improves as the information length in a coded block becomes longer. This principle is used in the next subclause.
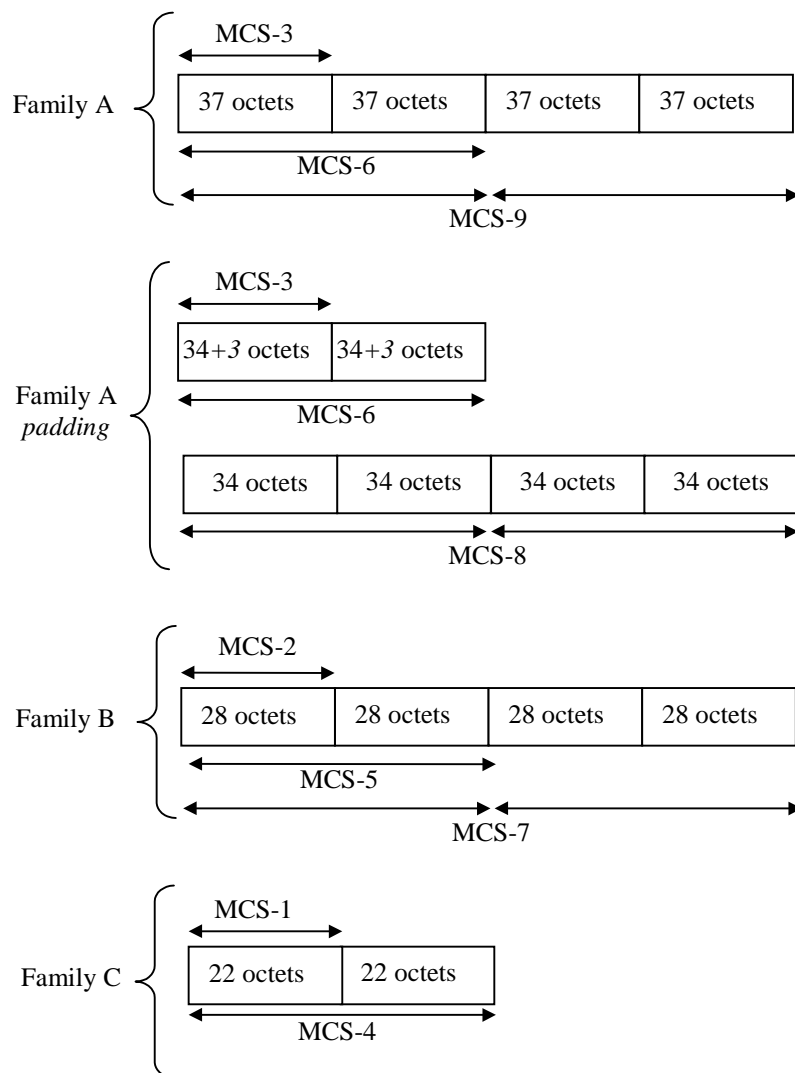
Figure 233: General description of the Modulation and Coding Schemes for EGPRS

8.8.3   Concept Proposal for ARQ with HOMTC

As we noted, in EGPRS the payloads for the higher MCSs were split to avoid the poorer performance when using higher coding rate blocks with convolutional coding. In this subclause we first examine the Turbo code structure, and note simulation data showing that for HOMTC, the performance is improved by encoding the payload as a single block. The proposal for management of ARQ and Link Adaptation is then discussed.

8.8.3.1   Turbo Coding Block Structure

The 3GPP RAN Turbo code is a Parallel concatenated code [15]. The structure is shown in figure 234. It is a Rate 1/3 code, with the output bits being systematic bits (the original information bits), plus 2 parity bits. There are 2 separate parity coding structures; the 1st encoder uses the information bits in the original order; the 2nd encoder uses the information bits after the internal Turbo interleaver. The internal interleaver causes the original bit order to be lost in parity 2 calculation - this produces a useful effect in terms of decoding in that, for the block lengths considered for HOMTC, we will not observe frame errors where only one half of the information data is in error. Either the complete block is correctly decoded, or neither half.

This behaviour was verified in simulation. The same is also seen when simulating MCS8 and MCS9 as single and double blocks.
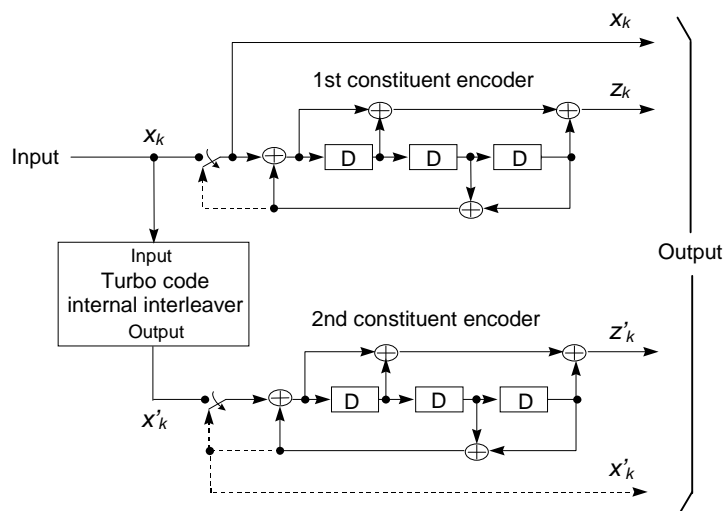
Figure 234: Structure of rate 1/3 Turbo coder (dotted lines apply for trellis termination only)

The comparison of performance for single and double RLC PDU blocks has been reported in [31]. It has been seen that, for Turbo coded configurations there is a clear advantage in encoding the information as a single RLC PDU. As was seen in the EDGE Feasibility study [37], this is not the case for convolutional coding, and so in the EDGE standardization process the data was split into 2 RLC PDUs for the higher MCSs.

The implication of this is that there is no reason to retain the split used in EGPRS for MCS7, MCS and MCS9 when using Turbo coding. As is seen in [31], performance degrades for shortened blocks.

8.8.3.2   RLC/MAC Operation for HOMTC

As with EGPRS, the transfer of RLC Data Blocks in the acknowledged RLC/MAC mode can be controlled by a selective type I ARQ mechanism, or by type II hybrid ARQ (incremental redundancy (IR)) mechanism, coupled with the numbering of the RLC Data Blocks within one Temporary Block Flow. The sending side (the MS or the network) transmits blocks within a window and the receiving side sends Packet Uplink Ack/Nack or Packet Downlink Ack/Nack message when needed.

The ARQ mechanism is considered for 3 cases:

    i)   Type I ARQ with Link Adaptation.

    ii)   Type II Hybrid ARQ with no intra block Link Adaptation.

iii) Type II Hybrid ARQ with intra block Link Adaptation.

8.8.3.2.1 Type I ARQ for HOMTC with Link Adaptation

The concept for Type I ARQ is almost identical to that for EGPRS. A slight modification is made to take advantage of the improved performance of Turbo coded blocks as the source code block length increases, and also to exploit the potential for higher throughput from the Higher order 16-ary modulation. The new MCSs are shown in table 93; for reference current EGPRS MCSs are shown in table 92.

Existing MCS7, MCS8 and MCS9 payloads are modified so the payload is encoded as a single PDU. These are configurations MCS7-T4-16APK, MCS8-T4-16APK and MCS9-T4-16APK in table 93.

The MCS10-T4-16APK and MCS11-T4-16APK coding schemes are included to provide higher throughputs. The payloads for these are now aligned with existing MCS families.

The usage of the family structure is then as for EGPRS.

Table 92: Modulation and Coding Schemes for EGPRS

Modulation and Coding Scheme	Data Code rate	RLC blocks per radio block	Raw Data (octets)	Interleaving depth	Data rate kb/s/slot	Family
MCS1	0.53	1	1x22	4	8.0	C
MCS2	0.66	1	1x28	4	11.2	B
MCS3	0.85	1	1x37 _34+3_	4	14.8	A
MCS4	1.0	1	1x44	4	16.0	C
MCS5	0.37	1	1x56	4	22.4	B
MCS6	0.49	1	1x74	4	29.6	A
MCS7	0.76	2	2x56	4	44.8	B
MCS8	0.92	2	2x68	2	54.4	A
MCS9	1.0	2	2x74	2	59.2	A

Table 93: Modulation and Coding Schemes for HOMTC

Modulation and Coding Scheme	Data Code rate	RLC blocks per radio block	Raw Data (octets)	Interleaving depth	Data rate kb/s	Family
MCS1-T4-8PSK (see note)	0.14	1	1x22	4	8.0	F
MCS2-T4-8PSK	0.18	1	1x28	4	11.2	E
MCS3-T4-8PSK	0.24	1	1x37 _34+3_	4	14.8	D
MCS4-T4-8PSK	0.28	1	2x22	4	16.0	F
MCS5-T4-8PSK	0.36	1	2x28	4	22.4	E
MCS6-T4-8PSK	0.48	1	2x37	4	29.6	D
MCS7-T4-16APK	0.55	1	4x28	4	44.8	E
MCS8-T4-16APK	0.67	1	4x34	4	54.4	D
MCS9-T4-16APK	0.73	1	4x37	4	59.2	D
MCS10-T4-16APK	0.82	1	6x28	4	67.2	E
MCS11-T4-16APK	1	1	6x34	4	81.6	D

NOTE. For code rates below R=0.33, the rate is an effective one created by repetition of bit according to 3GPP TS 25.212 rate matching. The Turbo code mother code rate is R=0.33.

8.8.3.2.2 Type II Hybrid ARQ for HOMTC

The method proposed for Type II HARQ with HOMTC is similar to that for EGPRS, however the limitation regarding how re-transmissions may be done is removed. Currently, on re-segmenting a payload, the new payload parts are separately re-encoded and the re-segmentation is signalled. This occurs for example on re-transmission of data from MCS6 block using MCS3 - 2 MCS3 blocks need to be transmitted to transfer the original, and no capability of incremental redundancy combining is available.

The following gives a description of how the modified HARQ would work. First we consider the case without LA, and then the case with LA.

8.8.3.2.2.1   No Link Adaptation

Consider a simplified example of a short block, ignoring tail bits also for simplicity. Suppose we have an information block of 16 information bits, $[s_0 s_1 ... s_{15}]$. This is encoded as:

$$[s_0 p_{00} p_{01} s_1 p_{10} p_{11} ... s_{15} p_{15,0} p_{15,1}]$$

where p_{k0} and p_{k1} are the parity bits output with the *kth* systematic bit. Suppose we transmit the code word using 16APK with initial code rate 1. Then, until the codeword is correctly decoded, the transmission redundancy versions might follow a pattern such as that shown below (see note). On the first transmission, 16 systematic bits are sent. If the block is not received correctly, Transmission 2 is sent using a punctured redundancy version of 16 bits. This can be combined at the receiver for an additional attempt to decode. If, again the block is not received correctly, Transmission 3 is sent using another redundancy version of the bits. At this point all bits have been transmitted at least once. Again, an attempt at decoding is made. Should this fail the redundancy version sequence is repeated until the block is correctly decoded. At each stage the newly received bits can be combined with those received in previous punctured versions of the block, in order to improve the initial data input to the Turbo decoder.

Transmission 1: $[s_0 s_1 ... s_{15}]$

Transmission 2: $[p_{00} p_{11} p_{20} p_{31} ... p_{14,0} p_{15,1}]$

Transmission 3: $[p_{01} p_{10} p_{21} p_{30} ... p_{14,1} p_{15,0}]$

NOTE.   The precise redundancy versions should be set to allow use of 3GPP RAN rate matching algorithms[15].

Table 94: Code Rate after each Transmission

Transmission Number	No intra-block LA		With intra-block LA	
	Modulation	Code Rate	Modulation	Code Rate
1	16APK	1	16APK	1
2	16APK	0.5	8PSK	0.57
3	16APK	0.33	8PSK	0.4
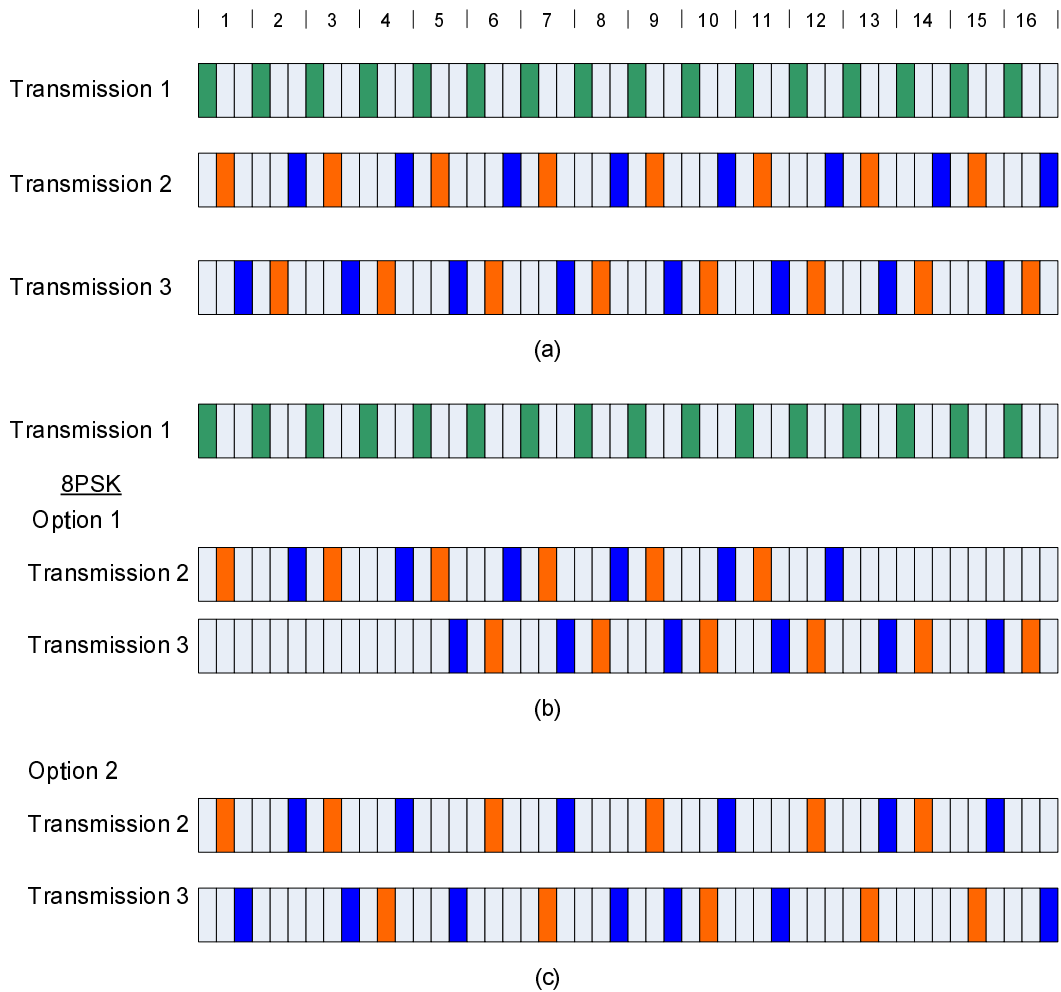
**Figure 235: Example of Redundancy versions for a) all 16APK transmissions;
b), c) transmissions with first 16APK, then 8PSK modulation**

8.8.3.2.2.2   With Link Adaptation

This subclause now considers an extension to the case of subclause 8.8.3.2.2.1, where in this case a change of modulation is allowed. As above, the first transmission of the block is as for Transmission 1. Suppose that LA now occurs, and the transmissions will be made using 8PSK instead of 16APK (see note).

> NOTE.   In the case of moving from 8PSK to GMSK (MCS6 to MCS3), this results in a loss of previously received data.

Instead of dumping previously transmitted data from the higher modulation (as happens in re-segmentation from MCS6 to MCS3), it would be preserved on switching modulation. The new modulation scheme, say 8PSK, is used as a medium to continue bit transfer of the coded data block that we have already started transmission using 16APK. The advance of the coding rate for the cases with and without modulation change is shown in table 94. This gives an advantage over EGPRS when switching modulations. Additionally, it is possible that the receiver will decode the source data after only one transmission over 8PSK, instead of 2 blocks over 8PSK as would be done using the EGPRS concept, thereby improving the throughput.

With regard to how to distribute the un-punctured bits for each re-transmission, a number of approaches could be taken. One possibility is to treat the 8PSK re-transmissions similar to split block, transmitting first the early part of the puncturing sequence, then on the next block transmitting the late part of the next sequence (see figure 235 (b)). Alternatively, the rate matching can be configured to distribute the un-punctured bits evenly throughout the coded block for each re-transmission (see figure 235 (c)). It is expected that Option 2 will give better performance.

8.8.3.2.3 Header Format

Some modification of the header format will be required to manage the signalling of a block using different modulation sequences.

Note that it is possible that the header of the first version of the BSN transmission is not decoded correctly, and then the modulation is changed. There are 2 options for how to handle this. The first option is to include in the ACK/NACK signalling a flag bit for each block not correctly received, that indicates if the header was decoded or not. A block whose header was not decoded yet, can be moved to a different MCS in the family as no redundancy information is yet stored at the receiver. Another option is not to signal this, and to allow the transmitter to change modulation in the middle of a block and allow the IR combining mechanism to reduce the code rate. It is anticipated that the second option is probably preferable. It avoids the modification to the ACK/NACK; and also the throughput performance is improved by using the longer source block length.

8.8.3.3 USF Signalling

In most cases that there are EGPRS and HOMTC MSs operating in the same cell, it will be possible to avoid any multiplexing loss. Strategies such as allocation to different hop sequences and timeslots, and intelligent alignments of signalling USFs for EGPRS only mobiles can mitigate most of the impact. However, there will be cases that there is no choice but to signal a USF to an EGPRS mobile on a block used for DL to a HOMTC mobile. In this case we should avoid the severe multiplexing loss that occurred by multiplexing in EGPRS over a previously GPRS service. If we were using MCS7 for transmission, then the EGPRS family would push us down to MCS2 to signal to a GPRS MS. However, in principle there is no reason to do this with HOMTC. As described in subclause 8.8.3.2.2.2, we can use 8PSK modulation to provide an additional redundancy version of a previously transmitted block with minimal impact on the throughput.

8.8a Modulation Order and symbol Rate Enhancement (MORE) [48]

In this subclause, the combination of higher order modulation with 20 % higher symbol rate is investigated.

8.8a.1 Concept Description

The concept includes the following elements :

- higher order modulations (16-ary and 32-ary modulations)

- higher symbol rate (the same as for HUGE, i.e. 325 ksymbols/s)

- slightly broader pulse shaping than the linearised GMSK (similar to HUGE)

- use of both convolutional and turbo codes

8.8a.2 Discussion of the Concept

8.8a.2.1 Benefits

Synergies between HUGE and MORE related to modulation, coding schemes, increased symbol rate and pulse shaping can be exploited.

MORE can be combined with MSRD to achieve good performance already at moderate C/I ratios and hence increase the spectral efficiency.

MORE can be combined with downlink dual carrier to achieve higher peak data rates on the downlink. Up to a quadrupling of the EDGE data rate is possible using 32-ary modulation, which would allow peak data rates of approximately 950 kbps for a MS with 4 TS.

A phased approach is proposed which allows for proper interoperability testing of mobiles with networks based on a phased implementation for both mobiles and networks.

MORE takes into account legacy networks by including improvements to throughput and spectral efficiency on basis of 8-PSK modulation.

Together with HUGE, MORE can provide both higher spectral efficiency and higher peak data rates for operators with scarce radio resources, relying on symmetrical single carrier traffic channel deployments. Hence the GERAN Evolution performance requirements are met.

In combination with improvements being standardized under the latency reductions work item, HUGE and MORE can provide bearers for support of bidirectional real-time data or conversational services over PS.

Hence MORE provides a future proof path for GSM/GERAN operators intending to deploy GERAN Evolution features.

8.8a.2.2   Drawbacks

Higher symbol rates with 16-ary and 32-ary modulations may not be supported on many legacy networks. However, as 8-PSK with 325 ksymbols/s is also considered as an option for the downlink, some legacy networks might be able to support at least the first level of the proposed downlink enhancements.

One additional work item is to be treated. However given synergies between HUGE and MORE, the additional standardisation effort due to MORE should be rather moderate and the standardization of MORE can even be time aligned with HUGE.

8.8a.3   Performance Estimation

In this section, the performance of an example coding scheme is studied at higher symbol rate and different bandwidths. Studying different bandwidths is of greater importance because it might be necessary to limit the bandwidth of transmission on the downlink to today's bandwidth despite the higher symbol rate as greater adjacent channel interference might have more impact on legacy mobiles unlike HUGE where most networks are expected to cope with the higher interference using diversity reception.

For this initial study, linearised GMSK pulse shaping is assumed. It is expected that the performance shown in this contribution could be bettered using enhanced pulse shapes. For the purpose of simulations, an ideal single antenna receiver for the downlink without RF impairments is assumed.

At this time no new coding schemes for higher symbol rate are defined. It should be noted that by using transmissions at higher symbol rate, there is space for more symbols in a given burst.

With 1.2 times the legacy symbol rate (325 ksymbols/s), we have 20 % more room for additional symbols and hence additional bits. One way of using this additional space is to have more robust coding for the data. Hence, for comparison, we selected two EGPRS coding schemes - MCS-8 @ 0.92 code rate and MCS-7 @0.76 code rate. Note that the relation between the code rates of the two coding schemes is a factor of 1.21 which is close to what could be gained using additional symbols from increased symbol rate. The performance of a legacy transmission using MCS-8 is then compared with that of MCS-7 with legacy and new pulse shape and the channel is run at higher symbol rate. The impact of additional inter symbol interference due to wider pulse shape in terms of symbol periods (depending on pulse width) is modeled. The delay spread of the channel in terms of symbol periods also increases at higher symbol rate and this effect is also modeled in the link simulator. Three different bandwidths are considered for the simulations as shown in Figure 232.b1. The spectra of the modulated signals are measured during the simulation and Figure 232.a1 shows the spectra. It can be seen that when 20 % higher bandwidth is allowed for the modulated signal, the spectrum mask cannot be met (red curve in). However, by reducing the bandwidth of the signal (green and blue curves) it is possible to meet the spectrum mask. The performance of these modulated signals is studied and is compared with transmission at legacy symbol rate (Figure 232.b1).
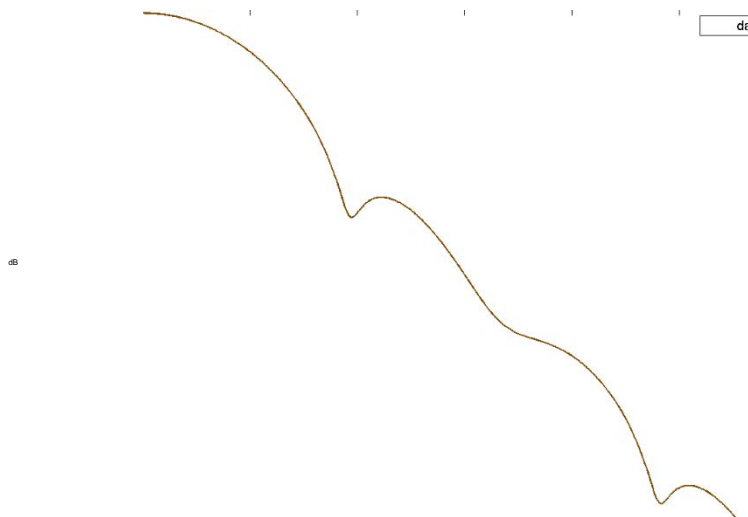
Figure 232.a1: Simulated spectra of the modulated signals
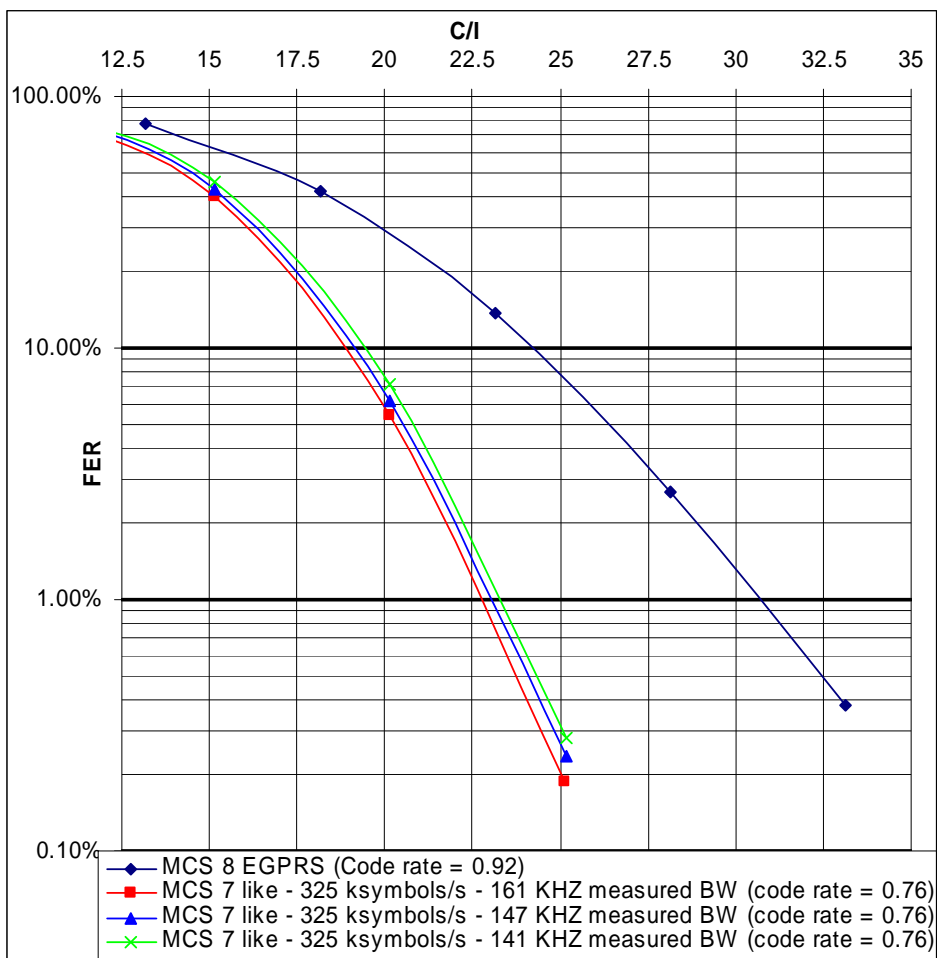
Figure 232.b1: Expected performance of higher symbol rate coding schemes

From the above results, it could be observed that though there is some loss (~ 0.5 to 1dB) in performance due to higher symbol rate without corresponding bandwidth increase; it is still possible to have huge gains (almost 5 dB in the simulated case @ 10% FER). Since most of the gain is coming because of additional code space, it is expected that such gains are not possible for all coding schemes (in particular coding schemes which are already robustly coded may have lesser gains). Under sensitivity limited conditions, a higher inter symbol interference will result in slightly lower

coverage as the peak to average ratio of the signal will then be slightly higher. However, as can be seen from the performance improvement shown in Figure 232.a, it is expected that a considerable improvement can still be achieved.

It can hence be concluded that even at the current bandwidth, the performance of the coding schemes at higher symbol rate is significantly better and thus it is expected that MORE could be deployed on the downlink with out any impact to the legacy mobiles.

8.9 Implementation Impact

There are a number of alternatives when applying higher order modulations with increasing degree of impact to consider:

    a) Replacing 8-PSK with 16-QAM for MCS-8 and MCS-9 only with the same user data rate (case B in subclause 8.4.1.3). The impact is mainly on the RF receiver and transmitter.

    b) Modify MCS-8 and MCS-9 as above and in addition add new coding scheme for 16-QAM to increase the available peak rate (case C in chapter 8.4.1.3). This option will increase the peak user data rate as well. Thus the handling of data flows with higher rates need to be considered.

    c) Modify MCS-8 and MCS-9 as above and in addition add new coding schemes for 16-QAM and 32-QAM (case D in subclause 8.4.1.3). The impact is similar to option b, but requests even better receiver/transmitter performance as well a handling of higher user data rates.

In addition the modifications could be applied to DL only or both UL and DL.

The improvement in performance and capacity due to higher order modulations will require modest increases in computational complexity at the receiver. The complexity of channel estimation, prefilter calculation, AFC etc. are in the same order as in the case of 8-PSK modulation. However, the equalizer complexity is increased depending on the modulation level. Depending on the implementation structure, the complexity increases between linearly and exponential. Using RSSE implementation may drastically reduce the complexity increase with moderate impact on performance, see subclauses 8.3.3 and 8.4.3.8.

To include improved performance and capacity due to higher order modulations will require EVM performance of the transmitter for these modulations to be comparable with that for 8-PSK. This may put more stringent requirements on PA linearity and, to some extent, on synthesizer noise characteristics.

8.9.1 Impacts on the Mobile Station

If higher order modulation is applied to DL only, then the main impact is the increased complexity of the receiver as described above.

The capability to receive and decode correctly QAM modulations need to be signalled in classmark 3 and MS-RAC, so the network know which coding schemes that could be used to each mobile. In addition, if new coding schemes are introduced, new capabilities for this need to be introduced.

If applied to UL as well, the challenge is to keep EVM low enough for the higher order modulations. Mainly this will put requirements on synthesizer noise and on PA linearity. The maximum output power may decrease by 2 dB compared to 8-PSK.

The capability to transmit QAM modulations need to be signalled in classmark 3 and MS-RAC.

8.9.2 Impacts on the BSS

If higher order modulation is applied to DL only, then the main impact is the potentially more stringent requirements on PA and synthesizer for keeping EVM approximately constant for all modulations. However, if only 16-QAM is considered, there is fair chance that the HW impact is small or none. The impact on HW depends on the performance of present 8-PSK BSS. The increase of PAR may reduce the available maximum output power for QAM-modulations by 2 dB compared to 8-PSK, assuming the power capability of present BTSs is unchanged.

If applied to UL as well, then the main impact is the increased complexity of the receiver as described above. If peak user data rate is increased, the handling of higher peak data flow also needs to be considered.

Thus introducing only 16-QAM on MCS-8 and MCS-9 will probably affect only SW.

8.9.3   Impacts on the Core Network

The impact on core network is negligible and only on SW. Addition of new signalling parameter is as simple as any other new feature.

8.9a   Implementation Aspects of MORE

8.9a.1   Mobile Stations

- Implementation of higher order modulations (16 ary and 32 ary) as discussed in the GERAN Evolution feasibility study.

- Implementation of a receiver taking into account the broader TX pulse shape (by e.g. using a matched filter).

- Implementation of a receiver processing higher symbol rate. For the symbol rate of 325ksymbols/s a complexity increase up to 50 % is expected.

- Implementation of turbo decoder.

8.9a.2   Network

- Implementation of higher order modulators, fulfilling tighter EVM requirements.

- Implementation of broader TX pulse shaping.

- Implementation of higher symbol rate transmitter.

- Optionally implementation of turbo encoder.

8.10   Impacts on the Specifications

Following specifications will be affected:

- 3GPP TS 24.008: "Mobile Radio Interface Layer 3 specification; Core Network Protocols; Stage 3".

- 3GPP TS 45.001: "Physical Layer on the Radio Path; General Description".

- 3GPP TS 45.002: "Multiplexing and Multiple Access on the Radio Path".

- 3GPP TS 45.003: "Channel Coding".

- 3GPP TS 45.004: "Modulation".

- 3GPP TS 45.005: "Radio Transmission and Reception".

- 3GPP TS 45.008: "Radio Subsystem Link Control".

- 3GPP TS 43.064: "Overall Description of the GPRS Radio Interface; Stage 2".

- 3GPP TS 44.060: "General Packet Radio Service (GPRS); Mobile Station (MS) - Base Station System (BSS) interface; Radio Link Control (RLC) / Medium Access Control (MAC) protocol".

- 3GPP TS 51.021: "Base Station System (BSS) Equipment Specification; Radio Aspects".

- 3GPP TS 51.010: "Mobile Station (MS) Conformance Specification".

8.11 References

[1]   AHGEV-050016, "Higher Order Modulations", source Ericsson.

[2]   AHGEV-050023, "3GPP TR ab.cde vx.y.z Feasibility Study on Future GERAN Evolution", Output document from Adhoc on GERAN evolution, Copenhagen, May 18th - 19th.

[3]   SMG2 EDGE 2E99-021 "Noise Model of Transmitter-Receiver Chain for EDGE", source Ericsson.

[4]   SMG2 331/97 "EDGE Feasibility Study; Work Item 184; Improved Data Rates through Optimised Modulation Version 1.0".

[5]   GP-042355 "Video Telephony over GERAN - C/I cdf in real NW", source TeliaSonera.

[6]   GP-052144 "Updates for New Modulation Schemes section of the Technical Report on Future GERAN Evolution", source Ericsson.

[7]   GP-052084 "16-QAM for GERAN Evolution", source Nokia.

[8]   GP-060258 "Performance Evaluation of 16QAM and Turbo Codes", source Ericsson.

[9]   GP-060784 "More results on 16QAM and turbo codes," source Ericsson.

[10]   GP-050977, "GERAN Continued Evolution", source Ericsson.

[11]   GP-052099, "GERAN Evolution - Proposed Text on New Coding Schemes for Technical Report", source Intel.

[12]   GP-052722, "GERAN Evolution - New Proposed Text on New Coding Schemes for Technical Report," source Intel.

[13]   GP-060186, "Additional Results for Turbo Coding and Higher Order Modulation", source Intel.

[14]   GP-060931, "GERAN Evolution - New Performance Data for Turbo Coding and Higher Order Modulation Schemes," source Intel.

[15]   3GPP TS 25.212, "Multiplexing and Channel Coding (FDD)".

[16]   GP-042667, "Enhanced Support for CS Video Telephony over GERAN - discussion paper", source Intel.

[17]   GP-051508, "GERAN Evolution - Proposed Text on New Modulation Schemes for technical report", source Ericsson.

[18]   GP-051546, "Dual-Carrier EGPRS for GERAN Evolution," source Nokia.

[19]   GP-052656, "Performance Evaluation of 16QAM and turbo codes," source Ericsson.

[20]   3GPP TS 45.003, "Channel Coding".

[21]   3GPP TS 45.005, "Radio Transmission and Reception".

[22]   3GPP TS 43.064, "Overall Description of GPRS Radio Interface; Stage 2".

[23]   3GPP TS 25.892, "Feasibility Study for Orthogonal Frequency Division Multiplexing (OFDM) for UTRAN," v6.0.0.

[24]   GP-060565, "Symbol Mapping of Turbo Coded Bits for 16-QAM Modulation", source Samsung.

[25]   3GPP TS 25.213 v7.0.0, "Spreading and Modulation (FDD)".

[26]   GP-060773, "Performance of 16-QAM and Turbo Codes with Mobile Station Receive Diversity", source Nokia.

[27]   3GPP TS 45.903, "Feasibility Study on Single Antenna Interference Cancellation (SAIC) for GSM networks".

[28]   GP-061232, "Increased Peak Throughput with 16QAM and Turbo Codes", source Ericsson.

[29]   AHGEV-060029, "Higher Order Modulation and Turbo Codes - Discussion and Some New Results", source Ericsson.

[30]   GP-061235, "16QAM with Alternative Transmit Pulse Shaping", source Ericsson.

[31]   GP-061242, "Comparison of Different Coding Configurations for Higher Order Modulation and Turbo Coding Schemes", source Intel.

[32]   GP-061171, "On Modified 16-ary Constellations for Higher Order Modulation and Turbo Coding Schemes", source Intel.

[33]   GP-060932, "16QAM Modulation Usage on the BCCH Carrier," source Intel.

[34]   C. Thomas, M. Weidner and S. Durrani, "Digital Amplitude-Phase Keying with M-ary Alphabets", IEEE Trans. Comm., Vol. Comm-22, pp. 168-180, Feb. 1974.

[35]   T. Hoa Vo and T. Le-Ngoc, "Power and Bandwidth Efficient Circular M-ary APK Schemes with Low PAR", Proc. of CCGEI, pp. 1527-1530, May 2003.

[36]   GP-061173, "Incremental Redundancy for Higher Order Modulation and Turbo Coding Schemes (HOMTC)", source Intel.

[37]   SMG2 WPA 127/99, WPB 003/99 (2A99-127.doc), "Two Burst Based Link Quality Control Proposal for EGPRS", source: A&T, Ericsson, Lucent, Nokia, Nortel.

[38]   3GPP TS 44.060, "GPRS; Radio Link Control/Medium Access Control (RLC/MAC) protocol".

[39]   Berrou, C., Glavieux, A. and Thitimajshima, P., "Near Shannon limit error-correcting coding and decoding: turbo codes," Proceedings of IEEE International Communications Conference '93, pp. 1064-1070, May 1993.

[40]   Vitthaladevuni, P.K.; Alouini, M.-S.; Kieffer, J.C, "Exact BER Computation for Cross QAM Modulations," IEEE Transactions on Wireless Communications, pp 3039-3050, vol 4, Issue 6, Nov 2005.

[41]   GP-061591, "Higher Order Modulation and Turbo Codes - Higher HOM", source Intel.

[42]   GP-061752, "Additional results for higher order modulation and turbo coding including 32QAM and IRC", source Ericsson.

[43]   GP-062120, "System level performance of HOT", source Ericsson.

[44]   GP-062121, "Blind modulation detection performance for HOT", source Ericsson.

[45]   GP-062122, "Impact of using HOT on the BCCH carrier", source Ericsson.

[46]   GP-062123, "Multiplexing HOT with legacy MS", source Ericsson.

[47]   GP-062209, "Blind Modulation Dectection performance for HOT", source Intel.

[48]   GP-062188, "MORE – Downlink Improvements for GERAN Evolution", source Siemens.

[49]   GP-062187, "Burst format for MORE compatible with USF decoding for legacy EGPRS MS", source Siemens.

9   Dual symbol rate and modified dual symbol rate

9.1 Introduction

This paragraph proposes two alternative uplink concepts: Dual Symbol Rate (DSR) and Modified Dual Symbol Rate (MDSR) for Future GERAN evolution to double bitrates in uplink. DSR doubles the modulation rate in the transmitter of the mobile station and MDSR combines higher symbol rate (3/2) with 16QAM and optionally with QPSK. Both options offer about similar bit rates and performance in uplink e.g. 1.8 to 1.9 times higher average bit rates at coverage and 1.7 to 1.9 times higher bit rates at interference limited scenarios.

The main benefit of MDSR is the narrower signal bandwidth of two 200 kHz GSM channels instead of three in the case of DSR. This could simplify dual transceiver implementation compared to DSR e.g. narrower channel filter may be applied and oscillators are not needed to tune out of 200 kHz channel raster.

It was found earlier that DSR and MDSR with 2.0 and 1.5 times higher symbol rates clearly exceed the given performance objectives on coverage and spectral efficiency but that two legacy TRX implementation option was not favoured. Optimisation of MDSR concept for single legacy TRX implementation may be done by removing the 100 kHz offset and reducing the symbol rate further e.g. to 1.2 (6/5) or 1.33 (4/3) times higher than the legacy symbol rate, to produce High Symbol Rate schemes (HSR). To meet peak throughput objectives, e.g. 32QAM modulation is then needed.

The BTS receiver needs to cope with wider transmission bandwidth and could beneficially utilise the gain of interference rejection combining (IRC) for reception of dual symbol rate. The receiver complexity for DSR is about up to 50 % more complex per bit than for 8PSK. The dual symbol rate applies to normal GSM frequency planning for all re-uses up to 1/1. Evolution in uplink bit rates is needed to support uploading of images or video from camera phones and also to maintain a balance in bit rates and in coverage with downlink enhancements e.g. with dual carrier.

9.1.1   Technology outline

The transmitter power of Mobile Station is limited e.g. by multi slot power reduction, thus more effective method than adding uplink timeslots or carriers (7.) is needed to improve uplink throughput. Interference Rejection Combining diversity algorithm is widely used in EDGE BSS and it has potentially some unused gain e.g. IRC could cope with higher amount of uplink interference.

9.1.2   Service outline

The EGPRS uplink bit rate evolution is needed to support e.g. imaging feature evolution in EGPRS mobile phones. Camera phones have couple of Mpixel resolution, high quality optics and integrated flash producing decent pictures for family use. In consequence camera phones are replacing point-and-shoot cameras - the biggest segment in the digital photography.

Although mobiles may have high capacity memory cards or even integrated hard disc drive, it would be likely irresistible not to send taken pictures or videos immediately to friends or family by email, post them to a web blog or a photo printing service with EGPRS phone in hand. As a bonus those camera phones would increase also downlink data traffic by peoples reading emails or visiting in blocks. So each camera phone owner would be a significant mobile content creator in terms of Mbytes and freshness of the created information.

Dual Symbol Rate EGPRS could approximately halve image upload times, or provide almost double bit rates or better uplink coverage for real time video sharing with DTM.

9.2 Concept description

The dual symbol rate and modified dual symbol rate double up link bit rates with minimal impact to mobile stations. The transmission bandwidth is widened and needs appropriate receiver in BTS. According to simulations both spectral efficiency and coverage can be enhanced significantly. With widened signal bandwidth it's possible to utilise properties of interference rejection combining diversity receiver for both DSR/MDSR reception and also to provide additional robustness against wideband interference to normal 8PSK and GMSK reception.

DSR or MDSR are likely not applicable in downlink until penetration of diversity MS's employing IRC is high enough to cope with widened bandwidth as base stations do in uplink.

A communication link equipped with multiple transmit and receive antennas (~MIMO, Multiple Input Multiple Output) can achieve higher link data rates. DSR can be seen as a "Multi User"-MIMO system, where multiple users, with single transmitter antenna for each, share the same uplink band width with simultaneous signals received by BTSs equipped with diversity antennas to achieve better spectral efficiency, as illustrated in figure 236.
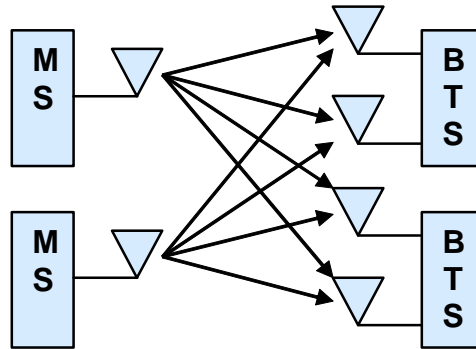
Figure 236:DSR is as a distributed MIMO scheme

9.2.1   Comparison with MIMO

A MIMO receiver needs at least as many Rx antennas as there are data streams occupying the same timeslot and channel. With DSR, spatial multiplexing is proposed without ensuring that this MIMO requirement is fulfilled. A BTS has typically 2 Rx antennas, but there may be more than two data streams in a given timeslot and channel. For instance see 101.

Moreover, the weighting coefficients of the two Rx antennas can only be set either for spatial filtering or for maximum ratio combining (MRC), but not for both at the same time. Hence, if the two Rx antennas are used for spatial filtering to separate a conventional GSM signal and a DSR signal which occupies the same channel, the two Rx antennas can no more be used to improve the SNR by MRC.

Since in MIMO the TX antennas are located on the same terminal, only the throughput of that single terminal suffers if spatial multiplexing fails (e.g. because of insufficient rank of the channel matrix), whereas with this proposal, since the two transmit antennas are on different terminals, a DSR user can jam the uplink of another MS's voice call (for more on voice impact see subclause 9.5.11.2).

9.2.2 Modulation

The Dual Symbol Rate could apply the existing 8PSK parameters excluding symbol rate and shaping filter. The Modified Dual Symbol Rate uses 16QAM modulation at 3/2 times higher symbol rate compared to GSM. QPSK is considered optionally for coverage extension. MDSR modulator could produce 100 kHz frequency offset to locate the MDSR carrier effectively in the middle of two GSM channels. The following table compares modulation parameters of 8PSK, DSR and MDSR. The signal bandwidths of DSR and MDSR are compared with three and two 8PSK carriers respectively in figures 237 and 238.

Table 95: Modulation parameter comparison

	8PSK	DSR	MDSR	
Symbol Rate	270 833 symbols/s (13 MHz / 48)	541 667 symbols/s (13 MHz / 24)	406 250 symbols/s (13 MHz / 32)	
Modulation	8PSK	8PSK	16QAM	QPSK(optional)
Rotation	3π/8	3π/8	-	π/4
Shaping pulse	Linearised Gaussian, BT=0.3	Hanning windowed Root raised cosine, roll-off= 0.29, length = 7 symbol periods	Hanning windowed Root Raised Cosine, roll-off = 0.29, length = 6 symbol periods	
Peak to Average Ratio (PAR)	3.2 dB	2.8 dB	5.1 dB	2.1 dB
Frequency shift	-	-	100 kHz	
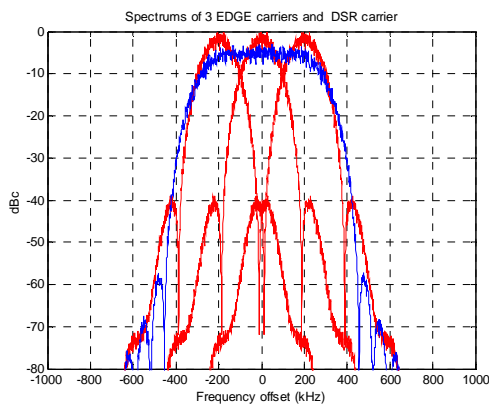
Figure 237: DSR spectrum
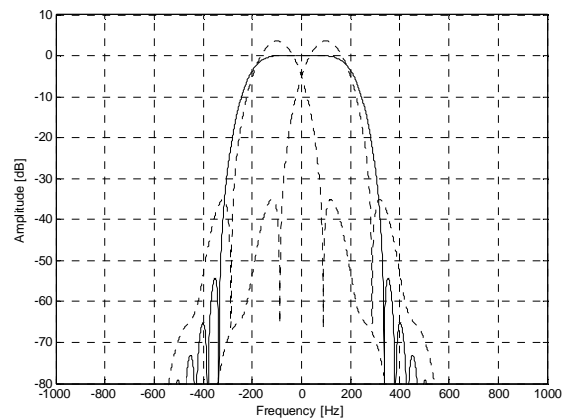
Figure 238: MDSR spectrum

Table 96 compares parameters of High Symbol Rate (HSR) schemes using 1.2 x symbol rate. It can be seen that the narrower shaping pulse would introduce 0.9 dB higher PAR and thus have an impact to coverage.

Table 96: Modulation parameters for 1.2 times higher symbol rate

Parameter	1.2 x 16QAM (240 kHz)	1.2 x 32QAM (240kHz)	1.2 x 16QAM (325 kHz)	1.2 x 32QAM (325 kHz)
Symbol Rate	325 000 symbols/s (13 MHz / 40)			
Modulation	16QAM	32QAM	16QAM	32QAM
Symbol rotation	-	-	-	-
Shaping pulse	Hanning windowed RRC, bandwidth = 0.74 roll-off = 0.3, length = 5 symbol periods		Hanning windowed RRC, bandwidth = 1.00 roll-off = 0.3, length = 5 symbol periods	
Peak to Average Ratio	6.0 dB	5.8 dB	5.1 dB	4.9 dB

9.2.3   Multiplexing

9.2.3.1   Burst format

In DSR burst one 8PSK modulated symbol corresponds to three Gray mapped bits as defined in 3GPP 45.004, subclause 3.2 Symbol mapping. In MDSR burst, one 16QAM modulated symbol corresponds to four Gray mapped bits, thus with 3/2 symbol rate MDSR burst carries double amount of bits (as in DSR) compared normal 8PSK. A particular bits within a timeslot are referenced by a Bit Number (BN), with the first bit being numbered 0, and the last (1/2) bit being numbered 937. The bits are mapped to symbols in ascending order according to 3GPP TS 45.004.The normal burst format has an equal structure in time with existing GMSK and 8PSK modulated normal bursts excluding

0.5 symbol periods longer tails for MDSR as shown in table 97. For optional QPSK the number of bits is the same as in EGPRS.

Table 97: Normal burst format for DSR and MDSR

DSR			MDSR			Contents
Bit number	Length in bits	Length in DSR symbols	Bit number	Length in bits	Length in MDSR symbols	
0 - 17	18	6	0 - 19	20	5	Tail bits
18 - 365	348	116	20 - 367	348	87	Payload bits
366 - 521	156	52	368 - 523	156	39	Training Sequence bits
522 - 869	348	116	525 - 871	348	87	Payload bits
870 - 887	18	6	872 - 891	20	5	Tail bits
888 - 936.5	49.5	16.5	892 - 936.5	45.5	11.375	Guard Period

The training sequence bits should be defined so that amplitude variations are minimized similar to 8PSK training sequences. Furthermore, the training sequence design should consider both autocorrelation and cross-correlations properties to achieve good channel estimation performance in high noise and interfering conditions. An example set of new sequences, based on exhaustive search, are proposed for DSR in table 98. The training sequence bits and tail bits for MDSR are FFS.

Table 98: DSR Training sequence bits

DSR TS number	DSR training sequence bits, (BN366 - BN521)
0	111 111 111 111 001 001 111 111 111 001 001 001 111 111 001 001 001 001 001 001 111 111 111 001 111 001 111 001 001 111 111 001 111 111 111 111 001 111 111 001 111 001 001 001 111 001 001 111 001 001 001 001
1	111 111 111 111 001 111 111 001 001 111 001 111 111 111 001 001 001 001 001 001 111 001 001 111 001 001 001 111 001 111 111 001 111 111 111 111 001 001 111 111 001 111 001 111 111 001 001 111 001 111 001 111
2	111 111 001 001 111 001 111 001 111 111 111 001 001 111 001 111 001 001 111 111 001 111 001 111 001 111 111 001 001 111 111 111 111 111 001 001 111 111 111 111 111 111 111 001 001 001 001 001 001 001 111 111
3	111 111 001 001 111 111 111 111 111 111 001 001 001 111 001 111 001 111 111 001 001 001 001 001 111 111 001 111 111 111 111 111 111 001 001 111 111 001 111 001 111 111 001 001 001 001 001 001 001 111 111 001
4	111 111 111 001 111 111 001 111 001 111 111 001 001 111 111 001 001 001 001 111 001 111 111 111 111 111 001 001 111 111 111 001 111 001 111 111 111 111 001 111 001 001 111 111 001 111 111 111 001 111 001 111
5	111 111 001 001 111 111 111 001 001 001 001 001 001 001 111 001 001 111 111 111 001 001 001 111 111 111 111 001 111 001 111 001 111 111 001 111 111 001 111 111 001 001 001 111 001 111 111 111 001 111 111 111
6	001 111 111 001 001 001 111 001 111 111 001 001 001 001 001 001 001 001 001 111 111 111 001 001 001 111 111 001 111 001 111 001 001 001 111 111 001 111 111 001 111 111 001 111 001 111 001 001 001 111 001 001
7	001 111 001 111 001 001 111 111 001 001 001 111 001 001 001 001 111 111 111 111 111 001 001 001 111 001 111 001 001 001 111 001 001 111 001 111 001 001 111 001 001 001 001 001 001 111 001 001 111 111 111 001

The tails (6 symbols each) are defined as modulating bits same as for 8PSK with the following states:

(BN0, BN1 .. BN17) = (1,1,1; 1,1,1; 1,1,1; 1,1,1; 1,1,1; 1,1,1)

(BN870, BN871 .. BN887) = (1,1,1; 1,1,1; 1,1,1; 1,1,1; 1,1,1; 1,1,1)

9.2.3.2 Blind symbol rate and modulation detection

A BSS needs to detect which symbol rate and modulation were used in the received burst. Detection may be enabled by orthogonal training sequences as in blind modulation detection between 8PSK and GMSK modulations as illustrated fin figure 239.
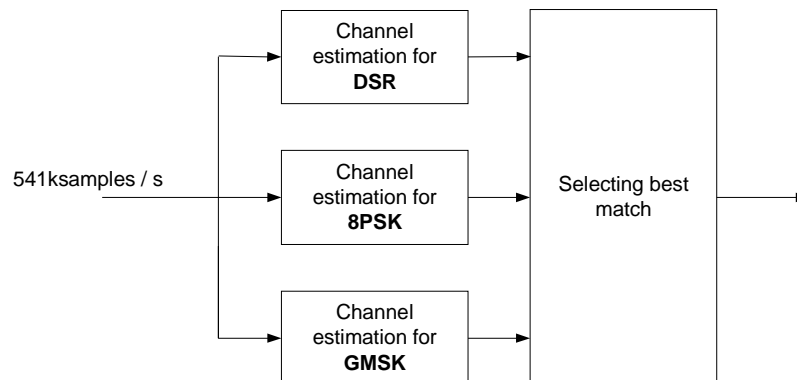
Figure 239: Illustration of blind symbol rate and modulation detection for received burst

Next, a simple procedure to perform channel estimation for each modulation and symbol rate option is presented shortly.

The received signal is presented by linear model $\mathbf{y}=\mathbf{Xh}+\mathbf{n}$. Narrowband channel filtering and rotation can be presented by multiplications of matrices $\mathbf{G}$ and $\mathbf{R}$, respectively. Thus LS estimator for each channel can be expressed in form of: $\mathbf{h} = \mathbf{Py}$, where $\mathbf{P} = (\mathbf{X}^H\mathbf{G}^H\mathbf{GX})^{-1}\mathbf{X}^H\mathbf{G}^H\mathbf{R}^H$ and is pre-calculated for each modulation and training sequence.

Thus further narrow band channel filtering, and also symbol rotation can be incorporated to the channel estimator. For MDSR the frequency offset could also be included.

Performance of blind detection is FFS.

In MDSR, the signal has a different symbol rate (1.5 times normal EDGE) and higher order modulation is also proposed. This has the following implications:

- The maximum output power is lower by 2 dB because of higher peak-to-average ratio (PAR).

- The energy per bit is lower by 1.8 dB because of shorter symbol period.

- The energy per bit is a further 1.2 dB lower because of higher number of bits per symbol.

The above implies that there is a total reduction of approximately 5 dB in terms of energy per bit and this has significant impact on the cell edge performance. Thus QPSK as an alternative modulation scheme is seen as mandatory for the concept to work with reasonable cell edge throughput. However, this would complicate the blind detection process for the MDSR and also traditional EGPRS MCS because of the choice between 4 different modulation formats: GMSK, 8-PSK, 16-QAM and QPSK, the latter two modulation formats being at 1.5 times the symbol rate and at 100 kHz offset from the center frequency of the former two modulation formats. One solution would be to define MCS selection rules in RLC retransmission, so that only one linear modulation in addition to GMSK is possible to send by MS assuming that the same set of MCS families are applied for each modulation. Thus number of modulations on blind detection is not increased compared to EGPRS. The performance of blind modulation detection especially at low C/I and low input level where EGPRS starts working (e.g. where MCS-1 has a BLER of 50 %) should be investigated to see the impact of such a new proposal on the uplink.

A BSS needs to detect which symbol rate and modulation was used in the received burst. It is possible, as is shown in table 99, to limit detection within two modulation alternatives as it is a case in EGPRS today. Thus number of modulations can be increased without increasing the complexity of blind modulation and symbol rate detection.

Table 99: Selection of modulation

Modulation of commanded MCS	Modulation for initial transmission	Modulation for re-transmission of GMSK modulated blocks	Modulation for re-transmission of 8PSK modulated blocks	Modulation for re-transmission of 1.2x16QAM modulated blocks	Modulation for re-transmission of 1.2x32QAM modulated blocks
GMSK	GMSK	GMSK	8PSK	8PSK	8PSK
GMSK with re-segmentation bit on	GMSK	GMSK	GMSK	GMSK	GMSK
8PSK	8PSK	GMSK	8PSK	8PSK	8PSK
1.2 x 16QAM	1.2 x 16QAM	GMSK	1.2 x 16QAM	1.2 x 16QAM	1.2 x 16QAM
1.2 x 32QAM	1.2 x 32QAM	GMSK	1.2 x 32QAM	1.2 x 32QAM	1.2 x 32QAM

9.2.3.3 Multi slot classes

Current 8PSK multi slot classes or DTM multi slot classes should apply for DSR and MDSR.

9.2.4 Channel coding

The channel coding of dual symbol rate should be carried out in a similar way as with existing 8PSK modulated coding schemes of EGPRS (MCS5-5 to 9), so that incremental redundancy (IR) can be supported between 8PSK and DSR or MDSR blocks.

Table 100 illustrates possible new modulation and coding schemes. The coding rate could be a bit lower than for relative 8PSK MCSs depending on the coding of header. The interleaving of RLC blocs could be optimised according to coding rate similarly as in EGPRS. Optional QPSK schemes are similar to existing EGPRS schemes except to the modulation and symbol rate.

Table 100: DSR and MDSR modulation and coding schemes

MCS DSR / MDSR / HSR	Family	Modulation DSR / MDSR	FEC	RLC Blocks [Bytes]	Interleaving [Bursts]	Bit rate [bit/s]
DCS-5 / MDCS-5 / HSR-5	B	8PSK / 16QAM	0.35 - 0.38	2 x 56	4	44 800
DCS-6 / MDCS-6 / HSR-6	A	8PSK / 16QAM	0.45 - 0.49	2 x 74	4	59 200
DCS-7 / MDCS-7 / HSR-7	B	8PSK / 16QAM	0.70 - 0.76	4 x 56	4	89 600
DCS-8 / MDCS-8 / HSR-8	A	8PSK / 16QAM	0.85 - 0.92	4 x 68	1 or 2	108 800
DCS-9 / MDCS-9 / HSR-9	A	8PSK / 16QAM	0.92 - 1.00	4 x 74	1	118 400

9.2.5 RLC/MAC

The RLC/MAC header need to carry information of 4 RLC blocks thus new header type is needed, but the EGPRS uplink RLC/MAC header type-1 could be re-used for 2 lowest DSR MCSs, without adding new bytes. Three highest DSR MCSs carrying 4 blocks would need the following additions to the EGPRS uplink RLC/MAC header type-1:

- 2 octets to indicate block sequence numbers (BSN3, BSN4).

- 5 bits to enhance Coding and Puncturing Scheme indicator field (CPS).

Detection of the new header type is FFS.

In downlink, *EGPRS MCS IE* needs to be enhanced by 1 bit to carry also DSR MCSes.

The DSR do not need changes to the existing RLC/MAC procedures and for example current uplink allocation methods e.g. dynamic allocation through USF and RRBP mechanisms should apply for DSR.

Current maximum RLC Window size for EGPRS (1024) should apply for DSR as well as for dual carrier (subclause 7.5.2.4).

The EGPRS link adaptation may be enhanced for DSR by adding new rules to for MCS selection for retransmission with and without re-segmentation enabling incremental redundancy and ensuring optimal performance.

The same RLC/MAC changes required for DSR applies also for MDSR, but impact of optional QPSK is FFS.

9.2.6   RRC

Introduction of new Radio Access Capability is needed.

9.2.7   Radio transmission and reception

It could be assumed that Dual Symbol Rate has quite similar properties as 8PSK and the same approach as used for specifying properties 8PSK could be applied, but some considerations are needed due to wider spectrum.

It is assumed that BTS uses IRC diversity allowing interferes to overlap from adjacent carriers. BTS performance for DSR should likely be specified with diversity, since that is typical BTS configuration. For performance evaluation and requirements the network interference scenario needs to be defined e.g. similar to DARP, but considering wider and thus overlapping bandwidth of DSR, IRC capability, uplink interference statistical distribution rather than just average and mixed voice and data traffic model.

9.2.7.1   Transmitter output power and power classes

No changes expected for DSR and existing E-power classes could be applied due to similar linearity requirements with 8PSK.

9.2.7.2   Modulation accuracy

Current EVM figures should likely apply for DSR with a note of different symbol rate and shaping filter. EVM for MDSR is FFS.

9.2.7.3   Power vs. time

No major changes are expected for DSR, since PAR is similar with current 8PSK and burst structure is specified according to the current 8PSK modulated normal burst. Due to the shaping filtering the lower limit during random data symbols may need to be removed due to possible zero crossings. PVT for MDSR is FFS.

9.2.7.4   Spectrum due to modulation

Spectrum due to modulation mask needs to be changed to apply for dual symbol rate. As an initial starting point the current spectrum mask for 8PSK could shifted by 200 kHz for DSR and 100 kHz for MDSR and relative amplitude normalized to correspond the same absolute power with 8PSK.

9.2.7.5   Spectrum due to transients

Spectrum due to transients needs to reflect changes in spectrum due to modulation.

9.2.7.6   Receiver blocking characteristics

Channel filtering of BTS transceiver is assumed to meet existing blocking characteristics for GMSK despite being wide enough to pass through DSR or MDSR signal.

9.2.7.7 AM suppression characteristics

No changes expected.

9.2.7.8 Inter-modulation characteristics

No changes expected.

9.2.7.9 Nominal Error Rates (NER)

Similar limits as for 8PSK could be applied.

9.2.7.10 Reference sensitivity level

Adding diversity cases need to be considered.

9.2.7.11 Reference interference level

Adding diversity cases need to be considered.

9.3 Modelling assumptions and requirements

9.3.1 MS transmitter modelling

Ideal transmitter was used in coverage and interference scenarios, but power amplifier model based on the GaAs HBT technology was used in spectrum due to modulation and adjacent channel power evaluations.

9.3.2 BTS receiver modelling

Uplink Interference Rejection Combining diversity (IRC) was used in simulations and some reference simulations were also performed with Maximum Ratio Combining (MRC) or without diversity. The effective noise figure was 5 dB, antenna branches were uncorrelated and no other impairments were included to receiver simulations, if not otherwise stated.

9.3.3 Simulation approach for interference modelling

As seen in figure 237 DSR spectrum overlaps over three normal 200 kHz carriers resulting in about 3 to 5 times more stringent interference situation for the BTS receiver. Thus conventional single interferer models (like CCI, ACI) or even the multi-interferer method used in SAIC cannot be used for DSR performance evaluations.

The interference modelling used burst-wise data recorded from dynamic system simulator in link simulator to simulate multiple interferers. This approach combines benefits of both simulation environments, providing accurate evaluation of IRC algorithm to cope with multiple interferers having variable bandwidth and modulation. The number of simultaneous interferers varied dynamically burst by burst up to more than 20 as depicted in a spectral snapshot in figure 101.

Network level results e.g. spectral efficiency was obtained by combining link results with wanted signal level statistics.

Burst-wise interference data from dynamic system simulator included MS Id, signal level and modulation information for co-channel, 1st and 2nd adjacent channel interferers, that enable to produce system level interference environment in link simulator using similar structure as in 6.3. The signal level information was averaged in system simulator so that fast fading was simulated only once in link simulator for both wanted and all interfering signals. DSR simulations were performed by changing 8PSK modulated bursts to be DSR-8PSK modulated.

Link adaptation was not dynamic, but MCS giving the best average throughput was selected for each signal level in link simulator. It is assumed to have better results with dynamic link adaptation.

The impact of dual symbol rate signal to TCH/AFS5.9 was simulated in link simulator.
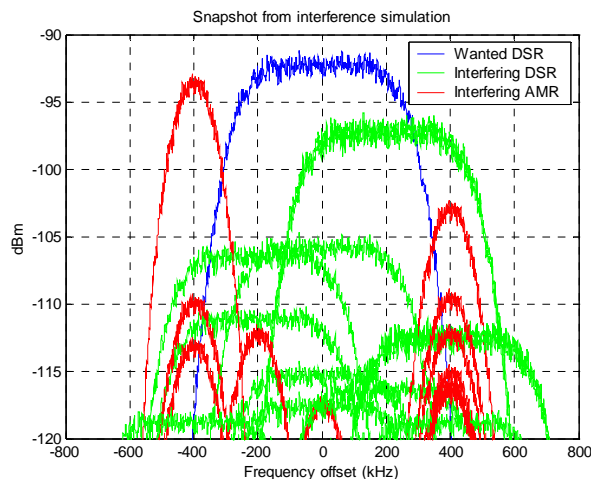
Figure 240: Spectral snapshot from simulated UL interferences at cell border for DSR

9.4 System level model

9.4.1 Network model and system scenarios

4 different system scenarios were used to collect burst-wise interference data and wanted signal statistics. Network configurations and simulation parameters are listed in the tables 101 and 102. Frequency re-use 4/12 was studied for BCCH, and reuses 1/1 (1/3 load), 1/3 and 3/9 for hopping layer. It should be noted that frequency re-use is determined for normal 200 kHz carrier and with overlapping DSR carrier it is effectively 2 times higher e.g. at re-use 1/1 case the effective re-use for DSR is about 2/1. Network load was about 75 % in all cases. In BCCH case it was assumed that all traffic is EGPRS data, whereas in TCH cases there were 4 TCH TRXs in each cell serving 19.2 voice Erlangs and about 210 kb/s for EGPRS traffic in average, yielding to 17 % to 25 % share of slots for data. Voice load alone introduced 20 % effective frequency load (EFL) for frequency re-uses 1/1 and 1/3.

Amount of recorded bursts was large enough to achieve statistically reliable results for evaluating relative DSR gain over EDGE, because exactly the same interference statistics was used within each data scenario. On the other hand accuracy is likely not sufficient with used files to make accurate absolute performance evaluations with other than 1/1 or 1/3 re-uses.

Site-to-site distance was 3 000 meters in interference scenarios and 12 000 meters in the coverage scenario. The propagation environment was typical urban at 3 km/h. DTX and power control algorithms were enabled for voice and EGPRS.

FTP traffic model with 120 kB file size was used for EGPRS and the same amount of traffic was assumed in UL and DL, causing sufficient uplink load. This FTP model corresponds to about 200 kB to 230 kB file size with DSR.

Table 101: Network model parameters

Parameter	Value
Site-to-Site distance	3 000m at interference scenarios 12 000m at coverage scenario
Frequency	900MHz
Sectors per site	3
Antenna pattern	65 degrees
Log. Normal Fading standard deviation	6dB
Correlation Distance	50m
Path loss exponent	3.67
Propagation model	Typical Urban, 3 km/h
Number of cells	75

Table 102: System Scenarios

Parameter	Scenario 1	Scenario 2	Scenario 3	Scenario 4
Reuse	4/12 (BCCH only)	1/3 (TCH only)	3/9 (TCH only)	1/1 (TCH only)
Bandwidth	2.4MHz	2.4MHz	7.2MHz	2.4 MHz
TRXs per cell	1	4	4	4 (1/3 load)
Hopping	No	Random RF	Random RF	Random RF
Synchronised BSS	Yes	Yes	Yes	Yes
Voice Load	0	19.2 Erl (AMR 5.9)	19.2 Erl (AMR 12.2)	19.2 Erl (AMR 5.9)
Voice Activity	60% (DTX on)	60% (DTX on)	60% (DTX on)	60% (DTX on)
Voice Power Control	Yes	Yes	Yes	Yes
EGPRS DL Load (served)	252 kbits/s (6.5 slots)	218 kbit/s (7.1 slots)	236kbit/s (6.6 slots)	217 kbit/s (8.1 slots)
EGPRS UL Load (served)	244 kbit/s (5.2 slots)	205 kbit/s (5.0 slots)	211 kbit/s (4.1 slots)	203 kbit/s (5.6 slots)
EGPRS UL Power Control	Yes	Yes	No	Yes
EGPRS Traffic Model	FTP (120 kB)	FTP (120 kB)	FTP (120 kB)	FTP (120 kB)
Number of recorded bursts	40 000 (200s)	30 000 (150s)	30 000 (150s)	30 000 (150s)

9.4.2 Network interference statistics

In figures 241, 242, 243 and 103 cumulative co- and adjacent channel interference distributions are shown for scenario 1 and scenario 2. Carrier level shows Rx levels measured from EGPRS connections. The percentage value after the interference number displays a probability of an interferer. The complete list of the interferer probabilities are shown in table 104. Note that probabilities for the 1st adjacent apply also for the 2nd adjacent interferer.
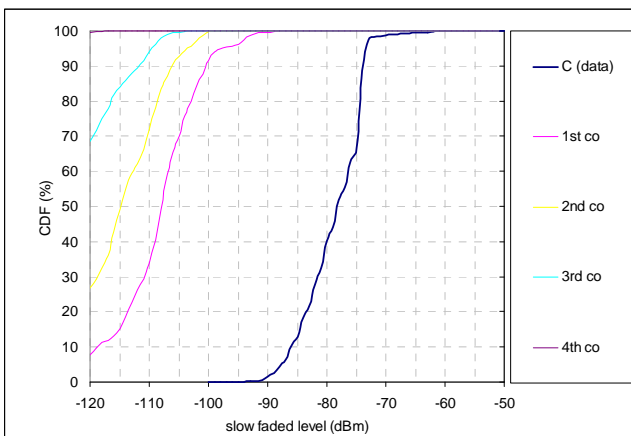
Figure 241: 4/12 co-channel I level cdf
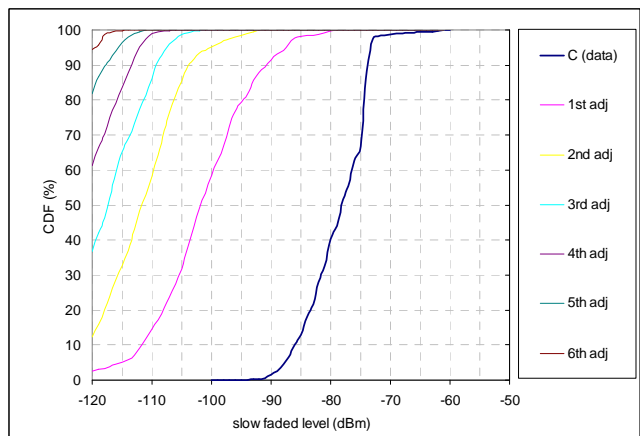
Figure 242: 4/12 adjacent channel I level cdf
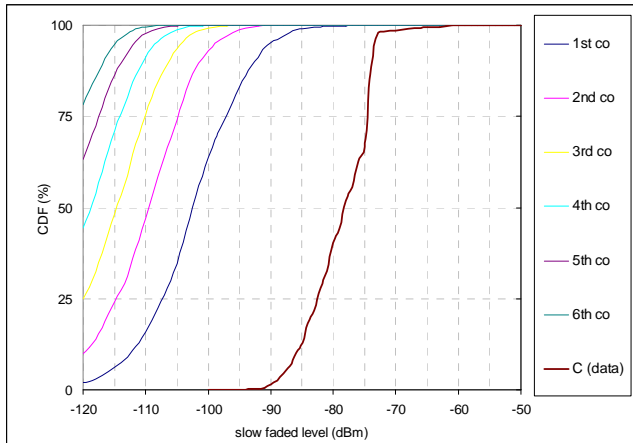
Figure 243: 1/3 co-channel I levels
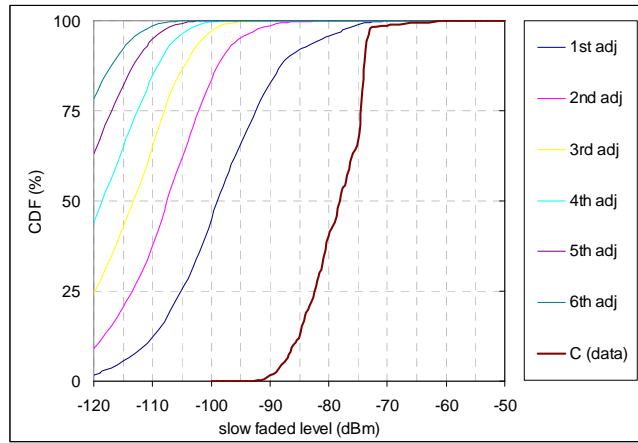
Figure 244: 1/3 adjacent channel I levels

Table 103: Signal Level statistics

	Scenario 1 (4/12)	Scenario 2 (1/3)	Scenario 3 (3/9)	Scenario 4 (1/1)	Coverage
95 % value	-87.7 dBm	-87.7 dBm	-87.5 dBm	-87.7 dBm	-108 dBm
50 % (median)	-78.2 dBm	-78.2 dBm	-77.3 dBm	-78.2 dBm	-98 dBm

Table 104: Probabilities for interferers to exceed -120 dBm

Ordinal number of interferer	Scenario 1 (4/12)		Scenario 2 (1/3)		Scenario 3 (3/9)		Scenario 4 (1/1)	
	Co-channel	Adjacent AC1, AC2	Co-channel	Adjacent AC1, AC2	Co-channel	Adjacent AC1, AC2	Co-channel	Adjacent AC1, AC2
Dominant	92 %	97 %	98 %	98 %	63 %	80 %	99 %	95 %
2nd	73 %	88 %	90 %	91 %	22 %	49 %	93 %	92 %
3rd	32 %	64 %	76 %	76 %	4.0 %	22 %	80 %	83 %
4th	0.6 %	39 %	56 %	56 %	0.5 %	8.6 %	61 %	68 %
5th		19 %	37 %	37 %	0.1 %	0.9 %	43 %	51 %
6th		5.6 %	22 %	22 %		0.3 %	28 %	35 %
7th			11 %	12 %		0.1 %	16 %	22 %
8th			4.9 %	5.3 %			8.0 %	13 %
9th			1.6 %	1.9 %			3.5 %	6.4 %
10th			0.4 %	0.6 %			1.2 %	2.8 %
11th			0.1 %	0.1 %			0.4 %	1.0 %
12th							0.1 %	0.3 %

9.5 Performance characterization

9.5.1 Spectrum due to modulation

Figure 246 shows simulated example of spectrum due to modulation with GaAs HBT PA model biased near to class-B resulting 35 % power added efficiency (PAE) for DSR. For comparison the spectrum due to modulation for 8PSK would kiss the existing limit line at 400 kHz offset with the same PA as depicted in figure 245.

The existing 8PSK spectrum mask was shifted by 200 kHz for DSR and is plotted as a reference to demonstrate the impact of DSR. The carrier power of DSR is corrected by 3dB to match with the same absolute power with 8PSK measured through the 30kHz filter.

This spectrum due to modulation is further analysed in subclause 9.5.2.
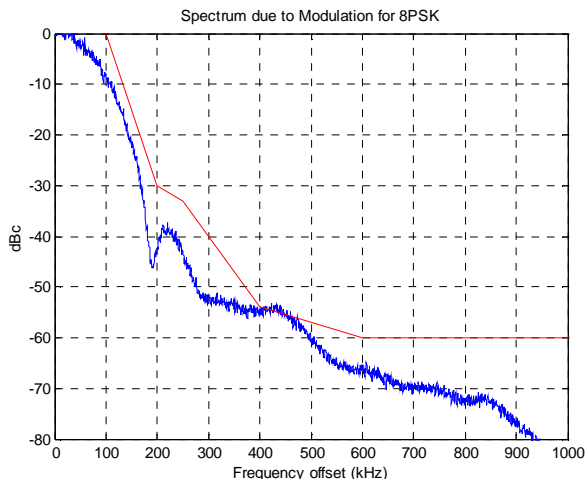
Figure 245: Simulated spectrum due to modulation for 8PSK
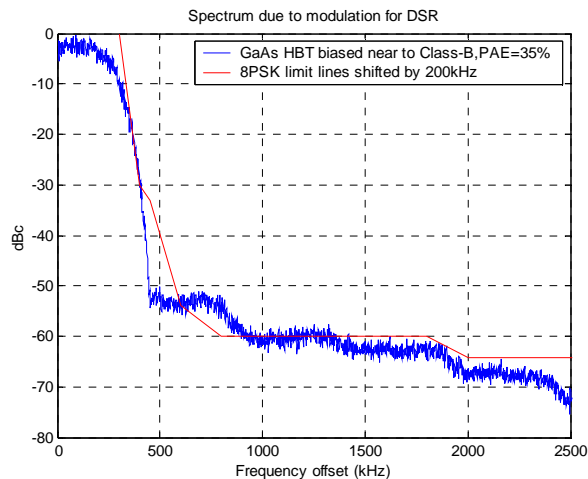
Figure 246: Simulated spectrum due to modulation for dual symbol rate

Figure 247 shows simulated example of spectrum due to modulation for MDSR 16PSK with the same PA model as used for DSR, but 2 dB higher output back-off. The existing 8PSK spectrum mask was shifted by 100 kHz and is plotted as a reference.
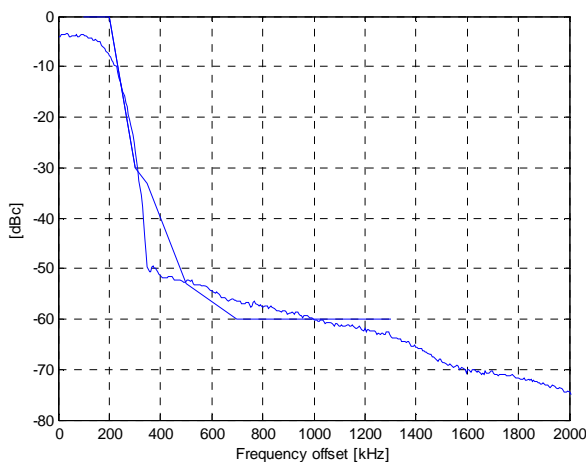
Figure 247: Simulated spectrum due to modulation for MDSR (16QAM)

9.5.2   Adjacent channel power

The adjacent channel power due to DSR transmission was evaluated by using GaAs HBT PA model biased near to class-B yielding to 35 % power added efficiency. Simulated spectrum is shown in figure 246.

9.5.2.1   Adjacent channel power to GSM/EDGE uplink

Adjacent Channel Power (ACP) for different offsets was estimated through 180 kHz rectangular filter compared to the total transmitted signal power. The adjacent channel power limits were derived from the reference interference level limits for 3 lowest offsets and from spectrum due to modulation mask for higher offsets. Indeed existing limits are shifted by 200 kHz.

Results are in table 248. Adjacent channel power due to DSR seems to comply with existing ACP limits excluding 800 kHz offset, where limit was exceeded by 2 dB and could likely be improved e.g. by compromising in power added efficiency. The system impact of this 2 dB exception at level of -56 dB would be likely negligible.

Table 105: Adjacent channel powers to GSM/EDGE uplink for DSR

	Offset										
	400 kHz	**600 kHz**	**800 kHz**	**1 000 kHz**	**1 200 kHz**	**1 400 kHz**	**2 000 kHz**	**1 800 kHz**	**2 000 kHz**	**2 200 kHz**	**2 400 kHz**
Simulated ACP @180 kHz BW	20 dB	55 dB	56 dB	62 dB	61 dB	63 dB	68 dB	64 dB	68 dB	69 dB	71 dB
Existing ACP limit @ 180 KHz shifted by 200kHz	18 dB	50 dB	58 dB	60 dB	60 dB	60 dB	63 dB	60 dB	63 dB	63 dB	63 dB
Margin	2 dB	5 dB	-2 dB	2 dB	1 dB	3dB	5 dB	4 dB	5 dB	6 dB	8 dB

The used guard band used between operators depends on regulatory requirements and possible agreements and typically does not exist or is single 200 kHz channel. Thus existing ACP between operators varies and is typically 18 dB or 50 dB. Similar ACP values for DSR can be obtained by 200 kHz or 400 kHz guard band.

To ensure 50 dB ACP, it is possible to use DSR at BCCH layer allocated in the middle of operator's frequency band, so that use of edge channels can be avoided. Or it is also possible to use restricted MA list for DSR/EGPRS avoiding edge channels of operator's frequency allocation, which still can be used for voice. Thus DSR can be used with existing guard band and without segregation in EGPRS, but may need some support from BSS resource allocation.

9.5.2.2   Adjacent channel power to WCDMA uplink

Adjacent channel power (ACP) was estimated through 3840 kHz rectangular filter compared to the total transmitted signal power. The impact to adjacent WCDMA uplink was estimated by determining ACP at 2.7 MHz offset and comparing it to allowed ACP of WCDMA transmitter at 5MHz offset.

As a result modelled PA has 19 dB margin on ACP introduced to adjacent WCDMA. So, dual symbol rate can be applied with current 200 kHz guard band adjacent to WCDMA.

Table 106: Adjacent channel power to WCDMA uplink at 2 700 kHz offset for DSR

Simulated ACP due to DSR	54 dB
Allowed ACP for WCDMA at 5 MHz offset (24 dBm)	33 dB
Margin (26 dBm for DSR)	19 dB

9.5.2.3   Spectrum mask and spurious emissions

At first glance, the spectrum of MDSR looks as wide as the spectrum of two adjacent GMSK modulated carriers. However, the adjacent channel performance is worse.

9.5.2.3.1   Adjacent channel protection

Today, the attenuation of the first adjacent channel interferer (±200 kHz) through reference, 180 kHz wide RX filter amounts to 18 dB. However, for MDSR, the attenuation in -200 kHz/+400 kHz offset would be only 16 dB as shown in table 117. 2 dB lower adjacent channel protection correspond to almost 60 % more power leaking into the adjacent channels.

9.5.2.3.2   Spectrum after PA and spectrum mask

The simulated spectrum after a PA model and the comparison with a spectrum mask, shifted by 100 kHz as shown in figure 247, shows that the mask is violated at 300 kHz and continuously between 500 kHz and 1 000 kHz carrier offset despite a 2 dB higher output power back-off than for 8-PSK. It can be concluded that:

- either the additional back-off of 2 dB is still too low; or

- a more linear and hence less efficient PA would be needed; or

- the constellation diagram needs to be optimized with respect to the peak-to-average and peak-to-minimum ratio; or

- more spectrum relaxation than just a horizontal shift of the mask will be needed, leading to more adjacent channel interference.

Furthermore, the wide band noise emissions of an MDSR Tx chain need to be investigated too, in particular the noise in the downlink band.

9.5.3 Coverage

The DSR and MDSR coverage was modelled with the following assumptions, resulting to level of -108 dBm at cell border (95 %).

Noise floor of BTS with NF=5dB - see note)	-115 dBm
Required E_b/N_o for EFR (FER < 1 %) with diversity	2 dB
Body loss difference between talk and data positions	3 dB
Power decrease for 8PSK related to GMSK	4 dB in UL 2 dB in DL
Power decrease for 16PSK related to GMSK	6 dB at highest power 4 dB at lower levels
Power decrease for QPSK related to GMSK	2 dB
Fading etc. margins	6 dB
NOTE: Noise figure of BTS is typically couple of dB lower yielding to -110 dBm at cell border, but NF=5dB is commonly used as a reference. So 2 dB implementation margin is effectively included to assumptions.	

Throughput versus received signal level is depicted in figure 79 for 8PSK with and without IRC and for DSR with and without incremental redundancy at TU3iFH conditions and in figure 249 for GMSK, EGPRS, DSR, MDSR including QPSK at TU3iFH conditions. 5 dB noise figure was assumed for BTS receiver, but no other impairments.

Table 107 shows throughputs and throughput gains with maximum multi slot power reduction for 1 to 4 uplink slots by using -98 dBm as a median level and -109 dBm at cell edge for single slot. The DSR could have one MCS more below DCS-5, which may improve the throughput gain at cell border. 16QAM used additional 2dB power reduction for single slot case only.

MDSR seems to provide about 1.7 to 1.9 times higher average throughput than EGPRS. At cell edge 16-QAM can not provide coverage gain, but with QPSK the throughput with single slot is 1.9 times higher than with EGPRS, although average gain of QPSK is not significant.

As a conclusion DSR provides 1.9 times higher throughput in coverage limited case and provides also higher throughput than could be obtained by doubling number of uplink timeslots with 8PSK, if maximum power reduction is assumed.

The used RRC modulation shaping filter has a bit relaxed bandwidth compared to the existing linearised GMSK filter resulting to almost 2 dB gain. Thus expectation to see about 3 dB loss due to halved energy per symbol in DSR is not a valid assumption for DSR.

The gain due to incremental redundancy is highest at the lowest signal levels. At cell border (95 %) the throughput gain due to IR was 49 %. In real life the IR gain would be even higher e.g. with non-ideal link adaptation and real FH.
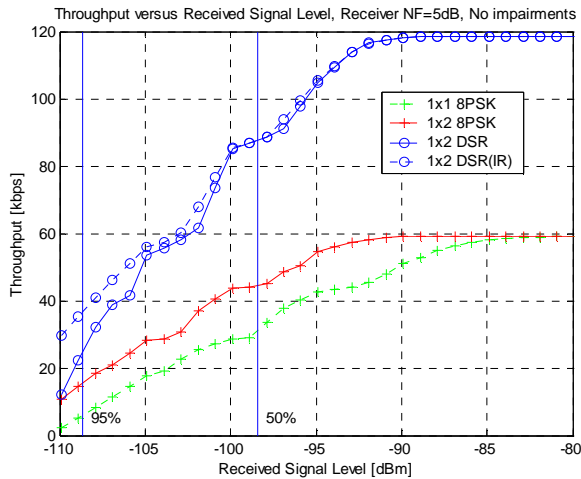
Figure 248: Throughput at coverage scenario TU3iFH
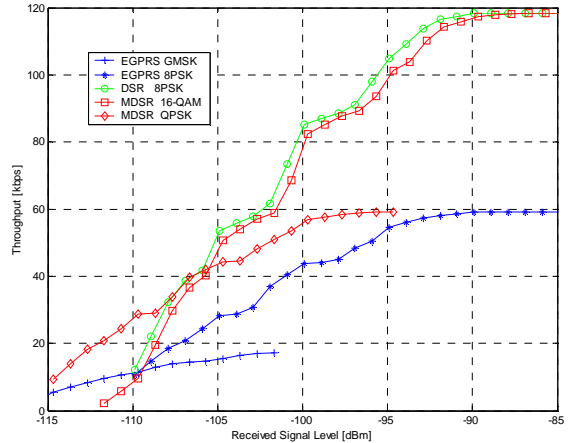
Figure 249 Throughput versus received signal level, TU3iFH, NF=5dB

Table 107: Throughputs with maximum multi slot power reduction at TU3iFH

Number of time slots	Cell border	Average			
	1 slot	1 slot	2 slots	3 slots	4 slots
Multi slot power reduction	0 dB	0 dB	3 dB	4.8 dB	6 dB
Power reduction for 16QAM	2 dB	2 dB	0 dB	0 dB	0 dB
EGPRS	15 kbps	44 kbps	74 kbps	95 kbps	117 kbps
DSR	22 kbps	84 kbps	139 kbps	178 kbps	216 kbps
MDSR (without QPSK)	5 kbps	70 kbps	131 kbps	168 kbps	200 kbps
MDSR (with QPSK)	29 kbps	73 kbps	135 kbps	178 kbps	215 kbps
DSR gain	1.5 x	1.9 x	1.9 x	1.9 x	1.9 x
MDSR gain (without / with QPSK)	- / 1.9 x	1.6 / 1.7 x	1.8 / 1.8 x	1.8 / 1.9 x	1.7 / 1.9 x

The throughput at cell border is 22 kbit/s for DSR and 14.6 kbit/s for 8PSK yielding to 51 % gain at the border of cell.

9.5.4   Performance at Hilly Terrain

The receiver performance was evaluated also at Hilly Terrain to ensure receiver's capability to cope with delay spreads at least up to 20 µs. As a result the DSR provides about 2 times higher average throughput than 8PSK at HT3 iFH conditions.
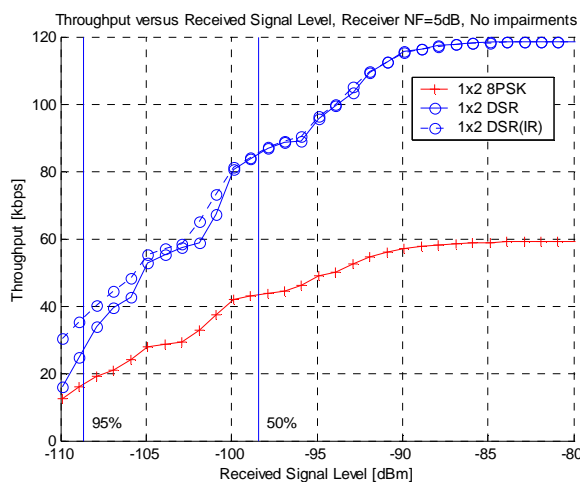
Figure 250: Throughput at Hilly Terrain 3km/h

The throughput at cell border is 25kbit/s for DSR and 15.8 kbit/s for 8PSK yielding to 57 % gain at the border of cell.

9.5.5 Performance at interference scenarios

Throughputs versus carrier level are shown in figures 251, 252, 253 and 254. Vertical lines mark 95 % and 50 % signal levels. Figure 109 summarises average throughputs at different system scenarios.
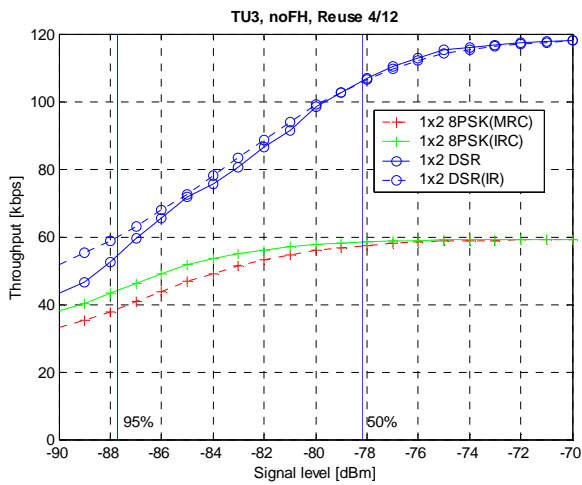
Figure 251: Throughput at scenario 1 (4/12)
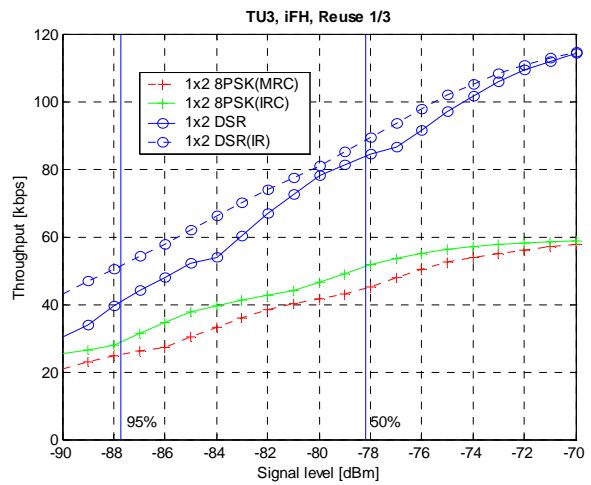
Figure 252: Throughput at Scenario 2 (1/3)
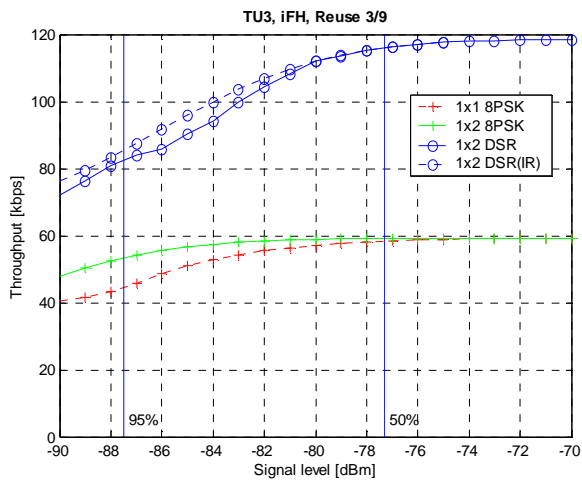
Figure 253: Throughput at Scenario 3 (3/9)
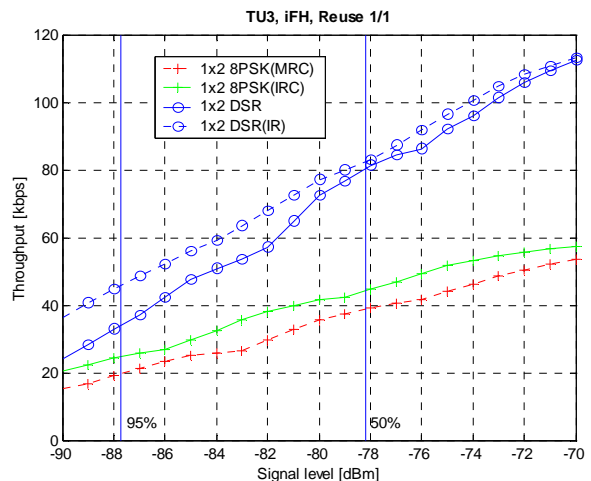
Figure 254: Throughput at Scenario 4 (1/1)
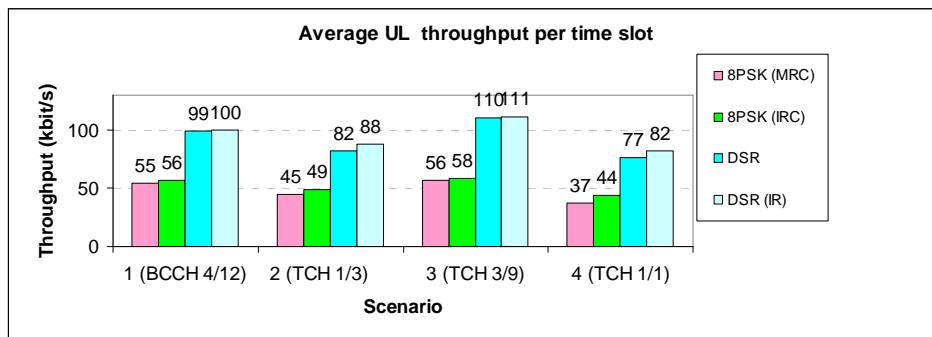
Figure 255: Average throughputs per time slot

Table 108: Summary for interference scenarios

	Scenario 1 (4/12)	Scenario 2 (1/3)	Scenario 3 (3/9)	Scenario 4 (1/1)
8PSK throughput per slot	56 kbps	49 kbps	58 kbps	44 kbps
DSR throughput per slot	99 kbps	82 kbps	110 kbps	77 kbps
Throughput gain	1.8 x	1.7 x	1.9 x	1.7 x

As conclusion DSR could provide 1.7 to 1.9 times higher average throughput in interference limited scenarios. At cell border the throughput gain was 54 % at reuse 3/9. The IR performance would likely be improved, if dynamic link adaptation were applied in simulations.

9.5.6 Spectral efficiency

The spectral efficiency of DSR was estimated only for BCCH re-use 4/12 (Scenario 1) providing 522 kbit/s average throughput per cell. Thus applying Dual Symbol Rate at BCCH layer may be attractive option.

Table 109: Spectral efficiency for Scenario 1 (BCCH 4/12)

Modulation	Spectral Efficiency
8PSK	124 kbits/s/MHz/Cell
DSR	219 kbits/s/MHz/Cell

By combining scenarios 1 and 2 it is possible to calculate cell level uplink throughput at 5 MHz bandwidth, which is 916 kbit/s + 19.2 Erl voice.

Spectral efficiency analysis in mixed data and voice scenarios is FFS.

9.5.7 Impact to voice users with 1/1 re-use

Simulation results presented later in this paragraph are with random resource allocation e.g. without any DSR specific RRM optimisation. Simulations show that DSR has similar impact to voice quality as EDGE at lower data load and smaller impact than EDGE with higher data load.

Simulations are performed at the worst case scenario, at re-use 1/1, which has also the best statistical accuracy. Re-use 3/9 has perfect voice performance even at cell border, thus this interference model is not suited for determining impacts at 3/9 with sufficient confidence level. The same would apply also for BCCH scenario.

Additionally possible DSR impact to voice users may be controlled by radio resource management, e.g.:

- Allocating DSR in BCCH carrier as EGPRS is possibly already and voice users in TCH carriers eliminates possible impact to voice users and provides 1.8 times higher spectral efficiency of BCCH UL as shown in scenario 1 in subclause 9.5.5. Possible voice users allocated to BCCH may not likely be impacted due to sparse frequency re-use e.g. 12.

- In synchronised BSS it is possible to allocate DSR synchronously to the same TCH radio slots to minimise possible impact. (FFS).

- In unsynchronised BSS it is possible to use different frequency reuse pattern or MA list or channel group for DSR to minimise possible impact.

- DSR power control e.g. lowering DSR power by 2 dB may ensure no impacts to voice quality or signalling performance.

The impact of DSR signal for voice users was studied by comparing FER of TCH/AFS5.9 with 8PSK and DSR interferes at interference scenario 4 (1/1 re-use). UL FER was also compared with DL SAIC FER to ensure that the assumption to have room for DSR interference is valid. Comparison has been made at 95 % signal level for both UL and DL as shown in figure 110. Note that the load was 430 kbit/s in uplink with DSR, 220 kbit/s in downlink and voice load 19.2 Erl.

The following findings can be listed at cell border:

- With similar UL cell throughput as in DL, DSR has similar impact to voice than EDGE.

- With 1.7 higher UL cell throughput DSR has 0.7 dB smaller impact to voice than EDGE.
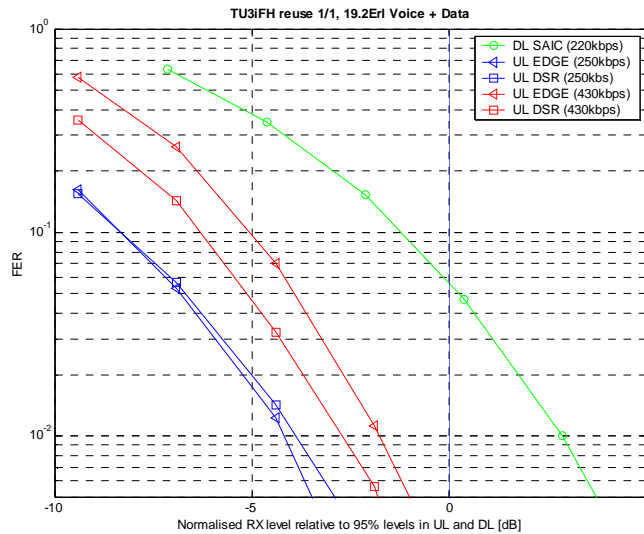
Figure 256: TCH/AFS5.9 FER at re-use 1/1

Table 110: Voice impact in UL due of DSR versus EDGE at 1% AFS5.9 FER

Cell Load	EDGE	DSR	DSR Gain
250 kbit/s	-3.9 dB	-3.5 dB	-0.4 dB
430 kbit/s	-1.6 dB	-2.3 dB	+0.7 dB

9.5.8 Impact to voice users C/I distribution with 1/3 re-use

The wider frequency spectrum of DSR will spread interference over a larger frequency range an increased interference on neighbouring channels. This is shown in figure 246 and table 111. The interference in the adjacent channel is just about 1 dB less than in the centre channel.

Table 111: Power distribution over 3 channels (1st lower adjacent channel, co-channel and 1st upper adjacent channel) measured with 180 kHz rectangular filter

Frequency offset [kHz]	-290 to -110	-90 to 90	110 to 290
Energy distribution DSR [dB]	-5.05	-3.91	-5.05

While this will not increase the total amount of emitted interference in the system (assuming that a DSR terminal uses the same transmit power as an EGPRS terminal), the interference will be distributed differently for DSR than for EGPRS. Since network frequency planning is optimised for regular 200 kHz GSM/EDGE carriers, the received interference levels may despite this be different in the two cases.

9.5.8.1 Simulation results for uplink

In order to investigate this effect, system simulations have been run. A mixed traffic scenario with 80 % speech traffic and 20 % data traffic was considered. The simulation parameters are summarised in table 112.

Table 112: Summary of system simulation parameters

Parameter	Value
Reuse	1/3
Traffic mix	80% speech, 20% data data is EGPRS data is DSR
Power control	Yes (for speech)
DTX	Yes (for speech)
Frequency load	10% and 20%
Receive diversity	IRC

The impact on uplink carrier-to-interference ratio (C/I) is shown in figure 257. The C/I for the speech users is 1 dB to 2 dB lower in the DSR case with 1.7x higher throughput than in the EGPRS case.
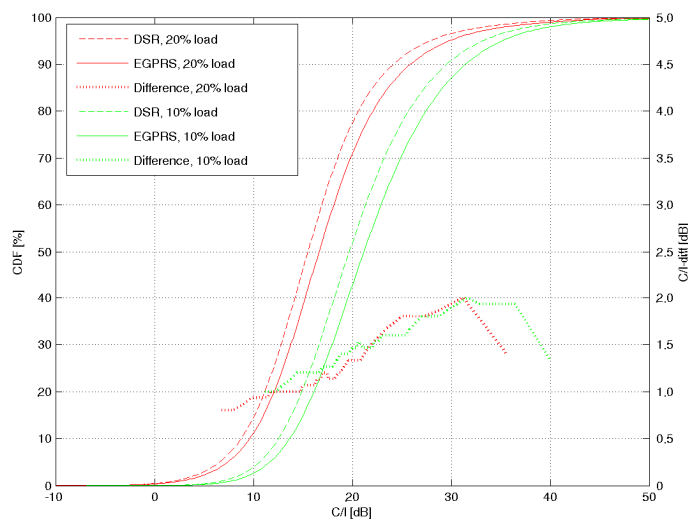
Figure 257: Uplink C/I distributions (left y-axis)
Also, the C/I difference is shown for the two cases (right y-axis)

The difference is caused by a blurred reuse in the DSR case. In an ordinary 1/3-reuse (as well as in a 1-reuse with MAIO planning), only adjacent channel interferers appear in the closest surrounding cells. If these are EDGE interferers, most of their energy will be in the adjacent channel and the receiver filter in the BTS will suppress it. In the DSR case however, the adjacent channel interferer will have a large part of its energy in the desired band (of the speech user) and the receiver filter in the BTS will not suppress it.

9.5.9 Uplink/downlink balance

It is earlier assumed that a degradation of uplink speech performance is not a problem, since the downlink performance is anyway limiting the overall performance. While this may be true in some scenarios, it is not always the case.

For instance, shadowing from buildings and other obstacles will impact the uplink-downlink balance. The effect of shadow fading is that the received signal strength will vary with the position of the receiver, the transmitters of the desired signal and interferers, and obstacles such as buildings. While the desired signal will be impacted equally in uplink and downlink by shadow fading, the interferers will not, since they do not originate from the same source (uplink interference from terminals, downlink interference from base stations).

One particular, but very relevant, example of this is indoor coverage, as illustrated in figure 259. The speech user is located in a building and connected to a macro-cell outside the building. Other interfering users are located elsewhere, outside the building. The building will attenuate the desired signal (uplink and downlink) by, say, 10 dB. The downlink interference coming from other base stations outside the building will be attenuated by the same amount. Therefore, the downlink C/I will not be impacted by the building. The uplink interference, on the other hand, coming from terminals outside the building, will not be attenuated. Therefore, the uplink C/I will be reduced by 10 dB. The consequence is that the indoor speech performance may be limited by the uplink, not the downlink.
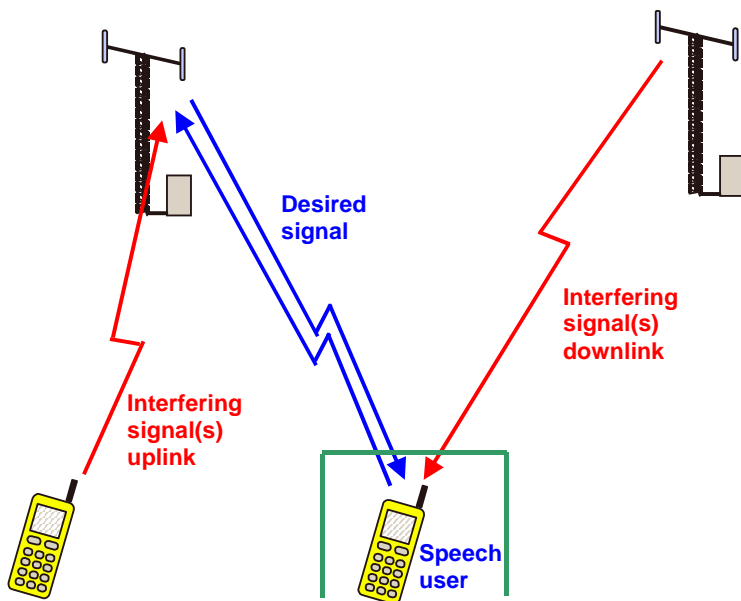
Figure 258: Indoor/outdoor interference scenario

To conclude, the increased interference levels due to DSR interference may degrade speech performance in some scenarios and areas, in particular indoors. On the other hand IRC can effectively reject the most dominant interferer, thus impact may be negligible in typical scenarios where most of users are in indoor locations e.g. 80 % (FFS).

9.5.10   Real Time service coverage

The coverage for real time data service was evaluated by using RLC un-ACK mode and next MCS exceeding 64 kbps with 2 uplink slots for both the EDGE and DSR resulting to 89.6 kbit/s. At 0.1 % target BLER the DSR gain was about 6.4 dB. It could be possible to develop optimised DSR coding schemes for real time.
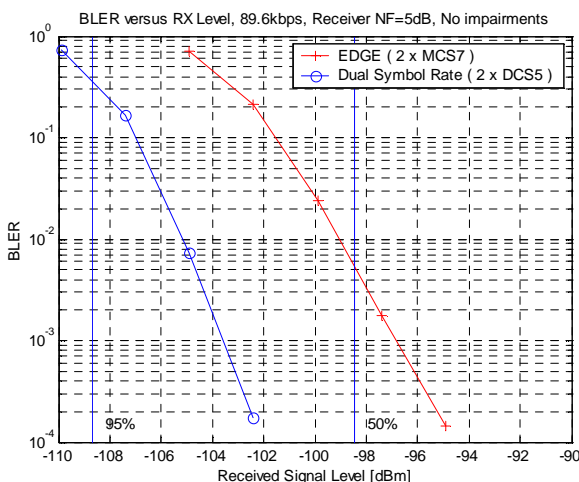
Figure 259: BLER vs. RX level

9.5.11   DSR and Speech Performance in Legacy MRC Network

Dual Symbol Rate performance in mixed voice and data interference scenario, with Interference Rejection Combining (IRC) in all the BTS receivers show 1.7 to 1.9 fold data capacity gain in uplink. In this subclause DSR performance is evaluated assuming legacy Maximum Ratio Combining (MRC) receivers for voice time slots in uplink and data time slots use IRC. So results would reflect the initial deployment case of DSR to the legacy GSM network.

In the presented simulations, the DSR transmitter power was adjusted by dynamic system simulator so that the same UL speech performance was achieved in both EGPRS and DSR cases i.e. DSR impact to voice was cleared out by DSR power control. Burst level information from system level simulator was collected separately for EGPRS and DSR, making simulation results more reliable.

9.5.11.1 DSR interference model for system simulation

Used dynamic system simulator calculates total received interference (for C/I definition) as a sum of co- and first adjacent channel interference levels through a reference, 180 kHz wide, RX filter, which provides 18 dB adjacent channel attenuation for EGPRS and GMSK interferers.

In the case of DSR interferer co-channel attenuation was 4.7 dB and adjacent channel attenuation 5.7 dB related to total DSR signal power. Impact of the second adjacent interferer (21.3 dB) was found to be negligible for the voice performance. The attenuation values of RX filter are also shown in table 113.

Table 113: Attenuation due to a reference RX channel filtering for EGPRS and DSR

Channel Offset	Attenuation due to channel filtering	
	EGPRS	DSR
0 kHz	0	4.7 dB
±200 kHz	18 dB	5.7 dB

9.5.11.2 UL speech performance in legacy MRC network

Dynamic system simulations were run with the frequency reuse of 1/3, which is basically the same as the DSR scenario 2.

At first, the reference EGPRS simulation was run (20 % EGPRS FTP data and 80 % AMR 5.9 kbit/s voice). Speech service quality was evaluated with the following criteria:

- Relative number of bad quality connections (connection average FER > 1 %).

- Relative number of bad quality samples (FER > 4 % measured for 2 seconds samples).

- Network level total average FER.

- Network level average UL TX power.

DSR simulation was first run with the exactly same power control parameters as used for EGPRS and with 2 dB and 4 dB lower power. Figure 260 presents network speech quality in terms of bad quality connections for different simulations. It is seen that without DSR power reduction the number of bad quality speech connections is slightly increased compared to reference EGPRS simulation. However, already 2 dB power reduction was enough to maintain speech performance at the reference level.

Table 114 presents required DSR power reduction values for all the examined speech quality criteria. It is seen that 2 dB power reduction was enough for all used criteria. Therefore, 2 dB power reduction was selected for the DSR data capacity evaluation. Required 2 dB power reduction is also in line with the C/I results presented in subclause 9.5.8.1, where it was found out that network C/I distribution increased about 1 dB to 2 dB due to DSR.
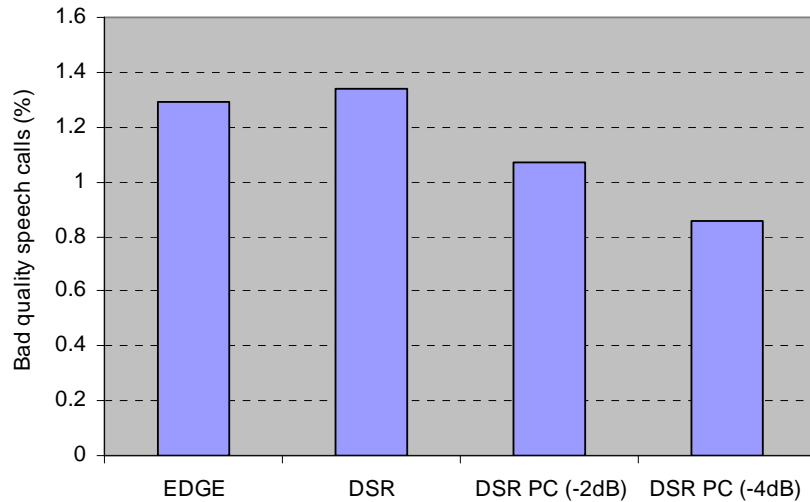
Figure 260: Percentage of bad quality voice calls for EGPRS and DSR with power offsets

**Table 114: DSR TX power reduction required to maintain reference voice quality
for different quality criteria**

Criteria	Power offset for DSR
Relative number of bad calls	-0.5 dB
Network average FER	-2 dB
Relative number of bad FER samples (2 s. period)	-1 dB
Average UL TX power	-2 dB

9.5.11.3   DSR performance in legacy MRC network

EGPRS and DSR data throughputs were studied with link level simulations based on recorded bursts resulting similar voice performance i.e. DSR TX power was limited by 2 dB. Median interference level and variance for 3 strongest co-channel interference levels and 2 strongest adjacent-channel interference levels are shown in tables 115 and 116. DSR TX power reduction is clearly seen in data interference levels. Strongest co-channel DSR interference is about 2.3 dB lower compared to strongest EGPRS interference. The difference between voice and data statistics is mainly due to quality based power control applied for voice.

Table 115: Interference statistics for voice

	DSR median	DSR variance	EDGE median	EDGE variance	Difference in median levels
Co1	-104.1	81.8	-103.8	77.3	0.3
Co2	-110.9	30.2	-110.1	30.4	0.7
Co3	-113.6	18.4	-112.8	21.9	0.9
Adj1	-100.6	82.1	-99.8	82.4	0.8
Adj2	-107.9	44.2	-107.6	47.1	0.3

Table 116: Interference statistics for data

	DSR median	DSR variance	EDGE median	EDGE variance	Difference in median levels
Co1	-104.9	44.4	-102.6	40.3	2.3
Co2	-110. 5	30.1	-108.0	28.8	2.4
Co3	-113.6	18.4	-112.8	21.9	0.9
Adj1	-99.2	72.8	-97.9	81.6	1.3
Adj2	-107.1	44.1	-105.7	54.1	1.4

Throughput versus received signal level is depicted in figure 261. 95 % signal level at the cell border is -88 dBm for EGPRS and -90 dBm for DSR. The DSR, with 2dB lower power, achieves 29 % better throughout at the capacity limited cell border than EGPRS (34 kbit/s for EGPRS and 44 kbit/s for DSR). It is expected that by more intelligent power control than just fixed 2 dB offset, the throughput gain at cell border could be in order of 50 %.

The cell level throughput values for EGPRS and DSR is presented in figure 263. DSR achieves 1.7 x higher data capacity compared to EGPRS.
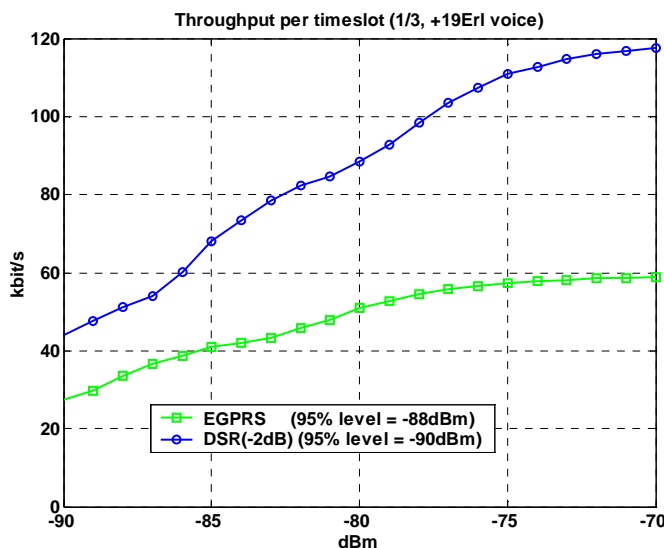
Figure 261: Throughput per TSL for DSR and EGPRS for reuse 1/3
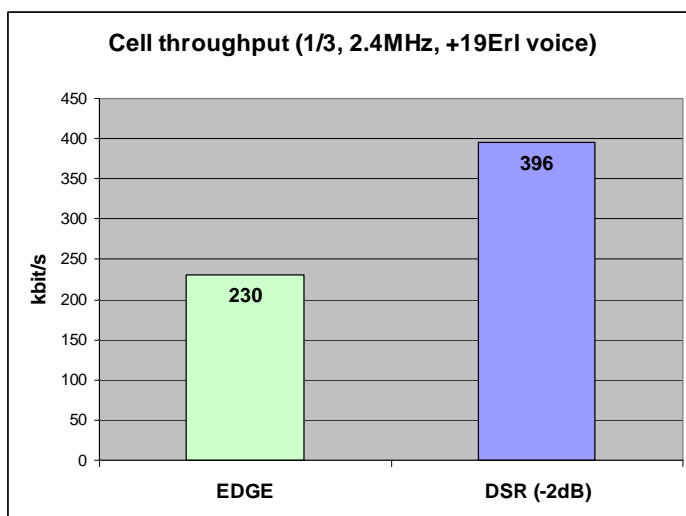
Figure 262: TCH layer (2.4MHz) throughput for 1/3 reuse, with average 4.5 time slots for data and 19 Erls voice traffic load

9.5.12   Impacts to the signalling

As shown in subclause 9.5.11, the DSR power control can be used to remove voice impacts due to DSR, thus it's expected that the same would apply also for signalling.

9.5.13 MDSR performance at interference scenario 2

9.5.13.1 Modelling assumptions and requirements

The modelling assumptions were the same as for DSR, excluding the following:

- MS use 2dB lower maximum power for 16QAM.

- Spectral properties, e.g. adjacent channel power levels of MDSR, were taken into account.

9.5.13.2 System level model

The system model and simulation approaches were the same as for DSR in purpose of compare MDSR to DSR. Only 1/3 re-use (the scenario 2) was studied assuming MRC for voice as in chapter 9.5.11. Power control was applied for MDSR so that voice performance is not reduced but rather improved related to EGPRS.

Two different MDSR loads were simulated:

- The same amount of timeslots as in EGPRS, to study cell capacity.

- The same cell throughput as in EGPRS, to study data rates at cell border.

Used dynamic system simulator calculates total received interference (for C/I definition) as a sum of co- and first adjacent channel interference levels through reference, 180 kHz wide RX filter. The attenuation values of RX filter for MDSR and EGPRS are shown in table 117.

Table 117: Attenuation due to reference RX channel filtering for EGPRS, DSR and MDSR

Channel Offset	Attenuation due to channel filtering		
	EGPRS	DSR	MDSR (+100 kHz)
0 kHz	0 dB	4.7 dB	3.7 dB
+200 kHz	18 dB	5.7 dB	3.7 dB
-200 kHz	18 dB	5.7 dB	16 dB
+400 kHz	47 dB	21 dB	16 dB

9.5.13.3 Performance at mixed voice and data interference scenario 2

Throughputs versus signal level at interference limited scenario are shown in figure 263. The following MDSR power control scheme was used to maintain the same or better voice quality than with EGPRS:

- Maximum MDSR power was 2 dB lower than EGPRS or DSR due to increased PAR.

- 4 dB power reduction related to EGPRS UL power control was applied at uplink levels higher than 86 dBm.

Due to difference in power control the cell edge and average levels are not the same for EGPRS, DSR and MDSR as shown in table 118. The MDSR performance with MRC instead of IRC was also simulated to demonstrate the role of IRC in MDSR performance.

TU3iFH, Reuse 1/3
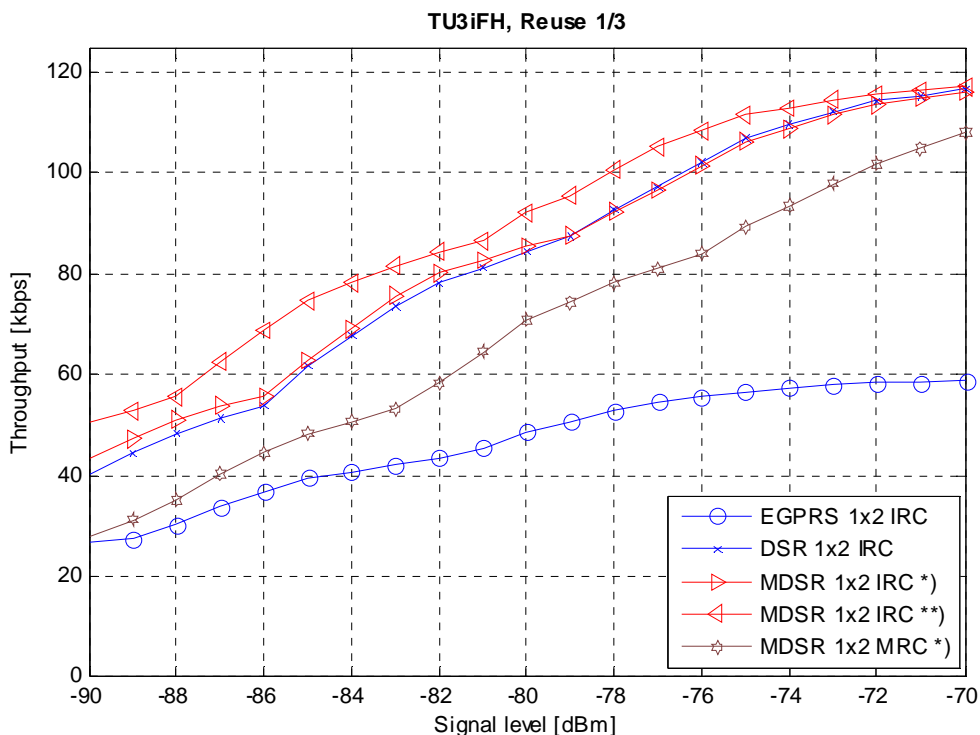
Figure 263: Throughput versus signal level at scenario 2 (1/3)

Table 118: Summary for interference scenario 2

	EGPRS	DSR (see note 1)	MDSR (see note 1)	MDSR (see note 2)	MDSR (see note 1)
Receiver	IRC	IRC	IRC	IRC	MRC
Cell edge level	88 dBm	89 dBm	90 dBm	90 dBm	90 dBm
Median level	80 dBm	82 dBm	82 dBm	82 dBm	82 dBm
Throughput per slot at cell edge	30 kbps	42 kbps	43 kbps	51 kbps	32 kbps
Average throughput per slot	50 kbps	77 kbps	79 kbps	86 kbps	60 kbps
Throughput gain at cell edge	-	40 %	43 %	67 %	6 %
Average cell throughput gain	-	1.6 x	1.6 x	1 x	1.2 x
NOTE 1: The same amount time slots for data as in EGPRS and equal voice quality.					
NOTE 2: The same cell throughput as for EGPRS and improved voice quality.					

As conclusion MDSR provided 1.6 times higher average cell throughput i.e. spectral efficiency with 1/3 re-use in interference limited scenario. At cell border the throughput gain was 67 %.

MDSR with MRC receiver has also reasonable performance against interference providing 20 % gain over EGPRS with IRC receiver. Thus IRC is not mandatory to obtain capacity gains by MDSR.

9.5.13.3.1   Impact of antenna correlation

The impact of receiver antenna correlation to MDSR throughput was studied by repeating scenario 2 by assuming RX antenna correlation of 0.7. This inclusion of interference distribution from system simulator instead of link level analysis should give realistic outcome. The results are plotted in figure 264.
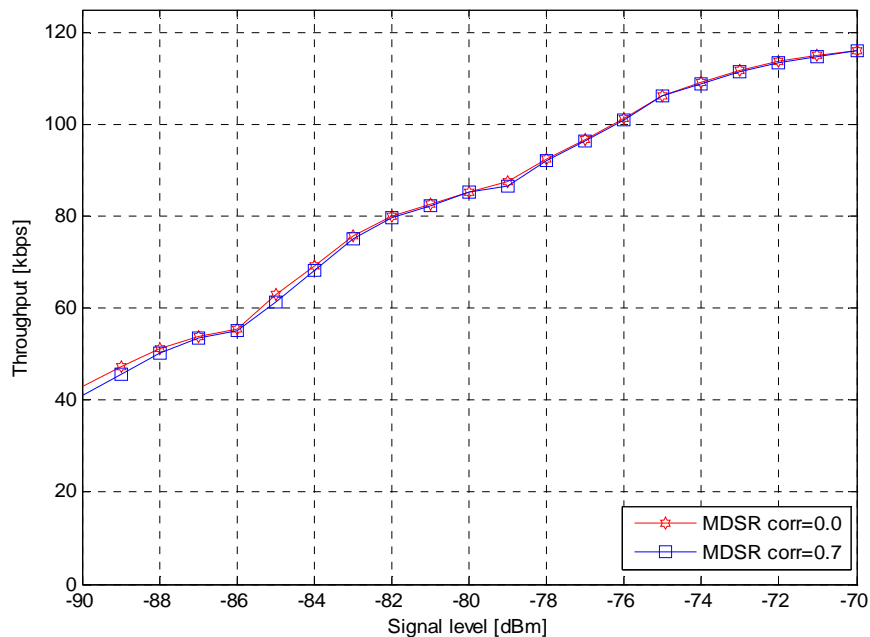
Figure 264: The impact of receiver antenna correlation 0.7 to MDSR throughput at scenario 2

9.5.13.4 Network performance at data only interference scenarios

MDSR network level performance was studied with dynamic system simulations. Wide MDSR carriers were modelled in the simulator e.g. carriers were shifted +100 kHz so that MDSR signal was overlapping with two basic 200 kHz carriers.

Presented simulation results are uplink results assuming 2-antenna diversity. MRC and IRC diversity receiver models were included in the simulations. Simulator uses well-known two phase link-to-system mapping method. At first, C/I of burst is mapped to a burst Bit Error Probability (BEP) and after that a Block Error Probability (BLEP) is estimated based on mean and standard deviation of the burst BEP values during the radio block period.

For the diversity simulations the mapping method was extended to include wanted and interfering signals for two antennas, and, furthermore, strongest interference levels were needed one by one for the IRC modelling. Verification simulations showed that the used modelling achieved high accuracy for all diversity cases. In figure 119 an example verification result is shown for MDSR IRC case. It can be seen that difference between the IRC model and actual link level simulation is less than 0.5 dB for the BLER values higher than 1.0 %.
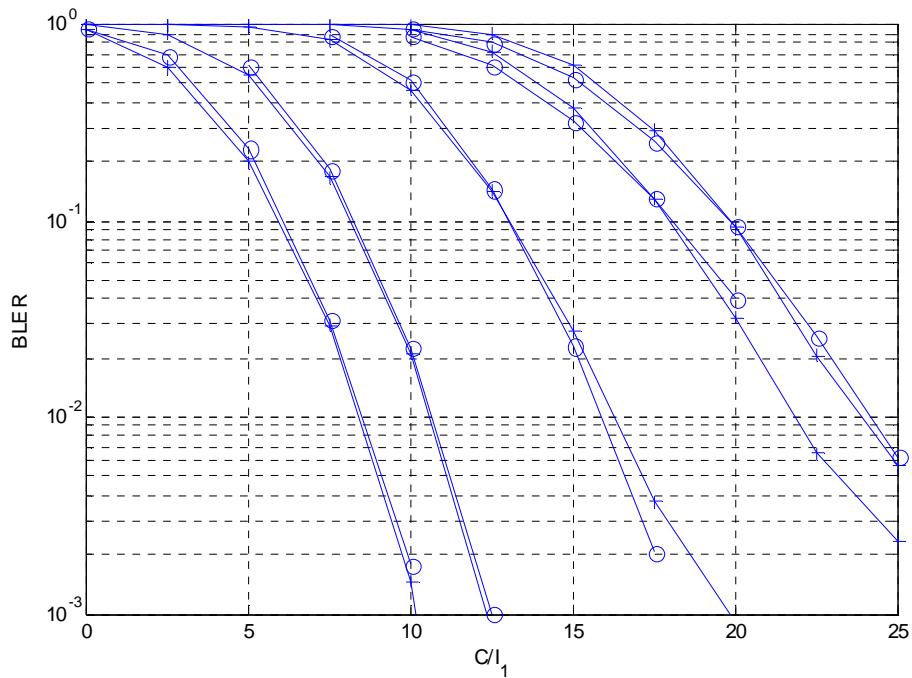
Figure 265: Verification of IRC model in system simulator at modified scenario DTS-2, with wanted and interfering signals MDSR modulated, is shown as BLER vs. C/I$_1$ for MDCS 5 to 9 IRC model is marked by circles and link simulations by crosses

The frequency re-uses 4/12, 1/3 and 3/9 were simulated. Only data traffic was included in the simulations in order to determine spectral efficiency gains according to agreed method in [4]. In the following results 10th percentile (worst) connection average bit rates are shown. 2-antenna diversity was assumed for all cases. For EGPRS both MRC and IRC were studied, while MDSR was studied with IRC only.

The network capacity gains were measured versus average session bit rate for the worst 10th percentile of the connections. Simulation parameters for respective scenarios 5, 6, and 7 are shown in table 119. Scenario 5 is BCCH layer simulation with one non hopping TRX and scenarios 6 and 7 are hopping layer simulations with 4 TRX per cell. In scenario 6 also 2-TRX MDSR implementation was studied. Note, that QPSK was not included in the simulations, which is expected to improve session bitrates below 120 kbps.

Table 119: Data only system scenarios

Parameter	Scenario 5	Scenario 6	Scenario 7
Reuse	4/12 (BCCH only)	1/3 (TCH only)	3/9 (TCH only)
Bandwidth	2.4 MHz (see note)	2.4 MHz (see note)	7.2 MHz (see note)
TRXs per cell	1	4	4
Hopping	No	Random RF	Random RF
Synchronised BSS	Yes	Yes	Yes
Simultaneous Voice Load	No	No	No
EGPRS DL Load	Variable	Variable	Variable
EGPRS UL Load	Variable	Variable	Variable
EGPRS UL Power Control	Yes	Yes	No
EGPRS Traffic Model	FTP (120 kB)	FTP (120 kB)	FTP (120 kB)
QPSK included to MDSR	No	No	No
NOTE: In spectral efficiency estimates, it was taken into account that MDSR actually uses 200 kHz wider spectrum, i.e. 2.6MHz for Scenarios 5 and 6 and 7.4MHz for Scenario 7.			

9.5.13.4.1 Performance at scenario 5 (4/12 re-use)

Figure 268 depicts reuse 4/12 simulation results. 10th percentile of connection bit rates are shown for EGPRS with MRC, EGPRS with IRC and MDSR versus offered FTP load. Then, MDSR capacity gains are compared to EGPRS with MRC and IRC are shown for different 10th percentile session bit rate requirements. Network capacity gain is 200 % to 270 % for 100 kbps requirement and 340 % to 550 % for the 144 kbps connection average bit rate requirement.

The simulation was an example BCCH layer data traffic capacity simulation. BCCH layer was more radio resource than spectrum limited for both EGPRS and MDSR in this example simulation. It can be seen, for example, that worst 10th percentile of the connections achieved as high as 220 kbps average bit rate in case of MDSR whereas only 50 kbps was obtained in case of EGPRS at the same traffic load.
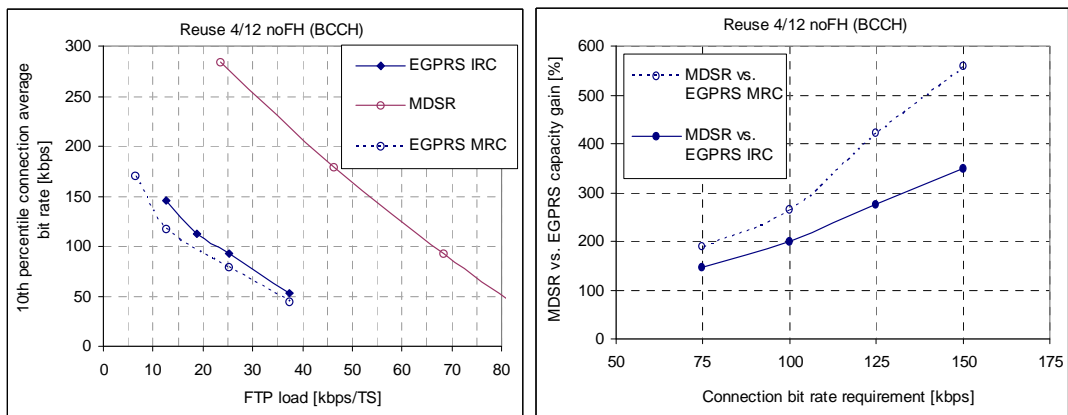
Figure 266: System simulation results for scenario 5 (4/12)

9.5.13.4.2 Performance at scenario 6 (1/3 re-use)

In case of re-use 1/3 capacity gain at 100 kbps session bit rate is 120 % to 190 % for 4-TRX implementation and 90 % to 150 % for 2-TRX implementation. For the 144 kbps bit rate requirement gains are 180 % to 420 % and 140 % to 340 %, respectively. Reuse 1/3 was found to be spectrum limited and therefore 2-TRX implementation achieved nearly the same network performance than with 1-TRX MDSR implementation.
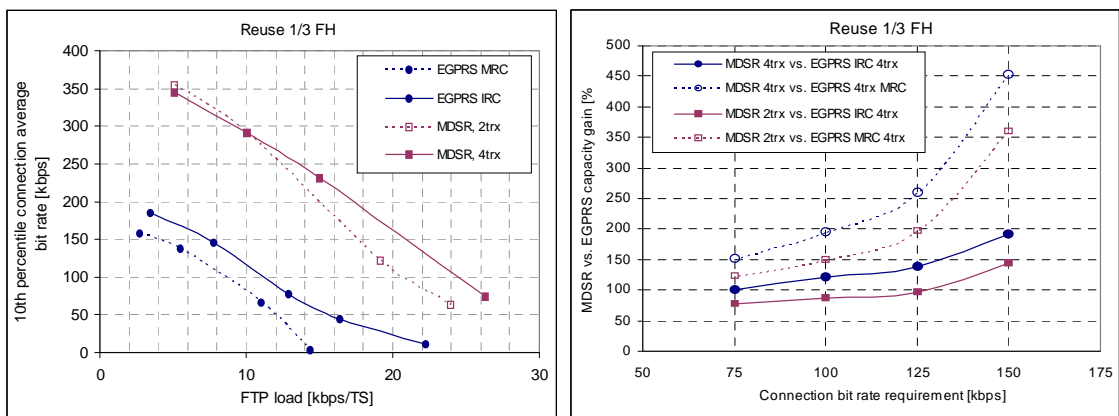
Figure 267: System simulation results for scenario 6 (1/3)

9.5.13.4.3 Performance at scenario 7 (3/9 re-use)

In case of re-use 3/9, capacity gain at 150 kbps session bit rate is about 150 % compared to EGPRS with IRC and 300 % compared to EGPRS with MRC.
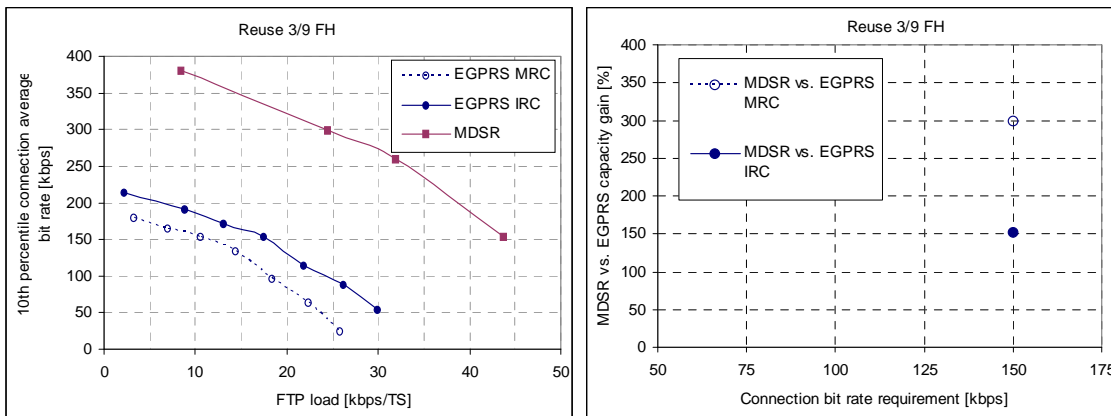
Figure 268: System simulation results for scenario 7 (3/9)

9.5.13.5 Performance of two transceiver implementation

This paragraph presents a dual TRX performance at DTS-2 scenario with impairments.

Two conventional receivers e.g. like used in the first generation GSM BTS over decade ago were assumed. Both receivers have independent impairments as listed in table 120. The used channel filter has 200 kHz bandwidth and in addition to that a random phase offset between receivers was generated for every burst.

Table 120: Receiver impairments

Impairment	Value
I/Q gain imbalance	0.125 dB
I/Q phase mismatch	1°
DC offset	-30 dBc
Phase noise	1.2° RMS

The DTS-2 link level interference scenario, illustrated in figure 269 and table 121, was used for both EGPRS and MDSR. In the case of MDSR, the frequency of adjacent-1 interference was chosen so that, it became as 3rd co-channel interference for MDSR with +3dB power level. Thus, it was not attenuated by channel filter providing adjacent channel protection like in the case of EGPRS. The used noise bandwidth was 271 kHz in both cases, i.e. it is -15.2 dB for 405 kHz bandwidth. Despite of these hardenings, interference levels in simulations referred to the level of co-channel-1 for both EGPRS and MDSR.
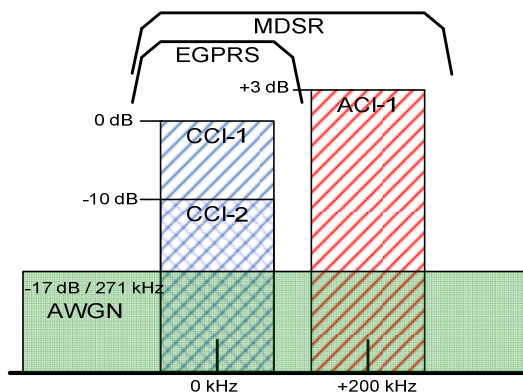
Figure 269: DTS-2 Link scenario for EGPRS and MDSR

Table 121: DTS-2 Link scenario for EGPRS and MDSR

Interfering Signal	Relative Level	Notes for MDSR
Co-channel 1	0 dB	
Co-channel 2	-10 dB	
Adjacent channel 1 (+200kHz)	+3 dB	"Co-channel-3" at +3 dB level
AWGN (BW=271 kHz)	-17 dB	-15.2 dB at 405 kHz BW
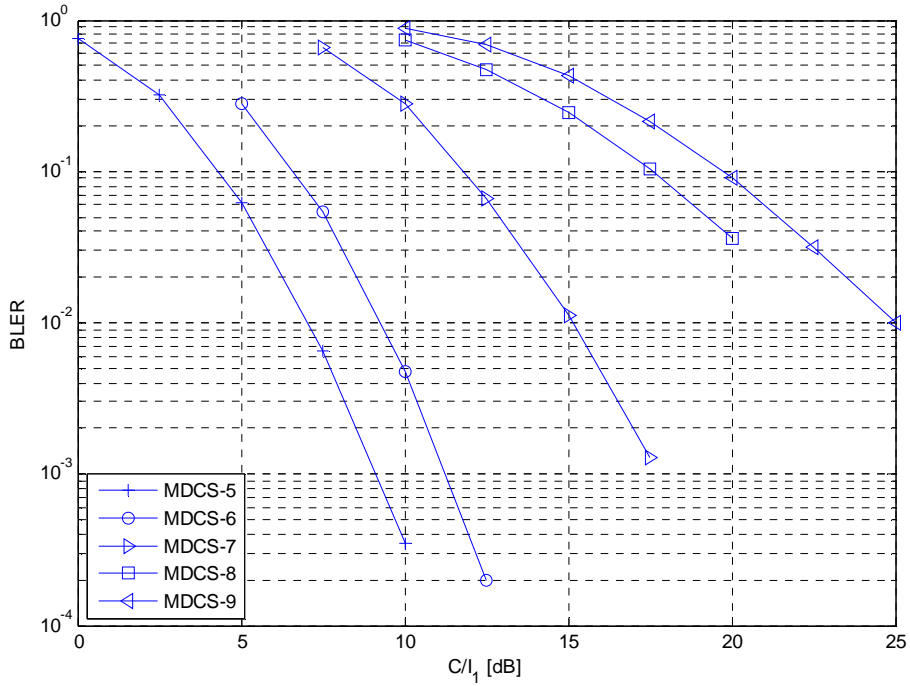
Figure 270: BLER versus C/I_1 with impairments at link scenario DTS-2
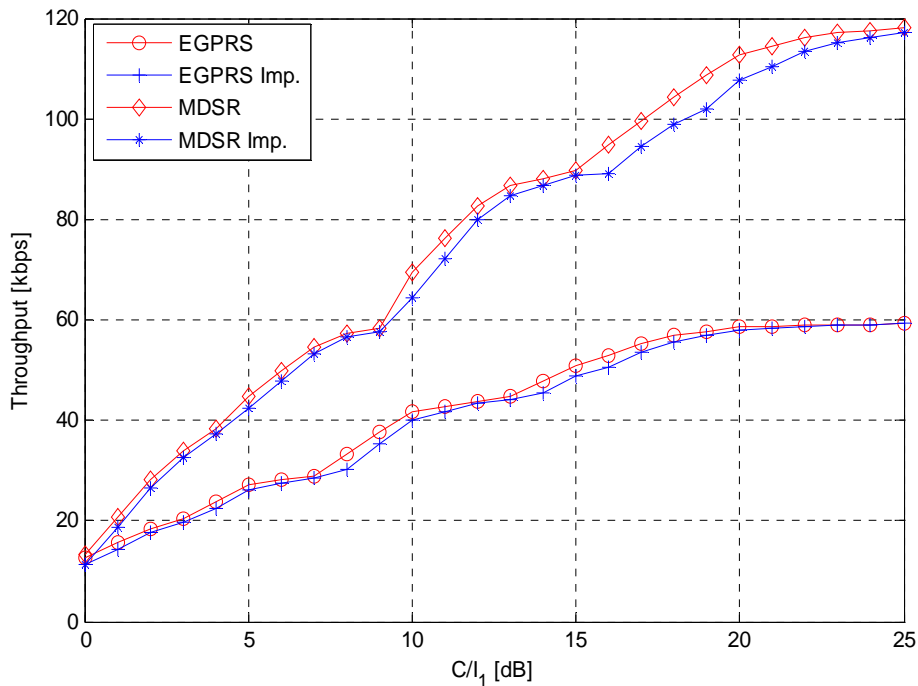
Figure 271: Throughput versus C/I_1 at DTS-2 with and without dual RX impairments

9.5.13.6   Voice and higher symbol rate in asynchronous interference scenario

This subclause presents some results for voice performance with asynchronous MDSR interference that has no 100 kHz offset. Offset was removed since two TRX implementation option found to have low interest. In addition IRC performance at low SNR conditions is also evaluated.

Simulations shown, 1.5 times higher symbol rate has lower voice impact than EGPRS with legacy MRC receiver.

9.5.13.6.1   Simulation assumptions

General modelling assumptions were:

- MRC and IRC receivers were used for AMR 5.9.

- Asynchronous and synchronous DTS-2 scenarios were used.

- Interfering signal were 8PSK and 16QAM with 1.5 symbol rate.

- Low SNR simulation was modelled with noise floor at 0dB instead of -17dB from I_1.

- Receiver impairments were included.

9.5.13.6.1.1   Receiver impairments

Table 122 lists used receiver impairments that were used in the receiver performance simulations.

Table 122: Receiver impairments

Impairment	Value
I/Q gain imbalance	0.125 dB
I/Q phase mismatch	1°
DC offset	-30 dBc
Phase noise	1.2° RMS
Total receiver noise figure	5 dB

9.5.13.6.1.12   DTS-2 interference scenario

The DTS-2 link level interference scenario is illustrated in figure 272 and table 124. Note that DTS-2 provides a link level approximation of system interference of a typical interference limited network for speech, which was agreed in TSG-GERAN for testing SAIC performance. The interference distribution for mixed speech and data on the uplink may therefore be different.

A random time offset was used for asynchronous interferers per frame. Two consecutive bursts with independent fast fading were generated to provide the same average interference power over the burst length as in the synchronous case.
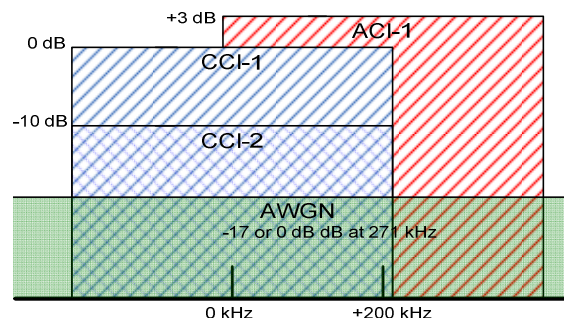
Figure 272: DTS-2 Link scenario with higher symbol rate interference

Table 123: DTS-2 Link scenario for EGPRS and MDSR

Interfering Signal	Relative Level
Co-channel 1	0 dB
Co-channel 2	-10 dB
Adjacent channel 1 (+200 kHz)	+3 dB
AWGN (BW=271 kHz)	-17 dB or 0 dB

9.5.13.6.2 Performance characterization

9.5.13.6.2.1 Voice performance at asynchronous and synchronous scenario

It can be seen from DTS-2 results with MRC that higher symbol has a bit smaller impact to voice than EGPRS interference at 1 % FER.

In asynchronous scenario MDSR interference has about similar impact to voice as EGPRS. But with IRC and in synchronous scenario, voice performance was degraded by 0.3 dB with MDSR interference (without 100 kHz offset) compared to EGPRS.
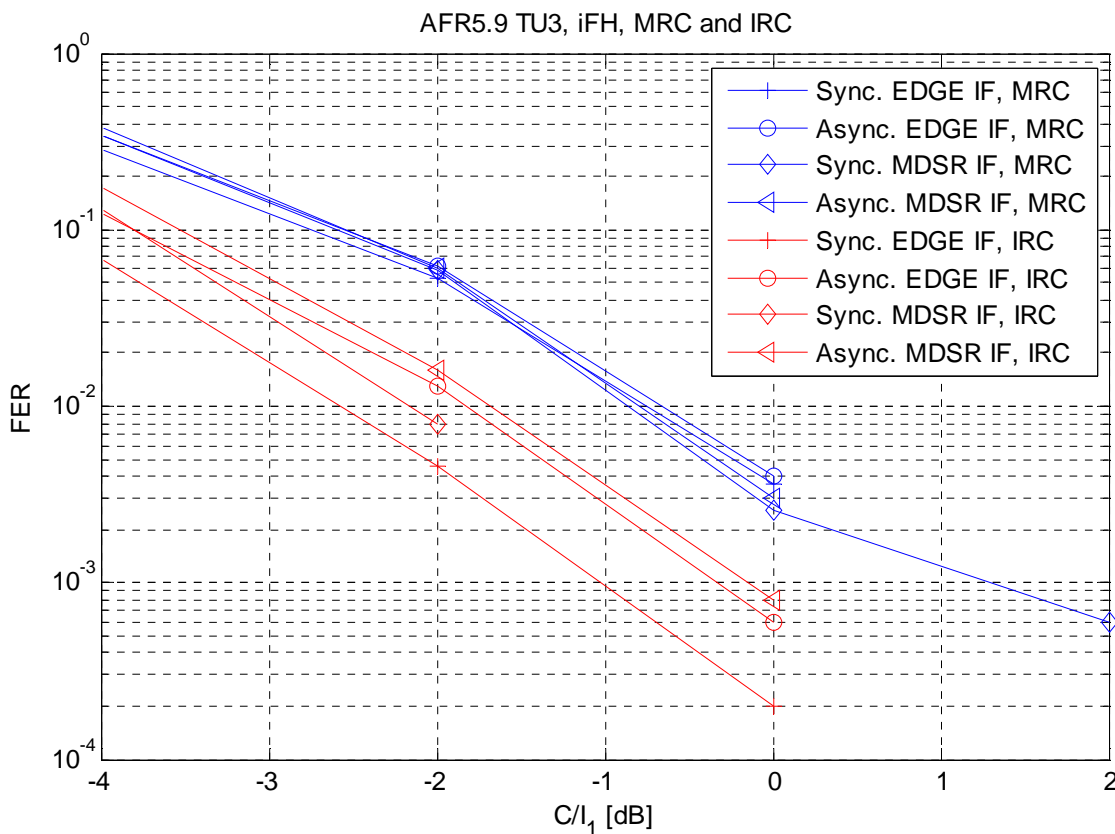
Figure 273: Voice impact with IRC and MRC

9.5.13.6.2.2 Voice performance at low SNR with MRC

Simulations with DTS-2 scenario at low SNR conditions show that higher symbol rate has 0.7 dB lower impact to voice than EGPRS.
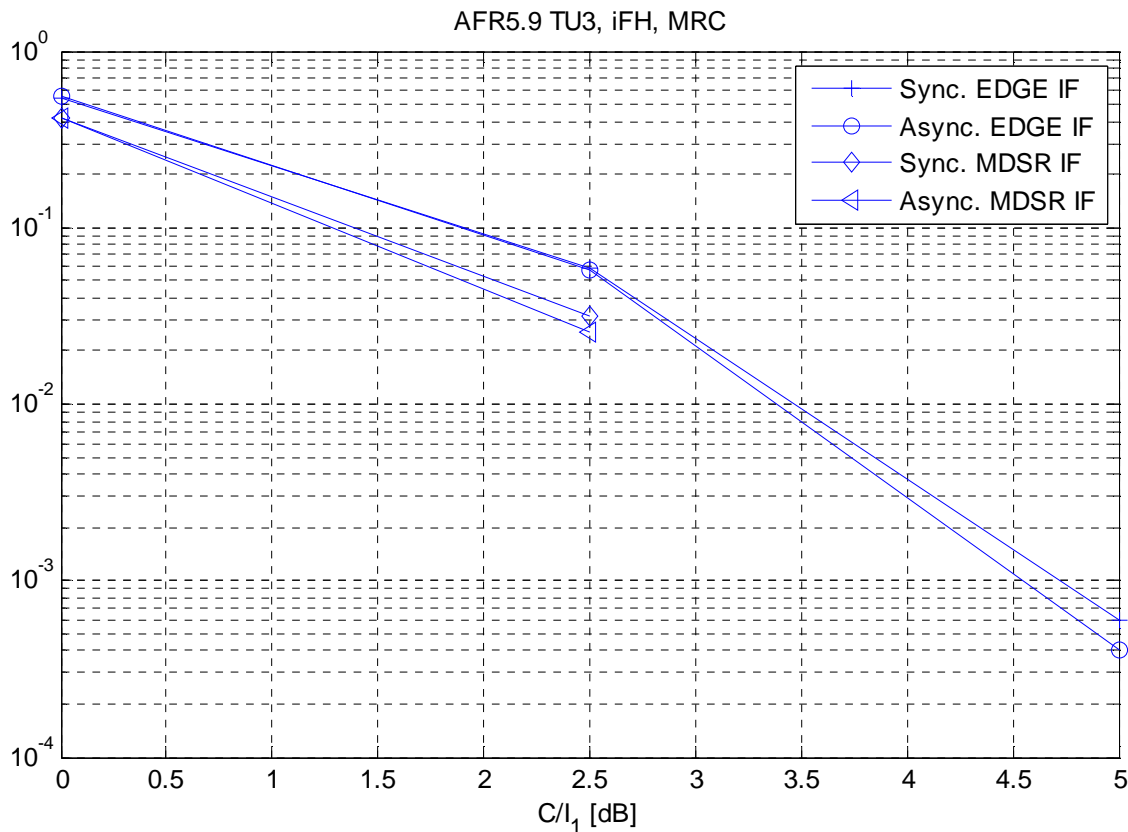
Figure 274: Voice performance at low SNR (noise power at 270 kHz equal to I_1 power)

9.5.14 High Symbol Rate (HSR) performance

Evaluated concept uses 1.2 times higher symbol rate i.e. 325 ksymbol/s and 32QAM modulation with convolution channel coding.

9.5.14.1 Modelling assumptions

Legacy EGPRS receiver SAW filter with 240 kHz BW (3GPP TR 45.912, subclause 9.7.1.1.1.1) was assumed. Two different transmitter shaping pulses were used with bandwidths of 240 kHz and 325 kHz to determine the performance impact of shaping filter.

The receiver performance modelling assumptions were:

In the receiver simulations BTS used legacy 8PSK receiver filter, a SAW filter model, with 240 kHz BW (subclause 9.7.1.1.1.1). Additionally receiver filter, which bandwidth was matched with the symbol rate was used as a reference.

Asynchronous DTS-2 scenario with 1.2 times higher symbol rate interferers was used.

Data performance was evaluated with Interference Rejection Combining (IRC) algorithm with 2 receiver antennas.

Voice impact (AMR 5.9) was analyzed with above mentioned asynchronous DTS-2 scenario with Maximum Ratio Combining (MRC) receiver.

Receiver impairments were included.

9.5.14.1.1 Receiver impairments

Table 124 lists used receiver impairments that were used in the receiver performance simulations.

Table 124: Receiver impairments

Impairment	Value
I/Q gain imbalance	0.125 dB
I/Q phase mismatch	1°
DC offset	-30 dBc
Phase noise	1.2° RMS
Total receiver noise figure	5 dB
SAW filter bandwidth	240 kHz

9.5.14.1.2 DTS-2 interference scenario

The DTS-2 link level interference scenario, illustrated in figure 275 and table 125, was used 1.2 times higher symbol rate with different shaping pulses and receiver filters.

A random time offset was used for asynchronous interferers per radio frame. Two consecutive bursts with independent fast fading were generated to provide the same average interference power over the burst period as in the synchronous case.
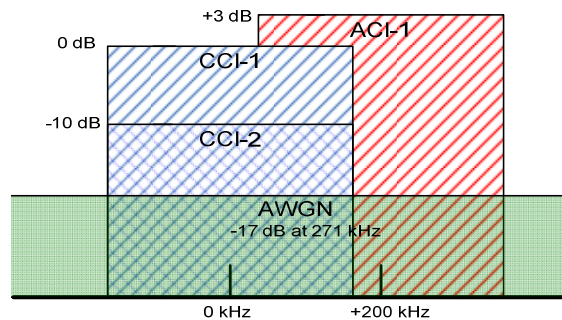
Figure 275: DTS-2 Link scenario for 1.2 times higher symbol rate

Table 125: DTS-2 Link scenario for EGPRS and MDSR

Interfering Signal	Relative Level
Co-channel 1	0 dB
Co-channel 2	-10 dB
Adjacent channel 1 (+200 kHz)	+3 dB
AWGN (BW=271 kHz)	-17 dB

9.5.14.2 Performance characterization

9.5.14.2.1 Coverage

Throughput versus received signal level is depicted in figure 276 for 1.2x32QAM with different shaping and receiver filters at TU3iFH conditions with receiver impairments given in table 124.

Table 126 shows average throughputs and throughput gains at -98 dBm median RX level. 1.2 x 32QAM used additional power due to higher PAR.

1.2x32QAM seems to provide up to 46 % higher average throughput than EGPRS with 325 kHz shaping pulse. It can be also seen that 32QAM is not sufficient and there is room for 1.2x16QAM below about 15 dB point.
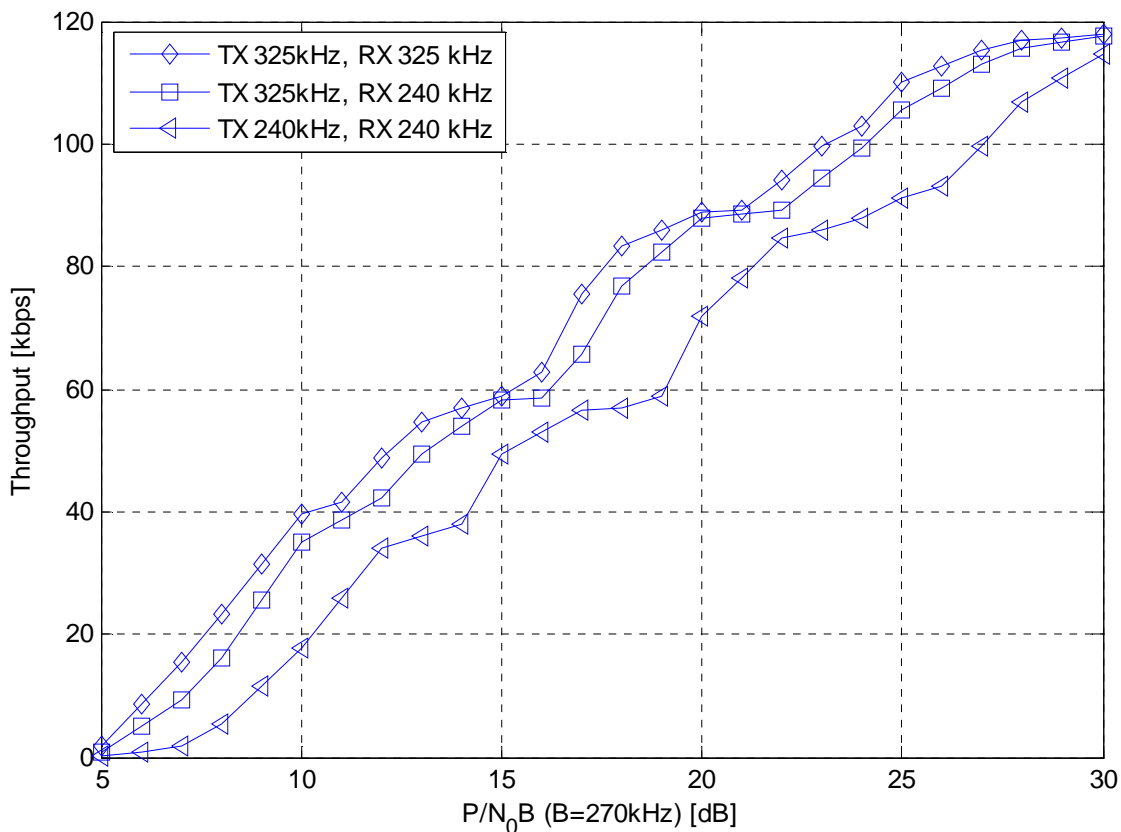
Figure 276: Throughput versus signal power per noise power at 270 kHz bandwidth, TU3iFH

Table 126: Average throughput per slot, TU3iFH

	EGPRS	1.2 x 32QAM		
Width of pulse shaping filter	180 kHz	325 kHz	325 kHz	240 kHz
Width of receiver filter	270 kHz	325 kHz	240 kHz	240 kHz
Peak to Average Ratio	3.2 dB	4.9 dB	4.9 dB	5.8 dB
Additional Power reduction related to EGPRS	N.A.	1.7 dB	1.7 dB	2.6 dB
Average throughput @ -98 dBm level with / without additional power reduction	44 kbps	58 kbps 65 kbps	56 kbps 60 kbps	37 kbps 53 kbps
Coverage gain over EGPRS with / without additional power reduction	N.A.	30% 46%	26% 34%	- 20%

9.5.14.2.2 Data performance in synchronous DTS-2 interference scenario

The throughput of 1.2 x 32QAM was evaluated in Figure 277 for the following cases:

- 1.2x32QAM with 325 kHz shaping filter and 325 kHz receiver filter.

- 12x32QAM with 325 kHz shaping filter and 240 kHz receiver filter.

- 12x32QAM with 240 kHz shaping filter and 240 kHz receiver filter.

It can be seen that wider shaping filter linked with wider receive filter outperforms other options and next best is wider shaping linked with narrow receiver filter.
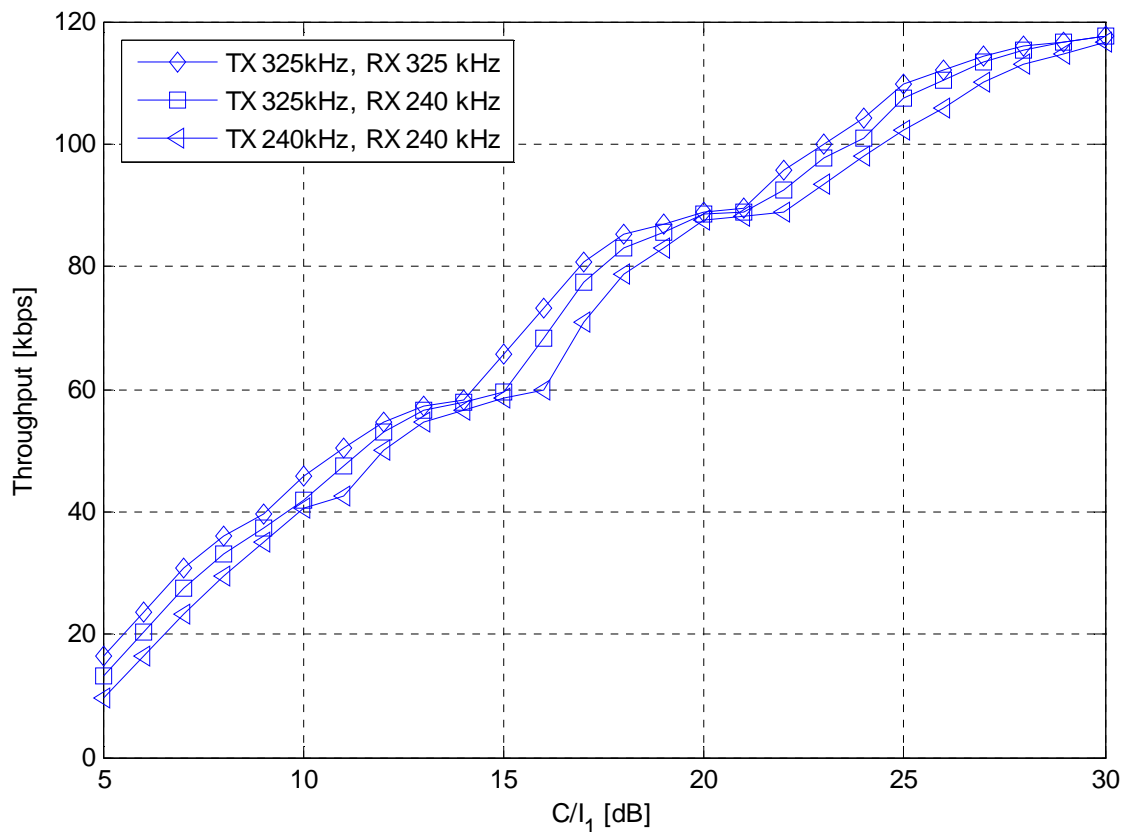
Figure 277: Throughput versus C/I₁ for different pulse shaping and receiver filters in synchronous DTS-2 scenario

9.5.14.2.3 Voice impact in asynchronous DTS-2 interference scenario

The AMR 5.9 FER was simulated with asynchronous DTS-2 scenario. Three curves are presented:

- AMR 5.9 FER with EGPRS interference.

- AMR 5.9 FER with 1.2x32QAM interference with 240 kHz shaping filter.

- AMR 5.9 FER with 1.2x32QAM interference with 325 kHz shaping filter.
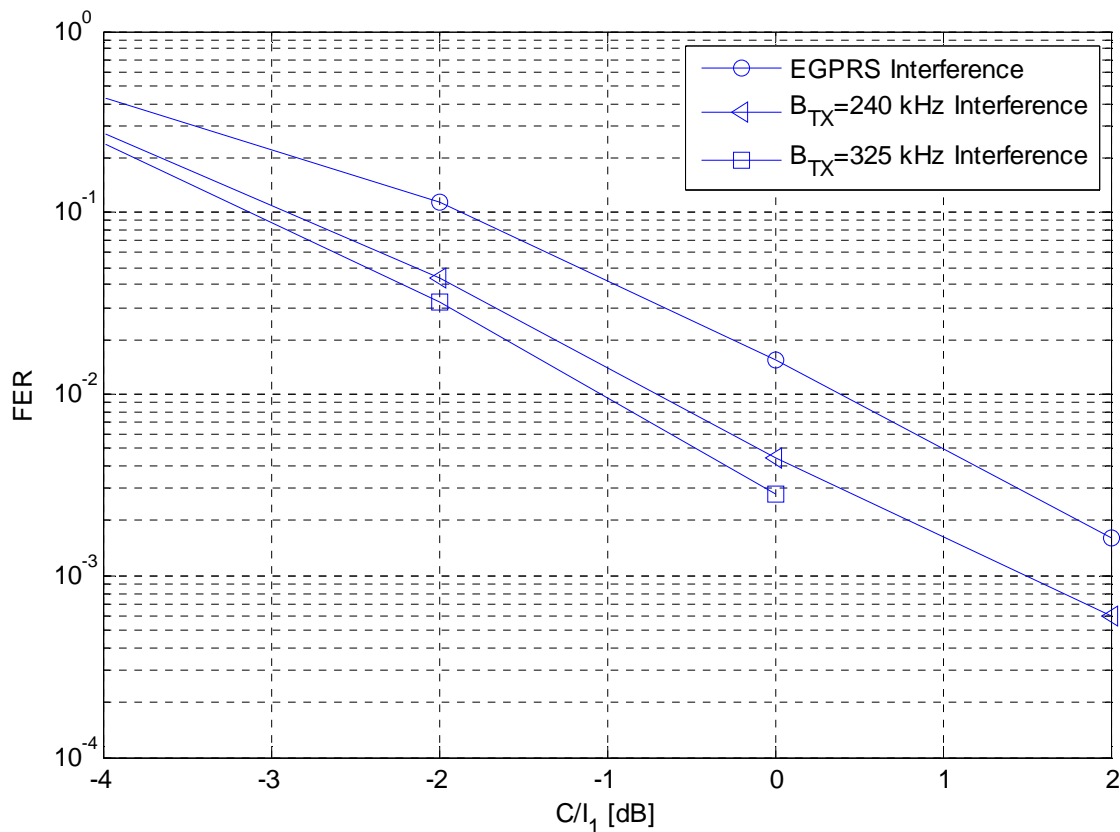
Figure 278: AMR 5.9 FER versus C/I$_1$ in asynchronous DTS-2 scenario

It can be seen that EGPRS as an interference seems to cause higher impact to AMR than 1.2 symbol rate. Indeed 240 kHz shaping filter seems to cause higher FER than 325 kHz shaping filter.

9.6 Impacts to the mobile station

9.6.1 DSR

Dual symbol rate has small impact to terminal e.g. HW changes could be limited to the modulator. Linearity requirements due to peak to average ratio are similar as for 8PSK. Requirements due to peak to minimum may be higher. Modulation spectrum mask at 800 kHz offset may need to be optimised allowing reasonable transmitter efficiency.

Encoding complexity of DSR is 2 times higher per timeslot than for 8PSK.

Switching between DSR and voice would be about similar than between GMSK and 8PSK today. Doubling the modulation rate is likely quite straightforward e.g. basic GSM clock 13 MHz is divided by 24 instead of 48, i.e. integer divider can be used. Existing guard band is sufficient for switching because length of shaping filter is not longer in time than that used for GMSK or 8PSK.

With DSR, the DAC would have to run at a higher sampling rate which would require a wider filter after the DAC. The wider Tx filter would in turn increase the Tx noise power [7].

NOTE: The impact of the higher Tx noise power on wide band noise and spurious emissions needs to be investigated [7].

9.6.2 MDSR

MDSR has small impact to terminal e.g. HW changes could be limited to the modulator. Generation of 100 kHz offset is considered to be done by the modulator on burst basis thus additional synthesizer settling time is not needed for it. Linearity requirements, e.g. due to peak to average ratio are a bit higher than for 8PSK. Encoding complexity of MDSR is 2 times higher per timeslot than for 8PSK, i.e. the same as for DSR.

9.6.2.1 MS implementation issues

To generate the MDSR modulation in the MS, it was proposed to apply an offset of 100 kHz in the baseband modulator. This means that the required baseband bandwidth will double although the symbol rate is only 50 % higher. The two different symbol rates and the doubled bandwidth may require a different, higher DAC sampling frequency and a wider filter bandwidth of the subsequent low-pass filters. A higher total noise power is expected. Therefore the achievable spectrum mask as well as wideband noise and spurious emissions should be investigated. If MDSR needs a relaxation of spectrum requirements, the MS should have the possibility to switch between two filter bandwidth settings, one for legacy EGPRS and one for MDSR.

Because of the higher PAR of 16-QAM, PAs with reasonable efficiency would need a higher output power back-off than for 8-PSK. New power classes would have to be defined. Furthermore, not only the higher PAR, but also the zero crossings may require higher linearity, and polar loops could not be used.

9.7 Impacts to the BSS

9.7.1 Impacts to the transceiver

The BTS receiver is required to have sufficient channel bandwidth and also should have sufficient processing power for double amount of uplink data. The sampling rate should be at least equal to the symbol rate. So DSR is not compatible with all legacy BTS hardware.

9.7.1.1 Two transceiver implementation for DSR

The secondary BTS transceiver implementation option may be based on the use of pair of legacy transceivers instead of one. This option utilises half band sampling where sampling rate can be half of DSR symbol rate and channel filter half of the BW of DSR i.e. like in EDGE. Indeed it is possible to share the DSP processing load over 2 transceivers for both equalizing and decoding and utilize Abis links of both transceivers. The main requirement in this option is to have inter-transceiver communication capability, almost similar to inter carrier interleaving, to share samples and detected soft-bits between 2 transceivers and possibility to tune receivers to offset from wanted DSR channel frequency. The radio performance would be similar to single transceiver option.
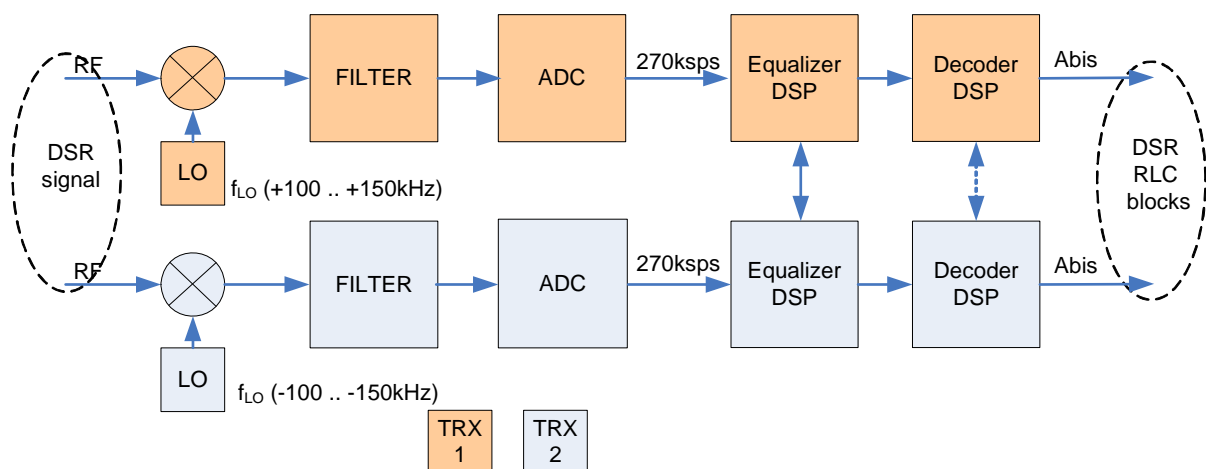
Figure 279: Optional DSR receiver implementation with pair of transceivers
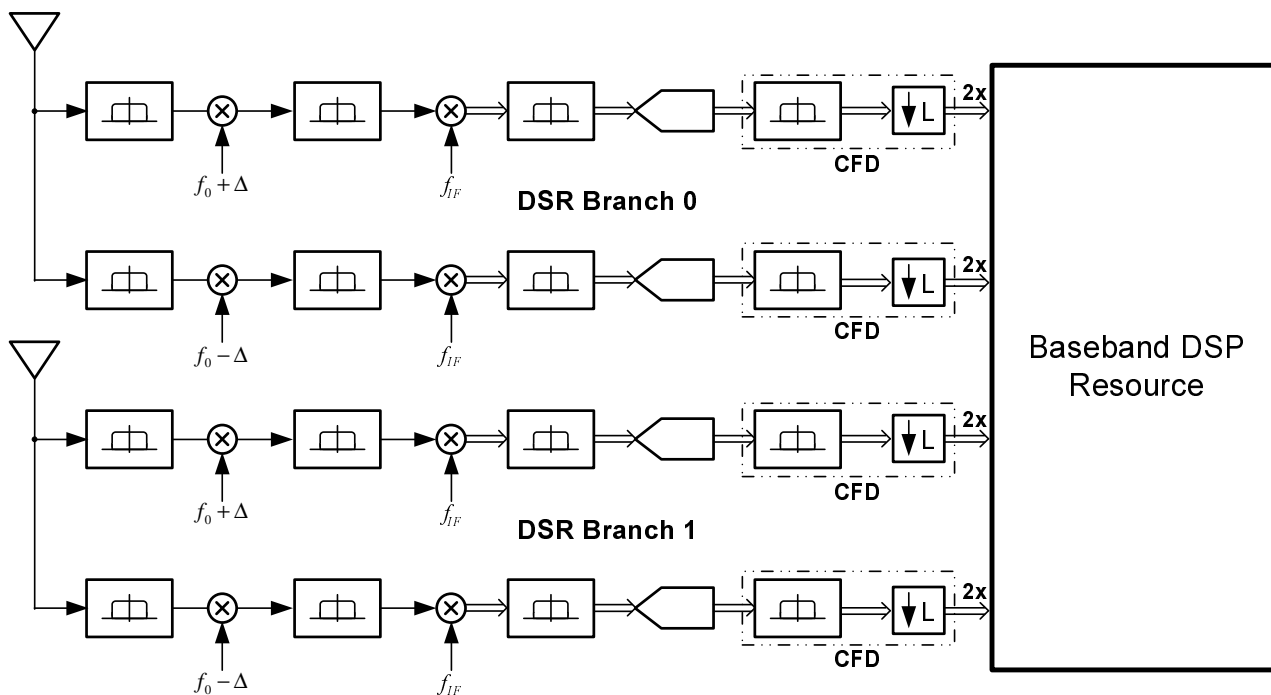
Figure 280: TRX reconfiguration for DSR receiver synthesis [8]

9.7.1.1.1 Performance impact of two TRX implementation

Uncoded DSR performance has been evaluated by simulations. A conventional DSR receiver is compared to a two TRX receiver. The DSR equalizer has the following characteristics.

- 11 channel taps.

- Synchronization window that handles time offsets comparable to the EDGE 8PSK equalizer.

- DFSE equaliser with 2 MLSE taps.

9.7.1.1.1.1 Impact of decreased receiver bandwidth

With a two TRX receiver, the signal is received through two separate receiver filters, each having a bandwidth optimised for a conventional GSM/EDGE carrier. Since a DSR signal has a bandwidth of 540 kHz, two GSM/EDGE receiver filters typically cannot receive the entire signal. In the simulations, the two receivers are assumed to be separated by 200 kHz and to have a filter bandwidth of 240 kHz each. This gives a total received bandwidth of 440 kHz. It is assumed that the signal can be perfectly reconstructed within this bandwidth from the two composite signals. Figure 281 shows the effect of the decreased bandwidth. This gives a lower bound on the losses due to bandwidth for a 2 TRX DSR receiver. The loss is at least 1 dB.
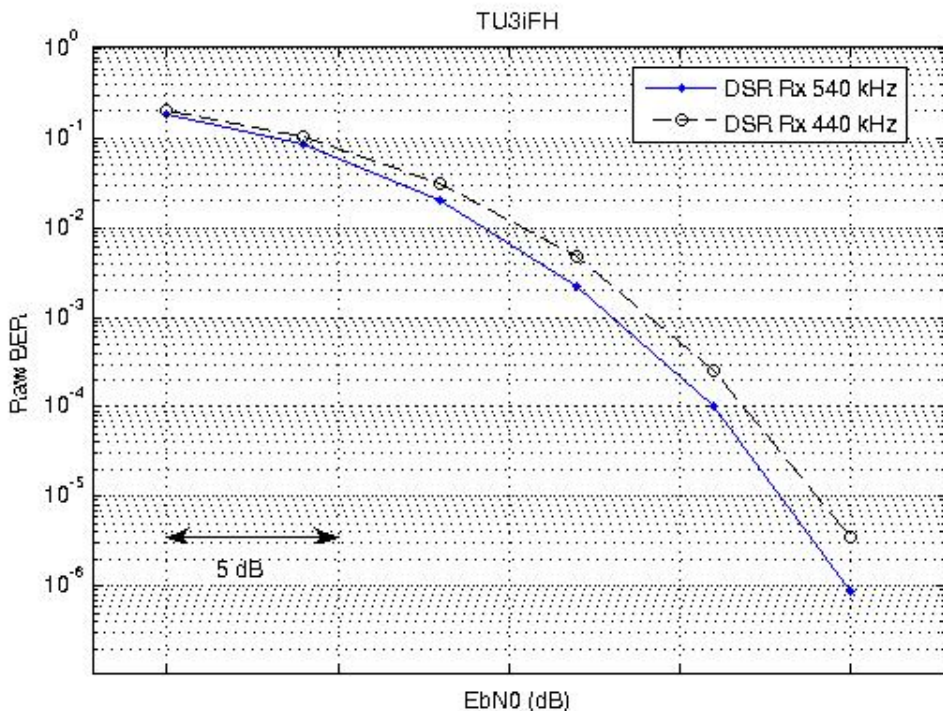
Figure 281: Performance loss due to limited receiver bandwidth

9.7.1.1.1.2 Impact of other analogue components

When two receivers are used to receive one wideband signal, a tight match of the analogue components of the two receivers is essential; otherwise the reconstructed signal will be distorted. The analogue parts of a GSM/EDGE receiver are designed for optimal reception of a single GSM/EDGE carrier and the tolerances of components are chosen to meet this requirement. With two receivers, deviations will be added, which may have an impact of the receiver performance.

One aspect of this was investigated by simulations. It was found that a loss of at least 2 dB (compared to a single TRX solution) can be expected due to this, with a catastrophic behaviour if the tolerances are exceeded. Other aspects that may further degrade performance are for further study.

> NOTE: This subclause is deliberately vague to avoid revealing implementation-specific details of the BTS architecture.

9.7.1.2 Processing complexity

The complexity increase due to DSR varies depending on the type and architecture of used receiver and performance requirements for DSR. Next is characterised the complexity of the receiver used for DSR simulations.
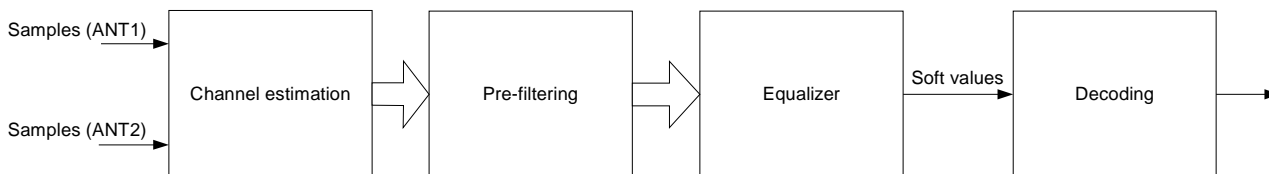
Table 127: Processing complexity estimation for dual symbol rate

Function	Processing demand relation to symbol rate (SR)	Relative to EDGE
Channel estimation	~ SR^2	4 x
Pre-filtering	~ SR^2	4 x
Equalizer	~ SR	2 x
De-coding	~ SR	2 x
Total		**2 - 3 x**

The channel estimate used in the simulated receiver has 11 taps i.e. about twice as much as in EDGE causing added complexity to the channel estimation and pre-filtering. The amount of equalizer states is the same as for EDGE receiver, thus the equalizer complexity is doubled due to symbol rate. The total complexity of inner receiver for DSR is about 3x higher than for EDGE.

The decoding complexity is 2 times higher per timeslot than for 8PSK due to doubled amount of bits.

Total processing complexity of DSR is in order of 2-3 times higher than for EDGE i.e. up to 50 % higher per bit.

9.7.1.2.1 Evaluation of receiver complexity

Above it stated that the receiver complexity for DSR is about up to 50% higher per bit under the condition that the simulated receiver has 11 taps. We think the complexity is different for different propagation models. For TU channel model, the maximum RMS delay is 5.0 μs, its influence to the taps number of channel estimation is smaller than the influence which the shaping pulse filter creates. So when the symbol rate doubles, the receiver taps number is nearly unchanged. But the max RMS delay of HT channel model is 20.0μs which will influence the receiver taps number more seriously than the shaping pulse filter dose, so the simulated receiver has 11 taps, some parameters of pre-filtering is also enlarged to make the complexity of pre-filtering about twice as much as in ordinary 8-PSK.
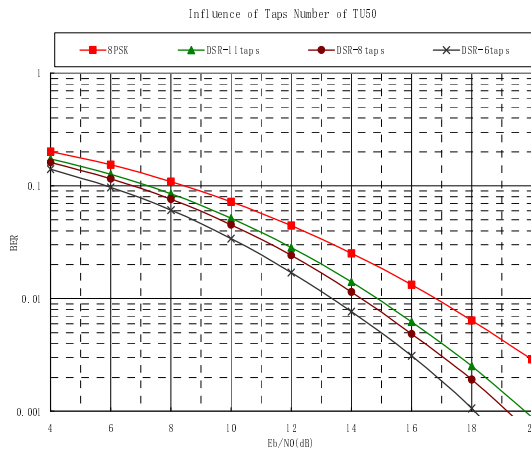
Figure 282: Influence of DSR receiver taps number in TU50 using single antenna
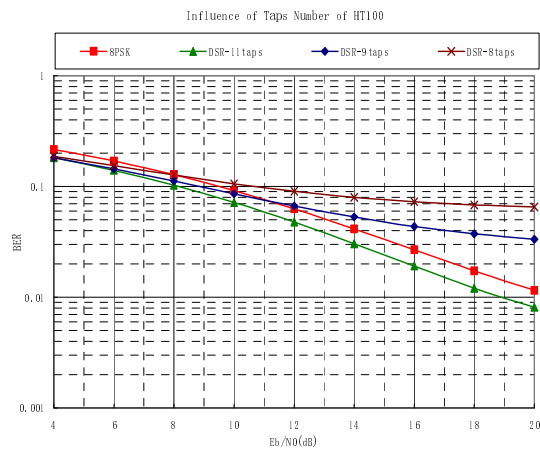
Figure 283: Influence of DSR receiver taps number in HT100 using single antenna
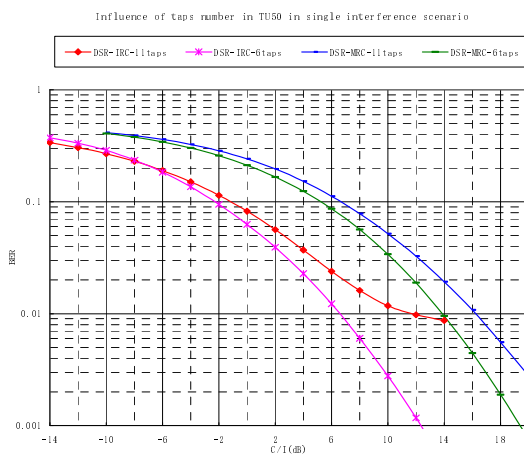
Figure 284: Influence of DSR receiver taps number in TU50 at single interference scenario using two antennas
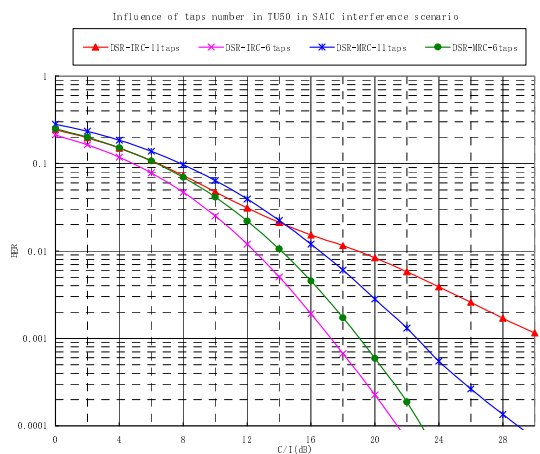
Figure 285: Influence of DSR receiver taps number in TU50 at SAIC interference scenario using two antennas

For convenience, only pay attention to the BER performance. Figure 282 shows the performance of 8-PSK with 6 taps and performance of DSR with taps equal to 6, 8 and 11 in TU50. It's obvious that the performance of DSR with 6 taps is best, just like analysed above. Figure 283 shows that in HT100 using 11 taps cause best performance, and as the number of taps decreases, the performance decreases quickly.

To show the inapplicability of 11 taps in TU50 more clearly, the influence of taps number using two antennas IRC/MRC is also presented, see figures 284 and 285. The performance shows that the influence of taps number is more sensitive when two antennas IRC is used. At high CIR level, performance of 11 taps is very bad and is almost near the performance limit, because 11 taps have exceeded the estimated TU channel length which is about 8T, and longer taps will introduce more noise. Table 128 will show the CIR gain(at BER=4%) using 6 taps against 11 taps at different scenarios.

Table 128: performance gain using 6 taps against 11 taps in TU50 at interference scenarios

Scenarios	Single interference IRC	Single interference MRC	SAIC interference IRC	SAIC interference MRC
Gain	2 dB	2 dB	2.5 dB	2 dB

In summary, for TU channel model the receiver complexity for DSR is as same as for EDGE receiver per bit, and for HT channel model the receiver complexity for DSR is about 50% higher per bit because the complexity of channel estimation and pre-filtering double.

Table 129: complexity estimation for DSR in TU and HT channel model

Function	Relative to EDGE in TU (per bit)	Relative to EDGE in HT (per bit)
Channel estimation	1×	2×
Pre-filtering	1×	2×
Equalizer	1×	1×
De-coding	1×	1×
Total	1×	1.5×

9.7.1.3 MDSR impacts to the transceiver

In simulations a Frequency Domain MMSE equalizer was used. The channel estimate used in the simulated receiver has 9 taps i.e. about 1.5 times as much as in EDGE. The decoding complexity is 2 times higher per timeslot than for 8PSK due to doubled amount of bits. Total processing complexity of MDSR is in order of 2 times higher than for EDGE. Thus it is not increased per bit.

The MDSR may also use two transceiver implementation proposed in [1] with the following changes:

- No need to tune receivers out of 200 kHz raster.

- Narrow reference channel filtering is sufficient.

Sampling rate conversion related symbol rate needs to be considered in DSP.

9.7.1.4 Network implementation issues

The IRC performance which was assumed in the MDSR simulations was based on synchronous networks. However, most networks are asynchronous. IRC performance in asynchronous networks may be lower. Since IRC is a prerequisite for full MDSR performance, simulations would be appreciated which prove that MDSR provides similar gains in asynchronous networks.

Since the MDSR signal occupies two channels, IRC will have to cope with a higher number of interferers, distributed over wider spectrum (at least 2 GSM channels). To assess the MDSR performance under more adverse conditions for IRC, simulations similar to those presented for DTS-2 scenario would be appreciated, however with 2 equally strong adjacent channel interferers at 0 dB power each instead of one adjacent channel interferer at +3 dB.

The MDSR spectrum occupies two channels. This means that MDSR cannot be used on the highest channel of an operator's frequency band. This restriction may have an impact on the frequency planning. MDSR may require other channel assignments or hopping sequences than legacy EGPRS.

Blind detection needs to be extended as shown in subclause 9.2.2.2.

The equaliser would have to cope with:

- a longer impulse response in terms of taps;

- more symbols and, in addition;

- more states per symbol.

9.7.2 Impacts to the PCU

PCU needs to be able to handle double amount of bits per radio slot in uplink. Other impacts to the PCU are minimal e.g. related to the RLC/MAC and resource management.

9.7.3 Impacts to the BSS radio network planning

Without any DSR specific RRM optimisation the DSR can be used for frequency reuses up to 1/1. IRC receiver can typically cope with increased UL interference and voice capacity is not decreased e.g. assuming existing networks employ MRC or have sufficient unused gain from IRC as shown in subclause 9.5.5.

Indeed it is possible to use DSR specific RRM e.g. power control as depicted in subclause 9.5.7, to ensure no impact to voice quality with legacy MRC transceivers.

Possibly some considerations would be needed for edge channels of the operator band e.g. use of DSR/EGPRS is restricted at edge channels by punctured MA list , i.e. the applicable MA list will depend of the service.

With the new punctured MA list, there will be collisions in the used frequencies in the hopping patterns because of unequal number of hopping frequencies in the hopping lists [7].

The dual symbol rate benefits from synchronised BSS for tightest frequency reuses, as does AMR with SAIC.

Performance in asynchronous networks is FFS. It could be assumed that DSR power control can be optimised for asynchronous networks as well.

Neighbouring base stations on the same band with DSR should preferably use interference rejection combining, and so would be more robust against uplink interference from other cells. This may not be possible by all legacy transceivers, e.g. MRC receivers thus RRM e.g. power control may be used to cope with it.

Thus DSR does not need changes on the existing frequency planning and DSR may be enabled like any plug and play feature to the existing networks.

9.8   Impacts to the core network

No impacts.

9.9 Impacts to the specification

The impacted 3GPP specifications are listed in table 130.

Table 130: Impacts to the 3GPP specifications

Specification	Description
3GPP TS 43.064	GPRS Stage 2
3GPP TS 44.018	Radio Resource Control (RRC) protocol
3GPP TS 44.060	Radio Link Control / Medium Access Control (RLC/MAC) protocol
3GPP TS 45.001	Physical layer one radio path; general description
3GPP TS 45.002	Multiplexing and multiple access on the radio path
3GPP TS 45.003	Channel Coding
3GPP TS 45.004	Modulation
3GPP TS 45.005	Radio Transmission and Reception
3GPP TS 45.008	Radio subsystem link control

9.10   Possible enhancements

9.10.1   Dual Symbol Rate in downlink

The deployment of DSR in DL as well would need either high diversity terminal penetration or dedicated band and radio resources for DSR users. Both of these are pretty unrealistic in release 7 timeline. Indeed dual carrier offers already similar throughput gain in DL.

9.11   Compliance to the objectives

Following tables summarise compliancy to the objectives given in subclauses 4.2 and 4.3.

Table 131: Compliance with performance objectives for DSR

Objective	Required value	Evaluated result for DSR	Compliance
Spectrum efficiency/capacity gain	> 50 %	80 % for data (in BCCH scenario)	Compliant
Peak data rate increase	100 %	100 %	Compliant
Sensitivity increase in DL	3 dB	N.A.	N.A.
Mean bit rate increase at cell edges	> 50 %	51 % to 57 %(coverage) 54 % (3/9 reuse scenario)	Compliant
Initial RTT (=Idle RTT)	< 500 ms	N.A.	N.A.
Active RTT	< 150 ms	N.A.	N.A.
In balance with RTT-bit rate-product and TCP window	N.A.	4 DSR slots need about 150 ms RTT	Compliant
In balanced with downlink improvements	N.A.	DSR is a counterpart of dual carrier	Compliant
Mean improvements relative to peak improvement	N.A.	"Mean to peak improvement ratio" is > 0.85	Compliant

Table 132: Compliance with performance objectives for MDSR

Objective	Required value	Evaluated result for MDSR	Compliance
Spectrum efficiency/capacity gain	> 50 %	120 % to 190 % at 10th (worst) percentile session bitrate of 100 kbit/s (90 % to 150 % for 2 TRX implementation)	Compliant
Peak data rate increase	100 %	100 %	Compliant
Mean bit rate increase at cell edges	> 50 %	90 % (coverage limited) 67 % (capacity limited)	Compliant

Table 133: Compliance with compatibility objectives for DSR

Objective	Evaluated result for DSR	Compliance
Coexist with existing legacy frequency planning	Applies to re-uses up to 1/1 (related to normal 200 kHz carrier). Only edge channels of operator band allocation need to be considered.	Partially compliant
Multiplexing with legacy EGPRS	Provides seamless UL multiplexing	Compliant
Avoid impacts on existing BTS, BSC and CN hardware (Upgradeable by SW only)	TRX DSP complexity is 2 - 3 x higher and TRX/RX path needs sufficient bandwidth and sampling rate.	FFS
Be based on the existing network architecture		Compliant
Be applicable also for Dual Transfer Mode	The DSR/GMSK switching can be performed within guard period.	Compliant
Be applicable for the A/Gb mode interface		Compliant

Table 134: Compliance with compatibility objectives for MDSR

Objective	Evaluated result for DSR	Compliance
Coexist with existing legacy frequency planning	1/3 evaluated. The uppermost channel of operator's band allocation may not be used.	Compliant
Multiplexing with legacy EGPRS	Provides seamless UL multiplexing and incremental redundancy with EGPRS.	Compliant
Avoid impacts on existing BTS, BSC and CN hardware (Upgradeable by SW only)	TRX DSP complexity is 2 times higher and 2 TRX option can be used.	Compliant
Be based on the existing network architecture		Compliant
Be applicable also for Dual Transfer Mode	The DSR/GMSK switching can be performed within guard period.	Compliant
Be applicable for the A/Gb mode interface		Compliant

9.12 References

[1]   AHGEV-010 "Dual Symbol Rate for GERAN evolution", Nokia.

[2]   3GPP TS 25.101 "User Equipment (UE) radio transmission and reception (FDD) (Release 6)".

[3]   GP-052657 "Uplink enhancements for GERAN evolution", Ericsson.

[4]   GP-060189: "DSR performance in legacy MRC network", Nokia.

[5]   GP-060775: "Modified Dual Symbol Rate Concept for Future GERAN Evolution", Nokia.

[6]   GP-060816: "Implementation aspects of Dual Symbol Rate", Ericsson.

[7]   GP-060817: "Updates to Dual Symbol Rate", Siemens.

[8]   GP-060729: "DSR Receiver Synthesis Using Dual-Carrier Architectures" Motorola.

[9]   GP-060699: "Dual Symbol Rate Link Level Simulation Results" Huawei.

10 Latency enhancements

10.1 Introduction

Four different enhancements are studied and evaluated:

-   Improved ACK/NACK reporting.

-   Reduced Transmission Time Interval (TTI).

-   Variable sized Radio Blocks.

-   Hybrid ARQ.

The enhancements reduce overall latency and have a second order effect on mean/average and peak bit rates as reduced latency (i.e. lowering the round trip time) may provide better throughput if the bit rate on the link becomes so high that the maximum buffer window size limits the transmission rate.

The improved ACK/NACK reporting and hybrid ARQ mainly provide reduced latency in non-ideal radio conditions, as the number of re-transmissions is almost zero in ideal conditions. The reduced TTI and Variable sized radio blocks takes effect in both non-ideal radio conditions and ideal radio conditions.

10.1.1 Performance gains

10.1.1.1 Web-browsing

Tests have been performed using a "frozen" CNN-test page of a size 137 kB built by 37 objects. Results of "time to download" the web page have been obtained as a function of different latency and bit rate combinations. The values are based on measured results in lab with interpolation of values in-between.

Figure 286 shows the download time as a function of throughput that are based on measurements with throughput 40 kbps (web download time 51 s; not shown in figure 286) and 200 kbps (web download time 25 s).
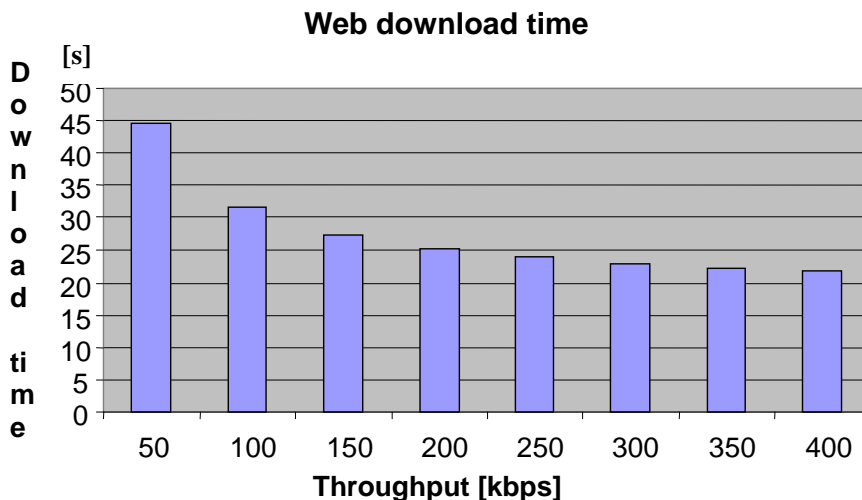
Web download time

**Figure 286: Web download time depending on throughput
with fixed latency/RTT of 400 ms as measured by PING**

At higher throughputs the gain is reduced since the latency becomes the limiting factor.

Figure 287 shows results for download time versus latency/RTT. The result is based on lab measurements with latency 400 ms (web download time 25 s) and 150 ms (web download time 12.5 s). The latency was measured by PING command.
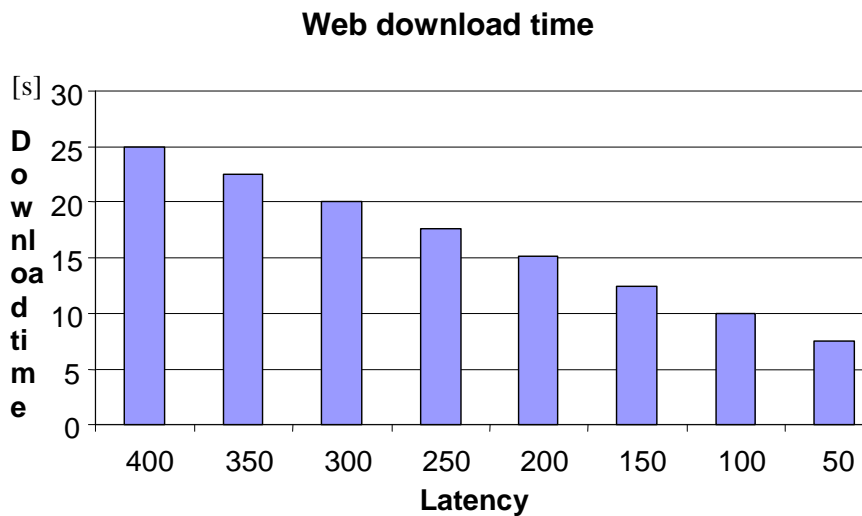
Web download time

Figure 287: Web download time depending on latency with fixed throughput of 200 kbps

Figure 287 shows that the download time is substantially decreased when latency is decreased. When latency reaches zero the download time will be limited by the throughput.

Figure 288 shows download time versus throughput. The RTT/latency have been fixed to 100 ms and the values are based on results from figures 286 and 287.
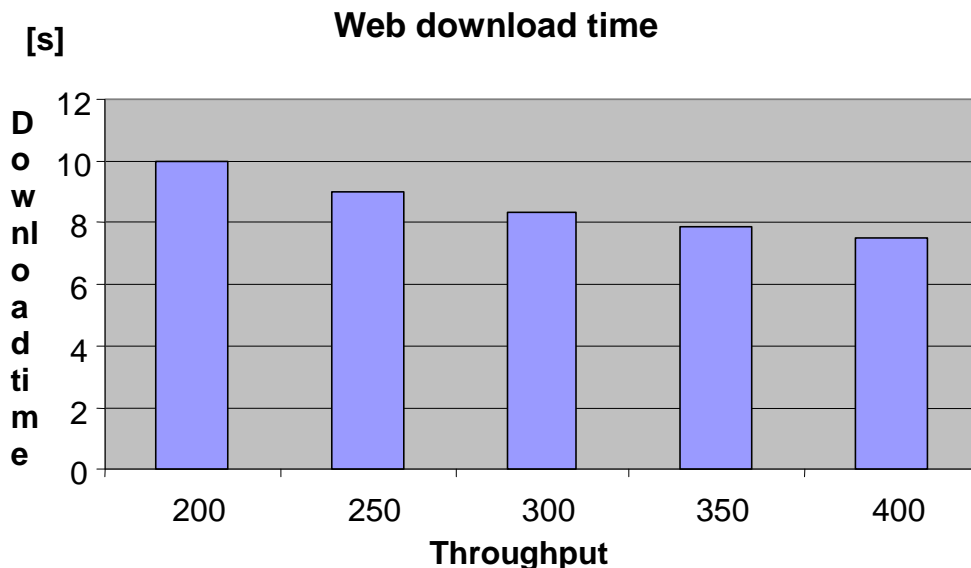
Figure 288: Web download time depending on throughput with fixed latency/RTT of 100 ms

10.1.1.2 Delay estimations

Figure 289 shows a sequence chart containing GERAN interfaces identifying the interfaces for possible delay reductions in GERAN, namely Abis and Um. The Abis interface is typically not a matter of standardisation but have an important role. Delay estimations for a few cases are shown below for different cases including a VoIP case end-to-end, i.e. mouth-to-ear. The latter case can be found in table 4. Note that these cases do not consider multiplexing issues between 10 ms and legacy 20 ms users.
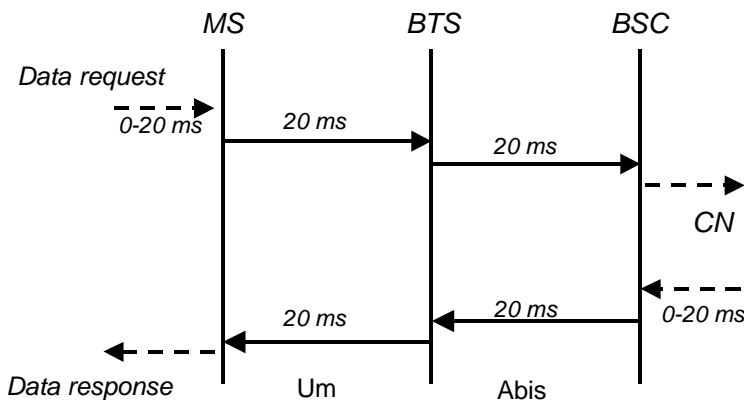
**Figure 289: Indicative delays in GERAN network for a time slot
Note that it is assumed that the Abis delay is the same as the TTI value**

Table 135 shows a delay scenario of typical existing deployments including assumed node delays. It is calculated from when a BSC/PCU has received a packet starting to send it to the MS assuming the RLC block included a poll with RRBP=13, and ending when an answer has been received.

Table 135: Round trip time existing specifications assuming an Abis of equal transmission time as on the radio interface. Node processing time is included (all values in [ms])

Direction	BSC/PCU	Abis	BTS	Um	MS	SUM [ms]
BSC/PCU→		20	< 5	20		40 to 45
←MS		20	< 5	20	40	80 to 85
SUM		40	< 10	40	40	120 to 130

With up to 5 ms BTS delay the RTT becomes 130 ms. It differs with 10 ms from the 120 ms value contained in 3GPP TS 44.060 [1].

Table 136 contains the same basic assumptions as in table 135, but shows instead the delay of transmitting a packet from the BSC/PCU to the MS when the first packet was received in error and a retransmission was needed.

Table 136: Round trip time with one retransmission (20 ms TTI in Um and Abis) (all values in [ms])

Direction	BSC/PCU	Abis	BTS	Um	MS	SUM [ms]
BSC→		20	< 5	20		40 to 45
←MS		20	< 5	20	40	80 to 85
BSC/PCU→	< 10	20	< 5	20		40 to 55
SUM	< 10	60	< 15	60	40	160 to 185

The resulting RTT is in the range 160 ms to 185 ms.

Table 137 determines the delay for the same scenario as in table 136 but using the latency enhancements in [2], i.e. a reduced TTI of 10 ms and also including an Abis delay reduction to the same level as the TTI. The reaction time of MS is one TTI period (similar to RRBP=8/9).

**Table 137: Latency enhancements of 10 ms TTI including reduced Abis delay
with one retransmission and event-based Ack/Nack (all values in [ms])**

Direction	BSC/PCU	Abis	BTS	Um	MS	SUM [ms]
BSC→		10	< 5	10		20 to 25
←MS		10	< 5	10	10	30 to 35
BSC/PCU→	< 10	10	< 5	10		20 to 35
SUM	< 10	30	< 15	30	20	70 to 95

Table 138 determines the delay for the same scenario as in table 136 but using the latency enhancements in [2], i.e. a reduced TTI of 10 ms and keeping the Abis delay to 20 ms. The reaction time of MS is one TTI period (similar to RRBP=8/9).

**Table 138: Latency enhancements of 10 ms TTI, 20 ms Abis, including
with one retransmission and event-based Ack/Nack (all values in [ms])**

Direction	BSC/PCU	Abis	BTS	Um	MS	SUM [ms]
BSC→		20	< 5	10		30 to 35
←MS		20	< 5	10	10	40 to 45
BSC/PCU→	< 10	20	< 5	10		30 to 45
SUM	< 10	60	< 15	30	20	100 to 125

The resulting RTT (BSC->MS->BSC) is in the range 50 ms to 60 ms and assuming one retransmission the total transmission time is in the range of 70 ms to 95 ms.

Table 139 shows a end-to-end delay, mouth-to-ear, for a VoIP service that utilises the latency enhancements and if these are not used (legacy case). Note that it is assumed that one retransmission is enough, as incremental redundancy would enable feasible frame error rates for speech. The use of the IR functionality allows for a better radio resource usage than using a pure un-acknowledgement mode.

**Table 139: Delay budget for end-to-end conversational delay (VoIP)
for shorter TTI case and the legacy case**

Leg	Delay (shorter TTI etc.)	Delay (normal TTI etc.)
A-party MS/GERAN	95 ms	185 ms
CN/Transit including Gb	50 ms	50 ms
B-Party MS/GERAN	95 ms	185 ms
SUM	240 ms	420 ms

The result is in the order of 240 ms. The required value for satisfied users is around 200 ms to 300 ms according to ITU-T Recommendation G.114 [3]. The result in table 4 is within that range.

10.1.1.3 Email

There are number of email protocols defined, including X400, IMAP, and POP (ref [1]). Of these, the widest used are POP and IMAP. This document considers some performance issues of the POP3 protocol. First the use case of a user downloading email headers from a server is considered. Then the use case of a user downloading email content is considered.

10.1.1.3.1 Download of Email Headers

Initially the user is able to download the message headers, in order to quickly decide which emails should be downloaded in their entirety.

Assumptions are as follows:

Item	Value	Note
Coding Scheme on downlink	MCS-8 or MCS-9	permits at least 130 octets/ MAC PDU
Timeslot allocation	4 down, 1 up	
E-mail download protocol	POP3	
Average message header size	500 octets	Including protocol overhead. Requires 1 RLC frame period @ 4 slots

The POP3 command sequence used to download message headers is defined in ref [4], of which the following is an illustration (C: indicates command from client, S: response from Server):

```
C: TOP 1 2
S: +OK
<the POP3 server sends the headers of the message, a blank line, and the first 2 lines of the body
of message 1>
C: TOP 2 2
S: +OK
<the POP3 server sends the headers of the message, a blank line, and the first 2 lines of the body
of message 2>
… etc
```

Assuming that there are N email messages, the number of application layer message and radio data transfer time T_{trnsf} is as shown below:

Message	Size	Time/msg	Number	Total Time
TOP command from client	small	20ms	N	$N \times$ 20ms
response to TOPfrom server	500 octets	20ms	N	$N \times$ 20ms
Total (T_{trnsf})				$N \times$ **40ms**

The number of synchronous application protocol turnarounds (i.e. events where an application level transmitter has to wait for a response before proceeding), is denoted, P_t and:

$$P_t = 2N$$

That is, between the TOP and the subsequent response there is one synchronous turnaround event, as the client waits for the server to respond. Then there is another turnaround event before the client sends the subsequent TOP command, and so on.

Existing value of 20 ms TTI

Assuming the availability of high speed broadband links, it is assumed that transaction time is dominated by the radio interface. The minimum transaction time on the radio interface is computed by:

(time for data transfer T_{trnsf})+ (minimum protocol turnaround time)

$= N \times 40$ ms $+ P_t \times$ (minimum wait for next RLC block period)

$= N \times 40$ ms $+ 2N \times 20$ ms

For 100 email message headers, this yields 8 sec.

Advantage of 10 ms TTI

In this case minimum wait for next RLC block period is 10ms. Minimum transaction time is:

$= N \times 40 \text{ ms} + 2 \, N \times 10 \text{ ms}$

For 100 email message headers, this yields 6 sec

From the point of view of the user, the waiting time is reduced by a perceptible 25 %.

Note that this analysis assumes the TTI reduction on the radio interface can also be supported in on other parts of the network. Also note also that the time to transfer should be reduced to 30 ms (=20 ms + 10 ms) since assumption should be that TTI for both uplink and downlink is 10ms, and the small request message can be transmitted uplink in this time.

10.1.1.3.2　　　Download of Email Content

After the download of the email headers, the client typically downloads the emails. This may take place in the background, allowing the user to examine the headers for priority. Nevertheless, the faster this can be done the better.

Assumptions are as follows:

Item	Value	Note
Coding Scheme on downlink	MCS-8 or MCS-9	permits at least 130 octets/ MAC PDU
Timeslot allocation	4 down, 1 up	
E-mail download protocol	POP3	
Average message download size	3 000 octets	Including protocol overhead. Requires 1 RLC frame period @ 4 slots

In order to very large messages blocking smaller ones for unlimited periods of time, it is assumed that some strategy is adopted such as limiting the download message size. Other strategies may be used, for example modifying email content at the server to suit mobile device characteristics. Therefore in this analysis the time taken to download a set of messages of average size 3 000 octets is considered.

The POP3 command sequence used to download messages is illustrated in ref [4], of which the following is an extract (C: indicates command from client, S: response from Server):

```
C:    RETR 1
S:    +OK 120 octets
S:    <the POP3 server sends message 1>
S:    .
C:    DELE 1
S:    +OK message 1 deleted
C:    RETR 2
S:    +OK 200 octets
S:    <the POP3 server sends message 2>
S:    .
C:    DELE 2
S:    +OK message 2 deleted
   (etc, repeated once for each message)
C:    QUIT
```

Assuming that there are N messages, the number of application layer message and radio transmission time is as shown below:

Message	Size	Time/msg	Number	Total Time
RETR from client	small	20ms	N	$N \times$ 20ms
response to RETR from server	3000 bytes	120ms	N	$N \times$ 120ms
DELE from client	small	20ms	N	$N \times$ 20ms
response to DELE from server	small	20ms	N	$N \times$ 20ms
Total				$N \times$ **180ms**

The number of synchronous application protocol turnarounds (i.e. events where an application level transmitter has to wait for a response before proceeding), is denoted, P_t and since there are 2 commands and 2 responses sent per email:

$$P_t = 4N$$

By the same reasoning as above, the time to receive 100 message would be the following:

- At 20ms TTI: 26 sec.

- At 10 ms TTI: 22 sec (15 % improvement).

- At 5 ms TTI: 20 sec (23 % improvement).

Note that this analysis assumes client request messages are short and 10 ms TTI should be allowed for uplink transmission. Transmission time above should thus be 160 ms instead of 180 ms.

10.1.1.4 Impact to TCP performance

10.1.1.4.1 Introduction

Reducing the latency is not only important for VoIP but also for other services, notably those run over TCP/IP. The purpose of this subclause is to show that reduced latency is also important for FTP and HTTP applications that use TCP. To this end, simulations have been made on a model of the BSS and CN to obtain values of the user bit rate and download times for these applications.

10.1.1.4.2 System model and TCP parameters

We begin by describing the simulation network topology and method.

RTT simulations using constant bit rates are performed using a simplified model of GERAN and the CN, see figure 290. We only consider RLC retransmissions, the most important loop.
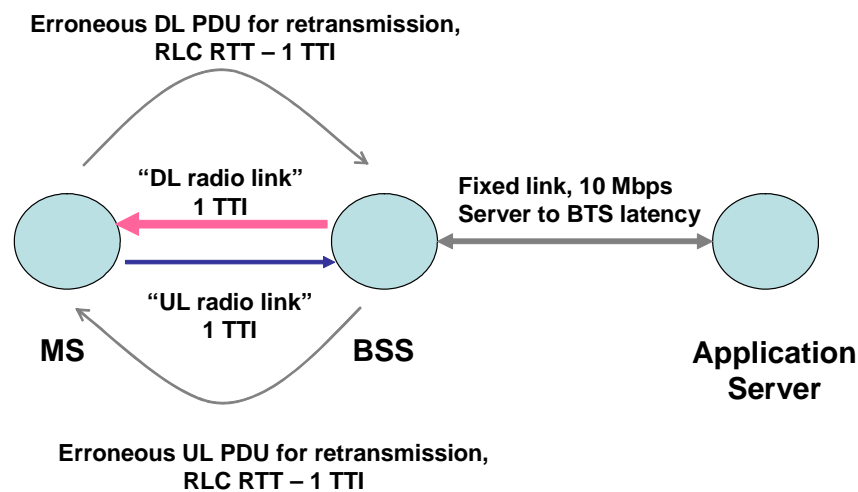
Figure 290: Simulation network topology

The purpose of the simulations is to obtain end-2-end bit rates and download times as functions of RLC RTT and "Server to BTS latency". The latter is a one way delay, whereas RLC RTT is a delay loop in UL and DL. More precisely, the RLC RTT is the delay from a TTI is received until erroneous PDUs are filtered out for retransmission plus one TTI, i.e. it includes processing delay, delay for sending RLC NACKs/ACKs and an immediate retransmission. Furthermore, Server to BTS latency is the time from an IP packet is sent from the server to it is available in the buffer for the first transmission over the radio.

The radio link model can be described as follows: IP packets are segmented into PDUs in the BTS node, and a TTI contains a number of PDUs. The number of PDUs depends on the channel bit rate and PDU size. The simulator waits TTI ms and determines which PDUs are erroneous. The erroneous PDUs are scheduled for retransmission (RLC RTT - 1 TTI) ms later.

A PDU is determined to be erroneous or not by drawing a uniformly distributed random number between 1 and 100. If the random number is less than a constant "target number" (BLER), this PDU is considered as erroneous, and is thus scheduled for retransmission (RLC RTT - 1 TTI) ms later. The errors of the following PDUs are independently generated. We assume that an unlimited number of retransmissions can occur, and that the RLC buffer and window size are unlimited. PDUs for retransmission are prioritized over PDUs that are waiting for a first transmission. The possibility that NACKS are erroneously interpreted in the Node B (which would lead to unnecessary RLC retransmissions) is **not** modelled. IP packets are forwarded to the upper layers in-sequence.

The DL and UL bit rates are assumed to be constant. Two sets of rates are used in order to show the impact of RTT on the PHY improvements suggested. To this end, standard MCS-6 EDGE rates in a 4+2 timeslot configuration is compared to an GERAN Evolution counterpart with four times higher bit rate.

The radio link parameters are summarized in table 140.

Table 140: System parameters

Parameters	GERAN ev.	EDGE
DL bit rate [kbps]	454.4	113.6
UL bit rate [kbps]	227.2	56.8
DL PDU size [bytes]	142	71
UL PDU size [bytes]	71	71
In sequence delivery	Yes	Yes
TTI [ms]	20	20
DL and UL BLER [%]	10	10

The BLER value is important: a reduction to 1% will essentially remove the impact of RLC RTT, but the capacity will be lower. We only use a 20 ms TTI value here, this is not important for the performance results shown later. However, a 10 ms TTI would enable lower RLC RTT values; these are just assumed below.

The TCP settings are shown in table 141.

Table 141: TCP settings

TCP settings	
TCP version	NewReno
Packet size [bytes]	1500
TCP initial cwnd [packets]	2
TCP max cwnd [packets]	42
TCP ssthresh [packets]	40
ACK delay at receiver [ms]	100
Min RTO [sec]	1.0

There are no packet losses in the network. The TCP ssthresh is the window size at which TCP enters congestion avoidance. Hence, up to ssthresh TCP window increases exponentially and after ssthresh the TCP window increases linearly. Generally, TCP is in the exponentially increasing phase at all times in the simulations performed in this contribution.

The TCP timeout timer (Retransmission Timeout, RTO) is set to 1 s, timeouts do only occur for the largest values of RLC RTT.

10.1.1.4.3 FTP performance

First we consider an ftp application. An ftp download of 100 kB application data is performed 10 times. Figure 291 displays the end-2-end average bit rates for EDGE MCS-6. Rates above 90 kbps are obtained for RLC below 100 ms if the Server to BTS delay (one way) is low, but the decay of the bit rate with delay is rather slow for these PHY (radio link) rates as expected.

Higher PHY rates are more sensitive to delays as shown in figure 292, which shows the corresponding results for the four times faster GERAN Evolution (GEV) radio link. For low latencies peak rates exceed 280 kbps, and these are substantially reduced if the RTT is higher. The reductions are of the order of 30 % to 40 % if the RLC RTT increases from 50 ms to 300 ms depending on the Server to BTS latency. The gains are larger if the latter (one-way) delay is smaller: up to 80 % in some cases by reducing the RLC RTT from 300 ms to 50 ms.

Figure 293 displays the GEV result in a different form. The jerk in the curve at 300 ms RLC RTT and 50 ms Server to BTS latency is due to a TCP timeout occurring once out of 10 simulations.

It is concluded that reducing the RLC RTT to exploit the increased link rates in GEV is important also for the FTP application. It is also important to reduce the Server to BTS delay.
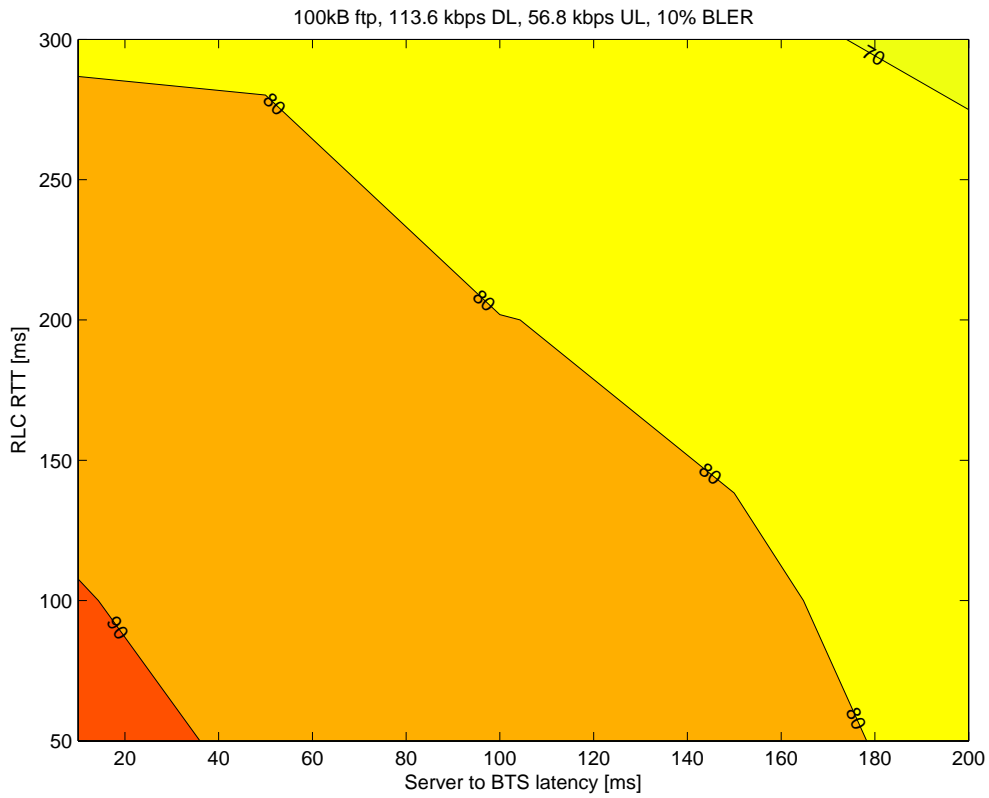
Figure 291: Ftp: average bit rate in kbps for EDGE.
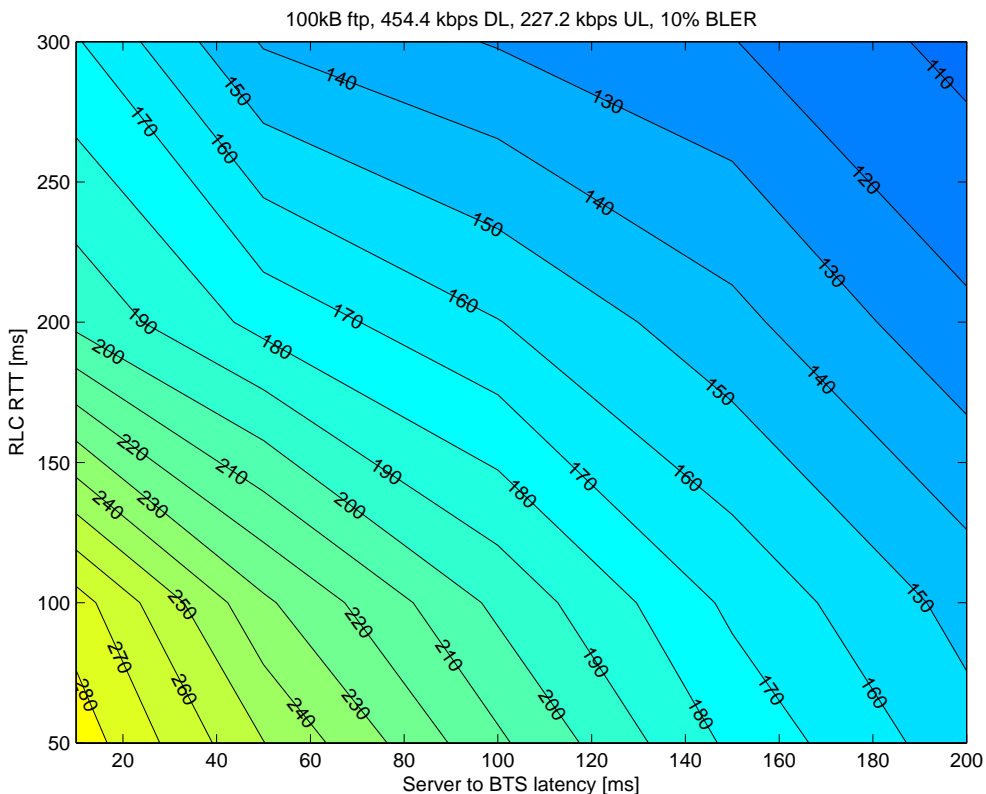
Figure 292: Ftp: average bit rate in kbps for GEV.
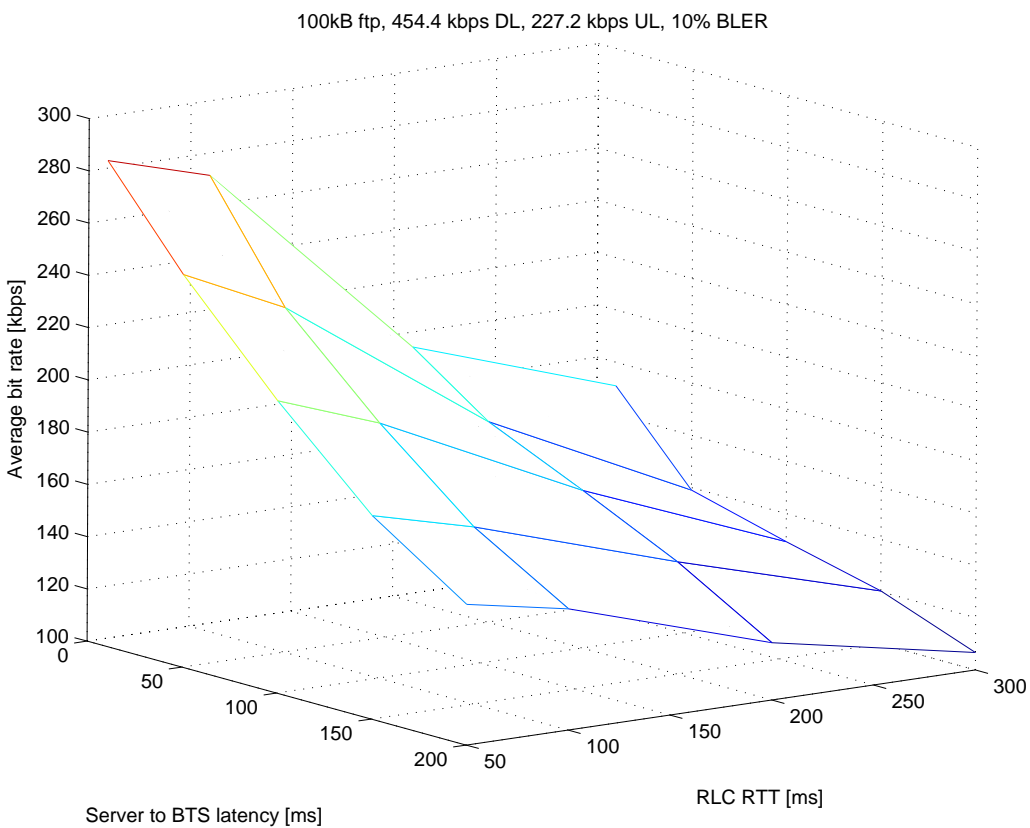
Figure 293: Ftp: average bit rate in kbps for GEV.

10.1.1.4.4 HTTP download

Next we consider download of a WEB page (http). The format of the web page is shown in table 142.

Table 142: WEB page

WEB page	
Number of objects	8
Packet size [bytes]	1 500
Size object 1 [packets]	41
Size object 2 [packets]	45
Size object 3 [packets]	8
Size object 4 [packets]	7
Size object 5 [packets]	4
Size object 6 [packets]	4
Size object 7 [packets]	3
Size object 8 [packets]	2

The HTTP download is only performed once. The WEB page objects are downloaded in sequence, i.e. the download of the second object starts after the first object has been completely downloaded. For the HTTP we show download times rather than bit rates to get an indication of the user experience.

The download time for the WEB page in table 135 is shown in figure 294 as a function of the Server to BTS latency. The reduction of download time varies between 40 % to 60 % as server to BTS latency is reduced from 200 ms to 10 ms, with lager reductions the lower the RLC RTT.

The same results for constant Server to BTS delays are shown in figure 295. The reduction of download time varies between 25 % to 50% if RLC RTT is reduced from 300 ms to 50 ms, with larger reductions the lower the Server to BTS latency.

In the extreme case the download reduces from 30.3 sec to 8.8 sec if both RLC RTT and Server to BTS latency is reduced simultaneously.
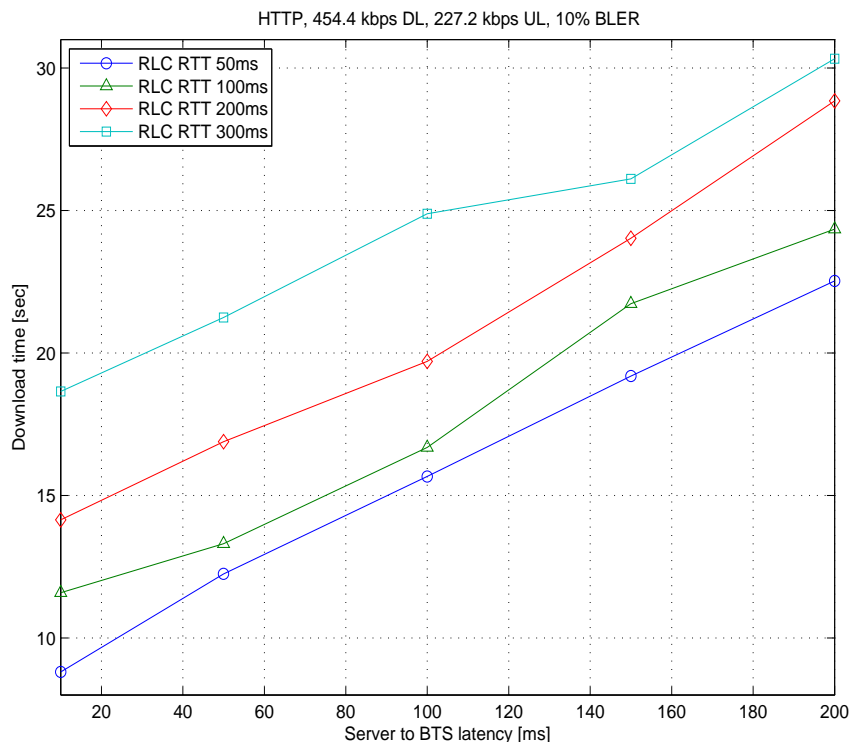
Figure 294: HTTP download time
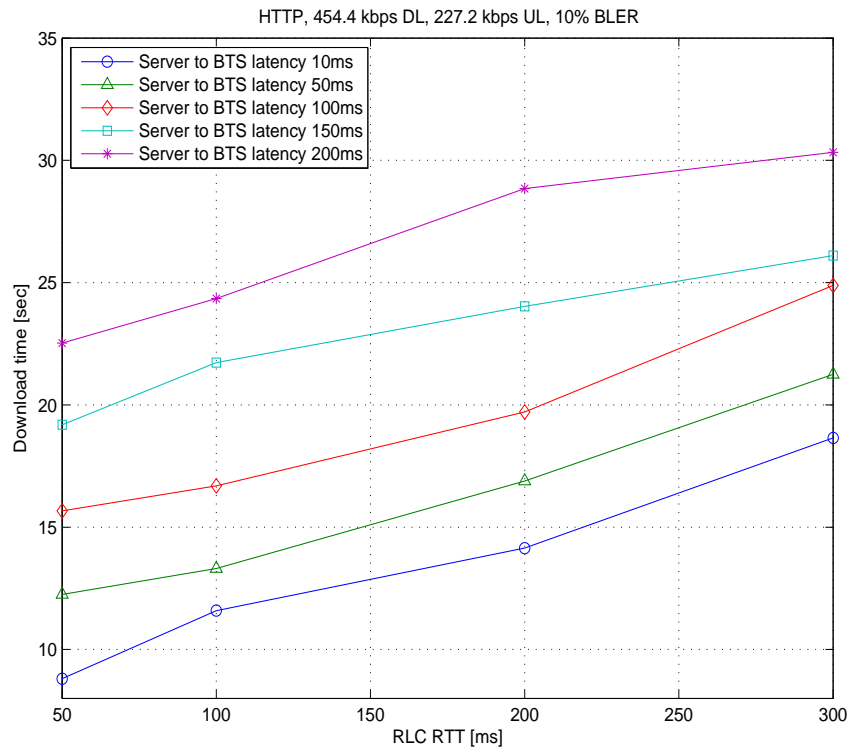
Figure 295: HTTP download time.

Like for the FTP application, it is concluded that the HTTP application will also benefit from the GEV PHY if the latency is reduced.

It is noted that the TCP performance as a function of the delays defined above will not change if the TTI is reduced, but a reduction of the TTI will make it possible to attain lower values of the RLC RTT and the Server to BTS latency. The gains will increase then, and the GEV PHY improvements will be exploited.

10.1.1.4.5 Measured delays in BSS and CN

The above results have shown the importance of reducing the RLC RTT and Server to BTS latency. The BSS to MS delay is indeed the major contributor to the delay, at least in the current network implementations.

To give an idea about the delay values some measurement data is presented below. The measurements were taken using a Nokia 6230 TEMS connected to a PC in a lab environment with a single EDGE capable TRX and a 4*64 kbps dynamic ABIS pool. 855 PING (32 Bytes) requests were captured. There was no other traffic in the network.

The results show that the CN delay (RTT_Gb_Gb: observed on Gb uplink to seen on Gb downlink) is about 1.5 % of the total PING delay to the DNS server. The downlink BSC delay is larger than UL due to TBF allocations.

The RTT_MS_MS (total round trip) varied between 540 ms to 1 200 ms, whereas the RTT_Abis_Abis (Abis up to Abis down) varied from about 70 ms to 190 ms. Hence the BSS to MS is the major contributor to the end-2-end delay.

The measurements indicated that the RLC_RTT constitutes the main part of the delay. It is likely that the PC-MS PPP link delay and the MS processing delay is significant, but that could not be measured.

10.1.1.4.6 The importance of the PING size

The average end-2-end RTT is important for TCP, but the smaller PING sizes do not show the impact of the RLC RTT for TCP. A 64 byte PING will be contained in a single PDU, whereas a 1 500 Byte PING is segmented into many PDUs where the probability that at least one of them is retransmitted is substantially higher.

To show this effect we consider PING sizes of 64 and 1 500 Bytes, respectively. In the simulations, the end-2-end RTT is measured 50 times and the time between the pings are set to 2.002 sec. By the 2 ms extra wait between the PINGs, the time that the IP packets arrive to the buffer for first transmission over the radio is phase shifted compared to the TTI clock. Hence, in average each packet will wait ½ TTI before next TTI is sent.

Figure 296 shows the average end-2-end delay as a function of the RLC RTT and the Server to BTS latency for a 64 Byte PING. Note that there is hardly any dependence on the RLC RTT since retransmissions occurs infrequently. Even though the GERAN evolution RTT requirement is 100 ms, it is worth to notice that at 50 ms RLC RTT and 10 ms Server to BTS latency the average end-2-end RTT is around 90 ms.
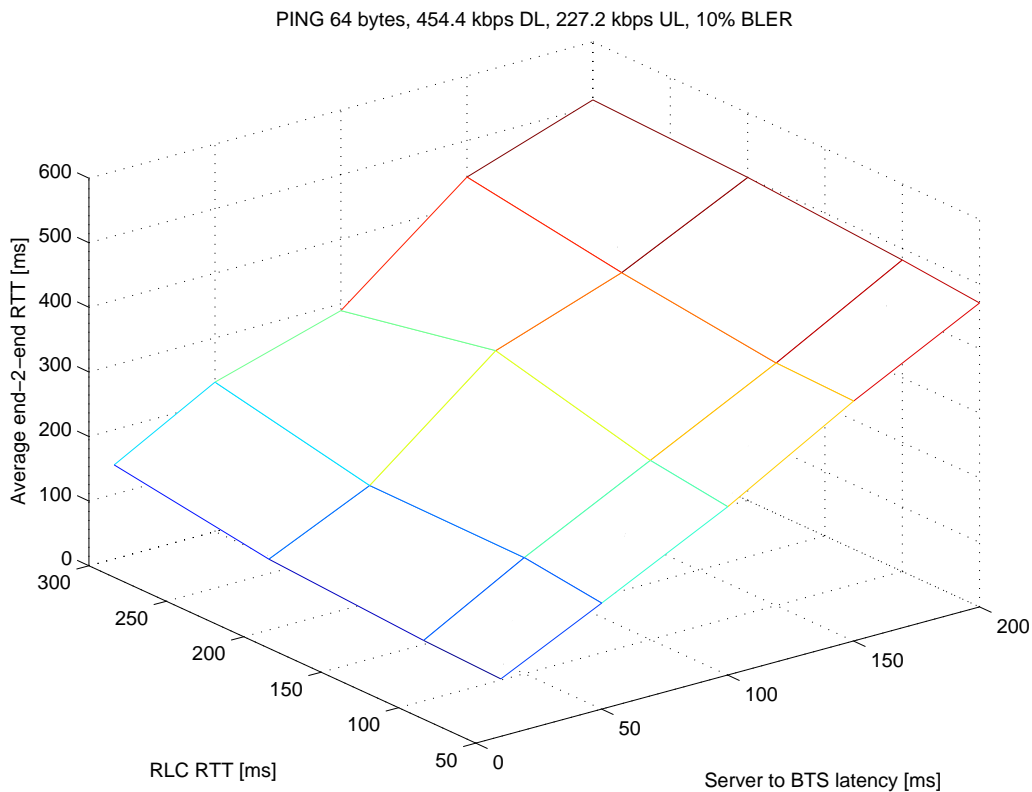
Figure 296: Average end-2-end RTT

The results for a 1 500 Byte PING are shown in figure 297, which clearly shows the effect of an increased RLC RTT on the average end-2-end RTT.

Figures 298 and 299 show the minimum observed end-2-end delay. For the 64 Byte PING there are no retransmissions over the radio link and essentially no dependence on RLC RTT. The increase of the delay for higher RLC RTT that can be observed in figure 299 are due to none of the 50 IP packets are transferred without RLC retransmissions, which indicates the high probability of retransmissions for large IP packets. Thus, for TCP traffic, it is not enough to put a requirement on PING RTT of small packets, since RLC RTT may be high and give poor TCP throughput.

PING 1500 bytes, 454.4 kbps DL, 227.2 kbps UL, 10% BLER
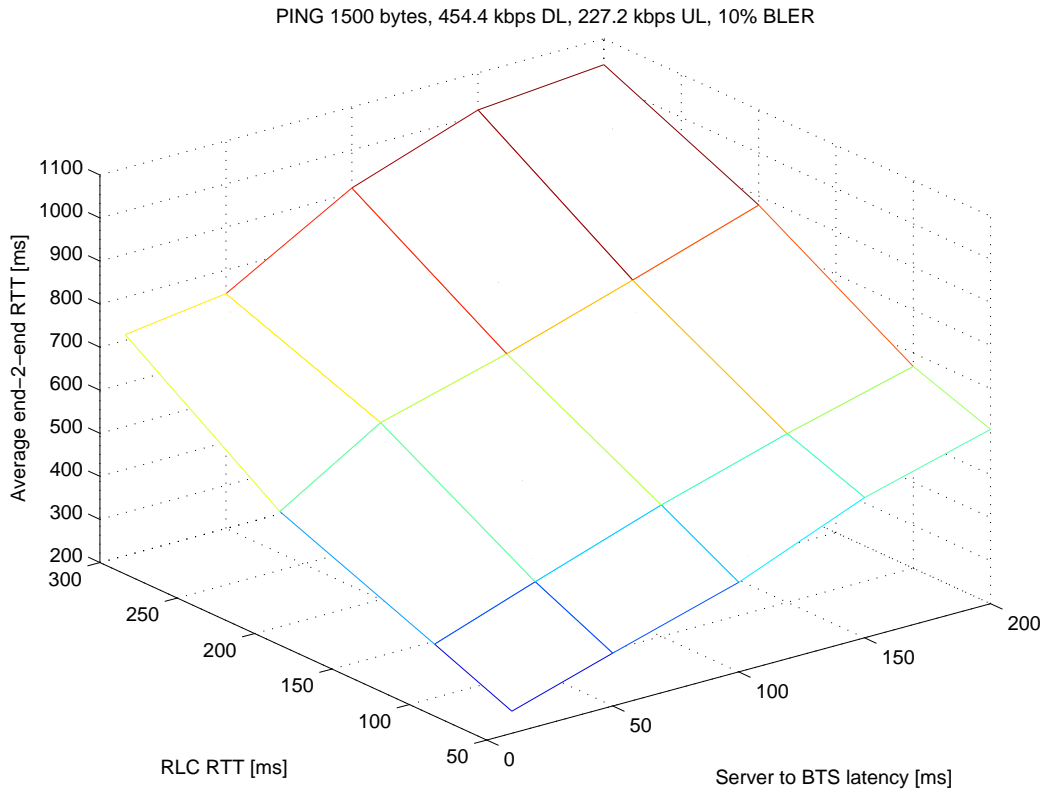
Figure 297: Average end-2-end RTT for 1 500 bytes IP packets (including header)

PING 64 bytes, 454.4 kbps DL, 227.2 kbps UL, 10% BLER
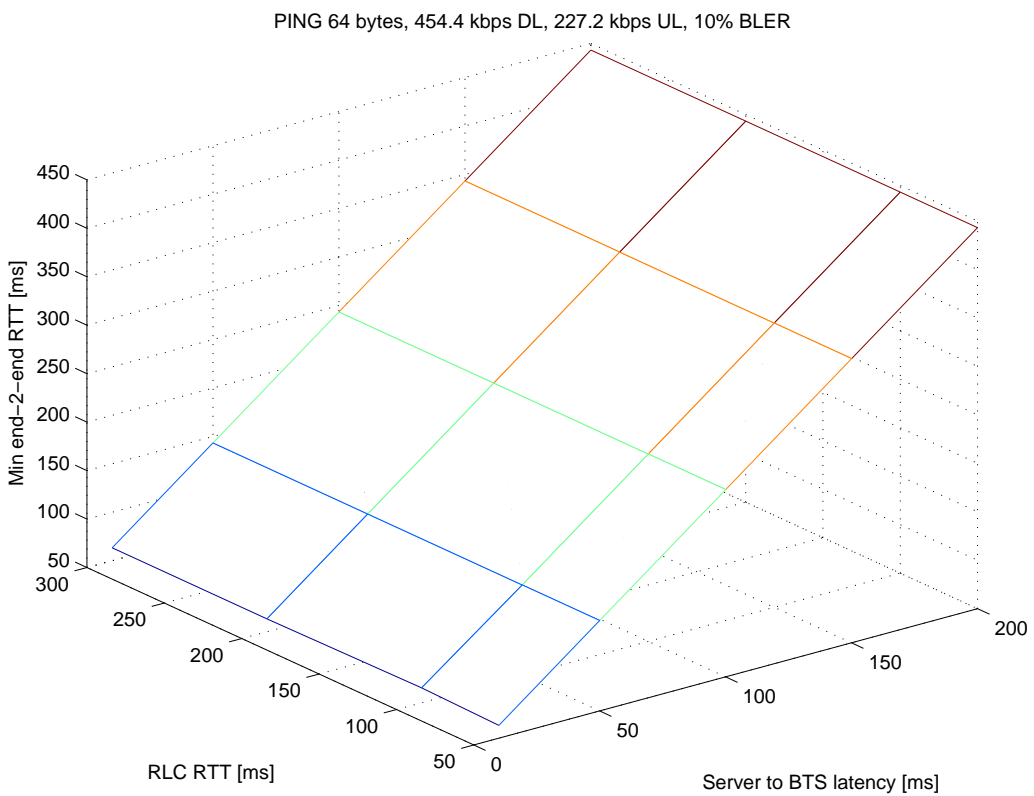
Figure 298: Minimal observed end-2-end RTT for 64 bytes IP packets (including header)
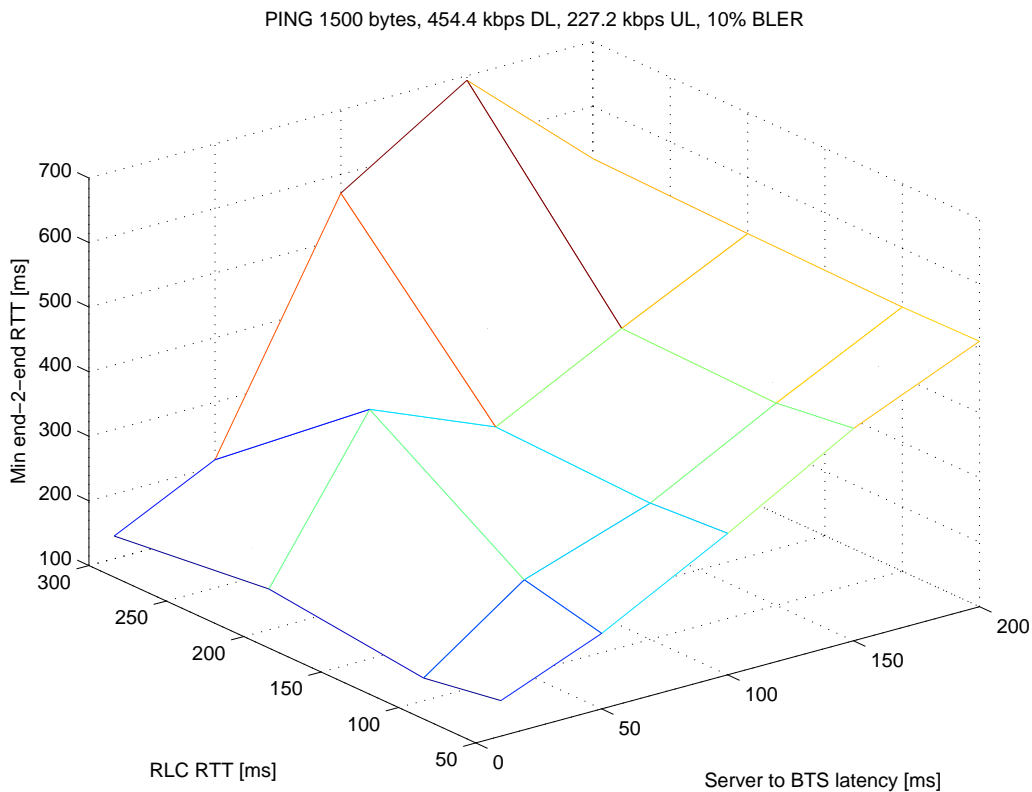
Figure 299: Minimal observed end-2-end RTT for 1 500 bytes IP packets (including header)

10.2   Improved ACK/NACK reporting

10.2.1   Concept description

10.2.1.1   Event based RLC ACK/NACK reports

Currently, the RLC/MAC ACK/NACK reporting is a time consuming procedure. This is especially true for downlink transfers. The procedure for DL transfers is that the BSS periodically (RRBP) polls the mobile for ACK/NACK reports. Considering the periodicity for the polling, it is realistic that it takes in the order of 150 ms to 250 ms from an RLC block is considered lost in the MS until the PCU realises it. This is a large problem especially considering delay sensitive applications such as Push-To-Talk over Cellular (PoC) and Voice over IP (VoIP). Consider also that in RLC Acknowledged mode the LLC layer in the receiver applies "in-order-delivery" to upper layers, which means that a single lost RLC data block will delay all consecutive LLC packets until this RLC data block has been successfully transmitted. A high-level example of the procedure is shown in figure 300 assuming a regular poll at every 12th RLC block.
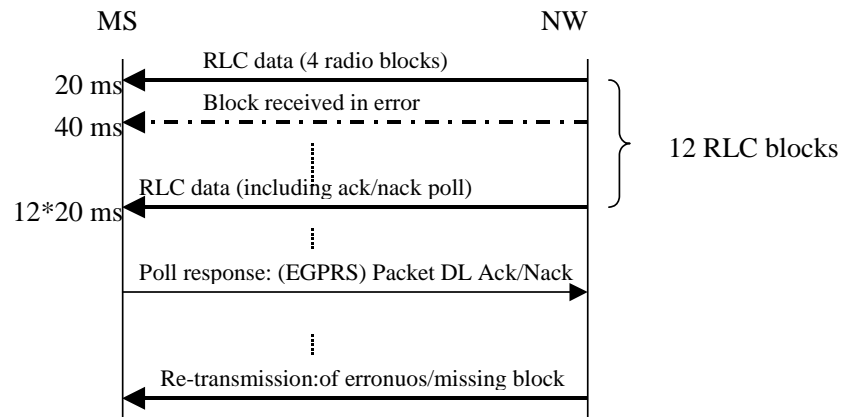
Figure 300: The principle of ARQ handling of DL RLC/MAC data block transmission assuming a poll every 12th RLC data block

"RRBP poll" in this context means a BSS ordered periodic poll for DL ACK/NACK from the MS. "USF scheduling" is the procedure for BSS to allow a specific MS to send data uplink on the specified UL channel.

Two methods to improve ACK/NACK reporting are:

- Event based RLC ACK/NACK reports.

- Downlink ACK/NACK in uplink data.

Those are detailed in next sub-chapters.

It is also possible to reduce the delay for the regular polling method. The scheduling of the "RRBP poll" can set a lowest possible value for an answer to 13 TDMA frames after the start of the reception. This could be lowered to 4 or 5 frames instead with a possible reduction of the delay of around 40 milliseconds.

10.2.1.2   Event based RLC ACK/NACK reports

A different approach to the periodic polls from the BSS would be that when the receiver (MS) realises that a RLC data block is missing - from BSN sequence out of order or, in the EGPRS case, when the BSN is successfully decoded but the RLC data is not - it could report this to the BSS without waiting for a regular poll. The "event" is occurring when the mobile station discovers a missing/erroneous RLC block. To avoid collisions on the shared UL physical channel(s) the event based ACK/NACK would have to be scheduled by BSS, and thus sent as a response to an USF scheduling. To let the BSS still have control over the balance between payload and ACK/NACKs in the UL direction, it may be desired that the BSS still control the mobile station usage also if the MS will be using the USF method. This can be done for example by setting a maximum ratio between ACK/NACK and payload, and/or set how many RLC data blocks that shall be missing before an event based DL ACK/NACK is sent. This would let the BSS dynamically control the DL ACK/NACK reporting depending on what is currently the main payload direction and also considering QoS requirements. In addition, by using USF scheduling the BSS would also have control over multiplexing of different users versus DL ACK/NACK reporting. Figure 301 gives an example of a possible event based ACK/NACK protocol sequence.
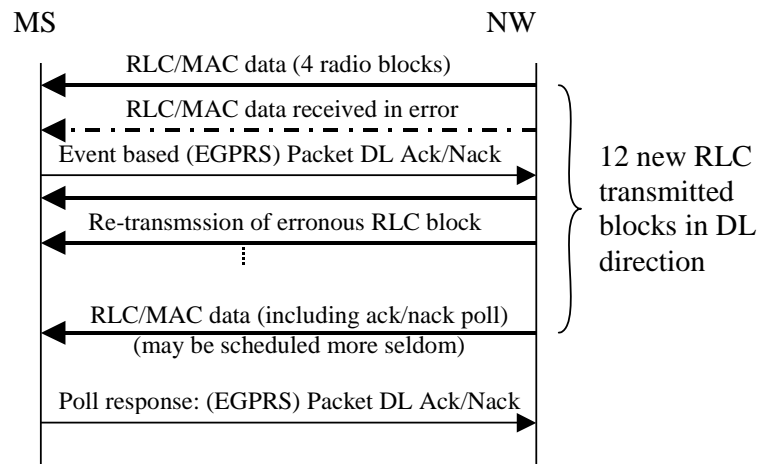
Figure 301: The principle of event based ARQ handling of DL RLC data block transmission including a regular poll defined to occur at every 12th RLC data block transmission

The regular poll is still expected to be needed even when using the event based ACK/NACK procedure, e.g. because there could be no or very few errors and the network could need ACKs, "I'm alive function", and performance feedback, but it could be sent less often and not be dependent on neither #errors nor QoS requirements. It is assumed that the event based ACK/NACK uses the same message as the answer to the regular poll, i.e. the Packet Downlink ACK/NACK. Since the response from the mobile station contains enough information, the network side knows when the ACK/NACK message was constructed and sent, the BSS RLC/MAC scheduling can avoid any duplicated re-transmission despite that the same error may be reported twice before retransmitted on the first occasion, e.g. reported by both the regular RRBP poll and the event based method.

It is assumed that an UL TBF exists. Typically this is true in many use cases (together with Extended UL TBF). If an UL TBF does not exist a "TBF/USF" could be established for the ACK/NACK procedure or the conventional polling need to be used.

10.2.1.3 ACK/NACK in Uplink Data

There are two ways how ACK/NACK information can be included (piggy-backed) into RLC data blocks:

- Include ACK/NACK in the header of an RLC data block.

- Include the ACK/NACK in the payload part of an RLC data block.

10.2.1.3.1 ACK/NACK in RLC header

There are spare bits in the RLC/MAC header for EGPRS uplink data blocks. These could be used for ACK/NACK blocks for the DL TBF. The method should be event based as described in subclause 10.2.1.2, which means that the bits shall be used only if there are lost blocks. Since there are very little room for sending BSN, the exact meaning of the bits needs to be defined.

The advantages with this method may be:

- Immediate NACK of lost RLC block possible -> low latency.

- No reduction of uplink capacity.

This method should be regarded as a complement to the method described in subclause 10.2.1.2.

10.2.1.3.2 Fast Ack/Nack reporting sending Ack/Nack in payload of an RLC data block

Due to the very little room in the header of EGPRS uplink RLC data blocks, an alternative to the solution outlined in the sub-clause above (subclause 10.2.1.3.1) is to reuse part of the payload of an EGPRS uplink RLC data block to convey signalling information.

10.2.1.3.2.1 Short bitmap in an RLC data block

The principle is that, instead of sending back to the transmitter a long bitmap in a dedicated radio block (i.e. the PDAN), the receiver could send back a very short bitmap, embedded in a normal RLC data block, leaving a lot of space to carry user plane data in the reverse direction.

The short bitmap would contain information about the recently received radio blocks, independently of their Block Sequence Number. The new bitmap would therefore be no longer indexed by a Starting Sequence Number, but on a time basis. More precisely, if a polling indication is received in radio block at time x, the mobile station would send back a short bitmap indicating the status of all the radio blocks received in all the assigned timeslots at time x, x-1, etc. depending on the size of the short bitmap and the number of assigned timeslots. The network as the sender knows the BSNs of the corresponding RLC blocks, when receiving the short bitmap, so that the correct information can be derived.

The length of the short bitmap has to be linked to the maximum number of RLC blocks that can be submitted during two successive pollings, and should take into account that some polling requests/short bitmaps might get lost. A suitable size for the short bitmap (which is anyway suggested to be fixed) is expected to be 4 octets.

Note that size of short bitmap is also linked to the acceptable TBF multiplexing level. Once the size of the short bitmap is fixed, also the maximum allowed TBF multiplexing level is fixed (on the timeslots where the Fast Ack/Nack reporting scheme is used).

Since there might be two RLC data blocks per radio block (in case of MCS 7/8/9), two bits per radio block are needed in the bitmap. For every radio block received in the assigned timeslots, the receiver shall set the pair of bits in the short bitmap in the following way:

0 0	-	failed header decoding
	-	header correctly received but with a different DL TFI
	-	header correctly received (with the correct DL TFI) but failed decoding of the payload of the RLC block (or blocks, in case of MCS 7/8/9)
0 1		header correctly received (with the correct DL TFI), failed decoding of the first RLC data block, correct decoding of the second RLC data block
1 0		header correctly received (with the correct DL TFI), correct decoding of the first RLC data block, failed decoding of the second RLC data block
1 1		correct decoding of the payload of the RLC block, or correct decoding of both the first and second RLC data blocks

In case of multiple TBFs, the same bitmap could carry the information for all the TBFs. In this case bits would be set to 1 for RLC blocks correctly received with any of the assigned DL TFIs. This would further optimize the procedure since feedback for all the TBFs could be provided at the same time.

If the polling is received in a radio block at time x, the first pair of bits in the short bitmap shall refer to the radio block received on the first assigned timeslot at time x, the second pair of bits shall refer to the radio block received on the second assigned timeslot at time x, etc. If there is still free space in the bitmap, the next pair of shall refer to the radio block received on the first assigned timeslot at time x-1 (i.e. in the previous 20 ms) and so on.

Note that the option of polling in different radio blocks with different RRBP values pointing at the same frame in the UL should not be allowed in this case. Note also that to minimize the effect of the MS reaction time, a further option could be to include in the bitmap information about the radio blocks received between the polling request and the polling response.

In figure 302 and the example is shown, referring to a DL TBF allocated on timeslots 0, 1, 2 and 3 (TBF1) and multiplexed with other TBFs (TBF2 and TBF3). The length of the short bitmap is assumed to be of only 2 octets in this example.
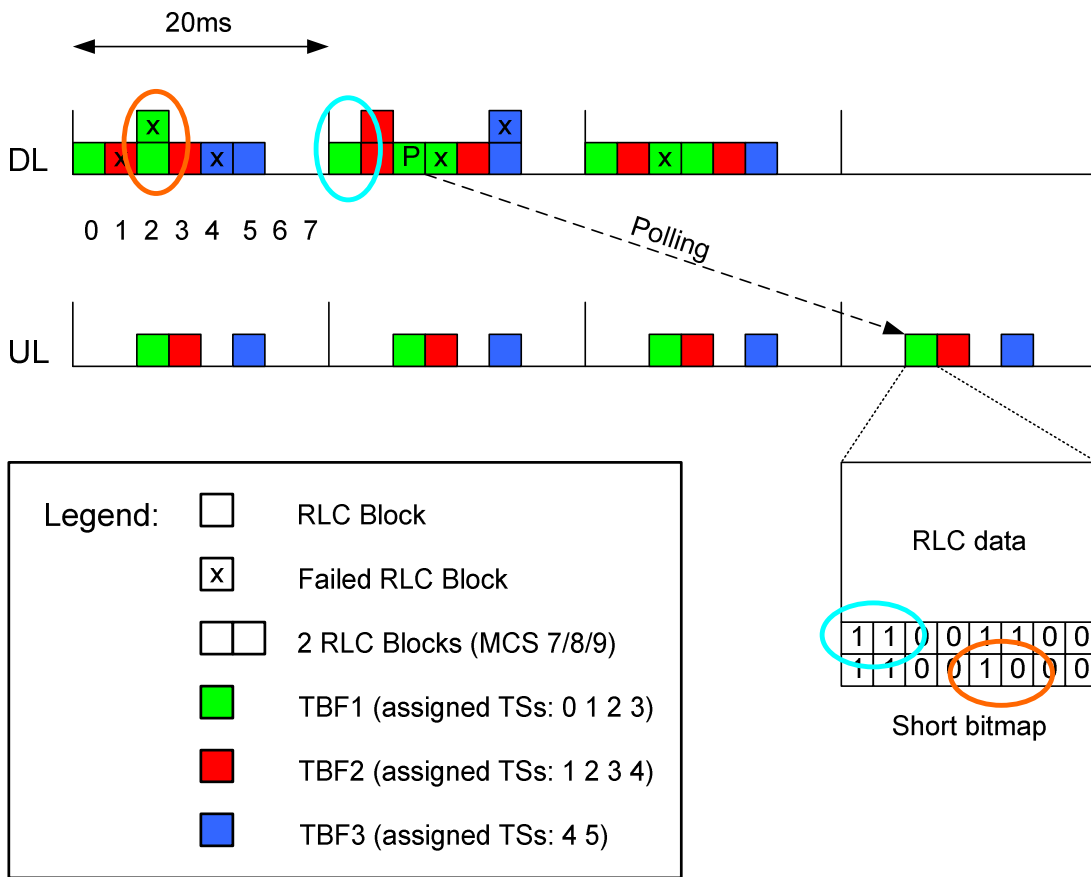
Figure 302: Example of fast ack/nack reporting operation

EGPRS uplink RLC data block would be formatted according to the figure below, where the insertion of the optional Short Bitmap field would depend on the presence of a polling indication in the previous corresponding DL radio block. This would also be signalled by a bit indicator reusing one of the spare bits in the UL RLC data block header.
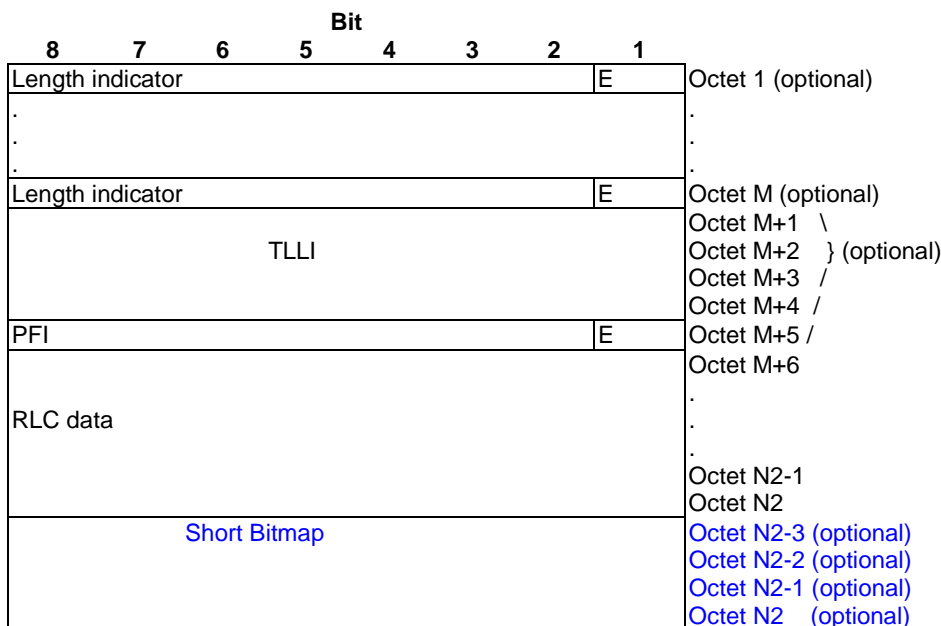
Figure 303: New Uplink EGPRS RLC data block

To preserve normal RLC operation, if an UL RLC data block has to be retransmitted, the size of the data part will have to remain the same as before. A different short bitmap shall anyway be included (independently of polling from the network) if the original transmission contained one. In case of EGPRS this means that if the new bit indicator in the UL RLC data block header indicates that the last 4 octets of the payload contain a Short Bitmap, the corresponding octets shall not be used when joint decoding is applied.

When Incremental redundancy is used, soft combining / depuncturing before convolutional decoding shall be applied only to the RLC data part (which remains the same for all the retransmissions). Incremental redundancy is not used for the decoding of octets of the short bitmap: only the last retransmission is used.

This is highlighted in the following diagram, that shows the encoded bits for two repetitions of the same RLC block:
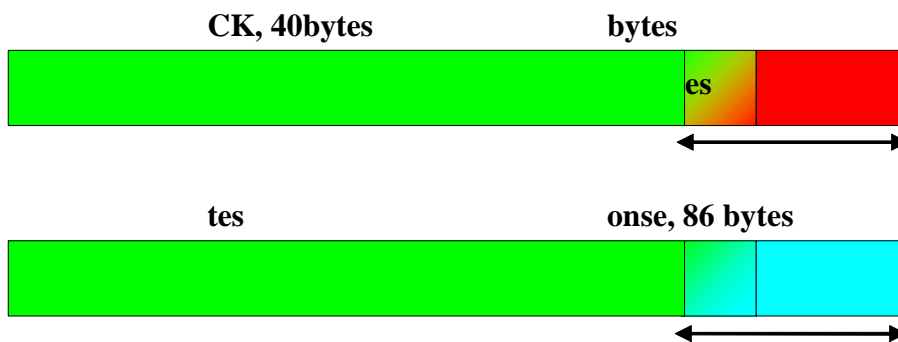
In case of repetitions, only the bits in the completely green part can be used for soft combining. Other bits should be excluded from the soft combining process. Note that this would result in a different (lower) decoding performance for the last k bits of the data part (where k is the constraint length) since soft combining cannot be used to derive their values.

An alternative would be to reduce the length of the data part by k bits by setting the last k bits to zero. In this case the encoded bits for two repetitions of the same RLC block are shown in the following diagram:

rives from the short bitmap   t combining

art derives from data part
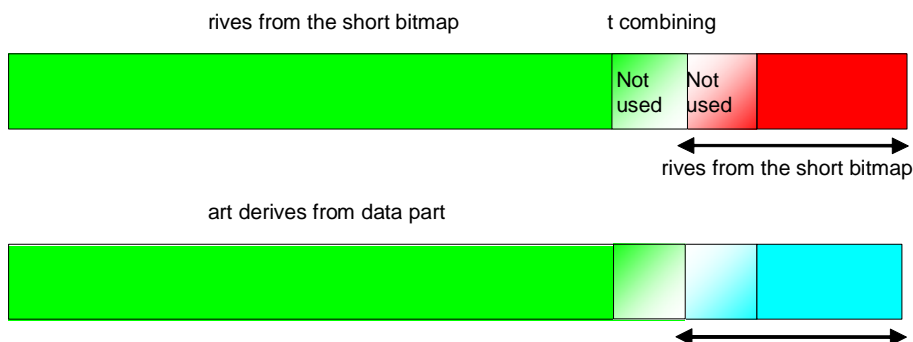
In this case it is possible to apply soft combining to derive all the bits of the data part so that decoding performance would not be affected. In practice, with this solution, it would be possible to keep the convolutional decoding algorithms unchanged: in other words, convolutional decoding could be performed over the whole block length, and the '0' bits would ensure that the Viterbi algorithm trellis is properly terminated at the end of the data part, and the last M decoded bits (where M is the length of the short bitmap) could just be discarded. Obviously, the short bitmap would need to be decoded separately.

10.2.1.3.2.2 Short bitmap in a single burst

A further possibility is the alternative submission of the short bitmap in a single burst (e.g. a newly formatted normal burst), if no other data and/or measurement reports have to be submitted.

As soon as the MS has no additional data payload to submit, e.g. during the Extended UL TBF phase, the MS could send a single burst carrying the short bitmap. This could save MS battery life and keep the UL interference low in the network, since only 1 out of 4 bursts of a radio block might be used.

10.2.1.3.2.3 Reduced MS reaction time

The other proposal is to reduce the minimum reaction time during the polling procedure, bringing it from 13 TDMA frames to 8 (or 9) TDMA frames, thus gaining 20 ms.

10.2.1.3.2.4 Co-existence with legacy procedures

In any case the new reporting mechanism based on the short bitmap has to co-exist with the old one. This is needed for instance when several subsequent polling requests/short bitmaps are not received (by the MS or the network). To obtain feedback information from the MS the only possibility in this case would be to ask for the normal PDAN message.

This can be done by a redefinition of the RRBP and ES/P fields in the header of EGPRS DL data blocks. The RRBP field could be split into 2 field: a new RRBP field (defining only two possible values: 20 ms and 40 ms reaction time) and a RS field defining the Reporting Scheme.

Bit

8	7	6	5	4	3	2	1	Octet
TFI	RRBP	RS	ES/P		USF			1
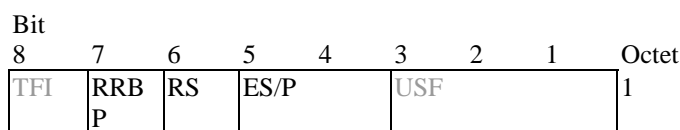
Figure 304: RRBP, RS and ES/P fields in modified EGPRS downlink RLC data block headers

And the meaning of the RRBP, RS and ES/P fields would be interpreted according to the tables below.

Table 143: new RRBP field

bit 6-5	Full-rate PDCH uplink block with TDMA frame number
0	(N+8 or N+9) mod 2715648
1	(N+13) mod 2715648

Table 144: RS field

bit 6-5	Full-rate PDCH uplink block with TDMA frame number
0	Normal ack/nack reporting scheme
1	Fast ack/nack reporting scheme

Table 145: ES/P field

Bits 5 4	ES/P
0 0	RRBP field is not valid (no Polling)
0 1	RRBP field is valid - Extended Ack/Nack bitmap type FPB (see note)
1 0	RRBP field is valid - Extended Ack/Nack bitmap type NPB (see note)
1 1	RRBP field is valid - Ack/Nack bitmap type NPB, measurement report included (see note)
NOTE:	This applies only if the RS bit is set to 0.

With this approach the network could dynamically request either the short bitmap (default case) or the conventional Ack/Nack message when necessary to recover from the loss of several successive polling requests / polling responses.

10.2.1.4 Fast Ack/Nack reporting in UL and DL

Piggybacking Ack/Nack reporting in both Uplink and downlink can be done by locating the Ack/Nack data in the payload. An example is shown in subclause 10.2.1.3.2 for piggybacking in UL. This subchapter describes a method to do it in both UL and DL; including a BSN based short Ack/Nack structure.

10.2.1.4.1 BSN based short Ack/Nack report

The suggested report has the size of n*3 byte, where n is the minimum number of segments that are needed for a report. Each segment of 3 byte consists of 5 fields, as shown in Table 9. One segment of 3 bytes is normally sufficient if errors are close together and belong to only one TBF, but it can be extended if needed for reports of different TBFs allocated to the same MS to allow for a combined Ack/Nack report to be sent or reporting of several erroneous BSN:s with large separation.

The Ack/Nack report is placed in the data field of the radio block, and is covered by the current channel coding and CRC. However, even if errors are detected in the data field, there should still be a good chance that the Ack/Nack report is correct. A separate CRC is therefore proposed for each Ack/Nack segment, so that the segments can be used if correct. If the radio block is erroneous, the Ack/Nack report will also be retransmitted together with the data, and IR is used for decoding of the second transmission.

Table 146: Data fields in one Ack/Nack report segment

Field	Size	Usage
Address	0 bit to 3 bits	TBF of the Ack/Nack information (identified by TFI). The size is a function of the number of active TBF:s for the user.
BSN_NACK	11 bits	BSN of a radio block that has not been correctly received.
BSN_MAP	6 bits to 9 bits	Ack/Nack bitmap of the block sequence numbers following BSN_NACK
Extension bit	1 bit	0: Report is complete, 1: A new Ack/Nack segment follows, using the same format.
CRC	3 bits	CRC covering the 3 byte segment

EXAMPLE: A user has 2 allocated TBFs and shall send a short Ack/Nack report of the current status. Acknowledged mode is used, so all errors should be reported. (If non-persistent mode had been used, only the most recent errors would be reported.) The TBF with lowest ID have received BSN 1, 2, 4 and 7 without error. The BSNs 3, 5 and 6 was erroneous while BSN 8 and higher numbers have not yet arrived.

The TBF with highest ID has received BSNs 1, 3, 4, 5, 8, 9, 10, 11, 12 and 15. The BSNs 2, 6, 7, 13, 14 and 16 was erroneous while BSN 17 and higher have not yet arrived.

In table 147 the Ack/Nack report is shown. Three segments are needed: one for the first TBF and two segments for the second TBF. Note that for the second TBF, BSN 11 and 12 are not covered by any of the two bitmaps. That is not needed, since they are implicitly acknowledged when the BSN_NACK number in the third segment is larger.

Table 147: Ack/Nack report for the MS described in the example

Seg.	Field	Size	Value	Meaning
1	Address	1 bit	0	The TBF with lowest ID.
1	BSN_NACK	11	3	BSN 3 is not yet received correctly.
1	BSN_MAP	8 bits	1001 0000	Ack/Nack bitmap for BSN 4-11 1=correctly received
1	Extension bit	1 bit	1	More Ack/Nack data follows
1	CRC	3 bit		CRC covering the first 3 byte segment
2	Address	1 bit	1	The TBF with highest ID.
2	BSN_NACK	11	2	BSN 2 is not yet received correctly.
2	BSN_MAP	8 bits	1110 0111	Ack/Nack bitmap for BSN 3-10 1=correctly received
2	Extension bit	1 bit	1	More Ack/Nack data follows
2	CRC	3 bit		CRC covering the second 3 byte segment
3	Address	1 bit	1	The TBF with highest ID.
3	BSN_NACK	11	13	BSN 3 is not yet received correctly.
3	BSN_MAP	8 bits	0100 0000	Ack/Nack bitmap for BSN 13-20 1=correctly received
3	Extension bit	1 bit	0	No more Ack/Nack data follows
3	CRC 2	3 bit		CRC covering the last 3 byte segment

The size of the short Ack/Nack report is variable in steps of 3 Bytes. An example of the new EGPRS Uplink and Downlink RLC data blocks can be found in figures 305 and 306 respectively. The minimum size of 3 Bytes has been used. Note that the location of the short Ack/Nack report immediately after the header is shown as an example. The only requirement is to have it located at a known place in an RLC data block.
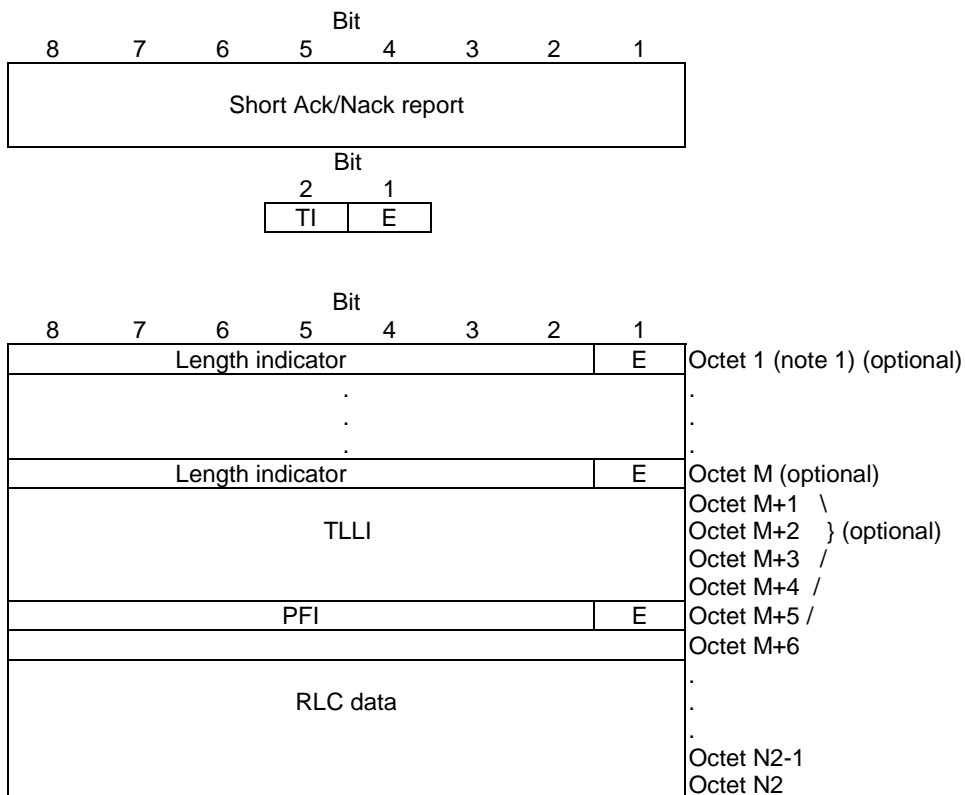
Figure 305: Modified Uplink EGPRS RLC data block

Bit

8	7	6	5	4	3	2	1
			Short Ack/Nack report				

Bit

2	1
FBI	E

Bit

8	7	6	5	4	3	2	1	
		Length indicator					E	Octet 1 (note) (optional)
		.					.	.
		.					.	.
		.					.	.
		Length indicator					E	Octet M (optional)
								Octet M+1
		RLC data						.
								.
								.
								Octet N2-1
								Octet N2
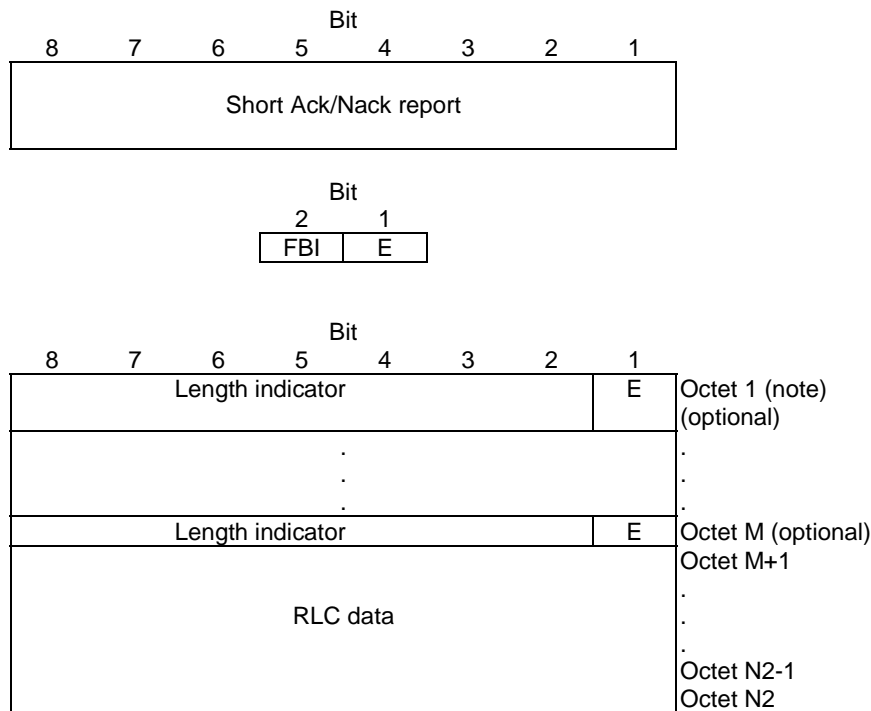
Figure 306: Modified EGPRS Downlink RLC data block

10.2.1.4.2 Ack/Nack reporting sent in UL direction

Subclause 10.2.1.3.2 describes a method how to do fast reporting in the UL direction by using piggybacking if data blocks are to be sent and it reuses the polling mechanisms with a slightly modified header such that legacy operation is still possible.

Legacy polling is still needed in order to support legacy MSs and as well as for keep-alive and Link Quality Control (LQC) purposes for mobile that support fast Ack/Nack reporting. The result would be a (substantially) reduced legacy polling repetition rate being applied for MSs that support fast Ack/Nack reporting compared to MSs that only support the legacy Packet Ack/Nack reporting scheme. Using the proposed short bitmap in [5], also described in option 1 of Chapter 2, the repetition rate of the legacy polling need also to be chosen to cater for the case when the short bitmap moves outside the short bit map window with errors. This is not the case if the Ack/Nack report is based on sequence numbers as suggested in option 2 of chapter 2.

The objective is to keep the network in control of how often an MS is allowed to send Ack/Nack reports. The reporting is performed as follows using the poll (RRBP) and USF fields in the downlink direction. If a mobile station has received a:

- RRBP (identified by the poll-bit) + USF for the same UL block period as identified in the poll (RRBP) the MS shall send:

    - A piggybacked DL Ack/Nack with data payload if one or more RLC data blocks have been received in error and are still outstanding.

    - A normal RLC data block (no piggybacking of Ack/Nack) if RLC data block have been received in error.

    - Normal (legacy) Ack/Nack report if there are no data payload to be sent.

- RRBP (identified by the poll-bit) and no USF in same period, the MS shall send a Normal Ack/Nack report (legacy case).

Thus, the network remains in control of the reporting (as in legacy case). In addition to the above scheme it could also be possible for the MS to report on its own (i.e. independent of RRBP) but then it needs to do this only when it is USF-scheduled. This should be limited to the case when there is space left in the UL data block or there is no data block to be sent in order to reduce potential increase of signalling and reduced overall performance. The event-driven MS controlled reporting could be allowed by the network so an operator could set a parameter at TBF set-up or, in general such as on a per cell basis, if this should be allowed or not.

The mobile station may, typically, need to prepare in advance both a short piggy-backed Ack/Nack report and a normal, non-piggybacked Ack/Nack report (where the non-piggybacked report may be a short Ack/Nack report or a full report) when the polling bit is received since a USF may or may not be allocated immediately before the report is to be transmitted in uplink direction.

In order for the receiver to know if there is a short (piggybacked) Ack/Nack report included in the UL RLC data block a header bit is needed to indicate if a piggy-backed Ack/Nack is added to the data block. A spare bit in the RLC/MAC header is used to indicate if a piggy-backed Ack/Nack is included in the UL RLC data block or not. A spare bit exists in all three EGPRS header types and will be used for this case. The different Header types are shown in figures 307 to 309 (taken from 3GPP TS 44.060).
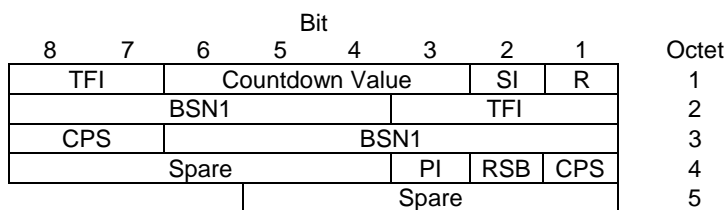
Figure 307: EGPRS uplink RLC data block header for MCS-5 and MCS-6
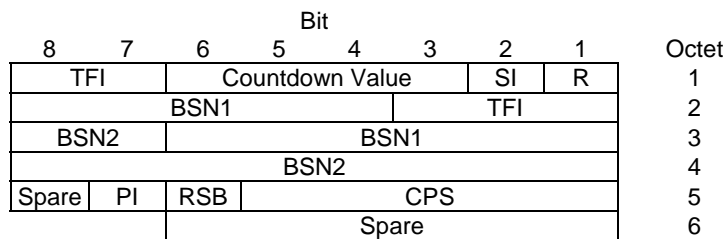
Figure 308: EGPRS uplink RLC data block header for MCS-7, MCS-8 and MCS-9
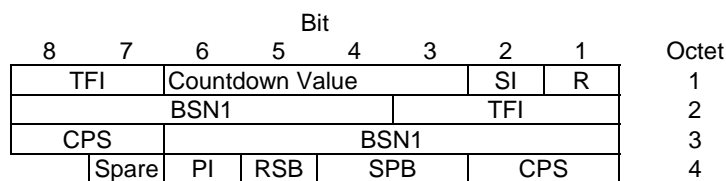
Figure 309: EGPRS uplink RLC data block header for MCS-1, MCS-2, MCS-3 and MCS-4

10.2.1.4.3 Ack/Nack reporting sent in DL direction

In order for the mobile station to determine that a short Ack/Nack report is included in the data block, the receiver need to know determine this, if possible without any double decoding. A bit in the header would indicate this. A redefinition of the RRBP and ES/P fields in the header of the EGPRS DL data blocks can be utilised (in [5] the same principle is used in another way to support UL piggybacking). The RRBP field is split into 2 fields: a new RRBP field (defining only two possible values: 20 ms and 40 ms reaction time) and an Ack/Nack field indicating a short Ack/Nack bitmap has been included in the data part, see figure 310.
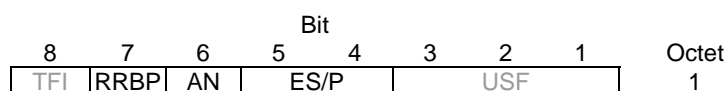
Figure 310: RRBP, AN and ES/P fields in modified EGPRS downlink RLC data block headers

The meaning of the RRBP, RS and ES/P fields would be interpreted according to tables 148 to 150 (note that the "Bit" or "Bits" indicates the #bits and individual order and not the actual bit position in the header). Note that the modification is backward compatible as used only for MSs capable of this reporting. The legacy header structure will still remain for legacy MSs and if fast reporting is not needed.

Table 148: new RRBP field

Bit 1	Full-rate PDCH uplink block with TDMA frame number
0	(N+8 or N+9) mod 2715648
1	(N+13) mod 2715648

Table 149: NEW AN field

Bit 1	Full-rate PDCH uplink block with TDMA frame number
0	No piggy-backed Ack/Nack included
1	Piggy-backed Ack/Nack included

Table 150: ES/P field

Bits 2 1	ES/P
0 0	RRBP field is not valid (no Polling)
0 1	RRBP field is valid - Extended Ack/Nack bitmap type FPB
1 0	RRBP field is valid - Extended Ack/Nack bitmap type NPB
1 1	RRBP field is valid - Ack/Nack bitmap type NPB, measurement report included

It is assumed that the RRBP can be reduced for this case of reporting. The old reporting scheme could very easily be supported by initialising this at e.g. TBF set-up, if necessary.

10.2.1.5   Possible usage

A possible use of the improved ACK/NACK procedures is (considering data transmitted in downlink):

UL TBF exist:

- If UL data is sent → use the "ACK/NACK in uplink data" / "Fast Ack/Nack reporting" mechanism.

- If UL data is not sent → use the Packet Downlink Ack/Nack message as a response to a USF/ "Fast Ack/Nack reporting" mechanism by sending a short bitmap/short Ack/Nack report in a single burst.

UL TBF does not exist:

- The normal poll mechanism, i.e. use the Packet Downlink Ack/Nack message as a response to a "RRBP poll" / "Fast Ack/Nack reporting" mechanism by sending a short bitmap/short Ack/Nack report in a single burst.

- In case of data sent in the uplink, the network can decide whether or not to piggy-back the Ack/Nack reports in downlink RLC data blocks, if there is such possibility, since network performs the scheduling.

10.2.2   Modelling assumptions and requirements

The simulation environment is shown in figure 311. It is a single user RLC protocol simulator where the LLC packet sizes, MCS, multislot and polling could be set. The radio channel is modelled by a BLER setting that also includes incremental redundancy. The feedback channel is ideal. The radio channel introduces the radio transmission delay (TTI).
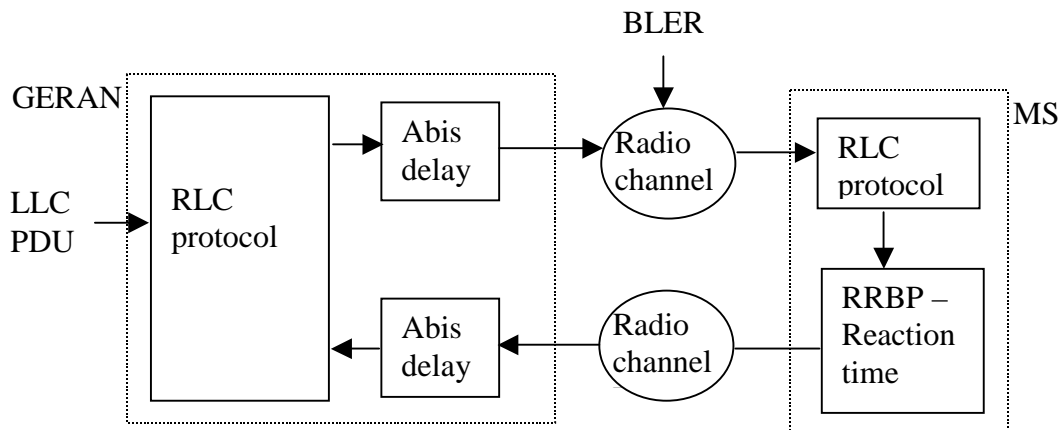
Figure 311: Overall protocol simulation model

Simulation parameters:

Parameter	Value(s)	Comments
LLC size	500 Bytes and 1 500 Bytes	
MCS	6 and 9	
Multislot	1	
Ack/Nack method	Polling @ every 12 RLC block or event based	Polling is the reference case. With event based, a Nack is sent when an erroneous block is received.
Incremental redundancy	Yes	
BLER [first, second, third]	[20 %, 2.5 %, 0 %]	The first BLER is for the first transmission of a RLC block, the second BLER is for a re-transmission, etc.
Abis delay	20 ms	
TTI	20 ms	
RRBP	13	Used in Polling case Same delay as for event based case.
MS reaction time	40 ms	Used in event based case Same MS reaction delay as in Polling case
Simulation length	50,000 LLC frames	
NOTE: Polling every 12 transmitted RLC block has been assumed.		

10.2.3   Performance characterization

10.2.3.1   Performance gain of "Event based RLC Ack/Nack reports"

The performance results are shown in figures 312 and 313. The reference case is when polling is used (a poll is executed every 12th RLC block). For each case of the cases, i.e. event based and polling, a poll is also done on the last RLC block in the RLC send buffer.
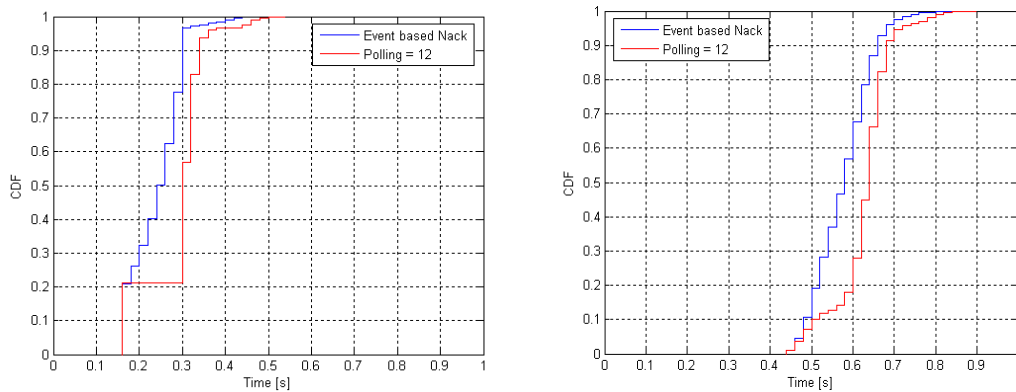
Figure 312: CDF vs. time to correctly receive a LLC packet. MCS-6 with LLC block sizes, 500 Bytes in left figure and 1 500 Bytes in right figure
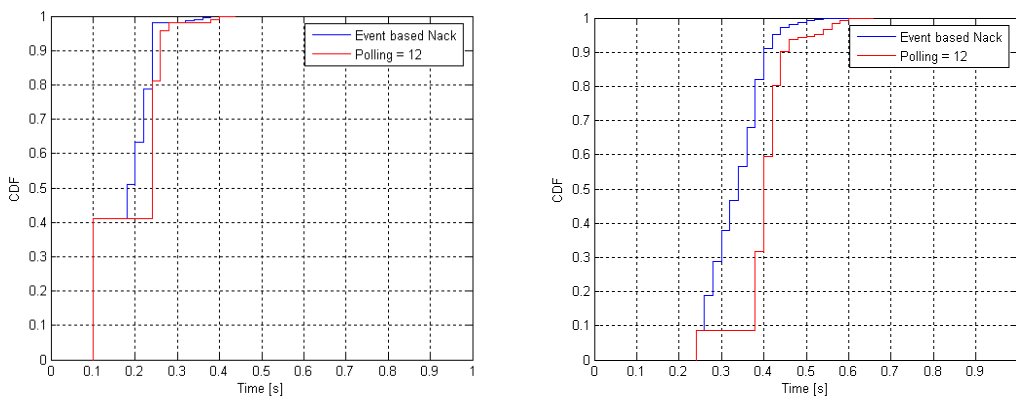
Figure 313: CDF vs. time to correctly receive a LLC packet. MCS-9 with LLC block sizes, 500 Bytes in left figure and 1 500 Bytes in right figure

The performance gain of having an event-based scheme is obvious. Table 151 summarises the gain at the median and 90 % CDF levels. The gain for the Event based Ack/Nack is relative the polling case.

Table 151

Case	Time [s] Poll = 12 CDF levels		Time [s] Event Ack/Nack CDF levels		Event Ack/Nack Gain [%]	
	50 %	**90 %**	**50 %**	**90 %**	**50 %**	**90 %**
500B, MCS-6	0.3	0.34	0.24	0.3	20	11
500B, MCS-9	0.24	0.26	0.18	0.24	25	8
1 500B, MCS-6	0.64	0.68	0.58	0.66	9	6
1 500B, MCS-9	0.4	0.44	0.34	0.4	15	9

Table 152 shows the number of average sent Ack/Nack reports for the different simulated cases. Note also that so called "final" Ack/Nack reports are included in the figures (i.e. for the poll sent in the last RLC block in sent buffer). Table 152 also shows the relative increase of Ack/Nack reports for the event case compared to the simulated polling case.

Table 152

Case	Average number of Ack/Nack per LLC block		Event/Poll ratio
	Poll	Event	
500B MCS-6 (7 radio blocks)	1.8	3.4	1.8
500B MCS-9 (4 radio blocks)	1.6	2.4	1.5
1 500B MCS-6 (21 radio blocks)	3.1	6.2	2.0
1 500B MCS-9 (11 radio blocks)	2.0	4.1	2.0

The event/poll ratio shows that between 1.5 up to 2 times more reports are sent. How the increase in number of Ack/Nack events will affect the radio resource usage depends if, and how much, event based reports can be sent within any UL data blocks.

Table153 summarizes the gains from a time perspective, i.e. how many users have received the data without errors within a specific time. The specific time instants are taken at the 50 % CDF level for regular polling and are shown in table 151.

Table 153

Case	Percentage of users [%]	
	poll	event
500B, MCS-6; #user's LLC ≤ 0.3 s	56	96
500B, MCS-9; #user's LLC ≤ 0.24 s	82	98
1500B, MCS-6; #user's LLC ≤ 0.64 s	66	86
1500B, MCS-9; #user's LLC ≤ 0.4 s	60	92

The gains are quite substantial and a larger number of users receive an LLC packet within a certain time limit than with a regular polling (here assumed set to 12).

NOTE: Gain does not assume similar uplink loads (feedback channel) between regular poll and the event-based approach.

10.2.3.2 Performance gain of the "Fast Ack/Nack reporting" mechanism

The following assumption are considered:

- The intrinsic *RLC RTT* (i.e. the time to cross two times the A-bis and Um interfaces plus the processing delay of network nodes) is assumed to be of 100 ms.

- The considered multislot allocation is 4 (DL) + 1 (UL).

- In case of conventional Ack/Nack reporting procedure, the polling period is 12 RLC blocks, i.e. the polling bit is set every 60 ms. The minimum (legacy) RRBP value is considered, leading to an MS reaction time of 40 ms.

- In case of the proposed fast Ack/Nack reporting strategy, the polling is set at every radio block (i.e. every 20 ms). The minimum new RRBP value is considered, leading to an MS reaction time of 20 ms.

Based on these values, the table below reports, for the conventional and the new proposed schemes:

the maximum time (*RLC RTT + MS React Time + (Polling Period - 20 ms)*) in order to receive a retransmission (when a lost RLC block is detected) the percentage of available bandwidth for data transmission on the UL TBF.

	Conventional reporting	*Fast reporting*
Maximum retransmission time	100+40+40= **180 ms**	100+20 = **120 ms**
Percentage of available bandwidth in the UL	66.6%	**80%** (MCS1) **94.6%** (MCS6) **97.3%** (MCS9)

The example indicates that a huge benefit is expected in terms of reduced transfer delay since the retransmission time of single RLC block is reduced by one third. At the same time a consistent improvement is expected in terms of uplink capacity that would increase from 66.6 % (with respect to the theoretically available one) to 80 % in the worst case, up to 95 % to 97 % if higher MCSs are used in the UL.

10.2.4 Impacts to the mobile station

The mobile station needs be able to schedule and send event based ACK/NACK.

The mobile station needs be able to insert a short bitmap or a short Ack/Nack report in an UL RLC data block when polled accordingly.

The mobile station needs to be able to receive a short Ack/Nack report in a DL RLC data block.

10.2.5 Impacts to the BSS

The PCU needs to be updated to handle new ACK/NACK scheme. Reuse of existing signalling messages except for the case using ACK/NACK in uplink data/"Fast Ack/Nack reporting" mechanism. There is an impact on BTS algorithms to exploit Incremental Redundancy in case of the "Fast Ack/Nack reporting" mechanism.. No impacts to the BTS. Potentially some new parameter setting ACK/NACK reporting constraints need to be signalled to the Mobile station

10.2.6 Impacts to the Core Network

No impacts.

10.2.7 Impacts to the specifications

The impacted 3GPP specifications are listed in table 154.

Table 154: Impacted 3GPP specifications.

Specification	Description	Comments
3GPP TS 43.064	GPRS Stage 2	
3GPP TS 44.060	Radio Link Control / Medium Access Control (RLC/MAC) protocol	

10.2.8 Open issues

Definition of the spare bits in the UL RLC/MAC header to report erroneous/missing blocks in DL (including aspects of multiple TBF handling).

10.3 Reduced transmission time interval

10.3.1 Concept description

A reduced transmission time interval (TTI) will reduce the Round Trip Time. The present situation (assuming ideal radio conditions) is shown in figure 314 where the delay related to the radio block period of 20 ms is shown. Depending on the MS capability and the radio conditions one or more radio blocks are necessary to send a Ping. By reducing the TTI the time needed to complete a Ping will be lowered.
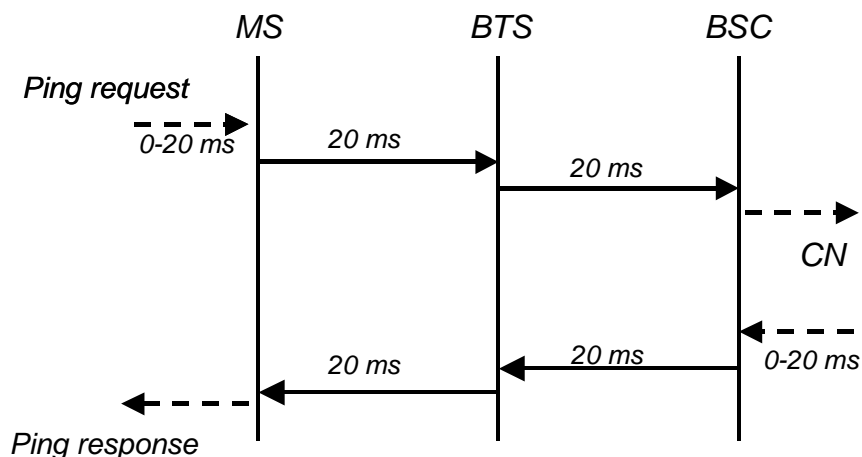
Figure 314: Typical delay figures related to the TTI of 20 ms in ideal radio conditions (note that the delay over Abis depends on configuration). In addition, node processing delay, core network delay and internet delay will contribute to the end-to-end delay

Today a radio block is divided into four bursts that are mapped onto four consecutive TDMA frames using one timeslot per frame, giving a TTI of 20 ms. This together with frequency hopping provides frequency diversity since coding and interleaving is done over one radio block. There are two ways to extend this to become more generic and reduce the delay for one radio block: in time-slot domain and in frequency domain.

10.3.1.1 Radio block mapping in time-slot domain

Figure 315 shows two examples of radio block mapping in time-slot domain.
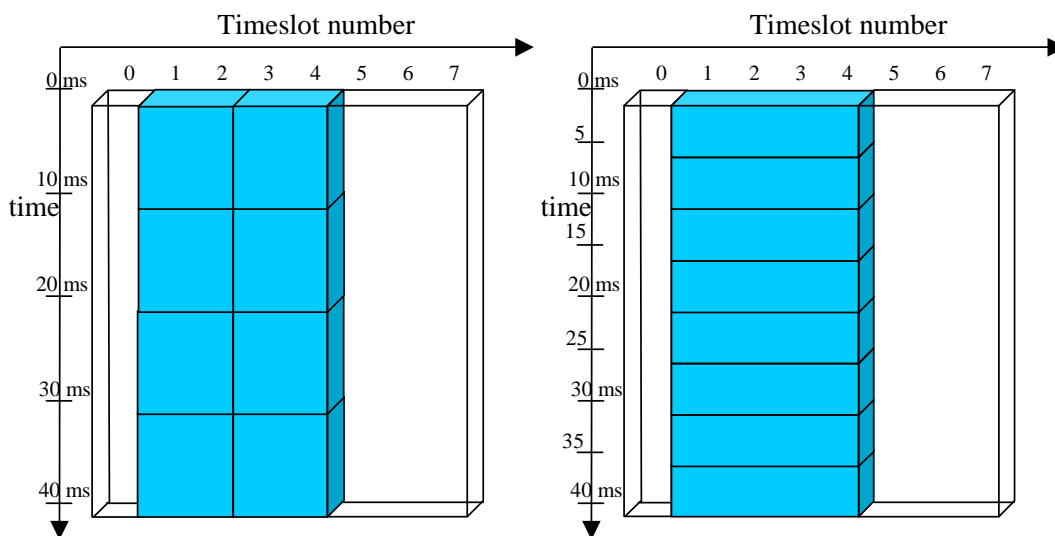
Figure 315: Different mappings in time-slot domain of four bursts onto a radio block

The mapping of the four bursts to a radio block consists of:

    i)   two consecutive TDMA frames and two consecutive timeslots (left figure).

    ii) one TDMA frame and four consecutive timeslots (right figure).

Alternative (i) reduces the TTI from 20 ms to 10 ms and alternative (ii) to 5 ms.

10.3.1.2 Radio block mapping in frequency domain (inter-carrier interleaving)

By mapping the four bursts of a radio block onto two consecutive TDMA frames on two separate carriers, the TTI can be reduced to 10 ms - without sacrificing frequency diversity. Similarly, quadruple-carrier EGPRS can be used to reduce the TTI to 5 ms. This is illustrated in figure 316. In order to avoid losing frequency diversity, the carriers should not be adjacent in frequency (in figure 316, they are depicted as adjacent only for simplicity).
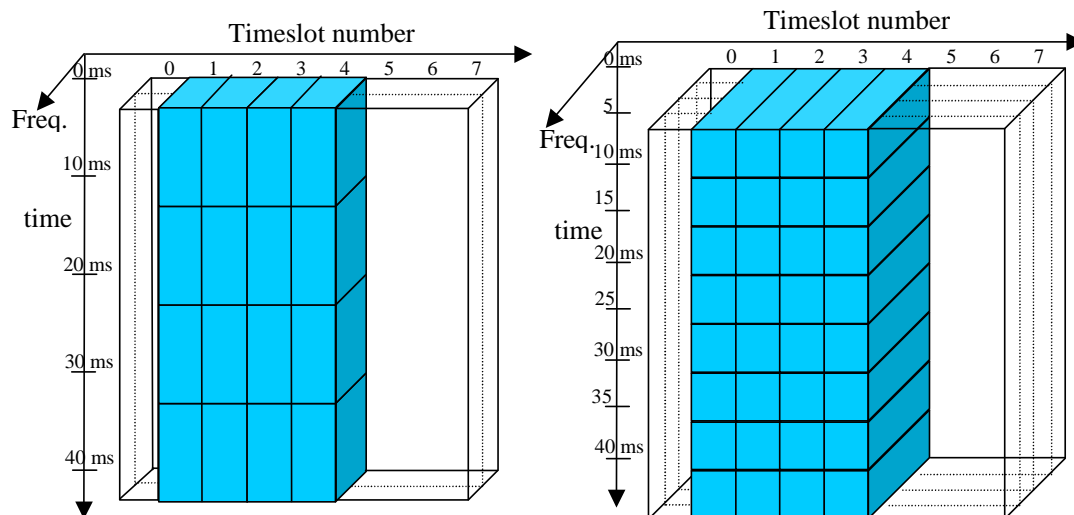
Figure 316: Different mappings in frequency domain of four bursts onto a radio block

The mapping of the four bursts to a radio block consists of:

    i)   two consecutive TDMA frames and two non-adjacent frequencies (left figure);

    ii) one TDMA frame and four non-adjacent frequencies (right figure).

Alternative (iii) reduces the TTI from 20 ms to 10 ms and alternative (iv) to 5 ms.

Frequency hopping can be applied as in the single-carrier case by assigning the same hopping sequence but different offsets (MAIO:s) to the different carriers.

10.3.1.3 USF scheduling of shorter TTI and legacy mobile stations

10.3.1.3.1 Basic principle

In order to support legacy mobile stations the USF structure must remain the same. This means that also the new, shorter TTI mobile stations need to adhere to the basic principle, possibly including some backward compatible additions if needed. However, one simple and backward compatible way is to completely rely on the existing USF scheduling method.

With this method, all USFs are always sent in the same dimension as the traditional USF, i.e. using a 20 ms USF allocation period for the next UL data period of 20 ms (that may be subdivided into 10 or even 5 ms TTIs). The USFs belonging to mobile stations with a lower TTI, such as 10 ms, are redefined so that an USF on carrier 1 corresponds to the first 10 ms radio block in the coming 20 ms period, while an USF on PDCH 2 corresponds to the second 10 ms period. In table 155 an allocation example is shown. Mobile stations "A" and "D" is using 10 ms TTI. Mobile stations "B" and "C" are legacy mobile stations having 20 ms TTI. The downlink data blocks can be sent to any mobile station and the 10 ms and 20 ms (legacy) TTI mobile stations can be multiplexed freely. Chapter 2.2 investigates potential issues related to USF decoding in downlink when 10 ms and 20 ms TTIs data blocks are multiplexed on same DL PDCH. Note that all UL frames can be allocated if within each 20 ms block period the same TTI is used. That is, it is only possible to change TTI at 20 ms intervals (this is also valid for DL data frames).

Table 155: Example of a 12-frame sequence with USF allocation, B and C are legacy users (20 ms) while users A and D are 10 ms TTI users (note that TDMA frame numbering is only based on data carrying frames)

TDMA Frame	PDCH/DL 1 USF	PDCH/DL 2 USF	PDCH/UL 1	PDCH/UL 2
1	USF-B	USF-C		
2	USF-B	USF-C		
3	USF-B	USF-C		
4	USF-B	USF-C		
5	USF-A	USF-D	B-burst	C-Burst
6	USF-A	USF-D	B-burst	C-Burst
7	USF-A	USF-D	B-burst	C-Burst
8	USF-A	USF-D	B-burst	C-Burst
9	USF-B	USF-C	A-Burst	A-Burst
10	USF-B	USF-C	A-Burst	A-Burst
11	USF-B	USF-C	D-Burst	D-Burst
12	USF-B	USF-C	D-Burst	D-Burst

.

10.3.1.3.2 Decoding USF in downlink when having both 10 ms and 20 ms TTIs

The issue investigated is if USF and Stealing Flags (SF) can still be used for the different multiplexing possibilities deployed in downlink (i.e. multiplexing of 10 ms and 20 ms TTIs). Tables 156 and 157 give an analysis and solutions. Based on the analysis and solutions it can be concluded that there is no real problems to multiplex different TTIs in downlink direction.

It should also be understood that legacy mobile stations cannot decode the relevant SF and USF portions if the modulation method (GMSK or 8PSK) changes from one 10 ms TTI to another during a 20 ms legacy block period so modulation method in DL needs to remain the same within each such legacy block boundary.

Table 156: GMSK bursts and position of stealing flags and USF

GMSK	Legacy stealing flags (SF)	Legacy USF
CS-1 to 4, MCS-1 to 4	Pos 57,58 in each burst CS-1: 11111111 CS-2: 11001000 CS-3: 00100001 CS-4: 00010110 MCS-1 to 4: as CS-4	CS-1: According to SACCH interleaving CS-2 to 4: burst 1: pos [0 50 100] burst 2: pos [34 84 98] burst 3: pos [18 68 82] burst 4: pos [2 52 66]
Solution:	Set legacy SF to indicate CS-4 when 10 ms TTI DL block is sent → legacy GPRS and EGPRS MS can decode the legacy USF	Put according to above

Table 157: 8PSK bursts and position of stealing flags and USF

8PSK	Legacy SF	Legacy USF
MCS-5 to 9	Pos 174,175 in each burst MCS-5/6: 00000000 MCS-7/8/9: 11100111	Pos 150, 151, 168, 169, 171, 172, 177, 178, 195 in each burst
Solution:	Legacy SF is not needed to decode legacy USF. SF can be reused to differentiate header types with 10 ms TTI in the new direction.	Put according to above

10.3.1.4 Introducing 2-burst radio block option

One of the advantages of reducing the TTI by transmitting 4 bursts in parallel onto 2 different timeslots is that legacy MCSs could be probably maintained, although changes would anyway be needed to the header and the interleaving scheme. Note that the assumption is that the header would be distributed across the 2 timeslots in this case.

But for low bandwidth applications such as VoIP it makes sense to define 2-burst radio blocks, i.e. radio blocks with a TTI of 10 ms transmitted on a single timeslot, as depicted in Figure 22. These radio blocks could be used in case of higher quality over the radio interface. In this case, assuming that such radio blocks could transport an IP packet (containing an AMR frame) every 20 ms, we could achieve a timeslot utilization of 50 %, also in case of continuous voice transmission (i.e. without considering any form of DTX). The spare bandwidth could be used by other TBFs, not necessarily carrying Conversational Services.
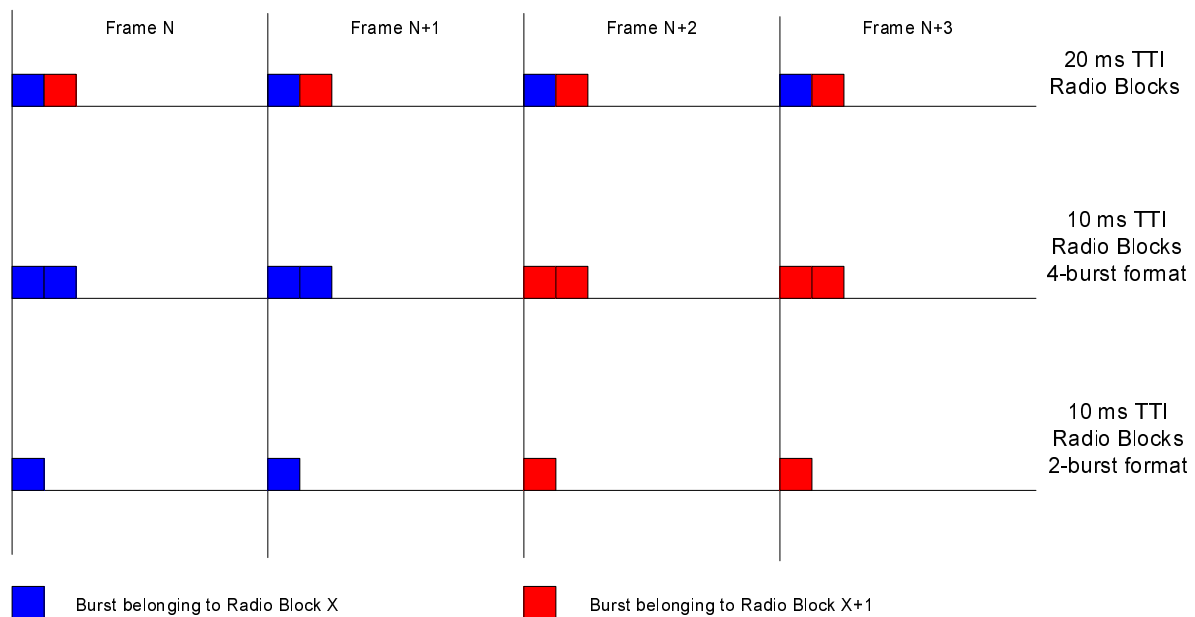
Figure 317: Conventional and RTTI radio blocks

10.3.1.5 Detailed proposal for a 5 ms TTI solution

The problem of a "5 ms TTI" solution is that it is apparently not possible to have a symmetric solution (i.e. a solution which is valid for both the downlink and the uplink) due to impossibility for (single-carrier) mobile stations to receive and transmit on 4 timeslots in the same TDMA frame.

But receiving and transmitting a radio block in the same TDMA frame is not strictly necessary to help reduce the latency. A solution that allows mobile stations to alternate between receiving a radio block in a TDMA frame and then transmitting a radio block in the subsequent TDMA frame would also yield significant benefit.

This is possible as outlined in figure 318.

Nothing can be received by the MS here
-> nothing will be transmitted by the BSS
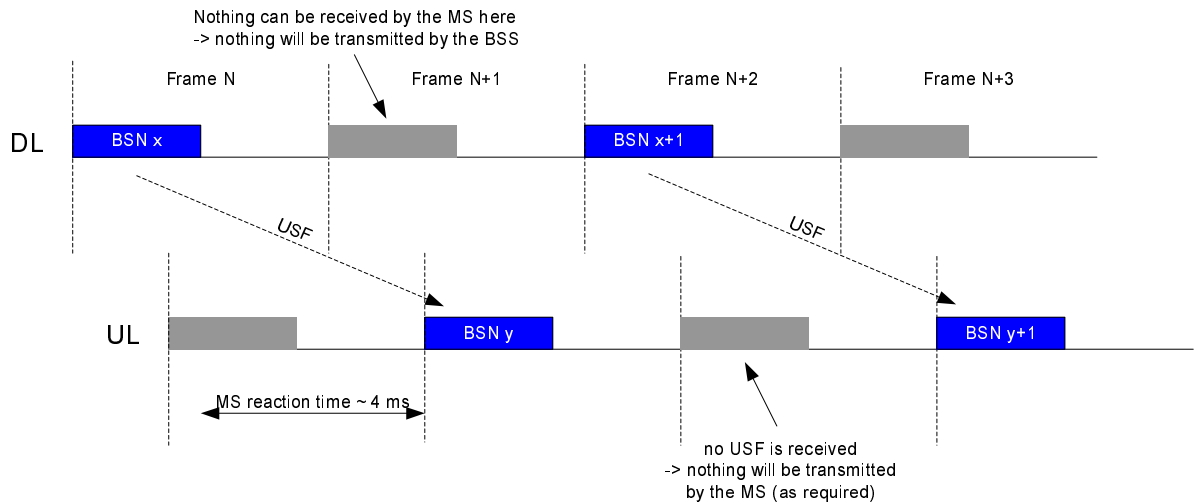
Figure 318: 5 ms TTI solution: transmission/reception in DL and UL

In the figure a DL radio block is sent in TDMA frame N, also containing the USF to allow transmission in the next uplink TDMA frame (N+1). If the mobile station needs to transmit in frame N+1 it might not be able (depending on MS capabilities) to monitor all the needed DL timeslots in the same TDMA frame. But we could easily specify that in this case (i.e. when the mobile station needs to transmit in a given frame) the mobile station is not mandated to read (all of) the DL timeslots in the same frame. This could be very similar to the current rule for EDA.

Referring again to figure 318, since the mobile station cannot receive any USF in the TDMA frame N+1, it will not transmit anything in the TDMA frame N+2 and therefore will be allowed to receive a further DL radio block in the same period, and so on.

The only constraint of this solution is that it will not be possible for both the network and the mobile station to transmit radio blocks onto two consecutive TDMA frames (this restriction is valid with currently available MS capabilities, but can be overcome with dual-carrier configurations).

The overall effect is that, even if 4 timeslots are allocated to a given mobile station in both directions, they can be used (if there is the need to maintain the same bandwidth in UL and DL) only every other frame. Therefore, the corresponding maximum throughput equals the one that can be achieved with a 2 DL + 2 UL configuration. But the benefit would be in terms of reduced latency.

Furthermore, even though the 4 allocated timeslots can only be used every other frame for a given mobile station, other mobile stations in RTTI TBF mode can be easily multiplexed on the same radio resources, thus reducing the risk of radio inefficiencies.

Figure 319 shows the scheduling opportunities for 2 RTTI TBFs on the same resources: the resources that cannot be used by a given TBF can be used by the other one.
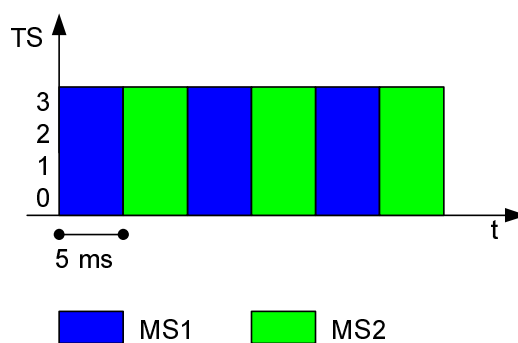
Figure 319: 5 ms TTI solution: Scheduling opportunities for 2 RTTI TBFs on the same resources

The benefit of this approach in terms of latency reduction is evident when deriving the corresponding RLC RTT.

Assuming that the "MS reaction time" (time between setting a polling indication in the DL and sending a feedback information in the UL) could be lower than one TDMA frame (as shown in Figure 23), the RLC RTT would result in:

$$\text{RLC RTT} = \text{BSC delay (10)} + 2\text{x Abis delay (5)} + 2\text{x BTS delay (< 5)} + 2\text{x Um delay (5)} + \text{MS reaction time (< 4)} = \sim\!40 \text{ ms}$$

The gain is also evident from table 158, where the transmission delay an RLC block transmitted 1, 2 and 3 times is shown in three different cases: a legacy, a "10 ms TTI" and a "5 ms TTI" TBF.

Table 158: Delay budget for an RLC block transmitted 1, 2 and 3 times with legacy (black) / 10 ms TTI (red) / 5 ms TTI (blue) TBFs

Drection	BSC/PCU	Abis	BTS	Um	MS	Sum
BSC →	10	20/10/5	< 5	20/10/5		55/35/25
← MS		20/10/5	< 5	20/10/5	40[(1)]/10[(2)]/<4	
BSC →	10	20/10/5	< 5	20/10/5		195/105/65
← MS		20/10/5	< 5	20/10/5	40/10/<4	
BSC →	10	20/10/5	< 5	20/10/5		335/175/105
NOTE 1: Currently minimum possible MS reaction time.						
NOTE 2: Value considered in other parts of this document for the "10 ms TTI" option (could be set to <4 for a better comparison).						

The consideration that the restriction to transmit every other frame would limit the benefit of the proposal is only partly true, as shown in the simulations contained in subclause 10.7.6, where this effect is taken into account.

Furthermore, although not discussed here in detail, the same considerations outlined in subclause 10.3.1.6 for the "10 ms TTI" approach remain valid for the "5 ms TTI" solution:

- It is possible to define both "4-burst" and "2-burst" RTTI radio blocks. In this case 2-burst RTTI radio blocks would be sent by using just two timeslots in the same TDMA frame (and the restriction to transmit every other frame could thus be limited/avoided).

- The rules regarding the stealing flags settings can be easily adapted.

- The rules regarding the USF scheduling can also be easily adapted.

10.3.1.6 Coexistence of legacy and RTTI TBFs (including 4-burst and 2-burst options)

10.3.1.6.1 Stealing Flags setting and decoding

For RTTI blocks transmitted with GMSK there is the need to specify how the MS could distinguish them from GPRS Coding Schemes (CS1-4) and EGPRS ones (MCS1-4), and in particular how the MS could distinguish between the 2-burst or 4-burst format of RTTI blocks.

The solution could reuse the same approach adopted when EGPRS was introduced: for MCS1-4 all the "legacy" stealing flags are set to indicate CS4, while four extra stealing flags (i.e. 1 per burst) are set to '0,0,0,0' to identify MCS1-4 (see definition of q(8),q(9),…,q(11) in subclause 5.1.5.1.5 of TS 45.003). Anyway, a mobile station in EGPRS TBF mode will always assume that MCS1-4 are used if "legacy" stealing flags indicating CS4 are detected.

Starting from the 2 following considerations:

1. Legacy MSs assume that transmission of radio blocks is synchronized on a 20 ms TTI basis. This means that the basic "time unit" should remain 20 ms. If an RTTI block is transmitted in the first 10 ms of a 20 ms time unit, then another RTTI block must follow (and not a normal radio block, since it would break the synchronization rule).

2. Two RTTI blocks transmitted in the same time unit of 20 ms have to use the same modulation (this is needed at least to allow legacy MSs to perform USF decoding).

It is assumed that, if 2 consecutive RTTI blocks are sent in the same 20 ms time unit using GMSK all the "legacy" stealing flags have to be set to indicate CS4.

The following basic rule could therefore be defined:

- When detecting the "legacy" stealing flags set to indicate CS4, a mobile station in RTTI TBF mode will always assume that 2 consecutive GMSK RTTI blocks are sent in the 20 ms time unit.

Additionally, the four extra stealing flags (i.e. $q(8),q(9),\ldots,q(11)$ in subclause 5.1.5.1.5 of 3GPP TS 45.003) could be set to discriminate between "4-burst RTTI blocks" (extra stealing flags set to '0') and "2-burst RTTI blocks" (extra stealing flags set to '1').

To decrease the risk of erroneous detection, 4 additional "RTTI-type" stealing flags are defined, one per burst in the 20 ms time unit, as shown in figure 320.
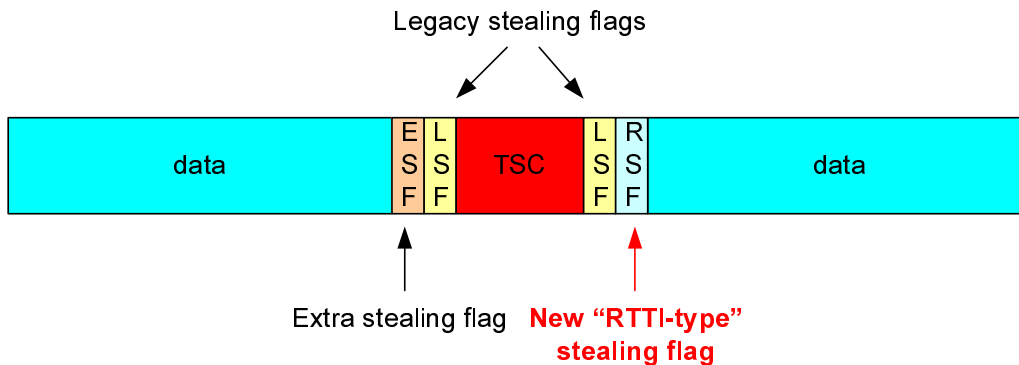
Figure 320: burst format for RTTI blocks.

The four additional "RTTI-type" stealing flags could be set to the same value as the extra stealing flags to discriminate between "4-burst RTTI blocks" ("RTTI-type" stealing flags set to '0') and "2-burst RTTI blocks" ("RTTI-type" stealing flags set to '1').

The overall rule that a mobile station in RTTI TBF mode should follow to detect different types of radio blocks would be then the following:

- **A MS in RTTI TBF mode will identify a block as a "GMSK 2-burst RTTI block" (after 10 ms, as required) by detecting:**

  - **(part of) the "legacy" stealing flags set to indicate CS4**:

    - For the first RTTI block in the 20 ms time unit, the MS would have to discriminate between '0,0,0,1' (first 4 stealing flags to indicate CS4) and the other initial 4-bit configurations to indicate CS1/CS2/CS3.

    - For the second RTTI block in the 20 ms time unit, the MS could use all the stealing flags in the 20 ms time unit, i.e. it could discriminate between '0,0,0,1,0,1,1,0' (stealing flags to indicate CS4) and the other stealing flags settings indicating CS1/CS2/CS3.

  - *plus 4 stealing flags set to '1'*, **i.e.**:

    - 2 extra stealing flags (those that can be read in the 10 ms time unit); plus

    - 2 additional "RTTI-type" stealing flags (those that can be read in the 10 ms time unit).

- **Similarly, a MS in RTTI TBF mode will identify a block as a "GMSK 4-burst RTTI block" (after 10 ms, as required) by detecting:**

  - **(part of) the "legacy" stealing flags set to indicate CS4** (as described above);

  - *plus 8 stealing flags set to '0'*, **i.e.**:

    - 4 extra stealing flags (the 2 that can be read in the 10 ms time unit on a given timeslot and the 2 on the subsequently allocated one); plus

    - 4 additional "RTTI-type" stealing flags (the 2 that can be read in the 10 ms time unit on a given timeslot and the 2 on the subsequently allocated one).

- **In any case a MS in RTTI TBF mode will be able to read a CS1-coded block (after 20 ms) by detecting the "legacy" stealing flags set to indicate CS1.**

This is needed to allow a mobile station to read distribution messages (CS1 coded).

The behaviour of a mobile station depending on the setting of legacy, extra and newly introduced "RTTI-type" stealing flags is summarized in table 159, according to the specific TBF mode.

Table 159: MS behaviour depending on stealing flags settings

Type of transmitted block	Stealing flag settings	Behaviour of the MS according to the specific TBF mode		
		GPRS TBF	**EGPRS TBF**	**RTTI TBF**
CS1 block	- Legacy stealing flags set to CS1	CS1 decoding	CS1 decoding	CS1 decoding
CS2-3 block	- Legacy stealing flags set to CS2-3	CS2-3 decoding	No decoding	No decoding
CS4 block	- Legacy stealing flags set to CS4	CS4 decoding	MCS1-4 decoding [decoding will fail]	"GMSK 2/4-burst RTTI block" decoding [decoding will fail]
MCS1-4 block	- Legacy stealing flags set to CS4 - Extra stealing flags set to '0,0,0,0'	CS4 decoding [decoding will fail]	MCS1-4 decoding	"GMSK 2/4-burst RTTI block" decoding [decoding will fail]
"GMSK 2-burst RTTI" block	- Legacy stealing flags set to CS4 - 2 extra stealing flags set to '1' - 2 additional "RTTI-type" stealing flags set to '1'	CS4 decoding [decoding will fail]	MCS1-4 decoding?? [if performed, decoding will fail]	"GMSK 2-burst RTTI block" decoding (after 10 ms)
"GMSK 4-burst RTTI" block	- Legacy stealing flags set to CS4 - 4 extra stealing flags set to '0' (2 on a given timeslot and 2 on the subsequently allocated one) - 4 additional "RTTI-type" stealing flags set to '0' (2 on a given timeslot and 2 on the subsequently allocated one)	CS4 decoding [decoding will fail]	MCS1-4 decoding?? [if performed, decoding will fail]	"GMSK 4-burst RTTI block" decoding (after 10 ms)

Regarding 8-PSK modulation, it can be assumed that when 8-PSK RTTI blocks are sent, the legacy stealing flags are set to one of the currently defined values - i.e. '0,0,0,0,0,0,0,0' (indicating MCS5 and 6) or '1,1,1,0,0,1,1,1' (indicating MCS7, 8 and 9). This would indicate the USF positions for a legacy MS (and also for a MS in RTTI TBF mode).

The first basic rule for 8-PSK modulated blocks would be the following:

- **When detecting the legacy stealing flags set to indicate MCS5&6 or MCS7,8&9, a mobile station in RTTI TBF mode will always assume that 2 consecutive 8-PSK RTTI blocks are sent in the 20 ms time unit.**

However, "extra" stealing flags are not defined for MCS5-9. Hence, we can define a whole set of 8 "RTTI-type" stealing flags for 8-PSK RTTI blocks, to discriminate between "8-PSK 4-burst RTTI blocks" ("RTTI-type" stealing flags set to '0') and "8-PSK 2-burst RTTI blocks" ("RTTI-type" stealing flags set to '1').

The overall rule that a mobile station in RTTI TBF mode should follow to detect different types of 8-PSK modulated radio blocks would be then the following:

- **A MS in RTTI TBF mode will identify a block as a "8-PSK 2-burst RTTI block" (after 10 ms, as required) by detecting:**

  - **(part of) the "legacy" stealing flags set to indicate MCS5&6 or MCS7,8&9:**

    - For the first RTTI block in the 20 ms time unit, the MS would have to discriminate between '0,0,0,0' (first 4 stealing flags to indicate MCS5&6) and the other initial 4-bit configurations to indicate MCS7,8&9, i.e. '1,1,1,0'.

    - For the second RTTI block in the 20 ms time unit, the MS could use all the stealing flags in the 20 ms time unit, i.e. it could discriminate between '0,0,0,0,0,0,0,0' (stealing flags to indicate MCS5&6) and the other stealing flags settings indicating MCS7,8&9, i.e. '1,1,1,0,0,0,0,1'.

- *plus 4 additional "RTTI-type" stealing flags set to '1'* (the four that can be read in the 10 ms time unit)

- **Similarly, a MS in RTTI TBF mode will identify a block as a "8-PSK 4-burst RTTI block" (after 10 ms, as required) by detecting:**

  - **(part of) the "legacy" stealing flags set to indicate MCS5&6 or MCS7,8&9** (as described above).

  - *plus 8 additional "RTTI-type" stealing flags set to '0'* (the four that can be read in the 10 ms time unit on a given timeslot and the four on the subsequently allocated one).

The description above refers to the MS behaviour for downlink transmission. In case of uplink transmission, the behaviour of the receiver in network would be similar (the network has more information though, since it controls the UL transmission via the USF scheduling).

10.3.1.6.2 USF setting and decoding

NOTE: This subclause addresses the issue handled in subclause above, but when the 2-burst radio blocks option is considered.

Another problem to solve is to allow legacy USF decoding (which needs 20 ms), in conjunction with fast (10ms) USF scheduling for RTTI TBFs.

The solution could be to have both a normal USF (read also by legacy MSs) plus 2 "10 ms USFs" (read only by MSs in RTTI TBF mode) defined in the 20 ms time unit on a given timeslot. Clearly, if the normal USF is set to a valid value, the 2 "10 ms USFs" will have to be set to an undefined value, and vice versa.

Note that the assumption here is that the "10 ms USFs" is defined per timeslot, regardless of the 2-burst or 4-burst RTTI block format of the DL RTTI block containing it.

- If a MS in RTTI TBF mode reads the corresponding "10 ms USFs" on a given timeslot it will be allowed to send a "2-burst RTTI blocks" on the corresponding timeslot.

- If a MS in RTTI TBF mode reads the corresponding "10 ms USFs" on a given timeslot and also on the subsequently allocated one, it will be allowed to send either a "4-burst RTTI blocks", or 2 different "2-burst RTTI blocks" on the two timeslots.

Furthermore, a normal USF could be assigned to an RTTI TBF as well. This would allow to transmit legacy blocks in the DL (with legacy USF), but still schedule RTTI blocks in the UL:

- If a MS in RTTI TBF mode reads the corresponding normal USF in a legacy downlink radio block on a given timeslot, it will be allowed to send 2 consecutive "2-burst RTTI blocks" on the corresponding timeslot.

- If a MS in RTTI TBF mode reads the corresponding normal USF in 2 legacy downlink radio blocks transmitted on a given timeslot and on the subsequently allocated one, in addition to the options above it will be also allowed to send 2 consecutive "4-burst RTTI blocks".

It has to be noticed that the "10 ms USF" would anyway refer to a point in time 20 ms ahead (not 10), to allow multiplexing with legacy MSs. This is shown in figure 321. The benefit of the proposal would be mainly in the higher scheduling flexibility.
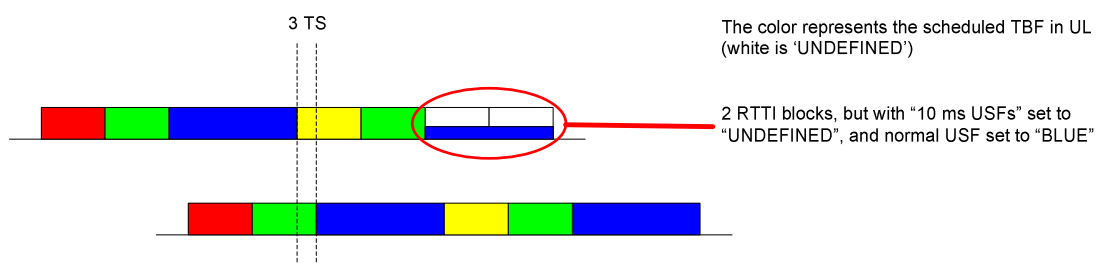
Figure 321: USF scheduling in case of multiplexing with legacy TBFs

Things would change if multiplexing with legacy MSs were not required. In this case it is not necessary to maintain the normal USF (to be read in 20 ms) and RTTI blocks could just carry 1 or 2 "10 ms USF" (1 in case of "2-burst format", 2 in case of "4-burst format"). In this case the USF would refer to a point in time 10 ms ahead allowing a further 10 ms reduction in latency. This is shown in figure 322.
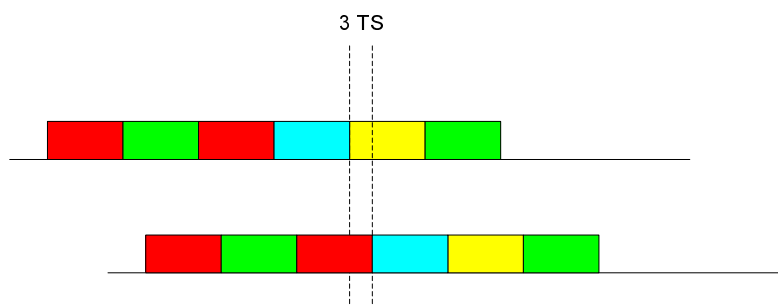
Figure 322: USF scheduling in case of no multiplexing with legacy TBFs

A further proposal is therefore to allow the possibility to define, in the RTTI TBF establishment phase, whether the "10 ms USF" has to be considered as a pointer to 20 ms ahead (scenario where multiplexing with legacy MSs is needed) or as a pointer to 10 ms ahead (scenario where multiplexing with legacy MSs is not needed).

10.3.1.7 Coexistence of legacy and RTTI TBFs (simplified RTTI solution)

The introduction of all the options in 10.3.1.6 would increase the complexity of the RTTI proposal:

- The 5 ms TTI solution would imply a 4 DL + 4 UL timeslots capable mobile station (although it would not be required to transmit AND receive on 4 timeslots during the same TDMA frame, see [6]). Furthermore the 5 ms TTI option would be hardly compatible with a DTM configuration.

- The introduction of the 2-burst radio block option would lead to the definition of:

  - completely new modulation and coding schemes;

  - the need to introduce additional stealing flags to signal the new radio block formats, see [7];

  - the need to add additional USF fields in a DL RTTI block, see [7].

In the following we assume that only the "4-bursts radio blocks with 10 ms TTI" option is supported. As has already described this can be achieved by transmitting 4 bursts in parallel onto 2 different timeslots.

The basic advantage of this approach is that legacy MCSs can be maintained, apart from the interleaving scheme. If the RTTI solution is combined with the Fast Ack/Nack Reporting proposal, some modifications will anyway be needed to the payload coding, in case where an RLC data block needs to contain a short bitmap.

In any case no additional stealing flags would have to be defined, nor additional USF fields in DL RTTI blocks, as described in the following.

10.3.1.7.1 The Stealing Flags problem

For RTTI blocks transmitted with GMSK there is the need to specify how the MS could distinguish them from GPRS Coding Schemes (CS1-4) and EGPRS ones (MCS1-4).

The solution is simple and reuses the same approach adopted when EGPRS was introduced: for MCS1-4 all the legacy stealing flags are set to indicate CS4, while four extra stealing flags (i.e. 1 per burst) are set to '0,0,0,0' to identify MCS1-4 (see definition of q(8),q(9),…,q(11) in subclause 5.1.5.1.5 of 3GPP TS 45.003). Anyway, a mobile station in EGPRS TBF mode will always assume that MCS1-4 are used if legacy stealing flags indicating CS4 are detected.

Starting from the 3 following considerations:

1. Legacy MSs assume that transmission of radio blocks is synchronized on a 20 ms TTI basis. This means that the basic "time unit" should remain 20 ms. If an RTTI block is transmitted in the first 10 ms of a 20 ms time unit, then another RTTI block must follow (and not a normal radio block, since it would break the synchronization rule).

2. Two RTTI blocks transmitted in the same time unit of 20 ms have to use the same modulation (this is needed at least to allow legacy MSs to perform USF decoding).

3. A MS in RTTI TBF mode doesn't have to distinguish between EGPRS MCSs and RTTI MCSs on the same resources.

We can assume that, if 2 consecutive RTTI blocks are sent in the same 20 ms time unit using GMSK all the legacy stealing flags - on both timeslots - have to be set to indicate CS4 (while the four extra stealing could be set again to '0', see note).

NOTE. This is possible considering the assumption 3 above.

Correspondingly, in case of GMSK modulation, a MS in RTTI TBF mode will only have to distinguish between two different cases:

- **A MS in RTTI TBF mode will identify a block as a "GMSK RTTI block" (after 10 ms, as required) by detecting (part of) the legacy stealing flags set to indicate CS4:**

    - For the first RTTI block in the 20 ms time unit, the MS would have to discriminate between '0,0,0,1' (first 4 stealing flags to indicate CS4) and the other initial 4-bit configurations to indicate CS1/CS2/CS3 (on both timeslots).

    - For the second RTTI block in the 20 ms time unit, the MS could use all the stealing flags in the 20 ms time unit, i.e. it could discriminate between '0,0,0,1,0,1,1,0' (stealing flags to indicate CS4) and the other stealing flags settings indicating CS1/CS2/CS3 (on both timeslots).

- **A MS in RTTI TBF mode will be able to read a CS1-coded block (after 20 ms) by detecting the legacy stealing flags set to indicate CS1:**

    - This is needed to allow a mobile station to read distribution messages (CS1 coded).

The behaviour of a mobile station depending on the setting of the stealing flags is summarized in the table below, according to the specific TBF mode.

Type of transmitted block	Stealing flag settings	Behaviour of the MS according to the specific TBF mode		
		GPRS TBF	**EGPRS TBF**	**RTTI TBF**
CS1 block	Legacy stealing flags set to CS1	CS1 decoding	CS1 decoding	CS1 decoding
CS2-3 block	Legacy stealing flags set to CS2-3	CS2-3 decoding	No decoding	No decoding
CS4 block	Legacy stealing flags set to CS4	CS4 decoding	MCS1-4 decoding [decoding will fail]	"GMSK RTTI block" decoding [decoding will fail]
MCS1-4 block	Legacy stealing flags set to CS4 Extra stealing flags set to '0,0,0,0'	CS4 decoding [decoding will fail]	MCS1-4 decoding	"GMSK RTTI block" decoding [decoding will fail]
GMSK RTTI block	Legacy stealing flags set to CS4 Extra stealing flags set to '0,0,0,0'	CS4 decoding [decoding will fail]	MCS1-4 decoding [decoding will fail]	"GMSK RTTI block" decoding (after 10 ms)

This shows that the behaviour of a mobile station in RTTI TBF mode is the same with respect to a mobile station in EGPRS TBF mode (i.e. the same complexity is expected).

Regarding 8-PSK modulation, we can assume that when 8-PSK RTTI blocks are sent, the legacy stealing flags are set to one of the currently defined values - i.e. '0,0,0,0,0,0,0,0' (indicating MCS5/6) or '1,1,1,0,0,1,1,1' (indicating MCS7/8/9). This would indicate the USF positions for a legacy MS (and also for a MS in RTTI TBF mode).

Correspondingly, in case of 8-PSK modulation, a MS in RTTI TBF mode will only have to distinguish between two different cases:

- A MS in RTTI TBF mode will identify a block as a "MCS5/6 RTTI block" (after 10 ms, as required) by detecting (part of) the legacy stealing flags set to indicate MCS5/6.

- Alternatively, a MS in RTTI TBF mode will identify a block as a "MCS7/8/9 RTTI block" (after 10 ms, as required) by detecting (part of) the legacy stealing flags set to indicate MCS7/8/9.

    NOTE 1:   For the first RTTI block in the 20 ms time unit, the MS would have to discriminate between '0,0,0,0' (first 4 stealing flags to indicate MCS5&6) and the other initial 4-bit configurations to indicate MCS7,8&9, i.e. '1,1,1,0' (on both timeslots).

    NOTE 2:   For the second RTTI block in the 20 ms time unit, the MS could use all the stealing flags in the 20 ms time unit, i.e. it could discriminate between '0,0,0,0,0,0,0,0' (stealing flags to indicate MCS5&6) and the other stealing flags settings indicating MCS7,8&9, i.e. '1,1,1,0,0,0,0,1' (on both timeslots).

The description above refers to the MS behaviour for downlink transmission. In case of uplink transmission, the behaviour of the receiver in network would be similar (the network has more information though, since it controls the UL transmission via the USF scheduling).

10.3.1.7.2   The USF decoding problem

Another problem to solve is to allow legacy USF decoding (which needs 20 ms), in conjunction with the need to schedule RTTI blocks in the UL every 10 ms.

A simple solution - already included in the Feasibility Study on GERAN Evolution - is to specify that MS in RTTI TBF mode will read:

- the USF allowing UL transmission in the first 10 ms of the next 20 ms time unit during 4 TDMA frames (i.e. legacy USF decoding) on the first allocated DL timeslot;

- the USF allowing UL transmission in the second 10 ms of the next 20 ms time unit during 4 TDMA frames (i.e. legacy USF decoding) on the second allocated DL timeslot.

With this proposal a MS in RTTI TBF mode would have to wait 20 ms to read the 2 USFs on the 2 allocated DL timeslots, so the USF would anyway refer to a point in time 20 ms ahead (not 10). This would not necessarily impact the RLC RTT (i.e. the time to perform an RLC retransmission) and would only slightly impact the upper layer RTT (e.g. the ping delay). In any case full interworking with legacy TBFs and full UL scheduling flexibility for RTTI blocks would be guaranteed.

The USF decoding procedure could be further optimized in case multiplexing with legacy TBFs is not required.

In this case it is not necessary to maintain the legacy USF decoding (i.e. USF to be read in 20 ms). Instead, the USF could be coded using the same 4 bursts used for a DL RTTI block (i.e. 4 bursts transmitted in parallel onto 2 different timeslots in 10 ms).

In this case a MS in RTTI TBF mode will read the USF allowing UL transmission in the next 10 ms time unit during 10 ms on 2 different DL timeslots. The USF would therefore refer to a point in time 10 ms ahead allowing a further 10 ms reduction in the upper layer RTT (e.g. the ping delay).

    NOTE: Another possible improvement, in case multiplexing with legacy TBFs is not required, is the possibility to change modulation in DL every 10 ms, further increasing the DL scheduling flexibility.

In both cases (i.e. where multiplexing with legacy TBFs is / is not required) the structure of the DL RTTI blocks would be the same. Only the way the USF is interleaved would change (during 20 ms on a single timeslot OR during 10 ms on 2 different timeslots). Considering this, it is possible to define in the RTTI TBF establishment phase whether the USF has to be read per timeslot in 20 ms (scenario where multiplexing with legacy TBFs is needed) or in 10 ms on 2 different timeslots (scenario where multiplexing with legacy TBFs is not needed).

10.3.2   Link level performance

10.3.2.1   Modelling Assumptions and Requirements

The following EGPRS services have been simulated for the timeslot mapping option; MCS-1, MCS-4, MCS-5 and MCS-9. Each simulation point has been run with 10 000 radio blocks (40 000 bursts).

Simulated radio scenarios:

-   Sensitivity: TU50iFH.

-   Co-channel interference: TU3iFH and TU3noFH.

Other simulator settings:

-   Blind detection of modulation was used.

-   RX impairments typical to a base transceiver station were used.

-   Uplink direction.

-   No antenna diversity.

-   When multiple time-slots are used in a TDMA frame, they are adjacent in time.

-   When multiple frequencies are used, they are separated in frequency to give independent multi-path fading.

10.3.2.2   Performance Characterization

The link level performance for case i, ii, iii and iv (as described in subclause 10.3.2.1) is summarised in tables 160 and 161. Reference performance with the regular radio block mapping is also shown. Detailed results can be found in Annex A. BLER means the total BLER, i.e. both header BLER and data BLER are considered. A '-' means the case has not been simulated. Note: different IP packet sizes (different types of services) could be considered further.

Table 160: Sensitivity performance, Es/No [dB] @ BLER=10^{-1}

	TU50iFH				
	Ref.	**i**	**ii**	**iii**	**iv**
MCS1	5.4	6.8	8.5	5.4	5.4
MCS4	16.9	16.1	15.2	16.9	16.9
MCS5	13.2	14.4	16.7	13.2	13.2
MCS9	27.2	25.8	25.8	27.2	27.2

Table 161: Co-channel performance, C/Ic [dB] @ BLER=10^{-1}

	TU3iFH					TU3noFH				
	Ref.	**i**	**ii**	**iii**	**iv**	**Ref.**	**i**	**ii**	**iii**	**iv**
MCS1	6.6	7.4	8.7	6.6	6.6	9.9	-	-	-	6.6
MCS4	17.7	17.4	16.7	17.7	17.7	15.2	-	-	-	17.7
MCS5	11.6	12.6	14.4	11.6	11.6	16.0	-	-	-	11.6
MCS9	26.3	25.8	25.7	26.3	26.3	24.7	-	-	-	26.3

The following observations of the performance relative to the regular radio block mapping can be made:

-   Radio block mapping in time-slot domain:

    -   With ideal frequency hopping, performance is degraded by up to 3.5 dB for MCS-1 and MCS-5 since they have strong channel coding and frequency diversity is reduced, whereas performance is improved by up to 1.7 dB for MCS-4 and MCS-9 since they have no channel coding.

-   Radio block mapping in frequency domain:

- With ideal frequency hopping, performance is unchanged for all MCS:s since frequency diversity is maintained.

- Without frequency hopping, case iv has the same performance as with ideal frequency hopping since interleaving is done over four frequencies.

10.3.2.3   Conversational services with reduced TTI

10.3.2.3.1   Introduction

This subclause aims at evaluating some worst case scenarios compared to TU3iFH. From the link level results some conclusions are drawn on the effects on application level.

The losses at more severe radio conditions are relevant regardless of the service. However, for other services than VoIP, the reference is legacy EGPRS, for which the losses will be the same as with reduced TTI. Therefore, the relative latency gains will be approximately the same regardless of the speed and channel profile. For VoIP, on the other hand, the latency gain relative to legacy EGPRS is not the main interest; instead it is necessary to fulfil an absolute latency requirement with sufficient coverage. The reference for VoIP is rather circuit switched speech. Therefore, this contribution focuses at VoIP, and consequently the performance loss after one retransmission is of interest (recall that it is possible to send one retransmission within the delay budget with a TTI of 10 ms).

10.3.2.3.2   Application Level Effects

In the previous Ericsson contributions a reduced transmission time interval (RTTI) of 10 ms was evaluated where the reduction in transmission time was achieved in the downlink by dual carrier and in the uplink by dual time slot transmission. Therefore, the link level simulations in this contribution have both been evaluated with the conventional radio block format, i.e. a radio block is transmitted on one time slot in four consecutive TDMA frames, but also with a dual time slot format where two time slots are used in two consecutive TDMA frames. These two alternatives are referred to as radio block format 1 and 2 respectively. The performance of the dual carrier scheme will be identical to radio block format 1 if ideal frequency hopping is utilized.

Previously it has been shown that the worse radio conditions experienced by the terminal the harder it is to fulfil the latency requirements of the chosen service, see [8]. Thus, the performance losses or gains are evaluated at the cell border where a C/I of 9 dB is assumed. The performance measure is loss/gain in coverage compared to TU3iFH.

At present time no protocol level simulations have been conducted to verify the effects on the application layer. Thus, only preliminary conclusions can be made.

10.3.2.3.3   Simulator settings

A state-of-the art link level simulator has been used for the evaluation of the different channel models. The parameter settings are shown in table 162. Thus, the frequency band is kept at 900 MHz for all simulations. However, since RA250noFH is simulated, the faster fading experienced at higher frequency bands is assumed to be somewhat covered.

NOTE.   RA250 at 800/900 MHz is replaced by RA130 at 1800/1900 MHz in the receiver performance requirements in 3GPP TS 45.005. Therefore, this is the channel with the maximum Doppler frequency.

Table 162: Link simulator settings

Parameter	Value
Channel profile	Typical Urban (TU) Rural Area (RA) Hilly Terrain (HT)
Terminal speed	3 km/h (TU) 100 km/h (HT) 250 km/h (RA)
Frequency band	900 MHz
Frequency hopping	Ideal (TU) No (TU, RA, HT)
Interference	Single co-channel interferer
Direction	Uplink
Antenna diversity	No
Incremental redundancy	Yes
Radio block format	1) One time slot on four consecutive TDMA frames (conventional transmission) 2) Dual time slot. Two time slots on two consecutive TDMA frames.
Impairments: - Phase noise - I/Q gain balance -I/Q phase imbalance - DC offset - Frequency error - PA model	Tx / Rx 0.8 / 1.0 [degrees (RMS)] 0.1 / 0.2 [dB] 0.2 / 1.5 [degrees] -45 / -40 [dBc] - / 25 [Hz] Yes/ -

The simulations have been conducted with incremental redundancy, IR. For the cases where there is no frequency hopping between the bursts within a radio block, there is a delay between the different IR transmissions to account for the time it takes for the control signalling (the round-trip time). This time has been chosen to be 70 ms and 120 ms for 10 ms and 20 ms TTI respectively.

10.3.2.3.4 Simulation results

Simulations have been performed on different channel profiles with different speeds depending on the channel used. For the evaluation of each channel model, TU3iFH is used as reference.

RA250noFH

In figure 323 the performance of MCS-2 on Rural Area channel at terminal speed 250 km/h is shown when radio block format 1 is used (conventional radio block transmission).
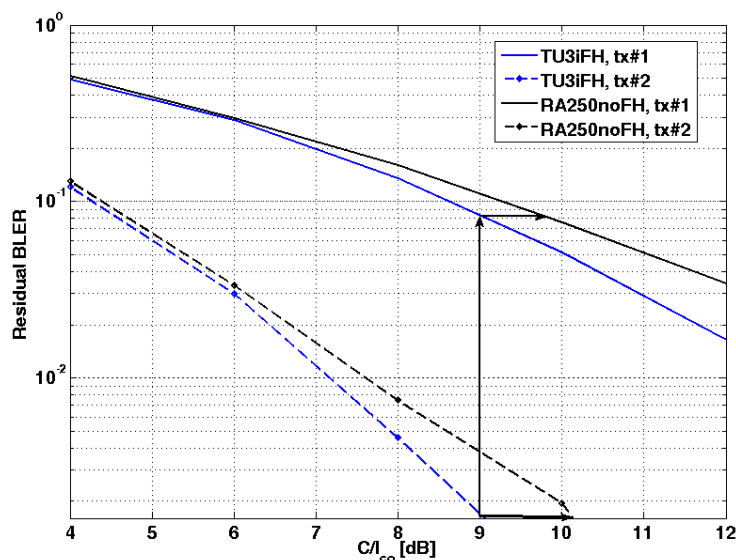
**Figure 323: Link performance of MCS-2 for TU3iFH and RA250noFH
when incremental redundancy and radio block format 1 is used**

It is seen that the coverage loss at the cell border could be expected to be at the most 1.2 dB for the first IR retransmission. In the first transmission the loss is approximately 0.7 dB. Also MCS-1 and MCS-5 has been evaluated, see table 163.

Figure 324 shows the corresponding plots when radio block format 2 has been used. It is seen that the loss is somewhat larger than for radio block format 1 with a coverage loss of 1 dB in the first transmission and 1.3 dB in the second transmission.
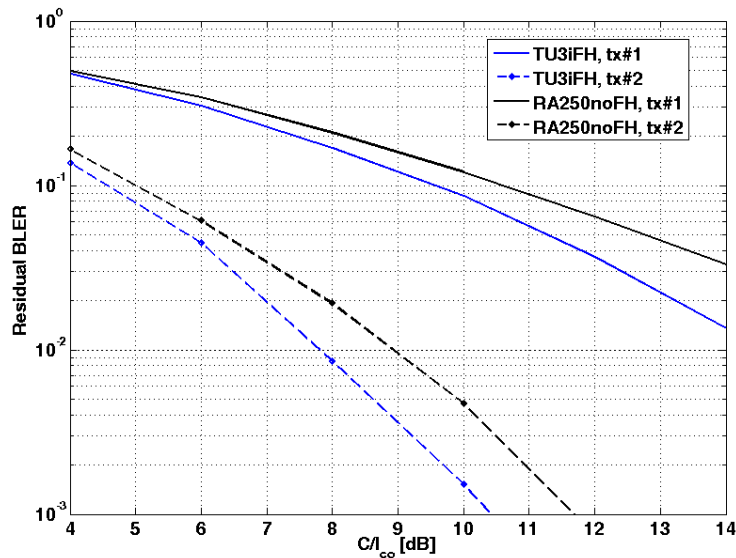
**Figure 324: Link performance of MCS-2 for TU3iFH and RA250noFH
when incremental redundancy and radio block format 2 is used**

Thus, it seems that the RA250noFH channel model degrades the performance of coded MCSs compared to TU3iFH, which was expected. The performance loss is at the most 1.3 dB for MCS-2 using radio block format 2 in the first IR retransmission. However, for the most coded MCSs, MCS-1 and MCS-5, the degradation is not as large probably since the time diversity from the high speed can be used. Note that according to GP-060753 and G2-060186, the end-to-end latency requirement is fulfilled with minimised resource utilisation with MCS-5 at 9 dB C/I on a TU3iFH channel. Therefore, with MCS-5 it will also be fulfilled on a RA250noFH channel, but at 9.3 dB C/I.

The results are summarized in table 163.

Table 163: Coverage loss of RA250noFH compared to TU3iFH.

| | Coverage loss (see note) [dB] | | | |
| | Radio block format 1 | | Radio block format 2 | |
	tx#1	tx#2	tx#1	tx#2
MCS-1	0.8	-	1.2	-
MCS-2	0.7	1.2	1.0	1.3
MCS-5	0.0	0.2	0.4	0.3

NOTE. The coverage loss has been measured given a BLER for TU3iFH @ C/I=9 dB

HT100noFH

For the Hilly Terrain model with a user speed of 100 km/h the coverage loss is listed in table 164.

Table 164: Coverage loss of HT100noFH compared to TU3iFH

| | Coverage loss (see note) [dB] | | | |
| | Radio block format 1 | | Radio block format 2 | |
	tx#1	tx#2	tx#1	tx#2
MCS-1	1.3	-	2.0	2.2
MCS-2	1.3	1.3	1.8	2.1
MCS-5	2.2	2.2	2.6	2.8

NOTE. The coverage loss has been measured given a BLER for TU3iFH @ C/I=9 dB

It is seen that the losses are larger than for RA250noFH but the difference in loss between the first and second transmission is approximately the same. For this channel model the loss is largest for MCS-5 with a loss of, at the most, 2.8 dB. This could be explained by Hilly Terrain having a larger time dispersion than Typical Urban. Since the 8-PSK equalizer has fewer taps than the GMSK-equalizer it is more susceptible to Inter Symbol Interference, ISI. According to GP-060753 and G2-060186, the end-to-end latency requirement is fulfilled with MCS-2 at 9 dB C/I on a TU3iFH channel. Therefore, with MCS-2 it will also be fulfilled on a RA250noFH channel, but at 11.1 dB C/I.

10.3.2.4 Reduced TTI and fast ACK/NACK

10.3.2.4.1 Definition of the new coding schemes

New RTTI coding schemes are defined as shown in table 165.

Table 165: Definition of new coding schemes

		RTTI 2 w/o bitmap	RTTI 2 w/ bitmap	RTTI 3 w/o bitmap	RTTI 3 w/ bitmap	RTTI 5 w/o bitmap	RTTI 5 w/ bitmap	RTTI 6 w/o bitmap	RTTI 6 w/ bitmap
Raw	Header	31	31	31	31	37	37	37	**37**
	Bitmap	0	20	0	20	0	20	0	**20**
	Data	**226**	**194**	**298**	**266**	**450**	**386**	**594**	530
Coded (+CRCs)	Header	117	117	117	117	135	135	135	**135**
	Bitmap	0	78	0	78	0	78	0	**78**
	Data	732	636	948	852	1 404	1 212	1 836	**1 644**
Punctured	Header	80	80	80	80	136	136	136	**136**
	Bitmap	**0**	**54**	**0**	**54**	**0**	**78**	**0**	78
	Data	**372**	**318**	**372**	**318**	**1 248**	**1 170**	**1 248**	1 170
Over head		12	12	12	12	8	8	8	**8**
Total		464	464	464	464	1 392	13 92	1 392	**1 392**

The Header coding is kept unchanged:
The bitmap is independently coded (with a 6 bit CRC). Data has 12 bit CRC. USF bits are included in the header (the coding of USF is unchanged). Over head refers to stealing flags (and extra stealing flags in case of MCS 1-4). The coding of the data for RTTI-MCS 2 and RTTI-MCS 3 with bitmap is slightly less robust than the corresponding coding schemes without bitmap. The coding of the data for RTTI-MCS 5 and RTTI-MCS 6 with bitmap is slightly more robust than the corresponding coding schemes without bitmap. The coding schemes for RTTI MCS schemes without bitmap is kept exactly same as the current MCS schemes (Only the burst mapping changes to allow RTTI option).

The new (RTTI 5 and RTTI 6) coding schemes are defined in such a way that there is always a possibility of retransmission using RTTI 2 and RTTI 3 coding schemes respectively, should link adaptation change the coding scheme by the time of retransmission.

10.3.2.4.2 Header coding

The coding of the header is kept unchanged. Only the burst mapping changes in order to allow reduced TTI operation. In other words, the header bits are mapped on to four bursts and the first two bursts are transmitted in the same TDMA frame in a multislot transmission and the other two bursts are transmitted in the next TDMA frame. The process is illustrated in figure 325.

Normal MCS transmission

RTTI transmission
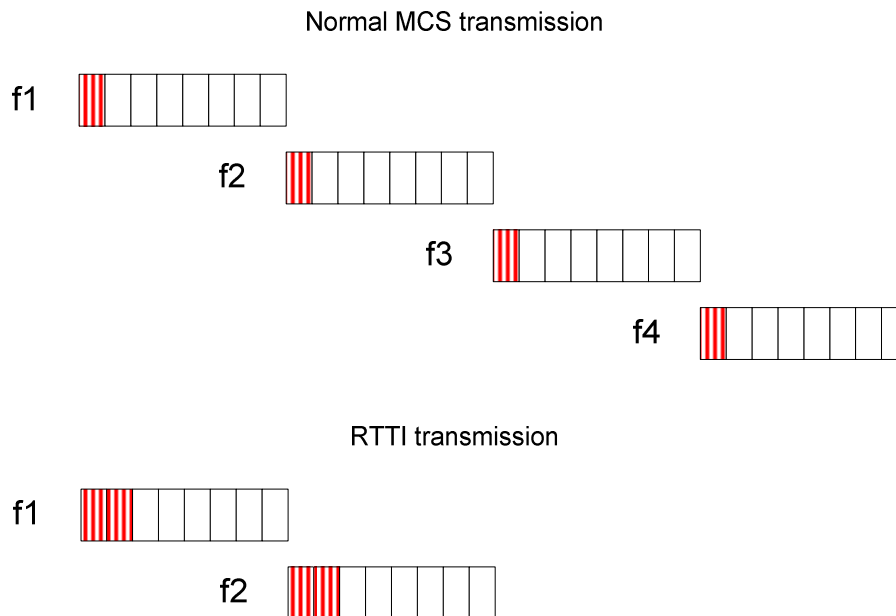
Figure 325: Reduced TTI burst mapping

10.3.2.4.3 Bitmap coding

A constant number of bits (20) per block are assumed as the payload size of the bitmap. The coding of the bitmap is done independently.

10.3.2.4.4 Block code

A 6 bit CRC is added to the 20 bitmap bits. The method used for generating the CRC bits of TCH/AFS logical channels is reused for this purpose. The result is a block of 26 bits.

10.3.2.4.5 Convolutional code

Tail biting convolutional code of 1/3 rate is used to encode the resultant 26 bits (from the block coding mentioned above) the code polynomials used for MCS-1 header coding are used for this purpose. The result is a block of 78 bits.

10.3.2.4.6 Puncturing

For RTTI 2 and RTTI 3 type logical channels, the convolutionally coded bitmap data bits are punctured from 78 bits to 54 bits. A pseudo random uniform puncturing pattern is used for this purpose.

10.3.2.4.7 Interleaving and burst mapping

The bitmap is interleaved as if it is part of data. The method is described in figure 326.
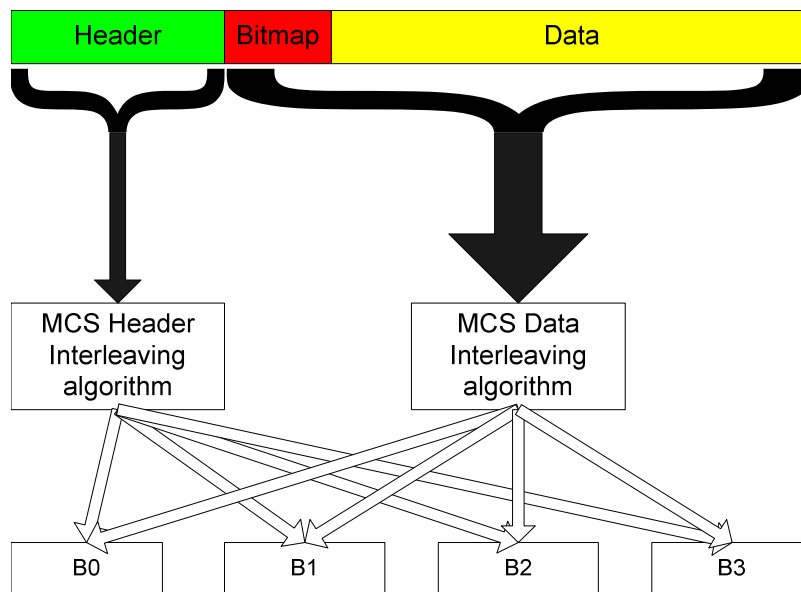
Figure 326: Interleaving of RTTI type data

10.3.2.4.8   Data coding

The size of the payload for each RTTI scheme is as shown in table 165. The basic coding scheme of the data is kept unchanged. (i.e. block coding, convolutional coding etc). However the algorithms operate on blocks of different sizes. The puncturing is done again using a pseudo random uniform puncturing pattern. The interleaving and burst mapping is done as specified in subclause 10.3.2.4.7.

10.3.2.4.9   Simulation results

Simulations are done for RTTI 3 and RTTI 6 type coding schemes for TU3 and TU 50 ideal frequency hopping channels for low band (GSM 800) and also for TU 50 in upper band (GSM 1800/1900). The results are shown in this subclause. The RTTI type coding schemes are assumed to always have the bitmap for first and second transmissions. A comparison is made against standard MCS schemes as defined currently. The idea is to have an insight of the performance achieved by the new coding schemes and the loss in the performance due to loss of frequency diversity.
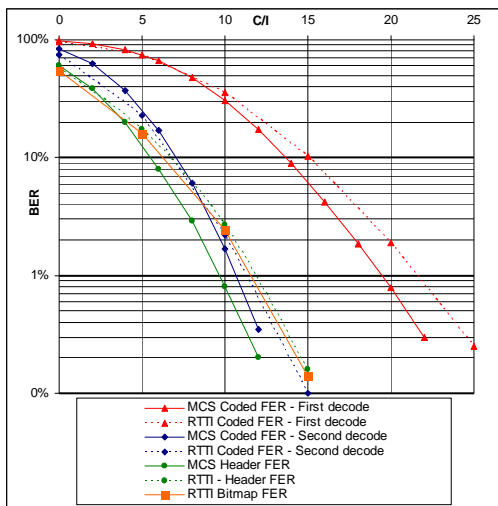
**Figure 327: MCS 3 like coding scheme -
TU 3 ideal FH**
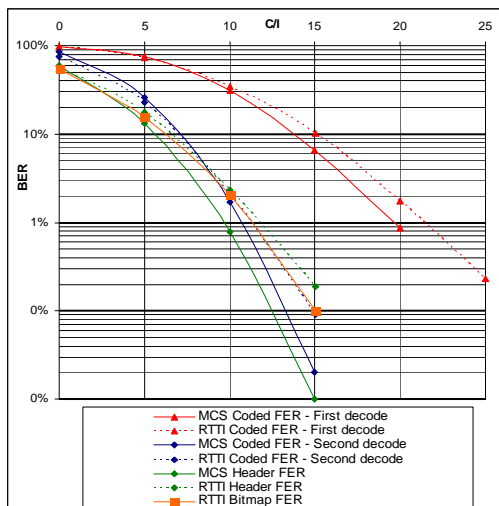
**Figure 328: MCS 3 like coding scheme -
TU 50 ideal FH**
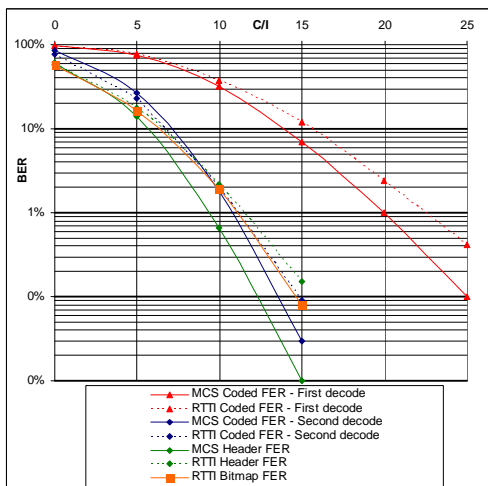
**Figure 329: MCS 3 like coding scheme -
TU 50 ideal FH - GSM 1800/1900**
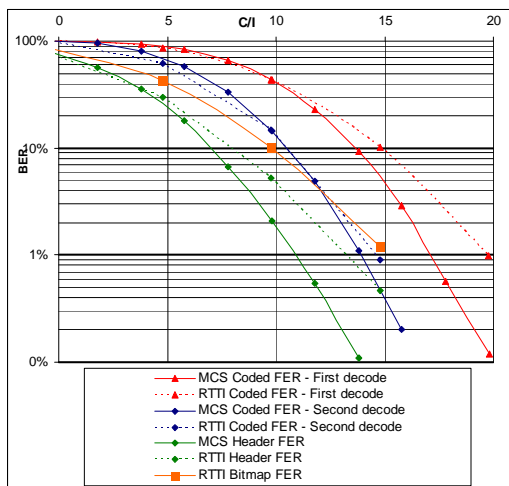
**Figure 330: MCS 6 like coding scheme -
TU 3 ideal FH**
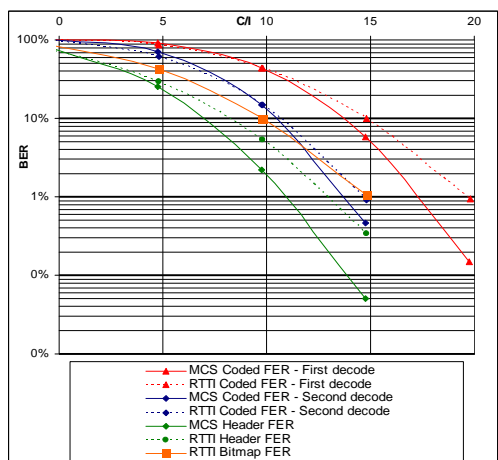
**Figure 331: MCS 6 like coding scheme -
TU 50 ideal FH**
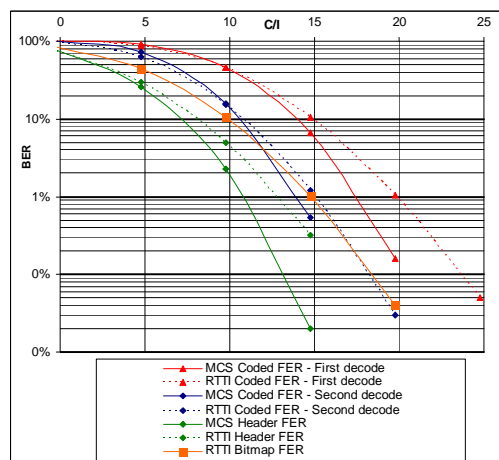
**Figure 332: MCS 3 like coding scheme -
TU 50 ideal FH - GSM 1800/1900**

10.3.3   Application performance

This subclause makes an evaluation of five traffic cases with use of a simulator:

1. End-to-end latency with Ping.

2. Conversational service over packet data (VoIP).

3. E-mail receiving and sending, using POP3 and SMTP respectively.

4. E-mail synchronization, using IMAP.

5. Web page download, using HTTP/1.1 without Pipelining.

The Ping analysis could be seen as a background to any further discussions whether a Reduced TTI has any potential to give gains to end-user services or not.

The analysis is made for single-user cases as well as for multiplexing of users in multiple-user cases. The RTT mode used is "active RTT", which means that TBF setup procedures are not considered.

10.3.3.1   Modelling Assumptions and Requirements

Table 166 gives the simulation assumptions. Any further assumptions are defined in direct relation to the results in next subclause.

Table 166: Simulation parameters used in the simulations

Type	Value	Comment
Radio Conditions	TU3iFH, C/I 9dB and 15dB	-
RLC re-transmission scheme	RLC acknowledged mode	Unlimited number of re-transmissions.
RRBP	**20ms TTI:** 20ms response time 10ms TTI: 20ms response time	The RRBP for both 20ms and 10ms TTI is set to 20ms reaction time in the mobile for an RRBP poll (after reception of the RRBP poll block). Thus 20ms reaction time is valid for both 20ms and 10ms TTI, for a fair comparison. Note that this implies a reduced RRBP compared to the legacy case (which is 40ms).
AMR encoding delay	40+15 = 55ms	Only applicable to the VoIP cases. 40ms speech (2*AMR frames) packed into one IP packet plus 15ms processing time.
AMR decoding delay	15ms	Only applicable to the VoIP cases. Processing time.
MS delay, UL/DL	**Both cases:** 5/5 = 10ms	Processing time.
Abis, UL/DL	**10ms TTI:** 10/10 = 20ms 20ms TTI: 20/20 = 40ms	Product implementation. 20ms reduction from product improvement, for a round-trip.
TTI	10ms and 20ms	Applicable both to data and RLC/MAC control signalling.
Core Network + server delay, UL/DL	**Both cases:** 5/5 = 10ms	Processing and transport time.
BSS buffers, UL/DL	**10ms TTI:** 0/10 = 10ms 20ms TTI: 0/20 = 20ms	Product implementation. Processing time rounded up to the nearest TTI.
Application data to Um synchronization, UL/DL	**10ms TTI:** 0..10/0..10 = 0..20ms 20ms TTI: 0..20/0..20 = 0..40ms	Um slot waiting time UL and DL in a single-user case. In multi-user cases scheduling principles apply as well.

Different Ack/Nack (RRBP) polling strategies were applied for VoIP compared to the other traffic cases. In case of VoIP a frequent polling strategy was applied, whereas a relaxed frequency was applied for the other traffic cases.

10.3.3.2 Performance Characterization

10.3.3.2.1 Single-user cases

10.3.3.2.1.1 Introduction

Single-user cases have been analysed with simulations for Ping, VoIP and e-mail sending and receiving. Single-user means, in this context, that there is only one mobile reserved per packet channel. Thus, more users can be served by one base station or cell (and even TRX) and the results in this subclause are still applicable.

The mobile is reserved with 4 timeslots downlink and 4 timeslots uplink in all scenarios for a fair comparison. For the VoIP cases, this is applicable to both the talker and the listener. For the RTTI cases, Dual-carrier is used in the downlink, whereas Dual-timeslot is used in the uplink to achieve the 10ms TTI. Thus a two TDMA frame interleaving scheme is applicable. The only used Ack/Nack enhancement is a shorter RRBP. Neither event based Ack/Nack nor piggy-backing of Ack/Nacks are included in the simulations. RLC/MAC control signalling is transmitted with the same TTI as the data blocks. Since the RTT mode is "Active RTT", only non-distribution RLC/MAC control signalling is applicable.

10.3.3.2.1.2 Ping

End-to-end latency is typically benchmarked with a Ping traffic case. The default Ping size is 32 bytes which typically ends up with 70 bytes of RLC data: 32 bytes ICMP payload, 8 bytes ICMP header, 20 bytes IP header and 10 bytes LLC/SNDCP header. 70 bytes is valid both for request and response. The simulations performed uses 70 bytes as RLC data payload in uplink as well as downlink, and the Pings are sent back-to-back.

The simulation parameters used in the Ping simulations are listed in table 166.

The results from the simulations are summarized in table 167.

Table 167: Results for the single-user Ping simulations (milliseconds)

		MCS-5					MCS-6					MCS-7				
		Min	Med-ian	Ave	95th	< 100 ms	Min	Med-ian	Ave	95th	< 100 ms	Min	Med-ian	Ave	95th	< 100 ms
C/I 9dB	20ms TTI	129	164	208	387	0%	129	264	225	386	0%					
	10ms TTI	81	125	133	223	39%	72	144	124	216	43%					
	Gain [%]	37%	24%	37%	42%		45%	46%	45%	44%						
C/I 15dB	20ms TTI											130	263	213	270	0%
	10ms TTI											72	143	119	166	45%
	Gain [%]											45%	46%	44%	39%	

The "< 100 ms" column in table 167 shows the number of samples with Ping times below 100 ms. It is expected that the number of samples below 100 ms will be even higher (for the RTTI case) when a more robust MCS is chosen. This shows that the 100 ms objective (for GERAN Evolution) is reached for a large portion of the samples, even with an aggressive MCS, in non-ideal radio conditions.

10.3.3.2.1.3 PS Conversation Service, VoIP

A conversational service over GERAN packet data is analysed in this subclause. The scenario analysed is a mobile to mobile conversation, and the results are presented in mouth-to-ear delay for the different scenarios.

The VoIP scenarios assume 2 AMR 7.95 frames per IP packet, which correspond to 40 ms of speech per IP packet. It also assumes in-order-delivery of LLC packets and TCP/IP header compression, which makes one LLC fit into an MCS-5 (or higher) RLC data block.

The simulation parameters used in the VoIP simulations are listed in table 166.

The results, expressed as mouth-to-ear delay, from the simulations are summarized in tables 168 and 169.

Table 168: Results for the single-user VoIP simulations (milliseconds), C/I 9 dB

C/I [dB]	TTI [ms]	MCS1			MCS2			MCS5			MCS6		
		Min	Med	98th	Min	Med	98th	Min	Med	98th	Min	Med	98th
9	10	146	173	306	127	154	280	127	170	276	127	207	317
	20	174	216	412	174	239	431	174	269	420	174	312	510
	Gain [%]	16	20	26	27	36	35	27	37	34	27	34	38

Table 169: Results for the single-user VoIP simulations (milliseconds), C/I 15 dB

C/I [dB]	TTI [ms]	MCS5			MCS6			MCS7			MCS8			MCS9		
		Min	Med	98th	Min	Med	98th	Min	Med	98th	Min	Med	98th	Min	Med	98th
15	10	127	137	182	127	139	212	127	189	232	127	206	284	128	209	284
	20	174	187	278	174	190	311	174	285	331	174	307	430	177	310	433
	Gain [%]	27	27	35	27	27	32	27	34	30	27	33	34	28	33	34

The highlighted values in tables 168 and 169 are further discussed in Conclusions.

The VoIP service has, in average, the following timeslot utilization (10ms TTI):

- C/I 9dB: 18 % of the 4 timeslots => 0.72 timeslots.

- C/I 15dB: 14 % of the 4 timeslots => 0.56 timeslots.

10.3.3.2.1.4   E-mail

An e-mail service is analysed in this subclause. The scenarios analysed are sending of an e-mail using the SMTP protocol and reception of an e-mail using the POP3 protocol.

The simulation parameters used in the e-mail simulations are listed in table 166.

10.3.3.2.1.4.1   E-mail sending, SMTP

The scenario analysed is sending of an e-mail using the SMTP protocol. A flow-graph of a typical SMTP scenario is described in annex B.

The results, expressed as session time, from the simulations are summarized in tables 170 and 171.

Table 170: Result for the single-user SMTP simulations (milliseconds)
E-mail of 5 kbytes plain text

		MCS-5				MCS-6				MCS-7			
		Min	Med-ian	Ave	95th	Min	Med-ian	Ave	95th	Min	Med-ian	Ave	95th
C/I 9dB	20msTTI	3.24	4.09	4.10	4.60	3.74	4.60	4.60	5.11				
	10msTTI	2.41	2.88	2.90	3.24	2.48	3.03	3.05	3.45				
	Gain [%]	26%	30%	29%	30%	34%	34%	34%	32%				
C/I 15dB	20msTTI									3.09	3.79	3.82	4.30
	10msTTI									1.88	2.31	2.31	2.59
	Gain [%]									39%	39%	40%	40%

Table 171: Result for the single-user SMTP simulations (seconds)
E-mail of 5kbytes plain text plus 100 kbytes attachment

		MCS-5				MCS-6				MCS-7			
		Min	Med-ian	Ave	95th	Min	Med-ian	Ave	95th	Min	Med-ian	Ave	95th
C/I 9dB	20msTTI	19.5	20.3	20.3	21.2	19.2	20.7	20.7	21.6				
	10msTTI	18.7	19.5	19.4	19.9	17.9	18.7	18.7	19.3				
	Gain [%]	4%	4%	4%	6%	9%	9%	10%	11%				
C/I 15dB	20msTTI									13.1	13.9	13.9	14.7
	10msTTI									10.7	11.4	11.4	11.8
	Gain [%]									18%	18%	18%	20%

10.3.3.2.1.4.2   E-mail receiving, POP3

The scenario analysed is a reception of an e-mail using the POP3 protocol. A flow-graph of a typical POP3 scenario is described in annex B.

The results, expressed as session time, from the simulations are summarized in tables 172 and 173.

Table 172: Result for the single-user POP3 simulations (milliseconds) - E-mail of 5 kbytes plain text

		MCS-5				MCS-6				MCS-7			
		Min	Med-ian	Ave	95th	Min	Med-ian	Ave	95th	Min	Med-ian	Ave	95th
C/I 9dB	20msTTI	3.50	4.08	4.13	4.68	3.97	4.65	4.66	5.21				
	10msTTI	2.48	2.87	2.90	3.22	2.49	3.00	3.00	3.27				
	Gain [%]	29%	30%	30%	31%	36%	36%	36%	37%				
C/I 15dB	20msTTI									3.02	3.61	3.60	3.91
	10msTTI									1.87	2.24	2.23	2.46
	Gain [%]									38%	38%	38%	37%

Table 173: Result for the single-user POP3 simulations (seconds)
E-mail of 5 kbytes plain text plus 100 kbytes attachment

		MCS-5				MCS-6				MCS-7			
		Min	Med-ian	Ave	95th	Min	Med-ian	Ave	95th	Min	Med-ian	Ave	95th
C/I 9dB	20msTTI	26.1	27.4	27.4	28.6	27.3	28.9	28.8	29.6				
	10msTTI	20.6	21.8	21.7	22.2	21.0	22.6	22.5	23.1				
	Gain [%]	21%	20%	21%	22%	23%	22%	22%	22%				
C/I 15dB	20msTTI									18.6	19.3	19.3	19.9
	10msTTI									14.2	14.7	14.7	15.0
	Gain [%]									24%	24%	24%	25%

10.3.3.2.1.4.3   E-mail synchronization using IMAP

The scenario analyzed is a synchronization of an e-mail inbox using the IMAP protocol. The e-mail account consists of a number of folders, where only the Inbox is synchronized. The scenario starts with the e-mail client already running and when establishing a TCP connection. Then the e-mail client performs a login to the e-mail account. The scenario ends when all headers are downloaded and displayed in the e-mail client. Only the headers and flags (indicating "read"/"answered" etc) of the e-mails are downloaded. A flow-graph of a typical IMAP scenario is described in annex B.

Two Inbox scenarios are simulated, first where the Inbox consists of 100 e-mails where 27 of them are new since the last synchronization. Secondly, where the Inbox consists of 20 e-mails where 5 of them are new.

The results, expressed as session time, from the simulations are summarized in tables 174 and 175.

Table 174: Result for the single-user IMAP simulations (seconds)
100 e-mail headers where 27 are new

		MCS-5				MCS-6				MCS-7			
		Min	Med-ian	Ave	95th	Min	Med-ian	Ave	95th	Min	Med-ian	Ave	95th
C/I 9dB	20msTTI	5.75	6.80	6.81	7.52	6.35	7.64	7.65	8.41				
	10msTTI	4.39	5.02	5.03	5.45	4.76	5.38	5.38	5.81				
	Gain [%]	24%	26%	26%	28%	25%	30%	30%	31%				
C/I 15dB	20msTTI									4.69	5.66	5.64	6.10
	10msTTI									3.22	3.74	3.74	4.00
	Gain [%]									31%	34%	34%	34%

Table 175: Result for the single-user IMAP simulations (seconds)
20 e-mail headers where 5 are new

		MCS-5				MCS-6				MCS-7			
		Min	Med-ian	Ave	95th	Min	Med-ian	Ave	95th	Min	Med-ian	Ave	95th
C/I 9dB	20msTTI	3.18	3.95	3.96	4.50	3.36	4.41	4.43	5.02				
	10msTTI	2.21	2.76	2.77	3.08	2.45	2.96	2.97	3.30				
	Gain [%]	31%	30%	30%	32%	27%	33%	33%	34%				
C/I 15dB	20msTTI									2.69	3.52	3.52	3.92
	10msTTI									1.82	2.21	2.21	2.44
	Gain [%]									32%	37%	37%	38%

10.3.3.2.1.5 Web service

A large web page, consisting of 53 objects and 289 kbytes in total, was used in this analysis. HTTP/1.1 without Pipelining, as used for example by Microsoft Internet Explorer, was used for the analysis. Two parallel TCP connections are used to download the objects.

The results, expressed as session time, from the simulations are summarized in the table below. It should be noted that in a use case where the end-user uses links from a page to another page, the gain in seconds is applicable to all web pages. The gain in seconds is thus applicable to each move to a new page and can be very large in the end. As an example of 5 equally large web pages, the total gain in seconds would be 5*10=50 seconds (C/I 9dB).

Table 176: Result for the single-user Web download simulations (seconds)
Web page of 289 kbytes and 53 objects

		MCS-5				MCS-6				MCS-7			
		Min	Med-ian	Ave	95th	Min	Med-ian	Ave	95th	Min	Med-ian	Ave	95th
C/I 9dB	20msTTI	53.6	56.1	55.9	57.0	55.2	57.9	57.9	59.4				
	10msTTI	45.6	46.7	46.6	47.5	47.0	48.2	48.2	49.3				
	Gain [%]	15%	17%	17%	17%	15%	17%	17%	17%				
C/I 15dB	20msTTI									35.1	36.4	36.4	37.3
	10msTTI									29.7	30.3	30.3	30.8
	Gain [%]									15%	17%	17%	17%

10.3.3.2.2 Multiple-user cases

10.3.3.2.2.1 Introduction

Multiple-user cases have been analysed with simulations for Ping, VoIP and Web download. Multiple-user means, in this context, that there is more than one mobile reserved per packet channel. Thus, the results in this subclause are applicable when packet channel sharing applies. The purposes with the multi-user cases are to analyse the multiplexing delays introduced from scheduling and the possible resource segregation from multiplexing different users on the same packet channels.

Time-slot reservation in the multiple-user cases are done so that there are two mobiles reserved on each packet channel, where one of them is the reference mobile. The reference mobile(s) is the mobile(s) for which end-user performance is measured and presented. Thus, a packet channel sharing of 2 applies for all used packet channels throughout the sessions. The reference mobile(s) has a 4+4 reservation, as in the single user cases. For the legacy case, this thus assumes a type 2 mobile. For the VoIP cases, there are two reference mobiles, since the results are presented in mouth-to-ear delay for a mobile-to-mobile conversation. The same time-slot reservation principle apply, i.e. two mobiles reserved on each packet channel, where one of them is the reference mobile. The two reference mobiles are not multiplexed on the same packet channels.

For the RTTI cases, Dual-carrier is used in the downlink, whereas Dual-timeslot is used in the uplink to achieve the 10 ms TTI. Thus a two TDMA frame interleaving scheme is applicable. The only used Ack/Nack enhancement is a shorter RRBP. Neither event based Ack/Nack nor piggy-backing of Ack/Nacks are included in the simulations. RLC/MAC control signalling is transmitted with the same TTI as the data blocks.

MAC scheduling principles applied are of course important and might differ between implementations. In this context two scheduling principles are applicable: "round-robin" and "QoS-based". "Round-robin" means that the mobiles get an equal share of the packet channels' bandwidth. "QoS-based" means that the priority (relative or absolute) between mobiles are applied in MAC scheduling, which means, higher priority mobiles will get a higher share of the packet channels' bandwidth than lower priority mobiles. For simplicity, only one packet flow per mobile is applied.

Three different multiple-user cases are analysed:

    a) Reference mobile(s): 10ms TTI, Other mobiles: 20ms TTI.

    b) Reference mobile(s): 10ms TTI, Other mobiles: 10ms TTI.

    c) Reference mobile(s): 20ms TTI, Other mobiles: 20ms TTI.

Case c) is considered the reference case, where case a) and b) shall be compared to.

    NOTE: All the multiplexed users use the same Abis transmission time, for a fair comparison. That is, 10 ms Abis is used for case a and b and 20ms Abis is used for case c.

Multiplexing loss, used in the following chapters, is defined as how much of the timeslots that can not be utilised due to scheduling constraints, even though any transmitter has data buffered for transmitting.

10.3.3.2.2.2 Ping

The same Ping case is used as described in subclause 10.3.3.2.1.2. The reference mobile is performing Pings, whereas the other mobiles perform a constant UDP flow in both UL and DL. A "round-robin" MAC scheduling is applied to all mobiles, which means that all mobiles have the same priority.

The simulation parameters used in the Ping simulations are listed in table 166. Note that table 166 only shows the single-user delays. Any additional delay from multiplexing and USF scheduling is fully considered in the simulator.

The results from the simulations are summarized in table 177. The A, B and C cases are described in subclause 10.3.3.2.2.1.

Table 177: Results for the multiple-user Ping simulations (milliseconds)

		MCS-5						MCS-6						MCS-7					
		Min	Median	Ave	95th	Multiplexing Loss	<100 ms	Min	Median	Ave	95th	Multiplexing Loss	<100 ms	Min	Median	Ave	95th	Multiplexing Loss	<100 ms
C/I 9dB	A	102	189	180	274	5.2%	0%	81	156	151	249	8.1 %	29%						
	B	91	179	181	218	0%	8%	73	156	151	255	0%	27%						
	C	161	285	264	406	0%	0%	142	265	230	386	0%	0%						
	Gain A vs. C	37%	34%	32%	33%			43%	41%	34%	35%								
	Gain B vs. C	43%	37%	31%	46%			49%	41%	34%	34%								
C/I 15dB	A													81	154	142	216	4.5%	30%
	B													75	155	146	216	0%	26%
	C													142	264	222	308	0%	0%
	Gain A vs. C													43%	42%	36%	30%		
	Gain B vs. C													47%	41%	34%	30%		

10.3.3.2.2.3 PS Conversation Service, VoIP

The same VoIP case is used as described in chapter 10.3.3.2.1.3. There are two reference mobiles performing a mobile-to-mobile VoIP conversation, whereas the other mobiles perform a constant UDP flow in both UL and DL. A "QoS-based" MAC scheduling is applied to all mobiles. The reference mobiles have an absolute priority (for example QoS Conversational) over the other mobiles (for example QoS Interactive). The scenario analysed is a mobile to mobile conversation, and the results are presented in mouth-to-ear delay for the different scenarios.

The simulation parameters used in the VoIP simulations are listed in table 166. Note that table 166 only shows the single-user delays. Any additional delay from multiplexing and USF scheduling is fully considered in the simulator.

The results from the simulations are summarized in tables 178 and 179. The A, B and C cases are described in subclause 10.3.3.2.2.1.

Table 178: Results for the multiple-user VoIP simulations (milliseconds), C/I 9 dB

C/I [dB]	Scenario	MCS1				MCS2				MCS5				MCS6			
		Min	Med	98th	Multiple	Min	Med	98th	Multiple	Min	Med	98th	Multiple	Min	Med	98th	Multiple
9	A	146	198	358	3.3	130	187	336	4.6	128	190	308	11.0	128	227	379	10.2
	B	147	205	382	0	133	223	405	0	128	189	312	0	128	228	376	0
	C	179	247	472	0	178	348	594	0	175	284	455	0	175	332	534	0
	Gain A vs. C [%]	18	20	24		27	46	43		27	33	32		27	32	29	

Table 179: Results for the multiple-user VoIP simulations (milliseconds), C/I 15 dB

C/I [dB]	Scenario	MCS5				MCS6				MCS7			
		Min	Med	98th	Multiple…	Min	Med	98th	Multiple…	Min	Med	98th	Multiple…
15	A	127	141	195	13.1	127	145	224	12.6	127	204	249	12.2
	B	127	142	207	0	127	146	229	0	128	209	252	0
	C	174	188	297	0	174	191	315	0	175	297	361	0
	Gain A vs. C [%]	27	25	34		27	24	29		27	31	31	

C/I [dB]	Scenario	MCS8				MCS9			
		Min	Med	98th	Multiple…	Min	Med	98th	Multiple…
15	A	128	218	304	12.4	127	222	302	12.1
	B	128	222	305	0	132	226	306	0
	C	177	312	439	0	187	318	440	0
	Gain A vs. C [%]	28	30	31		32	30	31	

The highlighted values in tables178 and 179 are further discussed in Conclusions.

10.3.3.2.2.4 Web donwload

The same Web download case is used as described in subclause 10.3.3.2.1.5. The reference mobile is performing Web download, whereas the other mobiles perform a constant UDP flow in both UL and DL. A "round-robin" MAC scheduling is applied to all mobiles, which means that all mobiles have the same priority.

The simulation parameters used in the Web simulations are listed in table 166. Note that table 166 only shows the single-user delays. Any additional delay from multiplexing and USF scheduling is fully considered in the simulator.

The results from the simulations are summarized in table 180. The A, B and C cases are described in subclause 10.3.3.2.2.1.

Table 180: Results for the multiple-user Web download simulations (seconds)

		MCS-5					MCS-6					MCS-7				
		Min	Median	Ave	95th	Multiplexing Loss	Min	Median	Ave	95th	Multiplexing Loss	Min	Median	Ave	95th	Multiplexing Loss
C/I 9dB	A	81,1	82,6	82,4	83,2	0,2%	79,2	80,6	80,5	81,4	~0%					
	B	81,0	82,2	82,2	83,6	0%	78,9	80,2	80,3	81,2	0%					
	C	88,6	90,5	90,6	92,2	0%	86,8	88,5	88,8	91,1	0%					
	Gain A vs. C	8%	9%	9%	10%		9%	9%	9%	11%						
	Gain B vs. C	9%	9%	9%	9%		9%	9%	10%	11%						
C/I 15dB	A											48,6	49,4	49,4	49,9	~0%
	B											48,4	49,6	49,5	50,2	0%
	C											55,4	56,4	57,2	57,5	0%
	Gain A vs. C											12%	12%	14%	13%	
	Gain B vs. C											13%	12%	13%	13%	

10.3.3.2.3 Summary of Results

This subclause summarizes the gains achieved with the RTTI cases compared to the legacy cases. In table 181, the gains are shown for the single-user cases and table 182 shows the gains for multiple-user cases.

Table 181: Summary of results, single-user cases

Application	Relative Gain (legacy case vs RTTI case)	Absolute Gain (legacy case vs RTTI case)
Small e-mail send, SMTP	29 % to 40 %	~1.5 seconds
Large e-mail send, SMTP	4 % to 18 %	~2 seconds
Small e-mail receive, POP3	30 % to 38 %	~1.5 seconds
Large e-mail receive, POP3	21 % to 24 %	~6 seconds
Small Inbox synch, IMAP	30 % to 37 %	~1.5 seconds
Medium Inbox synch, IMAP	26 % to 34 %	~2.5 seconds
Large Web-page download	17%	~10 seconds
Ping	37 % to 45 %	~100 ms (40 % of samples below 100 ms)
VoIP	Not of significant interest	VoIP works at cell border (C/I 9 dB) Capacity increase potential at C/I 15 dB

Table 182: Summary of results, multiple-user cases

Application	Relative Gain (legacy case vs RTTI case)	Absolute Gain (legacy case vs RTTI case)
Large Web-page download	9 % to 14%	~8 seconds
Ping	32 % to 26 %	~80 ms (~30 % of samples below 100 ms)
VoIP	Not of significant interest	VoIP works at cell border (C/I 9 dB) Capacity increase potential at C/I 15 dB

10.3.3.2.4 Conclusions

10.3.3.2.4.1 General

The simulator has used a Reduced TTI, related Abis improvements (product implementation) and a shorter RRBP. The latency gains from Abis improvements are 20ms per round-trip, and the shorter RRBP improves every downlink re-transmission by 20 ms. The rest of the improvements, which is thus the major part, come from the Reduced TTI.

10.3.3.2.4.2 Single-user cases

Reduced TTI, shorter RRBP and related Abis improvement give an end-to-end latency gain (as measured with Ping) of around 40 % in the single-user cases. Approximately 40 % of the RTTI Ping samples meet the objective in (for GERAN Evolution) of a round-trip below 100 ms in non-ideal radio conditions with the given MCSs.

The improvement in roundtrip gives a significant gain to an e-mail service. For up/down-loading this is especially true for small e-mails/Inbox, where the relative gains decrease for larger e-mails/Inbox. The gains are:

- SMTP: 29 % to 40 % for small e-mails (5kbyte) and 4 % to 18 % for large e-mails (5 + 100 kbytes).

- POP3: 30 % to 38 % for small e-mails and 21 % to 24 % for large e-mails.

- IMAP: 30 % to 37 % for small Inbox and 26 % to 34 % for medium sized Inbox.

Conversational VoIP targets are assumed as:

- Mouth-to-ear delay target of ≤ 300 ms [3].

- FER target of ≤ 1 % per link => ≤ 2 % end-to-end [9] (for speech channels).

As can be seen from the result tables (and yellow marks), the legacy case does not meet the targets of 300ms@2% FER at all at C/I 9dB. The RTTI case meets these targets with MCS-5. At C/I 15dB the legacy case meets the targets with MCS-5 whereas the RTTI case meets the targets using MCS-9. This implies that RTTI is needed to meet the conversational targets at lower C/I, and that the RTTI cases gives significant capacity increase potential, since a higher MCS can be used and still meet the targets.

The improvement in round-trip also gives gains to a Web download. The Web download using HTTP/1.1 gives a gain of 17 % for a large Web page.

10.3.3.2.4.3   Multiple-user cases

Reduced TTI, shorter RRBP and related Abis improvement give an end-to-end latency gain (as measured with Ping) of around 35 % in the multiple-user cases. Note that the same Abis transmission time is used for all multiplexed mobiles, for a fair comparison.

For VoIP (as can be seen from the result tables and yellow marks), the legacy case does not meet the targets of 300ms@2% FER at all at C/I 9dB. The RTTI cases meets these targets with MCS-5 (308 ms). At C/I 15 dB the legacy case meets the targets with MCS-5 whereas the RTTI case meets the targets using MCS-9 (302 ms). This implies that RTTI is needed to meet the conversational targets at lower C/I, and that the RTTI cases gives significant capacity increase potential, since a higher MCS can be used and still meet the targets.

In the cases of multiplexing RTTI and legacy mobiles the multiplexing loss, or resource segregation, for the Ping cases are 5 % to 8 % and for the VoIP cases 3 % to 13 %. The loss is due to that the Ping and VoIP cases implies many starts and stops of data transfer (short bursts of payload), and could therefore be seen as worst case scenarios. Note also that the analysis considers only one RTTI mobile per packet channel. As can be concluded from the Web download cases, the multiplexing loss is very small, ≤ 0.2 %.

Modulation segregation (i.e. the same modulation needs to be used on both 10ms sub-slots to be able to USF schedule other mobiles) is not considered in this analysis, since fixed MCSs are used. Possible techniques to handle modulation segregation are discussed in ref [10].

10.3.3.2.4.4   Capacity gain

Even though capacity gains have not been explicitly evaluated, it is clear that a shorter session time gives a capacity gain, since any pooled resources may be re-used earlier, for other sessions, from the pool.

In the simplest model, where up-to one user is located in each cell, the gain per application can be directly translated into HW savings of any HW resources that are pooled between the cells. As an example, this would mean a HW saving of 4 % to 40 % for e-mail and web services.

The timeslot utilization, for the used VoIP model, has been shown to be 0.6 to 0.7 timeslots per user.

10.4   Variable-sized Radio Blocks

10.4.1   Introduction

One of the goals of GERAN Evolution is to reduce the latency between the mobile station and the Gi interface. Although a significant proportion of this latency is incurred in devices and interfaces which are outside the scope of standardization, we should not ignore the delay incurred over the radio interface.

This paper presents a proposal for Variable Sized Radio Blocks (VSRB) which could reduce the radio-interface delay for small amounts of PS data, both in the uplink and in the downlink.

10.4.2   Motivation

For the transfer of large amounts of data, the latency is primarily determined by the bandwidth available, and, for a given resource allocation and modulation/coding scheme, this is fixed. In fact, the delay (as noticed by the user) is only affected only by the delay of the *last* radio block in the LLC frame (since the LLC frame cannot be passed to higher layers before it has been reassembled).

For the last block in an LLC frame, and for small amounts of data in general, the limiting factor is the delay while the receiver waits for all four bursts to arrive. VSRB aims to reduce this delay in those situations where the amount of data to be sent is small (compared with the amount which could be transmitted in 4 bursts frames).

10.4.3   Concept Description

10.4.3.1   Overview

Under the proposed scheme, new burst mapping rules would be defined (using existing burst structures) which would allow a receiver to decode both the data and header parts of a frame using fewer than four bursts; the exact number would depend on the amount of data to be sent.

Convolutional encoding and puncturing would be used as in the current schemes, although with modified input and output block lengths.

The existing allocations (4 bursts over 4 TDMA frames) are used, which means there are no impacts on the scheduling algorithms or channel assignments, and hence no need for resource segregation.

10.4.3.2   Example: TCP ACK (52 octets)

Using the proposed scheme, an uncompressed TCP Acknowledgement (52 octets) could be mapped onto only 2 bursts, using either MCS-8 or MCS-9, allowing the receiver to decode the data and header 10 ms earlier than it would if using the existing burst mapping.

The new burst mapping for 'MCS-9_2' is shown below for the first two bursts (note that the normal burst structure is used unchanged):
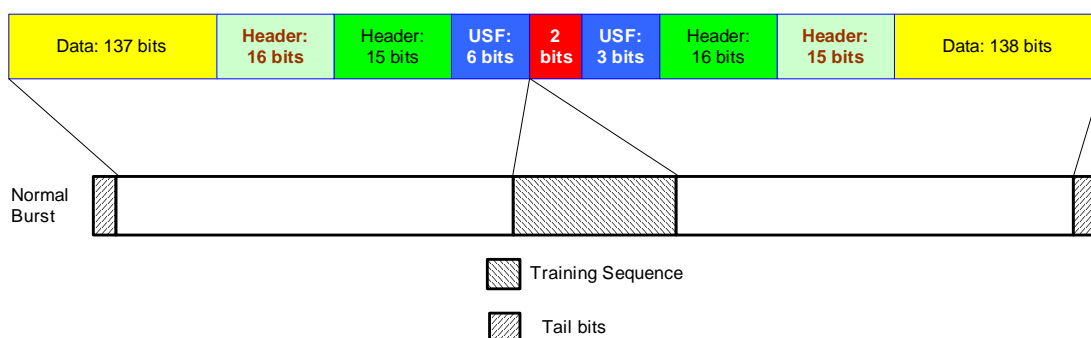
Figure 333: New burst mapping for 'MCS-9_2'

In order for the receiver to be able to decode the header using only two bursts, the header bits that are currently sent in bursts 3 and 4 would be sent in bursts 1 and 2. The current bit-swapping procedures would need to be modified to account for the additional header information in these bursts.

For reference, the current burst mapping is, for all four bursts:
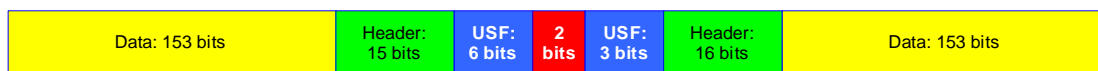
Figure 334: Current burst mapping

In this example, bursts 3 and 4 would not be needed by the receiver to decode the header and data. However, in order to ensure backwards-compatibility, the USF in downlink blocks must be mapped onto the bursts in the same way as currently. Furthermore it is proposed that 'unused' blocks contain redundant data (using Incremental Redundancy) so that if the receiver is unable to decode the data using just two bursts, it may use soft-combining to attempt to decode the data after all four blocks have been decoded. Note that other possibilities for the last two bursts could also be considered - e.g. sending additional data.

The timeline is shown below comparing existing and proposed schemes:
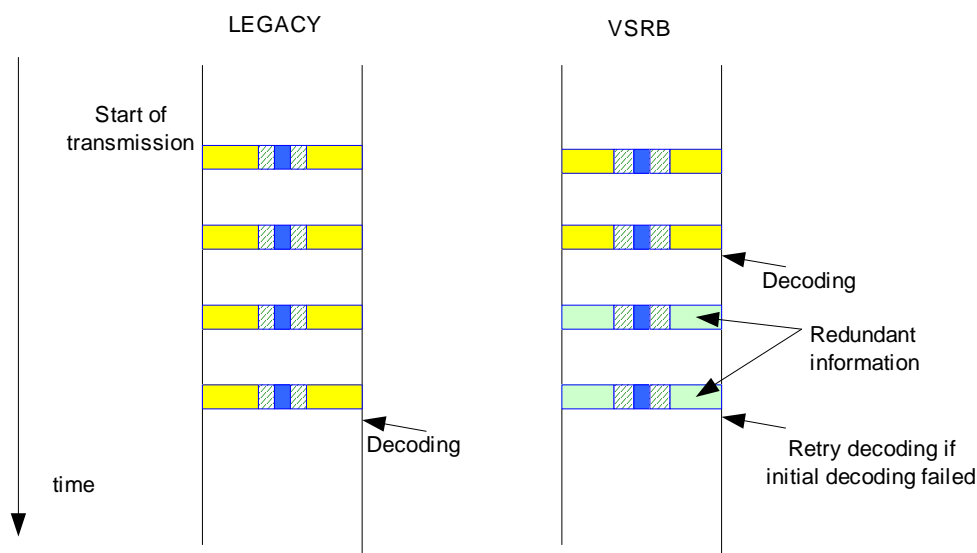
Figure 335: Comparison of existing and proposed schemes

10.4.3.3 Signalling/Detection

The signalling of the use of the new mapping schemes remains an open issue and FFS. Possible approaches may include:

- Using the stealing bits (subject to the restriction, obviously, that the receiver must be able to determine that this block should be decoded after *n* bursts, having received *2n* stealing bits).

- Blind detection (by attempting to decode the header).

- Indication in the previous block that the next block may use a shorter block.

If stealing flags were used, it may be possible to allow a legacy mobile to decode the header (and thereby determine that the block was not intended for them), by mapping header bits to all blocks as done currently, and defining stealing flag patterns so that a legacy mobile would 'correct' the new unknown pattern to a currently-defined pattern corresponding to the legacy 4-burst modulation/coding scheme.

Note that while indication in the previous block may be the most robust option, there remains a problem if the previous block is erroneous.

10.4.3.4 Radio Block Capacity

The amount of (uncoded) data that can be transmitted in each radio block is shown in the table below for MCS-7 to MCS-9.

EXAMPLE: If 18 octets (or fewer) are to be sent using MCS-7 coding and puncturing, this can be sent in one burst, allowing a reduction of 15ms in the one-way delay.

Table 183

Bursts used	Reduction in delay (ms)	RLC Blocks	MCS 7	MCS 8	MCS 9
1	15	1	144 (18)	77 (22)	194 (24)
2	10	1	401 (50)	487 (60)	530 (66)
3	5	1 (see note)	705 (88)	854 (106)	928 (116)
		2	2 x 343 = 686 (2 x 42)	2 x 418 = 836 (2 x 52)	2 x 455 = 910 (2 x 56)
4 (Legacy)	-	2	2 x 448 = 896	2 x 544 = 1 088	2 x 592 = 1 184
Numbers in (…) are octets, rounded down.					
NOTE: Because of the problem of retransmitting (see below) it is proposed that data sent in three bursts be sent as 2 RLC blocks.					

10.4.3.5 Retransmissions

Existing modulation and coding schemes belong to one of three families for the purpose of retransmissions. However, for the MCS7/8/9 1- and 2-burst options, the overall code rate (using all four bursts) would be lower than other code rates, and may not benefit from retransmission using a lower coding scheme.

For the 3-burst options (using 2 RLC blocks), retransmissions could be carried out using lower coding schemes in the families shown below (requiring some additional padding).

Table 184

Bursts used	RLC Blocks	MCS 7	MCS 8	MCS 9
3	2	C	B	A (possibly B)
4 (Legacy)	2	B	A	A
NOTE: "(possibly …)" indicates that the amount of data in the original block would need to be reduced slightly.				

10.4.3.6 Benefits

As stated in the introduction, the majority of the delay from MS to SGSN is incurred away from the air interface. However, the benefits described here may be combined with improvements to other interfaces/nodes.

As already stated, the latency for a TCP ACK can be reduced by 10ms; this benefit will apply (cumulatively) to *every* TCP ACK sent in a TCP session.

A similar reduction can be achieved for small RTP or IP packets, especially when using header compression. (e.g. 40 ms of G.729 VoIP data could be transmitted in 2 bursts of MCS 7, 8 or 9 using header compression [11]).

In addition, the use of incremental redundancy *within* the complete radio block would make such transmissions more robust than if sent using the legacy bit mapping (see subclause 10.5.4).

See subclause 10.10.1 for benefits of reduced latency on TCP layer.

10.4.4 Performance Characterization

10.4.4.1 Bandwidth Efficiency

Obviously this proposal increases the overhead as a proportion of the amount of data sent; however, since this scheme would only be used when there was no other data to send, the reduced efficiency is not an issue.

10.4.4.2 Latency

The delay incurred by a radio block currently is fixed at 20 ms. By using VSRB, the latency would be lower in those cases where fewer than four bursts are required to transmit the final radio block.

The figure below compares the total air interface delay for varying amounts of data to be sent. (The graph continues in a similar manner *ad infinitum*).
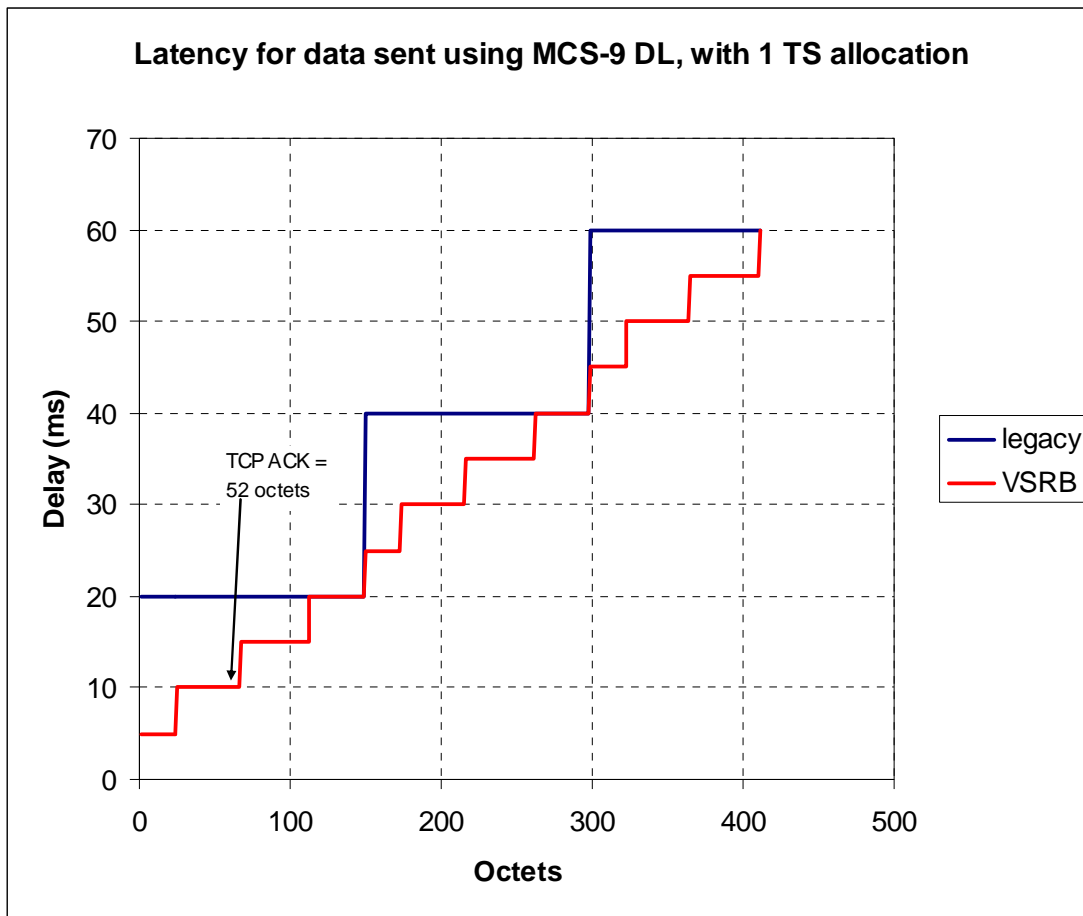
Figure 336: Delay / data sent

10.4.4.3   Block Error Probability

Because the code rate for the reduced-sized blocks will be the same as in the current coding schemes, the block error probability will be very similar, although because of reduced diversity, the probability that a block can be decoded with just the minimum number of bursts may be slightly lower than at present.

However, by using incremental redundancy in the 'unused' bursts, the resulting BLER (using all four bursts) will be lower than the legacy scheme (since the overall code rate including all four bursts will be lower than at present), making it less likely that the data must be retransmitted. This scheme may therefore be appropriate for use where, currently, the coding and modulation scheme would be changed (to a more robust scheme) for the last block of a TBF when a small amount of data is to be sent.

Although the motivation for this feature was the reduction of latency, it may be that the increased redundancy and lower code rate may make this suitable for use in low C/I scenarios.

10.4.4.4   Simulation results

10.4.4.4.1   Simulation Parameters

Simulations are performed for normal BTS and the physical channel used is the TU3 idFH channel. Interleaving is done by random permutation of the bits and new puncturing patterns are used to achieve the required number of output bits after coding for VSRB blocks. It should be noted that the performance of the VSRB might be further optimised by changing the interleaving and puncturing patterns. Simulations are run for 10 000 frames at each C/I point.

10.4.4.4.2 Header Error Rate

The proposed change in the way the header is mapped onto bursts is shown in figure 337. This allows the receiver to decode both the header and data having received only 2 bursts.
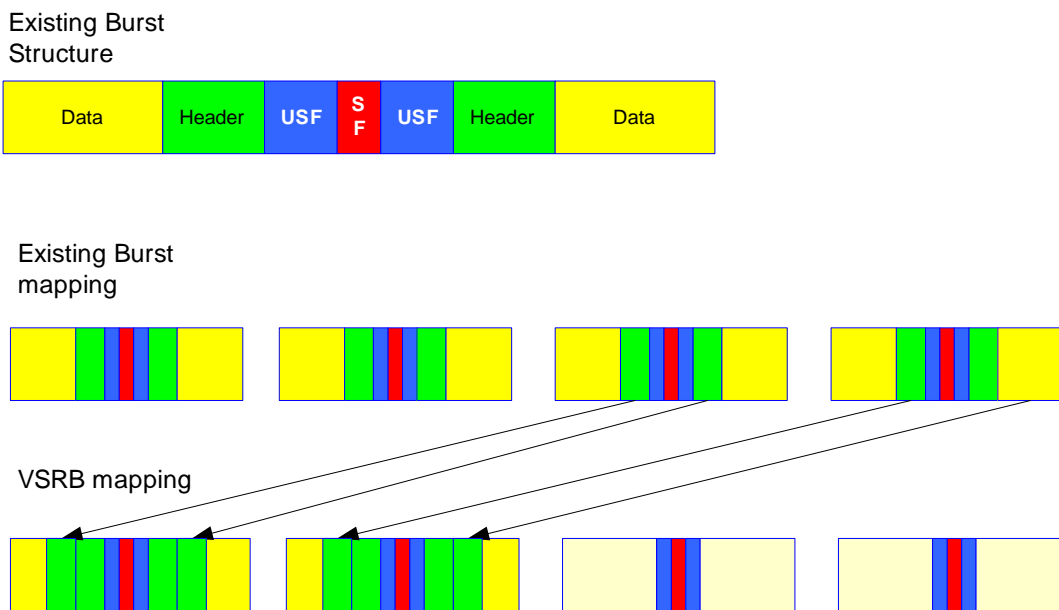
Figure 337: Header sent in first two bursts
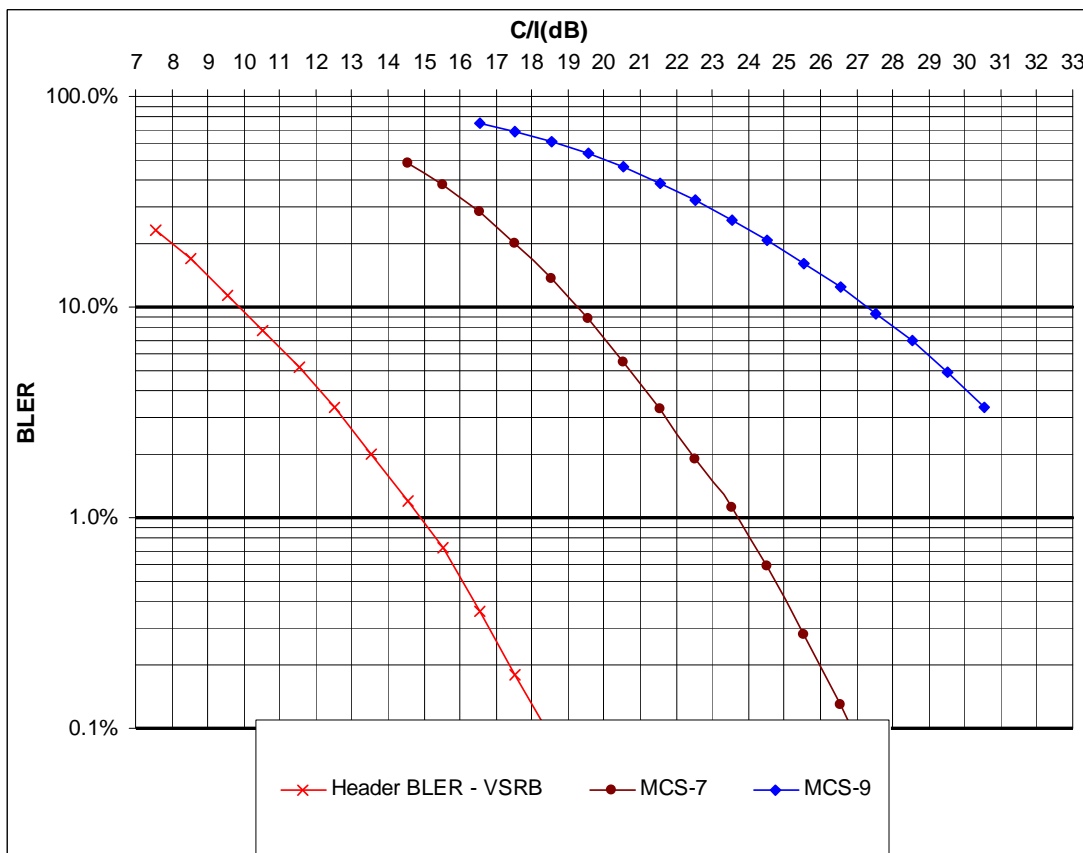
Figure 338: VSRB Header Probability

In figure 338 we plot the probability of (MCS-7/8/9) header error for TU3 with ideal frequency hopping. We also plot, for reference, the BLER for MCS-7 and MCS-9.

The probability of an error in the legacy header is negligible, and is not plotted.

As can be seen from the figure, the reduction of frequency diversity does have an impact on the probability of header error, however, this remains negligible compared to the overall probability that the data block will be received in error. It should be noted that the data error rate includes the header error rate. In other words, the entire data block is treated to be in error when there is a header error.

10.4.4.4.3 Equal Code Rate Comparison

As described in GP-052598, the underlying code rate for the data sent in the first two blocks would be the same as in the existing coding schemes. The proposed arrangement of data using VSRB is shown in figure 339.

Although the code rate will remain the same, the performance may suffer due to reduced frequency diversity.
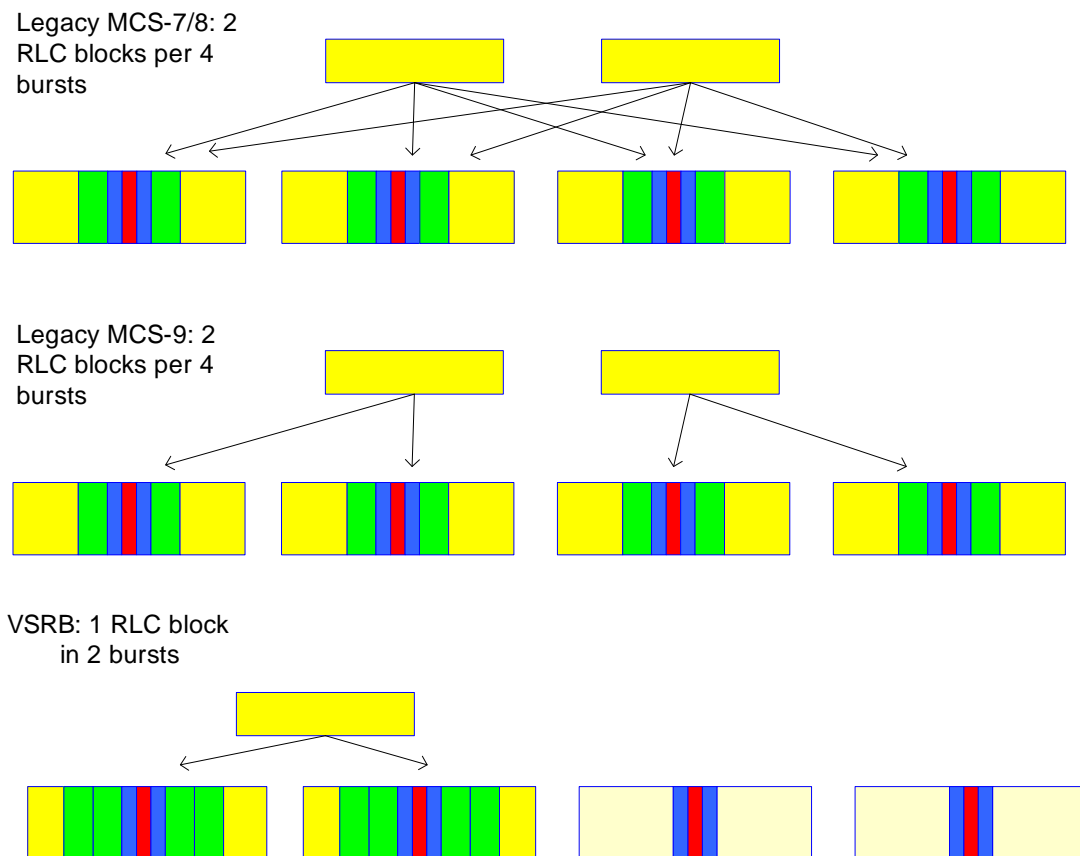
Figure 339: Arrangement of Data using VSRB
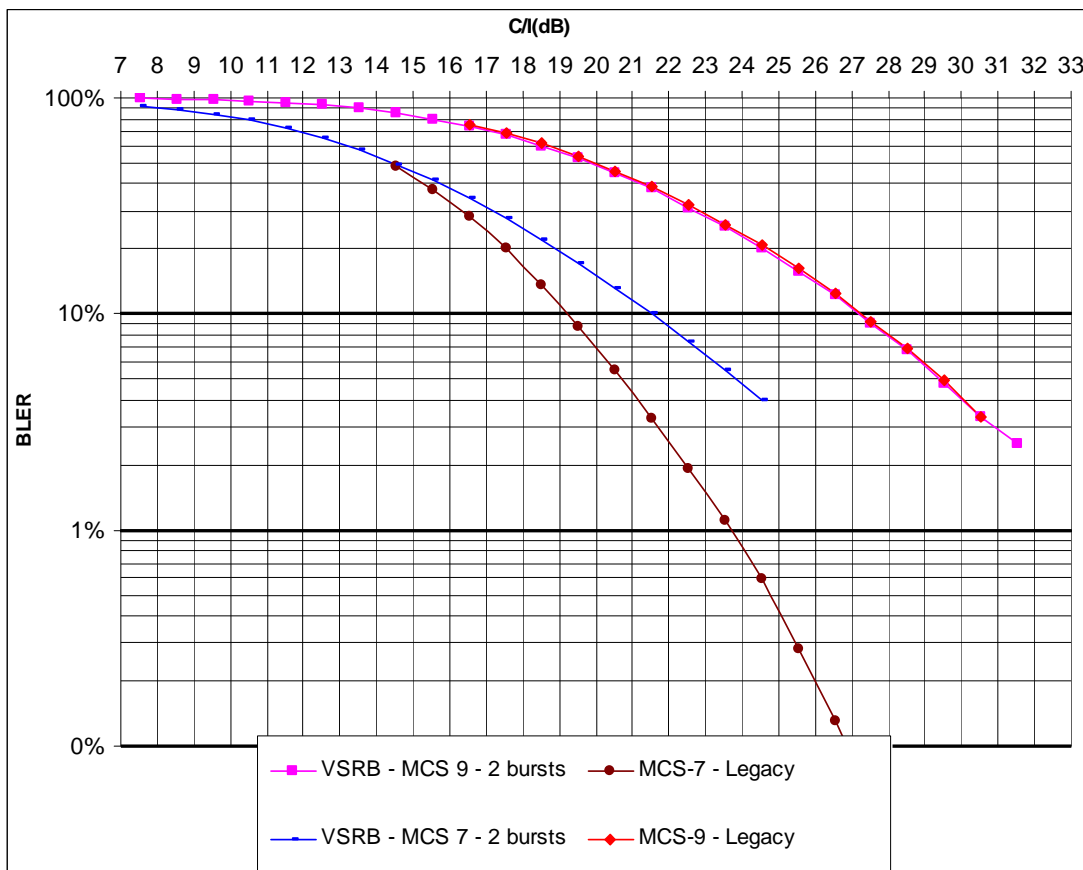
Figure 340: BLER Comparison between VSRB (2-bursts) and legacy MCS

Because there is no interleaving between the first and second pairs of bursts in MCS-9, there is no difference in the block error rate for VSRB-MCS-9 and legacy MCS-9.

For MCS-7, the legacy interleaving scheme spreads the data bits of a single block over all four bursts where as the new interleaving scheme spans only across two bursts; hence, there is some degradation of performance for VSRB compared with the legacy scheme: approximately 2 dB at 10 % BLER as shown in the above Figure. The loss is mainly due to the loss in frequency diversity in case of frequency hopping scenarios.

10.4.4.4.4   Equal Data Load Comparison

In practice, when transmitting small amounts of data, lower coding schemes may be used in preference to using a higher rate coding scheme with extra padding.

This has the benefit that small amounts of data are transmitted more robustly, reducing the probability that a retransmission will be required.

In order to give comparable performance, it is proposed that, for VSRB, redundant information is sent in the second pair of bursts; if decoding is not successful after two bursts, then incremental redundancy is used, as shown in figure 341.
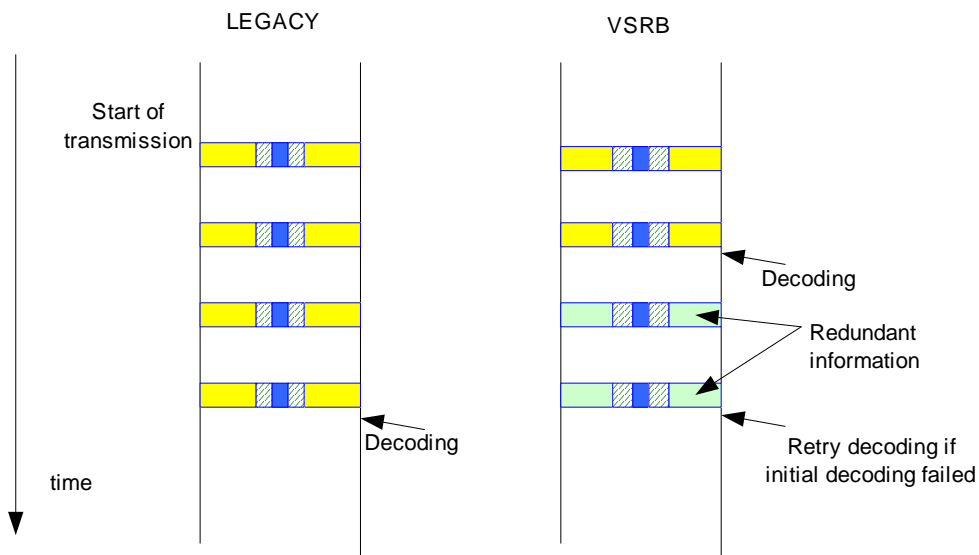
Figure 341: Use of Incremental Redundancy

VSRB-MCS-9 (2 bursts) can transmit approximately the same amount of data as MCS-6; VSRB-MCS-7 (2 bursts) can transmit approximately the same amount of data as MCS-5. In figure 342 we compare the BLER for each VSRB scheme, decoded after all four bursts have been received, and legacy MCS-5 and 6.
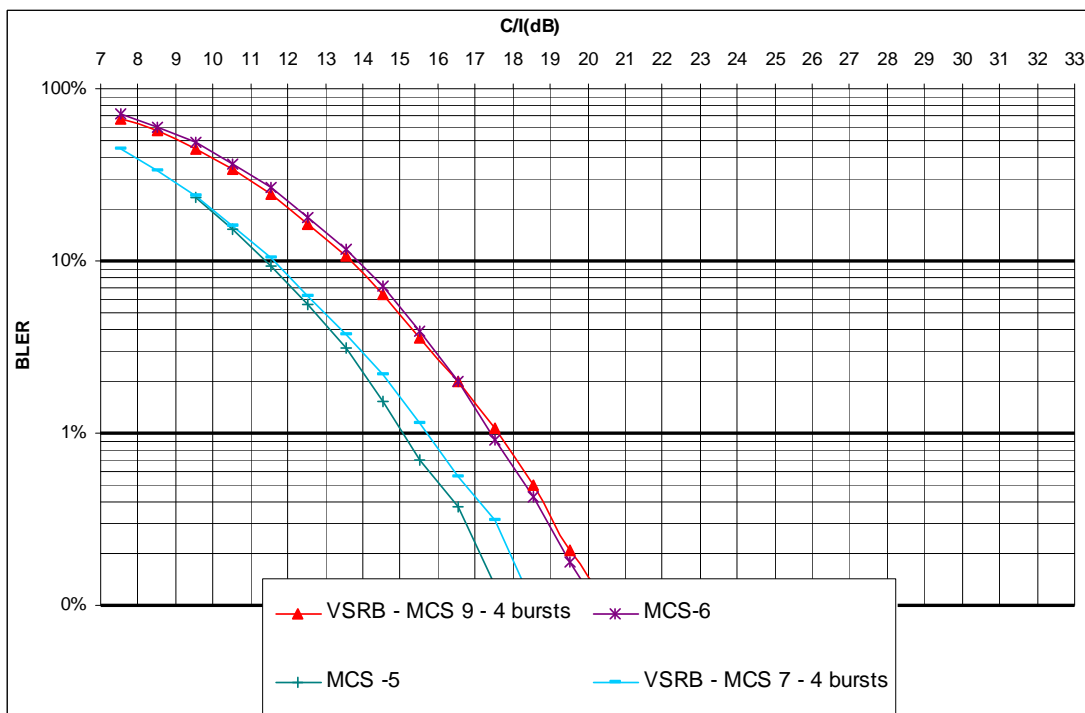
Figure 342: Comparison of BLER between VSRB (4-bursts) and legacy MCS

As can be seen from figure 342, there is almost no difference in performance between using VSRB with incremental redundancy, and the lower encoding scheme carrying the same amount of data.

10.4.5   Impacts on Network Entities and Standards

10.4.5.1   Impacts to the Mobile Station

The following modifications are required to the mobile station:

-    (Transmit) Addition of new interleaving and burst mapping schemes.

- (Receive) Addition of new de-interleaving schemes.

- (Receive) Addition of soft-combining using redundant data in 'end' bursts.

10.4.5.2   Impacts to the BSS

The impacts on the BSS are the same as for the mobile station.

10.4.5.3   Impacts to the Core Network

There is no impact on the core network

10.4.5.4   Impacts to the specifications

The impacted 3GPP specifications are listed in table 185.

Table 185

Specification	Description
3GPP TS 43.064	GPRS Stage 2
3GPP TS 44.060	Radio Link Control / Medium Access Control (RLC/MAC) protocol
3GPP TS 45.003	Channel coding

10.4.6   Comparison of VSRB and RTTI

In subclause 10.3 the use of a reduced TTI (RTTI) is described. In this subclause, we compare RTTI and VSRB. Figure 343 shows the delay incurred over the radio interface for sending data where the allocation is 2 TS per TDMA frame; for the RTTI scheme this allows a TTI of 10 ms.
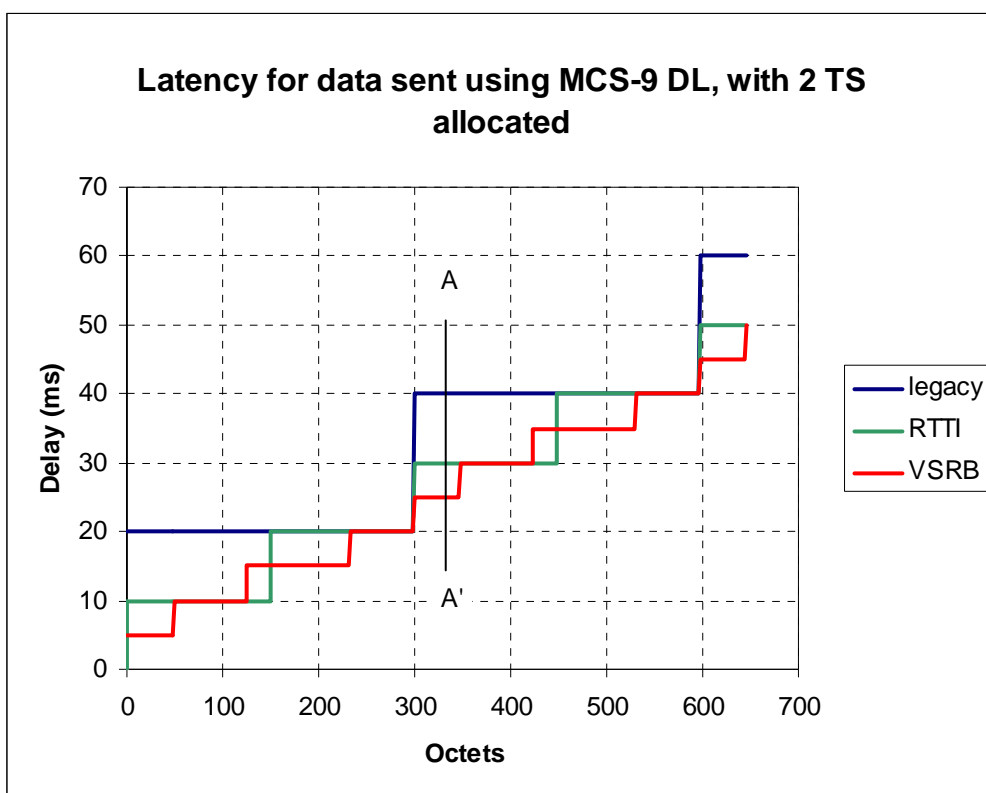
Figure 343: Delay over the radio interface / data sent

As can be seen, RTTI and VSRB provide broadly comparable delay improvements, although there are ranges over which the delay using VSRB is lower than with RTTI, and (for some small ranges) vice versa. (Explanation for the case at A-A' is shown in figure 344.)

If, for simplicity, the VSRB scheme is restricted to 4-burst or 2-burst blocks (i.e. 1-burst and 3-burst blocks not possible), the comparison is as shown in figure 344.
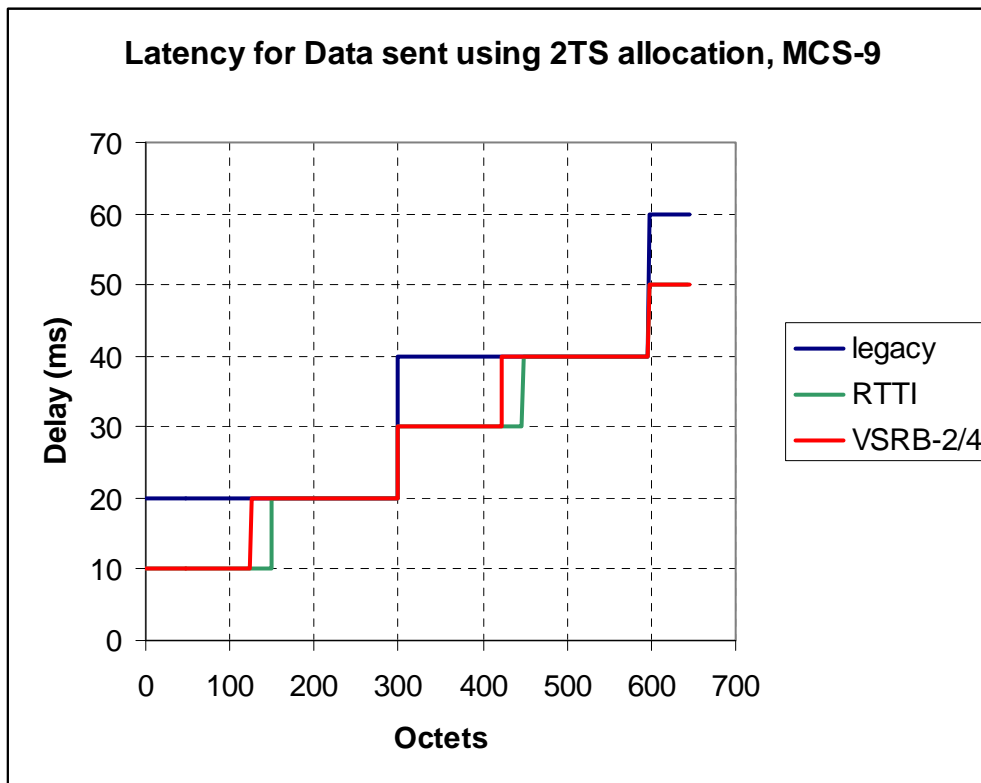
Figure 344: Delay over the radio interface / data sent (4-burst or 2-burst blocks)

One benefit of the RTTI scheme is that it does not reduce bandwidth efficiency; therefore, latency may be reduced for blocks even where more LLC data is buffered (in such circumstances, VSRB would most likely not be appropriate). However, in order to achieve this, new (multislot, or multi-carrier) channels must be defined; these would not be compatible with legacy mobiles, requiring resource segregation.

VSRB is fully backwards-compatible, as it uses existing allocation schemes and therefore does not need new channel definitions or resource segregation (a method of scheduling RTTI has also been proposed so that avoids resource segregation). However, as shown above, it can provide similar latency improvements (if not better) compared with RTTI. VSRB can also be applied where a single TS allocation is made (cf. RTTI requires an allocation of two or more timeslots).

10.5   Combining Methods

10.5.1   Preface

Latency can be improved during short transmissions by allowing earlier decoding of the final RLC block. As noted in [3] from Siemens, early decoding the final RLC block of a short transmission is a valuable contribution to reducing system latency since this decoding operation limits the earliest response time.

A number of methods have been proposed to GERAN which can lead to earlier decoding of the final RLC block. These include:

-    Methods which pack the RLC block into a shorter duration (measured in TDMA periods) by distributing the block on multiple frequencies within each TDMA period [12] and [13].

-    A concept introduced in GERAN#27 [14], called Variable Size Radio Block (VSRB), which shortens the block when it is not full.

This contribution shows how these concepts can be combined to achieve even earlier decoding of the final RLC block than would be possible individually.

10.5.2   Early Decode with Multi-Frequency

The use of multiple receiver frequencies inside the same TDMA period allows the early decode of a RLC frame as shown below, while maintaining a level of frequency diversity gain equivalent to legacy mobiles (diversity over 4 frequencies, denoted F1 to F4). In this case the mobile station must contain two receive paths capable of operating simultaneously. Unused blocks can contain redundancy information which can be combined with the used block to allow error correction.

The benefit of using Multiple frequencies in the same TDMA frame can also be applied to a single frequency receive path as illustrated in the following figure. In this case bursts are distributed on two frequencies in each TDMA frame by ensuring there is a 'gap' to retune within the TDMA frame (in the illustration below the mobile has 1 slot to re-tune). Then two bursts from each RLC block can be transmitted in a single TDMA period. In this case, where only one RLC frame needed to be transmitted, its decoding is brought forward by 10 ms without impact on frequency diversity gain.
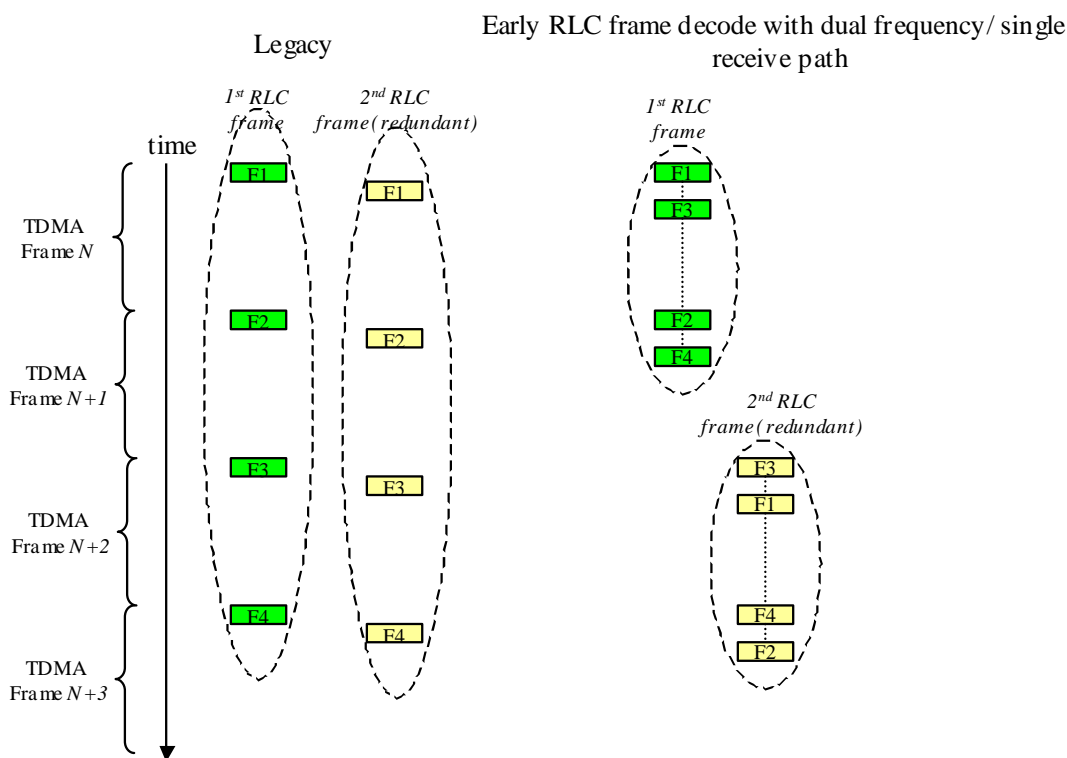
Figure 345: Early RLC frame decode with dual frequency/ single trx

The benefit of multiple frequency can be extended beyond the use of 2 frequencies in a TDMA frame. In the following figure early decode is illustrated in the case of a 4 frequency trx, where only 3 RLC frames need to be send in the final RLC block period. The final RLC frame can contain redundancy information. In the illustration below, where 3 out of 4 possible RLC frames contain data, the decode time is advanced by 5 ms compared with legacy receivers.

4-frequency trx,
with redundant frame
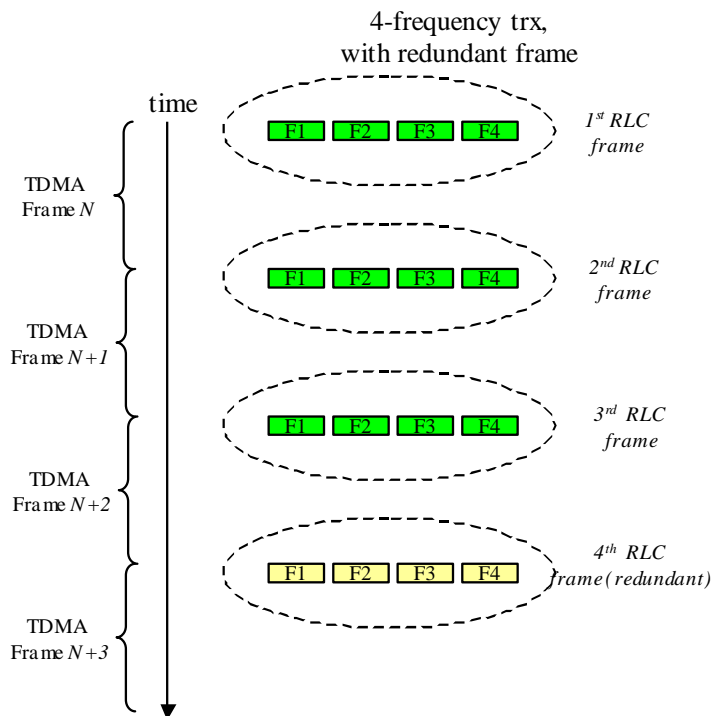
Figure 346: Early RLC frame decode with quad frequency

10.5.3 Early Decode with VSRB

Latency can be improved when the final RLC radio block of a transmission is only partially full. The basic idea, called VSRB, is to ensure all the information needed to decode the RLC block is contained in earliest bursts, provided it fits in these bursts.

VSRB is fully described in [14] but for convenience is illustrated below. It is assumed that enough information is in the first two bursts of the RLC block period for a decode attempt to take place. The second two bursts contain redundant information to allow further decode attempts using incremental redundancy decoding. Although frequency diversity is reduced for the first decode attempt, it is fully exploited during later attempts and on average earlier decoding can be expected.

EXAMPLE: If the radio block is half full it can be decoded up to 10 ms earlier with a consequent improvement in latency. This is illustrated in figure 347.
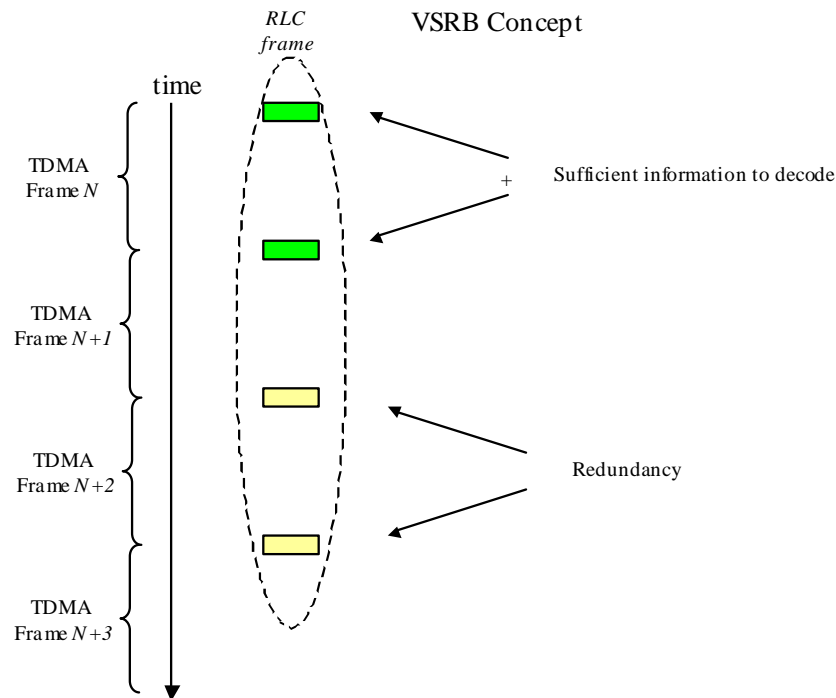
Figure 347: VSRB

10.5.4 Early Decode with combined VSRB and Multi-Frequency

VSRB can be combined with multiple frequency/ multislot operation. In this case *N* RLC frames are sent in a single RLC period, assuming *N* slots are used. With legacy mobiles, each burst of the RLC frames must be transmitted over a different one of the 4 TDMA frames otherwise frequency diversity gain is lost.

During the final RLC block period of a transmission, only a subset of the *N* available RLC frames may be actually needed for data (since the number of RLC frames transmitted is not necessarily an exact multiple of *N*); the remaining frames can contain redundancy information. With a legacy mobile, not capable of multi-frequency operation with one TDMA frame, none of the RLC frames can be decoded early, since all frames are spread over the entire RLC block period, i.e. 4 TDMA frames.

If the last RLC frame is not full, then multi-frequency operation can be combined with VSRB to deliver the last RLC frame even earlier. In the illustration below the last RLC frame is only 50% full, and is coded according to VSRB principles. A single receive path is assumed with multi-frequency operation achieved by using timeslots with time separation for retuning. In the illustration below, decoding of the final RLC frame is advanced by:

- 5 ms compared to pure dual-frequency without VSRB;

- 5 ms compared to pure VSRB without dual-frequency; and

- by 15ms compared to legacy mobiles.
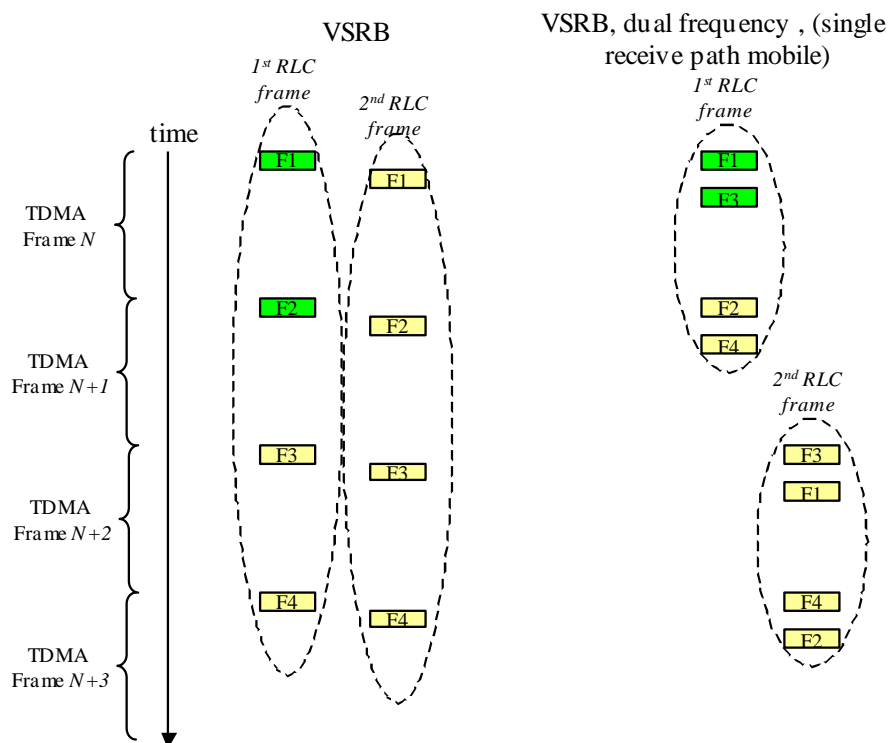
Figure 348: VSRB and dual frequency/ single trx

In summary, the following steps can be taken to reduce latency by advancing in time the decode of the final RLC frame of a multislot transmission:

1) Reduce the TTI of each RLC frame to 10ms (if two frequencies used) or 5 ms (if 4 frequencies used).

2) Use VSRB coding during the final RLC block period, if this would bring forward decode time.

10.6 Performance characterization of combined proposals

10.6.1 RTTI and Fast Ack/Nack Reporting

10.6.1.1 Simulation results for VoIP

In the following some results are shown regarding a VoIP service realized over a GERAN network that implements the following "latency reduction" features:

1. **Reduced TTI radio blocks**. Both "10 ms TTI" and "5 ms TTI" are considered. The "2-burst RTTI radio blocks" option is not taken into account. For the "5 ms TTI" case, the constraint described in subclause 10.3.1.5, mandating the transmission/reception of RTTI blocks every other TTI period (i.e. every other TDMA frame) is also considered in the simulations.

2. **A Fast Ack/Nack reporting scheme**, as described in subclause 10.2.1.3.2, i.e. the approach where a short bitmap is included in RLC data blocks.

3. **A shorter MS reaction time**: ~10 ms is assumed for the "10 ms TTI" case, while less than 1 TDMA frame is assumed for the "5 ms TTI" case, as described in subclause 10.3.1.5.

4. **TBFs operated in RLC Non-Persistent mode**. The maximum number of retransmissions per RLC block is set to 1 or 2 (i.e. the total number of transmissions for a given RLC block cannot exceed 2 or 3, respectively). The RLC Window Size is set to 6, i.e. a considerably lower value than the currently minimum possible of 64 (this issue is analyzed in more detail in GP-060780 (GERAN#29).

In addition, it is assumed that **SNDCP/LLC headers are reduced to 2 bytes**, as described in G2-022708 (GERAN WG2#11bis).

Four different low-latency scenarios are simulated, as described in table 186.

Table 186: Simulated scenarios

	Scenario 1	**Scenario 2**	**Scenario 3**	**Scenario 4**
TTI	10 ms	5 ms	5 ms	5 ms
RTTI blocks for a given user can be sent every TTI period?	Yes	Yes	No, only every other TTI period	No, only every other TTI period
Fast Ack/Nack Reporting	Enabled	Enabled	Enabled	Enabled
MS reaction time	~10 ms	< 4 ms	< 4 ms	< 4 ms
Total maximum # of transmissions per RLC block	2	3	3	2
RLC WS	6	6	6	6

The table below shows the corresponding transmission delay of an RLC block transmitted 1, 2 and 3 times, for the "10 ms TTI" and "5 ms TTI" case (the legacy case, **still assuming the fast ack/nack reporting scheme**, is also shown for comparison).

Table 187: Delay budget for an RLC block transmitted 1, 2 and 3 times with legacy (black) / 10 ms TTI (red) / 5 ms TTI TBFs (blue)

Direction	BSC/PCU	Abis	BTS	Um	MS	Sum
BSC →	10	20/10/5	<5	20/10/5		55/35/25
← MS		20/10/5	<5	20/10/5	40[(1)]/10[(2)]/<4	
BSC →	10	20/10/5	<5	20/10/5		195/105/65
← MS		20/10/5	<5	20/10/5	40/10/<4	
BSC →	10	20/10/5	<5	20/10/5		335/175/105
NOTE 1: Currently minimum possible MS reaction time.						
NOTE 2: Value considered in other parts of this document for the "10 ms TTI" option (could be set to <4 for a better comparison).						

To evaluate what can be considered a sort of worst-case scenario, it is assumed that the VoIP client puts a single 12.2 kbps AMR frame per IP packet, corresponding to 20ms of speech per IP packet. It is also assumed that ROHC is used (leading to an average IP headers compression size estimated in 3 bytes) therefore leading to 284 (244 payload + 40 IP+SNDCP/LLC headers) bits of RLC/MAC payload, that could fit in a single MCS-3 RLC data block. MCS-3 is therefore used for all the simulations, in a C/I condition of 9 dB (note: performance for MCS-3 in TU3iFH - 900MHz are used in the following, although the benefit of FH cannot be (completely) exploited in case of RTTI blocks).

Figure 349shows the CDF for both the RLC block and the LLC PDU transfer delays, in the Scenario 1 ("10 ms TTI"). It clearly shows the effect of the RLC in-sequence delivery feature, implying higher delays for LLC PDUs than the ones that could be erroneously expected by only considering the transmission delay for individual RLC blocks. **The 95-percentile delay for LLC PDUs is then around 120 ms**. **The corresponding IP packet loss** in this case (only 2 total transmissions allowed per RLC block) **is measured in 3 %**.
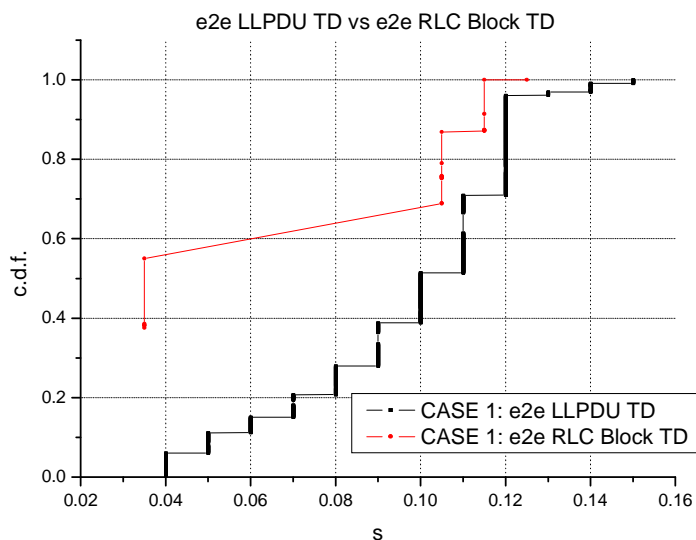
Figure 349: Case 1 ("10 ms TTI"), RLC vs LLC transfer delay.

In figure 350 the benefit of RLC Non-Persistent mode (with a reduced Window Size) over RLC Ack mode is shown, again for Scenario 1. **If RLC Ack mode were used, the LLC PDU transfer delay would increase, leading to a 95-percentile delay of around 180 ms**, definitely not acceptable for VoIP (reducing the Window Size for RLC Ack mode would not help, since it would increase the risk of stalling the transmit window).
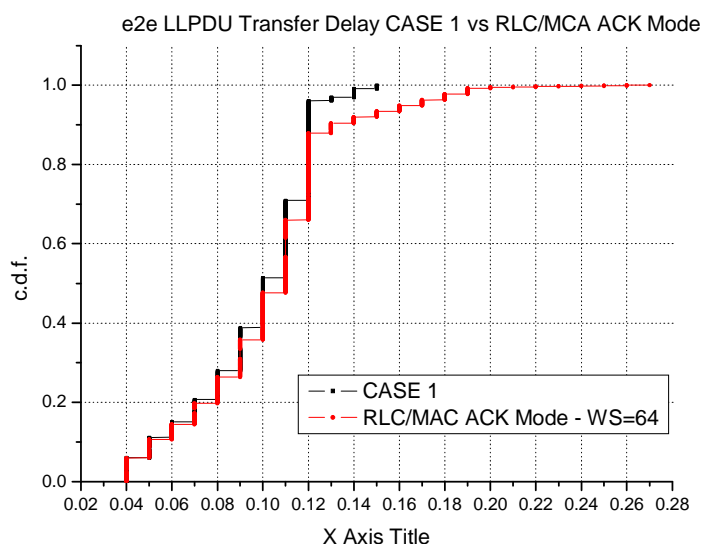
Figure 350: Case 1 ("10 ms TTI"), RLC Non-Persistent mode vs RLC Ack mode

To demonstrate the benefit of moving from a "10 ms TTI" to a "5 ms TTI" solution, figure 351 shows a comparison between Scenario 1 ("10 ms TTI") and Scenario 4 ("5 ms TTI"), where the total maximum number of allowed transmissions per RLC block is kept fixed to 2.
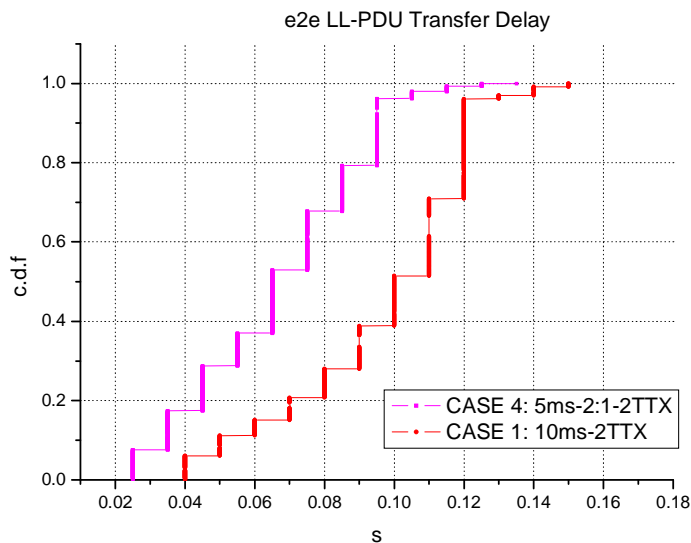
Figure 351: Case 1 ("10 ms TTI") vs Case 4 ("5 ms TTI")

The gain in terms of average LLC PDU transfer delay can be easily noticed. **In the "5 ms TTI" case also the 95-percentile delay is improved, going down to 95 ms, while the IP packet loss (not shown in the figure) remains the same, i.e. 3 %**.

But the "5 ms TTI" solution can also be used to lower the IP packet loss, by increasing the total maximum number of allowed transmissions per RLC block from 2 to 3. Figure 352 shows the comparison between Scenario 4 ("5 ms TTI", 2 Tx) and Scenario 3 ("5 ms TTI", 3 Tx). In case of maximum 3 transmissions the 95-percentile delay increases (as expected) reaching 120 ms (same value as in the "10 ms TTI" case with 2 transmissions), but the IP packet loss (not shown in the figure) decreases to 0.3 %.
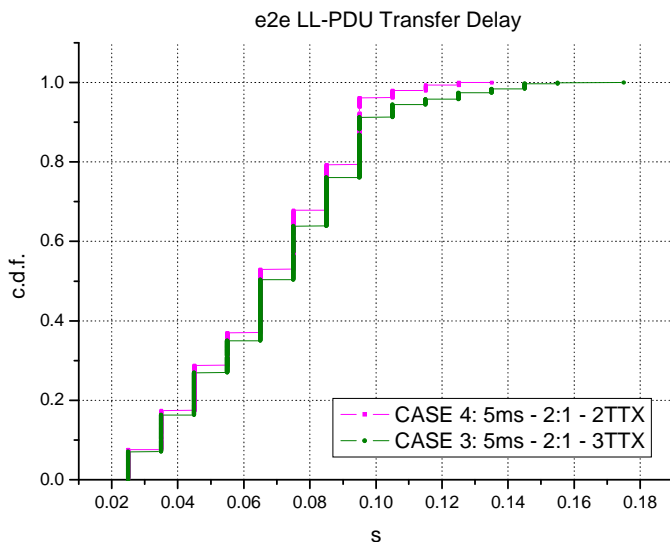
Figure 352: Case 4 ("5 ms TTI", 2 Tx) vs Case 3 ("5 ms TTI", 3 Tx)
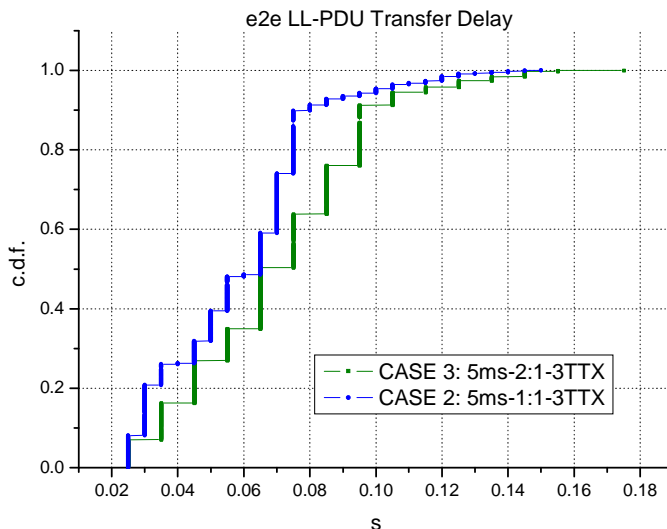
Figure 353: Case 3 ("5 ms TTI", 3 Tx) vs Case 2 ("5 ms TTI", 3 Tx, up to 1 RTTI block per TTI period)

Figure 353 shows the possible further improvement if "5 ms RTTI" blocks could be sent every TTI period (i.e. if a mobile station could receive and transmit on 4 timeslots in the same TDMA frame). Figure 353compares Scenario 3 ("5 ms TTI", 3 Tx) and Scenario 2 ("5 ms TTI", 3 Tx, up to 1 RTTI block per TTI period). Even here the gain in terms of average LLC PDU transfer delay can be easily noticed. **Also the 95-percentile delay is improved (100 ms compared to 120 ms), while the IP packet loss would further decrease from 0.3 % to 0.2 %**.

All these results, that could be made possible by the introduction in GERAN of the "reduced latency" features listed at the beginning, could be also compared with some evaluations made regarding a FLO-based solution for VoIP. The next table is taken from GP-023153 ("Link level performance comparison between Iu and enhanced A/Gb for VoIP", GERAN#12) and shows the C/I at 1 % of FER (TU3iFH - 900 MHz) for a VoIP over FLO solution, for both GERAN Iu and A/Gb mode, and for different AMR modes.

**Table 188: Link performance of VoIP over FLO using EEP
C/I at 1 % of FER (TU3iFH - 900 MHz)**

AMR	Iu mode	A/Gb mode	Difference
12.2 kbit/s	12.00 dB	12.65 dB	0.65 dB
7.4 kbit/s	7.50 dB	7.85 dB	0.35 dB
4.75 kbit/s	5.22 dB	5.60 dB	0.38 dB

The 12.2 kbps AMR solution over FLO (1% of FER @ C/I ~ 12 dB) can then be compared with the 12.2 kbps AMR solution over RTTI TBFs (0.3% of FER @ C/I = 9 dB, 95-percentile delay = 120 ms, as in Scenario 3), showing the improvement that can be achieved by the latter approach.

10.7 High Speed Hybrid ARQ

10.7.1 Introduction

A high speed hybrid ARQ (HS-HARQ) mechanism for the reduction of EGPRS latency is introduced. Several factors affect EGPRS latency in an ARQ mechanism including BLER, TTI, and rate of acknowledgement. The HS-HARQ mechanism increases the rate of acknowledgement by moving the ARQ mechanism from the PCU to the BTS and operating multiple Stop and Wait ARQ processes with synchronous acknowledgements. Terminating the ARQ protocol at the BTS would eliminate the backhaul delays between the BTS and the PCU from the ARQ loop. Operating the ARQ mechanism with synchronous acknowledgement would keep the acknowledgement delay constant and low. The synchronous nature of the acknowledgements would allow for a very small number of acknowledgement bits to be exchanged every block period.

The basic delay to transmit, acknowledge, and retransmit a block would be 60 msec in either uplink or downlink. By reformatting the EGPRS headers to use smaller BSNs and taking the remaining bits for piggybacked acknowledgements and other ARQ variables, the ARQ protocol overhead could be reduced to zero.

Maximum backward compatibility could be achieved by limiting the number of timeslots supported per TBF under the HS-HARQ protocol. Such TBFs in a multiple TBF environment are sufficient for VoIP, PoC, and videophone services.

10.7.2 Comparison of EGPRS ARQ, Fast ARQ, Reduced TTI, and HS-HARQ

Table 189 shows the round trip latency for a downlink block transmission, an acknowledgement, and a retransmission under the HS-HARQ scheme. A node delay of 5 msec is assumed at the BTS. The latency is calculated from when the BSC/PCU has started sending the block to the mobile and ends when the mobile receives the retransmission.

Table 189: HS-HARQ latency analysis (time to send transmission, acknowledgement and retransmission)

Direction	BSC/PCU	Abis	BTS	Um	MS	Sum (msec)
BSC ->		20	< 5	20		40 to 45
<-MS				20		20
BTS->				20		20
Sum (msec)		20	< 5	60		80 to 85

Table 190 compares the latency of several schemes in the same scenario. With the EGPRS ARQ, it is assumed that a poll is done every 60 msec, which leads to some blocks having higher latency than others.

Table 190: Latency comparison (time to send transmission, acknowledgement and retransmission)

	EGPRS ARQ*	Fast ARQ	TTI = 10 msec	HS-HARQ
Latency (msec)	160 to 225	140 to 165	70 to 95	80 to 85

Note that the HS-HARQ mechanism and a reduced TTI are compatible and may be combined. With a 10 msec TTI the latency for the combined scheme is 40 msec to 45 msec.

A mobile to mobile VoIP call with the HS-HARQ protocol has a single direction latency of approximately 220 msec. A mobile to mobile VoIP call with the HS-HARQ protocol combined with a 10 msec TTI has a single direction latency of approximately 140 msec.

10.7.3 HS-HARQ Proposal

Figure 354 shows the network architecture of the current EGPRS MAC and RLC protocols. Figure 355 shows the network architecture of the HS-HARQ mechanism. In the existing scheme the MAC and RLC protocols are both terminated at the PCU. Typically the PCU is located remote from the BTS at the BSC location or elsewhere.
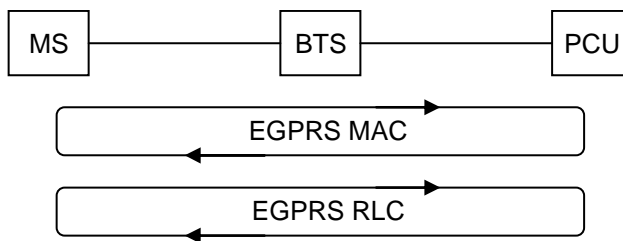
Figure 354: Legacy Network Architecture
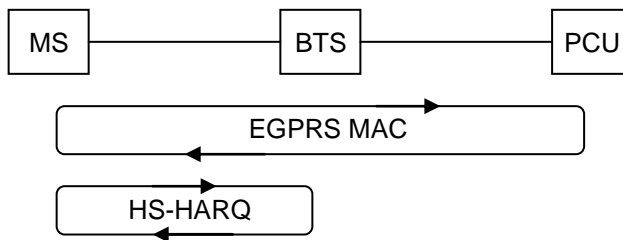
Figure 355: HS-HARQ Network Architecture

In the HS-HARQ scheme, the MAC is still terminated at the PCU but the ARQ is terminated at the BTS. The advantage of terminating the ARQ at the BTS is elimination of the backhaul delay between the BTS and PCU within the ARQ loop.

New functions which are supported in the BTS are:

- The HS-HARQ protocol.

- Block scheduling for timeslots managed by the HS-HARQ mechanism.

- Downlink data queuing.

- Radio link management.

- Polling management.

10.7.4 Channel Structures

HS-HARQ RLC data blocks have identical coding to EGPRS RLC data blocks (MSC1-MCS9) with modified header contents. HS-HARQ uses a synchronous ARQ mechanism for both downlink and uplink TBFs.

For a downlink TBF the timing between a transmission and its acknowledgement over the air interface is fixed. The downlink TBF timing is shown in figure 356. The acknowledgement always occurs in the block period following the transmission. A retransmission of the original block may occur in the following block period, allowing for a 60 msec transmission, acknowledgement, retransmission cycle.
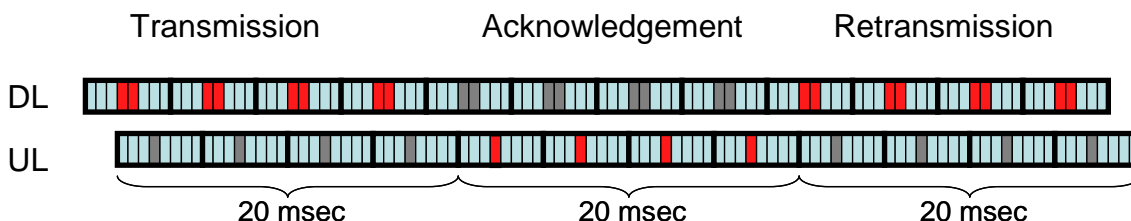
Figure 356: Downlink HS-HARQ ARQ timing

For an uplink TBF the timing between a transmission and its acknowledgement over the radio interface is fixed. The timing for an uplink TBF is shown in figure 357. The acknowledgement always occurs in the block period following the transmission. A retransmission of the original block may occur in the following block period, allowing for a 60 msec transmission, acknowledgement, retransmission cycle.
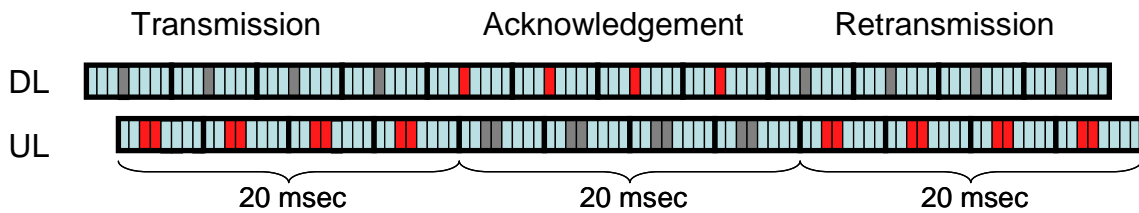
Figure 357: Uplink HS-HARQ ARQ timing

10.7.5 Stop and Wait ARQ

In order to limit latency for conversational services, the HS-HARQ mechanism could allow the number of retransmissions for each block to be limited. This limit could be negotiated or implied as part of the QoS negotiation and communicated from BSS to mobile during TBF establishment.

The HS-HARQ mechanism could utilize multiple stop and wait ARQ processes. Each process performs a simple stop and wait ARQ protocol to transfer several data blocks across the air interface at a time. Multiple processes operate in parallel to fill the pipeline formed by the transmit-ack-retransmit cycle of the air interface. This structure requires less hybrid ARQ soft decision memory and fewer block sequence numbers than a traditional selective repeat hybrid ARQ mechanism.

At the transmitter, blocks are fed into an array of stop and wait ARQ processes. These processes transfer blocks to the receiver using a simple stop and wait ARQ protocol, applying the optional per-block retransmission limit at each process. The receiver uses the block sequence numbers to reorder the blocks from the various ARQ processes. At the receiver a New Data bit indicates that the transmit process has moved on to a new block and facilitates detection of missed data blocks.

10.8 References

[1]   3GPP TS 44.060: "Mobile Station (MS) - Base Station System (BSS) interface; Radio Link Control/Medium Access Control (RLC/MAC) protocol," Rel-6, 2005-09.

[2]   3GPP TR 45.912: "Feasibility Study on Future GERAN Evolution," V0.2.0, output from 3GPP TSG GERAN#25, Schaumburg (Il.), U.S.A., August 29 - September 2, 2005.

[3]   ITU-T Recommendation G.114 (05/2003): "One-way transmission delay".

[4]   IETF RFC 1939: "Post Office Protocol-Version 3".

[5]   GP-060506: "Feasibility study for evolved GSM/EDGE Radio Access Network (GERAN) (Release 7)," 3GPP TR 45.912 v 0.5.0, April 2006.

[6]   GP-060781: "Proposal for a 5 ms TTI solution", Siemens, GERAN#29.

[7]   GP-060779: "RTTI approach for delay-sensitive applications", Siemens, GERAN#29.

[8]   G2-060186: "GERAN Evolution - Summary of Application Gains with RTTI and Shorter RRBP", Source: Ericsson.

[9]   3GPP TS 45.005: "Radio transmission and reception".

[10]   GP-060754: "GERAN Evolution - Considerations on Reduced TTI", Source: Ericsson, 3GPP TSG GERAN#29, San Jose del Cabo, Mexico.

[11]   IETF RFC 2508: "Compressing IP/UDP/RTP Headers for Low-Speed Serial Links".

[12]   Tdoc GP-051891: "GERAN evolution- Proposed text on Latency reduction for technical report", Panasonic.

[13]   Tdoc AHGEV-017: "Multi-carrier EDGE, GERAN Ad-Hoc on GERAN Evolution", Ericsson.

[14]   TD GP 052598: "Variable-sized Radio Blocks", Siemens.

11　　New burst structures and new slot formats

11.1　　Introduction

This subclause describes a candidate enhancement for the uplink based on the definition of a new set of transmission bursts deriving from the aggregation of timeslots at Layer 1. The aggregation relies on the removal of guard times and training sequences from a subset of bursts within a multislot allocation.

The new formats are therefore particularly suited for transmission on PS dedicated channels (uplink and downlink), or in the uplink, and are also applicable on downlink shared channels.

>　NOTE1.　PS dedicated channels are not defined in the Release 6 version of the specification, but a Work Item for their definition is currently open.

11.2　　Concept description

The idea articulates in two fundamental components: removal of training sequences and removal of guard times. The combination of these two aspects generates the new burst format.

Within a multislot allocation of n slots, the first component consists in the removal of training sequences from all slots except one. For example, in a 3-slot allocation, the TSC could be retained in the second slot, and disappear in the first and in the third. Similarly, the idea includes the removal of the stealing flags whenever the training sequence is removed, by operating under the assumption that the one remaining stealing flag will apply also to the other slots.

Further, extra room can be gained within a multislot allocation of n slots by allowing for data transmission also in the guard period, when the guard period falls within two timeslots allocated to the same user. In principle this would mean that the receiver would only ramp up before slot 1 and ramp down at the end of slot n. No further ramps would be present.

This would also allow for the removal of the tail bits wherever ramp up's and down's are removed. It is also interesting to note that, in the existing specification, there are no ramping requirements for base stations.

>　NOTE2.　From 3GPP TS 05.02 Subclause 5.2.8: "The guard period is provided because it is required for the MSs that transmission be attenuated for the period between bursts with the necessary ramp up and down occurring during the guard periods as defined in 3GPP TS 05.05. A base transceiver station is not required to have a capability to ramp down and up between adjacent bursts".

When the two aforementioned principles (removal of TSC and removal guard times) are combined, a new slot format for Evolved GERAN can be defined. The new slot format:

1)　Comes from the aggregation of the slots of a multislot allocation (i.e. from the removal of intermediate ramp up's and down's).

2)　Further, it contains only one training sequence, while the rest of the slot is an uninterrupted stream of data.

Obviously, one would define as many new slot formats as possible aggregations. Thus, assuming aggregations of 2, 3, and 4 timeslots are possible, three new slot formats would be defined. Figures 358 and 359 illustrate the principle for a 2-slot aggregation and a 3-slot aggregation.
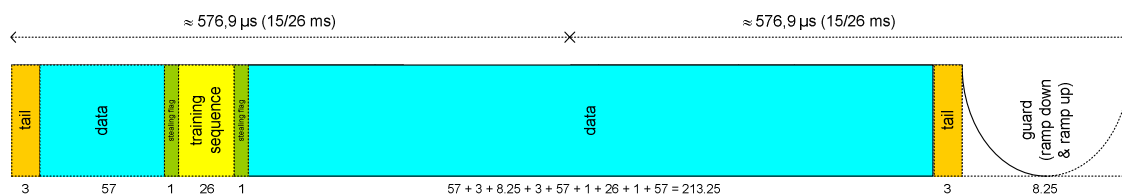
Figure 358: Proposed new slot format for evolved EDGE for a 2-slot aggregation
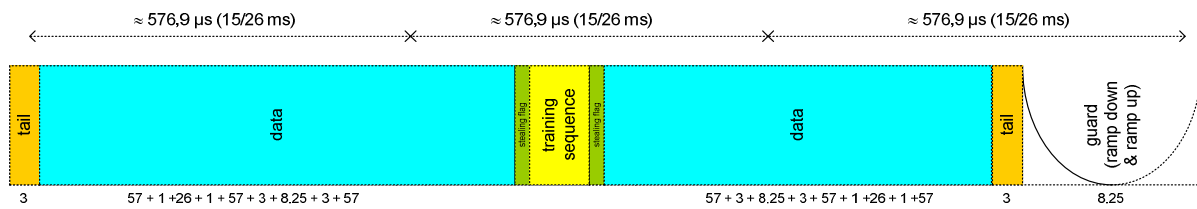
NOTE: Picture is not to scale w.r.t. figure 358.

Figure 359: Proposed new slot format for evolved EDGE for a 3-slot aggregation

The introduction of a new, larger, slot format, allows for some additional gain at Layer 2. In fact, it would now be possible to define larger radio blocks following a principle conceptually very similar to the Layer 1 timeslot aggregation. The radio blocks would still span four TDMA frames, but would now consist of four "aggregated" slots, instead of four ordinary slots. This would allow them to carry a larger proportion of data with respect to the header, since there would be no need for a RLC/MAC header in every single slot. Multiple RLC/MAC blocks could be multiplexed in one radio block, following the same principle already existent for MCS7-9. This is further discussed in subclause 11.3. Figure 360 illustrates the principle for a 2-slot allocation.
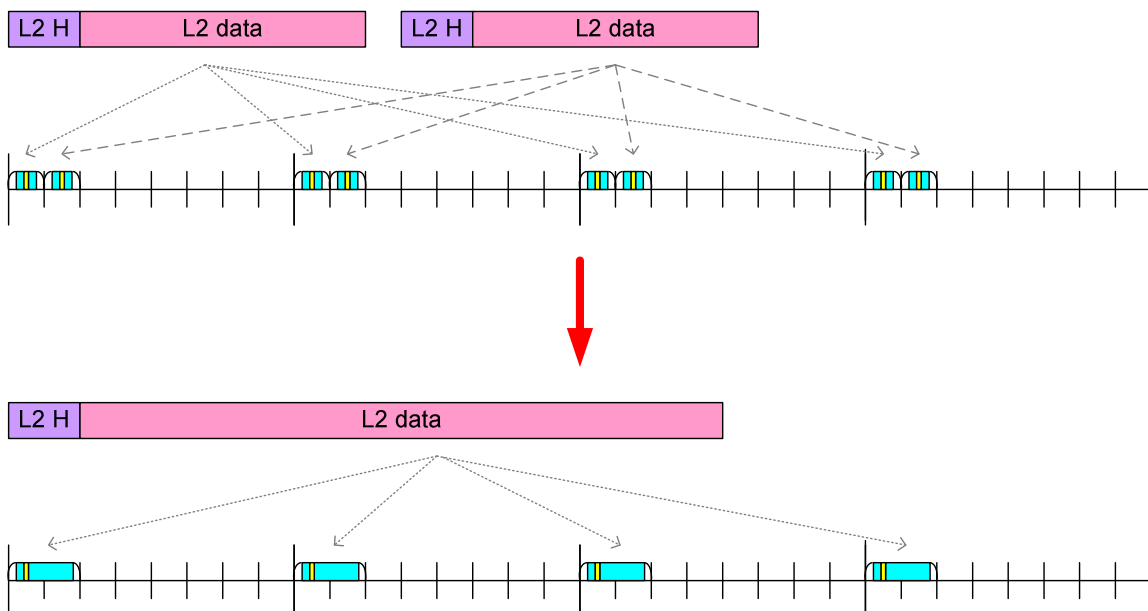
Figure 360: RLC/MAC level corresponding to a 2-slot aggregation

In the downlink, the removal of the RLC/MAC header from certain timeslots would include the removal of the USF, and therefore a reduction of scheduling opportunities in the uplink, since no USF scheduling of legacy mobiles can take place in correspondence of the aggregated timeslots. In the downlink a similar observation as for the USF does apply for the RRBP scheduling.

However, in the uplink, there is nor USF neither RRBP. Thus, the drawbacks identified above do not exist. The new burst formats can be used in the uplink whenever at least two or more adjacent timeslots are allocated to a mobile station.

11.3   RLC/MAC Aspects

11.3.1   Introduction

The following subclauses will consider the 2-slot aggregation as an example for the discussion of the RLC/MAC Aspects. However, the principles discussed here can be easily extended to an aggregation of multiple slots.

11.3.2   RLC/MAC and the New Burst Structures

When the physical layer uses the new burst structures, each TDMA frame offers to the MAC and RLC layers a larger number of bits.

Further, it is assumed that, in correspondence of a 2-slot aggregation, two RLC blocks will still be carried, i.e. one RLC block in correspondence of every timeslot, with the exception of MCS7-9. This is in line with the existing RLC behaviour.

Provided this, the additional bandwidth offered by the new burst formats can be exploited in the following ways:

1. Increase the RLC block size & keep the same code rate and the same mother code (convolutional).

2. Keep the same RLC block size & make the code rate more robust (keeping also the same mother code).

3. Trade-off between (1) and (2).

4. Increase the RLC block size & exploit the increased length with different coding, e.g. with turbo or LDPC codes.

Subclause 11.3.2.1 will illustrate option 1 ('Increased RLC block size for the 2-slot aggregation").

Subclause 11.3.2.2 will illustrate option 2 ("Reduced code rate for the 2-slot aggregation").

Option 3 can be to some extent inferred from the subclauses 11.3.2.1 and 11.3.2.2 and is not be discussed here.

Option 4 has been simulated and results are presented in subclause 11.4.2.5.

11.3.2.1   Option 1: Increased RLC block size for the 2-slot aggregation

11.3.2.1.1   Principles

The working principles and inter-relations of RLC, MAC, and physical layer for this option are summarized as follows for the case of the 2-slot aggregation.

-   Data comes uncoded from the upper layers (IP/SNDCP/LLC).

-   BCS (12 bits) is added.

-   Data is coded with the same convolutional mother code as EGPRS:

    -   Constraint length = 7.

-   Data is then punctured:

    -   Puncturing pattern dependent on MCS.

-   1 or 2 data blocks co-exist in a fourtet of timeslots (radio block):

    -   MCS1-6: 1 data block per radio block.

    -   MCS7-9: 2 data blocks per radio block.

-   Header is created & HCS is added to the header.

-   Header is coded with the same convolutional mother code and then punctured:

    -   Different puncturing pattern than data part.

-   Header & data part(s) are interleaved over the four timeslots.

-   Stealing flags (SF) are added.

-   Modulation is performed.

Additionally:

-   The header is assumed to be larger to indicate the multiple blocks.

-   Data (non coded) has to be a multiple of 8.

-   The BCS is increased from 12 to 16:

    -   Better error detection for slightly longer blocks.

-   12 Stealing Flags (SF) were accounted for the New Formats:

    -   Cope with eventual definition of additional MCS's for reduced TTI.

-   A, B. C indicates the EGPRS family. The same concept has been maintained.

-   The code rate has been kept the same as old format.

-   Data part is ~21 % larger consistently for all MCS.

11.3.2.1.2   Pictorial representations

Figure 361 is a pictorial representation of the coding/puncturing/multiplexing process for MCS1-4 for larger block sizes.
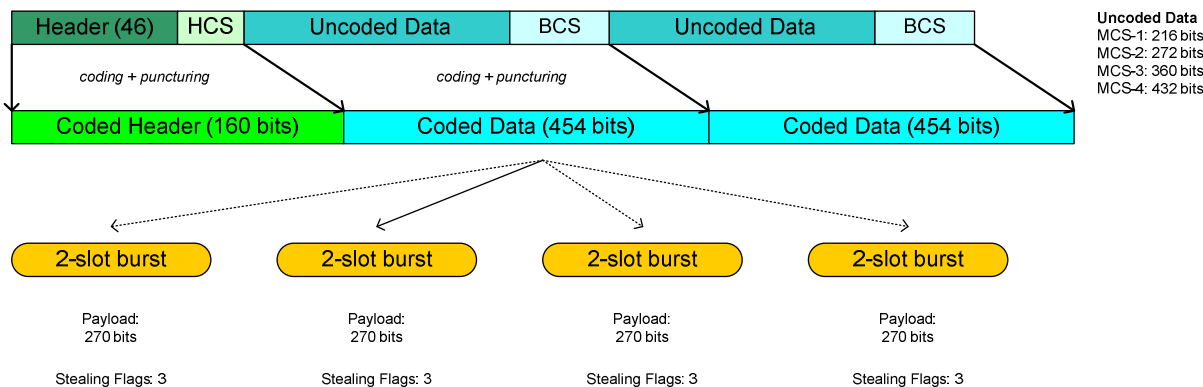
Figure 361: Pictorial representation of MCS1-4 for 2-slot aggregated bursts with increased RLC block size

Figure 362 is a pictorial representation of the coding/puncturing/multiplexing process for MCS5-6 for larger block sizes.
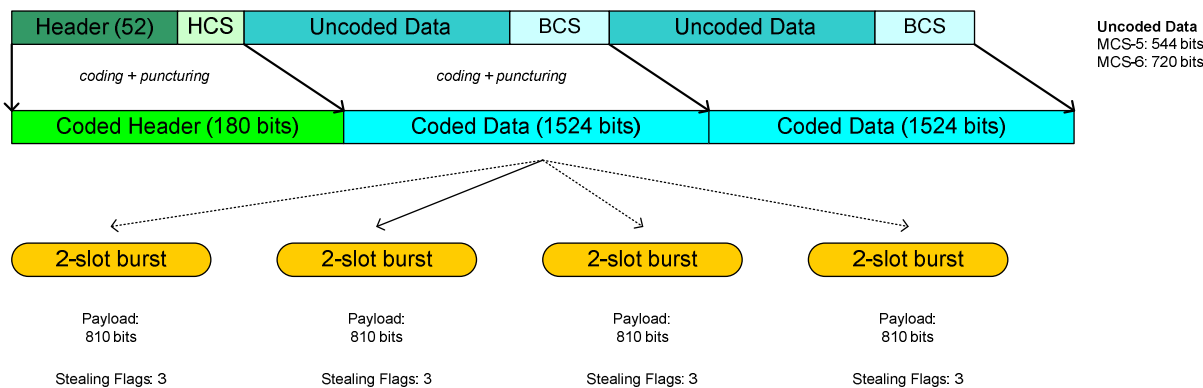
Figure 362: Pictorial representation of MCS5-6 for 2-slot aggregated bursts with increased RLC block size

Figure 363 is a pictorial representation of the coding/puncturing/multiplexing process for MCS7-9 for larger block sizes.
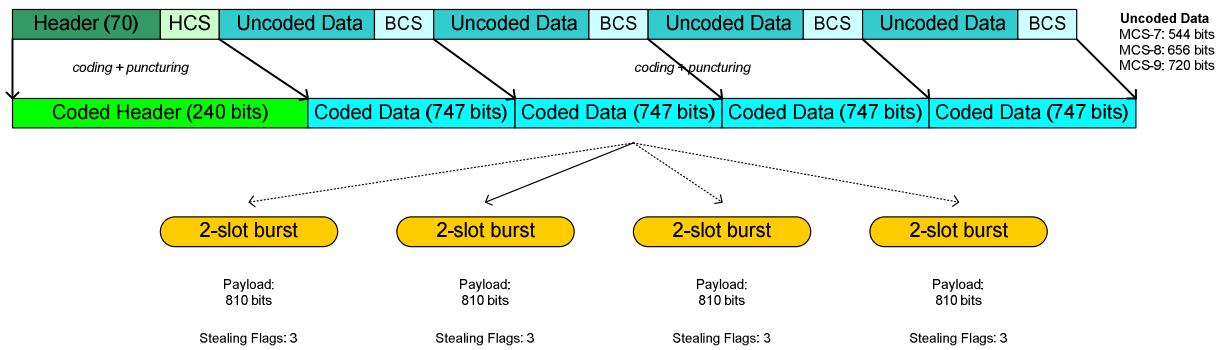
Figure 363: Pictorial representation of MCS7-9 for 2-slot aggregated bursts with increased RLC block size

11.3.2.1.3 A numerology

The following table summarizes the numerology associated with the schemes described in subclause 11.3.2.1.2. This table also captures the fact that MCSs are still grouped in families (A, B, C).

All figures in bits.

The nomenclature is as follows.

Uncoded Header: Header before coding. It changes for the GMSK blocks, the 8PSK blocks and the 8PSK blocks carrying two RLC blocks.
HCS: Protection for the header.

Uncoded Data: "raw" data, i.e. data coming from the upper layers before coding and puncturing. This is consistently larger than the corresponding value presented in subclause 2.5. In other words, all of the additional bandwidth coming from the timeslot aggregation has been employed to provide a larger RLC payload.
BCS: Protection for the data part.

Coded Header: Header + HCS after coding and puncturing.

Coded Data: Data + BCS after coding and puncturing.
Code rate: effective code rate for the data part (the mother code is the same, but the amount of puncturing changes from MCS to MCS). It shall be noted that the code rate is always equal to the code rate of the existing RLC blocks, as indicated in table 2.

Total: number of bits that are passed to the fourtet of timeslots are the physical layer.

Table 191: RLC/MAC Numerology for 2-slot aggregation with larger RLC blocks

	New Format (2-slot aggregation, larger RLC blocks)							
	Head	HCS	Uncoded Data	BCS	Coded Header	Coded Data	Data code rate	Total
MCS-1 (C)	46	8	2*216	2*16	160	2*454	~0.5	1 068
MCS-2 (B)	46	8	2*272	2*16	160	2*454	~0.63	1 068
MCS-3 (A)	46	8	2*360	2*16	160	2*454	~0.83	1 068
MCS-4 (C)	46	8	2*432	2*16	160	2*454	~1	1 068
MCS-5 (B)	52	12	2*544	2*16	180	2*1524	~0.37	3 228
MCS-6 (A)	52	12	2*720	2*16	180	2*1524	~0.48	3 228
MCS-7 (B)	70	12	4*544	4*16	240	4*747	~0.75	3 228
MCS-8 (A)	70	12	4*656	4*16	240	4*747	~0.9	3 228
MCS-9 (A)	70	12	4*720	4*16	240	4*747	~1	3 228

For this Option, new MCS schemes will be needed for this concept. Note that for different levels of aggregation at the physical layer, different set of MCS schemes may need to be defined - for instance, assuming that aggregation of 2 to 4 timeslots on uplink is proposed; it may be necessary to define a total of 27 new MCS schemes.

A change in the number of allotted timeslots on the uplink at the physical layer leads to an automatic change in the MCS scheme because of aggregated timeslot configurations and this is undesirable. This might need complicated inter layer communication between the physical layer and the RLC/MAC layer both at the sender and the receiver.

There will be some implications on the incremental redundancy support across different new MCS schemes and this would lead to further losses from the system perspective if seamless incremental redundancy support is not possible across all the new MCS schemes.

11.3.2.2 Option 2: Reduced code rate for the 2-slot aggregation

11.3.2.2.1 Principles

The working principles and inter-relations of RLC, MAC, and physical layer for this option are summarized as follows for the case of the 2-slot aggregation.

The same working principles illustrated in subclause 11.3.2.1.1 are maintained. Additionally:

- The header is assumed to be larger to indicate the multiple blocks.

- Data (non coded) has been kept the same as for the existing RLC/MAC blocks.

- 12 stealing flags (SF) were accounted for the New Formats:

    - Cope with eventual definition of additional MCS's for reduced TTI.

- A, B, C indicates the EGPRS family. The same concept remains the same.

- The code rate has been reduced for each MCS:

    - All of the bandwidth made available from the new burst format is used to reduce the code rate for the same payload size.

11.3.2.2.2 Pictorial representations

Figure 364 is a pictorial representation of the coding/puncturing/multiplexing process for MCS1-4 for reduced code rate.
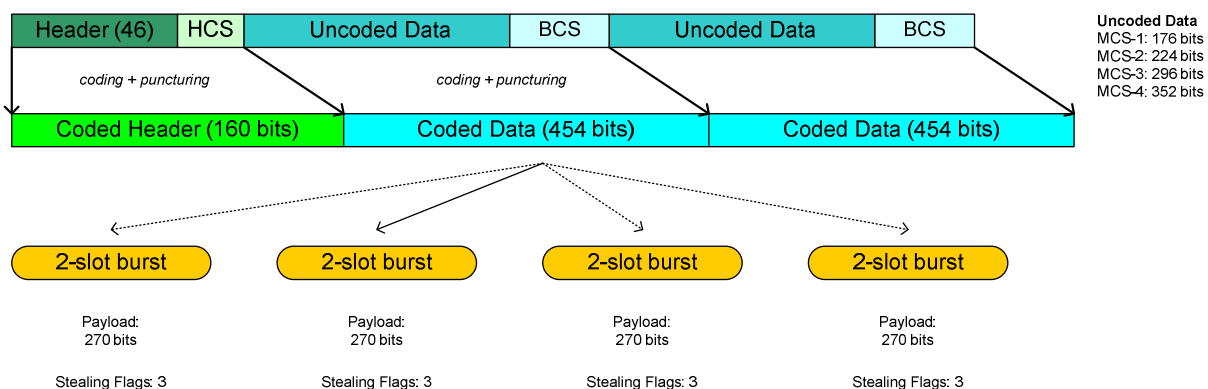
Figure 364: Pictorial representation of MCS1-4 for 2-slot aggregated bursts with reduced code rate

Figure 365 is a pictorial representation of the coding/puncturing/multiplexing process for MCS5-6 for reduced code rate.
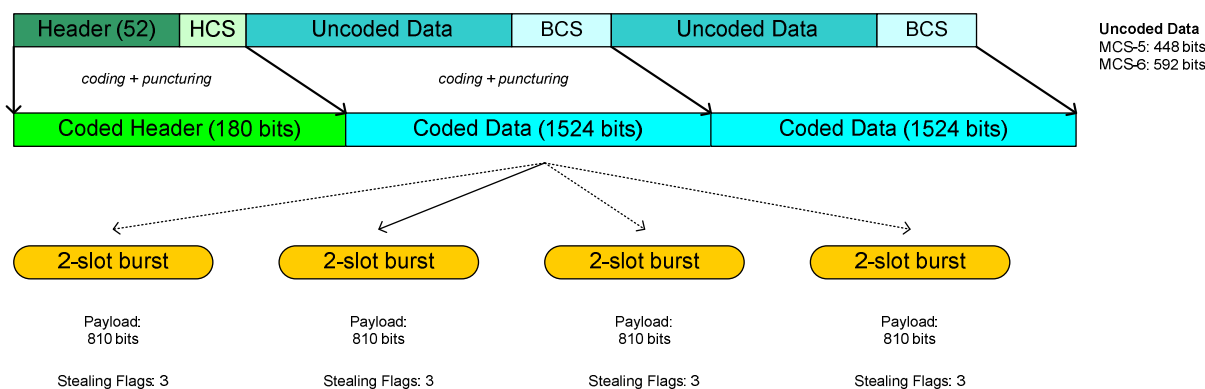
Figure 365: Pictorial representation of MCS5-6 for 2-slot aggregated bursts with reduced code rate

Figure 366 is a pictorial representation of the coding/puncturing/multiplexing process for MCS7-9 for reduced code rate.
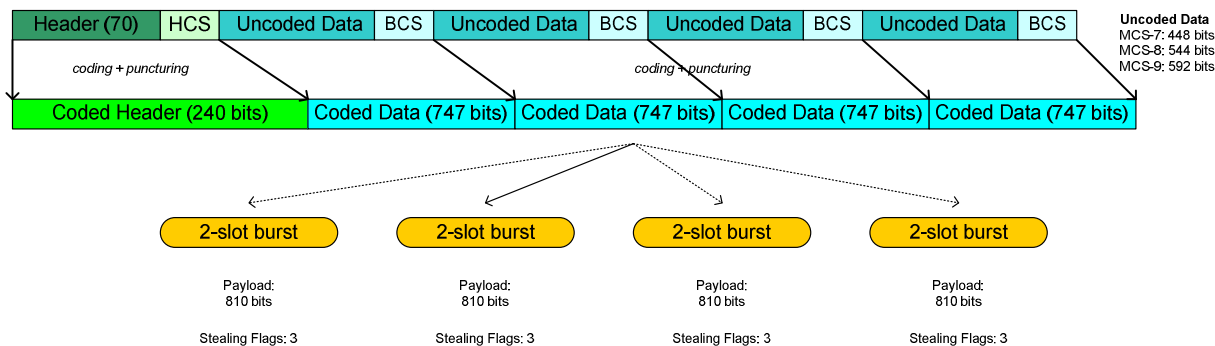
Figure 366: Pictorial representation of MCS7-9 for 2-slot aggregated bursts with reduced code rate

11.3.2.2.3   A numerology

The following table summarizes the numerology associated with the schemes described in subclause 11.3.2.2.2. This table also captures the fact that MCSs are still grouped in families (A, B, C).

All figures in bits.

The nomenclature is as follows.

Uncoded Header: Header before coding. It changes for the GMSK blocks, the 8PSK blocks and the 8PSK blocks carrying two RLC blocks.
HCS: Protection for the header.

Uncoded Data: "raw" data, i.e. data coming from the upper layers before coding and puncturing. This is the same as subclause 2.5.
BCS: Protection for the data part.

Coded Header: Header + HCS after coding and puncturing.

Coded Data: Data + BCS after coding and puncturing.
Code rate: effective code rate for the data part (the mother code is the same, but the amount puncturing changes from MCS to MCS). In other words, all of the additional bandwidth coming from the timeslot aggregation has been employed to reduce the code rate.

Total: number of bits that are passed to the fourtet of timeslots are the physical layer.

Table 192: RLC/MAC Numerology for 2-slot aggregation with reduced code rate

	New Format (2-slot aggregation, more robust code rate)							
	Head	HCS	Uncoded Data	BCS	Coded Header	Coded Data	Data code rate	Total
MCS-1 (C)	46	8	176	12	160	2*454	~0.365	1068
MCS-2 (B)	46	8	224	12	160	2*454	~0.49	1068
MCS-3 (A)	46	8	296	12	160	2*454	~0.65	1068
MCS-4 (C)	46	8	352	12	160	2*454	~0.775	1068
MCS-5 (B)	52	12	448	12	180	2*1524	~0.29	3228
MCS-6 (A)	52	12	592	12	180	2*1524	~0.388	3228
MCS-7 (B)	70	12	2*448	2*12	240	4*747	~0.6	3228
MCS-8 (A)	70	12	2*544	2*12	240	4*747	~0.73	3228
MCS-9 (A)	70	12	2*592	2*12	240	4*747	~0.79	3228

11.3.2.3   Discussion

The previous options are summarized by the following scheme.

Table 193: Summary of RLC/MAC options for Aggregated Bursts

	Option 1	Option 2	Option 3	Option 3
Basic Principle	**Increase** the RLC block size **Keep** the code rate unchanged	**Keep** the RLC block size unchanged **Reduce** the code rate	**Increase** the RLC block size **Reduce** the code rate (middle way between Option 1 and Option 2)	**Increase** the RLC block size **Change** the mother code (e.g. Turbo, LDPC)
Expected behaviour	Larger amount of data is transferred in a given radio block The BLER per radio block is expected to get slightly larger (slightly larger RLC block size for same or similar BER)	The BLER per radio block is expected to be reduced, thus improving the overall throughput		Larger amount of data is transferred in a given radio block The BLER per radio block is expected to be reduced, thus improving the overall throughput
Notes	There is still one RLC block per timeslot for MCS1-6 and two RLC blocks per timeslot for MCS7-9. New RLC block size have to be defined.	There is still one RLC block per timeslot for MCS1-6 and two RLC blocks per timeslot for MCS7-9. Further, the RLC block size is the same as for the legacy case, irrespective of the number of aggregated slots. The number of aggregated slots influences only the puncturing pattern		New RLC blocks and a new mother code have to be designed
Described in	Subclause 11.3.2.1	Subclause 11.3.2.2		Simulated in Subclause 11.4.2.5

Options 1 and 2 are describing a trade-off curve between larger block size and more robust code rate. The optimum point of this curve would most likely have to be found with simulations.

Option 4 is also attractive in case one is willing to pursue changes to the employed coding technique. This in any case would be worth an investigation.

Note that if one of the uplink timeslots is a CS timeslot, then it is likely that aggregation of that CS timeslot is not possible. In such a case, in order to make the aggregation among the PS timeslots feasible, the CS time slot has to be moved to either the beginning or to the end of the allotted uplink timeslots. Whilst this is not a problem in general, it should be noted that in some cases, the CS timeslot has to stay in between the uplink PS timeslots.

In EGPRS the control messages are transmitted using CS-1. The timeslots on which these control messages are sent can not be aggregated with other timeslots. Since the network does not know in advance when exactly a MS transmits a CS-1 coded control message, the network would have to find out by blind detection if all allotted timeslots are aggregated or if there is a separate CS-1 coded timeslot.

11.4 Performance Characterization

11.4.1 Performance calculations

For a two timeslot allocation the gain of the new slot format (consisting of removal of guard times and TSC) measured at L1 would be 18.53 %. Within a n-timeslot allocation the gain would therefore be proportional to n, as illustrated by table 194.

Table 194: Bandwidth gain of the new slot format (see note)

Allocated Timeslots	Symbols in new slot format	Gain
2	270.25	18.53 %
3	426.5	24.7 %
4	582.75	27.8 %

NOTE. Performance figures will have to be verified with respect to the identified issues (e.g. high speed case).

It is worth noting that the above-mentioned gain merely include the additional L1 bandwidth. It does not include the fact that the additional bandwidth could be exploited e.g. for better coding. In fact, while tail-biting convolutional coding with Viterbi decoding is optimal for small block sizes (up to 150 bits), other coding schemes, such as turbo codes or hyper-codes, outperform TB-convolutional for blocks larger than 150 bits. Further, we note that the power employed in correspondence of each timeslot is obviously increased, since more bits are transmitted (e.g. in correspondence of guard times). However, the transmitted energy per bit remains unchanged.

11.4.2 Link Level Simulations

11.4.2.1 GMSK Modulated Channels with legacy equalizers

11.4.2.1.1 First simulation run

Simulations have been run for the following settings:

- RawBER simulation results.

- Results based on SNR-limited scenarios (i.e. no variation of interference within the aggregated timeslot).

- Results expressed in terms of performance degradation (or lack of performance degradation) due to the timeslot aggregation, i.e. the penalty (or lack of penalty) paid on the link budget because of the timeslot expansion and correspondent training sequence removal:

  - E.g. "0 dB" means that the non-aggregated format and the aggregated format were found to have the same performance.

- UL Receiver (in the BTS) assumed to be the same as a MS receiver (likely a pessimistic assumption).

- Frequency tracking errors and various impairments not considered neither for the non-aggregated nor for the aggregated format:

  - The goal being to evaluate the equalizer performance against the proposed new formats.

- "EQ-A" is a reference GMSK equalizer employing MLSE.

- "EQ-B" is another reference GMSK equalizer, employing MLSE + LMS with Per-Survivor Processing.

The results are summarized by table 195.

No performance requirements for the uncoded case exists certain channels: these cases have been shaded dark grey in table 195.

Also, the specification does not say anything for the certain channels: these cases have been shaded light grey in table 195.

Table 195: GMSK SNR-limited RawBER results

		rawBER = 8%				rawBER = 1%			
		EQ-A		EQ-B		EQ-A		EQ-B	
		2-slot	3-slot	2-slot	3-slot	2-slot	3-slot	2-slot	3-slot
900 MHz	TU3	0 dB	0 dB	0 dB	0 dB	0 dB	0 dB	0 dB	0 dB
	TU50	0 dB	0 dB	0 dB	0 dB	1 dB	1 dB	0 dB	0 dB
	TU120	1 dB	1 dB	0 dB	0 dB	> 6dB	> 6dB	~1 dB	~1 dB
	RA130	~0.5 dB	~0.5 dB	0 dB	0 dB	N.A.	N.A.	N.A.	N.A.
	RA250	~3 dB	~4 dB	0 dB	0 dB	N.A.	N.A.	N.A.	N.A.
	HT100	~0.5 dB	~1 dB	0 dB	0 dB	N.A.	N.A.	0 dB	0 dB
1800 MHz	TU3	0 dB	0 dB	0 dB	0 dB	0 dB	0 dB	0 dB	0 dB
	TU50	~1 dB	~1 dB	0 dB	0 dB	N.A.	N.A.	0 dB	0 dB
	TU120	~5 dB	> 6 dB	~1 dB	~1 dB	N.A.	N.A.	N.A.	N.A.
	RA130	~3 dB	~4 dB	~1 dB	~1 dB	N.A.	N.A.	N.A.	N.A.
	RA250	N.A.	N.A.	~2 dB	~3 dB	N.A.	N.A.	N.A.	N.A.
	HT100	~4 dB	~5 dB	~0.5 dB	~0.5 dB	N.A.	N.A.	N.A.	N.A.

11.4.2.1.2 Second simulation run

Further simulations were run independently of the former.

Those confirmed that the BER performance of aggregated new burst became worse for certain scenarios. The performance degradation of 3 burst aggregation in co-channel interference condition is listed in table 196 for GMSK channels.

Table 196: BER degradation of 3 burst aggregation compared to legacy burst, GMSK

scenario	8 % BER	1 % BER
TU3iFH 900 Mhz	0 dB	0 dB
TU50 900 MHz	0 dB	0.3 dB
TU50 1 800 MHz	0.3 dB	1.8 dB
RA250 900 MHz	1.5 dB	> 3 dB

The equalizer here used is based on normal implementation complexity.

11.4.2.2 8PSK Modulated Channels with legacy equalizers

11.4.2.2.1 First simulation run

Simulations have been run with the same settings as subclause 11.4.2.1.1. Additionally

- "EQ-A" is a reference EDGE equalizer, essentially replicating the same performance of an EDGE mobile receiver available today.

- Note that the complexity of running EQ-A over a 2-slot aggregation is lower than running EQ-A twice over a non-aggregated slot, since some channel processing associated to the TSC reception is run only once per aggregation. (Same applies for a 3 slot aggregation).

- "EQ-B" is a variant of "EQ-A" with slightly more frequent channel tracking.

  - The complexity of running EQ-B over a 2-slot aggregation is only marginally higher than running EQ-A twice over a non-aggregated slot. In fact, while channel processing is more frequent, this is offset by the fact that more TSC processing would have been performed over adjacent non-aggregated slots. In other words, EQ-B entails little complexity increase compared to EQ-A.

The results are summarized by table 197.

No performance requirements for the uncoded case exists certain channels: these cases have been shaded dark grey in table 197.

Also, the specification does not say anything for the certain channels: these cases have been shaded light grey in table 197.

Table 197: 8PSK SNR-limited RawBER results

		rawBER = 8%				rawBER = 1%			
		EQ-A		EQ-B		EQ-A		EQ-B	
		2-slot	3-slot	2-slot	3-slot	2-slot	3-slot	2-slot	3-slot
900 MHz	**TU3**	0 dB	0 dB	0 dB	0 dB	0 dB	0 dB	0 dB	0 dB
	TU50	0 dB	0 dB	0 dB	0 dB	2 dB	3 dB	1.5 dB	2 dB
	TU120	~1.5 dB	~1.5 dB	~1 dB	~1 dB	> 6dB	> 6dB	> 6dB	> 6dB
	RA130	~0.5 dB	~0.5 dB	< 0.5 dB	< 0.5 dB	~6 dB	> 6 dB	~6 dB	> 6 dB
	RA250	~2 dB	~2.5 dB	~1.5 dB	~2.5 dB	N.A.	N.A.	N.A.	N.A.
	HT100	~1 dB	~1.5 dB	~1 dB	~1.5 dB	> 6dB	> 6dB	> 6dB	> 6dB
1800 MHz	**TU3**	0 dB	0 dB	0 dB	0 dB	0 dB	0 dB	0 dB	0 dB
	TU50	~1 dB	~1 dB	~1 dB	~1 dB	> 6dB	> 6dB	> 6dB	> 6dB
	TU120	~6 dB	> 6dB	~5 dB	~6 dB	> 6dB	> 6dB	> 6dB	> 6dB
	RA130	~2 dB	~2.5 dB	~2 dB	~2.5 dB	N.A.	N.A.	N.A.	N.A.
	RA250	> 6dB	> 6dB	> 6dB	> 6dB	N.A.	N.A.	N.A.	N.A.
	HT100	~5 dB	> 6dB	~4 dB	~6 dB	N.A.	N.A.	N.A.	N.A.

11.4.2.2.2 Second simulation run

Further simulations were run independently of the former.

Those confirmed that the BER performance of aggregated new burst became worse for certain scenarios. The performance degradation of 3 burst aggregation in co-channel interference condition is listed in table 198 for 8PSK channels.

Table 198: BER degradation of 3 burst aggregation compared to legacy burst, 8PSK

scenario	%8 BER	1% BER
TU3iFH 900 Mhz	0 dB	0 dB
TU50 900 MHz	0 dB	0.5 dB
TU50 1 800 MHz	1.0 dB	6.5 dB
RA250 900 MHz	6 dB	> 10 dB

The equalizer here used is based on normal implementation complexity.

11.4.2.3 8PSK Modulated Channels with advanced simulation settings

11.4.2.3.1 First simulation run

Simulations for more complex cases have been run with the same settings as subclause 11.4.2.1.1. Additionally, Random SNR variations on a per-timeslot basis were simulated.

Effectively, this has been done by applying a random variation (± 1 dB) around the "nominal SNR" on a per-timeslot basis within a 2-slot and a 3-slot aggregation.

Figure 367 illustrates this simulation principle.
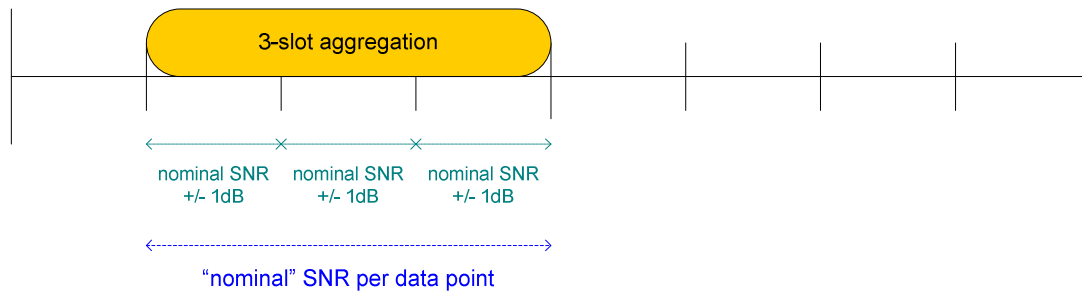
Figure 367: Per-timeslot SNR variations for a 3-slot aggregation

The simulation results can be summarized by the following table, expressed in terms of performance degradation (or lack of it) with respect to the "standard burst".

Note that for some profiles the standard has currently no performance requirements for the uncoded case.

In particular, no performance requirements for the uncoded case exist for RA130 and HT100. These cases have been shaded dark grey in table 199.

A rapid inspection of the results indicates that, for the evaluated cases (which obviously includes some amongst the most challenging ones, i.e. high speed at higher frequency), no difference exists from the cases where "non-advanced" simulation settings had been used.

This means that the simulated variation on a per-timeslot basis produced no discernible effect in the evaluation of the aggregated formats.

**Table 199: Performance delta between new burst formats and
the "standard burst" for 8PSK with EQ-A & EQ-B**

| | | rawBER = 8% | | rawBER = 1% | |
| | | EQ-B | | EQ-B | |
		2-slot	3-slot	2-slot	3-slot
1800 MHz	**TU3**	0 dB	0 dB	0 dB	0 dB
	TU50	~1 dB	~1 dB	> 6dB	> 6dB
	RA130	~2.5 dB	~3 dB	N.A.	N.A.
	HT100	~4 dB	~6 dB	N.A.	N.A.

11.4.2.4 Interference limited scenarios

Interference Limited scenarios are relevant to an evaluation of the new formats from two points of view.

First, the SINR could change within one aggregated slot in those scenarios where the interference conditions change on a per-timeslot basis.

Secondly, some interference cancellation implementation at the receiver (in the uplink) would have to cope with the removal of some of the training sequences within an aggregated format. This effect is difficult to study since uplink

interference cancellation techniques are proprietary and no details or performance requirements are available for it. The only reference of some relevance is DARP, i.e. downlink interference cancellation. It is therefore interesting to notice how DARP performance is tested in scenarios where the training sequence is removed, thus de-facto assuming that the interference cancellation algorithm will not, at least to achieve the required performance, rely on the TSC.

The interference scenario shown in figure 368 was simulated. All the interferer timeslots shown are assumed to be of same mean power.

Equalizer used for the simulations already includes channel tracking to compensate the channel variations during the longer burst.

Interference cancellation was not used.
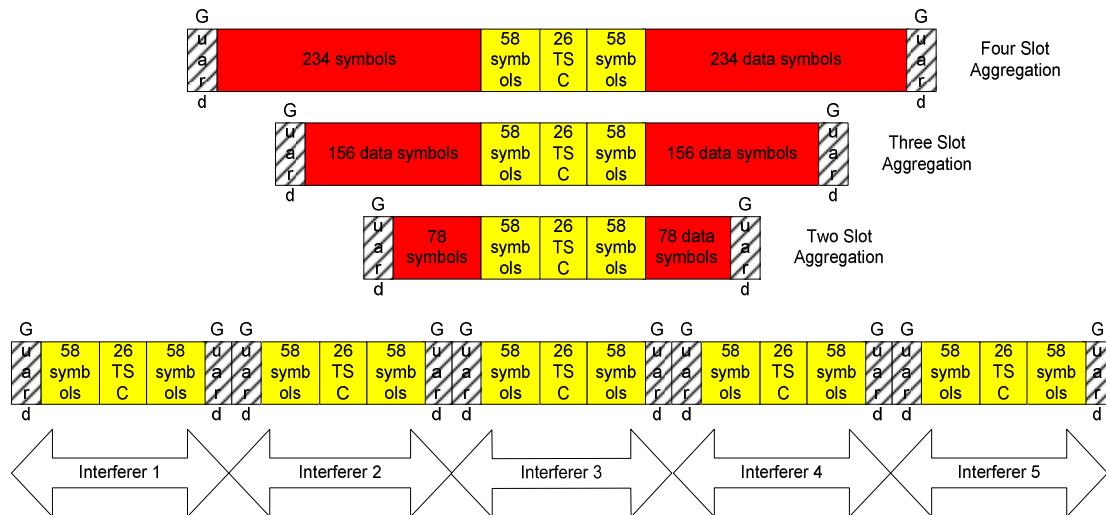
NOTE: The lengths of the burst shown above are not to the same scale.

Figure 368: Interference scenario simulated

The results are summarized in the table 200.

Table 200: Summary link level simulations with co-channel interference

	Loss in dB for TU 50 channel @ 1800 MHz			Loss in dB for RA 130 channel @ 1800 MHz		
	2 TS	3 TS	4 TS	2 TS	3 TS	4 TS
10% BER	0.7	1.6	2.7	3.8	13	> 20
8% BER	0.9	2	3.5	6	> 20	> 20
5 % BER	1.2	2.2	5	> 20	> 20	> 20

Such a link level loss would simply negate any gains achieved through timeslot aggregation for these high velocities at high frequency bands, when NO interference cancellation is used.

11.4.2.5 RLC Simulations

11.4.2.5.1 RLC Simulations with New Coding Schemes

As the aggregated RLC block can provide the longer data block length before channel coding, so using turbo codes as channel coding become realistic. In this subclause, turbo codes is introduced in the aggregated RLC data block and LA and IR simulation results are provided based on new defined coding schemes.

This subclause therefore corresponds to Option 4 of subclause 11.3.

Refer to the current EGPRS uplink MCS coding schemes, new uplink coding schemes is defined in the simulation, listed in table 201.

It is defined as the same data rate (per legacy burst) with legacy MCS. MB3MCS10 and MB3MCS11 are added to the coding schemes to reach peak data rate. In MB3MCS1 to MB3MCS9, the redundancy bit from burst aggregation and RLC aggregation are used as the protection bit in coding. Head length and coding schemes of new MCS type is the same with the legacy MCS in the simulation and it needs further study.

Table 201: New defined coding schemes for 3 burst aggregation

Legacy MCS type	New MCS (aggregation of 3 burst)	data rate per legacy burst (kbps)	Interleave depth (bursts)	Data block per RLC
MCS1	MB3MCS1	8.8	4	1
MCS2	MB3MCS2	11.2	4	1
MCS3	MB3MCS3	14.8	4	1
MCS4	MB3MCS4	17.6	4	1
MCS5	MB3MCS5	22.4	4	1
MCS6	MB3MCS6	29.6	4	1
MCS7	MB3MCS7	44.8	4	2
MCS8	MB3MCS8	54.4	2	2
MCS9	MB3MSC9	59.2	2	2
-	MB3MCS10	69.8	2	2
-	MB3MCS11	82.2	2	2

New burst of 3 aggregated legacy burst are considered in simulation and ideal LA (link adapt ion) and IR (incremental redundancy) assumed.

- Scenarios:

    - co-channel interference

- Equalizer type:

    - GMSK: MLSE + PSP (LMS)

    - 8PSK: RSSE + PSP (LMS)

    - The equalizer is not optimized and based on normal implementation complexity.

- TSC position:

    - In the middle of the new burst.

- Turbo code:

    - Take the turbo coding schemes and subsequent rate matching as it used in TSG RAN.

    - Max-log-map decoding algorithm used.

Simulations have been run for four channels.

- TU3iFH: 900 MHz.

- TU50: 900 MHz.

- RA250:   900 MHz.

- TU50: 1 800 MHz.

Table 202 shows the data throughput of new defined MCS and standard MCS. The CDF of C/I presented by TeliaSonera in *GP-042355*, indicates very few occurrences of C/I above 22 dB. According to the C/I pdf in *GP-042355*, the average data throughput can be calculated, the average gains are listed as following.

Table 202: Average throughput gain of new defined MCS with Turbo codes

Channel Type		Gains of LA	Gains of IR
TU3iFH	900 MHz	37 %	36 %
TU50	900 MHz	34 %	33 %
TU50	1 800 MHz	19 %	20 %
RA250	900 MHz	-9 %	2 %

The figures show that the data throughput gains of new coding schemes with turbo codes are very close to the theoretical gains with aggregated formats at L1 and L2.

11.5 Additional technical aspects

11.5.1 Influence of TSC Position

11.5.1.1 New slot formats in simulation

In modern mobile communication, coherent time T_c of the wireless channel is defined as [1].

$$T_c = \sqrt{\frac{9}{16\pi f_m^2}} \approx \frac{0.423}{f_m} = \frac{0.423\lambda}{v}$$

λ is the wave-length of carrier, v is the velocity of mobile terminal and f_m is the maximum Doppler frequency. At 250 km/h, T_c is about 2.03 ms for 900 MHz GSM system, a little shorter than the time duration of 4 legacy slots. So the maximum number of legacy slots we used in the new slot aggregation is 4 because the RA250 is the fastest fading channel in our simulation.

According to the rule of aggregation and the maximum number of slots, we use three new slot formats in the simulation, aggregation of two slots, three slots and four slots. As the current rule of aggregation, the position of TSC in the new slot is relatively not changed, and just remains in one of the legacy slots in the aggregation. In the new slot format we will find the lengths of data block before the TSC and data block following the TSC are not equal, and will induce the unbalance of channel estimation or channel tracking for the two data blocks. Furthermore, the unbalance will lead to demodulation and block error performance losses.

In order to evaluate the performance degradation, two types of new slot format are used in the simulation. One is that TSC remains in the first slot, denoted by Type A; another is that the TSC located at the middle of the new slot, denoted by Type B. Figures 369 to 371 show the details. As we know, the channel tracking makes the receiver more robust to the channel fluctuation and may influence the decision for the TSC position scheme. We include the LMS channel tracking in Viterbi algorithm [3] in our simulations to discuss this effect.

For the simulation convenience, the $0.25 \times n$ symbols of guard period (see note) form n legacy slots are moved into the new guard period in the new slot. For instance, the guard period in the aggregation of two slots is 8.5 symbols and the guard period in the aggregation of three slots is 8.75 symbols.

NOTE. The new slot is the aggregation of n legacy slots; n may equals 2, 3, 4 or more.

(a)Type A: TSC in the first slot

(b)Type B: TSC in the middle of new slot
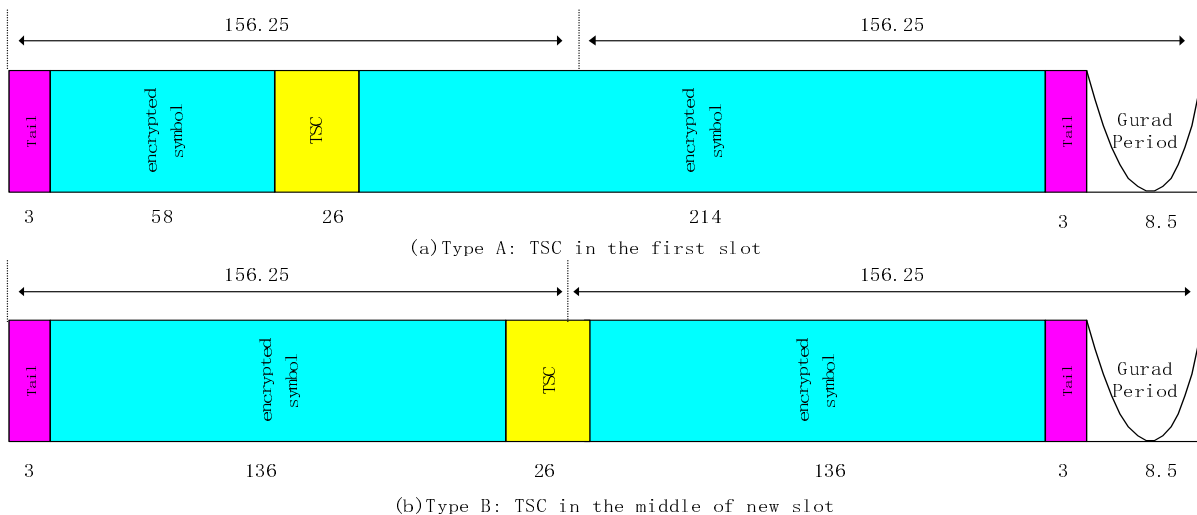
Figure 369: Aggregation of two slots

(a) Type A: TSC in the first slot

(b) Type B: TSC in the middle of new slot
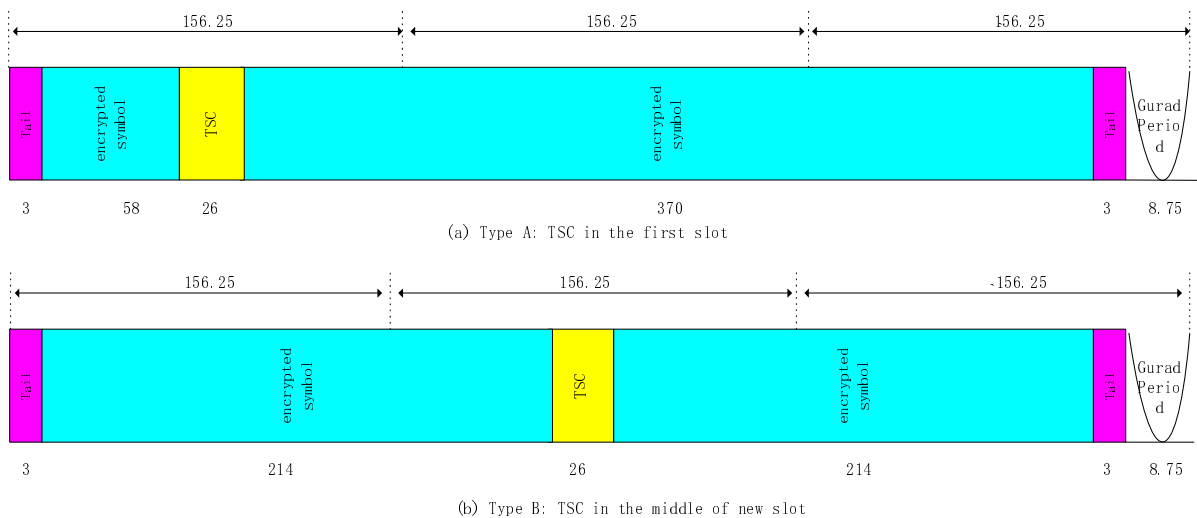
Figure 370: Aggregation of three slots

(a)Type A: TSC in the first slot

(b) Type B: TSC in the middle of new slot
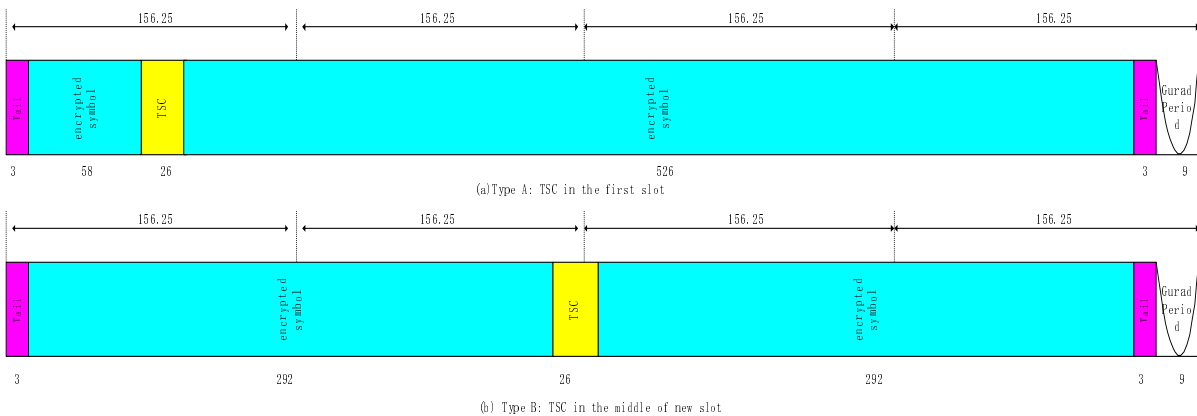
Figure 371: Aggregation of four slots

11.5.1.2 Simulation Results

In the following, the simulation results are presented to show the influence of the TSC position in the new slot on the link performance.

In the simulation, both GMSK and 8PSK modulation are applied. The wireless channel model used in the simulation is TU50, HT100 and RA250, which defined in [2].

Nomenclature is as follows.

Table 203: Description of curves

Type	Description
Type_A_ChTrac	TSC in the first slot and receiver with channel tracking
Type_B_ChTrac	TSC in the middle of new slot and receiver with channel tracking
Type_A_NoChTrac	TSC in the first slot and receiver without channel tracking
Type_B_NoChTrac	TSC in the middle of new slot and receiver without channel tracing

For convenience of compare, when the TSC is located in the middle of the new slot, the performance gains at BER level of 7 % for GMSK are summarised in the table 204.

Table 204: Performance gain (dB) at the BER level of 7 %, GMSK

Channel type	Aggregation of two slot		Aggregation of three slot		Aggregation of four slot	
	ChTrac	NoChTrac	ChTrac	NoChTrac	ChTrac	NoChTrac
TU50	0.0	0.1	0.1	0.2	0.2	0.5
HT100	0.1	0.3	0.5	1.5	1.2	> 3
RA250	0.7	1.5	2.0	> 3	> 3	> 3

It's obvious that receiver gets better performance when the TSC is located in middle of the new slot, especially under faster fading channel, such as RA250; for instance, at the BER level of 10 % for GMSK modulation, aggregation of four slots and receiver with channel tracking, the performance gain is about 3 dB under RA250, while 1.0 dB under HT100. More instances can be seen in table 204.

This phenomenon can be explained by following description. If the TSC is always located in the first slot, the lengths of data block before and behind the TSC are not equal, and the estimation error variance of the channel estimation for the two blocks is not equal. This will lead to the overall performance degradation of the receiver. While the TSC is located in the middle of new slot, the channel estimation for the two blocks is balanced. The fading in RA250 is faster than that in HT100. To the same new slot in which the TSC is located in the first slot, the unbalance of channel estimation in RA250 is more serious, and more improvement can be obtained by putting the TSC in the middle position of new slot.

At the same time, the performance gain is sensitive to the number of legacy slots in the new slot aggregation. The more legacy slots in the aggregation, the more gain will be obtained. For instance, at the 10 % BER for 8PSK modulation under HT100, the gain is 1.7 dB for aggregation of four slots and only 0.8 dB for aggregation of three slots, 0.1 dB for aggregation of two slots. And the statistical data in table 203 shows the gain's trend more clearly. To the new slot aggregation in which the TSC located in the first slot, the more slots used in new slot aggregation, the larger difference between the length of the two data blocks, and the more unbalance induced in channel estimation for two data blocks.

The simulation results also show that when the equalization receiver without channel tracking, the BER performance is more sensitive to the position of TSC in the new slot. Although the time duration of new slot in the simulations is shorter than the coherent time T_c, fading over the time duration is changing slowly. If the equalization does not track the slowly changing channel, the mismatch of channel estimation will be raised as the equalization processes. Hence, the BER unbalance of the receiver without channel tracking is more serious than that of receiver with channel tracking.

For real application, we may have more interest on the performance gain of 8PSK modulated new slot aggregation of two slots. At the BER level of 2 % under TU50, the performance gain is 0.3 dB for receiver with channel tracking, and 1.0 dB for receiver without channel tracking. More gains can be obtained under HT100 and RA250.

11.5.2   BER Distribution Aspects

With the aggregated bursts, the bit error rate would vary significantly over the whole burst. This is illustrated in figure 372.
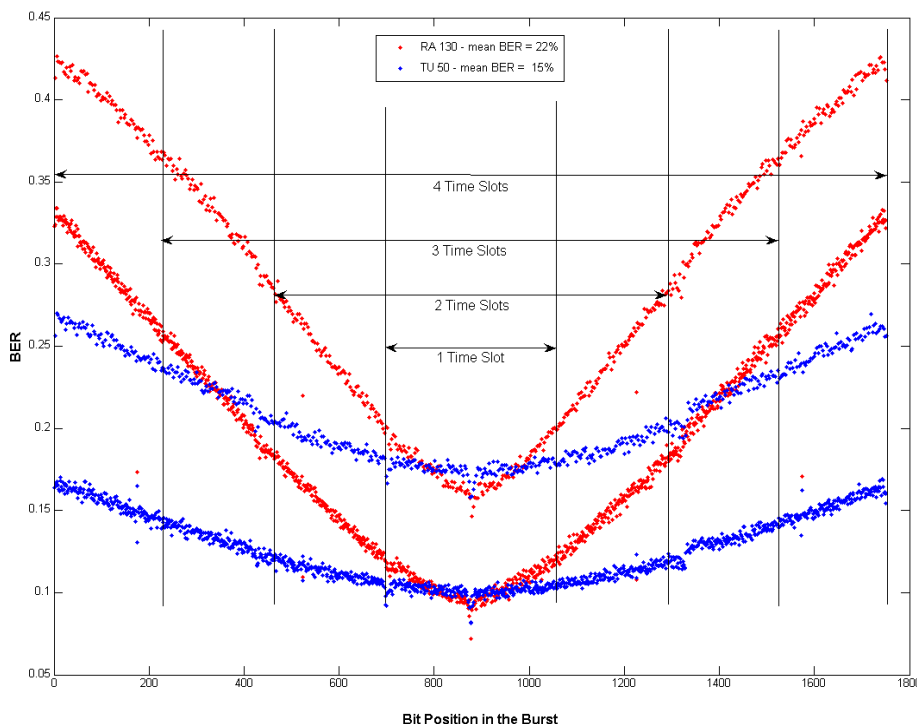
NOTE: Higher BER is experienced by every third bit in the 8 PSK symbol hence there are two distinct traces of BER profiles in the plot for each physical channel mode.

Figure 372: Bit error probability vs Position in the burst
(taken from the simulation of a 4 slot aggregated burst) - Cochannel interference

11.5.3   Relationship between performance penalty and aggregation size

11.5.3.1   Simulation Setting

The purpose of this subclause is to investigate the degradation structure of the new bursts.

The simulation is designed to have a 26-symbol training sequence in the middle of the aggregated burst, and 4 segments of symbols are placed on each side of the training sequence and 3 tail symbols on each end as shown in figure 373. The 4 segments correspond to the message symbols of the standard burst, 1st burst expansion, 2nd burst expansion, and 3rd burst expansion. The raw BER of the symmetric pairs of the symbol segments are collected. Name the pair closest to the training sequence the Segment-I and the pair that is 2nd closest to training sequence the Segment-II, and so on; giving us Segment-I, Segment-II, Segment-III, and Segment-IV, see figure 373.
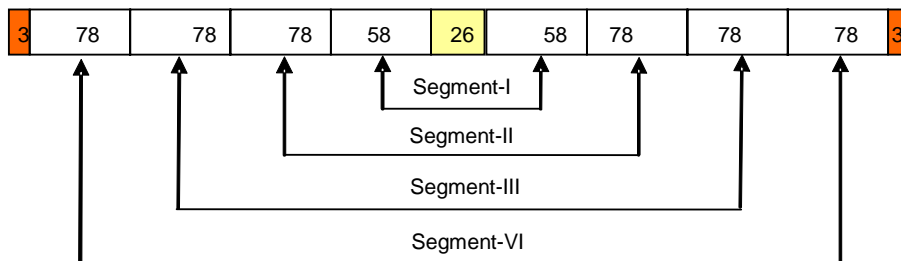
Figure 373: The burst structure used in the simulation analysis

11.5.3.2 Simulation Results and Analysis

The raw BER of the Segment-I, Segment-II, Segment-III, and Segment-IV are shown in figure 374.

The Segment-I performance can be considered as the performance of the standard burst. The equalizer is a well-known adaptive equalizer, which is per-survivor based adaptive RSSE. It is shown that the penalty accelerates as each legacy burst slot is added into the aggregated burst. On each step of the burst size expansion, the date rate increase of the expanded portion is (156-116)/116 = 34.5 %. The penalty of the expanded portion in difference levels of the expansion is given in table 205.
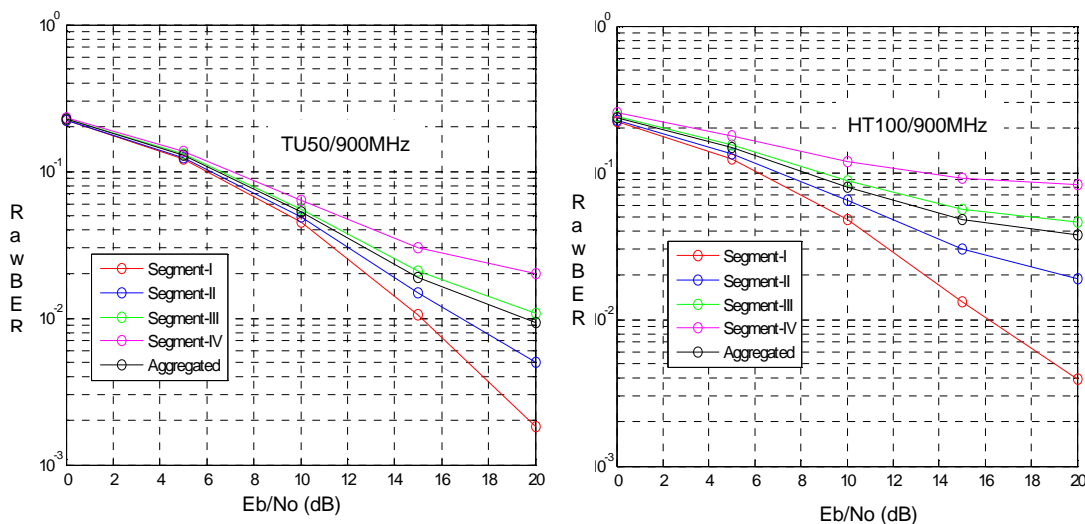
Figure 374: Raw BERs of Segment-I,II,II,IV, and aggregated burst

It is shown that the penalty accelerates as each legacy burst is added into the aggregated burst. The penalty will get worse for higher speed fading such as RA250. As the center frequency goes to 1 900 MHz, extra penalty can be expected. Although equalizer improvement can reduce the acceleration, the penalty structure will not be shifted dramatically. Thus as each legacy burst is added to the new burst, the value is diminishing, and it even could contribute negatively.

Table 205: Date rate increase on each level of expansion vs. its cost in TU50 and HT100

	1st expansion	2nd expansion	3rd expansion
Expand portion data rate increase	34.5 %	34.5 %	34.5 %
Penalty TU50@2%BER	1 dB	2.5 dB	7 dB
Penalty HT100@10%RBER	1 dB	2 dB	7 dB

The normalized goodputs of the different levels of aggregation are given in figure 375, which is defined as the product of the (1-RBER) multiplied by the ratio of number of information symbols to the total symbols sent.

It can be seen that 2-burst aggregation gives the most gain in terms of goodput. The value of expansion from 3-burst aggregation to 4-burst aggregation is minimal. Actually, for higher speed fading in 1 900 MHz, adding the 4th burst could contribute negatively.
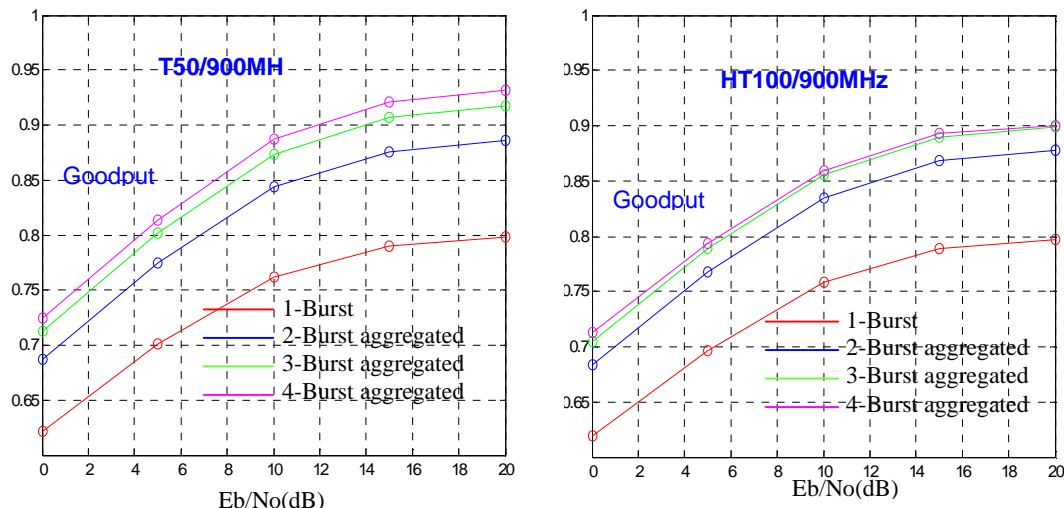
Figure 375: Goodput with different level of aggregation

It is important to point out that in interference limited cases, the penalty can be even worse since the variation of interferes across a standard burst boundary can be dramatic, which disturbs the equalizer tracking for the new burst structure.

11.6 New Burst Structures with Turbo Codes

According to the simulation results, even though the TSC is placed in the middle of the new burst, the BER performance of new burst structure will degrade under many scenarios, especially under faster fading channel. There are many ways to reduce the degradation, such as increasing the trellis size of the equalizer, using more frequently channel tracking algorithm or optimized channel tracking algorithm, but the degradation will still exist. The degraded BER performance will induce the degradation of upper layer BLER of channel decoding, so more powerful error corrective channel coding may be considered to use.

This paper presents performance on new defined coding schemes with turbo codes on new burst structure and some compatibility problems of new burst structure used in uplink.

11.6.1 BER Degradation of New Burst

The BER performance of aggregated new burst became worse. The performance degradation of 3 burst aggregation in co-channel interference condition is listed in tables 206 and 207.

Table 206: BER degradation of 3 burst aggregation compared to legacy burst, GMSK

Scenario		8 % BER	1 % BER
TU3iFH	900 MHz	0 dB	0 dB
TU50	900 MHz	0 dB	0.3 dB
TU50	1 800 MHz	0.3 dB	1.8 dB
RA250	900 MHz	1.5 dB	> 3 dB

Table 207: BER degradation of 3 burst aggregation compared to legacy burst, 8PSK

Scenario		8 % BER	1 % BER
TU3iFH	900 MHz	0 dB	0 dB
TU50	900 MHz	0 dB	0.5 dB
TU50	1 800 MHz	1.0 dB	6.5 dB
RA250	900 MHz	6 dB	> 10 dB

The equalizer here used is based on normal implementation complexity.

The coding scheme's BLER is sensitive to the BER, especially when higher coding rate. Very low level BER is needed to obtain peak data rate. Figures in table 1 and 2 show lager degradations at lower BER.

So more powerful error corrective channel coding may be used in upper layer when BER degradation can't be avoided.

11.6.2 New Coding schemes and Simulation

The target of GERAN evolution is to improve the data throughput. In [2], RLC aggregation is proposed to get more gains of data throughput, but the gains listed in the paper is the theoretical results. No proposals to get the gains are provided.

As the aggregated RLC block can provide the longer data block length before channel coding, so using turbo codes as channel coding become realistic. In this subclause, turbo codes is introduced in the aggregated RLC data block and LA and IR simulation results are provided based on new defined coding schemes.

11.6.2.1 Coding schemes

Refer to the current EGPRS uplink MCS coding schemes, new uplink coding schemes is defined in the simulation, listed in table 208. It is defined as the same data rate (per legacy burst) with legacy MCS. MB3MCS10 and MB3MCS11 are added to the coding schemes to reach peak data rate. In MB3MCS1 to MB3MCS9, the redundancy bit from burst aggregation and RLC aggregation are used as the protection bit in coding. Head length and coding schemes of new MCS type is the same with the legacy MCS in the simulation and it need further study.

Table 208: New defined coding schemes for 3 burst aggregation

Legacy MCS type	New MCS (aggregation of 3 burst)	data rate per legacy burst (kbps)	Interleave depth (bursts)	Data block per RLC
MCS1	MB3MCS1	8.8	4	1
MCS2	MB3MCS2	11.2	4	1
MCS3	MB3MCS3	14.8	4	1
MCS4	MB3MCS4	17.6	4	1
MCS5	MB3MCS5	22.4	4	1
MCS6	MB3MCS6	29.6	4	1
MCS7	MB3MCS7	44.8	4	2
MCS8	MB3MCS8	54.4	2	2
MCS9	MB3MSC9	59.2	2	2
-	MB3MCS10	69.8	2	2
-	MB3MCS11	82.2	2	2

11.6.2.2 Simulation setting

New burst of 3 aggregated legacy burst are considered in simulation and ideal LA (link adapt ion) and IR (incremental redundancy) assumed.

Scenarios:

- Co-channel interference.

Equalizer type:

- GMSK: MLSE + PSP (LMS).

- 8PSK: RSSE + PSP (LMS).

- The equalizer is not optimized and based on normal implementation complexity.

TSC position:

- In the middle of the new burst.

Turbo code:

- Take the turbo coding schemes and subsequent rate matching as it used in RAN [20].

- Max-log-map decoding algorithm used.

Curves are provided in four channels:

- TU3iFH: 900 MHz.

- TU50: 900 MHz.

- RA250: 900 MHz.

- TU50: 1 800 MHz.

11.6.2.3 Simulation results

The curves in figures 376 to 379 show data throughput vs. C/I of new defined MCS and standard MCS. Different gains of new defined MCS against standard MCS with different C/I can be seen in the figure. The CDF of C/I presented by TeliaSonera in [4] indicates very few occurrences of C/I above 22 dB. According to the C/I pdfi, average data throughput can be calculated, the average gains are listed as following.

Table 209: Average throughput gain of new defined MCS with Turbo codes

Channel Type		Gains of LA	Gains of IR
TU3iFH	900 MHz	37 %	36 %
TU50	900 MHz	34 %	33 %
TU50	1 800 MHz	19 %	20 %
RA250	900 MHz	-9 %	2 %

The overall gains in table 5 from [2] are listed here for comparison.

The figures in tables 209 and 210 show that the data throughput gains of new coding schemes with turbo codes are very close to the theoretical gains with aggregated formats at L1 and L2.

Table 210: Overall gain with aggregated formats at L1 and L2

Allocated Timeslots	Data symbols tx with legacy technique			Data symbols tx with new technique			Gain		
	MCS 1-4	**MCS 5-6**	**MCS 7-9**	**MCS 1-4**	**MCS 5-6**	**MCS 7-9**	**MCS 1-4**	**MCS 5-6**	**MCS 7-9**
3	1 128	1 232	1 208	1 626	1 660	1 652	44.1 %	34.7 %	36.8 %
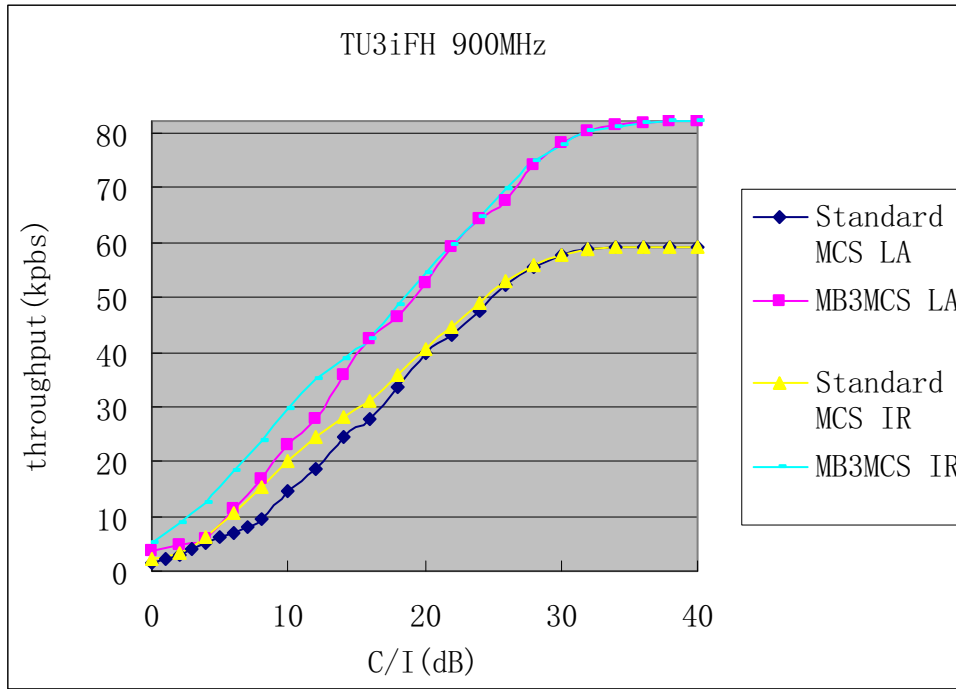
Figure 376: Throughput per standard burst under TU3iFH/900MHz
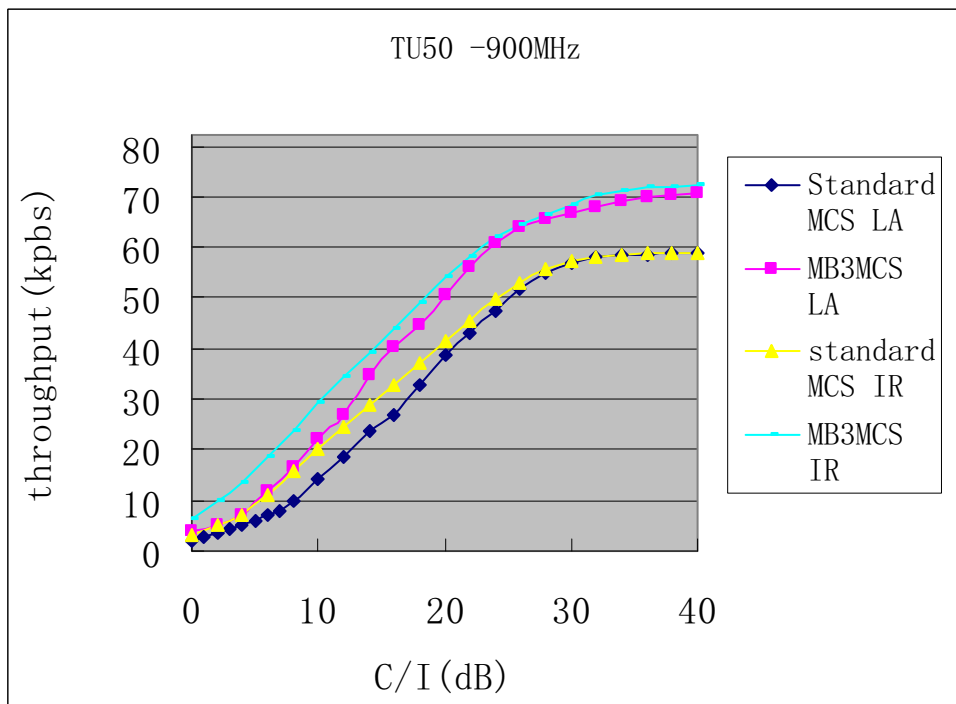
Figure 377: Throughput per standard burst under TU50/900MHz
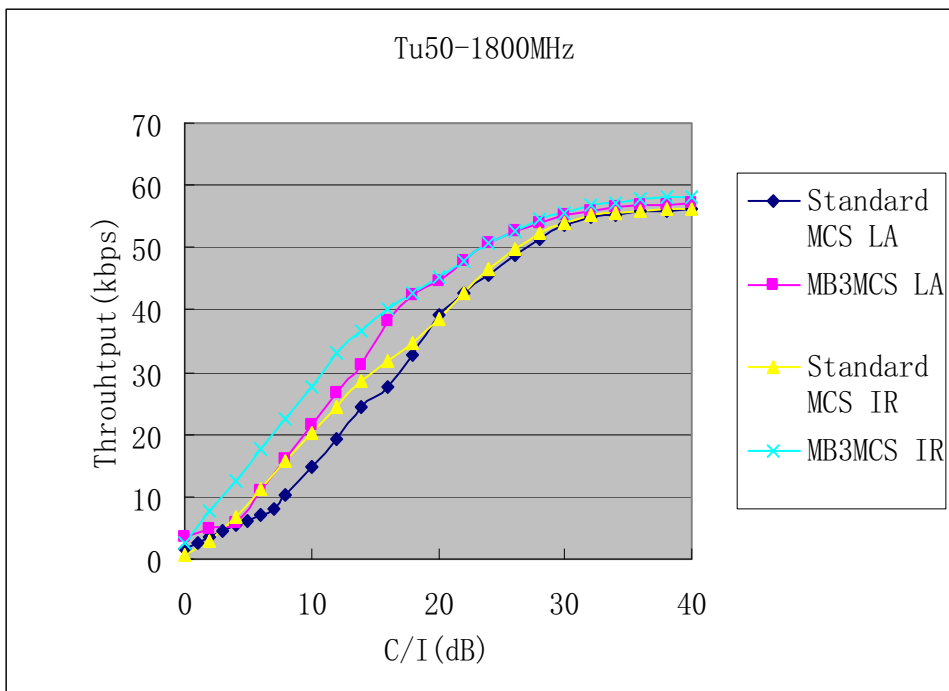
Figure 378: Throughput per standard burst under TU50/1800MHz
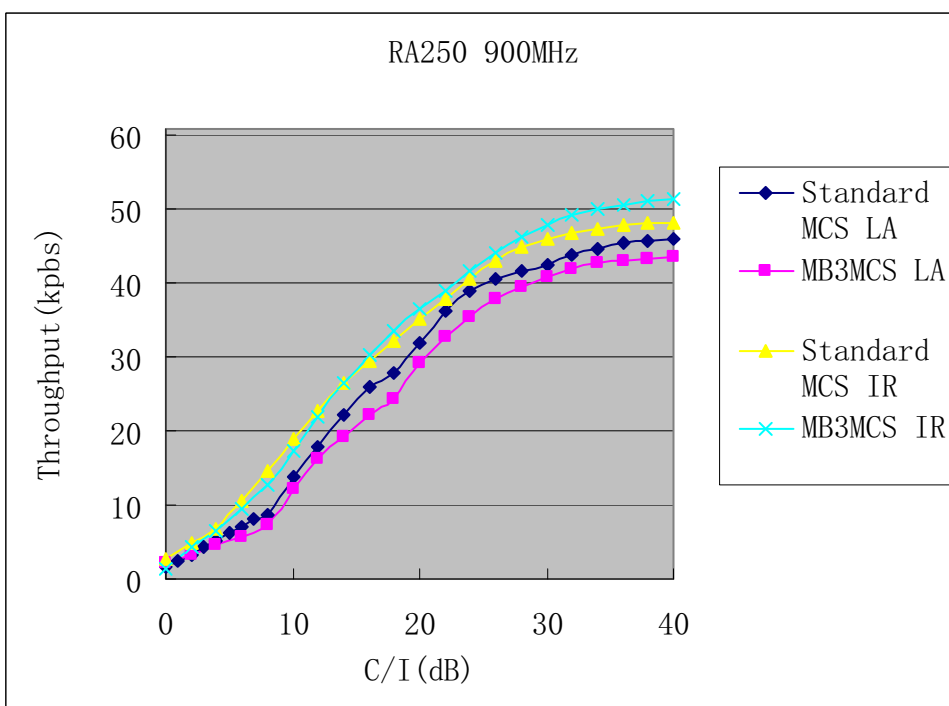
Figure 379: Throughput per standard burst under RA250/900MHz

11.6.3   Compatibility

Compatibility problems are reconsidered here.

11.6.3.1   Impact to the current frequency planning

Coexist with current frequency planning.

11.6.3.2 Multiplexing loss with legacy EGPRS

No loss in multiplexing with legacy EGPRS when used in uplink.

11.6.3.3 Impact to BTS

No hardware change needed. Turbo decoding can be implemented by software upgrade.

11.6.3.4 Applicable of DTM

Yes.

11.6.3.5 Applicable for the A/Gb mode interface

Yes.

11.6.3.6 Impact to the mobile station

For MS that already supports both GERAN and RAN, the existing Turbo coding capability can be re-used from RAN capability. Otherwise, the capability would need to be included.

11.7 Timeslot Aggregation for RTTI TBF and Link Performance

11.7.1 Introduction

Reduced TTI (RTTI) and Fast Ack/Nack Reporting (FANR) are accepted as effective enhancements to reduce latency [14], [15] and [16]. To get room for the FANR short bitmap, the coding schemes (convolution, puncturing and interleaving) of RLC data shall be modified due to the reduction of RLC data payload, or the RLC data code rate shall be increased. [17].

In this contribution, timeslot aggregation is introduced. A fat New Burst is formatted by aggregating the two uplink allocated timeslots of RTTI TBF and extra symbols are obtained. Some of the extra symbols are used to bear the short bitmap, thus the RLC data payload and its coding scheme can be maintained as before. The simulation results for the link performance of the legacy MCSs, RTTI + FANR and the New Burst + RTTI + FANR are also presented.

11.7.2 Timeslot aggregation for RTTI

At least two timeslots will be allocated to a RTTI TBF. If the two timeslots are consecutive, they can be aggregated to form a fat timeslot, thus can bear a fat burst. [18] That is, the radio blocks would still span two TDMA frames after aggregation, but would now consist of two "aggregated" bursts, instead of four ordinary bursts, as shown in figure 380.
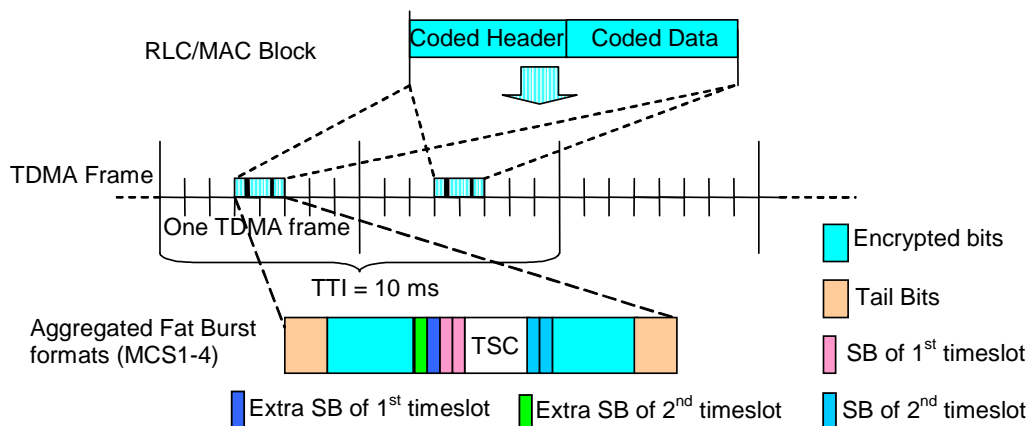
Figure 380: Normal Burst format after two timeslots aggregation for RTTI TBF

The stealing bits and extra stealing bits on both timeslots are preserved after aggregation because the block is composed of only two aggregated bursts. The preserved stealing bits and extra stealing bits are located next to the Training sequence as shown in figure 380. In case of MCS5-9, there will be no extra stealing bits. To improve the receiver performance, the TSC is located in the middle of new aggregated slot [19].

After the removal of Guard period and Tail Bits between the two bursts, and the Training Sequence of one burst, 40.25 extra symbols will be retrieved from each aggregated fat burst. Therefore, 80 or 240 extra bits will be retrieved for each block using MCS1-4 or MCS5-9 respectively.

The extra bits can be used to improve the throughput, or to reduce the RLC code rate, or to transfer the piggy-backed FANR bitmap.

In this contribution, some of the extra bits are used as FANR bitmap. For MCS1-4, all the 80 extra bits are used as the bitmap. For MCS 5-9, 120 bits are used, and the other 120 bits are used for redundancy or other purpose.

11.7.3   Definition of the new coding schemes

NBRTTI (New Burst RTTI) coding schemes are defined as shown in table 211.

Table 211: Definition of new coding schemes

		MCS-2 w/o bitmap	RTTI 2 w/ bitmap	NBRTTI 2 w bitmap	MCS-6 w/o bitmap	RTTI 6 w/ bitmap	NBRTTI 6 w/ bitmap
Raw	Header	31	31	31	37	37	37
	Bitmap	0	20	32[1]	0	20	32[1]
	Data	226	194	226	594	530	594
Coded (+CRCs)	Header	117	117	117	135	135	135
	Bitmap	0	78	120	0	78	120
	Data	732	636	732	1836	1644	1836
Punctured	Header	80	80	80	136	136	136
	Bitmap	0	54	80	0	78	120
	Data	372	318	372	1248	1170	1368(1248)[2]
Over head		12[3]	12[3]	12[3]	8[3]	8[3]	8[3]
Total		464	464	544	1392	1392	1632 [2]
NOTE 1: The 32 bit bitmap is independently coded (with an 8 bit CRC).							
NOTE 2: 120 bits out of 240 extra bits may be used as redundancy bits of RLC data, and in such case the puncturing scheme of RLC data shall be modified. In this contribution, the 120 bits are reserved as spare bits.							
NOTE 3: Over head refers to stealing flags (and extra stealing flags in case of MCS 1-4).							

11.7.4   Header and Data coding

The coding of RLC header and data is kept unchanged. Only the burst mapping is changed in order to allow Reduced TTI operation and aggregated bursts. The header and data bits are mapped on two aggregated fat bursts spanning two consecutive TDMA frames. The process is illustrated in the figure 380.

11.7.5   Bitmap coding

The bitmap payload has a length of 32 bits, thus is more robust or able to take more Ack/Nack information compared with 20 bits usually used for FANR. The coding of the bitmap is independent of RLC header and data.

To get a similar code rate as RLC header, 8 CRC bits are added to the bitmap payload. The method for generating the CRC and the convolutional coding polynomials of MCS header are reused here. For NBRTTI1-4, the convolutional coded bitmap data is uniformly punctured from 120 bits to 80 bits. For NBRTTI5-9, no bits are punctured from the coded bitmap. See table 211. After punctured, the bitmap is interleaved independently and mapped uniformly on the encryption bits. The method is described in the figure 381.
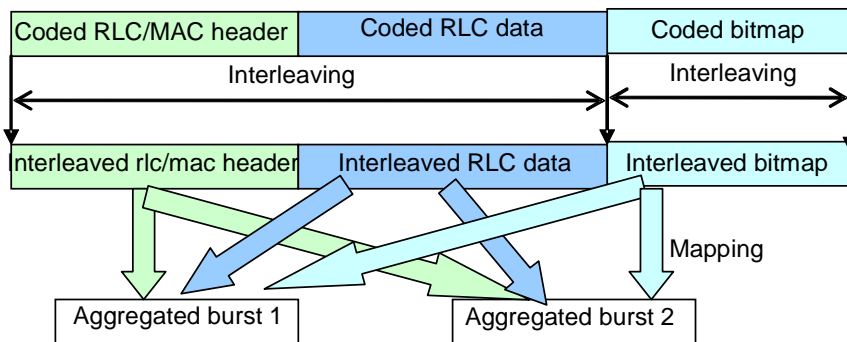
Figure 381: **Interleaving of NBRTTI type data**

11.7.6   Simulation results

Simulations are done for two types coding schemes (MCS-2-like and MCS-6-like) for TU3iFH and TU 50iFH channels for low band (GSM 900) and upper band (GSM 1800). Every type has three specific coding schemes: the standard MCS schemes, the RTTI type coding schemes assumed to have a 20-bit FANR bitmap, and the NBRTTI coding schemes assumed to have a 32-bit bitmap.

The idea is to have an insight of the performance achieved (e.g. higher throughput) through the NBRTTI coding schemes and the loss in the performance due to timeslot aggregation.

Figure 382 to 385 show the simulation results of the MCS-2-like coding schemes, including the data, header and the bitmap.
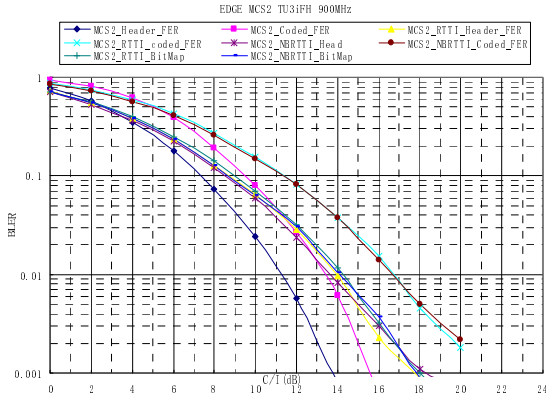
Figure 382: MCS2 like coding scheme - TU 3 ideal FH
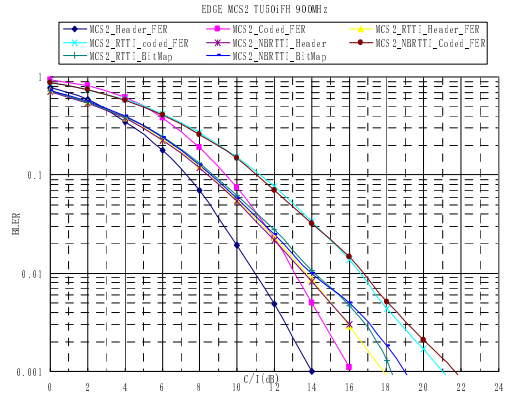
Figure 383: MCS 2 like coding scheme - TU 50 ideal FH
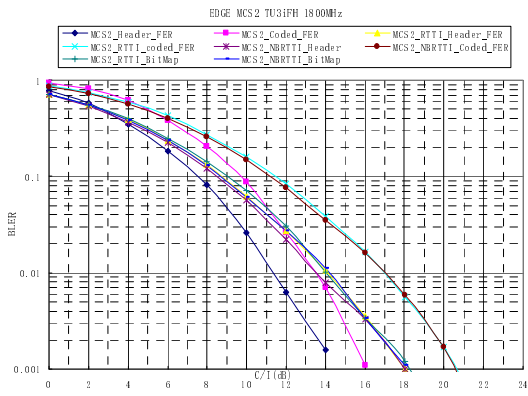
Figure 384 : MCS 2 like coding scheme - TU 3 ideal FH - GSM 1800
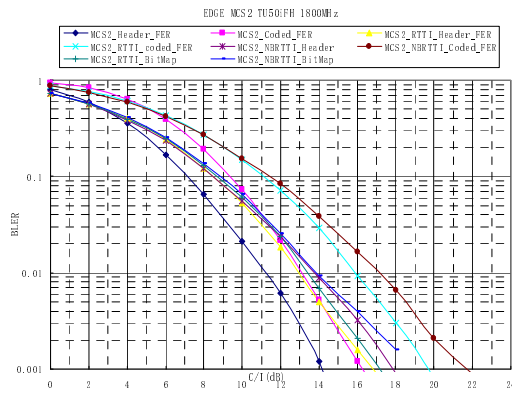
Figure 385: MCS 2 like coding scheme - TU 50 ideal FH - GSM 1800

Figure 386 to 389 show the simulation results of the MCS-6-like coding schemes, including the data, header and the bitmap.
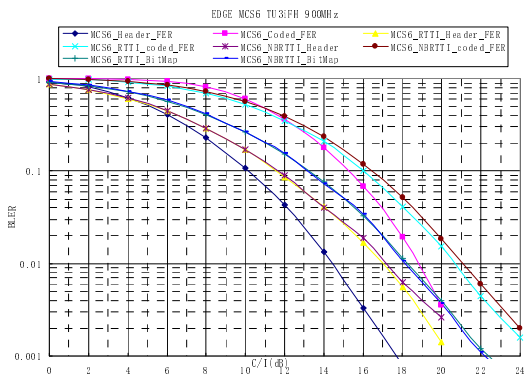
Figure 386: MCS 6 like coding scheme - TU 3 ideal FH
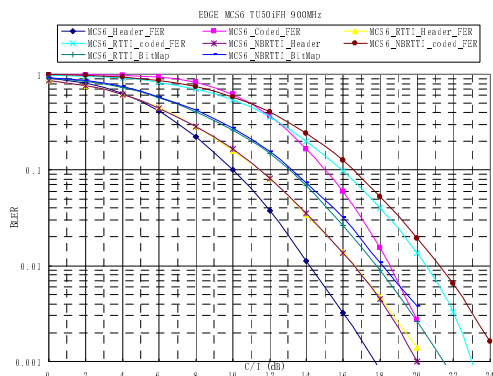
Figure 387: MCS 6 like coding scheme - TU 50 ideal FH
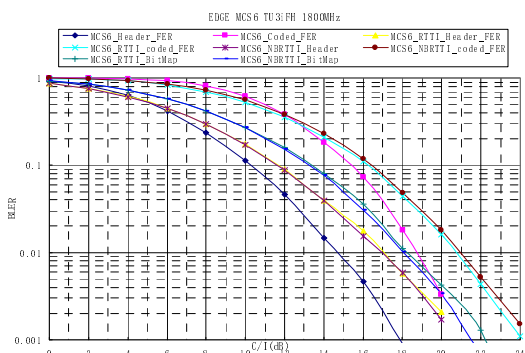
Figure 388: MCS 6 like coding scheme - TU 3 ideal FH - GSM 1800
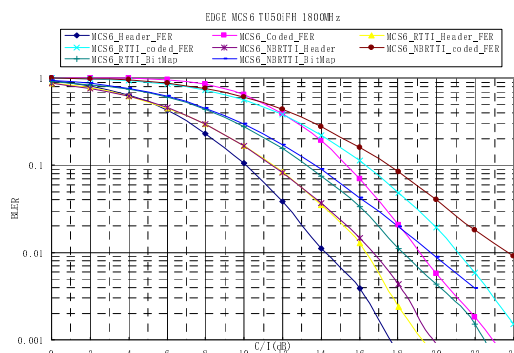
Figure 389: MCS 6 like coding scheme - TU 50 ideal FH - GSM 1800

Figure 390 and 391 show the throughput of the MCS-6-like coding schemes for low and upper band respectively.
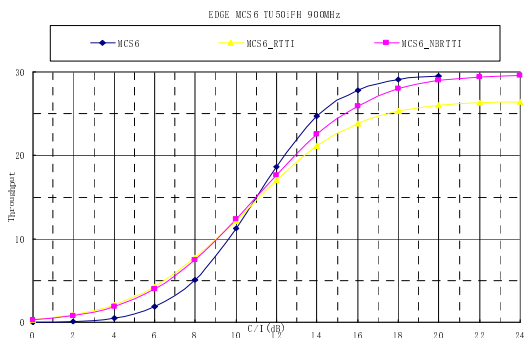
Figure 390: Throughput of MCS 6 like coding scheme - TU 50 ideal FH
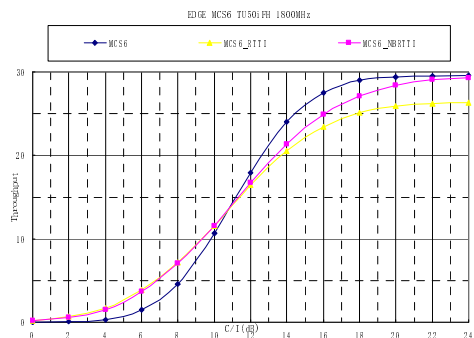
Figure 391:Throughput of MCS 6 like coding scheme - TU 50 ideal FH - GSM 1800

11.7 Impacts to the Mobile Station

From the point of view of the transmitter, implementation aspects may be simplified by the usage of the 157/156/156/156 transmission option, as referenced in subclause 5.7 of 3GPP TS 45.010 (see note), as this would remove the complication introduced by the 0.25 bit.

NOTE.   "Optionally, the BTS may use a timeslot length of 157 symbol periods on timeslots with TN = 0 and 4, and 156 symbol periods on timeslots with TN = 1, 2, 3, 5, 6, 7, rather than 156,25 symbol periods on all timeslots".

From the point of view of the receiver, the removal of the TSC will require enhanced receiver and equalization capabilities (for example channel tracking equalization). Resilience to higher Doppler and phase rotation will have to be investigated in particular for the high-speed case.

In an interference-limited scenario, the interference profile is likely to change within an aggregated timeslot (which would be subject to the interference from multiple independent bursts). This is not different from what interference cancellation algorithms (e.g. SAIC) already have to cope with today at the timeslot level in an asynchronous network. In general, we note that receiver capabilities in the mobile station have improved largely with DARP Phase 1.

From the point of view of the protocol stack on the transmission side, the proposal introduces some dependencies between the MAC layer and the RLC layer, as the RLC has to be aware of the ongoing timeslot aggregation.

11.8   Impacts to the BSS

From the point of view of transmission and reception, the impact is the same as in subclause 11.6.

Further, the BSS has to be able to handle received timeslots in a joint manner.

11.9   Impacts to the Core Network

The core network impact is minimal, e.g. indication of feature support.

11.10   Impacts to the Specification

A preliminary assessment of impacted specification follows. A more complete assessment can be done depending on whether the full set, or a subset, of components is pursued.

Table 212: Impacted 3GPP specifications

Specification	Description
3GPP TS 43.064	Overall description of the GPRS radio interface
3GPP TS 45.001	Physical Layer on the radio path: general description
3GPP TS 45.002	Multiplexing and multiple access on the radio path
3GPP TS 45.003	Channel Coding
3GPP TS 45.005	Radio transmission and reception
3GPP TS 44.018	Radio Resource Control (RRC) protocol
3GPP TS 44.060	Radio Link Control/Medium Access Control (RLC/MAC) protocol
3GPP TS 24.008	Mobile radio interface Layer 3 specification; Core network protocols; Stage 3 (Release 7)
3GPP TS 51.010	Mobile Station (MS) conformance specification

11.11   References

[1]   T. S. Rappaport: "Wireless Communications: Principles and Practice", Second Edition, Prentice Hall PTR, 2002.

[2]   3GPP Organizational Partners: "Radio transmission and reception", TS 05.05 V8.10.0, 2001/06.

[3]   R. Raheli, A. Polydoros and C. Tzou, "Per-survivor processing: a general approach to MLSE in uncertain environments", IEEE Trans. Commun., vol. 43, No. 2/3/4, pp. 354-364, Feb./Mar./Apr. 1995.

[4]   TeliaSonera: "Video telephony over GERAN - C/I cdf in real NW", GP-042355, 3GPP TSG GERAN 22, Nov 8-11, 2004.

[5] GP-061519" "New WID: Latency Reductions", Ericsson et al, GERAN#30.

[6] GP-061520: "New WID: Improved Ack/Nack reporting", Ericsson et al, GERAN#30.

[7] GP-061521: "New WID: Reduced TTI", Ericsson et al, GERAN#30.

[8] GP-061178: "Initial Link level results for RTTI coding schemes", Siemens, GERAN#30.

[9] GP-061570: "Feasibility study for evolved GSM/EDGE Radio Access Network (GERAN) (Release 7)", TR 45.912 (V1.1.0), GERAN#31.

[10] GP-060112: "The Influence of TSC Position in the New Slot on the Link Performance", Huawei, GERAN#28.

[11] 3GPP Organizational Partners: "Multiplexing and channel coding (FDD)", 3GPP TS 25.212 (V6.7.0), 2005-12.

12 Adaptation between mobile station receiver diversity and dual-carrier

12.1 Introduction

Within the context of the GERAN Physical Layer evolution, where one of the prime targets is a smooth evolutionary path, two proposed candidates are receive diversity (see clause 6), and dual/multi-carrier (see clause 7).

This Subclause deals with a proposed technique, referred to as Capabilities Switching, which is applicable if the two aforementioned candidates are introduced in the GERAN specification.

12.2 Concept description

The underlying assumption of the proposal outlined in this subclause is that, if and when Receive Diversity (RxDiv) and Multi-carrier GERAN (MC) are introduced in the specification, it makes sense to allow the existence of a class of mobiles operating with the following two constraints.

  a) RxDiv performances are required only when the terminal acts in single-carrier mode.

  b) Not more than two carriers are supported by the terminal when in Multi-carrier mode.

The existence of such a class of mobiles should be seen as the enabler for a faster and gradual implementation and introduction of the corresponding features. It shall not be seen as a limiting factor for further evolution steps.

The two constraints mentioned above can and should be exploited by the network to better control the performance of the terminals. This is possible by allowing the network to command the terminal whether to act in receive diversity (RxDiv) mode or in Dual/Multi-carrier mode (MC). In this context, the RxDiv mode implies that both antennas are tuned to the same carrier, and the MC mode implies that each antenna is tuned to a separate carrier.

  NOTE. The idea is in fact extensible to n antennas and n carriers.

The components of the idea are as follows:

  - The MS signals its capabilities are per point a) and b) above, associated with its switching capability.

  - By default, the terminal exploits the RxDiv capability:

    - Therefore, both antennas will be tuned to the same carrier and the MS performance will be increased as a consequence.

  - When appropriate, the network may signal to the MS to switch to the multi-carrier mode:

    - The signalling could be done in the assignment phase (e.g. in the EGPRS Packet Downlink Assignment), i.e. per MS.

- Consequently, the MS leaves the first antenna tuned to the first carrier, and tunes the second antenna to the second carrier.

- The network can switch between the two modes to trade-off capacity vs peak data rate.
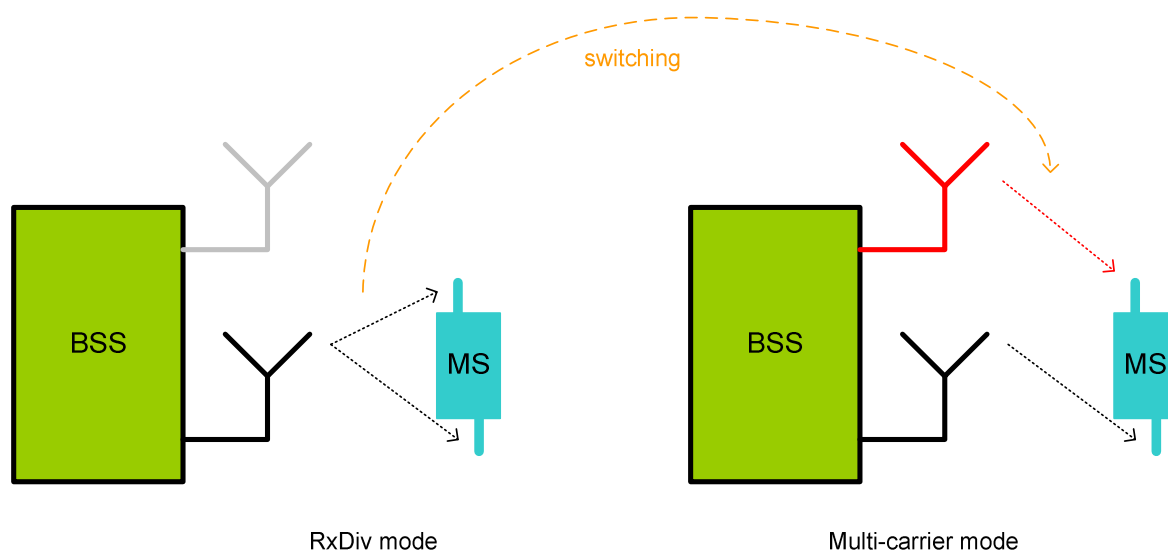
Figure 392: RxDiv - Multi-carrier switching

12.3 Performance Characterization

The performance of Capability Switching is the combination of the respective performances of Receive Diversity (see clause 6) and Dual/Multi-carrier (see clause 7). The combination depends on how the adaptation between the two modes is performed.

12.4 Impacts to the Mobile Station

The MS will have to support switching commands between the two modes, and will have to indicate the switching capability.

12.5 Impacts to the BSS

The BSS may have to add the switching option to its RRM algorithms.

12.6 Impacts to the Core Network

The CN will have support the signalling of the switching capability support.

12.7 Impacts to the Specification

The impact to specification is considered to be minimal, and depending on the specification impact of Receive Diversity and Dual/Multi-carrier.

13 Enhancements to resource allocation

13.1 Introduction

There are a number of allocation schemes defined for GPRS, including fixed allocation, Dynamic Allocation (DA) and Extended Dynamic Allocation (EDA). Of these EDA is the most capable since it permits the network to vary the weighting between transmit/receive slots from maximum downlink weighting to maximum uplink weighting. The other dynamic allocation scheme, namely DA, requires the mobile to monitor at least as many downlink slots as it transmits on the uplink, so using DA it cannot transmit more uplink slots than it can monitor downlink slots, even though the mobile may have hardware capable of such behaviour. The method of allocating uplink resources in EDA is explained in 3GPP TS 44.060, subclause 8.1.1.2.1.

The example below (figure 393) illustrates that sometimes EDA is inefficient at sharing uplink resources between mobiles. In this illustration the network needs to share allocated slots between two class 12 mobiles, MS1 and MS2, both of which are capable of using up to 4 slots in the downlink or uplink (the example applies equally to both downlink and uplink). Also, for purposes of illustration, we have assumed that only slots 0 to 5 are available for allocation (so we assume that slots 6 and 7 are being used for other mobiles).

There is a limitation of EDA that limits its efficiency when sharing resources between different mobiles. The limitation is that dynamic allocation can only grow "backwards", i.e. if the potentially transmitted slots are in the range $[N, M]$, where $0 \le N \le M \le 7$, then for slot k $(N \le k \le M)$ to be transmitted, all higher numbered slots (i.e. slots $k+1, k+2,... M$) must also be transmitted.

In the example, when using EDA, a 'fair' allocation might be to give MS2 an allocation starting at slot 0, and MS1 an allocation starting at slot 2. This is shown in the top illustration in figure 393. With such an allocation it is certain the MS2 can transmit at least 2 timeslots without blocking or being blocked by MS1. Also, both MS's can potentially transmit 4 slots, which is their maximum capability since they are multislot class 12 mobiles. But note that if MS2 transmits even one slot, then MS1 cannot transmit more then 2 slots without mutual blocking; this is an inefficiency of EDA.

In the second part of the illustration the new concept is shown, Back to Back Dynamic Allocation (B^2DA). The new approach is that allocation can proceed in an upward direction for some mobiles, but continue in the downward direction for other mobiles as in the existing standards.

It is easily seen that using this approach the likelihood of one mobile blocking the transmissions of the other is reduced; indeed in the example shown, provided both mobiles have three or less slots allocated they cannot block each other. However the number of timeslots required has not been increased; all that is done is to use them more efficiently.

Example for Class 12 Mobile
Note: illustration assumes slots 0-5 are available, slots 6, 7 used for other purposes. This example applies equally to uplink or downlink
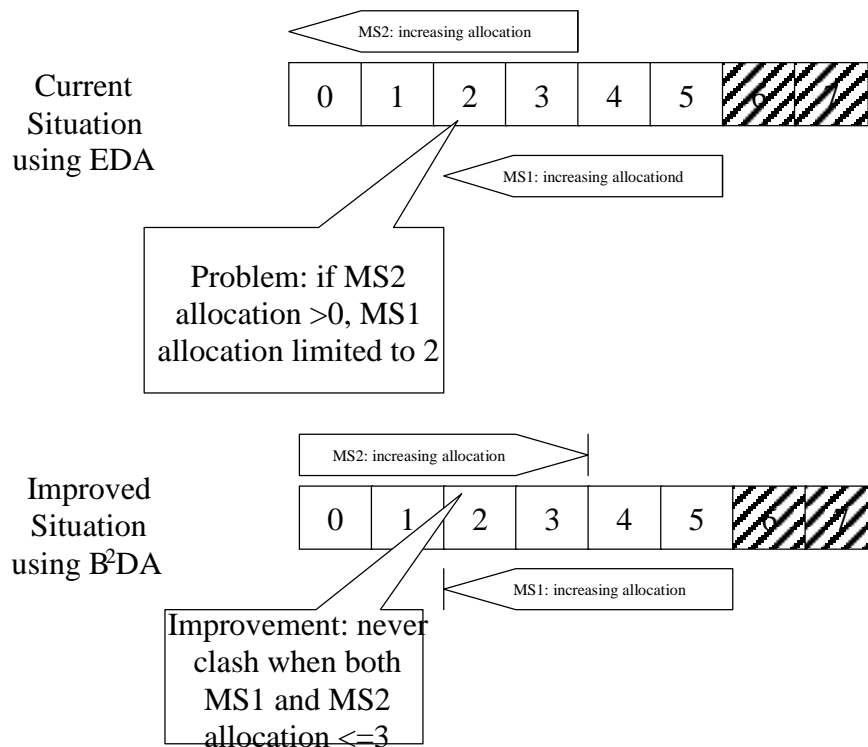
Figure 393: Advantage of B²DA operation

Clearly if this were adopted by the 3GPP standards a number of other issues would need to be addressed, for example mapping of USF to allocated timeslots (analogous to Special Extended Dynamic Allocation) and compatibility issues.

Note that this example assumes that resources are restricted to some degree and timeslot sharing between two mobiles is needed. If resources are not scarce and TS6 and 7 are available an alternative would be to exclusively allocate TS 6 and 7 to MS1. The general idea of GPRS is to allow sharing of limited resources as efficiently as possible between multiple mobile stations.

13.1.1   Benefits of the Solution

The proposed improvement will increase the statistical multiplexing efficiency of resource allocation on both the uplink and downlink during bursty packet data flows. It therefore constitutes a potential improvement to the 3GPP GPRS standards, enabling more efficient use of spectrum resources.

The benefit is likely to be greatest when a number of mobiles potentially have simultaneous requirements for dynamically allocated uplink resources, and uplink resources are limited due to the volume of traffic. An example situation might be if two mobiles are simultaneously requesting a web page download, or simultaneously servicing requests for data upload.

13.1.2   Details of Allocation Rule

For B2DA a new rule of allocation and USF monitoring is proposed as follows which is illustrated below:

"The mobile station shall monitor the lowest numbered assigned PDCH. If the mobile station detects an assigned USF value for an assigned PDCH on the lowest numbered PDCH, the mobile station shall transmit RLC/MAC blocks on all assigned PDCHs apart from the higher numbered assigned PDCHs."

In the illustration below, 4 uplink PDCHs are assigned, from slot 0 to slot 3. Therefore in this example the 'lowest numbered assigned PDCH' is 0 and the highest numbered assigned PDCH is 3. In order to distinguish the different allocations, different USF values may be used.

DL back/ UL forward allocation for a single class 12 mobile (B2DA)= assigment R1 T4
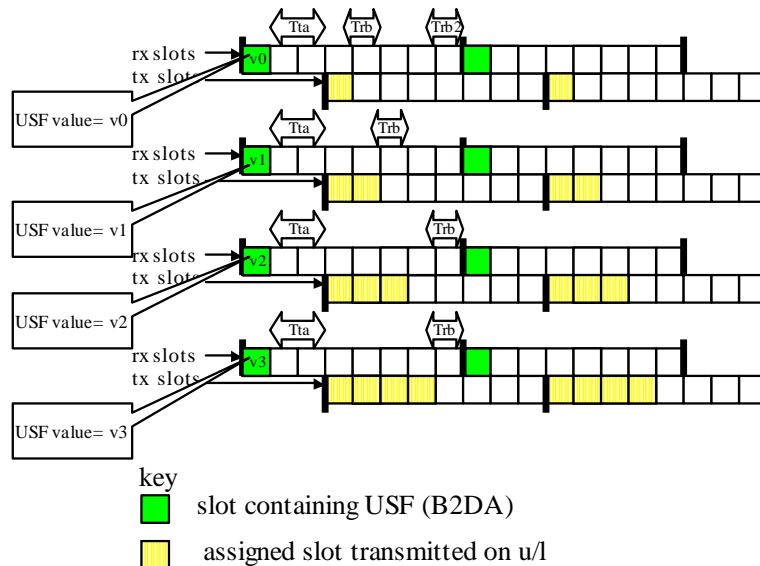
Figure 394: Illustration of B²DA allocation

Note that different USF values used to allow changing of dynamic allocations could reduce the multiplexing flexibility.

13.2 USF and Timeslot Resources

A combination of USF and timeslot can be considered as a resource. There are 7 USF values for allocation to each mobile station on each timeslot, hence there are 56 USF-TS resources available for sharing across various mobile stations. Both Dynamic Allocation and Extended Dynamic Allocation schemes use N USF-TS resources, where N is the number of uplink timeslots assigned to the mobile stations. The situation is different with B²DA.

In the example in figure 394, the USF values (v0-v3) for all assigned timeslots are transmitted on the lowest numbered assigned timeslots. It is proposed that either:

1) the value USF=FREE would be transmitted on the other timeslots allocated to the B²DA mobile, to prevent other mobiles using the uplink on those timeslots; or

2) some other USF value that is not significant to any other mobile could be transmitted (there are 7 such possible values apart from USF=FREE, and it is unlikely that 7 mobiles would multiplex onto one timeslot).

In summary, the B²DA mobile makes use of $2*N-1$ USF-TN resources, N of which are used exclusively for signalling allocation on the downlink on the lowest numbered assigned timeslot and $N-1$ for preventing other mobiles using the allocation on the remaining timeslots: . In the example in figure 394, The USF values (v0-v3) are available and can be transmitted and used as normal by another mobile on timeslots other than slot 0 (the lowest numbered timeslot assigned to the B²DA mobile).

With B²DA the USF-TN resources are concentrated on lowest numbered assigned timeslot and nearly twice the USF values are required. This may be considered a restriction but the advantages out weigh the disadvantages. In any case, with some other multislot class mobile stations it could be possible for the MS to monitor the lowest two assigned timeslots for USF, allowing the USF-TN resources to be distributed on two timeslots; this is for further study.

13.2.1 Co-existence with existing allocation schemes

In order that uplink resources can be allocated using dynamic allocation via the USF, two conditions must apply:

- the uplink resources are not also used by another mobile (since only one mobile can transmit on a given slot);

- the downlink slot on which the USF requires to be transmitted, in order to allocate the desired uplink resources, is not required to transmit the USF for another mobile.

In the following it is shown that B^{2}DA and EDA can co-exist and produce performance gains compared with homogenous allocations just using EDA, although some combinations are shown not to be possible. The following table shows possible configurations, where two mobiles are sharing slots 2 and 3 with timeslots 0, 1, 4 and 5 assigned to mobile 1 or mobile 2. In fact, the following combinations are possible, by combining EDA and B^{2}DA.

Table 213: showing permissible combinations of tx slots when two mobiles co-exist, "mobile 1" using EDA and "mobile 2" using B^{2}DA

No. of tx slots for mobile 2 (B^{2}DA) / Number of tx slots for mobile 1 (EDA)	0	1	2	3	4
0	Yes [-][-]	Yes [-][5]	Yes [-][4,5]	Yes [-][3,4,5]	Yes [-][2,3,4,5]
1	Yes [0][-]	Yes [0][5]	Yes [0][4,5]	Yes [0][3,4,5]	Yes [0][2,3,4,5]
2	**Yes [0,1][-]**	**Yes [0,1][5]**	Yes [0,1][4,5]	Yes [0,1][3,4,5]	Yes [0,1][2,3,4,5]
3	Yes [0,1,2][-]	Yes [0,1,2][5]	Yes [0,1,2][4,5]	Yes [0,1,2][3,4,5]	no
4	Yes [0,1,2,3][-]	Yes [0,1,2,3][5]	Yes [0,1,2,3][4,5]	no	no
Key: The cells show if configuration is possible and which timeslots are used by which mobile; [List of TS used by MS2][List of TS used by MS1].					

Note that very efficient uplink allocation is possible: specifically either one of them can transmit 4 slots, while the other is still able to transmit 2 slots. This is not possible in the EDA example allocating the same number of timeslots.

However, if EDA can only be combined with EDA, then only the following combinations are possible. As can be seen, if mobile 1 transmits 3 or more slots, mobile 2 cannot transmit any slots, and if mobile 2 transmits any slot, mobile 1 cannot transmit more than 2 slots.

**Table 214: permissible combinations of tx slots when two mobiles co-exist,
"mobile 1" using EDA and "mobile 2" using EDA**

No. of tx slots for mobile 2 (EDA) \ Number of tx slots for mobile 1 (EDA)	0	1	2	3	4
0	Yes [-][-]	Yes [-][5]	Yes [-][4,5]	Yes [-][3,4,5]	Yes [-][2,3,4,5]
1	Yes [3][-]	Yes [3][5]	Yes [3][4,5]	no (see note)	no
2	Yes [2,3][-]	Yes [2,3][5]	Yes [2,3][4,5]	no	no
3	Yes [1,2,3][-]	Yes [1,2,3][5]	Yes [1,2,3][4,5]	no	no
4	Yes [0,1,2,3][-]	Yes [0,1,2,3,4][5]	Yes [0,1,2,3,4][4,5]	no	no

NOTE. In these cases uplink slot 3 required by both MS1 and MS2.

In conclusion, by suitable combinations with EDA, the use of B^{2}DA can provide superior sharing of the uplink than can be achieved with homogeneous EDA allocation schemes.

13.3 Modelling Assumptions and Requirements

The proposal is likely to be beneficial when a number of users are employing data oriented services based on GPRS.

In order to quantify the benefits of the proposal the following modelling assumptions require to be specified:

- Modelling assumptions of traffic activity factors for uplink data services over GPRS. Note that detailed assumptions for uplink data traffic model parameters can be found in [1].

13.3.1 Illustration

In the following four scenarios are provided to show the potential use and advantages of B^{2}DA. The following is assumed in all cases.

- 6 slots are available for 2 mobiles.

- Both are sending variable rate encoded video data at 15 frames per sec (60 ms rate) with a video frame timing offset of 20 ms.

- Assume that the data rate is dimensioned for ~80 % average loading, i.e. 7 RLC blocks per video frame.

Scenario 1 shows that when data rates are fixed, resource sharing via EDA or B^{2}DA does not confer an advantage. Scenarios 2 and 3 show that resource sharing using EDA confers an advantage in the presence of variable data rates. Scenario 4 shows that B^{2}DA confers an even greater advantage.

Scenario 1: This illustrates the case where there is no sharing of resources, and no fluctuations in data rate.

The network assigns 3 slots to MS1, 3 slots to MS2, and the USF constantly allows transmission in both cases (the 'spare' blocks are transmitted with repeated data). As can be seen, there is a constant delay from 'frame available' to 'frame transmitted' is 60 ms.

Note that worst case delay from 'frame available' to 'frame transmitted' is 60 ms. In this case B2DA does not provide any additional advantage compared with EDA.
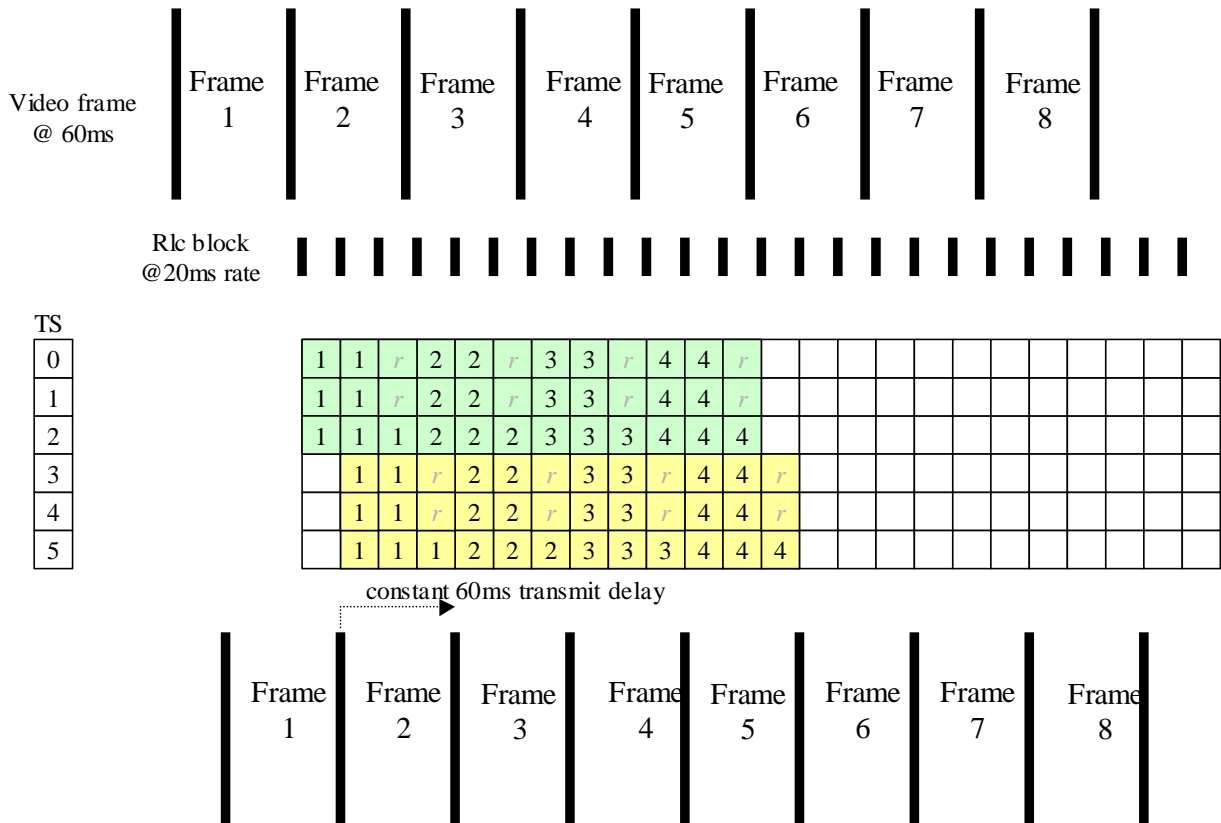
Note on terminology: blocks transmitted by MS1 shown in green, MS2 in yellow.

The number in the block indicates which video frame the block belongs to.

Repeated blocks (to fill up spare allocation) are marked "*r*"

Figure 395: Scenario 1: No resource sharing, constant data rate

Scenario 2: The resource allocation is identical to scenario 1, but this scenario shows the consequence of MS 2 wanting to send two 200 % 'overlong frames' in succession, i.e. two successive video frames requiring 21 RLC blocks each. After this, average length frames are sent.

In this example the transmit delay is increased to 220ms. In scenario 3, it will be shown how dynamic allocation improves this.

Note that the value of the Countdown Variable CV is shown for illustrative purposes.
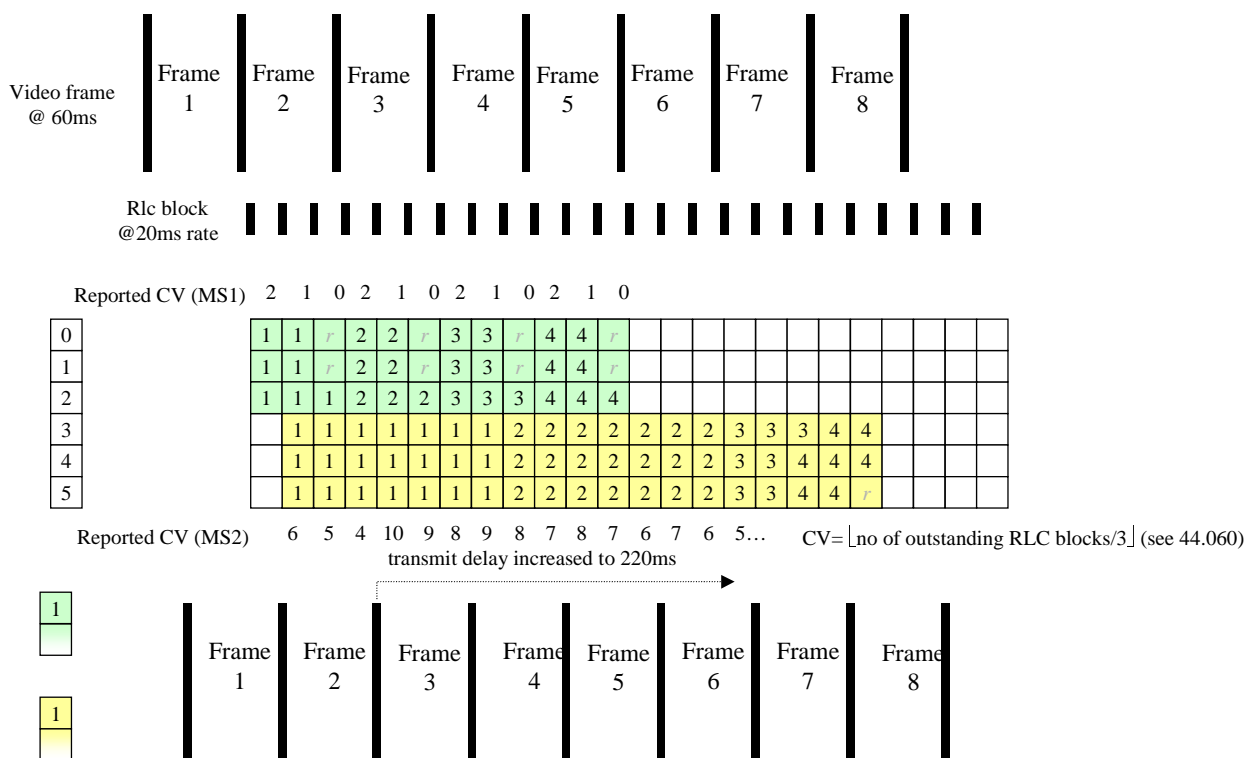
Figure 396: Scenario 2: No resource sharing, sudden data rate peak for MS2

Scenario 3: In this scenario there is the same data rate peak as scenario 2, (MS 2 wanting to send two 200 % 'overlong frames' in succession), but resources are shared using EDA. It is seen that there is some improvement regarding the peak transmit delay for MS2, but MS1 is severely impacted (in Scenario 4 this problem is solved by using B^2DA).

This scenario shows how: EDA can improve the maximum delay to MS2. It assumes uneven assignment, i.e. MS1 assigned slots 0 to 2 using EDA, and MS2 is assigned slots 2 to 5 using EDA (this allows 3-3 split without MS1 being blocked by MS2).

The CV is read by network and allocation provided to after a delay of 2 Radio blocks (i.e. 1 block for BS to decode the CV, 1 block to transmit USF corresponding to the subsequent block). The assumed network policy is to increase allocation of MS2 to 4 slots whenever CV≥5 (but with above time delay of 2 Radio blocks).

Then by using this scheme, we reduce the max delay of MS2 to 180 ms (down from 220 ms). However, the maximum delay of MS1 is severely impacted and is increased to 200 ms (from 80 ms).

Video frame @ 60ms

Frame 1 | Frame 2 | Frame 3 | Frame 4 | Frame 5 | Frame 6 | Frame 7 | Frame 8

Rlc block @20ms rate

frame 3 transmit delay of 200ms

0	1	1	r	2		2	r					3		3	3	4	r	
1	1	1	r	2		2	r					3		3	4	4	4	
2	1	1	1	2	1	2	2	1	1	2	2	2	3	3	3	4	4	4
3		1	1	1	1	1	1	2	2	2	2	2	2	3	3	4	4	r
4		1	1	1	1	1	1	2	2	2	2	2	2	3	3	4	4	r
5		1	1	1	1	1	1	2	2	2	2	2	2	3	3	4	4	4

MS2 Reported CV   5   4   3   8   7   6   6   5   4   5   4   3   4   3   2

frame 2 transmit delay of 180 ms

Arrows indicate blocks where allocation is increased due to reported value of CV

1

Frame 1 | Frame 2 | Frame 3 | Frame 4 | Frame 5 | Frame 6 | Frame 7 | Frame 8

1

Figure 397: Scenario 3:EDA, sudden data rate peak for MS2

Scenario 4: This shows the same data rate peak as scenarios 2 and 3, (MS 2 wanting to send two 200 % 'overlong frames' in succession), but resources are shared using B^{2}DA. It is seen that this gives the most improvement in the peak transmit delay. In this case the peak transmit delay for MS2 is 180 ms (identical with scenario 3), and the peak delay for MS1 is only 80 ms (considerably less than scenario 3).
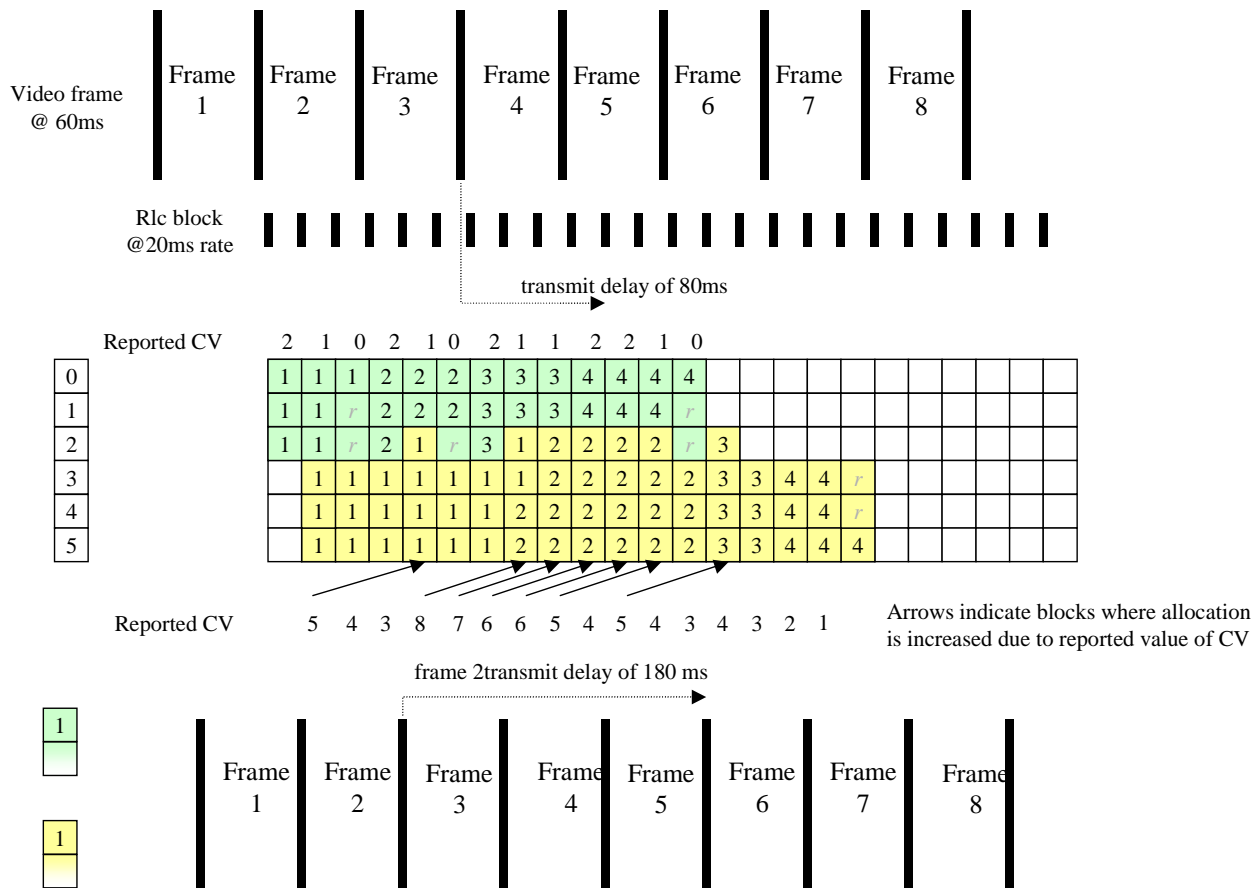
Figure 398: Scenario 4: B²DA, sudden data rate peak for MS2

Conclusion: The above scenarios show how B²DA can provide a performance benefit in the presence of fluctuating data rates.

13.4   Performance Characterization

Since a video stream is isochronous there is a "hard" deadline for every video frame by which time it must have been transmitted; any later and it becomes a missing frame in the video output. According to [2] the number of erased frames must be limited to at most 2 %, but the delay is also a key component of the QoS. In this analysis we assume the only reason for packet loss is excess transmit buffer delay; if the frame spends too long in the transmit buffer, it is thrown away. Provided the data is sent in acknowledged mode this is a realistic model.

The following figure is a typical extract from the 10 hour simulation sequence of two mobile stations transmitting MPEG4 data. For illustrative purposes it was assumed that two mobiles (MS1 and MS2) were sharing six available slots per radio block, as illustrated in figure 393. MS1 and MS2 were supplied with independent video sources and these were transmitted using both the EDA and the B²DA schemes to enable direct comparison. The coding scheme selected was MCS-1. The MPEG4 video source was scaled to represent the bits per video frame that would typically be found with QCIF video and streamed at a rate of 30 frames per second. For both EDA and B²DA, the allocation was identical (MS2 slots 0 to 2, MS1 slots 2 to 5). If MS2 CV was ≥ 5, and MS2 CV> MS1 CV, then allocation of MS2 was increased to 4 slots.

To assist comparison of EDA and B²DA, a trace of the number of pending RLC blocks in the uplink transmit buffer is shown for MS1 in figure 399. Similarly figure 400 shows the data for MS2. It can be seen from these results that B²DA gives a useful reduction in transmission delays when peak loads occur.
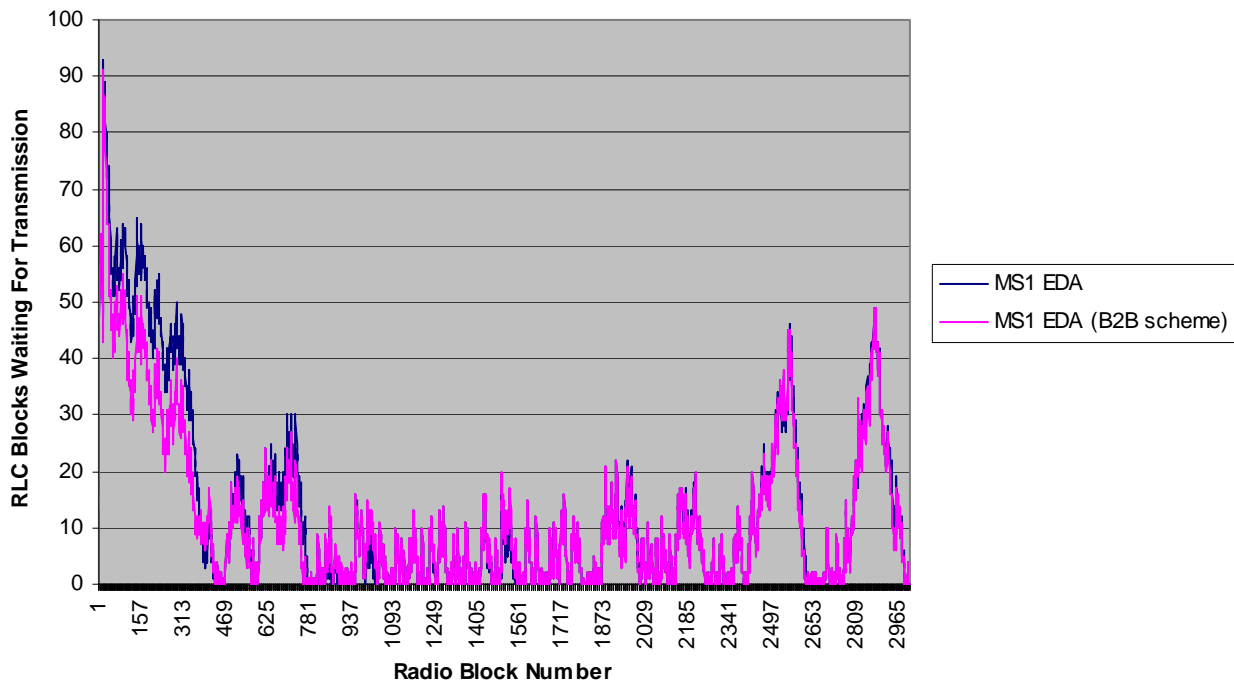
Figure 399: Trace of Uplink transmit buffer length for MS1s
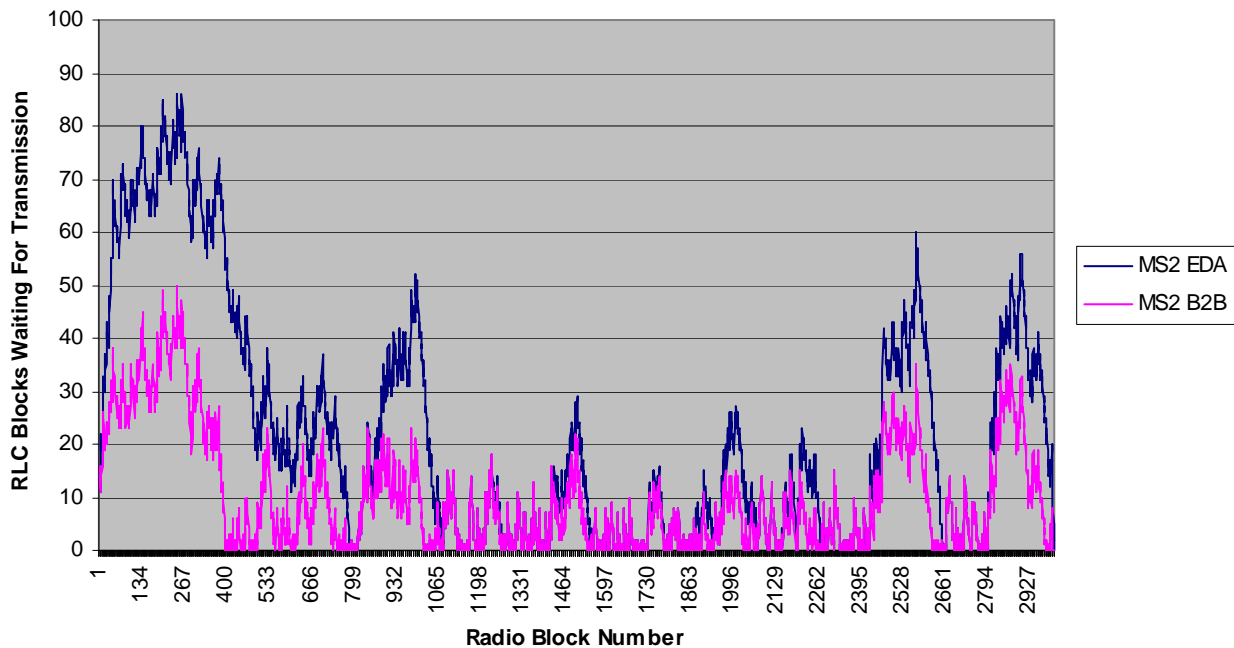
Figure 400: Trace of Uplink transmit buffer length for MS2s

13.4.1   Cumulative Probability Distribution- MCS-1, QCIF 30 FPS

In order to quantify this benefit the cumulative probability distribution function of the transmit buffer length of MS2 for 10 hours of MPEG4 is shown below in figure 401. The CDF in this figure shows the probability that transmit buffer length is less than given number of RLC blocks. This indicates that when only EDA is used, the transmission delay has a 2 % probability of exceeding 110 RLC block periods (2.2 seconds, which actually exceeds the time delay requirement stated in [2]). By contrast, when B^{2}DA is used, then transmission delay has a 2 % probability of exceeding 40 RLC Block periods (0.8 seconds). Assuming that packets with excess delay are deleted, and 2 % loss is acceptable, it is clear that the B^{2}DA scheme more than halves the required delay.
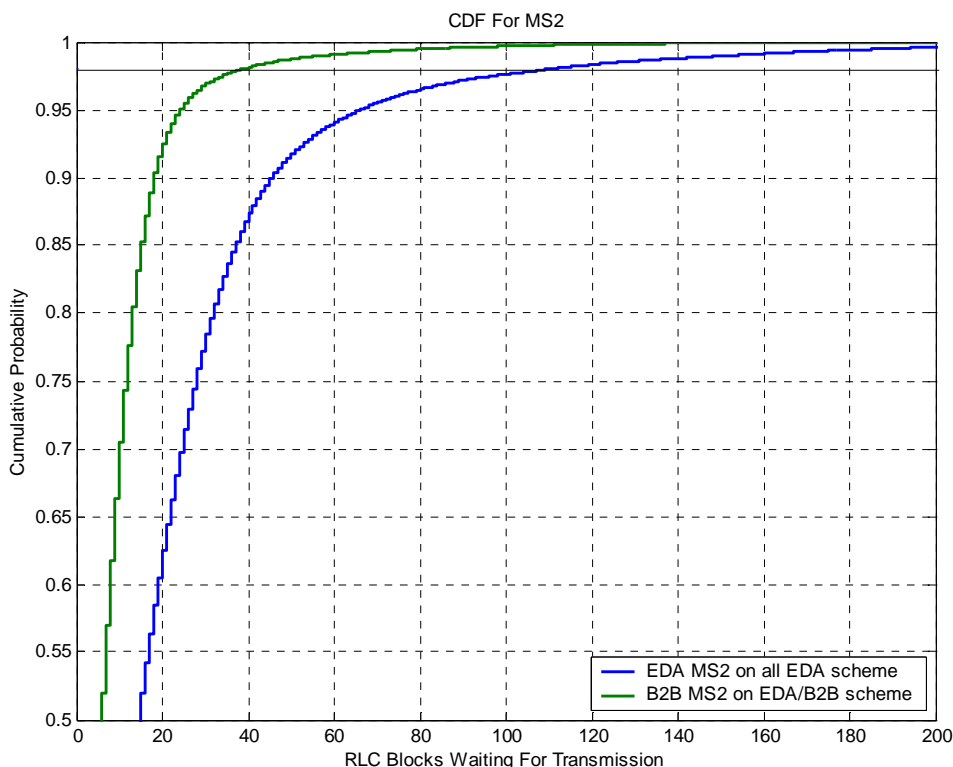
Figure 401: CDF of transmission buffer length for MS2 (QCIF 30 FPS)

As expected there is no significant difference in performance for MS1, since in both cases MS1 is using EDA, and only MS2 uses B^{2}DA (figure 402). The performance trend is very similar between MS1, and MS2 when using B^{2}DA, showing that MS1 and MS2 experience the same QoS when B^{2}DA is used in conjunction with EDA. This is clearly not the case when only EDA is used.
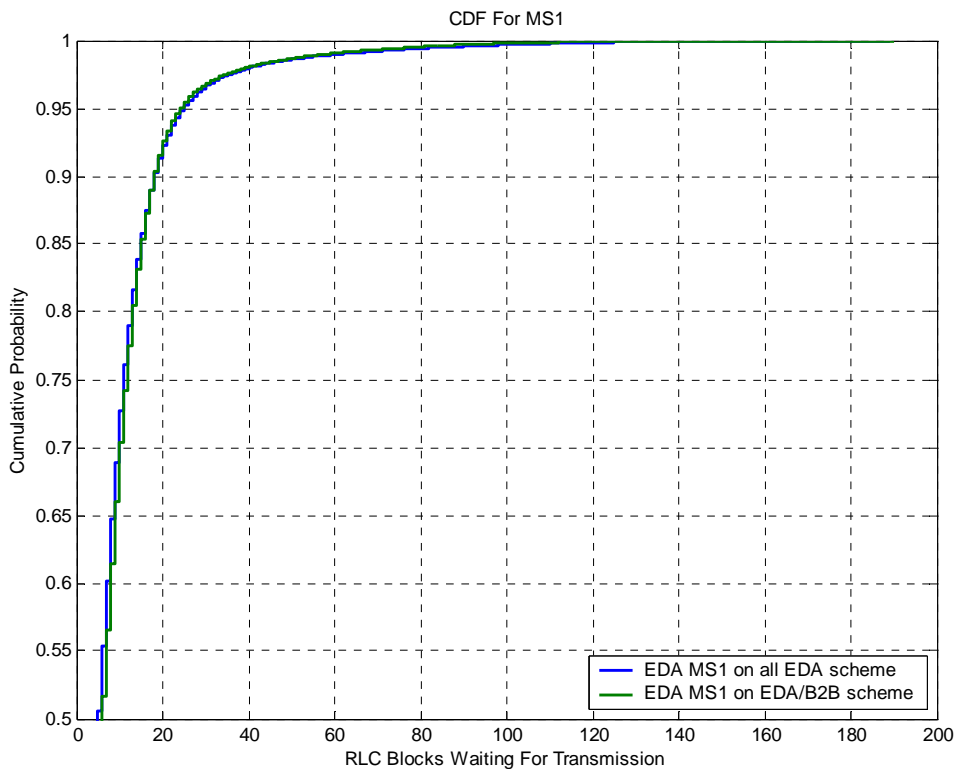
Figure 402: CDF of transmission buffer length for MS1

For completeness the CDF for the entire probability range 0 to 1 is shown below for MS1 and MS2.
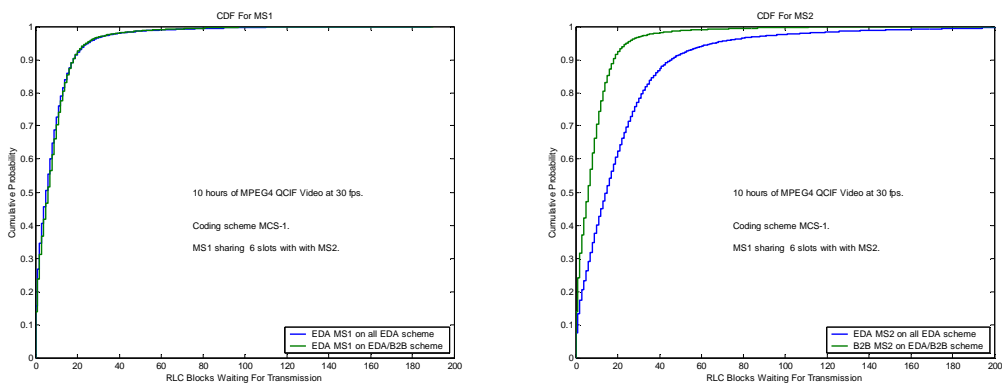
Figure 403: CDF for MS1, MS2

13.4.2   Cumulative Probability Distribution- MCS-5, CIF 15 FPS

In order to illustrate that the benefits apply to more than one coding scheme and configuration, analogous results are shown in figure 404 for a situation where two mobiles transmit CIF at 15 frames per second using MCS-5. Performance advantage is greater than 50 %.
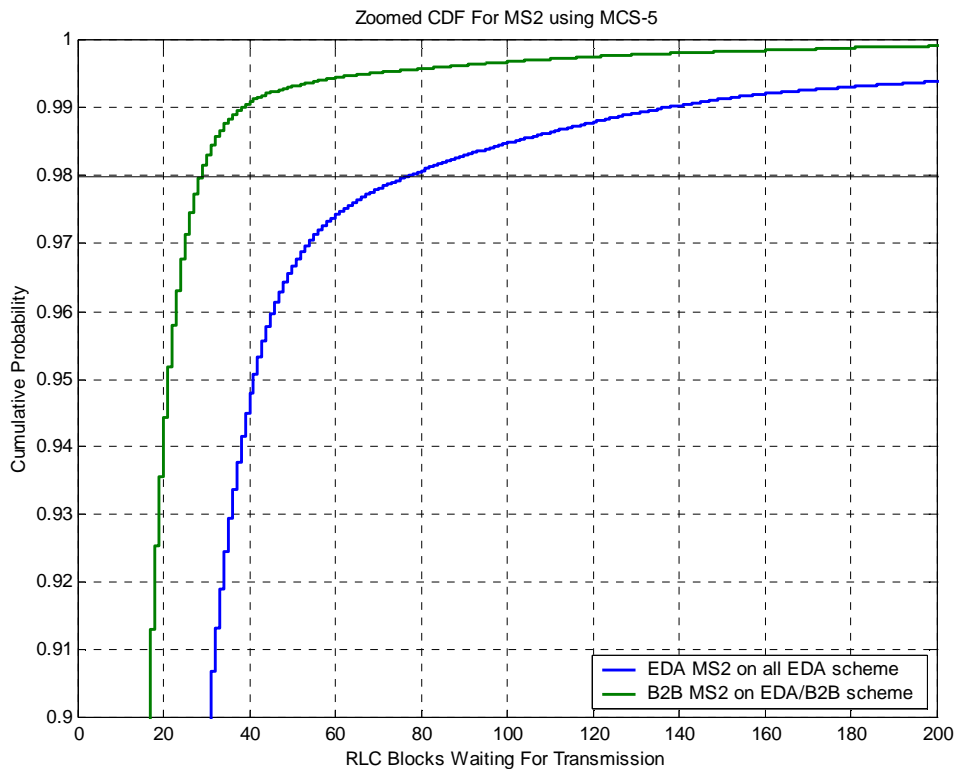
Figure 404: CDF of transmission buffer length for MS2 (MCS-5, CIF 15 FPS)

13.4.3   Summary of Performance Characterization

Using EDA alone, it would not be possible to share uplink resources between more than one mobile when transmitting variable rate delay sensitive real time streaming data such as MPEG4 video and expect both mobiles to receive a satisfactory QoS. For example, if each mobile individually needed 4 uplink slots, then the requirement for two mobiles would be 8 uplink slots. However using B^2DA it is possible to achieve 25 % multiplexing and achieve the same QoS; rather than 8 uplink slots, only 6 uplink slots are needed

To summarize, there is a 25 % improvement in data throughput efficiency in the given scenario.

13.5   Discussion: Improvement of B^2DA

13.5.1   Introduction

In order to enhance the resource allocation in GERAN Evolution, a new dynamic allocation scheme, Back to Back Dynamic Allocation, is presented above. B^2DA can grow assigned uplink timeslots "forwards" and reduce the mutual blocking when sharing resources between different mobiles during burst packet data flows.

As mentioned above, with B^2DA the number of USF values assigned to a mobile station is equal to the number of assigned uplink PDCHs, and these USF values are different from each other and concentrated on the lowest numbered timeslot. This will reduce the multiplexing flexibility as more than one USF value may be needed by one mobile on the lowest numbered timeslot while with existing schemes only one USF value is needed for one mobile on each assigned timeslot.

This subclause contains a proposal which aims to improve the multiplexing flexibility of B^2DA by using fewer amounts of USF values, and meanwhile not impact the efficient resource allocation as B^2DA. subclause 13.5.22 presents the detailed allocation scheme. Subclause 13.5.3 shows the benefits of this solution. Conclusions are given in subclause 13.5.4.

13.5.2 Details of proposed allocation scheme

13.5.2.1 New allocation rule based on B^{2}DA

The main idea is that, the network could reduce the number of USF values allocated to a mobile station, each different assigned USF value would represent a different allocation and one of these assigned USF values should indicate an allocation of all assigned uplink PDCHs. Due to the reduction of USF values, an adjusting rule of allocation and USF monitoring is proposed as follows.

The mobile station shall monitor the lowest numbered assigned PDCH. When an assigned USF value is detected on the lowest numbered PDCH, the mobile station shall transmit RLC/MAC blocks on all assigned PDCHs whose timeslot number is lower or equal to the corresponding assigned PDCH.

Considering a multislot class 12 mobile station, 4 uplink PDCHs are assigned, from slot 0 to slot 3. Only three different USF values, v0, v1 and v2, corresponding to PDCH0, PDCH1 and PDCH3 respectively, are assigned to the mobile station. USF value v0 indicates an allocation that the mobile can transmit RLC/MAC blocks on PDCH0, while v1 indicates PDCH0 to PDCH1, and v2 indicates all assigned PDCHs from PDCH0 to PDCH3. Figure 405 shows that three different USF values may be used to allocate PDCHs dynamically.
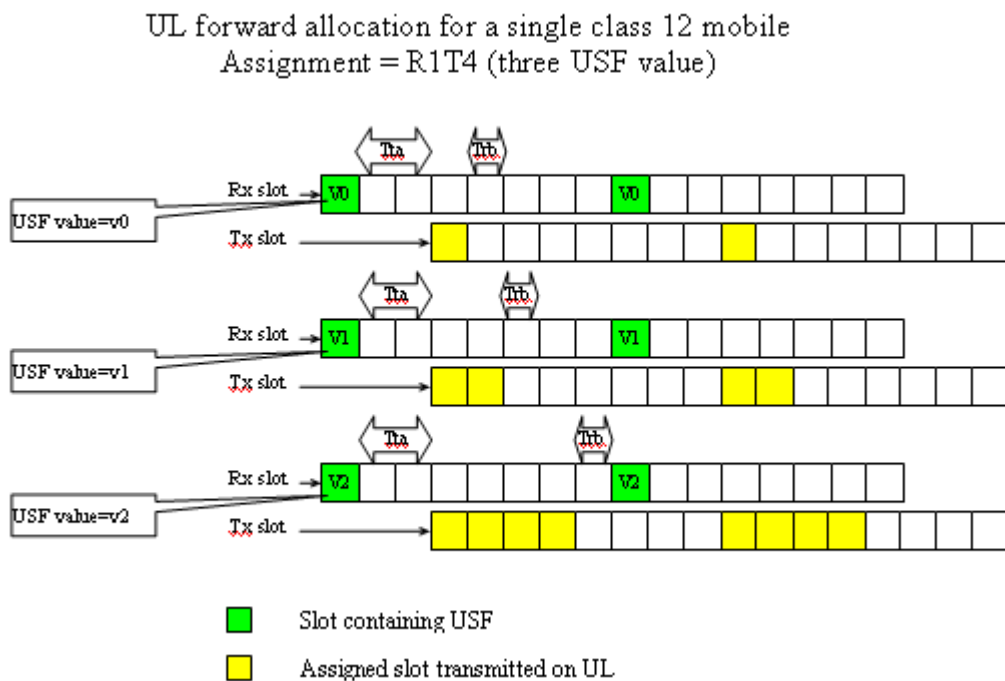
Figure 405: Illustration of the proposed allocation based on three USF values

13.5.2.1 USF resource

The amount of USF values remaining unused on the lowest numbered assigned PDCH will influence the potential applicability of B^{2}DA. However, it is possible to reduce the amount of USF values needed. The network can determine the amount of USF values needed in this allocation and establish the mapping of USF onto assigned PDCH according to the current situation including the USF recourse, the requesting service and etc. When the USF resource is limited, only two USF values are available for the situation illustrated in Figure below. One possible solution for the mapping of USF onto PDCH is shown in figure 406.

UL forward allocation for a single class 12 mobile
Assignment = R1T4 (two USF value)
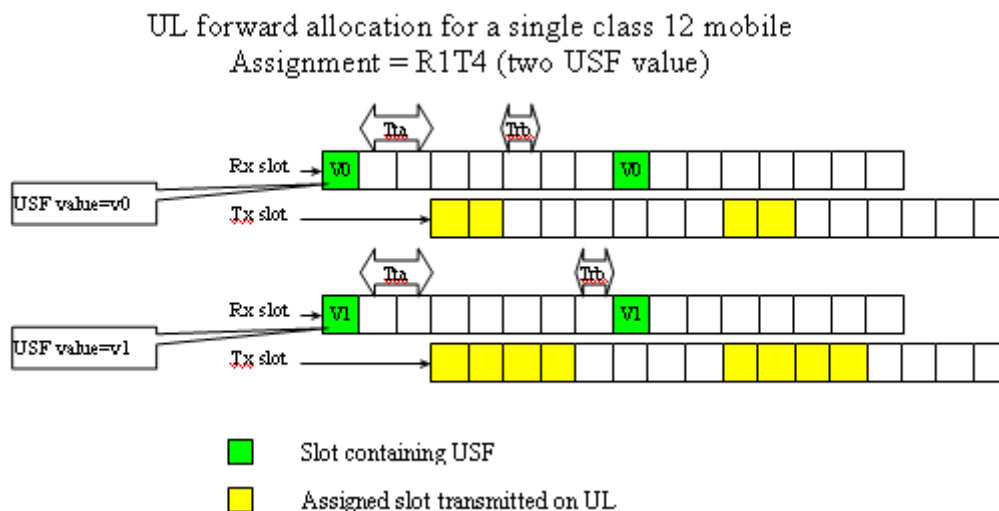
Figure 406: Illustration of the proposed allocation based on two USF values

13.5.3 Benefits of the Solution

The improvement reduces the amount of USF values needed on the lowest numbered assigned PDCH. This will increase the statistical multiplexing efficiency of resource allocation when a number of mobile stations simultaneously require for dynamically allocated uplink resources. This allocation can also co-exist with extended dynamic allocation to acquire performance gains compared with homogenous allocations just using EDA.

Elaborate allocation may be impossible with the proposed allocation in some situation. For example, it is impossible to allocate 3 uplink PDCHs in the instance as shown in figures 405 and 406. However, the proposed allocation make it possible for the BSS to use B^{2}DA in some USF resource limited situation.

Note that usage of USF-timeslot resources is increased in comparison to other dynamic allocation schemes, which require only *N* exclusive USF resources, by a factor of 100 %.

13.6 References

[1] Tdoc GP-052299: 3GPP TR 45.912 (V0.2.0): "Feasibility study for evolved GSM/EDGE Radio Access Network".

[2] 3GPP TS 22.105 (V6.3.0 - 2005-03): "Service Aspects: Services and Service Capabilities".

14 Modified MBMS Service

14.1 Introduction

Release 6 adds new components to the GSM/EDGE air interface in support of Multicast Broadcast Multimedia Subsystem (MBMS) operation, including MBMS-specific re-transmission protocols and enhanced outer coding techniques. Although new and efficient competitive technologies are becoming available for multimedia service delivery, re-use of the existing GSM infrastructure and mobile designs remains a highly cost-effective option for multimedia service delivery. Enhanced MBMS offers spectrally efficient operation in synchronous GSM networks through simulcast transmission in single-frequency network fashion. Provided the composite multipath channel impulse response is within the capabilities of the receiver, much higher signal-noise ratios (SNR's) can be achieved than for unicast traffic enabling high broadcast network spectral efficiency [1].

Note that use-cases may be needed to justify the introduction of modified MBMS with SFN in GERAN, since MBMS in GERAN is not intended to be a competing technology with e.g. DVB-H, but, conversely, a complementary technology.

14.2   Concept description

Contemporary network designs for the delivery of spectrally efficient broadcast services - such as DVB-H and MediaFLO, and even hybrid systems such as 3GPP2 BCMCS simulcast transmissions from individual cells in single-frequency network (SFN) fashion where the participating cells support sufficiently precise time- and frequency-synchronization to construct a single multipath channel from the network to the mobile device consisting of the sum of the individual per-cell channel impulse responses. Provided the composite multipath channel impulse response length is sufficiently small , broadcast receiver performance is limited not by co-channel interference, but rather by a) base station (BS) and MS implementation impairments (such as transmitter non-linearities, receiver thermal and phase noise, quadrature error etc.), b) adjacent channel interference, and c) any residual excess time-delay components.

14.3   Modelling Assumptions and Requirements

To evaluate the performance of single frequency network operation, the concatenated multipath channel experienced by the receiver must be characterised and then performance compared with unicast transmission. The following subclauses deal with modelling both methods of transmission in the same network for fair comparison.

14.3.1   Channel Modelling

The Root Mean Square (RMS) delay spread measure provides a crude means of assessing the amount of time dispersion in the resulting SFN. In order to assess the effect of the SFN operation on RMS delay spread, *System Configuration 2* defined in the GERAN SAIC Feasibility Study ([2], Clause 4) was used as the basis for assessing the RMS delay spread distribution of a simulated network. The primary parameters of the simulated network are given below in table 215.

Key parameters to note are the cell radius (1 000 m) and BS per-carrier radiated power level (43 dBm).

Figure 407 (left plot) shows an example composite Multipath Intensity Profile (MIP), with an RMS delay spread of 2.39 μs, constructed by combining the delayed MIP associated with each cell (i.e. sector) when the per-cell MIP is the 3GPP Typical Urban (TU) channel. The particular MIP shown in 407 was generated at position A in the network topology of figure 408. Figure 407 (right plot) shows the effective MIP generated by re-distributing the composite MIP onto a uniformly-sampled grid at 16x the GSM symbol rate. This approach will be used later to permit direct assessment of equalizer performance in the resulting composite channel.

Table 215: Simulated Network Parameters

Parameter	Units	Value	Comment
Number of Rings	Rings	3	
Total # Sites	Sites	37	
Sectors (cells) per site	Sectors	3	
Carrier Frequency	MHz	1900	
Cell Radius	m	1000	
BS Antenna Gain	dBi	17.0	
Sector Antenna Gain	dB	$-\min\left[12\left(\dfrac{\theta}{\theta_{3dB}}\right)^2, A_m\right]$	θ is angle w.r.t. antenna bore sight. θ_{3dB} is 3 dB antenna beam width
BS Front-Back Ratio (A_m)	dB	20.0	
Sector Antenna 3dB Beamwidth	degs	70.0	
Path Loss Model		$127.7 + 37.6\log_{10}[d(km)]$	UMTS 30.03, subclause B.1.4.1.3
Min. Path Loss	dB	70.0	
BTS Output Power	dBm	43.0	
MS Noise Figure	dB	10.0	
Shadowing Lognormal Standard Dev.	dB	8.0	
Shadowing Inter-site Correl. Coeff.		0.5	
Shadowing Intra-site Correl. Coeff.		1.0	
Power Control		Disabled	Maximum power radiated continuously per cell

Clearly, the composite MIP changes with each location in the network due to variation in path loss, shadow fading, antenna angle, relative BTS delay and so on. Figures 409 and 410 show the distribution of the composite RMS delay spread for all locations in the simulated network where sector 0 (see figure 408) of the centre cell is the best-serving cell (the serving cell distance is therefore distance to sector 0 of the centre site) and when a) the per-cell multipath channel is respectively TU and flat, and b) when all network cells are assumed to participate in the SFN. By comparing the figures, it can be seen that the distribution of RMS delay spread is dominated not by the per-cell MIP, but rather by the SFN dimensions.
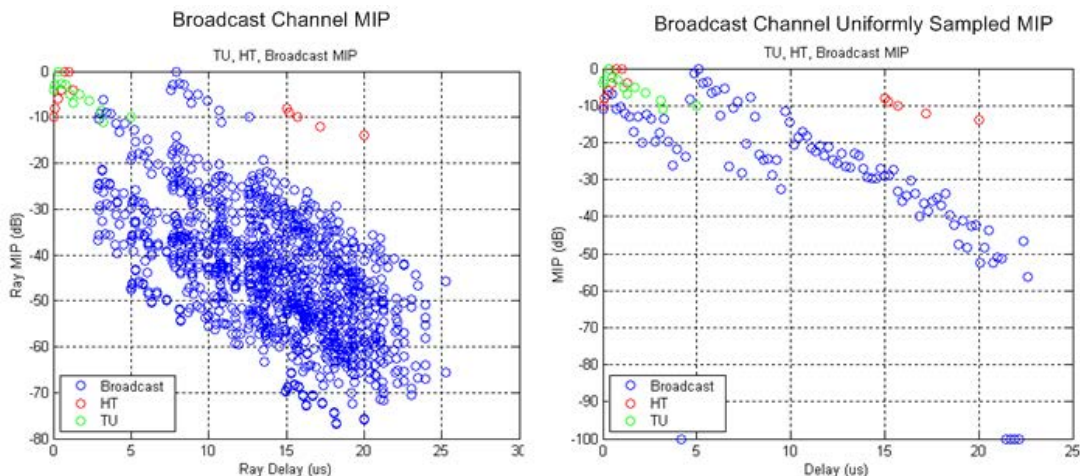
Figure 407: Broadcast channel example MIP
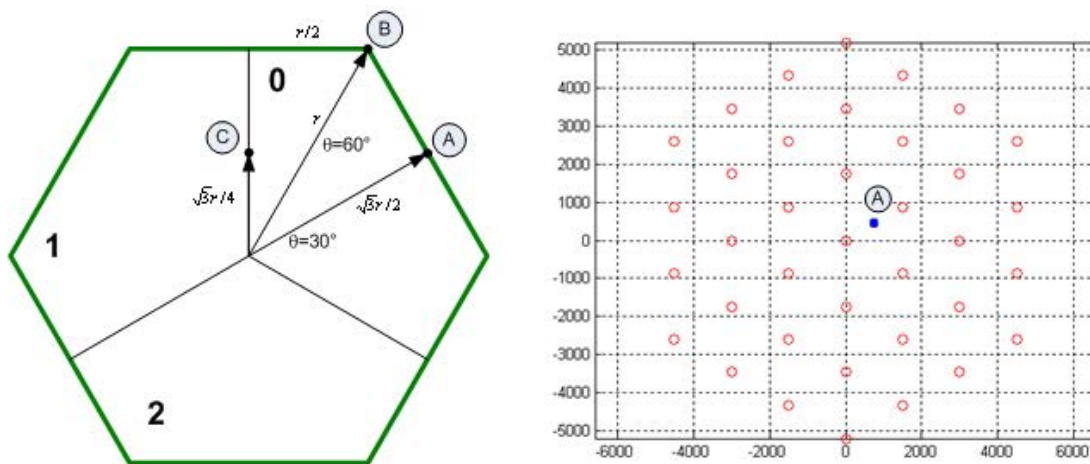
Figure 408: Example MIP reference location.
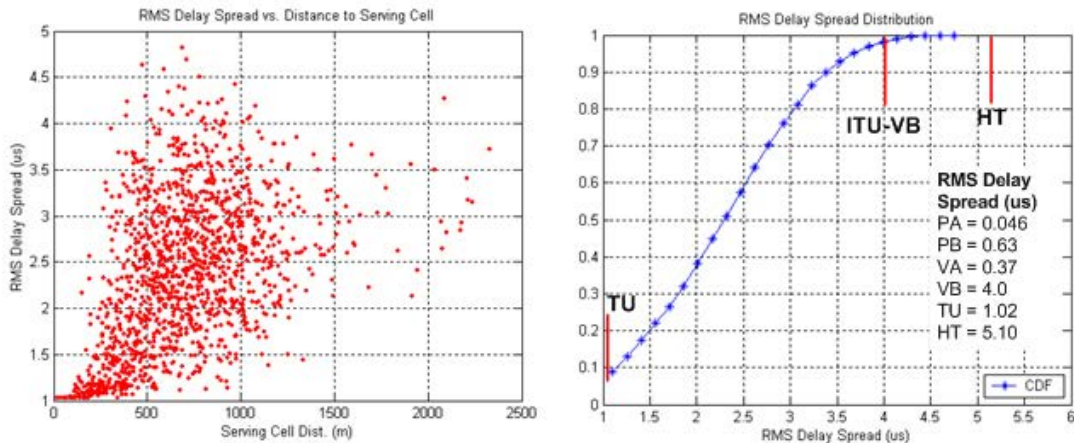
Figure 409: Broadcast RMS delay spread distribution - TU channel
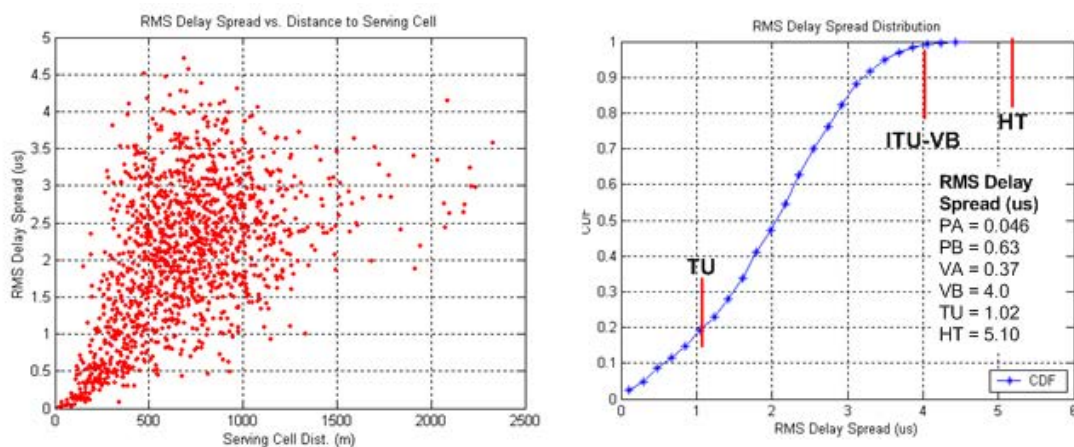
Figure 410: Broadcast RMS delay spread distribution - flat channel

The RMS delay spread of the standard 3GPP GSM (TU, HT) and ITU channel models (PA, PB, VA, VB) also appear in figures 409 and 410. It can be seen that the composite MIP of the broadcast network is generally distributed between the TU and HT RMS delay spread values of 1.02μs and 5.10μs respectively. The median delay spread for the broadcast network is 2.3μs for the TU channel case, and 2.0μs for the flat channel case. Accordingly, since GSM MS receiver conformance testing includes the HT channel condition, there is some indication that contemporary GSM mobile receivers could maintain good link performance in the presence of SFN-induced delay spread. This suggests a more detailed comparison with conventional re-use based interference avoidance broadcast modes.

14.3.2   Broadcast Network C/I and C/N Distributions

At the outset of the original GERAN MBMS work [3] the channel to interference plus noise ratios (CINR) characterising GERAN networks in a variety of re-use patterns were studied. The CINR distributions for the centre site (all sectors) of *System Configuration 2* of [2] assuming an MS noise-equivalent bandwidth of 200kHz appear in figure 411, where the triplet *(p,q,r)* corresponds to:

   a) *p* - site re-use group dimension;

   b) *q* - number of sectors per site;

   c) *r* - number of carrier frequency groups;

and where MS receiver impairments and BTS transmitter impairments are neglected, but the BTS antenna front-back ratio (20 dB) is included (as evidenced by the *(1,3,1)* reuse pattern whose asymptotic CINR is equal to the front-back ratio minus 3 dB).
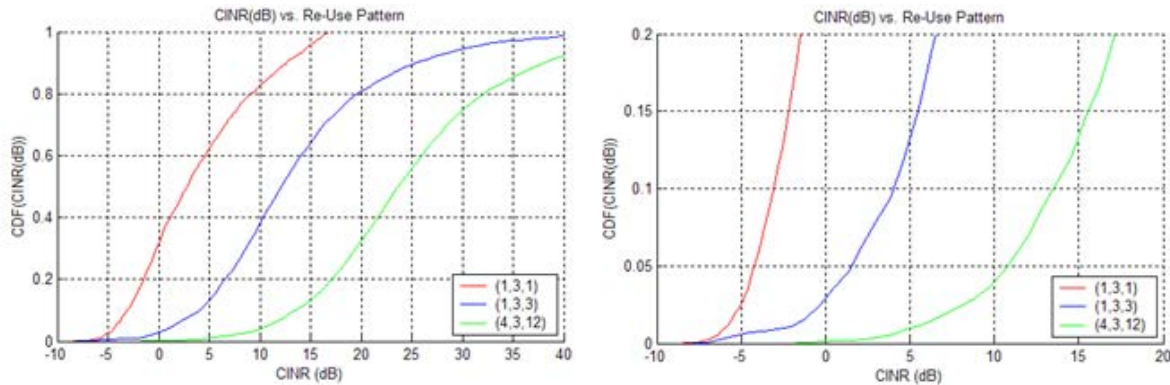
Figure 411: CINR distribution vs. re-use pattern

Assuming, say, 95 % broadcast channel coverage is required, the 5 %-ile CINR values for each re-use pattern appear in table 216. Note that for the system configuration parameters studied here, network operation is substantially interference-limited and so the CINR and CIR distributions are virtually identical.

Table 216: 5 %-ile CINR values

Re-use Pattern	5%-ile CINR (dB)
(1,3,1)	-4.2
(1,3,3)	1.5
(4,3,12)	10.7

Of course, in contemporary network design, the 5%-ile CINR values of table 216 are moderated by various techniques including fraction loading, discontinuous transmission, power control and so on. Nevertheless, application of these techniques here would reduce area spectral efficiency. Accordingly, for simplicity, the present analysis does not consider those approaches.

Further assuming that all of the cells in the simulated system are participating in the broadcast SFN, the performance-limiting C/I ratio is replaced with a signal to noise ratio distribution, or more usefully for link performance assessment, the ratio E_b/N_t of coded (i.e. transmitted) bit energy to receiver thermal noise density. Note again that it is assumed for the present purpose that other performance-limiting aspects - such as transmitter/receiver impairments, and adjacent channel interference - are neglected.

The resulting distribution of E_b/N_t for the center site (sector 0) of the simulated network appears in figure 412. It can be seen that the 5%-ile points for E_b/N_t at the GMSK and 8PSK coded bit rates are 38.6 dB and 33.8 dB respectively, although of course in this case, the broadcast channel has a larger delay spread than the underlying cell multipath channel.
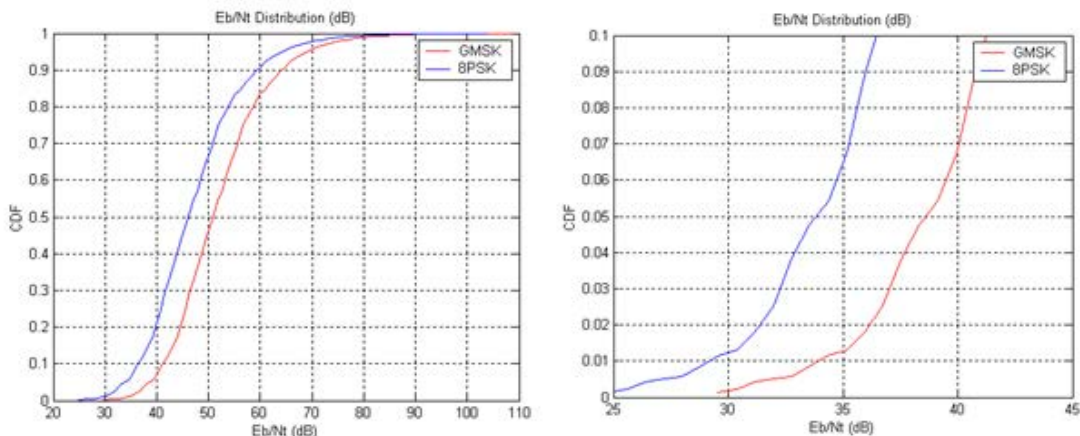
Figure 412: E_b/N_o distributions for centre cell

Accordingly, while the optimum approach to establishing broadcast channel coverage is to apply an appropriate link-system mapping at each point in the simulated network and then assessing the distribution of broadcast channel block error probability, a crude means of establishing broadcast channel coverage is to compare:

a) *Re-use Mode* - interference-limited performance at the C/I ratios specified in table 215 for the TU channel, and

b) *SFN Mode* - noise-limited performance at $E_b/N_t = \{38.6, 33.8\}$ for GMSK and 8PSK respectively, using a example broadcast channel such as that of figure 407.

Note that in the SFN mode b), however, the RMS delay spread of the composite MIP example of figure 407 is approximately equal to the median RMS delay spread of figure 409. Accordingly, an example composite MIP with larger delay spread equal to the 3.6 µs 95 %-ile point in figure 409 was selected. This MIP - which had an RMS delay spread of 3.68 µs (still 1.4 µs less RMS delay spread than the HT channel) - appears in figure 413. Note that the simultaneous assumption of 5 %-ile SNR and 95 %-ile delay spread is potentially pessimistic, although in practice these parameters would be correlated.
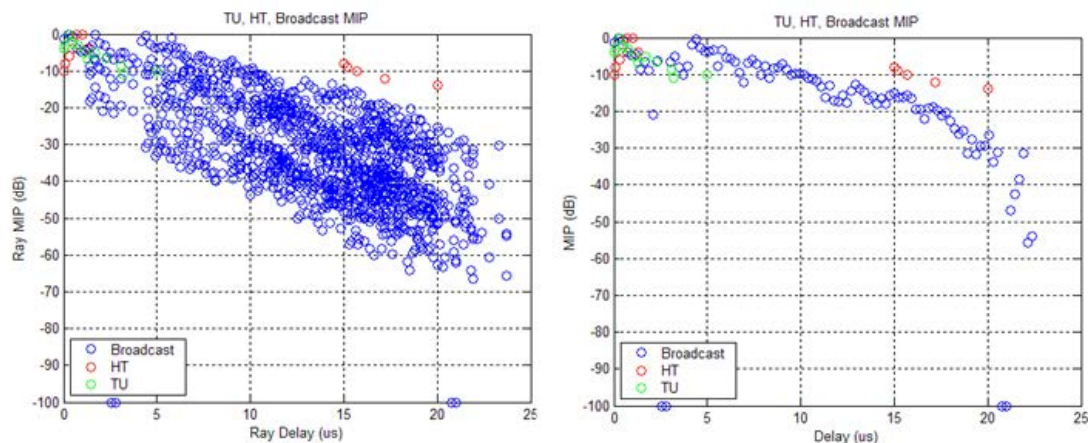
Figure 413: 95%-ile broadcast channel example MIP
(Left: simulated; right: uniformly sampled)

14.4   Receiver Link Performance

Table 217 lists C/I and E_b/N_o values required for operation at 10% radio link control (RLC) block error rate (BLER) under the SFN mode and re-use mode defined above for the example MIP's defined in figures 407 and 413 respectively. The specified values were derived from single-port receiver link simulations, but obviously dual-port (MSRD) receivers will offer better performance. Note that the selection of RLC block BLER was based on an assessment of potential application layer coding gain and H-ARQ, but this value could be further refined. Note also that the simulated values are ideal, since they disregard several significant implementation elements, but they do provide a useful guide to performance.

Here, it is assumed that the interference experienced in the conventional re-use case of figure 411 is structured according to the multi-interferer DARP model of TS 45.005, Annex L. For each MIP, ideal frequency hopping at 3km/h was applied.

Table 217: C/I **and** E_b/N_o **values required for 10% PDTCH BLER.**

MIP	TU	Broadcast - Fig. 1	Broadcast - Fig. 7
BLER = 10%	C/I (dB)	Eb/No (dB)	Eb/No (dB)
GMSK			
PDTCH MCS-1	8.5	8.3	8.6
PDTCH MCS-2	9.8	9.4	9.8
PDTCH MCS-3	13.3	12.7	12.9
PDTCH MCS-4	19.2	18.8	19.8
8PSK			
PDTCH MCS-5	14.4	10.2	10.8
PDTCH MCS-6	16.6	12.4	13.0
PDTCH MCS-7	21.5	17.1	17.9
PDTCH MCS-8	26.2	21.7	27.5
PDTCH MCS-9	29.1	24.7	N/A

Comparing the 95%-ile C/I values of table 215 with the required targets of table 217 suggest that for the conventional reuse system only relatively relaxed re-use patterns such as the *(4,3,12)* pattern are feasible at the required BLER. For the *(4,3,12)* pattern, MCS-2 is feasible. MCS-2 delivers an RLC PDU payload of 226 bits, which - neglecting H-ARQ re-transmissions - supports a per-cell throughput on the PDTCH logical channel of $R = (8slots.6block.226bits/block)/(26T_f) = 90.4kbps$ where T_f is the radio frame duration of 4.615ms. For the *(4,3,12)* re-use factor, this corresponds to an area spectral efficiency of $90.4/(12*0.2) = 37.7kbps/MHz/cell$.

Figure 412 and the 5%-ile 8PSK coded bit E_b/N_t of 33.8dB suggests that - again neglecting adjacent channel interference effects and BS/MS implementation SNR limitations - MCS-9 could be feasible for the median MIP of figure 407. MCS-9 delivers an RLC PDU payload of 1188 bits, and would therefore support a per-carrier throughput of $R = (8slots.6block.1188bits/block)/(26T_f) = 475.2kbps$. Since this could nominally be supported by a single carrier SFN, the area spectral efficiency is $475.2/0.2 = 2376kbps/MHz/cell$.

This represents an improvement in area spectral efficiency of $2376/37.7 = 63$-fold. It is again noted that the assumption of the *(4,3,12)* pattern may be a conservative assumption, and that the use of 'tighter' re-use patterns (such as *(1,3,1)* or *(1,3,3)*) with fraction loading etc. could result in higher spectral efficiencies for the re-use mode, but such modifications are not expected to match the spectral efficiency of the SFN.

The 95%-ile MIP of figure 413 gives marginally worse performance, suggesting support of only MCS-8 may be feasible at the 10 % RLC block error rate. This would slightly reduce the overall SFN spectral efficiency, but would not radically alter the conclusions.

14.5 Radio Resource Management

A number of options could be available for providing radio resources to support a GSM SFN broadcast mode.

In the simplest approach, one or more non-hopping radio frequency channels could be dedicated on a network-wide basis or over a local set Ω of cells to support the SFN, with a common training sequence code (TSC) applied to the common channel(s) at each participating cell (the TSC need not be tied to the Base Station Colour Codes, or BCC's). When the SFN is applied substantially over the entire network, there would appear to be relatively few TSC planning issues associated with such a deployment. When the SFN is constructed over a local set Ω of cells, TSC planning could be required at the edge of the SFN, but this challenge appears similar to conventional TSC planning (if used). In order to prevent adjacent channel interference of the BCCH pattern, the SFN radio channel or channels could be located non-adjacent to the BCCH carriers. Note that SFN operation would not be applicable to BCCH carrier frequencies since the SFN apparent *(1,3,1)* re-use pattern would deviate from conventional *(3,3,9)* or *(4,3,12)* (or larger) patterns, leading to an unallowed variation in the MS-observed RSSI on the BCCH carrier during timeslots devoted to broadcast use.

One drawback with such a configuration, however, is that an entire carrier frequency would be dedicated to the SFN. This could consume an excessive amount of radio frequency or BTS transceiver (TRX) resources in lightly resourced cells. As an alternative, individual timeslots on each non-hopping radio channel could be associated with the SFN on a per-timeslot basis, permitting improved granularity of radio resource assignment to the broadcast service. Of course, the associated SFN timeslot assignments would need to be coordinated between the participating cells in set Ω, but the required TRX hardware resources would be available for other logical channels (TCH/AxS, PDTCH, etc.) on timeslots not dedicated to SFN operation. For example, similar to conventional practice during the BCCH timeslot, the Mobile Allocation (MA) of MS's receiving a hopping TCH/AxS logical channel could be modified to exclude SFN-dedicated radio channels in any particular timeslot.

Neither of these approaches support, however, the use of frequency hopping which would entail a loss in performance for lower coding rates such as MCS5 and MCS6. Clearly, unidirectional broadcast services generally allow larger interleaving delays - and so improved time diversity - compared to real time services. This potentially allows the loss of hopping-induced frequency diversity benefits to be overcome. Reuse, however, of the current set of EDGE PDTCH MCS block structures (and 20 ms TTI) would minimise the impact of SFN operation on both the base and mobile station implementations. Notwithstanding, therefore, the marginal benefit (and occasional performance loss) of frequency hopping at very high code rates (e.g. MCS-4, MCS-9) the application of frequency hopping to a GSM SFN could offer performance benefits.

Permitting SFN frequency hopping over a set of cells Ω in a network supporting intra-cell orthogonal hopping such as GSM presents some obvious challenges. In order to maximise compatibility with existing specifications, the application of a common Hopping Sequence Number (HSN) and common TSC to the SFN over the set of participating cells Ω appears feasible. Contention or 'collisions' with other non-orthogonal transmissions from each cell could be handled by either a) defining a set of rules to permit arbitration of physical channel contention, or b) in the case of BTS' equipped with more than one transmit antenna (to support, for example, delay diversity), permit the broadcast burst to be transmitted on one antenna, and the contending burst on the second antenna.

Note that the impact on existing frequency planning need to be evaluated, since:

1. one or more non-hopping radio frequency channels are needed even in a NW fully supporting FH;

2. the SFN frequency allocation needs to take into account the BCCH carrier allocation.

Further, the worsening of radio performance for all the users whose FH set size is reduced, due to the introduction of SFN (without FH) in a NW fully supporting FH, needs to be evaluated as well as any increase in blocking probability in the CS domain and any increase in packet transfer delay in the PS domain needs.

14.6   Impacts to the Mobile Station

If the existing PDTCH MCS are retained for use in a GSM SFN broadcast channel mode, there would appear to be marginal impact to the MS RF subsystem specification, with the exception of the ability of the equalizer to deal with SFN-induced delay spread. However, as discussed in subclause 6.4, for contemporary medium- to small-cell GSM network deployments where spectral efficiency is most critical, the resulting composite channel delay spread does not appear to exceed the capability of current-generation MS'.

14.7   Impacts to the BSS

If the existing PDTCH MCS are retained for use in a GSM SFN broadcast channel mode, there would appear to be marginal impact on the BTS hardware, with the exception of the frequency hopping case. Existing transmitter designs capable of supporting error vector magnitudes consistent with MCS-9 transmission can clearly support adequate transmitter waveform qualities for MCS-9 delivery over SFN.

14.8   Impacts to the Core Network

Modified MBMS is seen as a feature that will enhance the performance of synchronous networks. It is not suitable for use in asynchronous networks.

14.9   Impacts to the Specification

The specifications listed in table 218 will be impacted by Modified MBMS.

Table 218: Impacted 3GPP Specifications

Specification	Description
3GPP TS 43.246	Multimedia Broadcast/Multicast Service (MBMS) in the GERAN; Stage2
3GPP TS 44.060	General Packet Radio Service (GPRS); Mobile Station (MS) - Base Station System (BSS) interface; Radio Link Control / Medium Access Control (RLC/MAC) protocol
3GPP TS 45.002	Multiplexing and multiple access on the radio path

14.10   Open Issues

Though RLC persistent mode in MBMS may be supported through unicast transmission using a separate resource, its impact on spectral efficiency has yet to be determined.

14.11   References

[1]   Y. Sun, R. Love, K. Stewart, K. Baum, B. Classon, V. Nangia, P. Sartori, "Cellular SFN broadcast network modelling and performance analysis", IEEE Vehic. Tech. Conf., Sept. 2005, pp. 2684-2690.

[2]   3GPP TR 45.903: "Feasibility Study on Single Antenna Interference Cancellation (SAIC) for GSM networks".

[3]   3GPP TR 25.992: "Multimedia Broadcast Multicast Service (MBMS); UTRAN/GERAN Requirements".

15   Uplink throughput enhancements with low standard impact

15.1   MS multislot capability switching

15.1.1   Introduction

For the downlink, two enhancements have been agreed as part of GERAN Evolution: Downlink dual carrier (see clause 7) doubles the peak data rate, and MSRD (see clause 6) increases both spectrum efficiency and data rate, the latter in particular at the cell edge. For balance between downlink and uplink, it would be desirable to find also an uplink enhancement that meets the objectives of the FS. Since (almost all) BTS have 2 Rx antennas with sufficiently low correlation, spectrum efficiency is already high in the uplink, compared with the downlink. Hence for the uplink, a method to increase data rates has higher priority than a method for higher spectrum efficiency.

Today, the typical EGPRS multislot class is 10 although the GSM standard allows for more than 2 uplink slots. If a few obstacles are removed and if some new multislot classes are defined, handsets supporting much higher uplink data rates can be brought onto the market without radical changes of the air interface.

15.1.2   Timeslot allocation

For type 1 MS which cannot transmit and receive at the same time, 6 uplink timeslots are a realistic limit if one timeslot is needed for the downlink, e.g. to transmit ACK/NACK messages. The following examples are based on a downlink dual carrier MS since MS supporting more than 4 Tx slots can be expected to support downlink dual carrier, too.

Downlink	1	2	3	4	5	6	7	0
f1	Mon.							
f2	PDTCH							
Uplink	6	7	0	1	2	3	4	5
f1'			PDTCH	PDTCH	PDTCH	PDTCH	PDTCH	PDTCH

Legend for the colours:

Neighbour cell monitoring	Downlink (MS receive)	Uplink (MS transmit)

In order not to require too short synthesiser lock time, the local oscillator for the Tx should be used for the monitoring in the following TDMA frame since monitoring need not start right at the beginning of the burst, and a small phase error does not matter either.

For DTM however, the synthesisers must be able to change the frequency between the end of the down-ramping and the beginning of an Rx burst. Furthermore, the time for monitoring may be shorter than one burst because of timing advance.

Downlink	1	2	3	4	5	6	7	0
f1	TCH/AFS							
f2	PDTCH	Mon.						
Uplink	6	7	0	1	2	3	4	5
f1'			PDTCH	TCH/AFS	PDTCH	PDTCH	PDTCH	PDTCH

Relaxations for BSIC decoding like those in 3GPP TS 45.008 may be needed.

To support 6 uplink timeslots and at the same time more than 2 downlink timeslots, the MS would need to be type 2 (full-duplex).

For applications such as Netmeeting, web browsing or file upload/download where either the uplink or the downlink clearly dominates, type 1 MS (half-duplex) are sufficient. Networks monitor which direction needs more bandwidth and they adapt the number of uplink and downlink timeslots accordingly.

For bidirectional video telephony however, high uplink and downlink data rates are needed simultaneously. The uplink transmission would either be limited to 4 timeslots (see subclause 7.6.1), or a full-duplex MS or a MS supporting dual carrier also in the uplink would be needed.

15.1.3   Full-duplex MS

When either the receiver or the transmitter is inactive, the duplex filter can be bypassed. However, during simultaneous reception and transmission, the duplex filter causes considerable insertion loss in both directions.

In the downlink, the duplex filter insertion loss and the Tx noise in the Rx band will lower the sensitivity. However, this desensitisation can now be compensated by the new feature MSRD. The intention of the multislot classes 13...18 was to allow for full-duplex operation. As long as the radio requirements do not take inevitable hardware limitations into account, the specified feature will never be implemented. Hence the sensitivity requirements for Rx slots which overlap with Tx slots should be relaxed by e.g. 4 dB for type 2 MS supporting MSRD. MSRD need not be supported simultaneously with downlink dual carrier, the more so as the downlink throughput also benefits from full-duplex operation.

For full-duplex operation, the relevant timeslot assignments will have at least 2 Tx slots. Hence a multislot power reduction by 3 dB would be allowed anyway if MULTISLOT_POWER_PROFILE 0 was chosen. This means that a lower output power due to the duplex filter insertion loss will not require a completely new relaxation. The objective should be that full-duplex MS need only reduce their nominal maximum output power by 3 dB, and this should be permitted. Even if the actual insertion loss of a duplex filter sample exceeds these 3 dB by 1...2 dB, the output power will still fit into the tolerance range.

The reduction may be limited to those Tx timeslots which overlap with Rx slots.

For further analysis of full-duplex MS, see subclause 15.2.

15.1.4   Tx power

From Rel-5 onwards, the MS sends multislot power profiles to the network which indicate for each modulation separately the need for lower output power under multislot uplink operation.

With regard to average current drawn from the battery and radiated power, a multislot power reduction will probably continue to be needed for GMSK, at least for more than two uplink slots.

For 8-PSK however, the output power of the usual power class E2 is much lower than the typical GMSK output power. Hence overheating - which was the reason for the introduction of multislot power reduction - is for 8-PSK a little bit less critical than for GMSK. Moreover, the risk that an MS might in the end overheat if it was operated under extreme conditions is not a convincing reason to always apply an output power reduction and a lower multislot class, even at normal conditions where overheating would be no issue. If overheating really becomes imminent, the MS has still the possibility to reduce its RAC to that RAC which it would have declared otherwise right from the beginning. Currently the mobile stations have to declare a RAC which, even at 55 °C ambient temperature, is sustainable over more than 15 minutes (test case 13.15.3). This makes it impossible to exploit the possibility to transmit on a higher number of timeslots, under normal conditions as well as under extreme conditions for the initial duration as long as heating is not a problem.

Hence it is suggested to usually signal 8-PSK_MULTISLOT_POWER_PROFILE 3, which allows for an 8-PSK output power of:

# uplink slots	low band	high band
6	27 dBm	26 dBm
8	26 dBm	26 dBm

(Even the GMSK output power should not be higher than what is listed above.)

Uplink dual carrier MS can support even more than 8 effective uplink slots. For designs using two PAs, the 8-PSK output power of each carrier should be also according to range defined in 3GPP TS 45.005 for power class E2 with 8-PSK_MULTISLOT_POWER_PROFILE 3.

Type 2 MS would have to reduce the maximum 8-PSK power to 24 dBm (± tolerances) in low band and 23 dBm (± tolerances) in high band during full-duplex operation. This reduction should be allowed without forcing type 2 MS to generally declare a lower power class or a lower multislot power profile.

15.1.5   Data rate increase

Under interference limited conditions where Tx power is not limiting the throughput, the throughput will scale with the number of uplink timeslots. If an MS supporting 6 uplink slots is compared with an MS supporting 4 uplink slots, the link-level throughput increase is 50 %.

In many cases, the link-level throughput gain will be higher under coverage limited conditions than under interference limited conditions since a higher 8-PSK multislot output power than assumed in the reference will be achievable. In addition to the higher number of uplink slots, the throughput per timeslot will also be higher if higher Tx power is used. This is illustrated based on figure 2 of [2] (coverage limited scenario, -98 dBm) where the green curve represents today's EGPRS with maximum multislot output power reduction and where the red curve shows what the combination of full Tx power (8-PSK only) with up to 6 timeslots can achieve - unless the MS overheats. The blue curves were left in the diagram just to show that a similar throughput can be achieved without radical changes of GSM's physical layer.
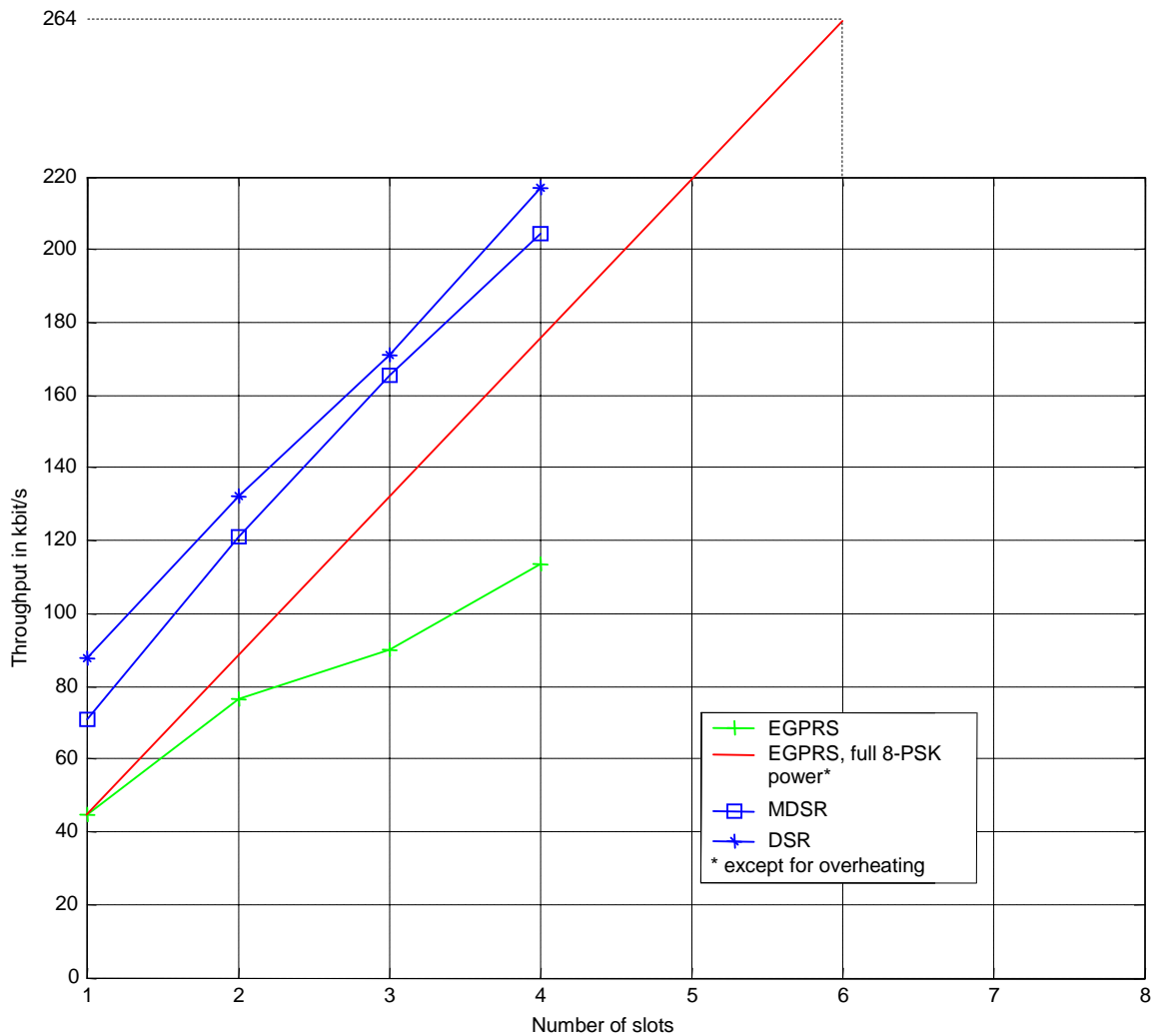
Figure 414: Uplink throughput comparison

15.1.6 Data rate increase at the cell edge

In this subclause, the throughput curves of [1] and the assumption of an Rx level of -109 dBm at the cell edge [1] are used.

The MS is assumed to support 6 uplink slots 8-PSK without output power reduction. This MS is compared with a reference MS that supports 4 uplink slots with 6 dB power reduction as in [1]. The MS's single slot output power is assumed to be 27 dBm for 8-PSK and 33 dBm for GMSK, i.e. 6 dB higher. Hence the Rx level at the BTS will rise by 6 dB after a link adaptation from 8-PSK to GMSK.

Table 219

MS	with multislot class 12 and output power reduction (baseline)	with higher multislot class and with full output power (new)
Number of uplink slots	4	6 (except for overheating)
Multislot power reduction	6 dB	0 dB for 8-PSK
Rx level at BTS for 8-PSK	-109 dBm - 6 dB = -115 dBm	-109 dBm - 0 dB = -109 dBm
Rx level at BTS for GMSK	-115 dBm + 6 dB = -109 dBm	*LA to GMSK not needed in this case*
Throughput per timeslot	13 kbit/s (GMSK)	15 kbit/s* (8-PSK)
Total throughput	52 kbit/s	90 kbit/s
NOTE: See [1], table 5, line "EGPRS", column "Cell border", and figure 3.		

The throughput gain amounts to 73 %. However, in the case of overheating, the MS would have to reduce its multislot class and fall back to the baseline (0 % gain). The requirement for mean bit rate increase by 50 % at the cell edge is exceeded if the gain of 73 % is available on average during 70 % of the time.

Under normal conditions (25 °C, no load mismatch), it is expected that a typical MS won't overheat. Under extreme conditions (55 °C, no load mismatch), it is expected that an MS could continuously transmit on 6 timeslots at 27 dBm 8-PSK for 10 minutes before it overheats. At 90 kbit/s, this would correspond to an upload of 6 MB. For files < 6 MB, the throughput gain would be 73 %, and for files > 8 MB, the throughput gain would be < 50 %. Since file uploads > 8 MB (or uninterrupted sending of more than 25 MMS at 300 kB each) are not deemed typical, we conclude that the requirement of 50 % higher mean bit rate at the cell edge will be fulfilled for the uplink.

15.1.7   Impacts on mobile stations

The MS needs to have one or more temperature sensors to detect if overheating is imminent. However, a temperature sensor in the RF part is already state of the art.

Under normal conditions - 25 °C and 50 Ω load at the antenna port - handsets can be designed to support up to six 8-PSK modulated Tx slots at 27 dBm without overheating. However, in the unlikely event that at least two of the following adverse, unusual circumstances coincide:

-    high ambient temperature;

-    substantial load mismatch;

-    long uplink transmissions without interruption.

The MS will have to downgrade either the multislot or the power class by a RAU with the new MS RAC IE [3], the reduction of the multislot class being much more efficient than a power reduction. Although a downgrade of RAC is expected to be a rare exception, MS manufacturers need to be sure that the network reacts to a multislot class reduction within a reasonable period of time. Otherwise, the mobile station might have to stop transmitting. To avoid such a situation, it is suggested to add an appropriate network test in 3GPP TS 51.021.

The peak current will not increase, but the average current that the battery needs to support will increase, depending on the multislot class, in particular for type 2 MS.

Typical EGPRS PAs are specified for supporting the maximum GMSK output power (without multislot power reduction) at a duty cycle of 50 %. Hence it can be expected that the support of 8-PSK at 27 dBm with a duty cycle of 75 % requires only an amendment of the PA specification, not a PA redesign.

The matching of PA and antenna should be designed such that an antenna mismatch, e.g. by a piece of metal close to the antenna, does not increase the heat dissipation in the MS. This may be not achievable for all channels, in particular for quad-band terminals, but even under load mismatch, the transmission can at least start with the full data rate.

Faster or more synthesizers will be needed to support more than 5 uplink slots, in particular if more than one downlink slot shall be supported at the same time (e.g. for DTM). Progress in digital frequency synthesis such as fast locking fractional-N synthesisers allows for faster switching between reception, transmission and monitoring.

New multislot classes need to be supported by the chipset and the software. Today, most chipsets support multislot class 12.

For uplink dual carrier MS, see clause 7.

15.1.7.1   Full-duplex MS

Full-duplex MS will need a duplex filter with bypasses for Rx and Tx direction, and Rx and Tx synthesisers will have to run at the same time. (For the GSM-R band, a duplex filter may be not feasible.)

The I/Q interface between the baseband and the transceiver chip needs to support simultaneous reception and transmission.

If the antenna switch causes harmonics during Tx operation, the harmonics could mix down with blockers, and blocking performance might be lower during full-duplex operation. In this case, another relaxation of the GSM specification could be required.

15.1.8 Impacts on the BSS

New multislot classes need to be implemented.

15.1.9 Impacts on the core network

No impacts expected.

15.1.10 Impacts on the specification

Since the standard already allows:

-   different output power reductions for GMSK and 8-PSK from Rel-5 onwards;

-   the possibility to reduce the multislot or power class if really needed; and

-   full-duplex MS;

-   only a few amendments are necessary;

-   definition of new multislot classes: 3GPP TS 45.002;

-   Rx performance relaxation during full-duplex operation: 3GPP TS 45.005;

-   MS maximum Tx power during full-duplex operation: 3GPP TS 45.005;

-   possibility to change the MS RAC during Tx tests: 3GPP TS 51.010;

-   test of Rx performance during full-duplex operation: 3GPP TS 51.010;

-   test of Tx power during full-duplex operation: 3GPP TS 51.010;

-   test that network supports change of MS RAC during an active PDP context: 3GPP TS 51.021.

15.1.11 Summary

In order to increase the uplink throughput, it is proposed that half-duplex MS use up to 6 uplink timeslots and that full-duplex MS use up to 8 uplink timeslots. Half-duplex EGPRS handsets with RLC/MAC uplink data rates of up to 355 kbit/s and full-duplex EGPRS handsets with RLC/MAC uplink data rates of up to 473 kbit/s will be feasible. Even legacy GPRS networks can benefit from the higher number of timeslots. Moreover, the coverage of 8-PSK multislot uplink transmissions will become larger since multislot output power reduction usually need not be applied. This will help EGPRS extend the coverage of 3G services. In the rare case of imminent overheating, the MS can dynamically adapt its multislot or power class by a routing area update.

This proposal is based on features which are already part of the GSM standard, but which should be amended in order to become usable. Only a few changes in the standard are required which can be completed in time for Release 7.

15.2 Type 2 MS Implementation

15.2.1 Concept Description

Full duplex operation is defined as the simultaneous transmission and reception of a signal. This technique requires a duplex filter in order to isolate receive and transmit paths.

Small ceramic, SAW, Film Bulk Acoustic Resonator (FBAR), and Bulk Acoustic Wave (BAW) based duplexers are available today and exhibit reasonably good isolation in a small package, which improves the possibility of implementing a type 2 mobile station. In addition, advanced receiver techniques such as DARP and mobile station receiver diversity (see clause 6) can help to overcome the loss in receiver sensitivity.

Enabling a type 2 mobile offers the possibility of transmitting more uplink slots while not affecting the downlink slot allocation. Type 2 mobiles also permit full flexibility in scheduling uplink timeslots (one or more) which can ease scheduling restrictions.

15.2.2   Void

15.2.2a   Interference Frequencies

15.2.2a.1   Introduction and Purpose

One of the types of interference in the receive band of a type 2 GSM mobile results from non-linear components in the receiver (such as the LNA and the mixer) combining the attenuated signal from the transmitter with other unwanted signals. These unwanted signals are typically called intermodulation interference or blocking signals. The products of these signals with the transmitter signal fall into the receive frequency band of the mobile station and can cause the receiver to behave non-linearly or can impact the receiver's sensitivity. This discussion document looks at the intermodulation interference frequencies that are of concern with four common GSM frequency bands. This information is referred to for the analysis of the intermodulation interference immunity of different type 2 MS architectures.

15.2.2a.2   Frequencies of Interest

Not all interference or blocking signals cause products that affect the GSM receive band. The first task therefore is to identify the frequency bands for interfering signals that pollute the receive GSM band when mixed with the transmit signal.

Let the transmitter signal be represented by $A_{TX} \cos \omega_{TX} t$, where A_{TX} is the amplitude of the transmit signal, and ω_{TX} represents the angular frequency of the transmit signal. Similarly the interferer signal is represented by $A_I \cos \omega_I t$, where A_I is the amplitude of the interferer signal and ω_I is the frequency.

Non-linearity in a receiver is typically modelled by a power series expansion (and limiting the expansion to only the first, second, and third order terms):

$$V = k_0 + k_1 V_{in} + k_2 V_{in}{}^2 + k_3 V_{in}{}^3$$

where V is the receiver output voltage; V_{in} is the receiver input voltage; k_1, k_2, and k_3 are the first, second, and third order voltage gain terms respectively; and k_0 is a DC offset term.

Substituting $V_{in} = A_{TX} \cos \omega_{TX} t + A_I \cos \omega_I t$ into the above equation gives:

$$V = k_0 + k_1 \left(A_{TX} \cos \omega_{TX} t + A_I \cos \omega_I t\right) + k_2 \left(A_{TX} \cos \omega_{TX} t + A_I \cos \omega_I t\right)^2 + k_3 \left(A_{TX} \cos \omega_{TX} t + A_I \cos \omega_I t\right)^3$$

Expanding out the power terms gives the following:

$$V = k_0 + k_1 \left(A_{TX} \cos \omega_{TX} t \quad + \quad A_I \cos \omega_I t \right) \quad + \ldots$$

$$k_2 \left(A_{TX}^2 \frac{1+\cos 2\omega_{TX} t}{2} \quad + \quad A_I^2 \frac{1+\cos 2\omega_I t}{2} \quad + \quad \underset{\text{2nd Order Intermod}}{2 A_{TX} A_I \frac{\cos(\omega_{TX} + \omega_I)t + \cos(\omega_{TX} - \omega_I)t}{2}} \right) \quad + \ldots$$

$$k_3 \left(A_{TX}^3 \left(\frac{3}{4} \cos \omega_{TX} t \quad + \quad \frac{1}{4} \cos 3\omega_{TX} t \right) \quad + \quad A_I^3 \left(\frac{3}{4} \cos \omega_I t \quad + \quad \frac{1}{4} \cos 3\omega_I t \right) \right) \quad + \ldots$$

$$k_3 A_{TX}^2 A_I \left(\frac{3}{2} \cos \omega_I t \right) + \underset{\text{3rd Order Intermod}}{\left(\frac{3}{4} \cos(2\omega_{TX} + \omega_I)t \quad + \quad \frac{3}{4} \cos(2\omega_{TX} - \omega_I)t \right)} \quad + \ldots$$

$$k_3 A_I^2 A_{TX} \left(\frac{3}{2} \cos \omega_{TX} t \quad + \quad \frac{3}{4} \cos(2\omega_I + \omega_{TX})t \quad + \quad \frac{3}{4} \cos(2\omega_I - \omega_{TX})t \right)$$

The second and third order intermodulation terms are of concern, since they can be close to the band of interest. Harmonics typically fall far out of band and are easily rejected with filtering. The cross modulation product on the interferer frequency is very critical where the interference frequency is close to the receive band (i.e. adjacent channel interferers). This is discussed in more detail in 15.2.2a.5.

15.2.2a.3   Intermodulation Interference

15.2.2a.3.1   Second Order Intermodulation Term

Looking first at the 2nd order intermodulation term:

$$2 A_{TX} A_I \frac{\cos(\omega_{TX} + \omega_I)t + \cos(\omega_{TX} - \omega_I)t}{2}$$

The frequencies terms of interest are $\omega_{TX} + \omega_I$ and $\omega_{TX} - \omega_I$. Because of the Even-Odd trigonometric identity cos(-x)=cos(x), the frequency term $\omega_I - \omega_{TX}$ needs to be considered as well. Next, solve for the interferer frequencies, where these terms fall into the RX band:

$$\begin{array}{ccc} \omega_{RX} = \omega_{TX} + \omega_I & \omega_{RX} = \omega_{TX} - \omega_I & \omega_{RX} = \omega_I - \omega_{TX} \\ \omega_I = \omega_{RX} - \omega_{TX} \quad [1] & \omega_I = \omega_{TX} - \omega_{RX} \quad [2] & \omega_I = \omega_{RX} + \omega_{TX} \quad [3] \end{array}$$

Cases [1] and [3] represent valid interference frequencies. Case [2] results in a negative frequency, because $\omega_{RX} > \omega_{TX}$, and is therefore discarded.

15.2.2a.3.2   Third Order Intermodulation Terms

Consider next the 3rd order intermodulation terms:

$$\frac{3}{4} k_3 A_{TX}^2 A_I \cos(2\omega_{TX} + \omega_I)t \quad + \quad \frac{3}{4} k_3 A_{TX}^2 A_I \cos(2\omega_{TX} - \omega_I)t \quad \text{, and}$$

$$\frac{3}{4} k_3 A_I^2 A_{TX} \cos(2\omega_I + \omega_{TX})t \quad + \quad \frac{3}{4} k_3 A_I^2 A_{TX} \cos(2\omega_I - \omega_{TX})t$$

The frequencies terms of interest are $2\omega_{TX} + \omega_I$, $2\omega_{TX} - \omega_I$, $2\omega_I + \omega_{TX}$, and $2\omega_I - \omega_{TX}$. Again because of the Even-Odd trigonometric identity cos(-x)=cos(x), the frequency terms $\omega_I - 2\omega_{TX}$ and $\omega_{TX} - 2\omega_I$ need to be considered as well. Next, solve for the interferer frequency, where these terms fall into the RX band:

$$\begin{aligned}\omega_{RX} &= 2\omega_{TX} + \omega_I \\ \omega_I &= \omega_{RX} - 2\omega_{TX}\end{aligned} \quad [4]$$
$$\begin{aligned}\omega_{RX} &= 2\omega_{TX} - \omega_I \\ \omega_I &= 2\omega_{TX} - \omega_{RX}\end{aligned} \quad [5]$$
$$\begin{aligned}\omega_{RX} &= 2\omega_I + \omega_{TX} \\ \omega_I &= \frac{\omega_{RX} - \omega_{TX}}{2}\end{aligned} \quad [6]$$

$$\begin{aligned}\omega_{RX} &= 2\omega_I - \omega_{TX} \\ \omega_I &= \frac{\omega_{RX} + \omega_{TX}}{2}\end{aligned} \quad [7]$$
$$\begin{aligned}\omega_{RX} &= \omega_I - 2\omega_{TX} \\ \omega_I &= \omega_{RX} + 2\omega_{TX}\end{aligned} \quad [8]$$
$$\begin{aligned}\omega_{RX} &= \omega_{TX} - 2\omega_I \\ \omega_I &= \frac{\omega_{TX} - \omega_{RX}}{2}\end{aligned} \quad [9]$$

Case [4] and case [9] result in negative frequencies and are therefore discarded.

15.2.2a.4   Intermodulation Frequency Bands

Now treating each frequency band as having a given bandwidth, the following substitutions can be made:

$$\omega_{RX} \Rightarrow F_{RXH} - F_{RXL} \qquad \omega_{TX} \Rightarrow F_{TXH} - F_{TXL} \qquad \omega_I \Rightarrow F_{IH} - F_{IL}$$

ω_{RX} and ω_{TX} can be any frequencies within a given GSM RX and TX band respectively. The intermodulation interference band frequency ranges are shown in Figure 417.
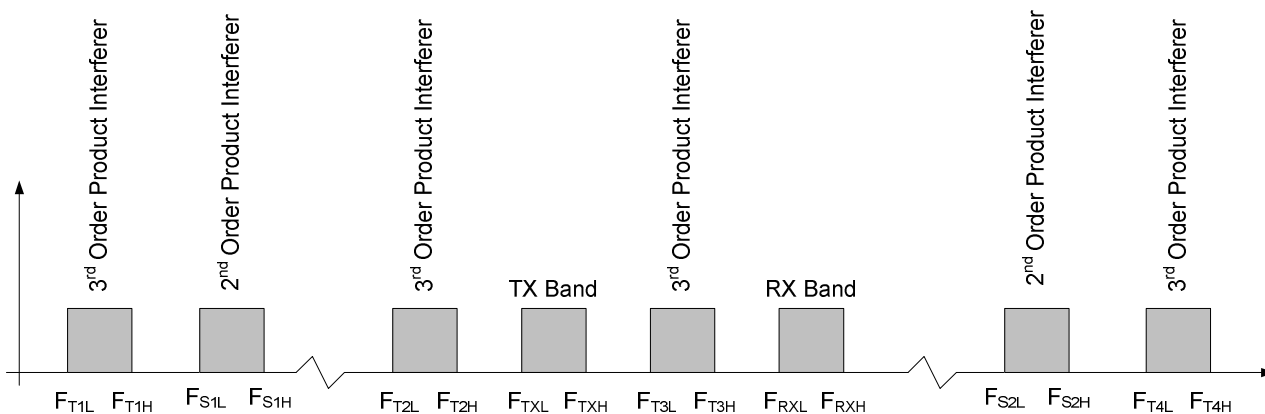
Figure 417: Intermodulation Interference Bands

The interference band frequency ranges are bounded by considering the extreme frequencies of each receive and transmit band. This method is described by the equations in Table 224. The angular frequencies (ω) have been replaced with ordinary frequencies using the relationship $F = \dfrac{\omega}{2\pi}$.

Table 224: Interference Band Edge Frequency Definitions

Product	Band Edge	Frequency
3rd Order	F_{T1L}	$(F_{RXL} - F_{TXH})/2$
	F_{T1H}	$(F_{RXH} - F_{TXL})/2$
2nd Order	F_{S1L}	$F_{RXL} - F_{TXH}$
	F_{S1H}	$F_{RXH} - F_{TXL}$
3rd Order	F_{T2L}	$2F_{TXL} - F_{RXH}$
	F_{T2H}	$2F_{TXH} - F_{RXL}$
3rd Order	F_{T3L}	$(F_{TXL} + F_{RXL})/2$
	F_{T3H}	$(F_{TXH} + F_{RXH})/2$
2nd Order	F_{S2L}	$F_{TXL} + F_{RXL}$
	F_{S2H}	$F_{TXH} + F_{RXH}$
3rd Order	F_{T4L}	$2F_{TxL} + F_{RXL}$
	F_{T4H}	$2F_{TxH} + F_{RXH}$

Applying the definitions in Table 224 for each GSM band gives the intermodulation interference frequencies shown in Table 225.

Table 225: Intermodulation Interfering Frequencies for Common GSM Bands

Product	Band Edge	Frequency Band			
		GSM 850 *Tx 824-849* *Rx 869-894*	**EGSM 900** *Tx 880-915* *Rx 925-960*	**DCS1800** *Tx 1710-1785* *Rx 1805-1880*	**PCS1900** *Tx 1850-1910* *Rx 1930-1990*
		Frequency (MHz)	**Frequency (MHz)**	**Frequency (MHz)**	**Frequency (MHz)**
3rd Order	ΔF_{T1}	10 – 35	5 – 40	10 -85	10 – 70
2nd Order	ΔF_{S1}	20 – 70	10 – 80	20 – 170	20 – 140
3rd Order	ΔF_{T2}	**754 – 829**	**800 – 905**	**1540 – 1765**	**1710 – 1890**
3rd Order	ΔF_{T3}	**846.5 – 871.5**	**902.5 – 937.5**	**1757.5 – 1832.5**	**1890 – 1950**
2nd Order	ΔF_{S2}	1693 – 1743	1805 - 1875	3515 - 3665	3780 - 3900
3rd Order	ΔF_{T4}	2517 - 2592	2685 - 2790	5225 - 5450	5630 - 5810

In each of the GSM bands there is overlap between the band F_{T2} and the TX band. Also there is overlap between the F_{T3} band and both the TX and RX bands. These two 3rd order product bands may prove to be the most troublesome. While the F_{T2} product band can be rejected by the filtering in the receiver, the F_{T3} product band will not be well rejected as it lies directly across the transition band of the duplexer and receive filter as well as in a portion of the Rx band where there is no duplexer and filter rejection.

The interference signal power levels that may be seen in these frequency ranges will vary depending on the RF environment. However the blocking signal levels that the MS must handle are specified in Section 5.1 of [8]. The document specifies blocking tone powers for each GSM band and classifies them as "in-band" (frequencies near or in the receive band) or "out-of-band" (frequencies farther away from the receive band). For DCS1800 and PCS1900 the out-of-band frequencies are subdivided into sections (a), (b), (c), and (d). The blocker powers and frequencies as stated in [8] are given in Table 226.

Table 226: Blocker Tone Frequencies and Powers

GSM Band	Frequency Band	Frequency (MHz)	Maximum Blocker Power
GSM850	in-band	849 – 914	-23dBm
	out-of-band	0.1– 849 and 914 – 12750	0dBm
EGSM900	in-band	915 – 980	-23dBm
	out-of-band	0.1 – 915 and 980 – 12750	0dBm
DCS1800	in-band	1785 – 1920	-26dBm
	out-of-band (a) and (d)	0.1 – 1705 and 1980 – 12750	0dBm
	out-of-band (b) and (c)	1705 – 1785 and 1920 – 1980	-12dBm
PCS1900	in-band	1910 – 2010	-26dBm
	out-of-band (a) and (d)	0.1 – 1830 and 2070 – 12750	0dBm
	out-of-band (b) and (c)	1830 – 1910 and 2010 – 2070	-12dBm

15.2.2a.5 Cross Modulation Interference

Cross modulation is caused by the transfer of the amplitude modulation of a strong signal (like the transmitter in a handset) onto another signal (the adjacent channel) in a nonlinear processing block (i.e. the LNA). There can be cross modulation between any two signals if one or both have some form of amplitude modulation. In this case, we are interested in the cross modulation from the transmitter signal of the mobile (which is relatively strong) and an adjacent channel interferer in the mobile. This is shown in Figure 418.
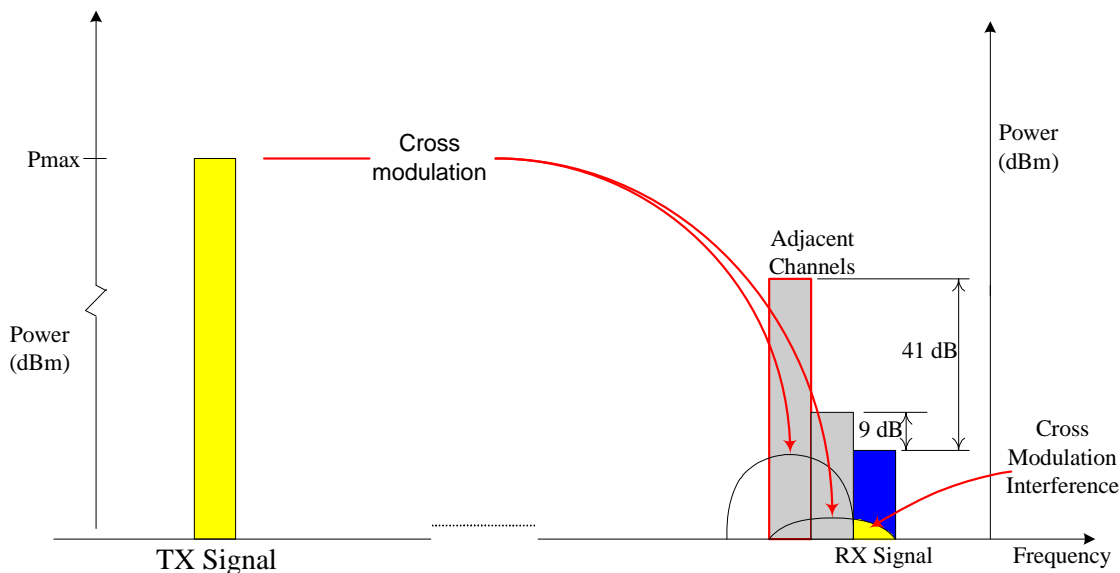
Figure 418: Cross modulation of the Adjacent Channel Signal by the TX Signal Causes Interference with the RX Signal.

Cross modulation power is proportional to the adjacent channel power and proportional to the square of the TX power (in Watts). Cross modulation is often the driver for linearity requirements in full duplex technologies such as CDMA. Analyzing this effect accurately requires statistic modelling of the modulated signal. The effect of cross modulation is not discussed at this time.

15.2.2a.6 Summary

This section defines the interference frequency bands that will combine with the TX signal and cause interference in the receiver. Some of these interference frequency bands lie close or even inside the TX and RX bands. It also reiterates the blocking requirements set by [8].

Other interference bands are far from the operating frequencies of the MS and should be strongly rejected by the MS antenna. However, as the transceiver requirements set out in [8] state that interference signal power levels must be considered at the antenna connector, the filtering benefits provided by the antenna cannot be accounted for in subsequent analysis.

15.2.3 Void

15.2.3a Transmitter Output Power Levels

Three cases for the transmitter output power levels are considered.

15.2.3a.1 No Maximum Output Power Reduction

The first case illustrates the situation where the type 2 mobile is expected to meet the maximum output power requirements as specified for the mobile class in [8]. In order to meet this specification the PA must exceed the specified maximum power (33 dBm for 850/900 MHz and 30 dBm for 1800/1900 MHz) by the total passive loss to the antenna port of the switchplexer. This output power case illustrates the worst situation for receiver interference in this frequency band, as the maximum amount of TX power will leak through to the RX chain.

As an example, consider the basic type 2 architecture outlined in Section 15.2.6a in the GSM 850 band. The SPDT maximum insertion loss is 0.45 dB, the maximum insertion loss of the duplexer in the TX path is 2.3dB and the maximum insertion loss of the SP4T switchplexer is 0.85 dB. This means that the maximum power at the PA output needs to be 33dBm + 0.85 dB + 2.3 dB + 0.45 dB = **36.6** dBm.

In order to achieve this elevated output power, the size of the PA would have to be increased significantly, and there would be a substantial increase in current consumption. The current consumption can be estimated with the equation:

$$I = \frac{[P_{out} - P_{in}]}{[Eff * V]}$$

P_{out} is in Watts, P_{in} can be ignored as the gain is high, Eff is the efficiency (assumed 50% for GMSK, and V is the applied voltage (assume 3.8 volts).

Consider the GSM 850 band; with a type 1 mobile, the maximum loss after the PA is approximately 0.2 dB for the harmonic filter, and 0.7 dB for the SP6T switch. Therefore the power at the output of the PA is 33 dBm + 0.9 dB = **33.9** dBm. The current draw for this output power is 1.29 A (during transmit).

Next look at the example described above with the basic type 2 architecture operating in the GSM850 frequency band. With the output power increased to **36.6** dBm, the current draw increases to 2.41 A (during transmit). Power consumption has almost doubled, which will have a significant impact on talk time. Furthermore, the acoustic duplex filters are not designed to tolerate such a high applied power level, and it is expected that this situation would significantly decrease the life of the duplex filter. However for compliance to the specifications this output power level should be analyzed.

15.2.3a.2 No Change in PA Capabilities

The second case that is considered is where the PA puts out the same maximum output power as it does with the current type 1 GSM architecture. As described in Section 15.2.3a.1, for GSM 850 the maximum power at the output of the PA is **33.9** dB. In DCS and PCS bands the maximum power measured at the PA output (based on typical type 1 mobile) is 30 dBm + 0.2 (harmonic filter) + 0.9 (max loss of SP6T switch in this frequency range) = **30.9** dBm. This output power is held constant.

As an example consider the basic type 2 architecture given in Section 15.2.6a. In this case, the maximum output power that the duplex filter sees is 33.9 dBm – 0.3 dB (typical insertion loss of the SPDT switch in this frequency range) =

33.6 dBm[1]. The maximum output power at the antenna port of the switchplexer varies depending on the duplexer and the switchplexer losses. For this architecture example in the GSM850 band it could vary between (33.6 dBm – 0.85 dB – 2.3 dB) = **30.45** dBm and (33.6 dBm – 0.7 dB – 2.0 dB) = **30.9** dBm. For the DCS/PCS band the maximum power at the TX port of the duplex filter is 30.9 dBm – 0.4 dB (typical insertion loss of the SPDT switch in this frequency range) = **30.5** dBm. The maximum output power at the antenna port of the switchplexer varies depending on the duplexer and the switchplexer loss. In both DCS and PCS band it would vary between (30.5 dBm – 0.8 dB – 2.1 dB) = **27.6** dBm and (30.5 dBm – 0.95 dB– 3.5 dB) = **26.05** dBm.

This power case assumption means that type 2 mobiles would require a maximum power reduction (even in single slot mode).

15.2.3a.3   Power Back Off based on Duplexer Power Tolerance

Duplex filters have a limit to how much input power they can tolerate. The specification for the GSM 850 SAW duplex filter (EPCOS B7638) states that it can handle 30 dBm CW in the TX band. The PCS band BAW duplex specification (EPCOS B7633) states that the filter can handle 29 dBm with a CDMA modulated signal in the TX Band. These parameters are incomplete. It is not specified whether these power limits are for RMS or peak power when a modulated signal is presented. The effect of duty cycle of the signal presented is not considered. Also, the percentage of the time that the signal is at or over the rated maximum is not considered.

Regardless of the limited information available, there is a possibility of damaging or reducing the life of the duplexer if the maximum rated power is exceeded. Therefore the analysis is repeated with the TX output power backed off to 29 dBm at the TX Port of the duplexer (30dBm for the GSM850 case).

The maximum output power at the antenna port of the switchplexer can vary depending on the duplexer and switchplexer loss. As an example consider the basic type 2 architecture given in Section 15.2.6a. In GSM850 band the maximum output power would vary between (30 dBm – 0.7 dB – 2.0 dB) = **27.3** dBm and (30 dBm – 0.85 dB – 2.3 dB) = **26.85** dBm. In EGSM900 it would vary between (29 dBm – 0.7 dB – 2.1 dB) = **26.2** dBm and (29 dBm – 0.85 dB – 3.5 dB) = **24.65** dBm. In PCS and DCS it would vary between **26.1** dBm and **24.55** dBm.

This power case assumption means that type 2 mobiles would require a maximum uplink power reduction (even in single slot mode).

15.2.4   Void

15.2.4a Analysis Assumptions

The interference and blocking signal frequencies and power levels are discussed in Section 15.2.2a.

Sensitivity requirements depend on the logical channel, the expected error rate, and the propagation environment. For AMR12.2 with FER 1%, the required SNR can easily vary between 8 dB and 16 dB depending on the channel conditions. For MCS-1 with 10% BLER, the required SNR can vary from 6 dB to 11 dB depending on the environment. To examine all the possible logical channels and environments at this feasibility stage is unrealistic. Hence the analysis in this document assumes that a signal to noise ratio of 10 dB is needed between the desired signal and cochannel noise and interferers in order to meet the bit error rate requirement with sufficient margin.

When verifying the immunity to blockers, the desired signal power is raised by 3dB to -99dBm. In a type 1 mobile there are typically only two components between the antenna and the receiver, the switchplexer and the RF filter. The maximum insertion loss of the switchplexer and receive filter occurs in the DCS/PCS bands and is equal to 4.6 dB. Therefore, the minimum signal power arriving at the receiver during blocker immunity testing is -99 dBm – 4.6 dB = **-103.6** dBm. If the cochannel noise and intermodulation products are to be 10 dB below the signal power, their combined power must not exceed -113.6 dBm.

The thermal noise in a single 200 kHz GSM channel is -121 dBm. Adding the maximum RF receiver noise figure (4.6 dB) to the thermal noise yields -116.4 dBm. Removing -116.4dBm from the permitted noise and interference level of -

---

[1] Note that this power level at the duplex filter may also affect reliability. The power handling ability of the duplexer needs to be examined in more detail.

113.6 dBm gives the maximum power intermodulation products can have without violating the 10 dB SNR requirement. This value works out to be -116.8 dBm.

This same analysis is done for the various architectures in each band, since the insertion losses of the components vary depending on the frequency, and different components are present in different architectures.

The receiver's tolerance to interference signal power is determined by the rejection provided by any receive band filtering, and by the linearity of the receiver. Based on the maximum interference signal level [9], the amount of transmitter power that leaks through to the receiver input, and the duplexer/filter performance [10], the receiver linearity (IIP2, IIP3, and the 1 dB compression point (C1dB)) required to prevent saturation by the transmit signal and degradation of the receiver sensitivity are determined.

In some cases, the passive losses degrade the receiver sensitivity to the point that the 10 dB SNR cannot be maintained at the receiver. In these cases, the input signal level must be increased to meet the performance requirements.

15.2.5   Duplexer and Receive Filter Requirements

15.2.5.1   Introduction

This section discusses the filter parameters that are used in the various analyses for different type 2 mobile architectures. Specifications that are used in these analyses are given. As type 2 GSM mobiles are not currently manufactured, some of the filters required are not available. Filter specifications for some bands had to be derived from existing filters.

15.2.5.2   Methodology

Frequency scaling allows filters with different centre frequencies to be compared. To estimate filter parameters, it is necessary to find a filter with similar scaled bandwidth and transition bands as the required filter. Figure 419 illustrates typical bandpass filter characteristics and defines parameters that are subsequently used in the equations.
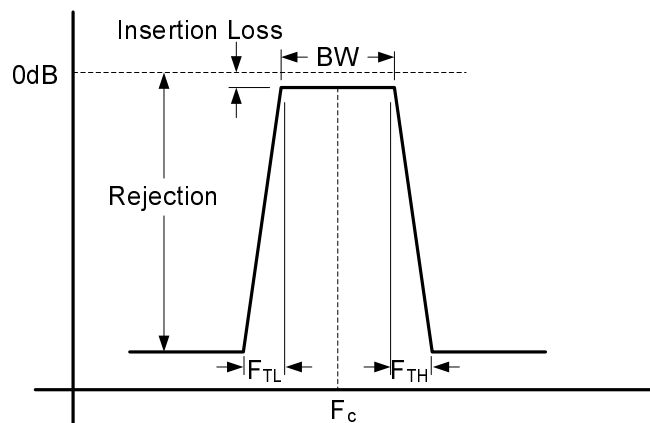
Figure 419: Diagram Showing Bandpass Filter Characteristics

The scaled bandwidth, the scaled transition band, and the shape factor are used to map filter requirements:

$$scaled\,bandwidth = \left(\frac{BW}{F_C} \right) \quad scaled\,transition\,band = \left(\frac{F_{TL}}{F_C} \right) \quad shape\,factor = \left(\frac{BW}{F_{TL} + BW} \right)$$

F_{TH} is not used in the above equations as it is on the high side of the RX band, away from the TX band, and therefore its value is not critical.

By matching the normalized bandwidth, normalized transition bands, and shape factor relatively closely, filter performance can be projected for other frequency bands. This method is just used to give approximate filter performance, and does not confirm that filters can be fabricated with these specifications.

The EGSM and DCS frequency bands did not have sample high TX rejection filters or duplexers available. The normalized bandwidth, transition bands and shape factor for EGSM and DCS are given in Table 227.

Table 227: Key Filter Parameters for the EGSM and DCS Band

	Filter for DCS		Filter for EGSM900	
	Actual	Scaled	Actual	Scaled
Centre Frequency	1842.5 MHz	1	942.5 MHz	1
Filter Bandwidth	75 MHz	0.041	35 MHz	0.037
Transition Band (F_{TL})	20 MHz	0.0109	10 MHz	0.0106
Shape Factor	0.789	-	0.778	-

15.2.5.3   Receiver Bandpass Filter Specifications

Two sets of receiver bandpass filters are considered in this analysis. Filters designed for current GSM receivers (i.e. type 1) have not been optimized for high rejection of the transmitter band since full duplex operation is not required. Sample filter specifications for these filters are given in Section 15.2.5.6.

For the GSM bands that are coincident with CDMA bands (i.e. GSM 850 and PCS 1900), there are sample high TX rejection filters targeted for the CDMA market that can be used for a type 2 mobile. The sample high TX rejection filter used in this analysis for the 850 MHz band is the EPCOS B9035. For PCS band the sample filter used is the EPCOS B9034. Filters were not found for the EGSM and DCS bands, so the filter specifications for these bands were derived from the B9034 according to the procedure described in Section 15.2.5.2.

Table 228 compares the normalized key filter parameters for the EGSM and DCS bands with those of the two high TX rejection filters.

Table 228: Key Filter Parameters for Each GSM Band

	B9035		B9034		DCS		EGSM 900	
	Actual (MHz)	Scaled	Actual (MHz)	Scaled	Actual (MHz)	Scaled	Actual (MHz)	Scaled
Centre Frequency	881.5	1	1960	1	1842.5	1	942.5	1
Filter Bandwidth	25	0.0284	58.8	0.03	75	0.041	35	0.037
Transition Band	20	0.0227	21.2	0.0108	20	0.0109	10	0.0106
Shape Factor	0.556	-	0.735	-	0.789	-	0.778	-

It can be seen that the scaled parameters and shape factor for the DCS and EGSM bands more closely match the B9034, therefore values for passband attenuation and rejection in the TX band for EGSM900 and DCS were taken directly from the B9034. For specifications outside of the RX and TX band frequencies, the frequency ranges were directly scaled by

the ratio of the centre frequencies; $F_{c-EGSM} \big/ F_{c-B9034}$ for the EGSM band, and $F_{c-DCS} \big/ F_{c-B9034}$ for the DCS band.

The high TX rejection bandpass specifications for all of the bands are given in Section 15.2.5.6.

15.2.5.4   Duplexer Filter Specifications

The EPCOS B7638 duplexer was available for the GSM 850 band and is used in this analysis. For the PCS band, the EPCOS BAW B7633 duplex filter for CDMA applications was used in this analysis. Duplex filters were not found for

the EGSM and DCS bands, so the filter specifications for these bands were derived from the B7633 according to the procedure described in Section 15.2.5.2.

Table 229 and Table 230 compare the normalized key filter parameters for the EGSM and DCS bands with those of the two high TX rejection filters.

Table 229: Key Duplexer Filter Parameters for TX-ANT

	B7638		B7633		DCS		EGSM 900	
	Actual (MHz)	Scaled	Actual (MHz)	Scaled	Actual (MHz)	Scaled	Actual (MHz)	Scaled
Centre Frequency	836.50	1	1880	1	1747.5	1	897.5	1
Filter Bandwidth	25	0.0299	58.8	0.0313	75	0.043	35	0.039
Transition Band	20	0.0239	21.2	0.0117	20	0.0114	10	0.0111
Scale Factor	0.556	-	0.735	-	0.789	-	0.778	-

Table 230: Key Duplexer Filter Parameters for ANT-RX

	B7638		B7633		DCS		EGSM 900	
	Actual	Scaled	Actual	Scaled	Actual	Scaled	Actual	Scaled
Centre Frequency	881.5	1	1960	1	1842.5	1	942.5	1
Filter Bandwidth	25	0.0284	58.8	0.03	75	0.0407	35	0.037
Transition Band	20	0.0227	21.2	0.0112	20	0.0109	10	0.0106
Scale Factor	0.556	-	0.735	-	0.789	-	0.778	-

It can be seen that the scaled parameters for both DCS and EGSM 900 bands more closely match the B7633, in both the transmit and receive path. Therefore values for TX-ANT attenuation, ANT-RX attenuation, and TX-RX isolation are taken from the B7633. For specifications outside of the RX and TX band frequencies, the frequency ranges were directly scaled by the ratio of the centre frequencies as described in Section 15.2.5.2.

While bandpass SAW filters are available for the EGSM and DCS bands (but just not optimized for TX rejection performance), it seems that making duplexers for these frequency band has not been tried. The methodology here is a way to estimate the performance of a duplexer in these bands, and is not a guarantee that the filter will have this performance in reality. In addition, the EGSM filter estimation is based on the PCS filter, which is fabricated using bulk acoustic wave (BAW) technology. However, it is more likely that the EGSM filter would be fabricated using SAW technology, similar to the filter for GSM 850. Similar performance would be expected.

The duplex filter specifications for all of the frequency bands are given Section 15.2.5.6.

15.2.5.5   Worst Case Assumption

For simplicity, only worst case conditions were considered. Minimum rejection figures over temperature were used for the filters and duplexers. Maximum in-band attenuation (insertion loss) figures were also used. If a particular frequency band of interest straddled two different rejection performance regions of a filter, the lowest rejection was assumed to apply to the entire frequency band.

15.2.5.6   Filter Specifications

The bandpass and duplex filter specifications are given in the following tables.

Bandpass Filter Specifications

Sample Standard GSM Bandpass Filters

Minimum Attenuation for Temperatures -30ºC to 85ºC

EGSM Filter		PCS Filter	
Frequency (MHz)	Attenuation (dB)	Frequency (MHz)	Attenuation (dB)
DC-880	48	DC-1830	30
880-905	30	1830-1910	10
905-915	17	2010-2070	10
980-1025	25	2070-2150	22
1025-2880	40	2150-3000	25
2880-6000	18	3000-6000	25
Maximum Insertion Loss 925-960 = 2.7 dB Typical Insertion Loss 925-960 = 1.8 dB		Maximum Insertion Loss 1930-1990 = 3.0 dB Typical Insertion Loss 1930-1990 = 1.8 dB	
GSM 850 Filter		DCS Filter	
DC-824	45	DC-1300	30
824-849	35	1300-1705	30
915-960	20	1705-1785	11
960-2000	35	1920-1980	18
2000-6000	18	1980-2500	22
		2500-3840	25
		3840-6000	25
Maximum Insertion Loss 869-894 = 2.4 dB Typical Insertion Loss 869-894 = 1.7 dB		Maximum Insertion Loss 1805-1880 = 3.0 dB Typical Insertion Loss 1805-1880 = 1.8 dB	

High TX Rejection Bandpass Filters

Minimum Attenuation for Temperatures -30ºC to 85ºC

B9035		B9034	
GSM 850 Filter		**PCS Filter**	
Frequency (MHz)	Attenuation (dB)	Frequency (MHz)	Attenuation (dB)
0.3 – 824	46	0 – 1850.6	40
824 – 849	46	1850.6 – 1909.4	46
914 – 950	20	2040 – 2070	35
950 – 1500	46	2070 – 4500	35
1500 – 2200	46	4500 – 5200	28
2200 – 3000	30	5200 – 6000	18
3000 – 4500	20		
4500 – 6000	15		
Maximum Insertion Loss 869-894 = 2.5 dB Typical Insertion Loss 869-894 = 2.1 dB		Maximum Insertion Loss 1930.6 – 1989.4 = 4.4 dB Typical Insertion Loss 1930.6 – 1989.4 = 2.7 dB	
EGSM900 Filter (Derived from B9034)		**DCS Filter (Derived from B9034)**	
Frequency (MHz)	Attenuation (dB)	Frequency (MHz)	Attenuation (dB)
0-880	40	0-1710	40
880-915	46	1710-1785	46
981-995	35	1918-1946	35
995-2164	35	1946-4230	35
2164-2501	28	4230-4888	28
2501-2885	18	4888-5640	18
Maximum Insertion Loss 925-960 = 4.4 dB Typical Insertion Loss 925-960 = 2.7 dB		Maximum Insertion Loss 1805-1880 = 4.4 dB Typical Insertion Loss 1805-1180 = 2.7 dB	

Duplex Filter Specifications

EPCOS B7638 Cellular Band Mobile Station Duplexer

Minimum Attenuation Performance for Temperature Range -30ºC to 85ºC

TX Port – Antenna Port		Antenna Port – RX Port		TX Port – RX Port	
Frequency (MHz)	Attenuation (dB)	Frequency (MHz)	Attenuation (dB)	Frequency (MHz)	Attenuation (dB)
100 – 698	35	100 – 804	35	100 – 800	50
698 – 746	36	824 – 849	54	824 – 849	55
746 – 804	30	954 – 1648	35	869 – 894	47
869 – 894	45	1648 – 1698	40	954 – 1700	45
954 – 1570	30	1698 – 2547	40		
1570 – 1698	40	2547 – 3000	35		
1698 – 2547	30				
2547 – 3000	20				
Maximum Insertion Loss 824-849 = 2.3 dB Typical Insertion Loss 824-849 = 2.0 dB		Maximum Insertion Loss 869-894 = 2.8 dB Typical Insertion Loss 824-849 = 2.4 dB			

EPCOS B7633 PCS Band BAW Duplexer

Minimum Attenuation Performance for Temperature Range -30ºC to 85ºC

TX– Ant.		Ant. – RX		TX – RX	
Frequency (MHz)	Atten. (dB)	Frequency (MHz)	Atten. (dB)	Frequency (MHz)	Atten. (dB)
0.3 – 1570	31	0.3 – 1770	33	0.3 – 1800	57
1570 – 1580	30	1770 – 1850.6	39	1850.6 – 1907	54
1580 – 1800	29	1850.6 – 1905.4	54	1907 – 1909.4	50
1930.6 – 1935	42	1905.0 – 1909.4	48	1930.6 – 1935	44
1935 – 1989.4	38	2010 – 2070	7	1935 – 1989.4	42
2400 – 2500	34	2070 – 2750	39	2070 – 4200	53
2500 - 3400	20	2750 - 3350	20		
3400 – 4400	25	3350 – 3500	39		
4400 – 5550	5	3500 – 4500	30		
5550 - 5730	5	4500 – 6000	20		
Maximum Insertion Loss 1850.6 – 1909.4 = 3.5 dB Typical Insertion Loss 1850.6 – 1909.4 = 2.1 dB		Maximum Insertion Loss 1930.6 – 1989.4 = 4.5 dB Typical Insertion Loss 1930.6 – 1989.4 = 3.1 dB			

Assumed EGSM900 Duplexer (based on EPCOS B7633 performance)

TX – Ant.		Ant. – RX		TX – RX	
Frequency (MHz)	Attenuation (dB)	Frequency (MHz)	Attenuation (dB)	Frequency (MHz)	Attenuation (dB)
0-750	31	0-851	33		
750-754	30	851 – 880	39		
754-859	29	890 – 912	54	0–859	57
925-928	42	912-915	48	880-913	54
928-960	38	967 – 995	7	913-915	50
1146-1193	34	995 –1322	39	922 – 924	44
1193-1623	20	1322 – 1611	20	924 – 950	42
1623-2101	25	1611 – 1683	39	988 – 2005	53
2101-2735	5	1683 – 2164	30		
		2164 – 2885	20		
Maximum Insertion Loss 880-915 = 3.5 dB Typical Insertion Loss 880-915 = 2.1 dB		Maximum Insertion Loss 925-960 = 4.5 dB Typical Insertion Loss 925-960 = 3.1 dB			

Assumed DCS Duplexer (based on EPCOS B7633 performance)

TX – Ant.		Ant. – RX		TX – RX	
Frequency (MHz)	Attenuation (dB)	Frequency (MHz)	Attenuation (dB)	Frequency (MHz)	Attenuation (dB)
0-1459	31	0– 1664	33		
1459-1469	30	1664 – 1710	39		
1469-1673	29	1710-1778	54	0-1673	57
1805-1811	42	1778-1785	48	1710-1781	54
1811-1880	38	1890-1946	7	1781-1785	50
2231-2324	34	1946 –2585	39	1805-1811	44
2324-3160	20	2585 – 3149	20	1811-1880	42
3160-4090	25	3149 – 3290	39	1924-3904	53
4090-5326	5	3290 – 4230	30		
		4230 – 5640	20		
Maximum Insertion Loss 1710-1785 = 3.5 dB Typical Insertion Loss 1710-1785 = 2.1 dB		Maximum Insertion Loss 1805-1880 = 4.5 dB Typical Insertion Loss 1805-1880 = 2.1 dB			

15.2.5.7 New Duplexer Arrangement for Lower Insertion Loss

In order to alleviate the tough requirements on the duplex filters' transition band slope which leads to high insertion loss, it is proposed to divide the receive/transmit band into two halves and to use different duplex filters for each half band. In this section the concept is explained with the example of EGSM900. However, the relationship between the guard band width and the carrier frequency is similar for DCS1800 or PCS1900. Hence the proposed solution could be attractive for the high bands as well.

15.2.5.7.1 Concept Description

The receive/transmit band is divided into two equal sub-bands. Each duplexer will then have a passband which is only half as wide, and a guard band which is increased by half the passband width. Therefore it can be implemented with a relatively simple filter design which will have very much reduced insertion loss. Extra signal routing switches are needed, but these do not add much loss.

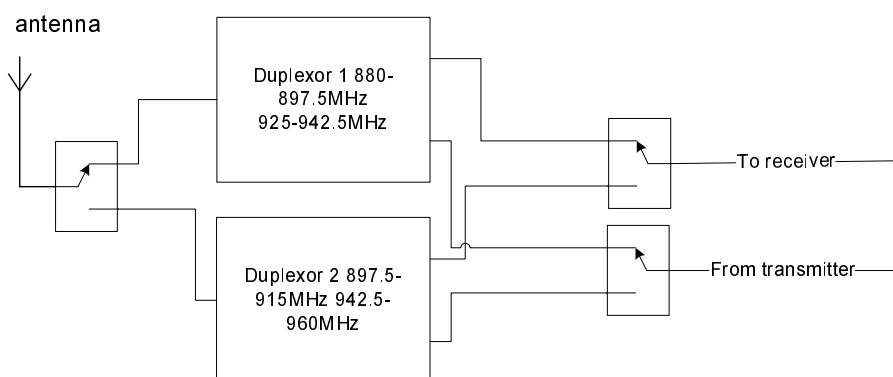Figure 419a and Figure 4196b show an EGSM900 example:

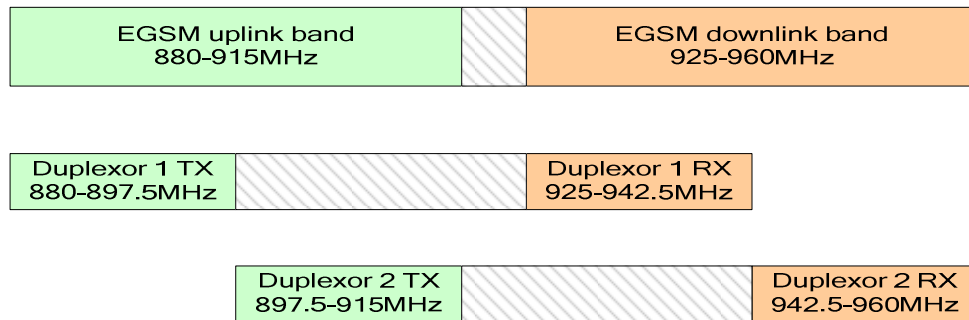**Figure 419a: Block diagram of new duplexer architecture**

Figure 419b: Frequency plan of new duplexer (EGSM band)

A lower insertion loss can be achieved since the transition band slope of each of the duplex filters does not need to be as steep as in the case of a duplex filter covering the whole band. Each of the new duplex filters needs fewer resonators than a conventional duplex filter. However, the total size may not decrease because the number of duplex filters doubles. This also depends on the size of individual duplex filters and this aspect is for further study.

15.2.5.7.2   Impacts on the Specification

There may be a need to change 45.002 annex B1 because the new technique can only support full duplex operation if the uplink and downlink channels are in the same half of the band. A problem will arise if the MS has to monitor a channel in the lower downlink half band (Duplexer 1 RX in Figure 419b) at the same time as transmitting in the upper uplink half band (Duplexer 2 TX in Figure 419b). To allow that the MS monitors all downlink channels with full sensitivity, there should be a point in time in every TDMA frame in which the network neither assigns an uplink nor a downlink slot – at least if the TX channel is in the upper half of the TX band. A similar problem may also occur with frequency hopping and this may further reduce the number of timeslots within a TDMA frame in which full duplex operation is possible using this architecture.

15.2.5.7.3   Impacts on the Analysis

Determination of the estimated filter parameters using this duplexer arrangement, and the subsequent analysis of the various architectures, is TBD.

15.2.6   Void

15.2.6a Basic Type 2 Architecture

15.2.6a.1   Introduction

This section discusses interference in the receive band of a type 2 mobile resulting from non-linearity in the receiver coupled with the presence of a transmit signal. Three different options for basic type 2 receiver architecture are discussed and analyzed. Using the duplexers and filters discussed in section 15.2.5, receiver linearity requirements are determined with respect to TX signal power leakage and interferer signal power (as discussed in section 15.2.2a).

15.2.6a.2   Receiver performance

The RF section receiver performance and linearity values were taken from a typical quad band GSM/EDGE chipset. The parameter values relevant to this analysis are given in Table 231.

Parameter	Value
Total Available Gain	46.0 dB
Maximum Receiver Noise Figure (RF section)	4.6 dB
Cascaded IIP3	-18.0 dBm
Cascaded IIP2	42.9 dBm
Estimated 1dB Compression Point	-28.0 dBm

15.2.6a.3   Mapping Filter Specifications

The duplexers used for this analysis are described in detail in section 15.2.5. The typical GSM receive bandpass filters and the high TX Rejection bandpass filters are also described in that section.

15.2.6a.4   Architecture Details

15.2.6a.4.1   Architecture 1 – The Basic Type 2 Mobile

The first analysis is performed using the architecture shown in Figure 420. This architecture assumes that there is no change in the transmission path regardless of whether the mobile is operating in half duplex mode (a type 1 mobile) or full duplex mode (a type 2 mobile).
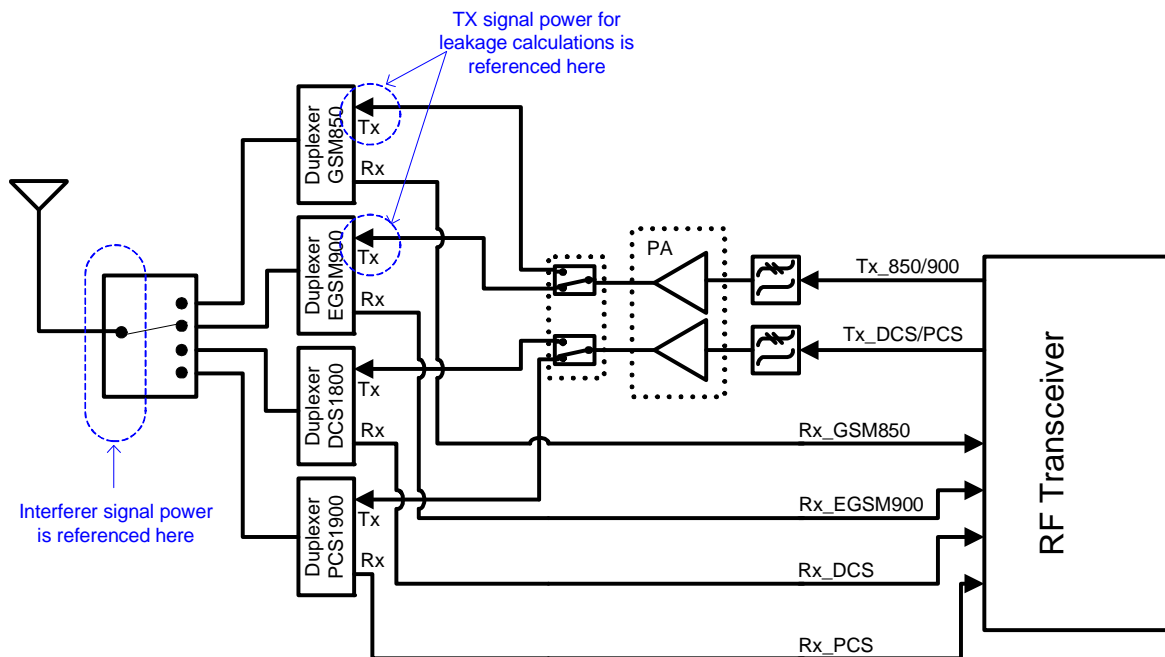
Figure 420: Basic Type 2 Architecture

The PA module shown in the figure comprises one PA for cellular band and one PA for PCS/DCS band. Since the duplex filters that follow the PA modules are band specific, this requires that SPDT switches [17] are placed after the PA. The insertion losses of the duplex filters are discussed in detail in section 15.2.5. The antenna switchplexer requires a SP4T switch [18]. The typical type 1 architecture requires a SP6T switchplexer [19] to support the TX and RX paths. The insertion losses of all the switches and switchplexers in the transmit or receive path are given in Table 232.

Table 232: Switch and Switchplexer Insertion Losses

Part	Application	Path	Cell Band		PCS Band	
			Typical	**Maximum**	**Typical**	**Maximum**
SPDT	Basic Type 2	Transmit	0.3 dB	0.45 dB	0.4 dB	0.6 dB
SP4T	Basic Type 2	Transmit	0.7 dB	0.85 dB	0.8 dB	0.95 dB
SP4T	Basic Type 2	Receive	0.7 dB	0.85 dB	0.8 dB	0.95 dB
SP6T	Type 1	Transmit	0.5 dB	0.7 dB	0.65 dB	0.9 dB
SP6T	Type 1	Receive	1.0 dB	1.2 dB	1.3 dB	1.6 dB

15.2.6a.4.2   Architecture 2 – The Basic Type 2 Mobile with Additional Filtering

In order to reduce the receiver linearity requirements, the TX signal power leakage and the intermodulation interferer power must be reduced. One way to do this is to add a bandpass filter between the duplexer and the receiver input, as shown in Figure 421.
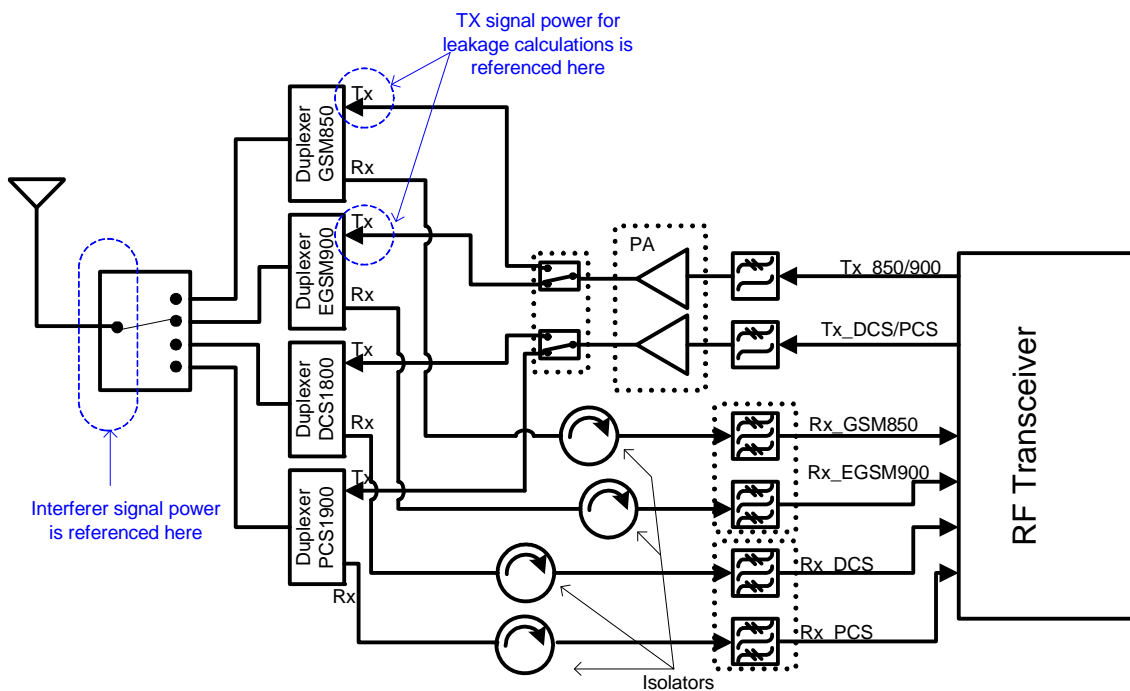

Figure 421: Basic Type 2 Architecture with Additional RX Filtering

The isolators between the duplexers and filters are included to provide a 50Ω impedance to the output of the duplexer and the input of the filter.[2]   They have a maximum insertion loss of 0.6 dB [20].

Two different choices of bandpass filters are analyzed. Typical filters used in type 1 GSM mobile stations are considered first. Then high TX rejection filters are considered.

15.2.6a.5   Analysis of the Basic Type 2 Architecture

This section looks at two different architectures for a basic type 2 GSM mobile. The first uses only the duplex filter for out of band rejection.   This architecture is illustrated in Figure 420 and discussed in section 15.2.6a.4.1. Full duplexer specifications are given in section 15.2.5.

The allowable intermodulation interference level for each band is determined using the method outlined in section 15.2.4a. The target SNR is achievable at the specified input level for all frequency bands, thus no change in the reference sensitivity level is required in this case. The maximum allowable intermodulation interference for each frequency band is given in Table 233.

Table 233: Maximum Allowable Intermodulation Interference for Duplexer Only Case

Frequency Band	GSM 850	EGSM 900	DCS 1800	PCS 1900
Input Signal Level in Interference	-99 dBm	-99 dBm	-99 dBm	-99 dBm
Maximum allowable intermodulation interference	-115.0 dBm	-118.6 dBm	-118.9 dBm	-118.9 dBm

Three cases for the transmitter output power levels are considered.

15.2.6a.5.1   No Maximum Output power Reduction

In this case, in order to meet this specification the PA must exceed the specified maximum power (33 dBm for 850/900 MHz and 30 dBm for 1800/1900 MHz) by the total passive loss to the output of the switchplexer. This output power case illustrates the worst situation for receiver interference in this frequency band, as the maximum amount of TX power will leak through to the RX chain.   The transmit signal power that reaches the receiver input is shown in Table 234.

Table 234: Transmit Signal Power at Receiver Input, Duplexer Only

	GSM Band			
	GSM850	EGSM900	DCS1800	PCS1900
Maximum Transmit Power at Duplexer TX port	36.15 dBm	37.35 dBm	34.45 dBm	34.45 dBm

---

[2] The isolator is likely needed to buffer the duplexer receiver port impedance in the duplexer antenna to Rx port stopband from the filter's input port impedance in the filter stopband. The duplexer and the filter stop bands are very large making the isolator's frequency range extremely broad. However the analysis results suggest that the receiver is most sensitive to interference in the frequency range 915MHz to 937.5MHz which falls inside the Rx band. In the other interference bands there is an enormous amount of margin. It therefore possible that the isolator need only operate well across the RX band, and across the TX band to keep the duplexer and filter rejection of the TX signal high. Only by measuring the cascaded performance of these two components without an isolator can it be conclusively determined if the isolator is needed.

Duplexer TX-RX Isolation in TX Band	55 dB	50 dB	50 dB	50 dB
Transmit Power at Receiver Input	-18.85 dBm	-12.65 dBm	-15.55 dBm	-15.55 dBm

As given in Table 231, the estimated 1 dB compression point of the receiver (C1dB) is -28 dBm. The transmit power at the receiver input exceeds C1dB for all frequency bands, therefore already it can be seen that this metric must be increased just due to TX power leakage alone.

Table 234 shows that the TX power leakage is greatest in the EGSM 900 band. Therefore intermodulation interference, which increases with increasing TX signal power, is also greatest in this band, and so this band is used to determine receiver requirements.

Table 235 shows the second order interferer power level limits (based on the degradation limit discussed in section 15.2.6a.5) for different IIP2 levels. The IIP2 of the typical transceiver chip (42.9 dBm) was far less than needed. To meet the specified blocker requirements with this basic architecture, an IIP2 of 76 dBm is required. This value is much higher than the approximately 60 dBm given in [21]; it is expected that this value is not readily achievable with an integrated receiver.

Table 235: Interferer Power Limits for 2nd Order Interference Bands for EGSM900 Receiver

	2nd Order Interference Bands for EGSM900 (Frequencies are in MHz)	
	10 – 80	1805 – 1875
Duplexer Isolation	33 dB	30 dB
Specified Blocker Power	0 dBm	0 dBm
Threshold Interference Power, IIP2 = 42.9 dBm	-30.1 dBm	-33.1 dBm
Threshold Interference Power, IIP2 = 76.0 dBm	3.1 dBm	0.1 dBm
Shading indicates the power limit is insufficient to meet the blocker specification.		

Table 236 shows maximum interferer power levels the receiver could handle for three different values of IIP3. The typical transceiver IIP3 (-18 dBm) was far less than was needed. The value IIP3 = 5 dBm value was considered as it represents approximately what is used in CDMA mobile chipsets [23]. This too was insufficient. An IIP3 of 36.8 dBm was required to meet the specified blocker levels. This value is much higher than the IIP3 demonstrated in [21]; it is expected that this value is not achievable.

Table 236: Interferer Power Limits for 3rd Order Interference Bands for EGSM900 Receiver

	3rd Order Interference Bands for EGSM900 (Frequencies are in MHz)				
	5 – 40	800 – 905	902.5 – 915	915 – 937.5	2685 - 2790
Duplexer Isolation	33 dB	33 dB	48 dB	3.1 dB	20 dB
Specified Blocker Power	0 dBm	0 dBm	0 dBm	-23 dBm	0 dBm
Interferer Power Limit, IIP3 = -18 dBm	-38.0 dBm	-96.3 dBm	-23.0 dBm	-67.9 dBm	-109.3 dBm
Interferer Power Limit, IIP3 = 5 dBm	-15.0 dBm	-50.3 dBm	0 dBm	-44.9 dBm	-63.3 dBm
Interferer Power Limit, IIP3 = 36.8 dBm	16.8 dBm	13.3 dBm	31.8 dBm	-13.0 dBm	0.3 dBm
Shading indicates the power limit is insufficient to meet the blocker specification.					

The results of this analysis are summarized in Table 237. The required linearity requirements are unrealistic.

Table 237: EGSM900 Linearity Requirements Duplexer Only, No Power Backoff

Receiver Linearity Parameter	Value
P$_{TX port}$	37.4 dBm
IIP2	76.0 dBm

IIP3	36.8 dBm
C1dB (IIP3 – 10dB)	26.8 dBm

15.2.6a.5.2   No Change in PA Capabilities

The second case that is considered is where the PA outputs the same maximum output power as it does with current GSM architectures. The EGSM band is still the hardest to meet because of the duplex filter characteristics. For a type 1 mobile, for EGSM band the maximum PA output power is 33dBm + 0.2 dB (harmonic filter) + 0.7 dB (SP6T switch) = 33.9 dBm. Therefore the maximum output power at the TX port of the duplex filter for the basic type 2 architecture is 33.9 dBm – 0.3 dB = 33.6 dB.

The required receiver linearity parameters for this case are summarized in Table 238.

Table 238: EGSM Linearity Requirements Duplexer Only, No Change in PA Output

Receiver Linearity Parameter	Value
$P_{TX\ port}$	33.6 dBm
IIP2	72.5 dBm
IIP3	33.1 dBm
C1dB (IIP3 – 10dB)	23.1 dBm

This reduction in output power does little to make the required linearity values more reasonable.

15.2.6a.5.3   Power Back Off based on Duplexer Power Tolerance

In this analysis, the TX output power is backed off to 29 dBm at the TX Port of the duplexer. The required receiver linearity parameters for this case are summarized in Table 239.

Table 239: Linearity Requirements Duplexer Only, Power Based on Duplexer Tolerance

Receiver Linearity Parameter	Value
$P_{TX\ port}$	29.0 dBm
IIP2	67.7 dBm
IIP3	28.3 dBm
C1dB (IIP3 – 10dB)	18.3 dBm

Even with this very significant back off in power, the linearity requirements are still very high. Clearly the duplex filter alone is insufficient for this application.

15.2.6a.6   Analysis of the Basic Type 2 Architecture with Typical GSM Receiver Filters

In order to reduce the receiver linearity requirements, the TX signal power leakage and the intermodulation interferer power must be reduced. One way to do this is to add a bandpass filter between the duplexer and the receiver input. This architecture is shown in Figure 421 and discussed in section 15.2.6a.4.2. This architecture will first be analyzed with typical filters used in type 1 GSM mobile stations. Full specifications for these filters are given in section 15.2.5.

The allowable intermodulation interference level for each band is determined using the method outlined in section 15.2.4a. The target SNR is not achievable at the specified input level for all frequency bands. The desired signal level needs to be increased by 3 dB to overcome the increased noise figure of the receiver in this architecture. Given the new input signal level (-96 dBm with interference), the maximum allowable intermodulation interference for each frequency band is given in Table 240.

Table 240: Maximum Allowable Intermodulation Interference for Duplexer + Standard GSM Filter Case

Frequency Band	GSM 850	EGSM 900	DCS 1800	PCS 1900
Input Signal Level in Interference	-96 dBm	-96 dBm	-96dBm	-96 dBm
Maximum allowable intermodulation interference	-114.0	-117.8 dBm	-118.9 dBm	-118.9 dBm

15.2.6a.6.1   No Maximum Output Power Reduction

Table 241 shows the TX signal power that reaches the receiver in this scenario.

Table 241: Transmit Signal Power at Receiver Input

	GSM Band			
	GSM850	EGSM900	DCS1800	PCS1900
Transmit Power at Duplexer TX port	36.15 dBm	37.35 dBm	34.45 dBm	34.45 dBm
Duplexer TX-RX Isolation in TX Band	55 dB	50 dB	50 dB	50 dB
Isolator Insertion Loss	0.6 dB	0.6 dB	0.6 dB	0.6 dB
Filter Rejection	35 dB	17 dB	11 dB	10 dB
Transmit Power at Receiver Input	-54.45 dBm	-30.25 dBm	-27.15 dBm	-26.15 dBm

In this combined filtering case, the TX signal power leakage was greatest in the PCS1900 band. Therefore intermodulation interference, which increases with increasing TX signal power, is also greatest in this band, and so this band is used to determine receiver requirements.

The rejection from the filter improved the second order interference tolerance to the point where the IIP2 performance is sufficient (Table 242).

Table 242: Interferer Power Limits for 2nd Order Interference Bands in the PCS1900 Receiver

	2nd Order Interference Bands for PCS1900 (Frequencies are in MHz)	
	20 – 140	3780 – 3900
Total Isolation (switchplexer + duplexer + isolator + filter)	64.3 dB	56.6 dB
Specified Blocker Power	0 dBm	0 dBm
Threshold Interference Power, IIP2 = 42.9 dBm	14.45 dBm	6.75 dBm

Analysis of third order interference tolerance indicated that IIP3 was insufficient. As shown in Table 243, an IIP3 of 17.2 dBm was required to meet the blocker power specifications. This represents an enormous upgrade in the receiver linearity (from the current -18 dBm). It is also well beyond the +5 dBm typically seen in CDMA receivers [23].

Table 243: Interferer Power Limits for 3rd Order Interference Bands for PCS1900 Receiver

3rd Order Interference Bands for PCS1900 (Frequencies are in MHz)

	10 – 70	1710 – 1830	1830 – 1890	1890 – 1910	1910 – 1950	5630 - 5810
Total Isolation (switchplexer + duplexer + isolator + filter)	64.3 dB	64.4 dB	50.6 dB	59.6 dB	5.5 dB	46.6 dB
Specified Blocker Power	0 dBm	0 dBm	-12 dBm	-12 dBm	-26 dBm	0 dBm
Int. Power Limit, IIP3 = -18 dBm	-0.1 dBm	-38.2 dBm	-52.2 dBm	-5.0 dBm	-58.1 dBm	-56 dBm
Int. Power Limit, IIP3 = 5 dBm	22.9 dBm	7.8 dBm	-6.2 dBm	18.0 dBm	-35.1 dBm	-10 dBm
Int. Power Limit, IIP3 = 17.2 dBm	35.1 dBm	32.2 dBm	18.2 dBm	30.2 dBm	-22.9 dBm	14.4 dBm
Shading indicates the power limit is insufficient to meet the blocker specification.						

The results of this analysis are summarized in Table 244.

Table 244: PCS Band Linearity Requirements Duplexer + Typical Filters, No Power Backoff

Receiver Linearity Parameter	Value
$P_{TX\ port}$	34.45 dBm
IIP2	42.9 dBm (spec)
IIP3	17.2 dBm
C1dB (IIP3 – 10dB)	7.2 dBm

15.2.6a.6.2   No Change in PA Capabilities

In this case the maximum power measured at the PA output for type 1 mobile is 30 dBm + 0.2 dB (harmonic filter) + 1.6 dB (switchplexer) = 31.8 dBm. Therefore the maximum power at the TX port of the duplexer is 31.8 dBm – 0.4 dB (minimum insertion loss of the SPDT) = 31.4

The required receiver linearity parameters for this case are summarized in Table 245.

Table 245: Linearity Requirements Duplexer + Typical Filter, No Change in PA Output

Receiver Linearity Parameter	Value
$P_{TX\ port}$	31.4 dBm
IIP2	42.9 dBm (spec)
IIP3	15.6 dBm
C1dB (IIP3 – 10dB)	5.6 dBm

The IIP3 requirement is still very high with this power back off.

15.2.6a.6.3   Power Back Off based on Duplexer Power Tolerance

In this analysis, the TX output power is backed off to 29 dBm at the TX Port of the duplexer (PCS band). The required receiver linearity parameters for this case are summarized in Table 246.

Table 246: Linearity Requirements Duplexer + Typical Filter, Power Based on Duplexer Tolerance

Receiver Linearity Parameter	Value
$P_{TX\ port}$	29.0dBm
IIP2	42.9 dBm (spec)

IIP3	14.4 dBm
C1dB (IIP3 – 10dB)	4.4 dBm

This small additional power reduction does little to change the requirements.

15.2.6a.7 Analysis of the Basic Type 2 Architecture with High TX Rejection Receiver Filters

TX signal power and intermodulation interference signal power at the receiver input can be further reduced by replacing the standard GSM filters with filters that offer a higher rejection in the TX frequency band. Such filters are available for the GSM800 and PCS1900 bands. The B9035 and B9034 filters from EPCOS are used in this analysis. As described in section 15.2.5, filter characteristics for the EGSM900 and DCS1800 frequency bands were estimated based on the performance of the B9034.

The allowable intermodulation interference level for each band is determined using the method outlined in section 15.2.4a. The target SNR is not achievable at the specified input level for all frequency bands. The desired signal level needs to be increased by 3 dB to overcome the increased noise figure of the receiver in this architecture. Given the new input signal level (-96 dBm with interference), the maximum allowable intermodulation interference for each frequency band is given in Table 247.

Table 247: Maximum Allowable Intermodulation Interference for Duplexer + High TX Rejection Filter Case

Frequency Band	GSM 850	EGSM 900	DCS 1800	PCS 1900
Input Signal Level in Interference	-96 dBm	-96 dBm	-96dBm	-96 dBm
Maximum allowable intermodulation interference	-114.2	-124.3 dBm	-125.1 dBm	-125.1 dBm

15.2.6a.7.1 No Maximum Output Power Reduction

Table 248 shows the TX signal power that reaches the receiver in this scenario.

Table 248: Transmit signal power at receiver input with High TX Rejection Filters

GSM Band			
GSM850	EGSM900	DCS1800	PCS1900

Transmit Power at Duplexer TX port	36.15 dBm	37.35 dBm	34.45 dBm	34.45 dBm
Duplexer TX-RX Isolation in TX Band	55 dB	50 dB	50 dB	50 dB
Isolator Insertion Loss	0.6 dB	0.6 dB	0.6 dB	0.6 dB
Filter Rejection	46 dB	46 dB	46 dB	46 dB
Transmit Power at Receiver Input	-65.45 dBm	-59.25 dBm	-62.15 dBm	-62.15 dBm

Due to the different filter rejections, the EGSM band is now the worst case. Examining IIP2 with the new filter rejection for this band illustrates that the IIP2 of the receiver is sufficient to meet the blocker specifications with ample margin (see Table 249).

Table 249: Power Limits for 2nd Order Interference Bands in the EGSM900 Receiver with High TX Rejection Filters

	2nd Order Interference Bands for EGSM900 (Frequencies are in MHz)	
	10 – 80	1805 – 1875
Total Isolation (switchplexer + duplexer + isolator + filter)	74.3 dB	66.4 dB
Specified Blocker Power	0 dBm	0 dBm
Threshold Interference Power, IIP2 = 42.9 dBm	52.15 dBm	44.25 dBm

Third order intermodulation interference was also greatly reduced with higher rejection filters. Table 250 shows a receiver IIP3 value of 2.5 dBm was sufficient to meet the blocker requirements. This value of IIP3 is in the range of values given in published CDMA receivers ([21], [22]), suggesting these linearity figures are reasonable for an integrated receiver.

Table 250: 3rd Order Intermodulation Threshold Levels for the EGSM900 Receiver with High TX Rejection Filters

	3rd Order Interference Bands for EGSM900 (Frequencies are in MHz)				
	5 – 40	800 – 905	902.5 – 915	915 – 937.5	2685 – 2790
Total Isolation (switchplexer + duplexer + isolator + filter)	74 dB	74 dB	95 dB	6.8 dB	39 dB
Specified Blocker Power	0 dBm	0 dBm	0 dBm	-23 dBm	0 dBm
Int. Power Limit, IIP3 = -18 dBm	23.8 dBm	32.5 dBm	44.8 dBm	-43.4 dBm	-2.2 dBm
Int. Power Limit, IIP3 = 2.5dBm	44.3 dBm	73.5 dBm	65.3 dBm	-23.0 dBm	40 dBm
Shading indicates the power limit is insufficient to meet the blocker specification.					

The results of this analysis are summarized in Table 251.

Table 251: EGSM Linearity Requirements Duplexer + High TX Rejection Filters, No Power Backoff

Receiver Linearity Parameter	Value
$P_{TX\ port}$	36.3 dBm
IIP2	42.9 (spec)
IIP3	2.5 dBm
C1dB (IIP3 – 10dB)	-7.5 dBm

15.2.6a.7.2   No Change in PA Capabilities

In this case the maximum power measured at the PA output is 34.05 dBm, and the maximum power at the TX port of the duplex filter is 33.9 dBm – 0.3 dB = 33.6 dBm[3].

The required receiver linearity parameters for this case are summarized in Table 252.

Table 252: EGSM Linearity Requirements Duplexer + High TX Rejection Filter, No Change in PA Output

Receiver Linearity Parameter	Value
$P_{TX\ port}$	33.6 dBm
IIP2	42.9 dBm (spec)
IIP3	0.6 dBm
C1dB (IIP3 – 10dB)	-9.4 dBm

These linearity figures are reasonable for an integrated receiver.

15.2.6a.7.3   Power Back Off based on Duplexer Power Tolerance

In this analysis, the TX output power is backed off to 29 dBm at the TX Port of the duplexer. The required receiver linearity parameters for this case are summarized in Table 253.

Table 253: EGSM Linearity Requirements Duplexer + High TX Rejection Filter, Power Based on Duplexer Tolerance

Receiver Linearity Parameter	Value
$P_{TX\ port}$	29 dBm
IIP2	42.9 dBm (spec)
IIP3	-1.7 dBm
C1dB (IIP3 – 10dB)	-11.7 dBm

These linearity figures are reasonable for an integrated receiver.

15.2.6a.8   Summary

This discussion document has looked at the intermodulation interference in a basic type 2 mobile. While this is a significant impairment in the receiver, there are other impairments that have not been analyzed here.

Considering only the intermodulation interference analyzed in this document, the analysis above has shown that it is likely possible to build a basic type 2 mobile receiver with sufficient intermodulation immunity given the architecture shown in Figure 421 and the assumptions described.

To address the intermodulation interference it seems that the IIP2 of a typical GSM RF transceiver is sufficient, however the IIP3 would need to be increased to approximately 2.5 dBm (in the case where the output power is not reduced). This value is typical for CDMA receivers and so is likely to be achievable in a highly integrated chipset. If it is permissible to reduce the output power to a level tolerated by the duplexers (30 dBm in GSM850, 29 dBm in EGSM, DCS and PCS bands at the duplexer TX port), then the IP3 requirement is reduced to approximately -1.7 dBm.

---

[3] Note that this power level at the duplex filter may also affect reliability. The power handling ability of the duplexer needs to be examined in more detail.

With this power reduction, the maximum output power at the antenna port of the switchplexer in GSM850 band is (30dBm - 2.0 dB - 0.7) = 27.3 dB. For EGSM900 the maximum output power would be (29dBm - 2.1 dB - 0.7 dB) = 26.2 dBm. For PCS and DCS the maximum output power would be (29 dBm – 2.1 dB - 0.8 dB) = 26.1. For GSM and EGSM a power backoff of about 7 dB is required for GMSK. For DCS/PCS a power back off of about 4 dB is required for GMSK.

The trade offs of building such a type 2 mobile are:

- Output power level must be significantly lowered to not violate duplexer limits. Receive signal power requires an increase of 4 dB to operate at the same S/ (N+I). Thus it is only appropriate in areas with strong signal coverage

- the increase IIP3 and C1dB of the receiver may result in a large receive IC and/or greater power consumption

- there are several new parts required for this architecture, which will increase the physical size and cost to manufacturer of mobiles regardless of the mode of operation

The gains achieved with type 2 operation needs to then be examined in light of the tradeoffs involved in the manufacturing of such a device with the basic architectures presented in this section.

15.2.7　Void

15.2.7a　Modified Type 2 Architecture

15.2.7a.1　Introduction

This section discusses interference in the receive band of a GSM850 and EGSM900 type 2 mobile resulting from non-linearity in the receiver coupled with the presence of a transmit signal. In section 15.2.6a, a basic receiver architecture that used a duplexer followed by a receive band filter is discussed. While this architecture placed seemingly achievable linearity requirements on the receiver active circuitry, it also reduced the receiver sensitivity. In this paper a receiver architecture that places an LNA between the duplexer and receive band filter is examined. Using the duplexers and filters discussed in section 15.2.5, LNA and receiver linearity requirements are determined with respect to TX signal power leakage and interferer signal power (as discussed in section 15.2.2a).

15.2.7a.2　LNA and Post-Filter Receiver Performance

Type 2 GSM mobile chipsets are not currently available; however the architecture presented here is similar to architectures proposed for CDMA receivers ([21] and [22]). The receiver presented in [21] is a good candidate for use in this analysis as it is a recent work and it is a zero-IF architecture, using only a few discrete components. Unfortunately, this receiver was targeted at the cell band (850MHz) only. Because the cell band frequencies are close to the EGSM900 band, it is assumed that a receiver could be fabricated with the same characteristics for the EGSM900 band. The PCS and DCS bands are at approximately twice the frequency of the cell band and will require separate analysis. Therefore this analysis is limited to the cell band and the LNA and post-filter receiver characteristics as presented in [21] are used (Table 254 and Table 255).

Table 254: Assumed LNA Performance Based on Measurements in [21]

Parameter	Nominal Value
Gain	15.5 dB
Noise Figure	1.2 dB
IIP3	11 dBm
IIP2	Unknown
Estimated 1dB Compression Point	1 dBm

Table 255: Assumed Post-Filter Receiver Performance Based on Measurements in [21]

Parameter	Value
Noise Figure	9 dB
Cascaded IIP3	9.2 dBm
Cascaded IIP2	60
Estimated 1dB Compression Point	-0.8 dBm

15.2.7a.3   Mapping Filter Specifications

The duplexers and filters used for this analysis are described in detail in section 15.2.5.

15.2.7a.4   Modified Architecture Details

The modified architecture is based on the basic architecture discussed in section 15.2.6a. An LNA is placed between the duplexer and filter in the receive chain as shown in Figure 422. This architecture assumes that there is no change in the transmitter or receive path regardless of whether the mobile is operating in half duplex mode (a type 1 mobile) or full duplex mode (a type 2 mobile).

The PA module shown in the figure comprises one PA for cellular band and one PA for PCS/DCS band. Since the duplex filters that follow the PA modules are band specific, SPDT switches [17] are placed after the PA. The antenna switchplexer requires a SP4T switch [18]. The specifications for the switches used in this application (and in type 1 mobiles for comparison) are given in Table 256. The duplex filters also have insertion losses associated with them. This is discussed in detail in section 15.2.5.

Table 256: Switch and Switchplexer Insertion Losses

Part	Application	Path	Cell Band		PCS Band	
			Typical	**Maximum**	**Typical**	**Maximum**
SPDT	Modified Type 2	Transmit	0.3 dB	0.45 dB	0.4 dB	0.6 dB
SPDT	Modified Type 2	Receive	0.3 dB	0.45 dB	0.4 dB	0.6 dB
SP4T	Modified Type 2	Transmit	0.7 dB	0.85 dB	0.8 dB	0.95 dB
SP4T	Modified Type 2	Receive	0.7 dB	0.85 dB	0.8 dB	0.95 dB
SP6T	Type 1	Transmit	0.5 dB	0.7 dB	0.65 dB	0.9 dB
SP6T	Type 1	Receive	1.0 dB	1.2 dB	1.3 dB	1.6 dB

In the receive chain, an LNA is placed between the duplexer and the receive band filter. A separate LNA is assumed for each GSM band. By placing switches at the inputs and outputs of the LNAs, it may be possible to use only two LNAs - a single LNA for GSM850 and EGSM900, and a single LNA for DCS1800 and PCS1900. Doing so would require four additional SPDT switches and would desensitize each receiver path by more than the loss of the SPDT switch. This option is not examined here.
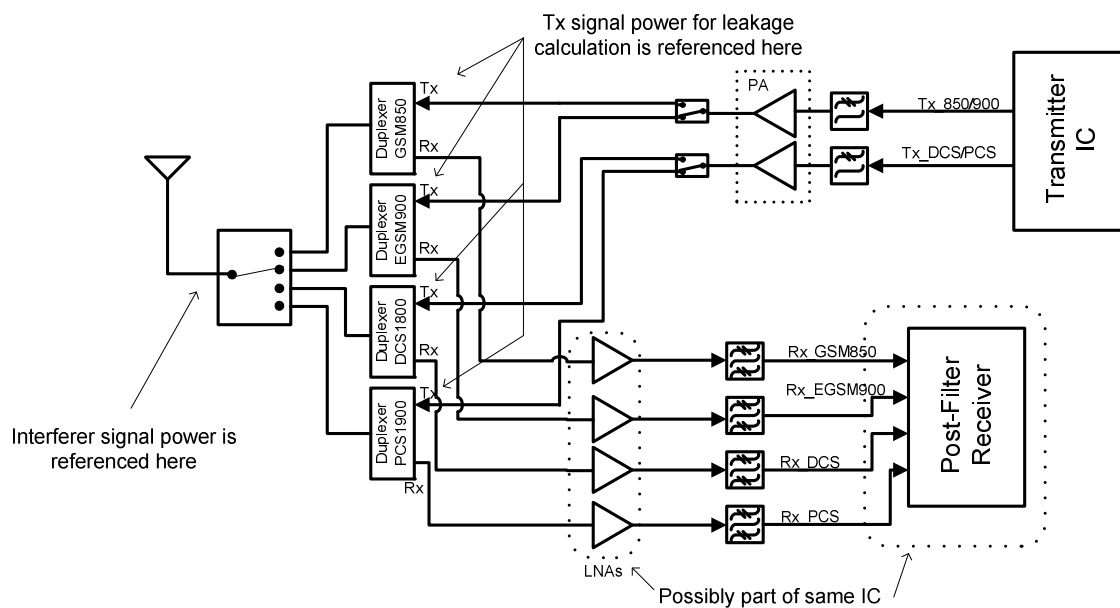
Figure 422: Modified Type 2 Architecture.

The integrated portions of the transmitter and receiver are shown as separate parts to avoid substrate coupling of noise from the transmitter to the receiver. More research is required to determine if it is necessary to separate the two parts, or if they could be integrated together.

15.2.7a.5   Receiver Sensitivity

The analysis assumptions are given in detail in section 15.2.4a.

The advantage to placing an LNA between the duplexer and filters (as shown in Figure 422) is improved sensitivity. Table 257 shows the minimum gain and the maximum noise figure of each component in the entire receive chain from the antenna to the output of the post-filter receiver.

Table 257: EGSM900 Receive Chain Gain and Noise Figure.

	Switchplexer	Duplexer	LNA	Receive Band Filter	Post-Filter Receiver	Cascaded Result
Minimum Gain	-0.85 dB	-4.5 dB	15.5 dB	-4.3 dB	48 dB	53.85 dB
Maximum Noise Figure	0.85 dB	4.5 dB	1.2 dB	4.3 dB	9 dB	8.12 dB

MS receiver sensitivity testing is conducted with a -102 dBm signal applied to the antenna connector [8]. Using the values in Table 257, the signal power at the output of the post-filter receiver is -48.15 dBm (-102 dBm + 53.85 dB). The total noise power at the output of the post-filter receiver is -59.03 dBm (-121 dBm (thermal noise in 200 kHz BW) + 8.12 dB (cascaded NF)[4] + 53.85 dB). The difference between the signal power and noise power at the output is 10.88

---

[4] This NF includes all the losses, gains, and active circuit noise from the antenna connector. Switchplexer loss, duplexer loss, LNA noise figure and gain, filter loss, and post-filter receiver noise figure are included.

dBm. Thus, during simple sensitivity testing, this receiver architecture meets the 10 dBm SNR goal assumed in this document.

15.2.7a.6   Transmitter Output Power Levels

Three cases for the transmitter output power levels are considered as described in section 15.2.3a. They are given again in Table 258 for the GSM 850 and EGSM 900 frequency bands.

Table 258: Transmitter Output Power Levels Considered

	GSM850	EGSM900
No maximum output power reduction	36.15 dBm	37.35 dBm
No change in PA capabilities	33.6 dBm	33.6 dBm
Power back off based on duplexer power tolerance	30 dBm	29 dBm

15.2.7a.7   Analysis Assumptions

The interference and blocking signal frequencies and power levels are discussed in section 15.2.2a.

GSM Type 1 mobile station receivers must pass a sensitivity test with -102 dBm of signal power.   The analysis assumes that a signal to noise ratio of 10 dB is needed between the desired signal and cochannel noise and interferers in order to meet the bit error rate requirement with sufficient margin (as described in section 15.2.3a).

When verifying the immunity to blockers, the desired signal power is raised by 3 dB to -99 dBm. As shown in Figure 422, between the antenna and the post-filter receiver are a switchplexer, a duplexer, an LNA, and an RF filter. The insertion loss of the switches, duplexers and filters is dependent on the GSM band in question. For the EGSM900 band the worst case switchplexer loss (0.85 dB), duplexer loss (4.5 dB), and filter loss (4.3 dB) combine to produce 9.65 dB of loss. Adding the LNA gain of 15.5 dB produces a desired signal level of -93.15 dBm. In keeping with the 10 dB SNR goal, noise and interferer power combined must not exceed -103.15 dBm.

In a 200 kHz bandwidth, there is -121 dBm of thermal noise. Using information from Table 257, the gain up to the input of the post-filter receiver is (-0.85 dB – 4.5 dB + 15.5 dB – 4.3 dB) = 5.85 dB and the cascaded noise figure is 8.12 dB. Adding these numbers gives the noise power referred to the post-filter receiver input (-121 dBm + 5.85 dB + 8.12 dB) = -107.03 dBm.

Converting -103.15 dBm and -107.03 dBm to linear units and subtracting the thermal noise from the total noise and interferer level gives the maximum allowable intermodulation interference before the target 10 dB SNR goal is violated; -105.44 dBm. This number is used to assess the immunity of the receiver to blockers in the intermodulation interference bands. If the power in the intermodulation product of the TX signal and the blocker exceeds -105.44 dBm in the following analysis, the LNA and/or post-filter receiver linearity are deemed insufficient.

Performing the same analysis for the GSM850 case reveals -100.9 dBm as the limit for intermodulation product power.

The receiver's tolerance to interference signal power is determined by the rejection provided by any filtering, and by the linearity of the receiver. Based on the maximum interference signal level, the amount of transmitter power that leaks through to the receiver input, and the duplexer/filter performance, the receiver linearity (IIP2, IIP3, and the 1 dB compression point (C1dB)) required to prevent saturation by the transmit signal and degradation of the receiver sensitivity are determined.

15.2.7a.8   Analysis of the Modified Type 2 Architecture

Analysis of this architecture concentrates on the EGSM900 band as its receiver linearity requirements are more stringent than those of the GSM850 band. There are three reasons for this:

-   The EGSM900 filters and duplexers used in this analysis offer less rejection of the TX signal and blockers than GSM850 filters (section 15.2.5).

- The EGSM900 duplexer has higher insertion loss in the transmit path than the GSM850 duplexer, requiring a stronger TX signal to achieve a given antenna port power. This results in higher TX power leakage to the receiver.

- The EGSM900 band has less SNR margin for intermodulation interference (-105.4 dBm vs. -100.9 dBm for GSM850).

Second and third order intermodulation interference signal power levels at the LNA input and at the input to the post-filter receiver are shown in Table 259 and Table 260. These values are used in the following sections to assess the receiver linearity and determine the required IIP2 and IIP3 values.

In this architecture, there is some flexibility in how gain and linearity is budgeted to the LNA and the post-filter receiver. Because a pre-existing LNA and post-filter receiver is used in this analysis, the gain and linearity budget is set. However, in the analysis that follows, minimum linearity values for the LNA and the post-filter receiver are given when the existing values prove insufficient.

The required IIP3 value for either the LNA or the post-filter receiver depends on the power of the TX signal, and on the power in the strongest interference signal in the third order intermodulation interference bands. As Table 260 shows, with the EGSM900 band duplexers and filters used in this analysis, the strongest third order intermodulation interference signal at the LNA input is in the frequency range 2685 MHz – 2790 MHz (see section 15.2.2a for more on the intermodulation interference frequencies). Over this frequency range, the duplexer provides only 20dB of rejection, much less than in any other interference band. Thus it is the third order intermodulation interference signal power and the TX signal power in this frequency range that dictate the required IIP3 for the LNA.

For the post-filter receiver, it is the third order intermodulation interference signal power that falls in the frequency range 915 MHz – 937.5 MHz that is strongest (Table 260). Thus this frequency range dictates the required IIP3 for the post-filter receiver.

Table 259: 2nd Order Intermodulation Interferer Power Levels and Rejection in EGSM900 Receiver Chain.

	2nd Order Interference Band (Frequencies are in MHz)	
	10 – 80	1805 – 1875
Blocker Power at Antenna Connector	0 dBm	0 dBm
Duplexer Rejection + Switchplexer Loss	33.7 dB	30.7 dB
Intermodulation Interference Power at LNA Input	**-33.7 dBm**	**-30.7 dBm**
LNA Gain	15.5dB	15.5 dB
Filter Rejection	40 dBm	35 dBm
Intermodulation Interference Power at Post-Filter Receiver Input	**-58.2 dBm**	**-50.2 dBm**

Table 260: 3rd Order Intermodulation Interferer Power Levels and Rejection in EGSM900 Receiver Chain.

	3rd Order Interference Band (Frequencies are in MHz)				
	5 – 40	800 - 905	902.5 - 915	915 – 937.5	2685 – 2790
Blocker Power at Antenna Connector	0 dBm	0 dBm	0 dBm	-23 dBm	0 dBm
Duplexer Rejection + Switchplexer Loss	33.7 dB	33.7 dB	48.7 dB	2.8 dB	20.7 dB
Intermodulation Interference Power at LNA Input	**-33.7 dBm**	**-33.7 dBm**	**-48.7 dBm**	**-25.8 dBm**	**-20.7 dBm**
LNA Gain	15.5 dB	15.5 dB	15.5 dB	15.5 dB	15.5 dB

Filter Rejection	40 dB	40 dB	46 dB	2.8 dB	18 dBm
Intermodulation Interference Power at Post-Filter Receiver Input	**-58.2 dBm**	**-58.2 dBm**	**-79.2 dBm**	**-13.1 dBm**	**-23.2 dBm**

15.2.7a.8.1 No Maximum Output power Reduction

With 37.35 dBm (Table 258) of TX signal power at the duplexer TX port for the EGSM900 case, the TX signal power levels shown in Table 261 are present in the receiver.

Table 261: Transmit Signal Power Levels and Rejection in Receiver Chain for EGSM900 with No Maximum Power Reduction.

Maximum Transmit Power at Duplexer TX port	37.35 dBm
Duplexer TX-RX Isolation in TX Band	50 dB
Transmit Power at LNA Input	**-12.65 dBm**
LNA Gain	15.5 dB
Filter TX Band Rejection	46 dBm
Transmit Power at Post-Filter Receiver Input	**-43.15 dBm**

The 1 dB compression point of both the LNA and post-filter receiver (C1dB$_{LNA}$ = 1 dBm and C1dB$_{PFR}$ = -0.8 dBm) is sufficient to handle the leaked TX signal power.

The IIP2 performance of the LNA is not given in [21]; therefore its immunity to intermodulation interference in the second order interference bands cannot be assessed. The analysis can be used to determine the required minimum value for IIP2. Table 259 shows the second order interferer power levels at the LNA input. Using the second order interferer with the highest power level at the LNA input (1805 MHz – 1875 MHz), the required minimum LNA IIP2 of 74.8 dBm is found. This value is very high and it may be difficult to achieve in the LNA.

The additive rejection of the duplexer and the filter reduces the maximum power levels in the second order interference bands to -50.2 dBm at the input to the post-filter receiver. This level is quite low, and the 60 dBm IIP2 of the post-filter receiver is adequate.

Considering the IIP3 performance, Table 262 shows maximum interferer power levels the receiver can tolerate for two different values of IIP3. The existing LNA and post-filter receiver IIP3 (11 dBm and 9.2 dBm respectively) are less than what is needed. The LNA IIP3 must increase to 36.1 dBm and the post-filter receiver IIP3 must increase to 18.1 dBm to tolerate the interference levels. These values are very high, likely beyond what is practical for the integration level of a GSM radio. The required LNA IIP3 is far beyond the demonstrated IIP3 in any of the integrated LNAs summarized in [25].

Table 262: Interferer Power Limits for 3rd Order Interference Bands for EGSM900 Receiver with No Maximum Power Reduction

	3rd Order Interference Bands for EGSM900 (Frequencies are in MHz)				
	5 – 40	800 – 905	902.5 – 915	915 – 937.5	2685 - 2790
Specified Blocker Power	0 dBm	0 dBm	0 dBm	-23 dBm	0 dBm
Interferer Power Limit, LNA IIP3 = 11 dBm Post-filter receiver IIP3 = 9.2 dBm	-8.0 dBm	-37.1 dBm	7.0 dBm	-39.0 dBm	-50.1 dBm
Interferer Power Limit, LNA IIP3 = 36.1 dBm Post-filter receiver IIP3=18.1 dBm	17.0 dBm	13.0 dBm	32.0 dBm	-23.0 dBm	0 dBm
Shading indicates the power limit is insufficient to meet the blocker specification.					

The results of this analysis are summarized in Table 263. The required linearity requirements are likely unrealistic.

Table 263: EGSM900 Linearity Requirements, No Maximum Power Reduction

Receiver Linearity Parameter	Value
$P_{TX\ port}$	37.35 dBm
LNA IIP2	74.8 dBm
Post-filter Receiver IIP2	60 dBm*
LNA IIP3	36.1 dBm
Post-filter Receiver IIP3	18.1 dBm
*Existing receiver value	

15.2.7a.8.2   No Change in PA Capabilities

As shown in Table 258 the TX signal power level at the duplexer TX port is 33.6 dBm. The TX signal power levels shown in Table 264 are present in the receiver.

Table 264: Transmit Signal Power Levels and Rejection in Receiver Chain for EGSM900 with No Change In PA Capabilities

Maximum Transmit Power at Duplexer TX port	33.6 dBm
Duplexer TX-RX Isolation in TX Band	50 dB
Transmit Power at LNA Input	**-16.4 dBm**
LNA Gain	15.5 dB
Filter TX Band Rejection	46 dBm
Transmit Power at Post-Filter Receiver Input	**-46.9 dBm**

With this power level reduction at the duplexer TX port, the required IIP2 of the LNA is reduced somewhat to 71 dBm. This IIP2 value may not be easily achieved in the LNA. The post-filter receiver's IIP2 value of 60dB is sufficient.

The reduction in duplexer TX port signal power reduces the susceptibility of the entire receiver to third order intermodulation interference. Table 265 shows that while the receiver used in this analysis does not have sufficient linearity, the required minimum IIP3 is considerably lower than in the no power reduction case. Minimum LNA and post-filter receiver IIP3 requirements are 32.3 dBm and 16.2 dBm respectively.

Table 265: Receiver 3rd Order Interferer Power Limits for EGSM900 Receiver with No Change In PA Capabilities

	3rd Order Interference Bands for EGSM900 (Frequencies are in MHz)				
	5 – 40	800 – 905	902.5 – 915	915 – 937.5	2685 - 2790
Specified Blocker Power	0 dBm	0 dBm	0 dBm	-23 dBm	0 dBm
Interferer Power Limit, LNA IIP3 = 11 dBm Post-filter receiver IIP3 = 9.2 dBm	-6.2 dBm	-29.6 dBm	8.8 dBm	-37.1 dBm	-42.6 dBm
Interferer Power Limit, LNA IIP3 = 32.3 dBm Post-filter receiver IIP3=16.2dBm	15.2 dBm	13.0 dBm	30.2 dBm	-23.0 dBm	0 dBm
Shading indicates the power limit is insufficient to meet the blocker specification.					

The results of this analysis are summarized in Table 266. The required linearity values are reduced considerably, but not enough to make them reasonable. The required LNA IIP3 in particular is still extremely high relative to recently published LNA performance [25].

Table 266: EGSM Linearity Requirements, No Change in PA Capabilities

Receiver Linearity Parameter	Value
$P_{TX\ port}$	33.6 dBm
LNA IIP2	71 dBm
Post-filter Receiver IIP2	60 dBm*
LNA IIP3	32.3 dBm
Post-filter Receiver IIP3	16.2 dBm
*Existing receiver value	

15.2.7a.8.3   Power Back Off based on Duplexer Power Tolerance

In this analysis, the TX output power is backed off to 29 dBm at the TX Port of the duplexer for EGSM900. For GSM850 the TX duplexer port power only needs to be relaxed to 30 dBm as the duplexer for this band can tolerate an extra 1dB of power. Even with this extra power the GSM850 case requires less IIP2 and IIP3 than the EGSM900 case, as the duplexer and receive band filter for GSM850 reject interfering signals more effectively than the EGSM900 duplexer and receive band filter (see section 15.2.5).

Table 267 shows the TX signal power levels for this case.

Table 267: Transmit Signal Power Levels and Rejection in Receiver Chain for EGSM900 with PA Output Power Reduced to 29 dBm

Maximum Transmit Power at Duplexer TX port	29 dBm
Duplexer TX-RX Isolation in TX Band	50 dB
Transmit Power at LNA Input	**-21 dBm**
LNA Gain	15.5 dB
Filter TX Band Rejection	46 dBm
Transmit Power at Post-Filter Receiver Input	**-51.5 dBm**

Using the TX power at the LNA input (Table 267) and the second order blocker power levels (Table 259), the LNA IIP2 requirement is found to be 66.5 dBm. This value is quite high, and whether it can be achieved in an integrated LNA is FFS. The 60 dBm IIP2 of the post-filter receiver is sufficient.

The reduction in TX power eases the IIP3 requirements slightly. As shown in Table 268, the required minimum LNA IIP3 is 27.8 dBm and the required minimum post-filter receiver IIP3 is 14.1 dBm.

Table 268: Receiver 3rd Order Interferer Power Limits for EGSM900 Receiver with PA Output Power Reduced to 29 dBm.

	3rd Order Interference Bands for EGSM900 (Frequencies are in MHz)				
	5 – 40	800 – 905	902.5 – 915	915 – 937.5	2685 - 2790
Specified Blocker Power	0 dBm	0 dBm	0 dBm	-23 dBm	0 dBm
Interferer Power Limit, LNA IIP3 = 11 dBm Post-filter receiver IIP3 = 9.2 dBm	-3.9 dBm	-20.4 dBm	11.1 dBm	-34.8 dBm	-33.4 dBm
Interferer Power Limit, LNA IIP3 = 27.7 dBm Post-filter receiver IIP3=14.1 dBm	12.9 dBm	13.0 dBm	27.9 dBm	-23.0 dBm	0 dBm
Shading indicates the power limit is insufficient to meet the blocker specification.					

The required receiver linearity parameters for this case are summarized in Table 269. The required IIP3 of the LNA is well beyond recently published results [25]. Even with this very significant back off in power, the post-filter receiver IIP3 requirements are still very high and are well beyond the performance of the receiver used in this analysis.

Table 269: Linearity Requirements of Receiver, PA Output Power Reduced to 29 dBm.

Receiver Linearity Parameter	Value
$P_{TX\ port}$	29 dBm
LNA IIP2	66.5 dBm
Post-filter Receiver IIP2	60 dBm*
LNA IIP3	27.8 dBm
Post-filter Receiver IIP3	14.1 dBm
*Existing receiver value	

15.2.7a.9   Blocker Power Reduction

As shown in section 15.2.7a.8, the integrated receiver together with the duplexers and filters used in this analysis were unable to provide the needed linearity. However this architecture is used in CDMA designs.   The applicability in one case but not the other relates to the way that GSM receivers are evaluated compared to CDMA receivers, in particular with respect to blocking specifications.

In [27], minimum performance of cdma2000 receivers is specified. Referring to section 3.5 of [27], it can be seen that blocker specifications are only given for Band Class 6 mobile stations. Band Class 6 mobile stations are for the 2GHz IMT - 2000 band (TX 1920-1980MHz and RX 2110-2170MHz). As given in table 3.5.5.2-1 of [27], the in-band blocker power is -56 dBm for close in blockers, and -44 dBm for other in-band blockers. Out of band blockers are defined in table 3.5.5.2-2 of [27]. The out of band blocker power varies depending on frequency offset. Closest to the desired frequency band the blocker level is given as -44 dBm. Slightly further out the blocker level increases to -30 dBm. Further out the blocker level rises to -15 dBm. However 24 exceptions are allowed where the blocker level requirement is subsequently dropped to -44 dBm.   Clearly these blocker levels are significantly lower than those specified in [8] for GSM.

In all other band classes except band 6, the single tone desensitization test applies. This test measures the receiver's ability to receive a CDMA signal on its assigned channel frequency in the presence of a single tone spaced at a given frequency offset from the center frequency of the assigned channel.

For the single tone desense test, the blocker power levels are -30 dBm and -40 dBm (depending on the frequency offset, see table 3.5.2.2-1 of [27]). As described in [23], the limiting factor in this test is typically cross modulation. The AM portion of the TX signal modulates the blocker tone which is close to the desired signal. This is the primary consideration given to TX signal related intermodulation in a CDMA MS.

It may be possible to make this architectural option applicable to GSM by reducing the blocker power levels as specified in [8]. For EGSM900, in-band and out of band blocker power levels are -23 dBm and 0 dBm respectively. For the case where the transmitter output power is reduced to 29 dBm, the blocker specifications need to be dropped to -34 dBm for out of band blockers and to -35 dBm for in-band blockers in order for the receiver, duplexers, and filters used in this analysis to have sufficient performance (see Table 268).

Maintaining the output power as per the specifications would require the in-band blocker level to be reduced to -39 dBm and out of band blocker level reduced to – 50 dBm.   Also, this does not consider the cross-modulation analysis,

which may further reduce the tolerable blocker levels.

Reducing blocker levels will decrease system capacity depending on factors such as cell radii, reuse pattern, and desense from other sources. Significant analysis would be required to determine if this is an acceptable approach.

15.2.7a.10   Summary

The analysis above has shown that it is likely not possible to build a type 2 mobile receiver (using the presented receiver architecture) with sufficient interferer immunity, based on currently available components and the current blocker specifications.

Even with the TX power backed off to the limit the duplexer can handle, the required LNA IIP3 is 27.8 dBm and the required post-filter receiver IIP3 is 14.1 dBm. The required LNA IIP3 is beyond recently published integrated LNA results [25]. Achieving this linearity in an integrated LNA while maintaining an acceptably low noise figure and reasonable power consumption may not be possible.

Achieving the required IIP3 performance required in the integrated post-filter receiver may, similarly, prove difficult trading off other performance metrics such as receiver noise figure, size, and current consumption.

The required LNA IIP2 is as high as 74.8 dBm (for the full TX power case) and as low as 66.5 dBm (for the TX power backed off to the duplexer limit). Recent publications regarding achievable IIP2 concentrate on mixer performance, as the mixer appears to be the limiting component in determining the overall IIP2 performance of a direct down conversion receiver [26]. There is little available literature concerning LNA IIP2 therefore more research is required to determine if the requirements determined in this document can be achieved.

With the additional suppression of the second order intermodulation interference bands provided by the filter, the post-filter receiver's IIP2 value was sufficient for all the TX power levels examined.

Improving the duplexer and filter rejection of the TX signal would reduce the linearity requirements of the LNA and post-filter receiver. Unfortunately there do not appear to be any duplexers or filters (SAW, BAW, or FBAR) currently available that offer significant improvement over the ones used in this analysis. It may be unrealistic to expect greater TX rejection, particularly from the duplexer. Reducing the blocker power levels may make this architecture useful for use in a type 2 mobile, however the consequences of reducing blocker power levels must be carefully considered. More analysis is need before this option can be considered.

The IIP3 and IIP2 values presented in this analysis considered only intermodulation interference involving the TX signal. Other issues such as cross modulation, and zero IF related baseband sensitivity degradation may require even higher values of IIP2 and IIP3.

15.2.8   Void

15.2.8a   Hybrid Type 2 Architecture

15.2.8a.1   Introduction

This section discusses interference in the receive band of a type 2 mobile resulting from non-linearity in the receiver coupled with the presence of a transmit signal. A hybrid architecture is discussed, which allows the mobile to operate as a type 2 mobile, but also permits it to operate in type 1 mode with less loss than the type 2 architecture imposes. Using the duplexers and filters discussed in section 15.2.5, receiver linearity requirements (for type 2 operation) are determined with respect to TX signal power leakage and interferer signal power (as discussed in section 15.2.2a). The performance in type 1 mode with the hybrid architecture is compared to that of a traditional quad-band GSM mobile to examine the additional losses. A variation is proposed to minimize the additional losses.

15.2.8a.2   Receiver performance

The RF section receiver performance and linearity values were taken from a typical Quad Band GSM/EDGE chipset. The parameter values relevant to this analysis are given in Table 270.

Table 270: Typical GSM/EDGE Receiver Performance Specifications

Parameter	Value
Total Available Gain	46.0 dB
Maximum Receiver Noise Figure	4.6 dB
Cascaded IIP3	-18.0 dBm
Cascaded IIP2	42.9 dBm
Overall 1dB Compression Point	-28.0 dBm

15.2.8a.3   Mapping Filter Specifications

The duplexers used for this analysis are described in detail in section 15.2.5. The typical GSM receive bandpass filters and the high TX Rejection bandpass filters are also described in that document.

15.2.8a.4   Architecture Details

15.2.8a.4.1   The Hybrid Type 2 Architecture

This section analyzes the intermodulation interference using the type 2 mobile architecture shown in Figure 423.   The motivation behind this hybrid architecture is to permit the mobile to operate in type 1 (i.e. half duplex) mode when appropriate, while minimizing the additional path loss.

As it was determined in section 15.2.6a that the standard GSM receiver filters used in type 1 mobiles were insufficient for type 2 operation, the receive filters considered in the hybrid architecture are the high TX rejection RX filters that are discussed in section 15.2.5. Because the insertion loss of these filters is slightly higher than that of the typical GSM receiver filters, and due to the higher insertion loss from the addition of the switches, the performance of the hybrid mobile when operating in type 1 mode will not be equivalent to a legacy type 1 mobile, however it will be significantly better than the performance of the basic type 2 architecture described in section 15.2.6a.
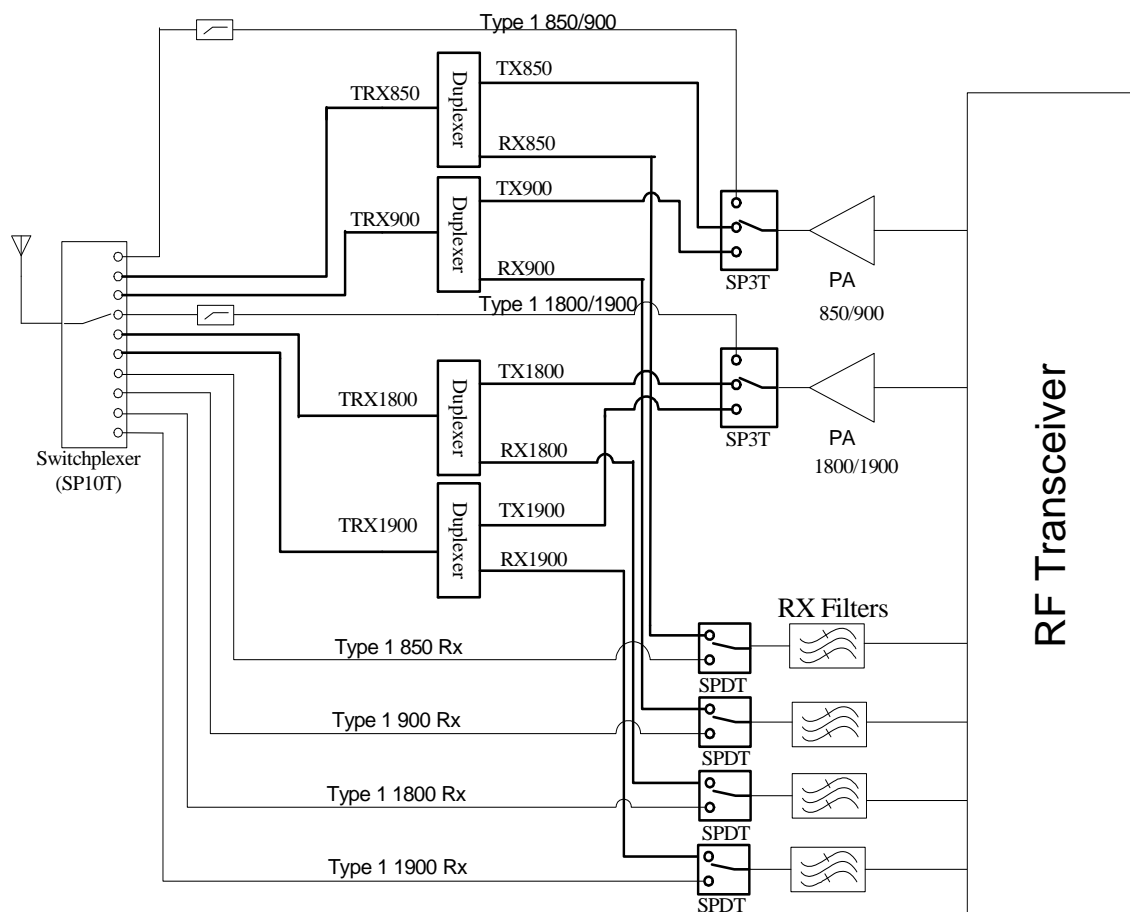
Figure 423: Hybrid Type 2 Architecture

The hybrid type 2 mobile architecture allows the duplexers to be switched out of the TX/RX path when not necessary. In the receive path, a SPDT switch [17] needs to be placed before the RX filters to allow a direct path from the antenna switch and the RF transceiver.

A SP3T switch [28] is required after the PA to allow for a bypass around the duplex filters.   When the duplexers are bypassed, a harmonic filter is required prior to the switchplexer. This is the same as in the type 1 architecture shown in Figure 424.

The switchplexer connecting the various RX and TX paths to the antenna requires a SP10T switch. An example for this part was not found; therefore the characteristics of this switch were taken from a SP9T switch [29].

The typical type 1 architecture requires a SP6T switchplexer [19] to support the TX and RX paths. The basic type 2 architecture requires a SP4T switchplexer [18]. The insertion losses of all the switches and switchplexers in the transmit or receive path are given in Table 271.

Table 271: Switch and Switchplexer Insertion Losses

Part	Application	Path	Cell Band		PCS Band	
			Typical	Maximum	Typical	Maximum
SPDT	Basic Type 2	Transmit	0.3 dB	0.45 dB	0.4 dB	0.6 dB
SPDT	Hybrid Type 2	Receive	0.3 dB	0.45 dB	0.4 dB	0.6 dB
SP3T	Hybrid Type 2	Transmit	0.3 dB	0.6 dB	0.3 dB	0.6 dB
SP10T	Hybrid Type 2	Transmit	0.9 dB	1.15 dB	1.15 dB	1.40 dB
SP10T	Hybrid Type 2	Receive	0.9 dB	1.1 dB	1.35 dB	1.55 dB
SP4T	Basic Type 2	Transmit	0.7 dB	0.85 dB	0.8 dB	0.95 dB
SP4T	Basic Type 2	Receive	0.7 dB	0.85 dB	0.8 dB	0.95 dB
SP6T	Type 1	Transmit	0.5 dB	0.7 dB	0.65 dB	0.9 dB
SP6T	Type 1	Receive	1.0 dB	1.2 dB	1.3 dB	1.6 dB

15.2.8a.4.2 Traditional Type 1 Architecture

The traditional type 1 architecture shown in Figure 424 is used as a performance benchmark for the hybrid architecture when operating in type 1 mode. The increased requirements for TX output power due to additional losses in the TX path, and the loss of sensitivity due to additional losses in the RX path are considered. The linearity requirements for this architecture are met with the standard GSM chipset specifications as given in Table 270.
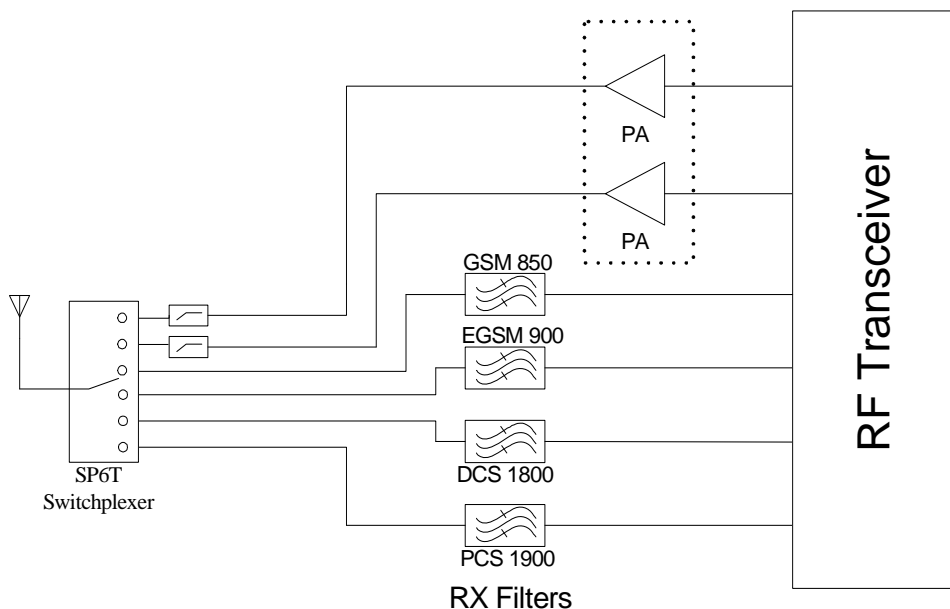
Figure 424: Typical Type 1 Architecture

15.2.8a.5 Type 2 Operation Analysis

15.2.8a.5.1 Assumptions

Three output power cases (as described in section 15.2.3a) for type 2 operation are considered. The interference and blocking signal frequencies and power levels are discussed in section 15.2.2a. Analysis assumptions are given in section 15.2.4a.

For this hybrid architecture, the required SNR is not achievable at the specified input level for all frequency bands. The desired signal level needs to be increased by 4 dB to overcome the increased noise figure of the receiver in this architecture. Given the new input signal level (-95 dBm with interference), the maximum allowable intermodulation interference for each frequency band is given in Table 272.

Table 272: Maximum Allowable Intermodulation Interference Hybrid Architecture

Frequency Band	GSM 850	EGSM 900	DCS 1800	PCS 1900
Input Signal Level in Interference	-95 dBm	-95 dBm	-95dBm	-95 dBm
Maximum allowable intermodulation interference	-113.7	-122.5	-127.2 dBm	-127.2 dBm

15.2.8a.5.2 No Maximum Output power Reduction

In this case, in order to meet this specification the PA must exceed the specified maximum power (33 dBm for 850/900 MHz and 30 dBm for 1800/1900 MHz) by the total passive loss to the output of the switchplexer. This output power case illustrates the worst situation for receiver interference in this frequency band, as the maximum amount of TX power will leak through to the RX chain.

Table 273: Transmit signal power at receiver input

	GSM Band			
	GSM850	EGSM900	DCS1800	PCS1900
Maximum Transmit Power at Duplexer TX port	36.45 dBm	36.75 dBm	34.9 dBm	34.9 dBm
Duplexer TX-RX Isolation in TX Band	55 dB	50 dB	50 dB	50 dB
SPDT Switch	0.3 dB	0.3 dB	0.4 dB	0.4 dB
High TX Rejection RX Filter	46	46	46	46
Transmit Power at Receiver Input	-64.85 dBm	-58.65 dBm	-61.5 dBm	-61.5 dBm

Table 273 shows that the TX power leakage is greatest in the EGSM 900 band. Therefore intermodulation interference, which increases with increasing TX signal power, is also greatest in this band, and so this band is used to determine receiver requirements.

Table 274 shows the second order interferer power level limits (based on the degradation limit discussed in section 15.2.8a.5.1) for different IIP2 levels. The second order input intermodulation point of the typical transceiver chip (42.9 dBm) was easily sufficient.

Table 274: EGSM 900, 2nd Order Intermodulation Threshold Levels for Type 2 Operation

	2nd Order Interference Bands for EGSM900 (Frequencies are in MHz)	
	10 – 80	1805 – 1875
Total Isolation (switchplexer + duplexer + SPDT + filter)	74.2 dB	66.8 dB
Specified Blocker Power	0 dBm	0 dBm
Threshold Interference Power, IIP2 = 42.9 dBm	53.2dBm	45.8 dBm

In the third order intermodulation interference analysis shown in Table 275, it is seen that a receiver IIP3 value of 2 dBm was sufficient to meet the blocker requirements. This value of IIP3 is in the range of values given in published CDMA receivers ([21],[22]), suggesting this linearity figure is likely reasonable for an integrated receiver.

Table 275: EGSM 900, 3rd Order Intermodulation Threshold Levels for Hybrid Type 2 Operation

	3rd Order Interference Bands for EGSM900 (Frequencies are in MHz)				
	5 – 40	800 – 905	902.5 – 915	915 – 937.5	2685 – 2790
Total Isolation (switchplexer + duplexer + SPDT + filter)	74.2 dB	74.2 dB	95.2 dB	7.0 dB	40.0 dB
Specified Blocker Power	0 dBm	0 dBm	0 dBm	-23 dBm	0 dBm
Int. Power Limit, IIP3 = -18 dBm	24.3 dBm	33.0 dBm	45.3 dBm	-43.0 dBm	-1.3 dBm
Int. Power Limit, IIP3 = 2.0 dBm	44.3 dBm	73.0 dBm	65.3 dBm	-23.0 dBm	38.7 dBm
Shading indicates the power limit is insufficient to meet the blocker specification.					

The results of this analysis are summarized in Table 276. The required linearity requirements are realistic.

Table 276: EGSM900 Linearity Requirements for Hybrid Architecture, No Power Backoff

Receiver Linearity Parameter	Value
$P_{TX\ port}$	37.6 dBm
IIP2	42.9 dBm (spec)
IIP3	2 dBm
C1dB (IIP3 – 10dB)	-8 dBm

15.2.8a.5.3 No Change in PA Capabilities

The required receiver linearity parameters for this case are summarized in Table 277. This reduction in output power makes the required linearity values slightly lower.

Table 277: EGSM Linearity Requirements for Hybrid Architecture, No Change in PA Output

Receiver Linearity Parameter	Value
$P_{TX\ port}$	33.6 dBm
IIP2	42.9 dBm (spec)
IIP3	0 dBm
C1dB (IIP3 – 10dB)	-10 dBm

15.2.8a.5.4 Power Back Off based on Duplexer Power Tolerance

Required receiver linearity parameters for this case are summarized in Table 277. This reduction in output power makes the required linearity values even lower.

Table 278: EGSM Linearity Requirements for Hybrid Architecture, Power Based on Duplexer Tolerance

Receiver Linearity Parameter	Value
$P_{TX\ port}$	29.0 dBm
IIP2	42,9 dBm (spec)
IIP3	-2.3 dBm
C1dB (IIP3 – 10dB)	-12.3 dBm

15.2.8a.6 Type 1 Operation – Comparison with Legacy Terminals

15.2.8a.6.1 Transmitter Path

The transmitter path of the legacy mobile and the transmitter path of the hybrid operating in type 1 mode differ in two ways. The SP3T switch after the PA is added, and the SP6T switchplexer is changed to an SP10T switch.

The SP3T switch has a maximum insertion loss of 0.6 dB. The maximum insertion loss of the SP6T switchplexer in the TX path is 0.9 dB, while the maximum insertion loss of the SP10T switch is 1.40 dB. Therefore there is a 0.5 dB increase loss increase due to the switch. The total increase in the transmit insertion loss for type 1 mode is 1.1 dB. The maximum insertion losses occur for the DCS/PCS band. For a type 1 mobile in DCS/PCS, the maximum power required at the output of the PA is (30 dBm + 0.2 dB (harmonic filter) + 0.9 B SP6T insertion loss) = 31.1 dBm. With the assumptions given in section 15.2.8a.5, the current draw for this output is 0.68 A (during TX, assuming 1/8 duty cycle, i.e. voice).

The increase of 1.1 dB means that the PA in a hybrid architecture operating in type 1 mode will need to put out 1.1 dB more power to have the same output power at the antenna port of the switchplexer. Therefore the output power is 32.2 dBm. The current draw for this output is 0.87 A. This represents an increase in power consumption during TX of approximately 29%. This will have an impact on talk time.

15.2.8a.6.2 Receiver Path

The receive path of the legacy mobile and the receive path of the hybrid operating in type 1 mode differ in two ways. The SPDT switch is added, and the SP6T switchplexer is changed to an SP10T switch. Also instead of typical GSM receive filters, high TX rejection filters have had to be used.

Maximum losses are in the DCS/PCS frequency band. The SPDT switch has a maximum insertion loss of 0.6 dB. The maximum insertion loss of the SP6T switchplexer in the RX path is 1.6 dB, while the maximum insertion loss of the SP10T switch is 1.55 dB, for a -0.05 dB difference. The typical GSM filter has a maximum insertion loss of 3.0 dB, while the high TX rejection filter has an insertion loss of 4.4 dB. Therefore the total increase in path loss for the hybrid architecture operating in type 1 mode (compared to a legacy mobile) is 1.95 dB.

15.2.8a.7 Type 1 Operation – Comparison with Legacy Terminals Using a Modified Hybrid Architecture

This increase can be significantly reduced by increasing the part count and rearranging the architecture slightly. The modified hybrid architecture is shown in Figure 425.
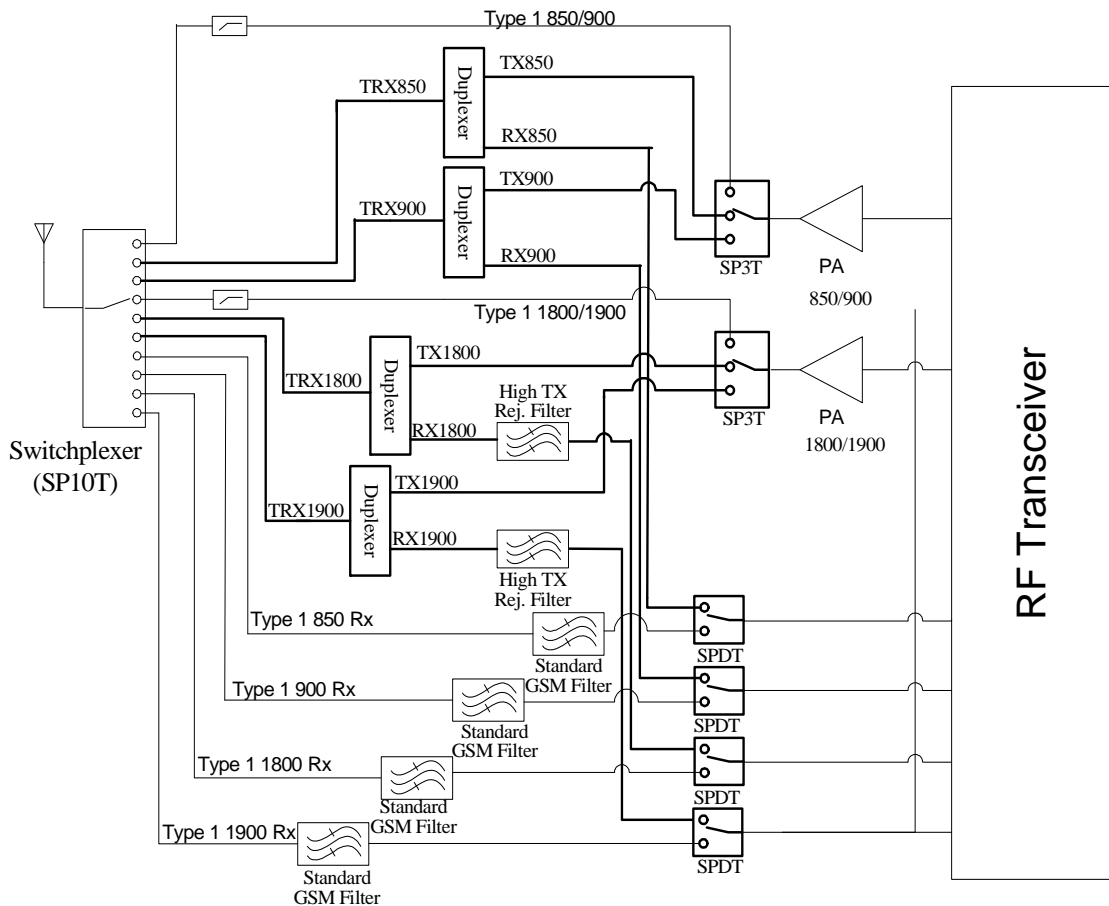
Figure 425 - Modified Hybrid Type 2 Architecture

The modification in this architecture places the standard GSM bandpass filters between the switchplexer and the SPDT switches on the type 1 path, and places the high TX rejection filters between the duplex filter and the SPDT switches on the type 2 paths. This means that when operating in type 1 mode, the mobile doesn't have to incur the additional insertion loss of the high TX rejection filters, which aren't needed in this mode in any case. This would save 1.4 dB of the 1.95 dB additional loss, making the different in receiver sensitivity only 0.55 dB. The architecture change does not improve the additional loss in the transmit path, and adding the two extra receive filters. However having two extra receive filters in the design increases the space requirements and the BOM costs, and the benefit would have to be weighed against these costs.

15.2.8a.8   Summary

This discussion document has looked at the intermodulation interference in a hybrid type 2 mobile. While this is a significant impairment in the receiver, there are other impairments that have not been analyzed here.

Considering only the intermodulation interference analyzed in this document, the analysis above has shown that it is likely possible to build a hybrid type 2 mobile receiver with sufficient intermodulation immunity. If the architecture shown in Figure 425 is utilized, the sensitivity degradation in type 1 mode can be reduced to just a little over 0.5 dB. To address the intermodulation interference it seems that the IIP2 of a typical GSM RF Transceiver is sufficient, however the IIP3 would need to be increased to approximately 2 dBm (in the case where the output power is not reduced). If it is permissible to reduce the output power to a level tolerated by the duplexers (30 dBm in GSM850, 29 dBm in EGSM, DCS and PCS bands at the duplexer TX port), then the IP3 requirement is reduced to approximately -2 dBm.

With this power reduction, the maximum output power at the antenna port of the switchplexer in GSM850 band is (30dBm - 2.0 dB - 0.9) = 27.1 dB. For EGSM900 the maximum output power would be (29dBm - 2.1 dB - 0.9 dB) = 26 dBm. For PCS and DCS the maximum output power would be (29 dBm – 2.1 dB - 1.15 dB) = 25.75. For GSM and EGSM a power backoff of 7 dB is required for GMSK. For DCS/PCS a power back off of 4.25 dB is required for GMSK.

The trade offs of building such a hybrid mobile are:

- type 2 mode of operation must operate at significantly lower output power and requires an increase of 4dB in the receive signal level for the same SNR. Thus it is only appropriate in areas of strong signal coverage

- the increase IIP3 and C1dB of the receiver may result in a large receive IC and/or greater power consumption

- type 1 mode of operation requires 1.1 dB greater PA output power to transmit at the same power level. This increases the current consumption when transmitting by approximately 29%.

- there are several new parts required for this architecture, which will increase the physical size and cost to manufacturer of mobiles regardless of the mode of operation

The remaining impairments need to be analyzed to determine the full requirements. The gains achieved with type 2 operation needs to then be examined in light of the tradeoffs involved in the manufacturing of such a device.

15.2.9   Areas for Further Study

There are several areas that need further study for this implementation. To name a few:

- It needs to be evaluated whether the attenuation in the paired frequency bands that is offered by the duplex filters is enough to meet spectral and interference requirements for GSM.

- The impact of the duplex filter return loss (both TX and RX port) on mismatch loss needs to be assessed.

- The impact of the inband ripple of the duplex filters (up to 3.0 dB at temperature extremes) on equalizer performance needs to be assessed.

- Current integrated circuits would have to be redesigned because of the changes in integration and routing in the major blocks.

- The mobile station would need to support power control in type 2 mode. The power level changes between slots and the initially power ramping all need to be done without impacting the receiver performance.

- Mobile type switching between slots should be evaluated.

- RX Band Noise from the PA leaking into the receiver should be evaluated band (likely insignificant, but would have an additive effect).

- Cross modulation effects when close in blockers or adjacent channels are present (likely significant, needs a thorough and statistical analysis).

- Reverse intermodulation products of the PA in the presence of an external blocker (may necessitate an isolator at the output of the PA, which would add more loss in the TX path).

15.3   References

[1]   AHGEV-060035, Modified Dual Symbol Rate Concept for Future GERAN Evolution, AdHoc on GERAN Evolution, May 2006

[2]   AHGEV-060016: "Discussion on Uplink Coverage," AdHoc on GERAN Evolution, May 2006

[3]   NP-010125, 3GPP TSG CN Plenary #11, Palm Springs, U.S.A, 14th - 16th March 2001

[4]   void

[5]   void

[6]   EPCOS Preliminary Data Sheet, "SAW Components - Preliminary Data Sheet B7638", October 2005.

[7]   void

[8]   3GPP TS 45.005, "Technical Specification; 3rd Generation Partnership Project; Technical Specification Group GSM/EDGE Radio Access Network; Radio Transmission and Reception", (3rd Generation Partnership Project (3GPP) Technical Specification).

[9]   TDoc GP-070113, "Interference Frequencies for Type 2 Mobiles", GERAN #33, Feb. 12-16, 2007.

[10]   TDoc GP-070114, "Duplexer and Receiver Filter Requirements for Type 2 Mobiles", GERAN #33, Feb. 12-16, 2007.

[11]   TDoc GP-070115, "MS Receiver Implementation Analysis for Basic Type 2 Architecture", GERAN #33, Feb. 12-16, 2007.

[12]   TDoc GP-070116, "MS Receiver Implementation Analysis for Modified Type 2 Architecture", GERAN #33, Feb. 12-16, 2007.

[13]   TDoc GP-070117, "MS Receiver Intermodulation Analysis for Hybrid Type 2 Architecture", GERAN #33, Feb. 12-16, 2007.

[14]   EPCOS data sheet, "SAW Components – BAW Duplexer, 1900 MHz CDMA (IS95), B7633", Version 2.0, August 17, 2006.

[15]   EPCOS data sheet, "SAW Components – SAW Rx Filter GSM 850, B9035", Version 2.0, Dec 06, 2005.

[16]   EPCOS data sheet, "SAW Components – SAW Rx Filter PCS/ WCDMA band II, B9034", Version 1.1, October 20, 2006.

[17]   Triquint Semiconductor Specification, "CSH210R; General Purpose SPDT Switch", Version 5.0, December 16, 2003.   http://www.triquint.com/docs/o/CSH210R/CSH210R.pdf

[18]   M/A-COM Electronics, "MASW-007813 V2 GaAs SP4T High Power Switch, DC-3GHz". http://www.macom.com/DataSheets/MASW-007813.pdf

[19]   M/A-COM Electronics, "MASWSS0091 GaAs SP6T 2.5V High Power Switch, Dual/Tri/Quad-band GSM Applications", Version 3.00. http://www.macom.com/data/datasheet/Final%20MASWSS0091%20Rev%203.pdf

[20]   TDK Electronics, "CU Series Isolators for Cellular Phone", TDK Data Sheet. http://www.tdk.com.hk/english/pdf/RF%20Comp/Isolator/e7711_CU.pdf

[21]   "A Fully Integrated Direct-Conversion Receiver for CDMA and GPS Applications", K. Lim et al, Future Communication IC (FCI) Inc., IEEE Journal of Solid-State Circuits, Vol. 41, No. 11, November 2006.

[22]   "High Performance RF Front-End Circuits for CDMA Receivers utilizing BiCMOS and Copper Technologies", G. Watanabe et. al., Motorola Semiconductor Products Sector, IEEE Radio and Wireless Conference, Sept. 10- Sept. 13, 2000.

[23]   "A Nightmare for CDMA RF Receivers: The Cross Modulation," B-K Ko et al., IEEE Asia Pacific Conference on ASICs Aug. 23 – Aug. 25, 1999, Seoul, South Korea.

[24]   "A 2GHz 16 dBm IIP3 Low Noise Amplifier in 0.25um CMOS Technology," 2003 IEEE International Solid-State Circuit Conference.

[25]   "A +7.9 dBm IIP3 LNA for CDMA2000 in a 90um Digital CMOS Process," D. Griffith, Radio Frequency Integrated Circuits (RFIC) Symposium, 2006

[26]   "A High IIP2 Direct-Conversion Mixer using an Even-Harmonic Reduction Technique for Cellular-CDMA/PCS/GPS Applications," M-.W. Hwang, et Al. Radio Frequency Integrated Circuits (RFIC) Symposium 6 – 8 June, 2004.

[27]   3GPP2 C.S0011-D_v2.0_061315, "Recommended Minimum Performance Standards for cdma20000 Spread Spectrum Mobile Stations, Release C, Version 2.0".

[28]   Sony Corporation, "CXG1174UR, High Power SP3T Switch with Logic Control"
              http://www.sony.co.jp/~semicon/english/img/sony01/a6805203.pdf.

[29]   Sony Corporation, "CXG1230EQ, SP9T GSM/UMTS Dual Mode Antenna Switch"
              http://www.sony.co.jp/~semicon/english/img/sony01/a6808768.pdf.

Annex A:
Plots for clause 7 (dual-carrier and multi-carrier)
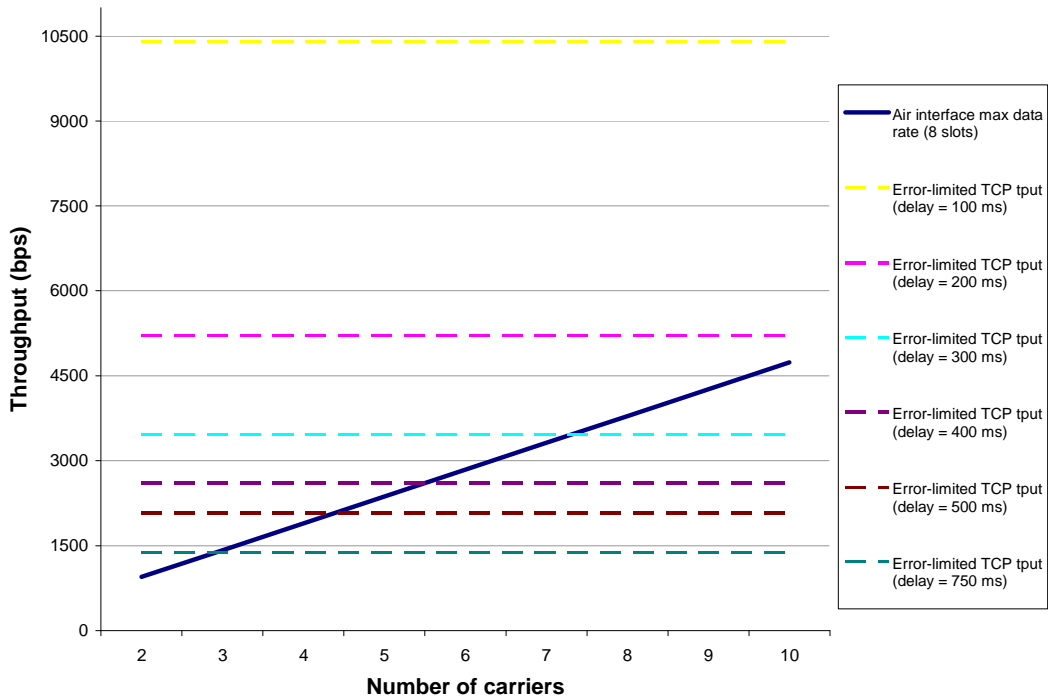
Figure A.1: TCP error limited throughput vs air interface peak data rate (8 slots, IP err = 10e-4)
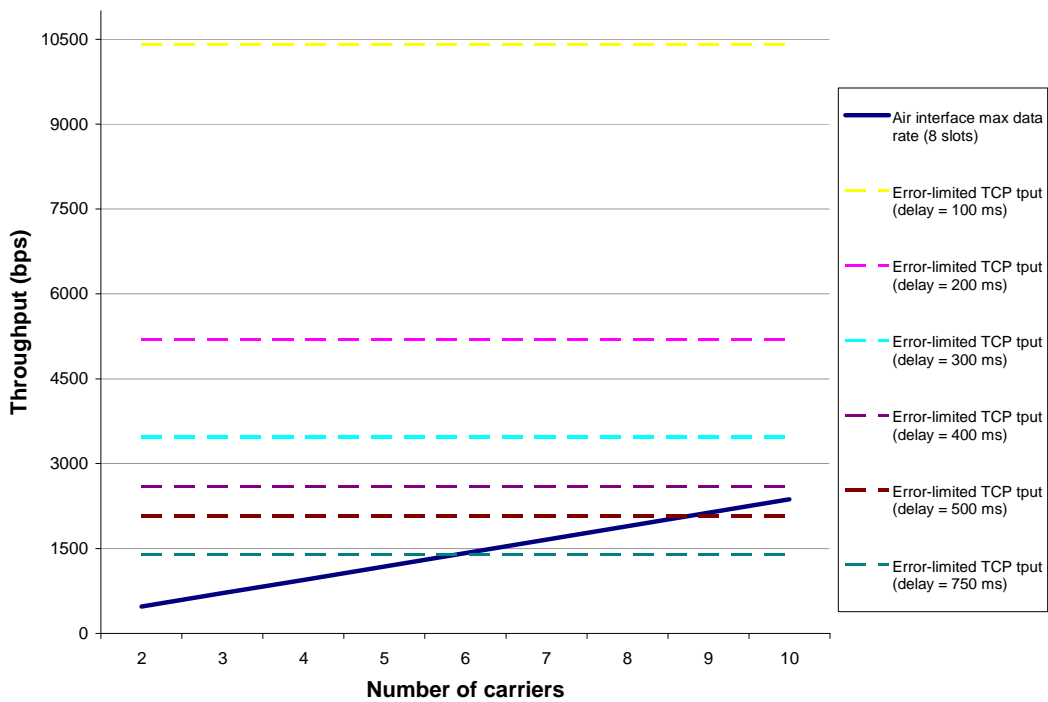
Figure A.2: TCP error limited throughput vs air interface peak data rate (4 slots, IP err = 10e-4)
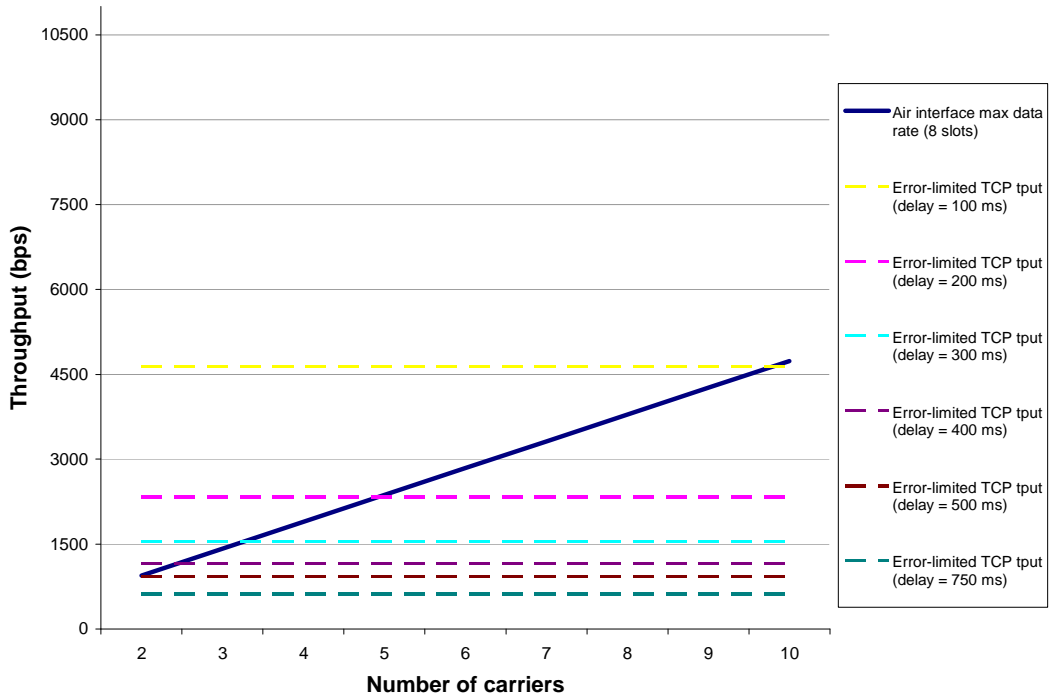
Figure A.3: TCP error limited throughput vs air interface peak data rate (8 slots, IP err = 5*10e-4)
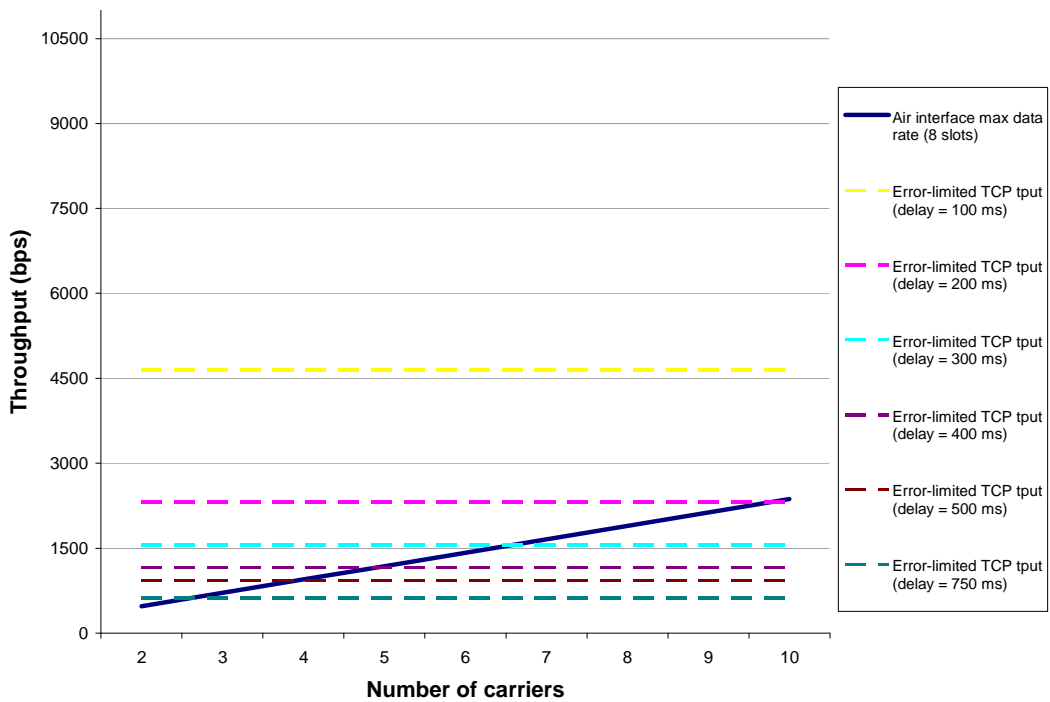
Figure A.4: TCP error limited throughput vs air interface peak data rate (4 slots, IP err = 5*10e-4)

Annex B:
Chapter 8 Link simulation results

These link simulation results are related to the data presented in Implementation Set C.

B.1 Link performance for 8-PSK and 16 QAM with and without turbo coding
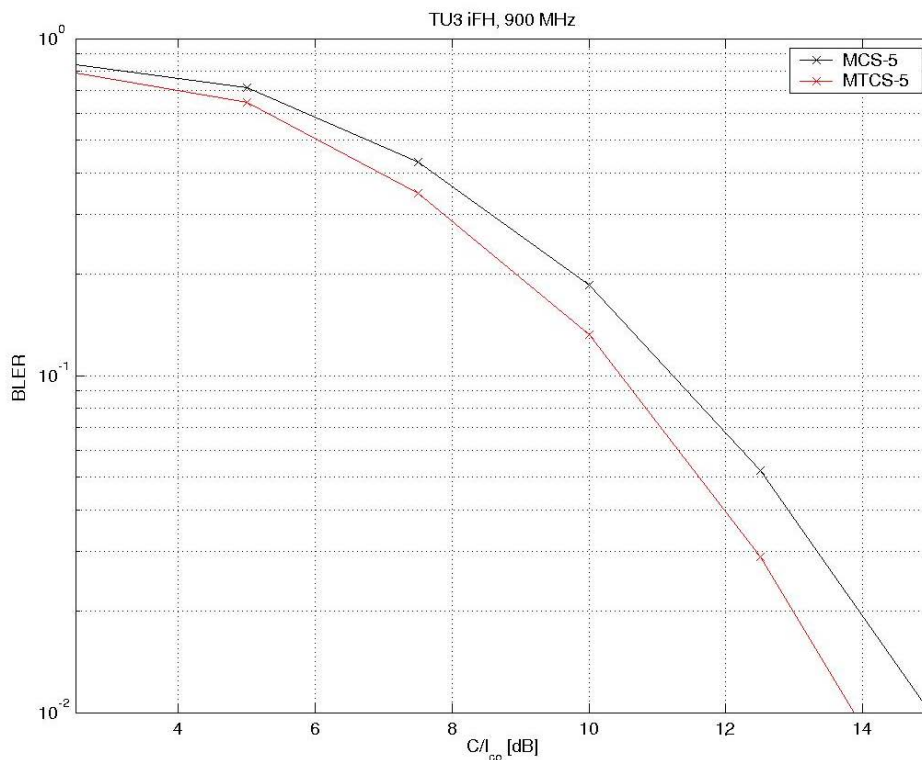
Figure B.1: MCS-5 and MTCS-5
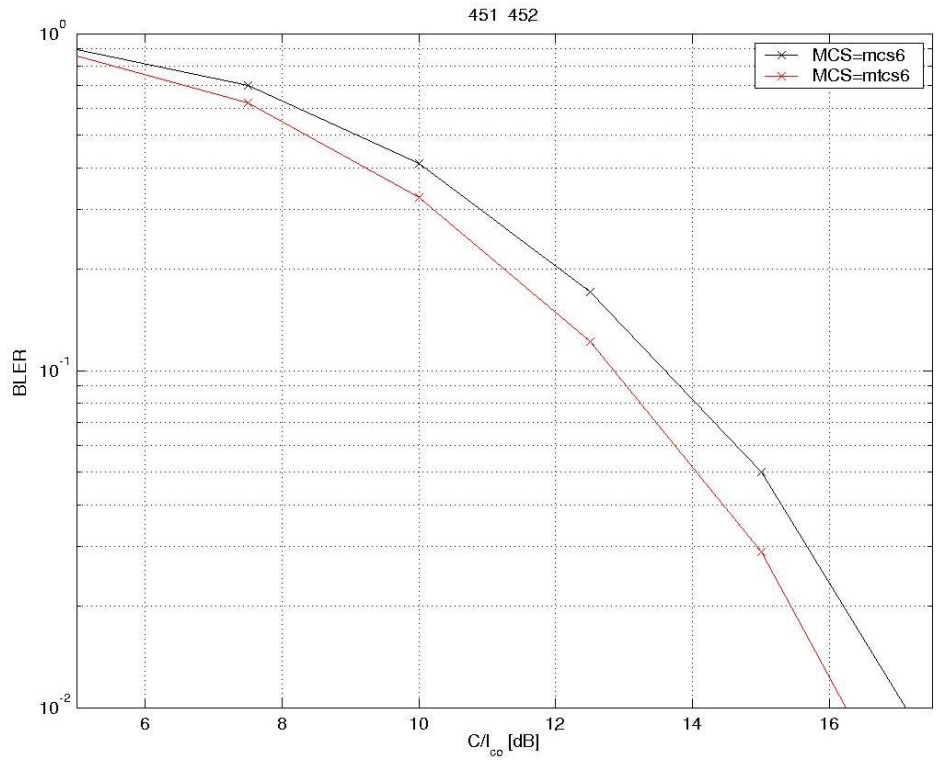
Figure B.2: MCS-6 and MTCS-6
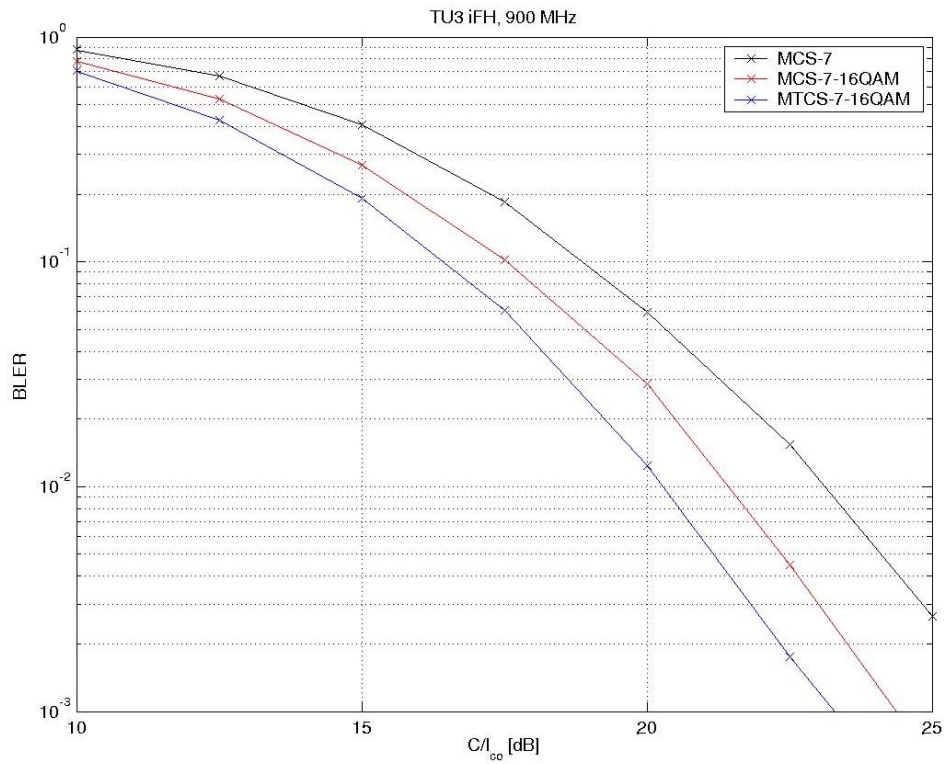
Figure B.3: MCS-7, MCS-7-16QAM and MTCS-7-16QAM
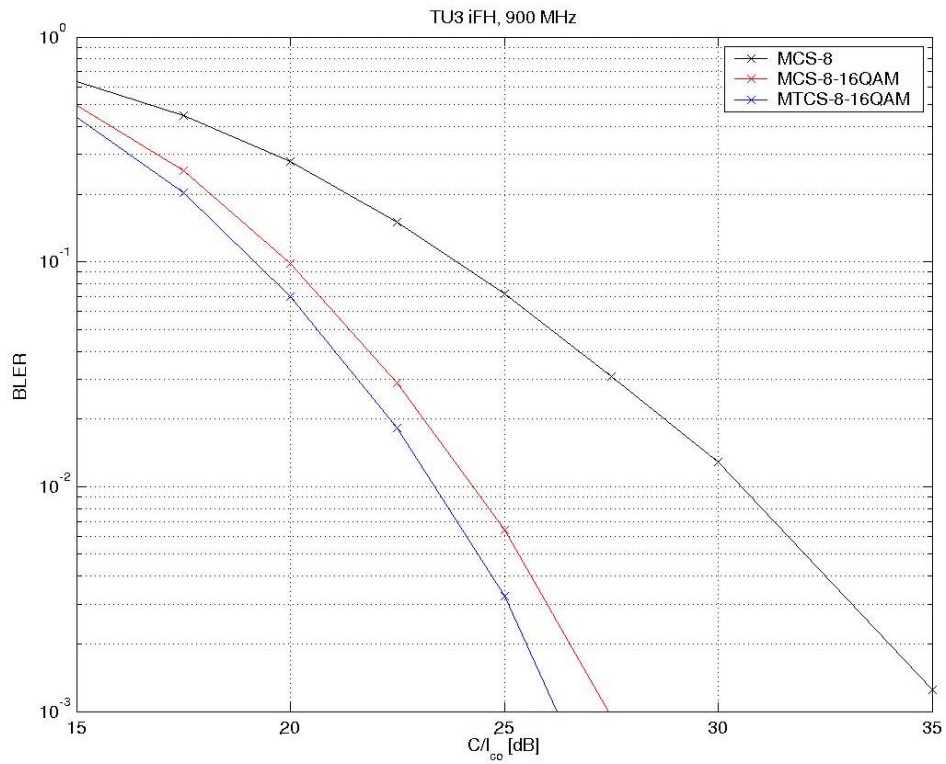
Figure B.4: MCS-8, MCS-8-16QAM and MTCS-8-16QAM
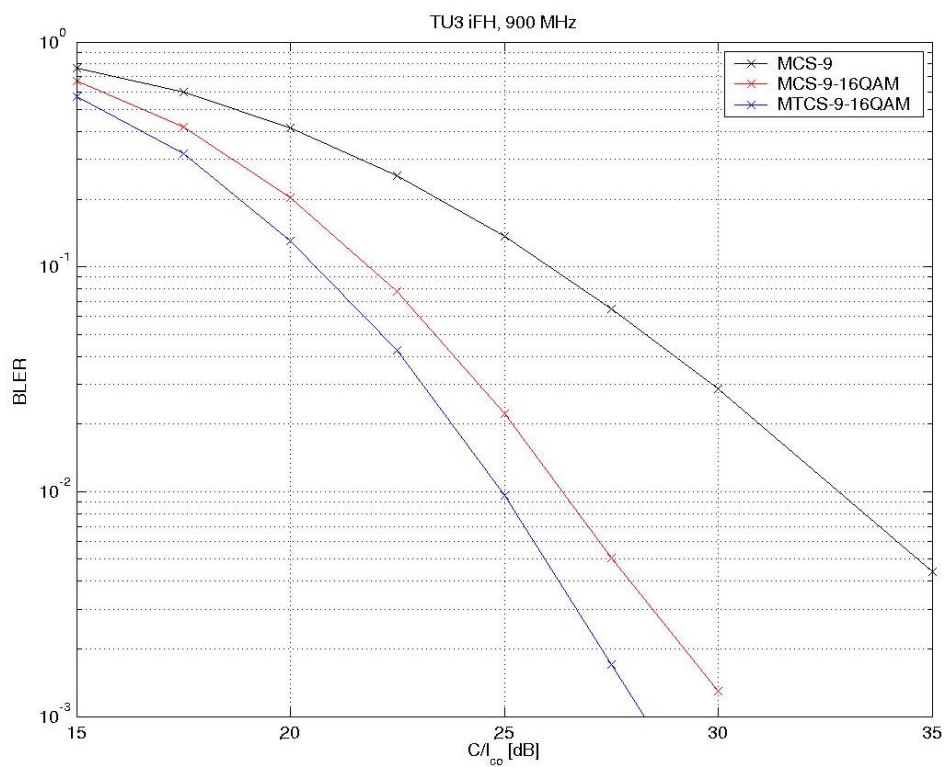
Figure B.5: MCS-9, MCS-9-16QAM and MTCS-9-16QAM
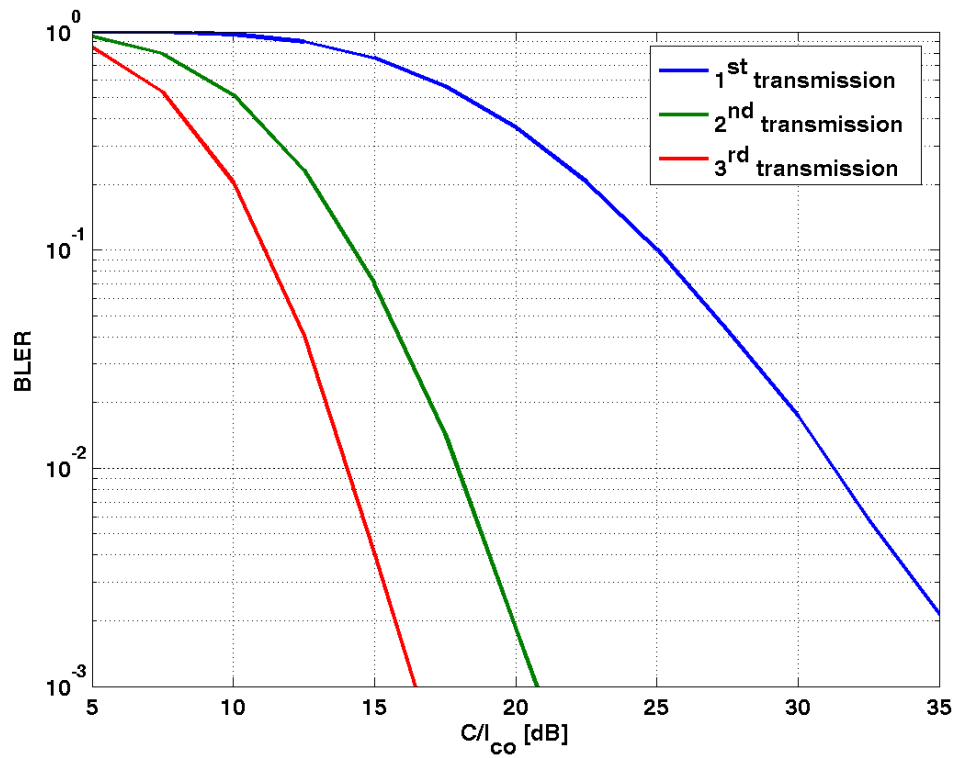
Figure B.6: Link performance with IR for MCS-10-16QAM on TU3iFH
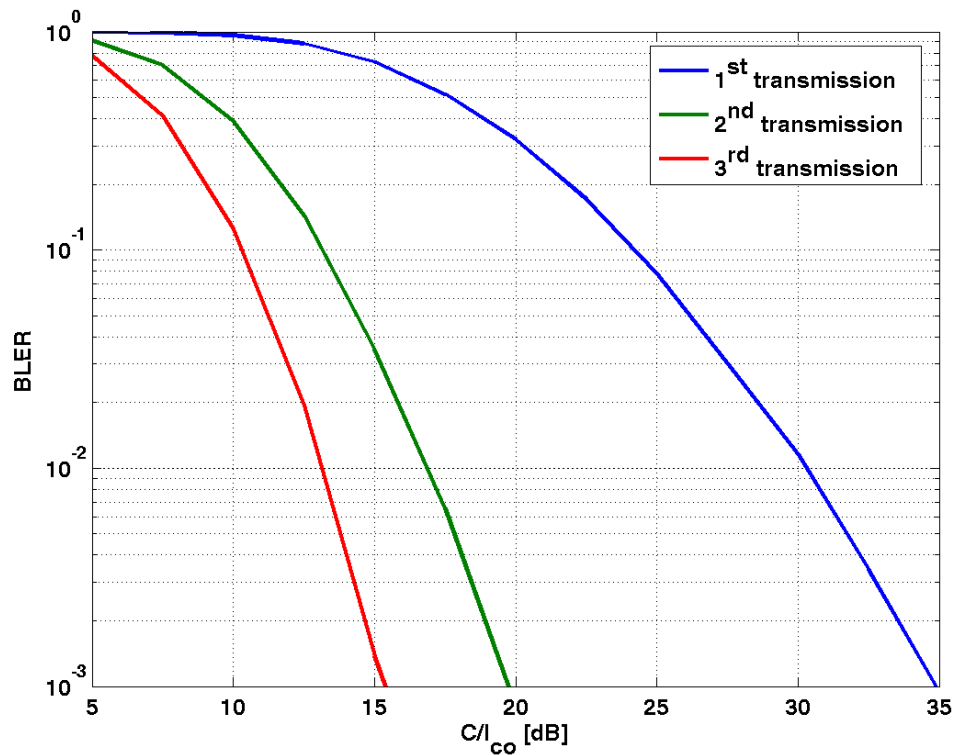
Figure B.7: Link performance with IR for MTCS-10-16QAM on TU3iFH
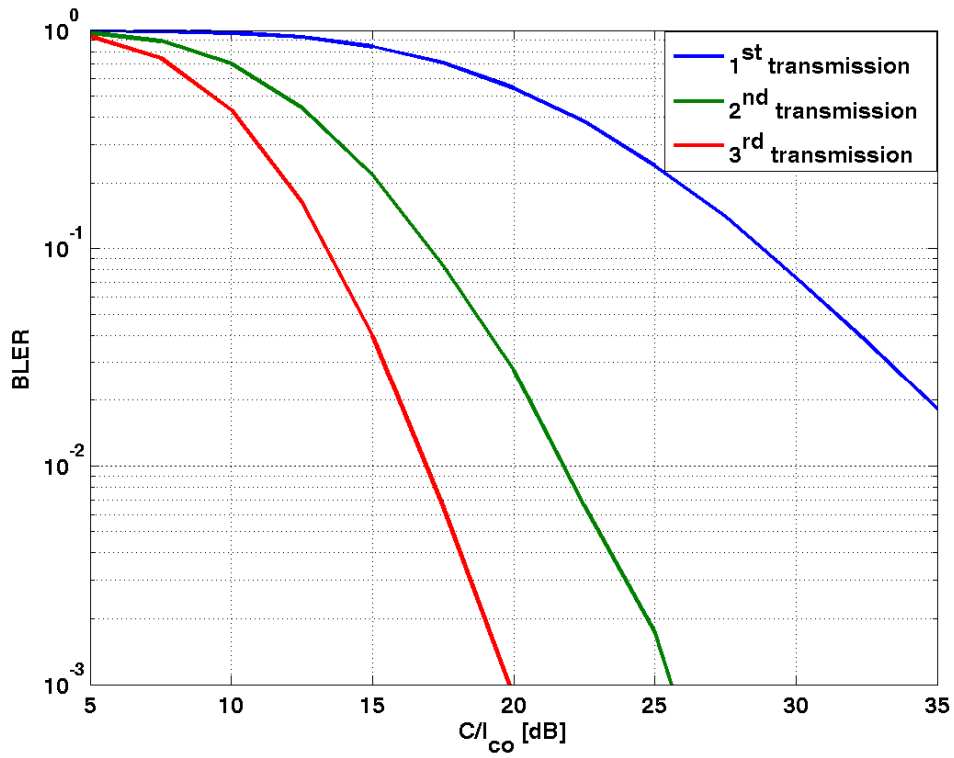
Figure B.8: Link performance with IR for MCS-11-16QAM on TU3iFH

B.2 C/I-distribution
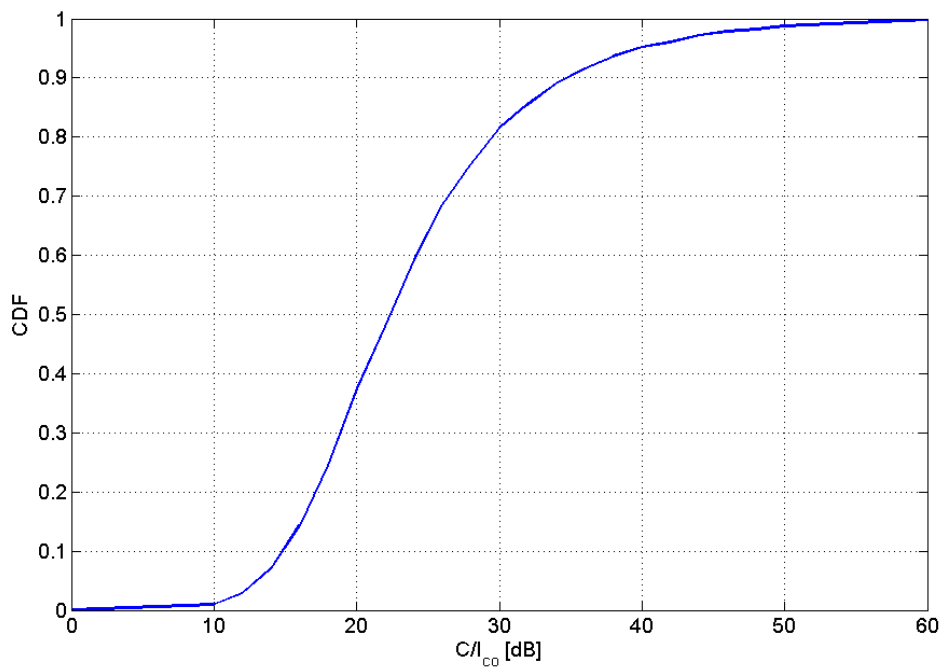
Figure B.9: C/I-distribution used when calculating mean user bit rates
Taken from a system simulation with a 3/9 freq. reuse and a 2 % blocking limit

B.3   Link performance 32QAM
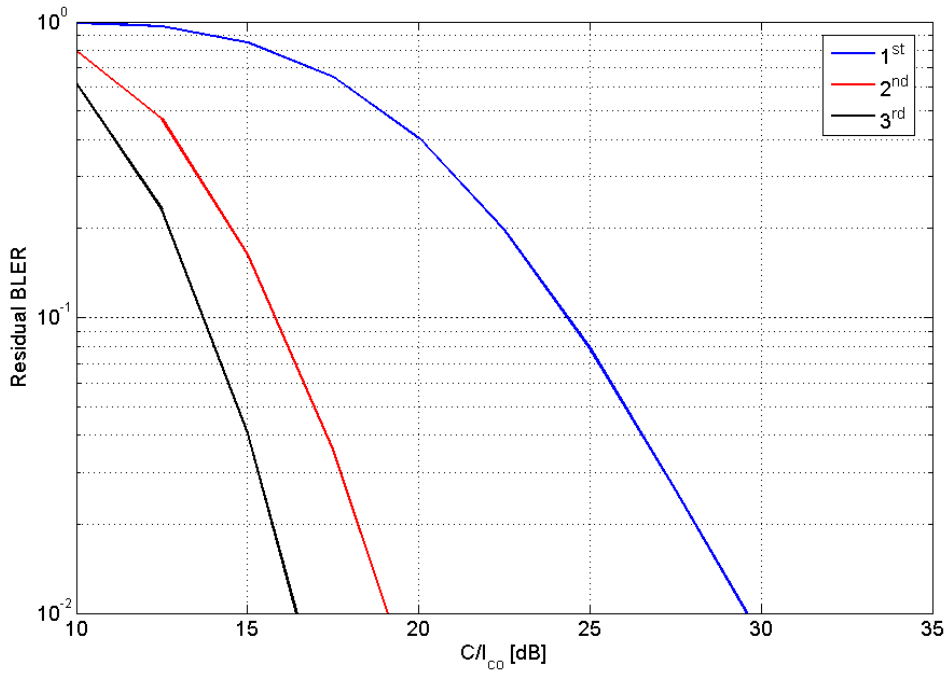
Figure B.10: Residual data block error for MCS-10-32QAM with IR
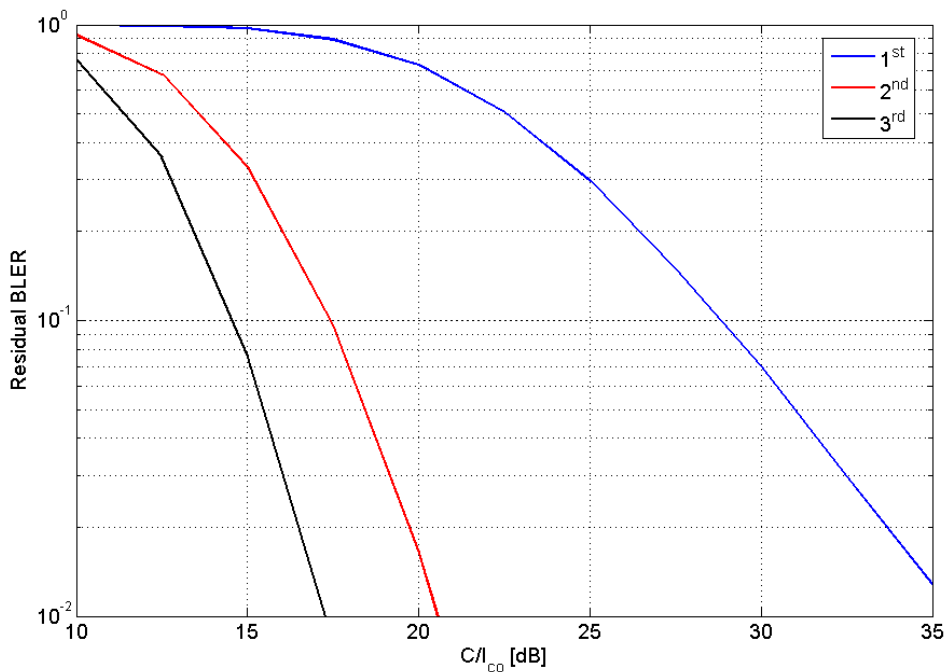
Figure B.11: Residual data block error for MCS-11-32QAM with IR
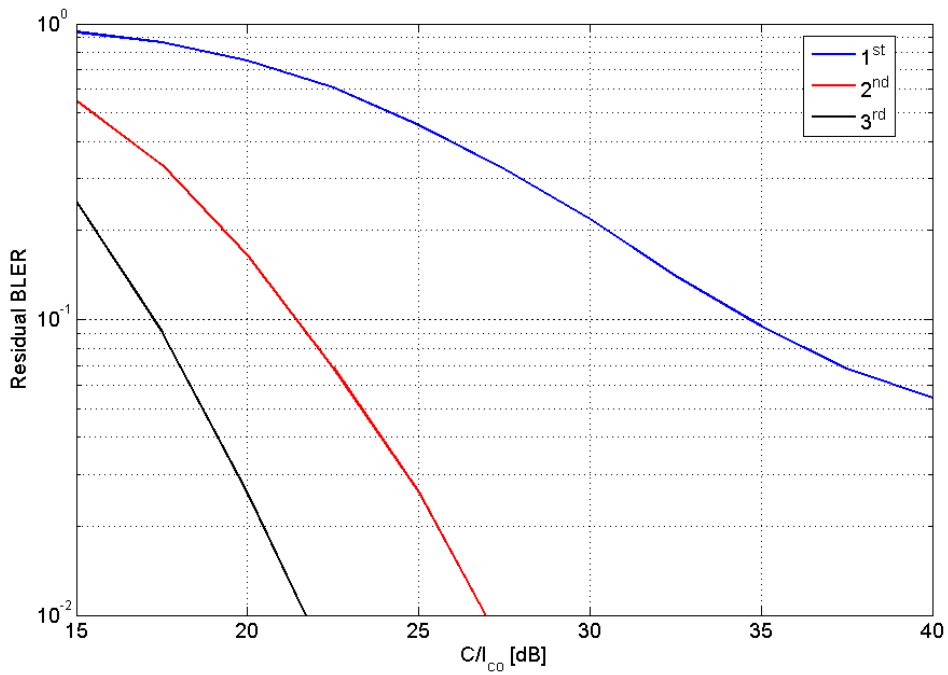
Figure B.12: Residual data block error for MCS-12-32QAM with IR
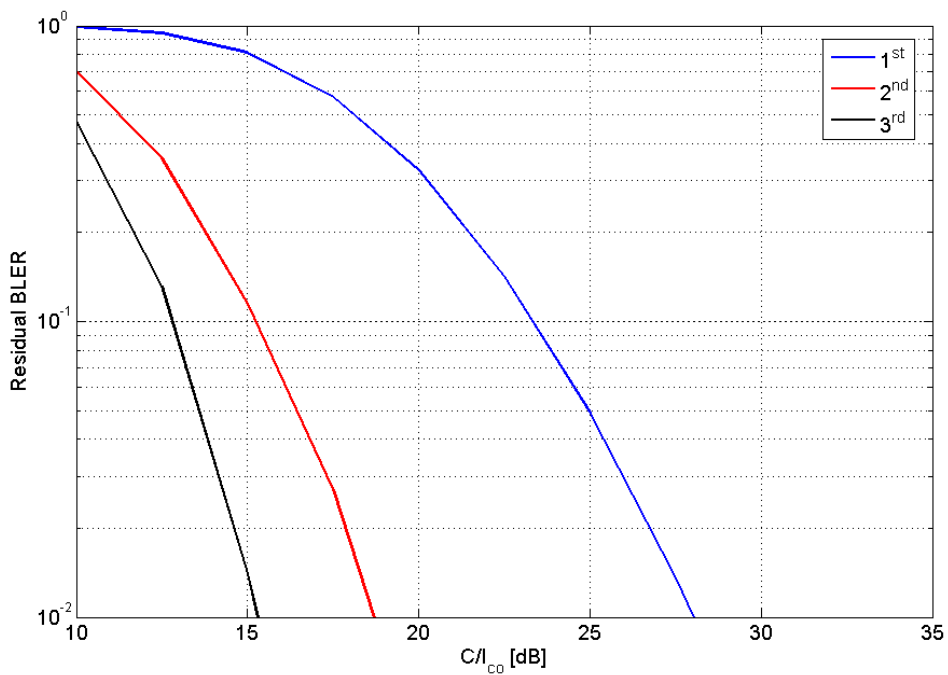
Figure B.13: Residual data block error for MTCS-10-32QAM with IR
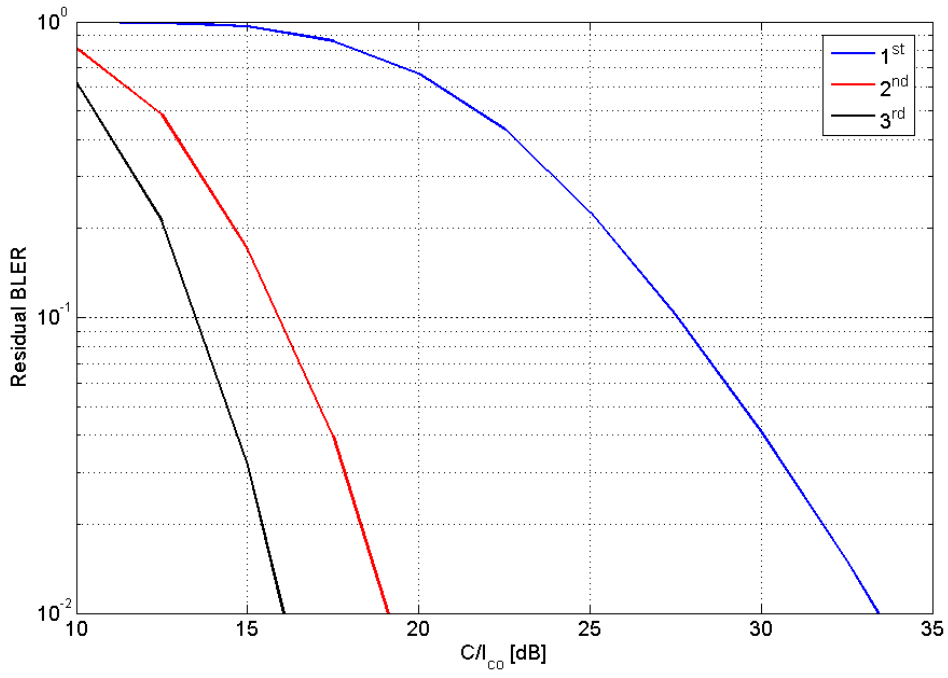
Figure B.14: Residual data block error for MTCS-11-32QAM with IR

Annex C:
Chapter 8 Link simulation results

These link simulation results are related to the data presented in Implementation Set D.

C.1 Detailed link performance results

Co-Channel Interferer (TU50 No Frequency Hopping).
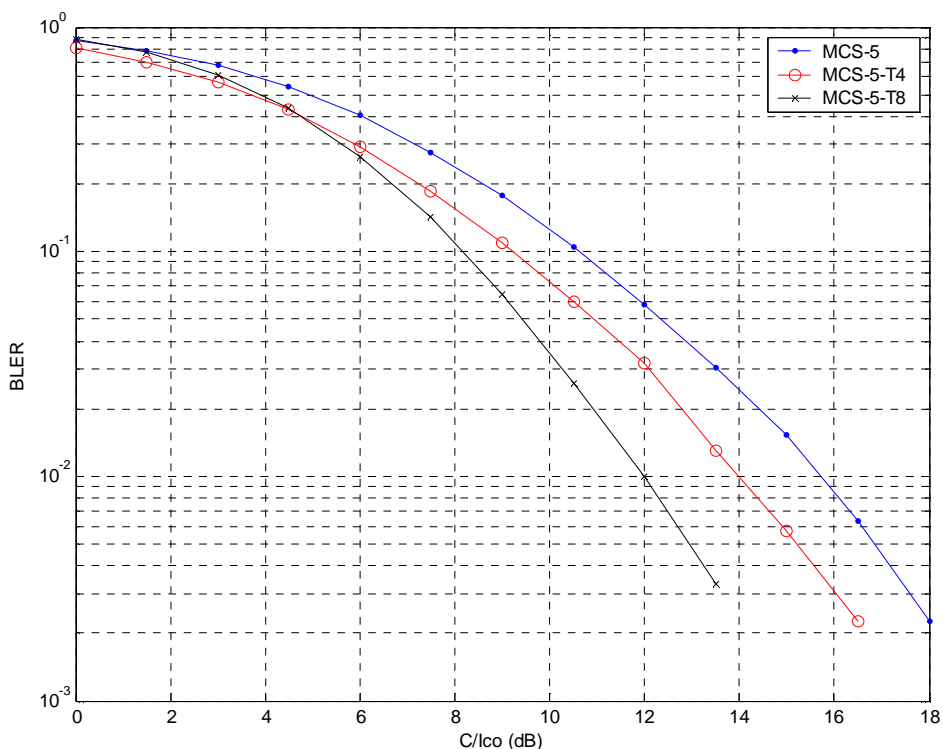
Figure C.1: TU50nH Co-Channel Performance (MCS-5)
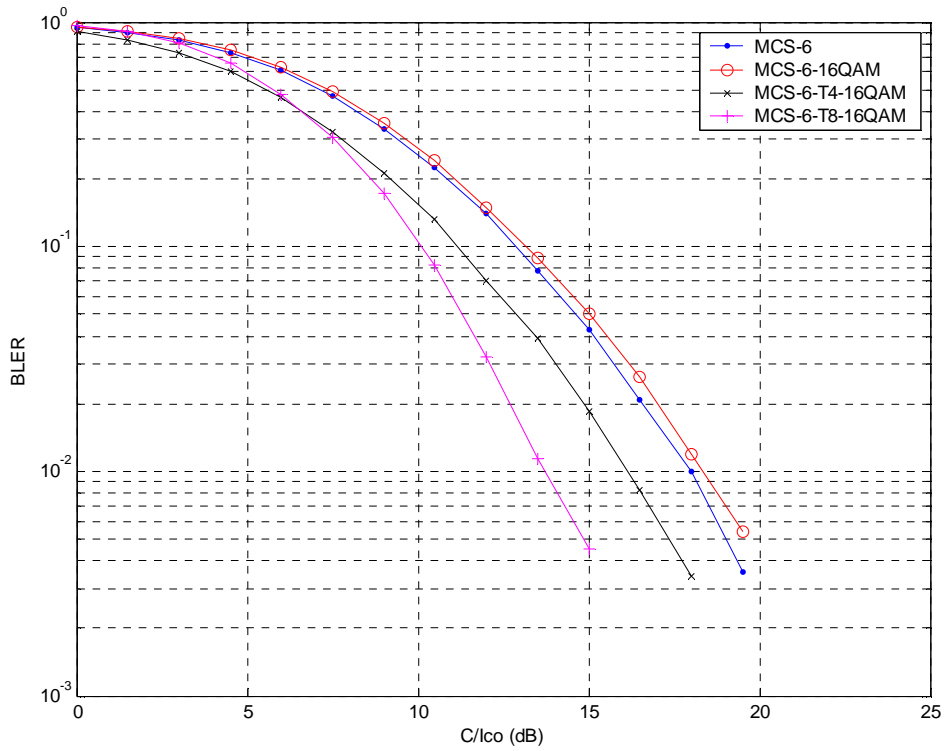
Figure C.2: TU50nH Co-Channel Performance (MCS-6)
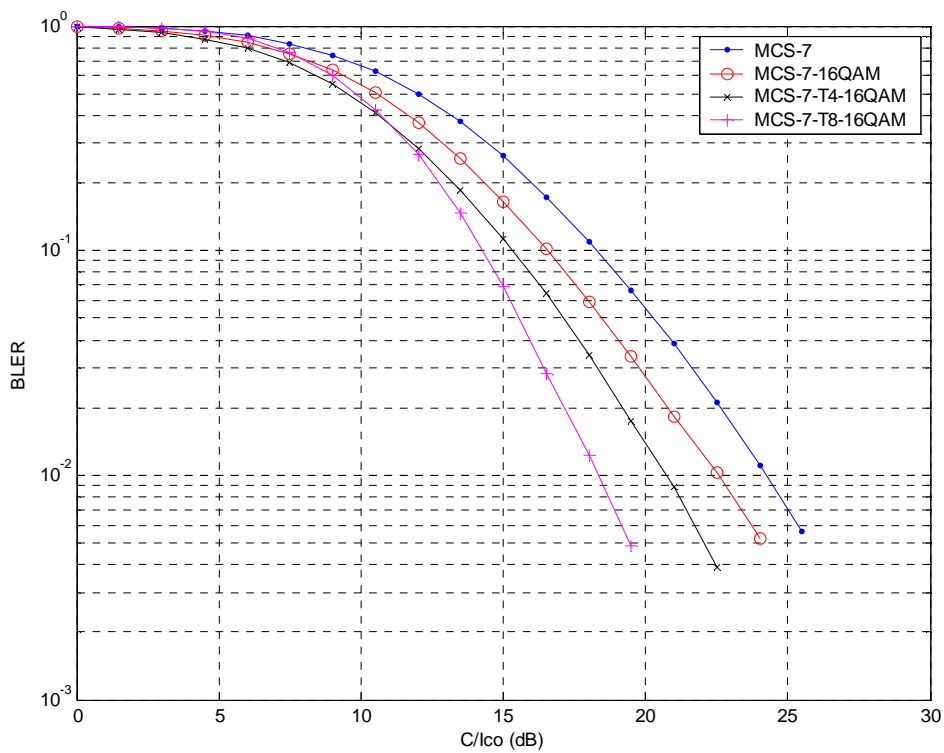
Figure C.3: TU50nH Co-Channel Performance (MCS-7)
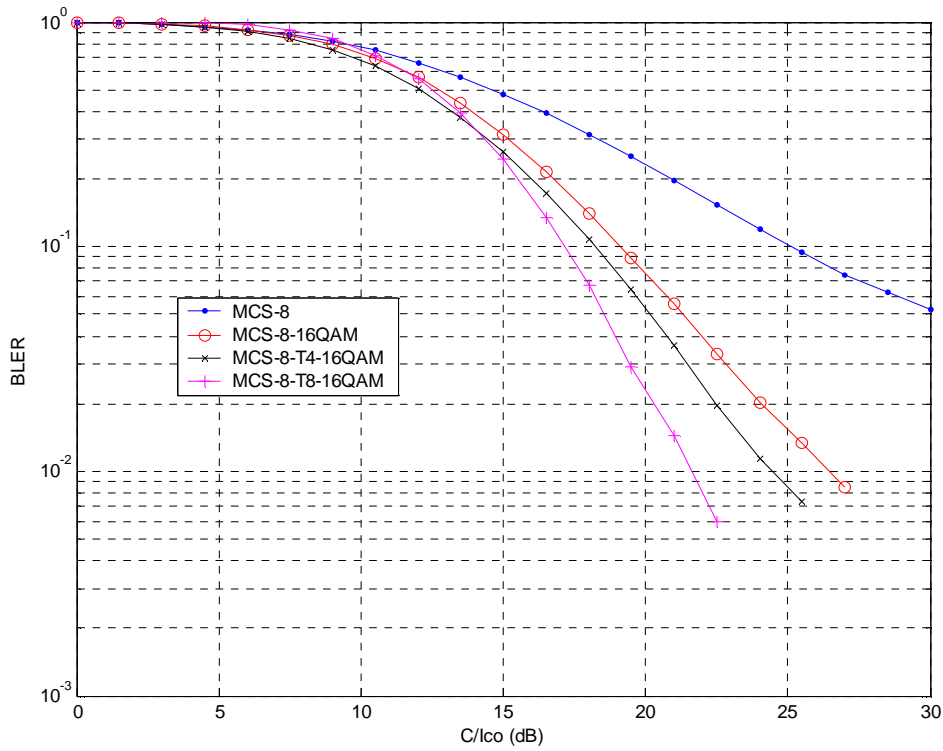
Figure C.4: TU50nH Co-Channel Performance (MCS-8)
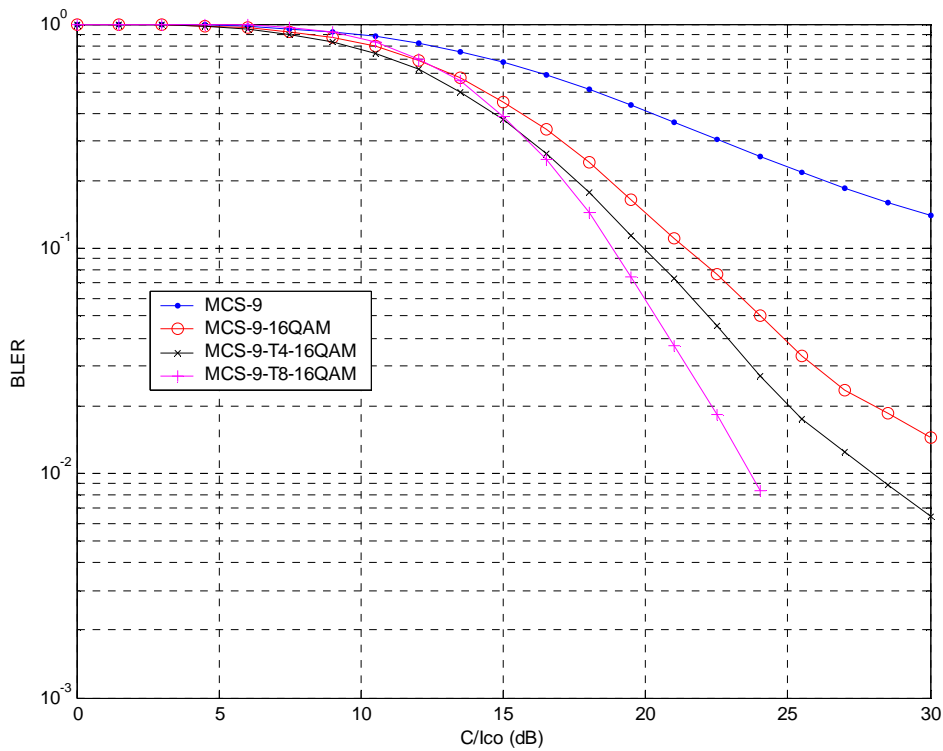
Figure C.5: TU50nH Co-Channel Performance (MCS-9)
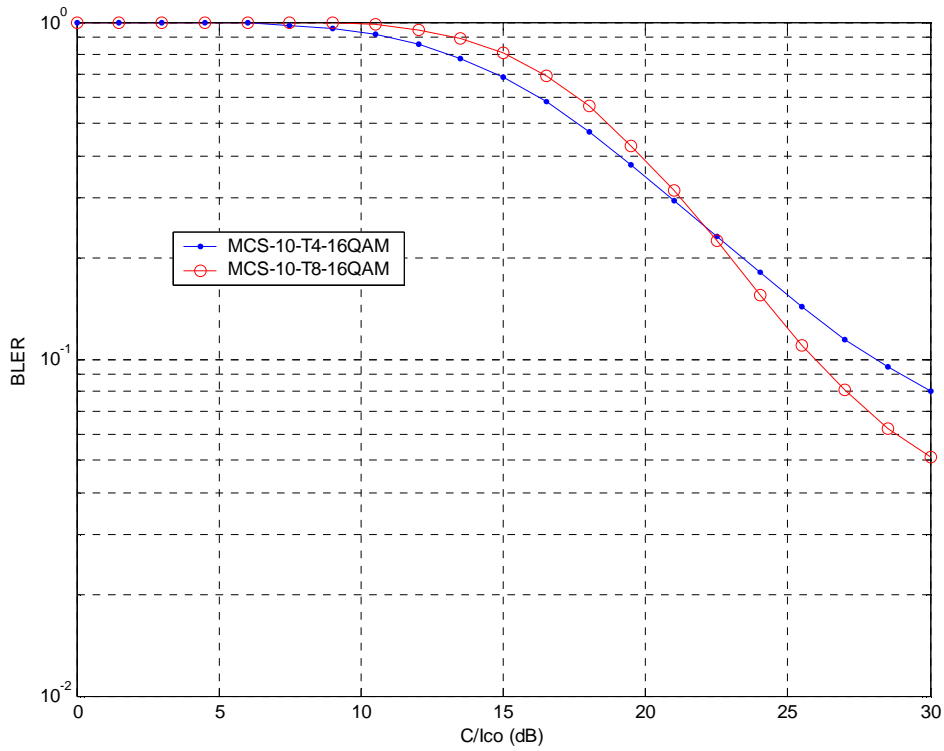
Figure C.6: TU50nH Co-Channel Performance (MCS-10 16-QAM)
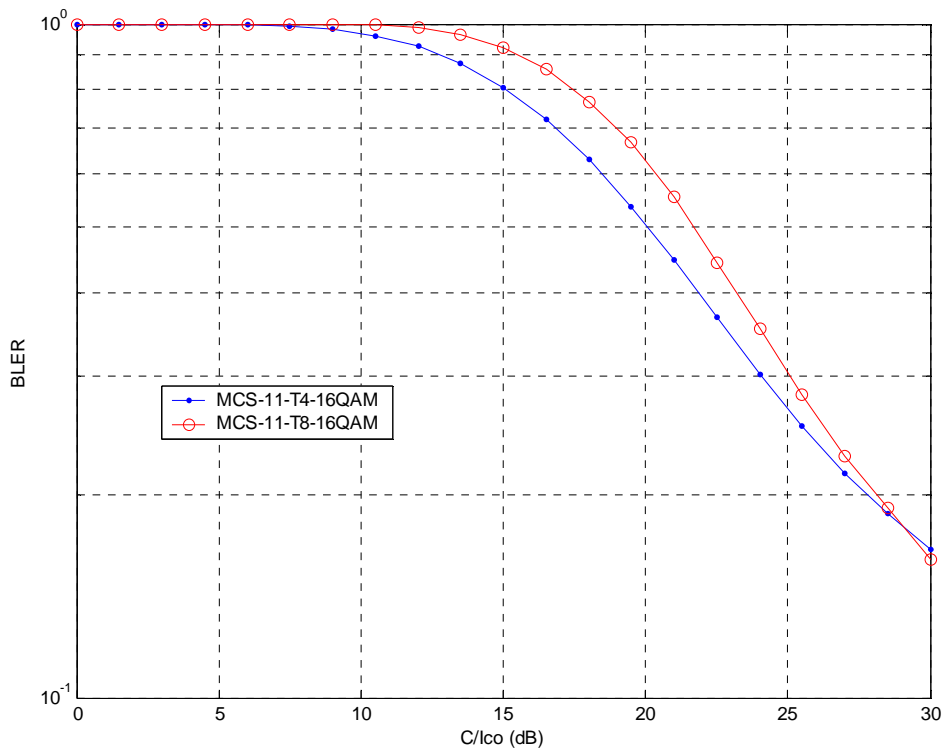
Figure C.7: TU50nH Co-Channel Performance (MCS-11 16-QAM)

C.2 Detailed modulation detection performance results
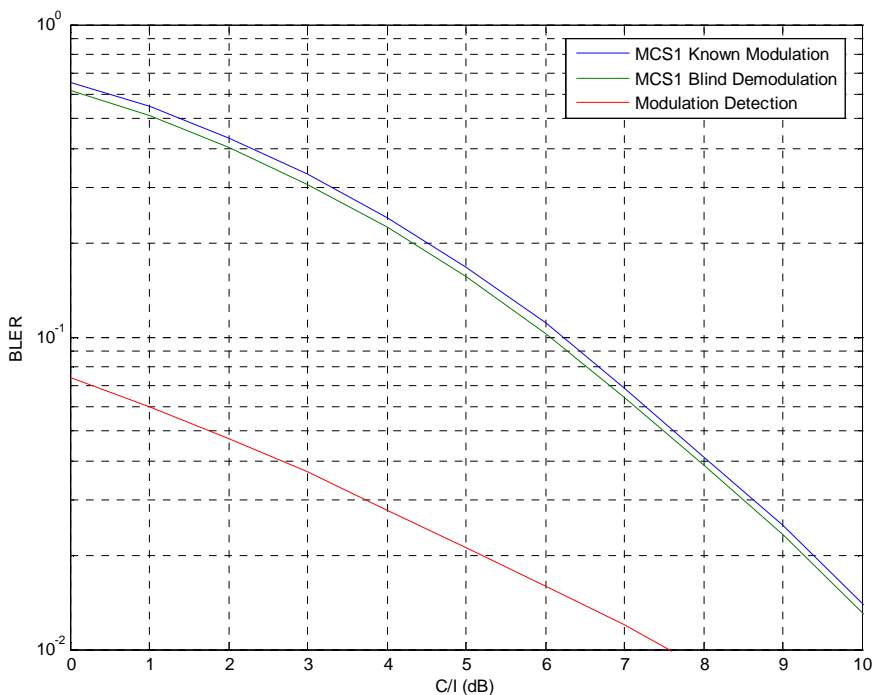
Figure C.8: MCS1, Co-channel, TU3iFH
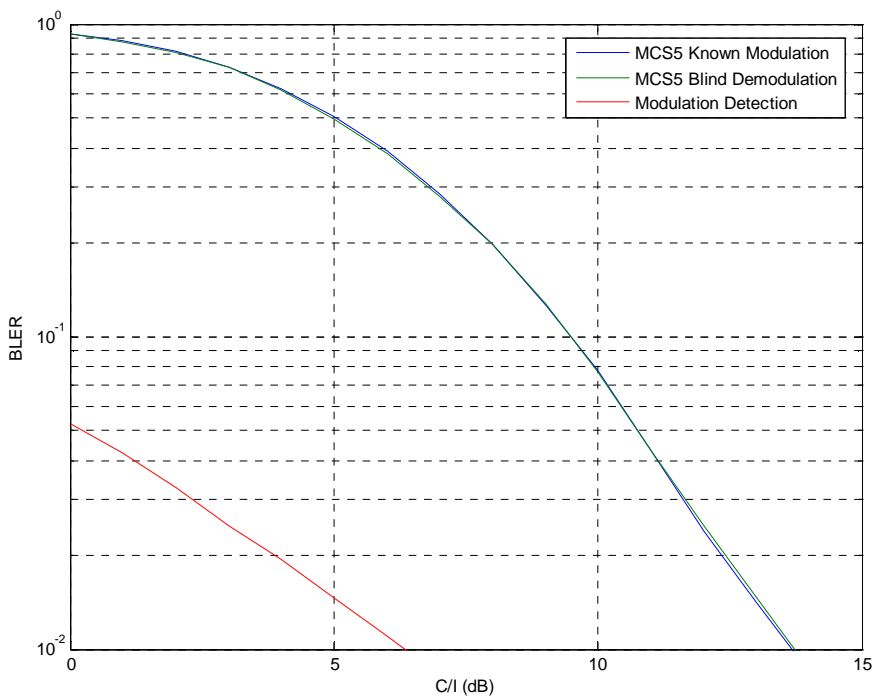
Figure C.9: MCS5, Co-channel, TU3iFH
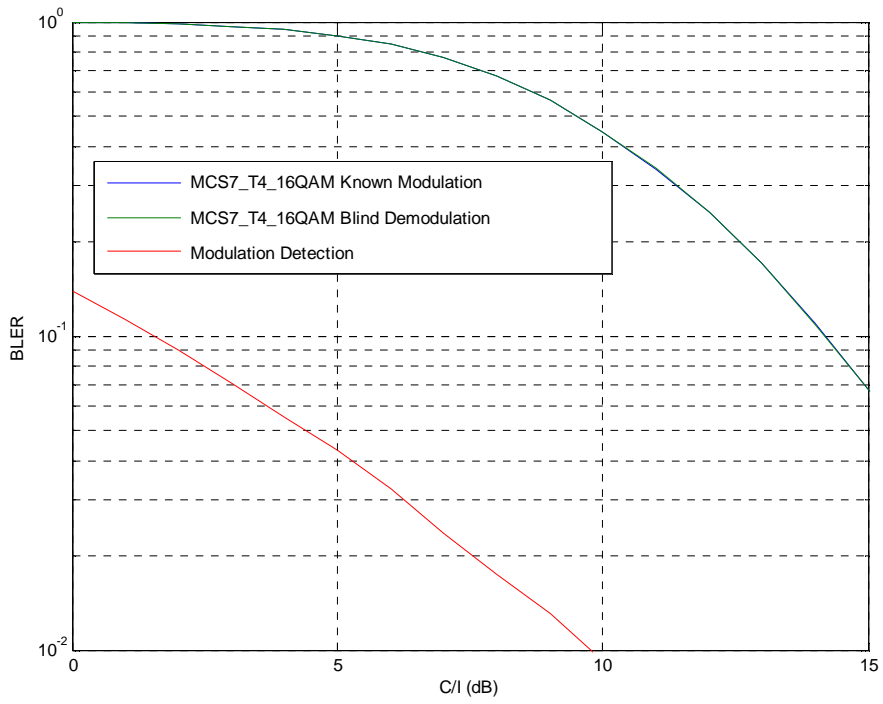
Figure C.10: MCS7-T4-16QAM, Co-channel, TU3iFH
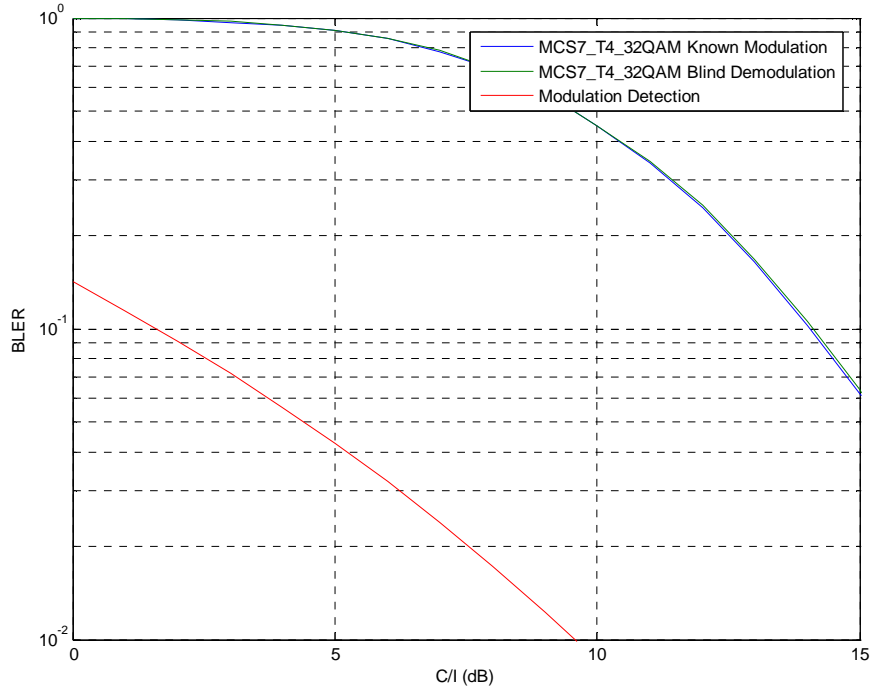
Figure C.11: MCS7-T4-32QAM, Co-channel, TU3iFH
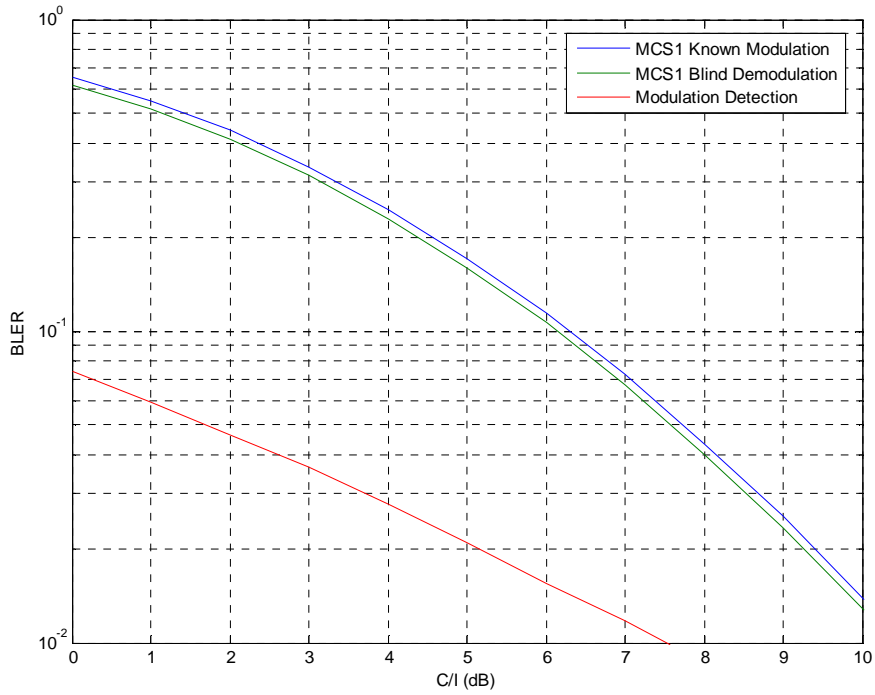
Figure C.12: MCS1, Co-channel, TU50iFH
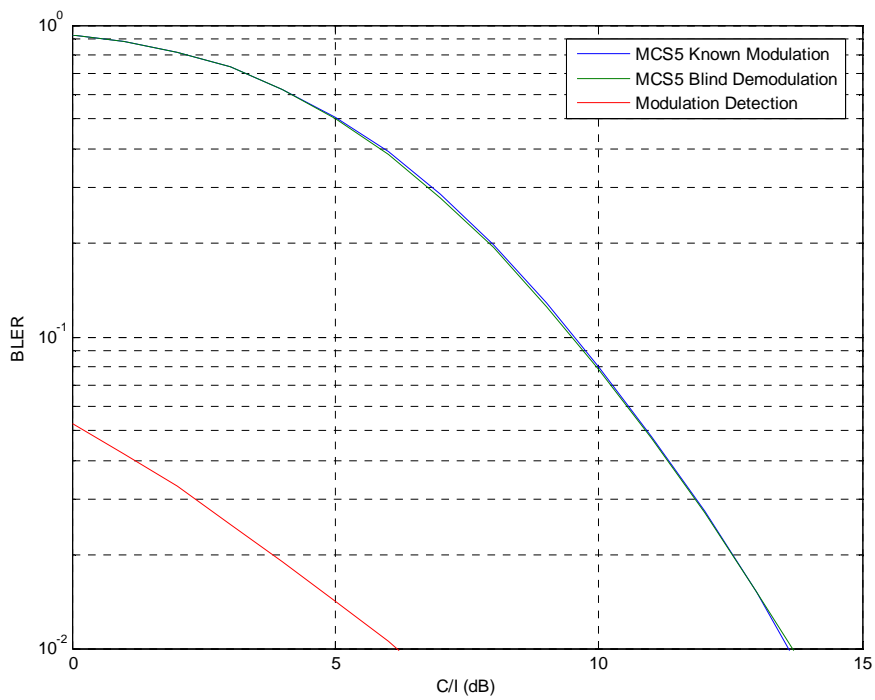
Figure C.13: MCS5, Co-channel, TU50iFH
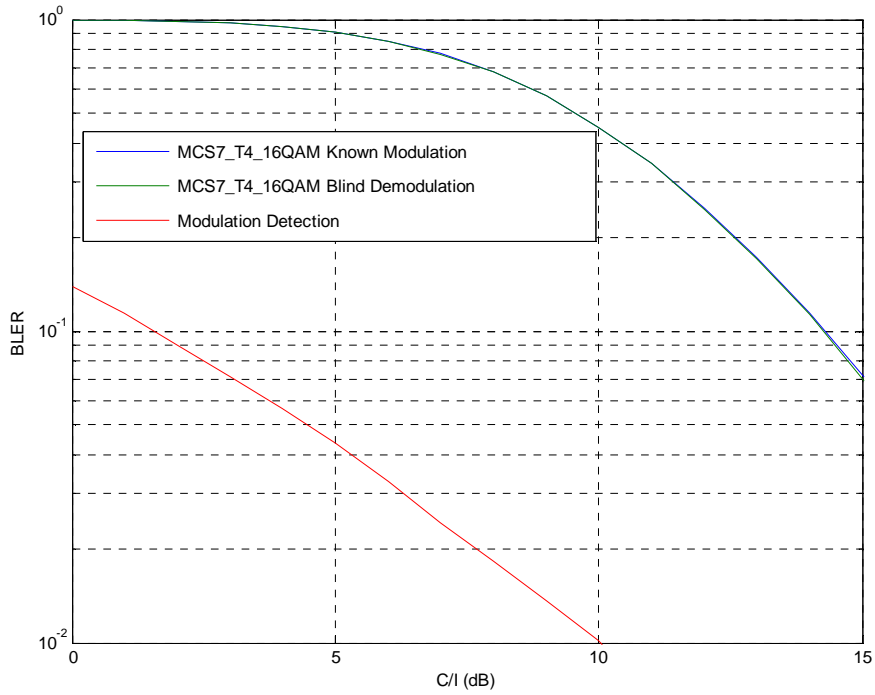
Figure C.14: MCS7-T4-16QAM, Co-channel, TU50iFH
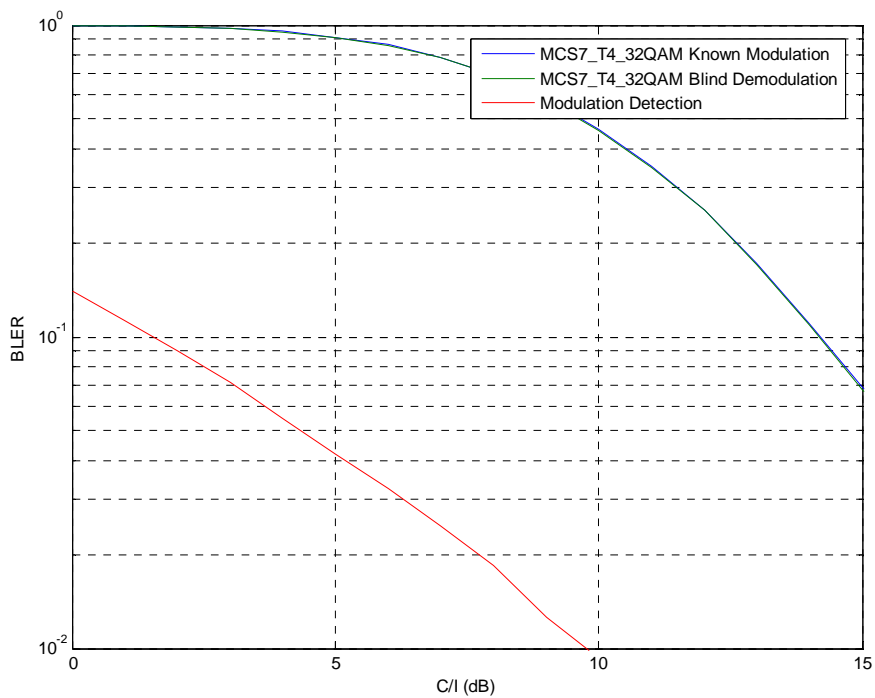
Figure C.15: MCS7-T4-32QAM, Co-channel, TU50iFH
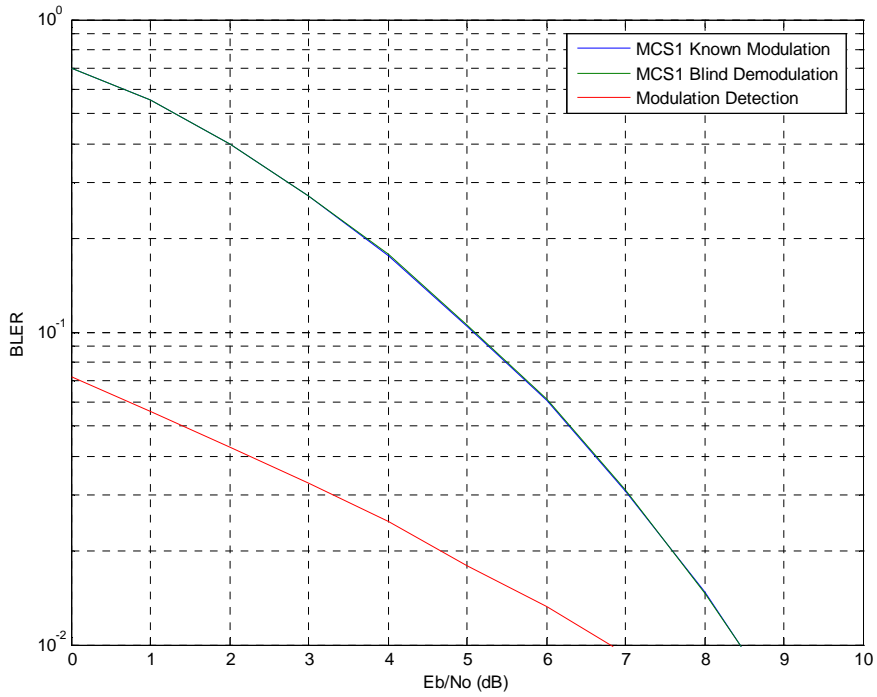
Figure C.16: MCS1, Sensitivity, TU50iFH
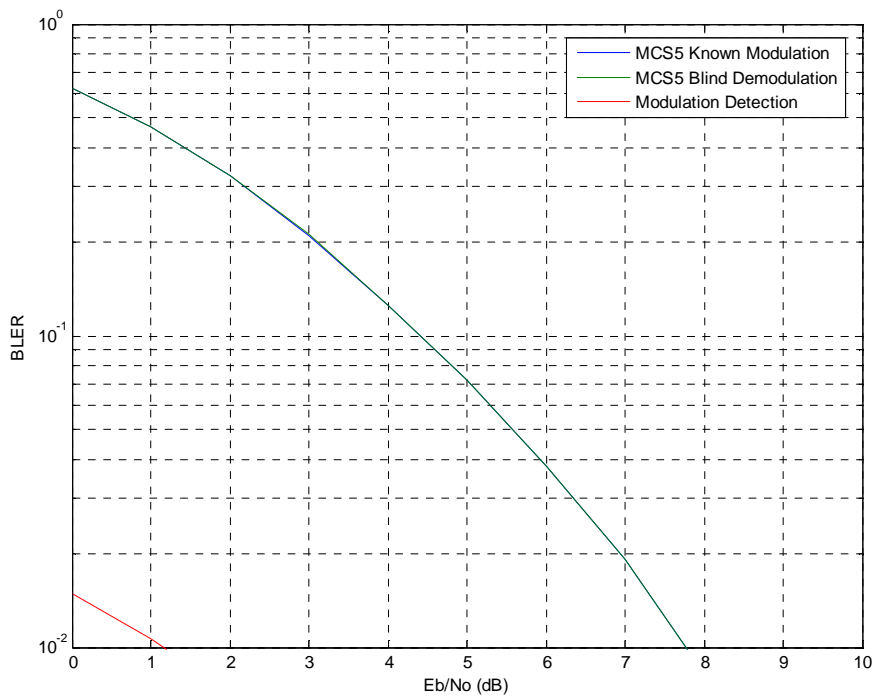
Figure C.17: MCS5, Sensitivity, TU50iFH
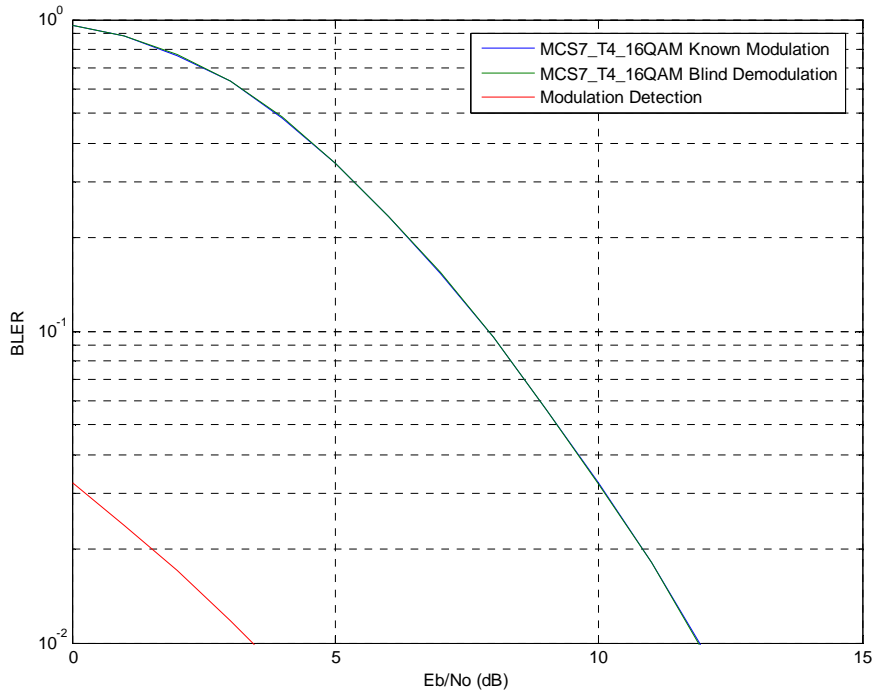
Figure C.18: MCS7-T4-16QAM, Sensitivity, TU50iFH
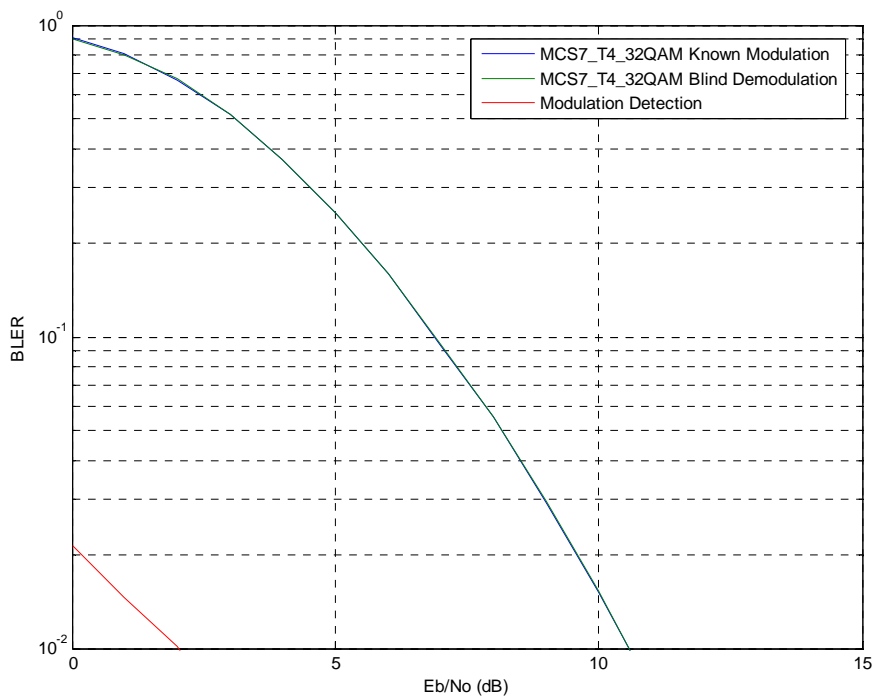
Figure C.19: MCS7-T4-32QAM, Sensitivity, TU50iFH
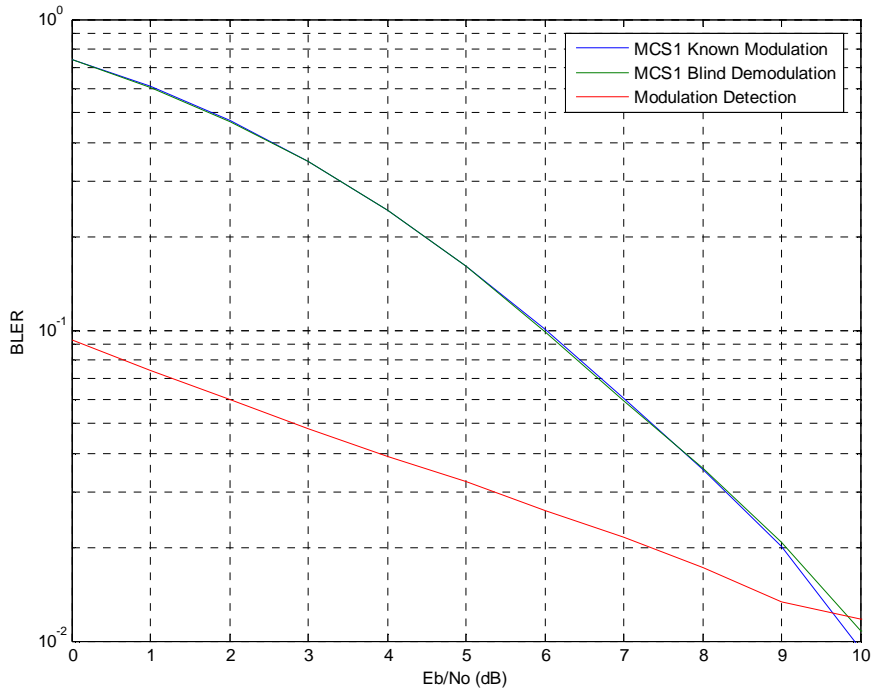
Figure C.20: MCS1, Sensitivity, HT100iFH
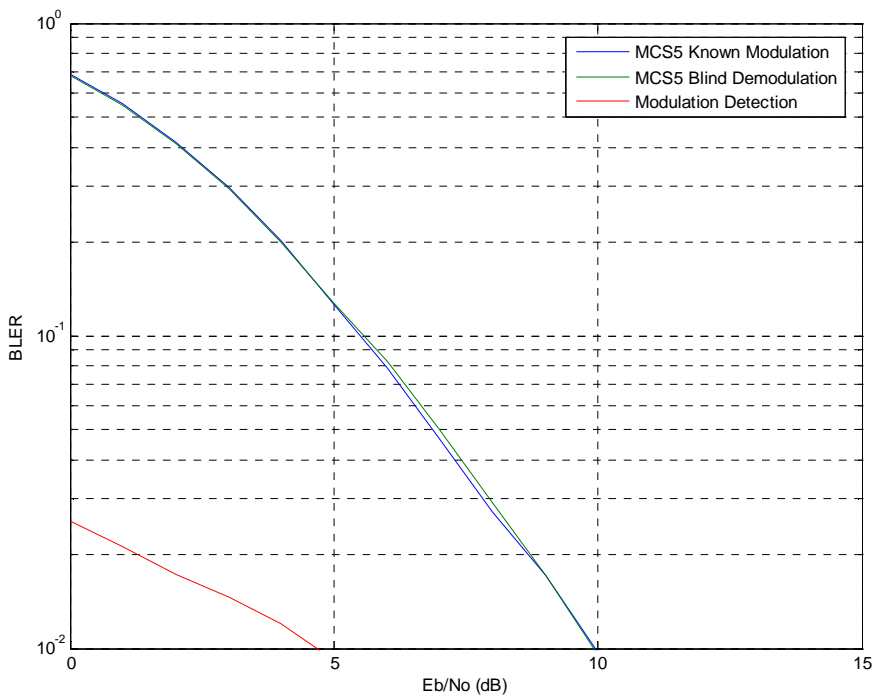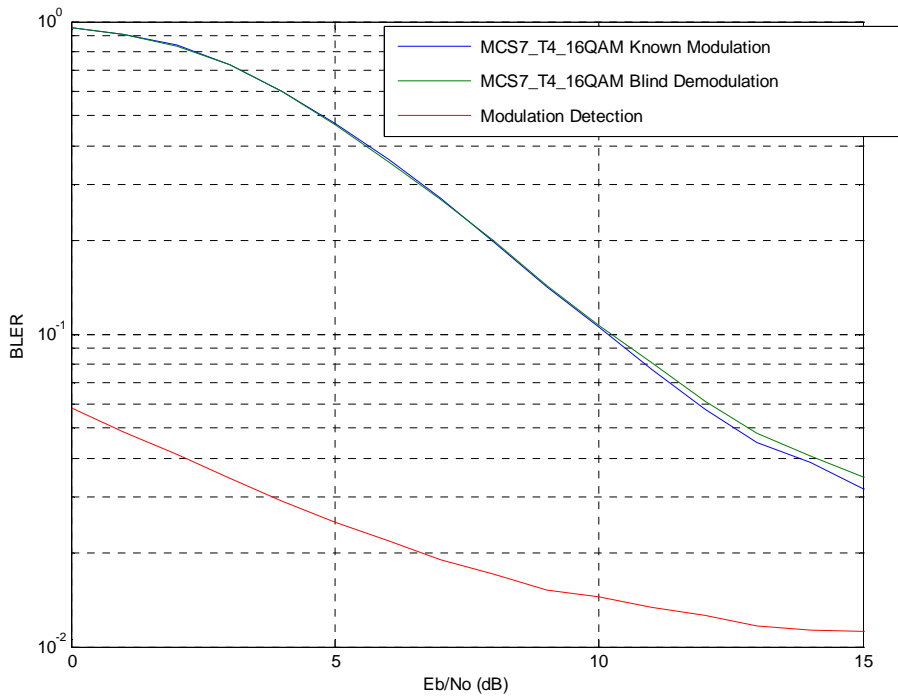

Figure C.21: MCS5, Sensitivity, HT100iFH
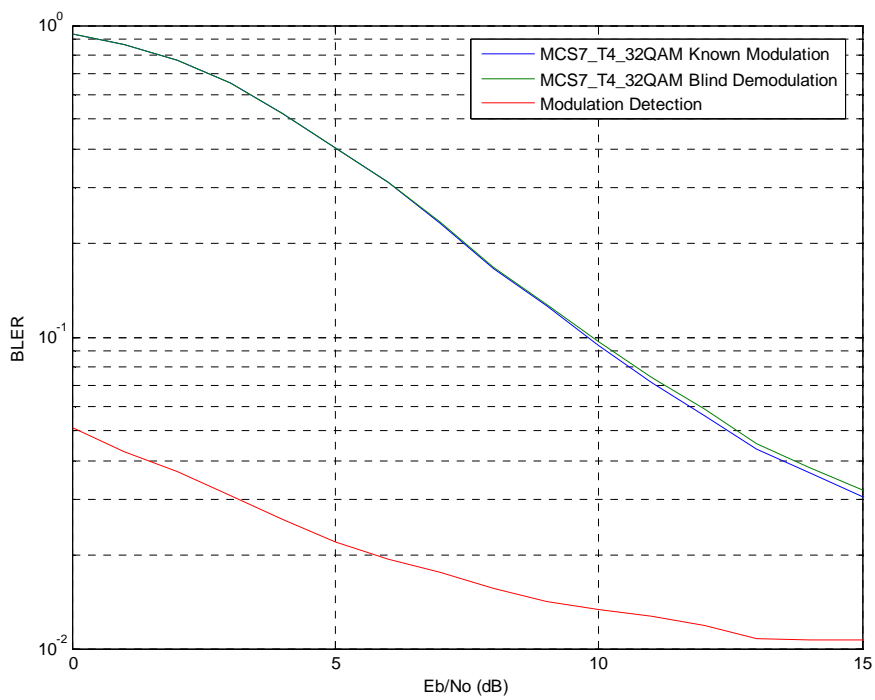
Figure C.22: MCS7-T4-16QAM, Sensitivity, HT100iFH
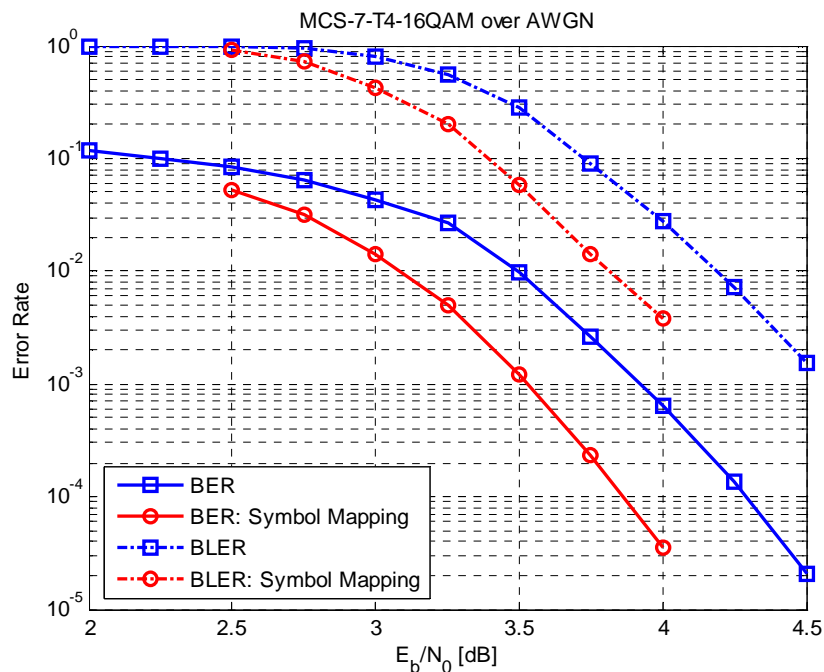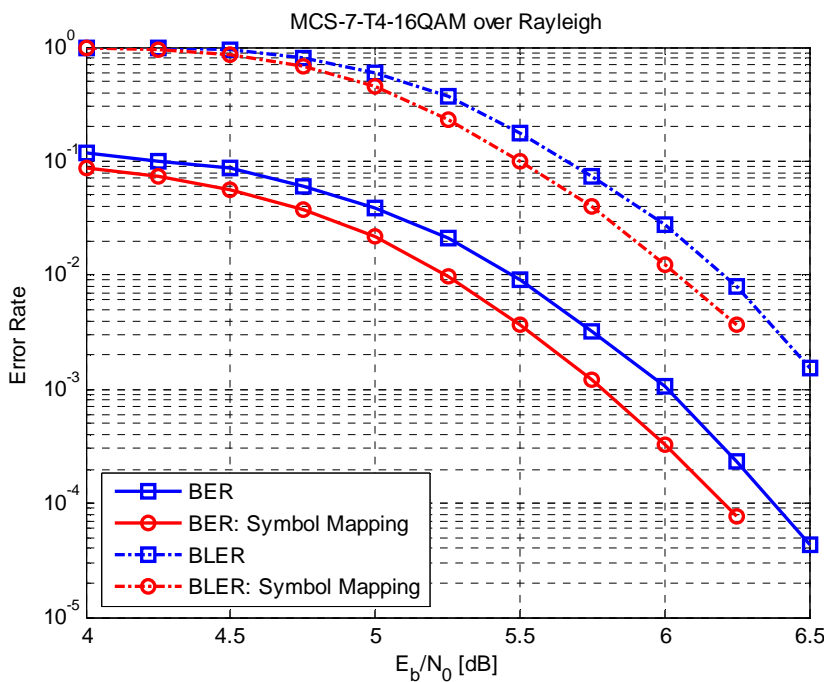

Figure C.23: MCS7-T4-32QAM, Sensitivity, HT100iFH

Annex D:
Chapter 8 Link simulation results

These simulation results are related to the investigation of performance when introducing a symbol mapping method according to subclause 8.5.
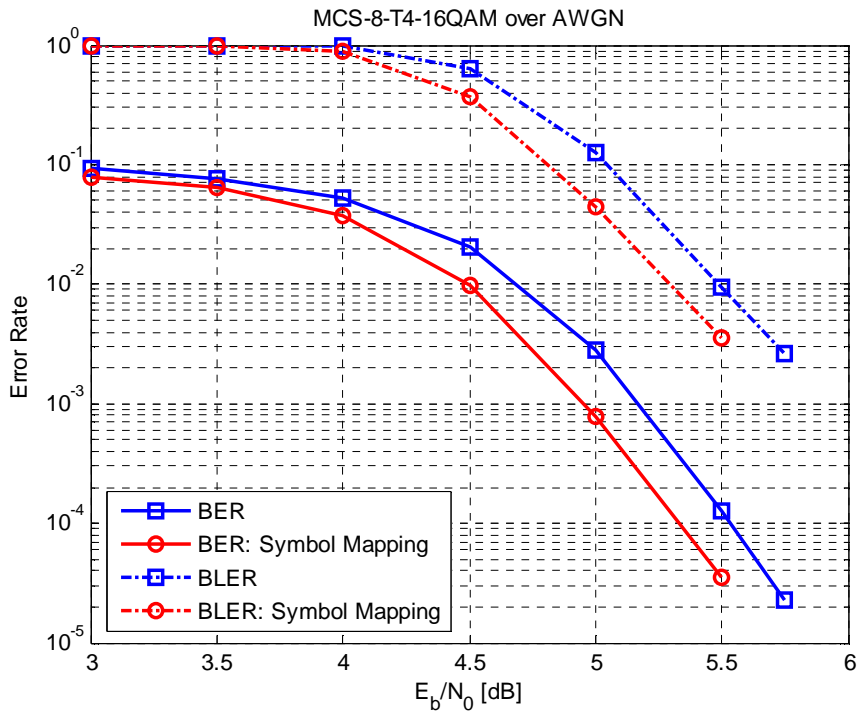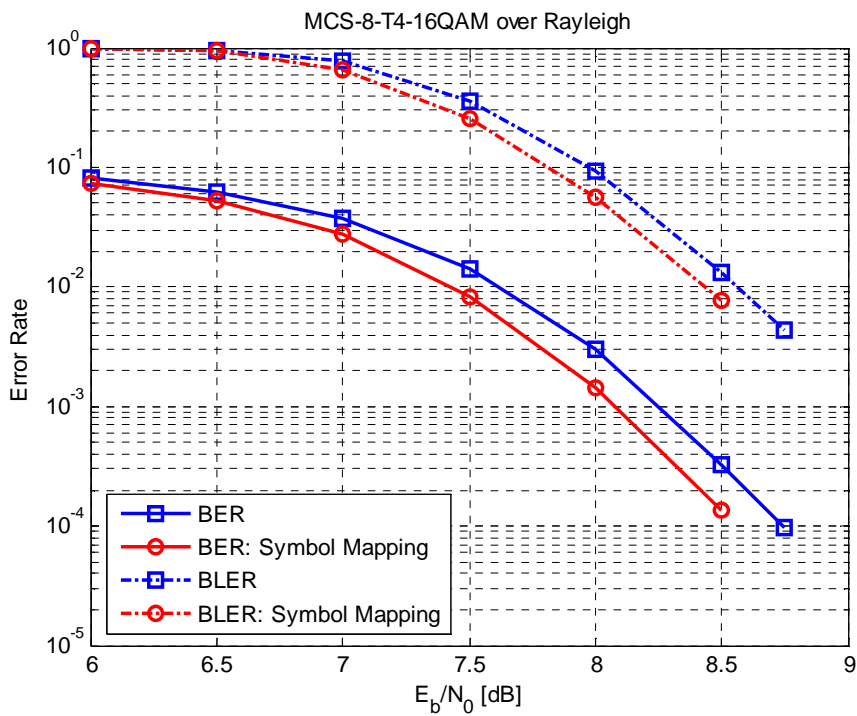

(a) AWGN channel

(b) Rayleigh channel

Figure D.1: BER and BLER of MCS-7-T4-16QAM

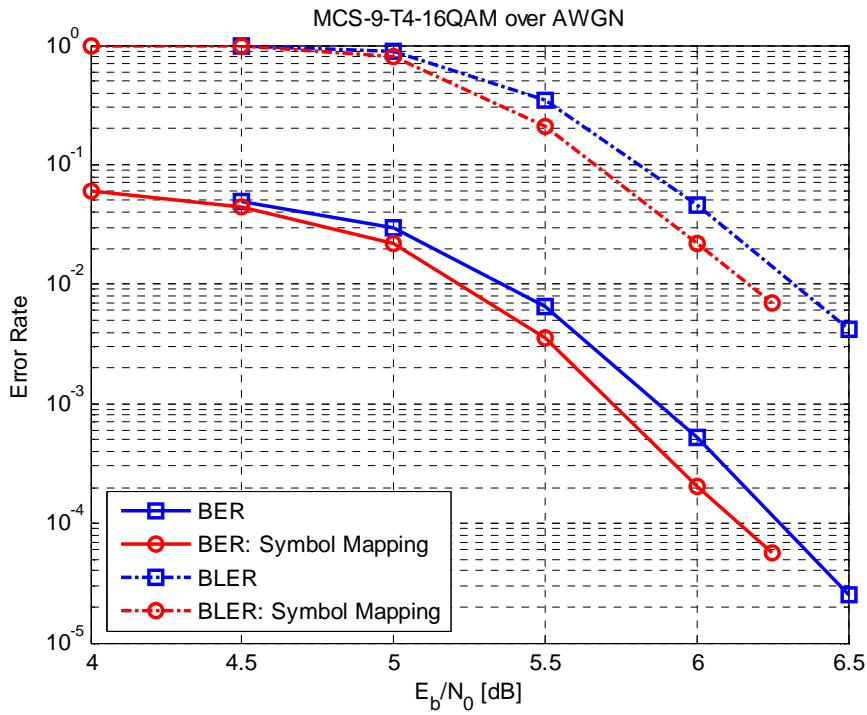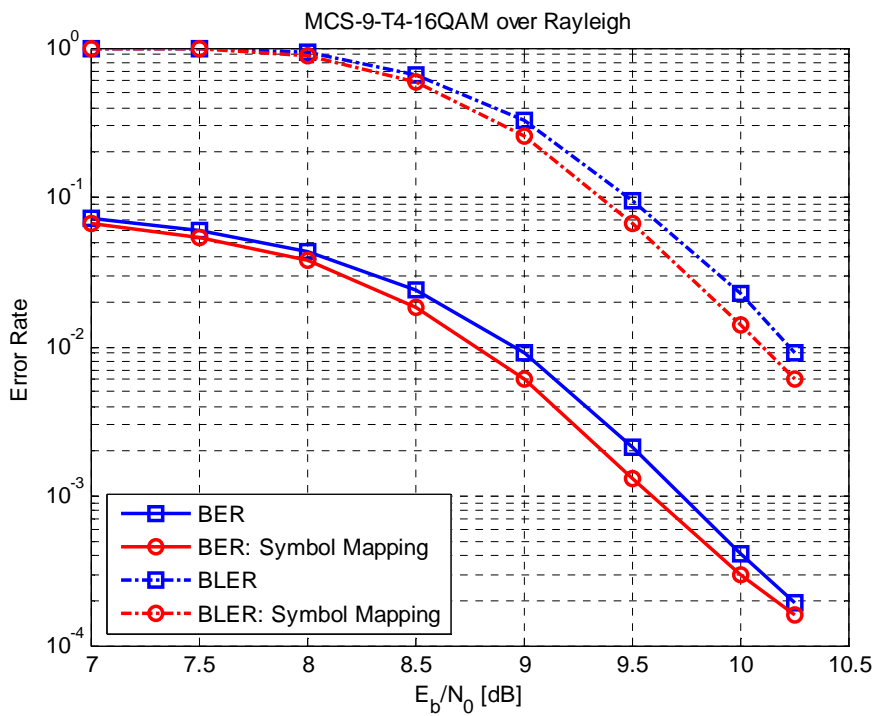**(a) AWGN channel**

(b) Rayleigh channel

Figure D.2: BER and BLER of MCS-8-T4-16QAM

MCS-9-T4-16QAM over AWGN

(a) AWGN channel

MCS-9-T4-16QAM over Rayleigh

(b) Rayleigh channel

Figure D.3: BER and BLER of MCS-9-T4-16QAM

Annex E:
Detailed simulation results for reduced transmission time interval (subclause 10.3.2)

This annex contains detailed simulation results for reduced transmission time interval. The following notation has been used in the legends:

Radio block format 1:	One timeslot in each of four consecutive TDMA frames (the regular radio block mapping).
Radio block format 2:	Two consecutive time-slots in each of two consecutive TDMA frames (case i in subclause 10.3).
Radio block format 3:	Four consecutive time-slots in one TDMA frame (case ii in subclause 10.3).

Results for inter-carrier interleaving (case iii and iv in subclause 10.3) with ideal frequency hopping are not included here since they are identical to results with radio block format 1. Results for inter-carrier interleaving without frequency hopping for case iv are not included since they are identical to results with radio block format 1 with ideal frequency hopping.

Figure E.1: Sensitivity performance for MCS-1 on TU50iFH

Figure E.2: Sensitivity performance for MCS-4 on TU50iFH

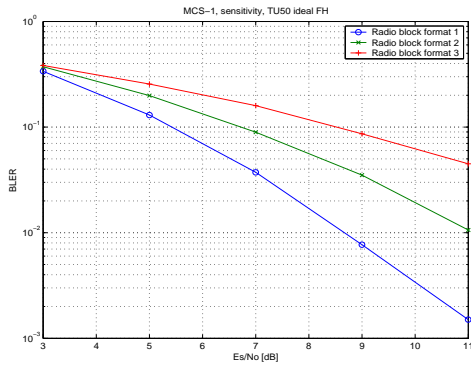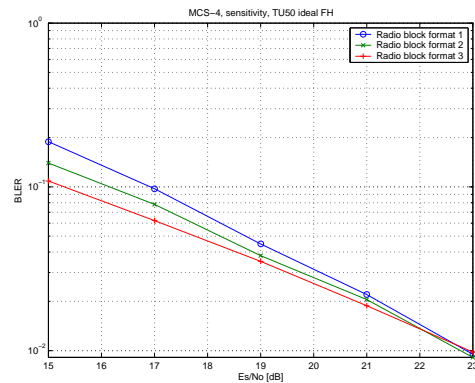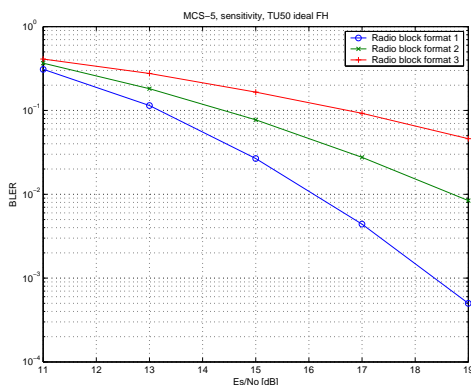**Figure E.3: Sensitivity performance for MCS-5 on TU50iFH**
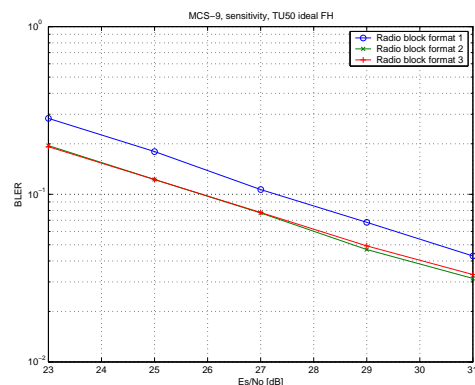
Figure E.4: Sensitivity performance for MCS-9 on TU50iFH
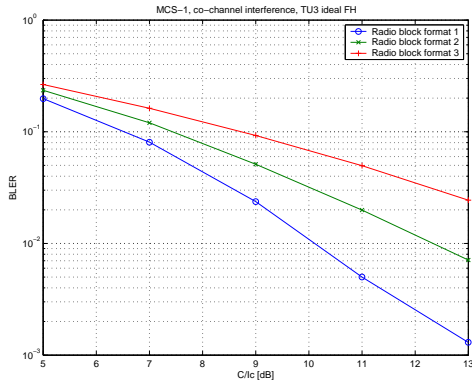
Figure E.5: Co-channel performance for MCS-1 on TU3iFH
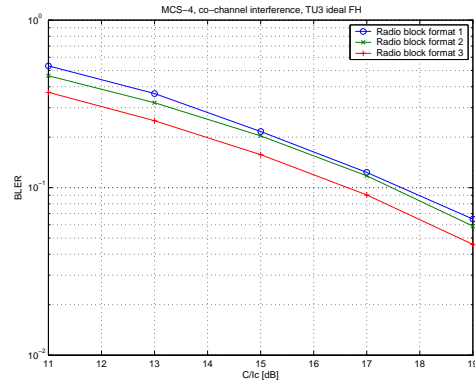
Figure E.6: Co-channel performance for MCS-4 on TU3iFH
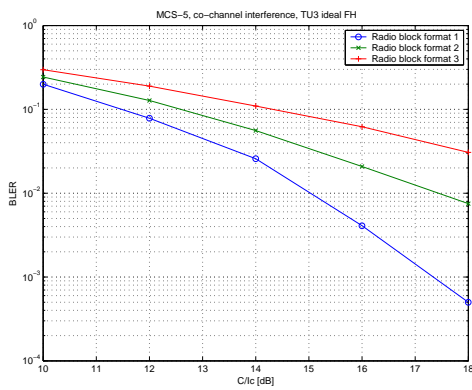
Figure E.7: Co-channel performance for MCS-5 on TU3iFH
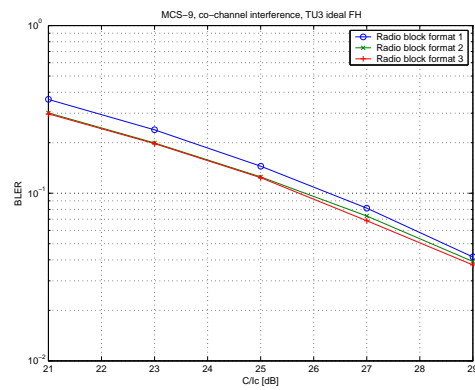
Figure E.8: Co-channel performance for MCS-9 on TU3iFH

Annex F:
Flow-graphs of SMTP and POP3 scenarios (subclause 10.3.3)

Figures F.1 and F.2 shows typical flow-graphs for the SMTP and POP3 scenarios respectively. All packet sizes are the IP packet lengths. TCP ACK/NACKs are left out for simplicity.
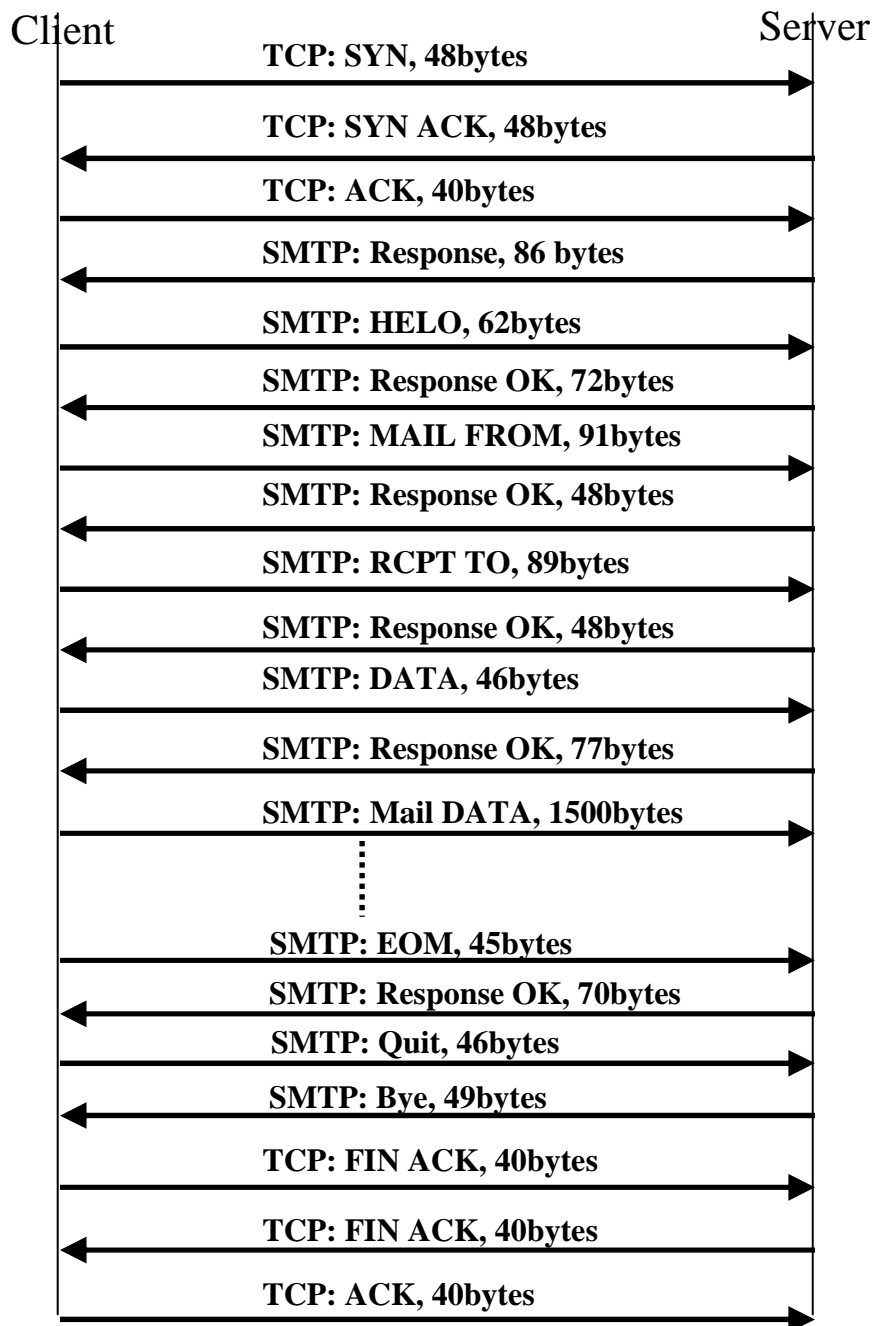
Figure F.1: Message flow-graph for e-mail sending using SMTP

Client   Server

Message	Direction
TCP: SYN, 48bytes	→
TCP: SYN ACK, 48bytes	←
TCP: ACK, 40bytes	→
POP3: Response, 91bytes	←
POP3: USER, 56bytes	→
POP3: Response, 81bytes	←
POP3: PASS, 56bytes	→
POP3: Response, 70bytes	←
POP3: STAT, 46bytes	→
POP3: Response, 54bytes	←
POP3: UIDL, 46bytes	→
POP3: Response, 87bytes	←
POP3: RETR, 48bytes	→
POP3: Mail DATA, 1500bytes	←
POP3: DELE, 48bytes	→
POP3: Response, 61bytes	←
POP3: Quit, 46bytes	→
POP3: Response, 54bytes	←
TCP: FIN ACK, 40bytes	→
TCP: FIN ACK, 40bytes	←
TCP: ACK, 40bytes	→

Figure F.2: Message flow-graph for e-mail reception using POP3

Client

	TCP: SYN, 48bytes →
← **TCP: SYN ACK, 48bytes**	
TCP: ACK, 40bytes →	
← **IMAP: Response, 150bytes**	
IMAP: Request Capability, 54bytes →	
← **IMAP: Capability, 170bytes**	
IMAP: Login, 80bytes →	
← **IMAP: Login Complete, 63bytes**	
IMAP: Namespace, 53bytes →	
← **IMAP: Response, 160bytes**	
IMAP: Request Folders, 55bytes →	
← **IMAP: Folders, 510bytes**	
IMAP: List Inbox, 59bytes →	
← **IMAP: Response, 83bytes**	
IMAP: Select Inbox, 58bytes →	
← **IMAP: Response, 210bytes**	
IMAP: Request Flags, 65bytes →	
← **IMAP: Flags, 1500bytes**	
⋮	
IMAP: Request New Headers, 200bytes →	
← **IMAP: New Headers, 1500bytes**	

Figure F.3: Message flow-graph for e-mail synchronization using IMAP

Annex G:
Change history

Change history								
Date	TSG #	TSG Doc.	CR	Rev	Subject/Comment		Old	New
2006-09	31	GP-061915			Feasibility study for evolved GERAN		2.0.2	7.0.0
2006-11	32	GP-062194	0001		Additional system level performance of HOT		7.0.0	7.1.0
2006-11	32	GP-062195	0002		Blind modulation detection performance for HOT		7.0.0	7.1.0
2006-11	32	GP-062196	0003		Impact of using HOT on the BCCH carrier		7.0.0	7.1.0
2006-11	32	GP-062197	0004		Multiplexing HOT with legacy MS		7.0.0	7.1.0
2006-11	32	GP-062385	0005	1	Correction of 16QAM results with alternative transmit pulse shaping		7.0.0	7.1.0
2006-11	32	GP-062383	0006	1	Blind Modulation Detection performance for HOT		7.0.0	7.1.0
2006-11	32	GP-062384	0007	1	Addition of MORE to chapter 8 on higher order modulations and turbo codes		7.0.0	7.1.0
2007-02	33	GP-070363	0010		Additional information regarding Type 2 MS Implementation		7.1.0	7.2.0
2008-12	40				Version for Release 8		7.2.0	8.0.0
2009-12	44				Version for Release 9		8.0.0	9.0.0
2011-03	49				Version for Release 10		9.0.0	10.0.0
2012-09	55				Version for Release 11		10.0.0	11.0.0
2014-09	63				Version for Release 12 (frozen at SP-65)		11.0.0	12.0.0
2015-12	68				Version for Release 13 (frozen at SP-70)		12.0.0	13.0.0

Change history							
Date	Meeting	TDoc	CR	Rev	Cat	Subject/Comment	New version
2017-03	RP-75	-	-	-	-	Version for Release 14 (frozen at TSG-75)	14.0.0
2018-06	RP-80	-	-	-	-	Version for Release 15 (frozen at TSG-80)	15.0.0
2020-07	RP-88e	-	-	-	-	Upgrade to Rel-16 version without technical change	16.0.0
2022-03	RP-95e	-	-	-	-	Upgrade to Rel-17 version without technical change	17.0.0

History

Document history		
V17.0.0	May 2022	Publication